

University of Strathclyde
Department of Bioengineering

**An investigation of the methodologies for biomechanical
assessment of stroke rehabilitation**

By

Enrica Papi (MSc, BSc)

This thesis is submitted in fulfilment of the requirements for the
degree of PhD in Bioengineering

2012

Copyright Statement

This thesis is the result of the author's original research. It has been composed by the author and has not been previously submitted for examination which has lead to the award of a degree.

The copyright of this thesis belongs to the author under the terms of the United Kingdom Copyright Acts as qualified by University of Strathclyde Regulation 3.50. Due acknowledgement must always be made of the use of any material contained in, or derived from, this thesis.

Signed:

Date:

Acknowledgments

If I am writing my acknowledgements it means I finally reached the light at the end of the PhD tunnel! For this priceless feeling thanks must be given to all the people who supported me, keeping me focused on my research while cheering me up when the light was totally off!

In particular, I would like to thank my supervisor Professor Philip Rowe for his guidance and the continuous challenges that made of my PhD a truly learning experience. Thanks for your support in completing my thesis.

My greatest gratitude and appreciation goes also to Mr Stephan Solomonidis for his precious advice, supervision and endless enthusiasms and encouragements.

I would also like to extend my appreciation to Mr Roy Bowers for making countless AFOs and for his inspiring clinical input to the project.

Thanks to Dr Chris Ugbolue and Dr Kostas Kaliarntas for their invaluable help during data collection in the biomechanics lab and for showing me a lovely friendship through these years.

Thanks to Mr Dave Smith and Mr John Maclean for their technical support, time dedicated to my material testing and strain gauges, and for kindly advising me in the discovery of the Scottish landscape. A big thanks also to Ms AnneMarie Baran for constantly and nicely helping me with the University paperwork.

Thanks to my 5th floor girls for making every day a more pleasant day at University. A heartily thanks to my mum and dad for transmitting me all their love day by day directly from Italy, that was essential to me to overcome all the difficulties. There are no words to describe my gratitude for your constant support and ever-patient capacity to listen and advice me in every circumstance and mostly when I was “*dazed and confused*”.

Thanks to my other two mums, Antonella and Manuela, to my beloved grandparents Gianna, Ciacci and Lara for feeding my thoughts with love and Italian delights!

My most special thanks to Beppe who kept me grounded to this achievement with his never-ending patience able to defeat the biggest of my mood thunderstorms. Thanks for being so considerate, supportive and guiding me towards the positive side against any biomechanical and maths theories.

A super smiling thanks to all my friends from Italy and all around the world who shared this experience with me and were always there when the PhD “*built me up or broke me down*”.

I would like to dedicate this thesis to my much-loved brother Carlo and cousin Lalli to encourage them to succeed at their objectives without ever giving up; even the biggest of the efforts will be paid back and the satisfaction in achieving something with your own abilities is priceless. It is worth to try, listen to the crazy one, “*fight the good fight*”! Thanks both of you for always believing in me.

“*You may say I’m a dreamer but I’m not the only one*”

GRAZIE

Enrica.

Abstract

Regaining satisfactory functional ambulation is one of the main aims of post stroke rehabilitation. Ankle foot orthoses (AFOs) are nowadays prescribed for the management of lower limb impairments following stroke onset. Their prescription and design however, is mainly empirical due to a lack of evidence-based research on their effects on gait and on their mechanical characteristics. Scientific data are crucial if the effects of rehabilitation are to be maximized.

The work presented in this thesis includes the investigation and development of methods that could be used to assess the effects of AFO on stroke survivors gait ability and, a feasibility study involving early stroke patients. The feasibility study aimed to evaluate the issues involved in a pilot randomised controlled trial (RCT) and when using a variety of outcome measures. The study also aimed to investigate, in a small group of stroke patients, the effect the provision of a solid polypropylene AFO has on gait biomechanics during the acute rehabilitation phase over a follow-up period of six months and, to measure the loads transmitted by the orthosis during gait.

Two gait analysis protocols, one allowing a full 3-D kinematics and kinetics evaluation of human gait and one for spatiotemporal parameters measurements, were introduced and their reliability explored. The feasibility of strain gauging an AFO for measuring orthotic loads was ascertained and the use of the uncontrolled manifold (UCM) approach to verify centre of mass (CM) control during gait was investigated. These methods were validated with tests on able-bodied subjects.

The application of such methodologies on stroke patients was successful. A comprehensive set of data collected was able to differentiate outcomes between walking with and without an AFO. Beneficial effects were shown when the subjects walked with the AFO at the ankle but also at the hip and knee level. Spatiotemporal parameters also improved when walking with an AFO. Gait strategy was clarified with the UCM approach with respect to CM position and the contribution of the AFO to the dorsiflexor moment was shown during early stance.

The methods proposed were capable of producing reliable results and being applied to early stroke patient to assess their walking capability. Conducting research

exploiting such methodologies will allow a better understanding of AFO properties and effects on gait, to promote recovery after stroke.

Difficulties were encountered in recruiting subjects and these are discussed along with suggestions for future studies.

Table of Contents

| | |
|--|-----------|
| Acknowledgments | iii |
| Abstract | v |
| List of Figures | x |
| List of Tables | xxiv |
| List of Abbreviations | xxviii |
| List of Publications | xxx |
| Introduction and Outline of the Thesis | 1 |
| Chapter 1: LITERATURE REVIEW | 5 |
| 1.1 Introduction | |
| 1.2 Stroke and blood supply to the brain | 5 |
| 1.3 Human burden of stroke and its consequences | 7 |
| 1.4 Stroke and gait abnormalities | 13 |
| 1.5 Orthotic management of stroke patients | 16 |
| 1.5.1 Introduction and biomechanical principles of ankle foot orthoses (AFOs) | 16 |
| 1.5.2 Research evidence on the use of AFO following stroke | 21 |
| 1.5.3 Mechanical properties of AFO: a survey of the literature | 33 |
| 1.6 Human locomotion and its analysis | 40 |
| 1.6.1 Basic principles of human motion analysis | 42 |
| 1.6.2 Joint Kinematics | 43 |
| 1.6.3 Associated errors to human movement analysis: Measurement and Compensation | 44 |
| 1.6.4 Clinical gait analysis protocol | 69 |
| 1.7 Literature Considerations | 74 |
| 1.8 Study Aims | 77 |
| Chapter 2: DEVELOPMENT AND ASSESMENT OF A NEW PROTOCOL FOR 3D GAIT ANALYSIS | 78 |
| 2.1 Introduction | 78 |
| 2.2 A new protocol and biomechanical model for gait analysis | 79 |
| 2.3 Comparative study of the proposed protocol and Plug-In-Gait protocol and two motion analysis capture systems | 94 |
| 2.3.1 Introduction | 94 |
| 2.3.2 Instrumentation and Methods | 95 |
| 2.3.3 Results | 100 |
| 2.3.4 Discussion and Conclusion | 112 |
| 2.4 Further developments of the cluster protocol | 117 |
| 2.4.1 Anatomical landmarks calibration | 117 |
| 2.4.2 Pelvic angles | 118 |
| 2.4.3 Joint moments | 119 |
| 2.5 Validation of the final stroke patient assessment protocol | 120 |
| 2.5.1 Introduction | 120 |
| 2.5.2 Methods | 120 |
| 2.5.3 Results | 124 |
| 2.5.4 Discussion and Conclusion | 133 |

| | |
|--|------------|
| Chapter 3: DESIGN OF A SIMPLIFIED VIDEO GAIT PROTOCOL FOR KINEMATIC AND TEMPORO SPATIAL PARAMETERS EVALUATION | 136 |
| 3.1 Introduction | 136 |
| 3.2 The video gait technique: Test apparatus | 137 |
| 3.3 Intra and Inter-rater reliability measurements of kinematic and temporo-spatial parameters of gait using a simple video gait technique | 139 |
| 3.3.1 Introduction | 139 |
| 3.3.2 Methods | 139 |
| 3.3.3 Results | 142 |
| 3.3.4 Discussion and Conclusion | 145 |
| 3.4 Evaluation of the concurrent validity of the new video system with the Vicon motion analysis system | 146 |
| 3.4.1 Introduction | 146 |
| 3.4.2 Methods | 146 |
| 3.4.3 Results | 150 |
| 3.4.4 Discussion and Conclusion | 151 |
| | |
| Chapter 4: ORTHOTIC LOAD MEASUREMENT | 152 |
| 4.1 Introduction | 152 |
| 4.2 Material testing | 153 |
| 4.2.1 Materials and Methods | 153 |
| 4.2.2 Results | 155 |
| 4.2.3 Discussion and Conclusion | 157 |
| 4.3 Strain gauge testing | 159 |
| 4.3.1 Materials and Methods | 159 |
| 4.3.2 Results | 161 |
| 4.3.3 Discussion and Conclusion | 165 |
| 4.4 Aluminium tests | 166 |
| 4.4.1 Materials and Methods | 166 |
| 4.4.2 Results | 169 |
| 4.4.3 Discussion and Conclusion | 171 |
| 4.5 Strain gauged AFO | 173 |
| 4.5.1 Materials and Measurement procedures | 173 |
| 4.5.2 Data Analysis | 176 |
| 4.5.3 Results | 179 |
| 4.5.4 Discussion and Conclusion | 182 |
| | |
| Chapter 5: RANDOMISED CONTROLLED STUDY METHODOLOGY | 184 |
| 5.1 Overview and Study design | 184 |
| 5.2 Study population | 184 |
| 5.3 Experimental procedures and outcome measures | 186 |
| 5.4 Management of outputs data and statistical analysis | 188 |
| | |
| Chapter 6: RESULTS | 190 |
| 6.1 Introduction | 190 |

| | |
|---|------------|
| 6.2 Study recruitment | 190 |
| 6.3 Clinical case studies | 191 |
| 6.3.1 Case study 1 | 192 |
| 6.3.2 Case study 2 | 220 |
| 6.3.3 Case study 3 | 230 |
| 6.4 Summary | 245 |
| Chapter 7: ANALYSIS OF GAIT DATA IN MANIFOLD SPACE | 246 |
| 7.1 Introduction | 246 |
| 7.2 Uncontrolled Manifold approach formulation | 248 |
| 7.3 Verification of the Uncontrolled Manifold approach | 253 |
| 7.4 Results | 255 |
| 7.4.1 Validation of the geometrical model | 255 |
| 7.4.2 UCM analysis for able-bodied subjects | 255 |
| 7.4.3 UCM analysis for stroke subjects | 258 |
| 7.5 Discussion | 262 |
| Chapter 8: DISCUSSION | 265 |
| 8.1 Introduction | 265 |
| 8.2 Case studies | 265 |
| 8.2.1 Gait analysis protocols outcomes discussion | 265 |
| 8.3 Methodological considerations | 274 |
| 8.3.1 Gait analysis protocols | 274 |
| 8.3.2 Orthotic load measurement | 277 |
| 8.3.3 Uncontrolled Manifold analysis | 278 |
| 8.3.4 Recruitment and RCT design | 280 |
| 8.4 Implications for clinical practice | 282 |
| Chapter 9: CONCLUSIONS AND RECOMMENDATIONS | 284 |
| 9.1 General Conclusions | 284 |
| 9.2 Recommendations for further study | 286 |
| REFERENCES | 288 |
| Appendix 1: Data Collection Sheet | 311 |
| Appendix 2: Index of Electronic Appendix | 314 |

List of Figures

| | |
|---|-----|
| Figure 1.1: Blood supply to the brain. Major arteries and circle of Willis are shown (Figure adapted from: http://brainmind.net/BrainLecture12.html). | 6A |
| Figure 1.2: Ischaemic stroke causes (Figure adapted from: http://brainmind.net/BrainLecture12.html). | 6A |
| Figure 1.3: Haemorrhagic stroke causes (Figure adapted from: http://brainmind.net/BrainLecture12.html). | 6A |
| Figure 1.4: Mortality rate for Scottish population between 2000 and 2009 standardised by age and gender (Table MS2 from www.isdscotland.org/isd/5782.html). | 8A |
| Figure 1.5: CVD rate for Scottish population between 2000 and 2010 standardised by age and gender (Table IS1 from www.isdscotland.org/isd/5782.html). | 8A |
| Figure 1.6: CVD incidence for Scottish population over 75 years old (a), and under 75 years old (b) (Table IS1 from www.isdscotland.org/isd/5782.html). | 8 |
| Figure 1.7: Mortality ratio standardised by age and The Scottish Index of Multiple Deprivation (SIMD). SIMD Decile: 1 most deprived to 10 least deprived area (Table DS1 from www.isdscotland.org/isd/5782.html). | 9A |
| Figure 1.8: Percentage of patients surviving for 30 days after emergency admission due to stroke. Figures are standardised by gender, age and deprivation. (http://www.indicators.scot.nhs.uk/TrendsJuly09/Stroke.html). | 9A |
| Figure 1.9: Why stroke affect only one side of the body: nerves cross over. (Figure adapted from: www.merckmanuals.com) | 9A |
| Figure 1.10: Cerebrum lobes subdivision (a) and associated functions description (b) (Martini, 2006). | 10A |
| Figure 1.11: Time course recovery of neurological (a) and functional (b) function in subjects with different severity of stroke (Jorgensen et al., 1995b). | 10A |
| Figure 1.12: AVERT protocol. Patients' assessment is conducted at arrival at hospital and after 3 and 12 months post stroke (AVERT Protocol Summary Version 1.0 - 4 April 2006). | 11 |
| Figure 1.13: Trend in Stroke Unit admission between 2005 and 2009. (Scottish Stroke Care Audit Report, 2010) | 12 |
| Figure 1.14: Example of a typical stance phase of stroke patients' hemiplegic leg. | 14A |

| | |
|--|-----|
| Figure 1.15: Equinovarus position of the foot: Foot inverted, adducted and plantarflexed. | 15A |
| Figure 1.16: Subject's assessment form to record range of motion and muscles power as introduced by the American Academy of Orthopaedic Surgeon. | 17A |
| Figure 1.17: Conventional double upright metal and leather AFO. | 17A |
| Figure 1.18: Example of plastic prefabricated AFOs (www.orthomerica.com ; www.optecusa.com). | 18A |
| Figure 1.19: Example of custom-made plastic AFOs: Spiral AFO (Condie and Meadows, 1993), Ground reaction orthosis and Solid AFO (Best Practice Statement, 2009) and articulated AFO (Best Practice Statement, 2009). | 18A |
| Figure 1.20: Example of three trimlines on a solid plastic AFO (Lehmann et al., 1983). | 18A |
| Figure 1.21: Three-force system (F_1 - F_2 - F_3) required to control plantarflexion at initial contact and mid swing. R represents the GRF (Condie and Turner, 1997). | 19A |
| Figure 1.22: Plastic ankle-foot orthosis with a single ankle strap (left) and 'figure-8' crossover strap (right) (Best Practice Statement, 2009). | 19A |
| Figure 1.23: Three-force system (R_1 - R_2 - R_3) to prevent supination of the foot (Condie and Meadows, 1993). | 19A |
| Figure 1.24: Force representations: vector acting in one point (left), distribution of multiple vectors over a broad area (right) (McHugh, 1999). | 20A |
| Figure 1.25: (a) Correction of knee hyperextension moment by realignment of GRF through knee joint centre; (b) AFO influence on hip moment: extension is created by the GRF (P) passing behind the hip (Condie and Meadows, 1993). | 20A |
| Figure 1.26: Adjustment of the GRF by tuning the AFO (Best Practice Statement, 2009). | 20A |
| Figure 1.27: Mean difference in walking speed during gait with AFO against barefoot walking or wearing shoes (Leung and Moseley, 2003). | 21A |
| Figure 1.28: Mean ambulation time for each task included in the mEFAP. Data for 3 conditions (No device, AFO, ODFS) are shown in seconds \pm SD (Sheffler et al., 2006). | 22 |
| Figure 1.29: Variation in gait velocity with provision of a polypropylene AFO (Rao et al., 2008). | 23 |

| | |
|---|-----|
| Figure 1.30: Step and Stride length (Perry, 1992). | 25A |
| Figure 1.31: Linear regression of gait velocity versus cadence in acute and chronic group patients (Rao et al., 2008). | 25A |
| Figure 1.32: Mean difference in cadence during gait with AFO against barefoot walking or wearing shoes (Leung and Moseley, 2003). | 25A |
| Figure 1.33: Mean difference in stride length during gait with AFO against barefoot walking or wearing shoes (Leung and Moseley, 2003). | 26 |
| Figure 1.34: Ankle, knee and hip sagittal plane angles for AFO benefit group walking with (light solid line) and without AFO (dark solid line) and AFO non-benefit group walking with (light dashed line) and without AFO (dark dashed line) (Bregman et al., 2010). | 27 |
| Figure 1.35: Comparison of normalised knee moment arm for the hemiplegic leg. Data are shown before treatment at 1 year and 4 years and for normal subject as reference. An extending moment arm is represented as a negative value (Butler et al., 1997). | 28A |
| Figure 1.36: Ankle moment and knee angles (positive values correspond to flexion) without AFO (a), AFO without springs (b), AFO with neutral plantar stopper (c), AFO with moderate stiffness at neutral initial angle (d), AFO with moderate stiffness at 7° dorsiflexed initial angle (e), AFO with slight stiffness at 7° dorsiflexed initial angle (f) (Miyazaki et al., 1997). | 28A |
| Figure 1.37: Three different designs of the ‘Gait Solution’ Orthosis as produced by Kawamura-Gishi Co. Ltd, Japan (http://www.kawamura-gishi.com/product/index.html) | 29 |
| Figure 1.38: Frequency distribution of Shank to Vertical Angle here referred as Shank to Floor angle (SAF), of tuned Ankle-Foot Orthosis Footwear Combinations by diagnosis (Owen, 2004). | 30A |
| Figure 1.39: Proposed algorithm for deciding AFO casting sagittal angle (Owen, 2005). | 31A |
| Figure 1.40: Effects of AFOs on energy cost and cardiorespiratory parameters (Franceschini et al., 2003). | 31A |
| Figure 1.41: Stiffness graph of a shoehorn type AFO. In the abscissa ankle joint angle is represented while the ordinate represents the AFO resistive movement (Yamamoto et al., 1993b). | 34A |
| Figure 1.42: Schematic overview of BRUCE (Bregman et al., 2009). | 34A |

| | |
|---|-----|
| Figure 1.43: (a) AFO types tested with strain gauges attached. The 5 AFOs are (from left) Flex, Standard, Moderate, Solid and Varus AFOs. A schematic view (b) of strain gauges positioning is shown in (from left) medial, posterior and lateral view (Chu and Feng, 1998). | 36A |
| Figure 1.44: Experimental AFO schematic view (Yamamoto et al., 1993b). | 38 |
| Figure 1.45: Étienne-Jules Marey's photochrononography (Figure adapted from http://comm02.wordpress.com/2011/02/08/etienne-jules-marey/). | 41 |
| Figure 1.46: Anatomical frames as defined by Cappozzo et al. (1995). | 42A |
| Figure 1.47: Schematization of the mechanism used by the triaxial goniometer which is identical to the Grood and Suntay's convention. (Chao, 1980). | 43A |
| Figure 1.48: Position artefacts trajectories of great trochanter (GT), lateral epicondyle (LE), head of the fibula (HF) and lateral malleolus (LM) skin markers during a walking cycle at natural cadence. (a) and (c) frontal plane, (b) and (d) sagittal plane (Cappozzo et al. 1996). | 45 |
| Figure 1.49: Rotational displacements of the surface marker based segment coordinate system with respect to the PST based segment coordinate system of 6 walking trials for three subjects (A, B, C) (Holden et al., 1997). | 47 |
| Figure 1.50: Angular deviation (α) between the real line and the one derived by two skin mounted markers (Tranberg and Karlsson 1998). | 49 |
| Figure 1.51: Attachment systems used: System A (a), B (b), C (c) (Südhoff et al., 2007). | 49 |
| Figure 1.52: RMS difference of knee rotations between 3D fluoroscopy and those evaluated with each cluster combination (ThT–ShT, ThP–ShT, ThC–ShT, ThD–ShT and ThD–ShD) expressed in percentage of the corresponding range. Black and grey bars referred to the two subjects analysed (Stagni et al. 2005). | 51 |
| Figure 1.53: Bone pose estimation steps using Double Calibration Technique: first (a) and new (b) methods. t_E and t_F refer to the instants of extension and flexion (Cappello et al., 1997;2005). | 52 |
| Figure 1.54: (a) Illustration of various marker sets tested. All the 11 sets employed are described on the table (b) (Manal et al.,2000). | 55 |
| Figure 1.55: Technical points considered to identify pelvic coordinate system. Axes convention is shown (Fukuchi et al.,2010). | 56 |
| Figure 1.56: Intra and inter-examiner precision (RMS values) of joint angles during upright posture (Della Croce et al., 1999). Values are in degree. | 58 |

| | |
|---|-----|
| Figure 1.57: The 3D location of the ALs using virtual palpation. | 59 |
| Figure 1.58: Inter-operator variability of the joint kinematics of one subject and one gait cycle (Donati et al., 2008). | 60 |
| Figure 1.59: Relationship between ab/adduction (a) and internal/external rotation (b) error and knee flexion angles (Kadaba et al., 1990). | 62 |
| Figure 1.60: Geometrical variables used in predictive methods (Della Croce et al., 2005). | 64 |
| Figure 1.61: Diagram of the propagation of HJC misallocation to hip and knee kinematics and kinetics (Stagni et al., 2000). | 67A |
| Figure 1.62: (a) Average of net knee moments from 18 subjects at 5 walking speeds (1 the lowest, 5 the fastest); (b) Mean values of KJC variation effect at 5 walking speeds (Holden and Stanhope 1998). | 68A |
| Figure 1.63: Flowchart representing a protocol design process. | 69 |
| Figure 1.64: Biomechanical model as for the Newington model (Baker et al., 1999). | 70A |
| Figure 1.65: Helen Hayes wand based marker set, anterior (left) and posterior (right). | 71A |
| Figure 1.66: Cleveland Clinic Foundation cluster based marker set, anterior (left) and posterior (right). | 71A |
| Figure 1.67: Schematic representation of OLGA optimisation procedure (Charlton et al., 2004). | 71 |
| Figure 1.68: (a) Marker set utilises in SAFLO protocol, with the particular of the knee wand shown. (b) Gait laboratory set up (4 cameras) and capture volume (Frigo et al., 1998). | 72A |
| Figure 1.69: (a) Plate-mounted marker configuration and calibrated anatomical landmark (.) (Benedetti et al., 1998); (b) Pointer calibration of the right lateral epicondyle (Cappozzo et al., 1995) | 72A |
| Figure 1.70: IOR Gait marker and calibration set up (Leardini et al., 2007). | 73 |
| Figure 1.71: LAMB markers set up: circles indicate anatomical markers, squares technical markers and triangles calibrated anatomical landmarks (Rabuffetti and Crenna, 2004). | 73 |
| Figure 1.72: Marker set used in Gillette functional model. The set up is the PiG markers (circles) with additional markers (triangles). NM1 and NM3 are arbitrarily placed (Schwartz and Rozumalski, 2005). | 74 |

| | |
|--|------|
| Figure 2.1: Diagram showing the designed marker set. A pointer with two markers used for calibration of anatomical landmarks (red circles) is also shown. | 83 |
| Figure 2.2: Example of how the technical frame was constructed based on the position of the markers in each cluster. | 84 |
| Figure 2.3: Example of AL position reconstruction. Knee Medial Epicondyle (ME) in two different instants of time is shown. The invariant position to the respect of the CTF is in blue font. | 86A |
| Figure 2.4: Body Planes. | 87 |
| Figure 2.5: Hip joint coordinate system. | 91A |
| Figure 2.6: Knee joint coordinate system. | 91A |
| Figure 2.7: Ankle joint coordinate system. | 92 |
| Figure 2.8: Laboratory configuration with camera on high tripods (Vicon 612) and camera on the wall trail (Vicon MX Giganet). Not all the cameras connected to the new system are visible. | 95 |
| Figure 2.9: Calibration tools: L-Frame (top left corner), 5-marker calibration wand (top right corner), dynamic calibration wand (centre). | 96 |
| Figure 2.10: Example of marker residual calculation with three camera rays, C1-D1, C2-D2 and C3-D3 (Motion Lab Systems, 2005). | 97 |
| Figure 2.11: Pointer used for anatomical landmark calibration in static trials. | 99 |
| Figure 2.12: Comparison of the two motion capture systems for PiG processed kinematics of a representative subject. <i>T</i> -test significant differences throughout the gait cycle are reported at the bottom as grey bars. | 103A |
| Figure 2.13: Comparison of the two motion capture systems for cluster method processed kinematics of a representative subject. <i>T</i> -test significant differences throughout the gait cycle are reported at the bottom as grey bars. | 103 |
| Figure 2.14: Hip joint angles about the three axes (X, Y, Z) as mean (\pm SD bars) over three gait cycles for PiG protocol (blue solid line) and cluster protocol (red solid line) of a representative subject. Statistical significant differences throughout the gait cycle are reported as grey bars. | 105A |
| Figure 2.15: Knee joint angles about the three axes (X, Y, Z) as mean (\pm SD bars) over three gait cycles for PiG protocol (blue solid line) and cluster protocol (red solid line) of a representative subject. Statistical significant differences throughout the gait cycle are reported as grey bars. | 105 |

| | |
|---|------|
| Figure 2.16: Ankle joint angles about the three axes (X, Y, Z) as mean (\pm SD bars) over three gait cycles for PiG protocol (blue solid line) and cluster protocol (red solid line) of a representative subject. Statistical significant differences throughout the gait cycle are reported as grey bars. | 106A |
| Figure 2.17: Knee Ab/Adduction angles of subject 1 as obtained by PiG (blue solid line) and Cluster protocol (red solid line). SD bars are also illustrated along each corresponding curve. | 107 |
| Figure 2.18: Hip, knee and ankle kinematics for PiG protocol as mean over 3 gait cycles for all 10 participants. SD bars are shown along each curve throughout the gait cycle. | 110A |
| Figure 2.19: Hip, knee and ankle kinematics for cluster protocol as mean over 3 gait cycles for all 10 participants. SD bars are shown along each curve throughout the gait cycle. | 110 |
| Figure 2.20: Flow chart diagram for the inverse dynamics approach (Hamill and Selbie, 2004). | 119 |
| Figure 2.21: Laboratory set up showing the 12 cameras, 4 force plates and the calibrated field of 6 m in length | 121 |
| Figure 2.22: Marker set used for data capture. Anatomical landmark markers used for calibration purposes are shown as blue circles. | 122 |
| Figure 2.23: Pelvis and lower limb joint angles in each plane as mean plus and minus SD over 10 gait cycles of the left (red solid line) and right (blue solid line) leg of one representative subject. | 124A |
| Figure 2.24: Hip, knee and ankle joint moments for left (red solid line) and right (blue solid line) leg of one representative subject. Mean and SD over ten walking cycles. | 127A |
| Figure 2.25: Right pelvis, hip, knee and ankle joint rotations in the three planes as mean over 10 repetitions of six subjects. Bars along the lines represent the SD. | 129A |
| Figure 2.26: Hip, knee and ankle joint moments mean and SD of the right leg of all six subjects. | 129 |
| Figure 2.27: Mean pelvic, hip and knee joint angle of the right leg over all subjects for pointer calibration method (red dotted line) and no pointer calibration (blue solid line). | 132 |
| Figure 3.1: Diagrammatic illustration of the test apparatus set up. | 137 |
| Figure 3.2: Sample of a Bull's eye marker. | 138 |

| | |
|---|------|
| Figure 3.3: Two segments goniometric rig set up with markers attached for data collection. | 147 |
| Figure 3.4: Lower limb marker set combining bull's eye markers and 14 mm diameter individual markers and rigid cluster. In red, markers on anatomical landmarks are shown. | 148 |
| Figure 3.5: Goniometric readings versus angle readings from AVPS (grey dotted line) and Vicon systems (black solid line). | 150 |
| Figure 4.1: Test sample dimensions as obtained from the 4.5 mm (a) and 6 mm (b) thick PP sheets. | 153A |
| Figure 4.2: Test protocol applied to PP samples with an Instron 5800R tensile testing machine. | 154 |
| Figure 4.3: Stress-strain graph of a selected polypropylene sample under tensile loads. | 155 |
| Figure 4.4: Stress-strain graph for the continuous tensile load test up to 1000 N (20 MPa). | 156A |
| Figure 4.5: Stress-strain graph of the last test protocol cycle of a typical polypropylene sample. Arrows indicate the loading and unloading path. Hysteresis is noticeable. | 156A |
| Figure 4.6: Creep during the 30 minutes hold step at 100N for a typical | 156A |
| Figure 4.7: A Strain gauged homopolymer polypropylene sample with particulars of strain gauges on the upper and lower surface and side view. | 159A |
| Figure 4.8: (a) Two-element 90° degrees rosette strain gauge used for strain measurement (Vishay Precision Group, Malvern, USA), (b) Wheatstone bridge circuit. | 159A |
| Figure 4.9: (a) Microstrain against time measured by the extensometer (blue curve) and strain gauges (red curve); (b) particular of plot (a) showing the approaching of a steady state. Data are from sample 2 test 1. | 162 |
| Figure 4.10: Microstrain against time during the 200 load cycles measured by the extensometer (blue curve) and strain gauges (red curve) for sample 1 test 2 (a) and sample 2 test 2 (b). | 163 |
| Figure 4.11: Microstrain peak values for the last cycle (200) as measured by strain gauges (grey bars) and extensometer (light grey bars) in the instrumented samples (2 samples, 2 test each). Mean (SD) bars are also shown relatively to the two systems for instrumented samples and for non strain gauged samples (green bar). | 164 |
| Figure 4.12: Test protocol applied to aluminium samples with the Instron tensile testing machine. | 167 |
| Figure 4.13: An aluminum strain gauged sample. A particular of the attached strain gauges is shown. | 167 |

| | |
|---|------|
| Figure 4.14: Test protocol applied to the strain gauged aluminium samples with the Instron tensile testing machine. | 168 |
| Figure 4.15: Stress/strain graph of a typical sample during the ramp loading steps from 500N to 4500N. On the side (right) the 3500N ramp is shown with the proportional limit being highlighted. | 169A |
| Figure 4.16: Stress/Strain graph of a typical sample during the entire test protocol. The different phases the material went through are highlighted and pictures of the samples shown at key points | 169A |
| Figure 4.17: Stress/Strain graph for sample 2, test 2 during the ramp cycles for extensometer (blue solid line) and strain gauges (red solid line). | 170 |
| Figure 4.18: (a) Microstrain measured by the extensometer (blue solid line) and strain gauges (red solid line) against time for the aluminium sample 2 test 2. (b) Particular period from graph (a) showing the variation in strain during the 1 minute hold block. | 170 |
| Figure 4.19: Medial and posterior view of the strain gauged AFO. | 173A |
| Figure 4.20: 45° three-element rosette (b) and two-element parallel strain gauge (a) used for strain measurements in the AFO (Vishay Precision Group, Malvern, USA). | 173A |
| Figure 4.21: AFO plantarflexion calibration set up. 1 kg weights are added on the hanger. For dorsiflexion calibration, the AFO is reversed. | 174 |
| Figure 4.22: Steps followed to transform the strain gauges outputs from the strain gauge reference frame (1) to the tibia reference frame (3). R indicates direction cosine matrix for axes system transformation. | 177 |
| Figure 4.23: Strain gauges outputs of the 0° (vertical) strain gauge of the 45° rosette against load for static AFO calibration in dorsiflexion (blue) and plantarflexion (red). | 179A |
| Figure 4.24: Strain gauges outputs of level A strain gauges against load for static AFO calibration in dorsiflexion (a) and plantarflexion (b). Results from the two calibrations conducted are plotted (blue and red curves). | 179A |
| Figure 4.25: Calibration of the four quarter bridges (1 to 4) obtained from the separation of the full Wheatstone bridge of the level A strain gauges for plantarflexion (Pla_1:4) and dorsiflexion (Dor_1:4). | 179 |
| Figure 4.26: Moment measured in the AFO as percentage of stance phase for all the steps recorded (1:8). Two steps for each walking trial were acquired. Positive values represent a plantarflexor moment. | 180 |
| Figure 4.27: Mean (\pm SD) total dorsiflexion/plantarflexion moment at the ankle for left leg with AFO (blue solid line) and right leg with shoe only (red solid line). | 181 |
| Figure 4.28: Total mean ankle moment of the left leg (blue solid line) and moment contribution of the AFO (red solid line) and anatomy (green solid line). | 182 |

| | |
|---|------|
| Figure 5.1: Schematic illustration of the study experimental protocol. | 186 |
| Figure 5.2: Solid ankle foot orthosis provided to the experimental group patients. | 187 |
| Figure 6.1: Walking speed at baseline, outcome and follow-up assessment for each condition tested. Bars indicate the SD over two trials. For shoes walking at baseline only one trial was performed. | 191 |
| Figure 6.2: Stance (diagonal pattern bars) and swing phase (white bars) duration of the affected leg with and without AFO for the three assessments of case study 1. Results of the <i>t</i> -test are shown for each compared bar. | 195A |
| Figure 6.3: Stance (diagonal pattern bars) and swing phase (white bars) duration of the unaffected leg with and without AFO for the three assessments of case study 1. Results of the <i>t</i> -test are shown for each compared bar. | 195A |
| Figure 6.4: Stance phase and swing phase duration of affected leg comparison across baseline (white bars), outcome (grey bars) and follow-up (diagonal pattern bars) assessments with and without AFO of case study 1. Results of the <i>t</i> -test are shown. | 196 |
| Figure 6.5: Stance phase and swing phase duration of unaffected leg comparison across baseline (white bars), outcome (grey bars) and follow-up (diagonal pattern bars) assessments with and without AFO of case study 1. Results of the <i>t</i> -test are shown. | 197A |
| Figure 6.6: Case study 1 baseline shank to vertical angle for affected leg at IC, FF, MS, HR and TC without (left) and with AFO (right). Angles in degree are reported with values of SD in brackets. | 198A |
| Figure 6.7: Case study 1 baseline shank to vertical angle for unaffected leg at IC, FF, MS, HR and TC without (left) and with AFO (right). Angles in degree are reported with values of SD in brackets. | 198A |
| Figure 6.8: Case study 1 outcome shank to vertical angle for affected leg at IC, FF, MS, HR and TC without (left) and with AFO (right). Angles in degree are reported with values of SD in brackets. | 198A |
| Figure 6.9: Case study 1 outcome shank to vertical angle for unaffected leg at IC, FF, MS, HR and TC without (left) and with AFO (right). Angles in degree are reported with values of SD in brackets. | 198 |
| Figure 6.10: Case study 1 follow-up shank to vertical angle for affected (a) and unaffected (b) leg at IC, FF, MS, HR and TC without (top) and with AFO (bottom). Angles in degree are reported with values of SD in brackets. | 199 |

| | |
|--|------|
| Figure 6.11: Pelvic tilt for baseline assessment of case study 1. Anterior tilt is positive. | 200A |
| Figure 6.12: Pelvic obliquity for baseline assessment of case study 1. Upward movement is positive in the vertical axis. | 200 |
| Figure 6.13: Pelvic rotation for baseline assessment of case study 1. Internal rotation is positive in the vertical axis. | 201A |
| Figure 6.14: Hip flexion/extension angle for baseline assessment of case study 1. Flexion positive on vertical axis. | 201 |
| Figure 6.15: Hip ab/adduction angle for baseline assessment of case study 1. Adduction is represented as positive on the vertical axis. | 202A |
| Figure 6.16: Hip internal/external rotation for baseline assessment of case study 1. Internal rotation is represented as positive on the vertical axis. | 202 |
| Figure 6.17: Knee flexion/extension angle for baseline assessment of case study 1. Flexion positive on vertical axis. | 203A |
| Figure 6.18: Knee ab/adduction angle for baseline assessment of case study 1. Adduction is represented as positive on the vertical axis. | 203 |
| Figure 6.19: Knee internal/external rotation for baseline assessment of case study 1. Internal rotation is represented as positive on the vertical axis. | 204A |
| Figure 6.20: Ankle dorsi/plantarflexion for baseline assessment of case study 1. Dorsiflexion is represented as positive on the vertical axis. | 204 |
| Figure 6.21: Ankle ab/adduction for baseline assessment of case study 1. Adduction is positive on the vertical axis. | 205A |
| Figure 6.22: Ankle inversion/eversion for baseline assessment of case study 1. Inversion is positive on the vertical axis. | 205 |
| Figure 6.23: Pelvis and lower limb kinematics at baseline assessment for case study 1. | 206A |
| Figure 6.24: Initial Contact: without AFO (left) and with AFO (right) at baseline assessment. | 206 |
| Figure 6.25: Heel Rise: without AFO (a) and with AFO (b) at baseline assessment. | 207 |
| Figure 6.26: Toe Off: without AFO (left) and with AFO (right) at baseline assessment. | 209 |
| Figure 6.27: Affected leg step length without (left) and with AFO (right). | 210 |

| | |
|--|------|
| Figure 6.28: Pelvis and lower limb kinematics at outcome assessment for case study 1. | 212A |
| Figure 6.29: Ankle Dorsi/Plantarflexion for baseline and outcome measurements during walking with (solid lines) and without (dotted lines) AFO for affected (left) and unaffected leg (right). Delays among curves can be noticed. | 212 |
| Figure 6.30: Pelvis and lower limb kinematics at follow-up assessment for case study 1. | 216A |
| Figure 6.31: Strain gauged AFO fitted on the subject's hemiplegic leg from a posterior view. | 218 |
| Figure 6.32: Dorsi/plantarflexion moments measured in the AFO as percentage of stance phase for all steps analysed (1 to 8). Plantarflexor moment is positive on the vertical axis. | 219A |
| Figure 6.33: Mean (\pm SD) over 4 steps of the total ankle dorsi/plantarflexion moment for affected (blue solid line) and unaffected (red solid line). | 219A |
| Figure 6.34: Total mean ankle moment of the affected leg (blue solid line) and contributions to the moment by the AFO (red solid line) and anatomy (green solid line). | 220 |
| Figure 6.35: Case study 2 baseline shank to vertical angle for affected (a) and unaffected (b) leg at IC, FF, MS, HR and TC without (top) and with AFO (bottom). Angles in degree are reported with values of SD in brackets. | 224A |
| Figure 6.36: Pelvis and lower limb kinematics at baseline assessment for case study 2. | 225A |
| Figure 6.37: Initial Contact through lateral side of the foot without AFO of the affected leg for case study 2. Sagittal and posterior view. | 225 |
| Figure 6.38: Initial to late stance phase of the unaffected leg during walking without AFO. | 227A |
| Figure 6.39: Case Study 2 initial contact frontal and lateral view and mid swing frontal view. | 227A |
| Figure 6.40: Case study 2 heel rise: without AFO (a) and with AFO (b) at baseline assessment. Thighs are reclined. | 228 |
| Figure 6.41: Walking speed at baseline and outcome assessment for each condition tested. Bars indicate the SD over two trials. | 231A |

| | |
|---|------|
| Figure 6.42: Sequence of instants of the unaffected leg without AFO preparing for swing phase initiation. Contralateral leg initial contact, the patient then raised a bit her body, moved the stick forward and finally raised the heel from the ground. | 233A |
| Figure 6.43: Sequence of instants of the unaffected leg with AFO preparing for swing phase initiation. Contralateral leg initial contact and heel rise simultaneous to the stick forward movement. | 233A |
| Figure 6.44: Stance (diagonal pattern bars) and swing phase (white bars) duration of the affected leg(a) and unaffected (b) with and without AFO for the two assessments of case study 3. Results of the t-test are shown for each compared bar. | 233 |
| Figure 6.45: Case study 3 baseline SVA for affected (a) and unaffected (b) leg at IC, FF, MS, HR and TC without (top) and with AFO (bottom). Angles in degree are reported with values of SD in brackets. | 236A |
| Figure 6.46: Case study 3 outcome SVA for affected (a) and unaffected (b) leg at IC, FF, MS, HR and TC without (top) and with AFO (bottom). Angles in degree are reported with values of SD in brackets. | 236A |
| Figure 6.47: pelvis and lower limb kinematics at baseline assessment for case study 3. | 237A |
| Figure 6.48: Initial contact for case study 3 without AFO (left) and with AFO (right) during baseline assessment. | 236 |
| Figure 6.49: Knee hyperextended and anterior tilt in stance phase without AFO (left) and relative instant with AFO (right) at baseline. | 237 |
| Figure 6.50: Mid Swing without AFO (left) and with AFO (right) at baseline test of patient 3. | 238 |
| Figure 6.51: pelvis and lower limb kinematics at outcome assessment for case study 3. | 242A |
| Figure 6.52: Sound leg mid stance just prior affected leg initial contact and increase unaffected knee flexion. | 243 |
| Figure 6.53: Knee internal/external rotation for outcome (blue solid line) and baseline (red solid line) AFO walking. | 244A |
| Figure 7.1: Uncontrolled manifolds graph from Schoner and Scholz, 2007. | 247 |
| Figure 7.2: Representation of the approximation of the centre of mass definition (yellow dot) and projection line connecting the mid points (red crosses) between anterior and posterior iliac spine. | 248A |
| Figure 7.3: Leg and foot stick model. | 248A |

| | |
|--|------|
| Figure 7.4: Positions of the foot on the ground at the identified 3 key points depending on θ_G value. | 249 |
| Figure 7.5: Hip, knee and ankle displacement in the x and y direction for one representative subject as obtained from the Cluster protocol and the geometric model. | 255A |
| Figure 7.6: Mean and SDs bars of sagittal hip, knee and ankle joint kinematics of six normal subjects during stance phase. | 256A |
| Figure 7.7: Mean centre of mass displacement during stance in the x and y directions for the six normal subjects. SD bars are shown. | 256 |
| Figure 7.8: Variance components within (Vucm, blue solid line) and perpendicular (Vort, red solid line) to the linearized UCM. | 257 |
| Figure 7.9: Balanced ratio for the six normal subjects. | 258A |
| Figure 7.10: Mean and SDs bars of sagittal hip, knee and ankle joint kinematics with (blue solid line) and without AFO (red solid line) for 3 stroke patients during their assessment. | 259A |
| Figure 7.11: Mean centre of mass displacement during stance in the x and y directions for the three stroke subjects. SD bars are shown. | 259 |
| Figure 7.12: Variance components within (Vucm, blue solid line) and perpendicular (Vort, red solid line) to the linearized UCM for the three stroke patients (P1,P2,P3). | 260 |
| Figure 7.13: Balanced ratio for case study 1. Mean balanced ratio of normal subjects is shown as reference. | 261A |
| Figure 7.14: Balanced ratio for case study 2. Mean balanced ratio of normal subjects is shown as reference. | 261A |
| Figure 7.15: Balanced ratio for case study 3. Mean balanced ratio of normal subjects is shown as reference. | 262 |

List of Tables

| | |
|--|------|
| Table 1.1: Stroke risk factors. | 7A |
| Table 1.2: Summary table of studies reporting STA assessment. | 48A |
| Table 2.1: Anatomical frames definitions. | 82A |
| Table 2.2: Marker set used during data collection. The name of each marker and its position is reported relatively to the body segment they are referred to. | 98 |
| Table 2.3: Joint angle parameters. Acronyms and corresponding definitions are reported. | 100 |
| Table 2.4: Reconstruction residuals for static trials for all lower limb markers as from Vicon612 cameras and Vicon MX cameras. Values are in mm. | 101 |
| Table 2.5: Reconstruction residuals for dynamic trials for all lower limb markers as from Vicon 612 cameras and Vicon MX cameras. Values are in mm. | 101 |
| Table 2.6: Hip joint angle parameters of a representative subject as mean (\pm SD) over 3 gait cycles calculated by the PiG and cluster protocol. | 105A |
| Table 2.7: Knee joint angle parameters of a representative subject as mean (\pm SD) over 3 gait cycles calculated by the PiG and cluster protocol. | 105 |
| Table 2.8: Ankle joint angle parameters of a representative subject as mean (\pm SD) over 3 gait cycles calculated by the PiG and cluster protocol. | 106A |
| Table 2.9: Mean (\pm SD) of knee adduction peak values in swing phase over 3 gait cycles expressed in degrees ($^{\circ}$) calculated with the PiG and cluster protocol for each participant (1 to 10). | 107 |
| Table 2.10: Mean ($^{\circ}$) and absolute mean (% of range of motion) of standard deviation values for hip joint angles for all study participants (1-10) for both PiG protocol and cluster protocol. | 109A |
| Table 2.11: Mean ($^{\circ}$) and absolute mean (% of range of motion) of standard deviation values for knee joint angles for all study participants (1-10) for both PiG protocol and cluster protocol. | 109A |
| Table 2.12: Mean ($^{\circ}$) and absolute mean (% of range of motion) of standard deviation values for ankle joint angles for all study participants (1-10) for both PiG protocol and cluster protocol. | 109 |
| Table 2.13: Mean (SD) for joint angle parameters across all subjects for PiG and cluster protocols. T-test results are shown in the last column. | 111 |

| | |
|---|------|
| Table 2.14: Mean (°) and absolute mean (%) values of angle standard deviation among the ten participants for both protocols. | 111 |
| Table 2.15: Anatomical landmarks static calibration markers, name and position are reported. | 118 |
| Table 2.16: Joint moment parameters. Acronyms and corresponding definitions are reported. | 123 |
| Table 2.17: Mean and standard deviation for the joint angle parameters over 10 repetitions of left (L) and right (R) leg of one subject. | 124 |
| Table 2.18: Mean values of angle standard deviation (°) and absolute standard deviation (%) throughout the gait cycle for joint angles in each plane for all study subjects. Left (L) and right (R) leg variability are reported. | 125 |
| Table 2.19: Joint moment parameters for the hip, knee and ankle of a representative subject's left (L) and right leg (R). Mean and standard deviation over 10 repetitions in Nm are reported. | 127 |
| Table 2.20: Mean values of joint moments standard deviation throughout stance phase duration for each plane and subjects' left (L) and right (R) leg. | 128 |
| Table 2.21: Joint angle parameters as mean and standard deviation of left (L) and right (R) leg of all subjects. | 130 |
| Table 2.22: Joint moments parameters as mean and standard deviation, in brackets, of left (L) and right (R) leg of all subjects. | 130 |
| Table 2.23: Mean values of the standard deviation over the gait cycle for left (L) and right (R) leg joint angles across the six participants, each walking 10 times. | 131 |
| Table 2.24: Mean values of the standard deviation over the stance phase for left (L) and right (R) leg joint moments across the six participants, each walking 10 times. | 132 |
| Table 2.25: Mean (SD) for joint angle parameters across all subjects as for pointer and no pointer calibration methods. In the last column <i>p</i> -values derived from a conducted <i>t</i> -test are reported. | 132A |
| Table 3.1: Representation of kinematic parameters, temporo-spatial parameters and tibia angle of inclination with respect to gait events showing the mean, and standard deviation for the three raters for the able-bodied and stroke survivors groups. | 142A |
| Table 3.2: Intra Rater Reliability (ICC value), Inter Rater Correlation and 95% Confidence Interval for the able bodied group for left and right side measurements. | 143 |

| | |
|---|------|
| Table 3.3: Inter-rater reliability for healthy participants and stroke survivors among the three raters. | 143 |
| Table 3.4: Intra Rater Reliability (ICC value), Inter Rater Correlation and 95% Confidence Interval for the stroke survivors group for left and right side measurements. | 144 |
| Table 3.5: Marker set used during data collection. Markers are classified in according to the capture system they are used for. | 148A |
| Table 3.6: Outcome parameters from the two systems averaged across the twelve participants. Mean, standard deviation and <i>p</i> -values are reported. | 151 |
| Table 4.1: Mean over 5 cycles of Young's Modulus values found experimentally for standard and perpendicular test samples of 4.5 mm thickness. In brackets the standard deviation is shown. | 157 |
| Table 4.2: Mean over 5 cycles of Young's Modulus values found experimentally for standard and UV treated test samples of 6 mm thickness. In brackets the standard deviation is shown. | 157 |
| Table 4.3: Average percentage differences between strain gauges and extensometer values of strain for the last 5 cycles of test in the two samples tested. | 162 |
| Table 4.4: Percentage differences between strain reference value and strain measured by strain gauges and extensometer for the peak values during cycle 200. | 164 |
| Table 4.5: Average percentage differences between strain gauges and extensometer values of strain for the last 5 cycles of test in the two aluminium samples tested. | 171 |
| Table 5.1: Research questions. | 184 |
| Table 5.2: Eligibility criteria for subjects' recruitment. | 185 |
| Table 6.1: Modified Rivermead Mobility Index (mRMI) and the Functional Ambulatory Category (FAC) for patient 1. | 192 |
| Table 6.2: Comparison of temporal parameters assessed with and without AFO for affected and unaffected leg for case study 1. | 194 |
| Table 6.3: Comparison of spatial parameters assessed with and without AFO for affected and unaffected leg of case study 1. | 197A |
| Table 6.4: Mean (°) and absolute mean (% of range of motion) of standard deviation values for each joint angles for both affected and unaffected leg during walking with and without AFO at baseline of case study 1. | 211 |

| | |
|--|------|
| Table 6.5: Mean (°) and absolute mean (% of range of motion) of standard deviation values for each joint angle for both affected and unaffected leg during walking with and without AFO at outcome assessment of case study 1. | 215 |
| Table 6.6: Ankle angle in degree and their occurrence as percentage of the gait cycle for outcome and follow up measurements with and without AFO of case study 1. | 216 |
| Table 6.7: Mean (°) and absolute mean (% of range of motion) of standard deviation values for each joint angle for both affected and unaffected leg during walking with and without AFO at follow-up assessment of case study 1. | 217 |
| Table 6.8: Comparison of temporal parameters assessed with and without AFO for affected and unaffected leg during baseline assessment for patient 2. | 222 |
| Table 6.9: Comparison of spatial parameters assessed with and without AFO for affected and unaffected leg during baseline assessment for case study 2. | 223 |
| Table 6.10: Mean (°) and absolute mean (% of range of motion) of standard deviation values for each joint angle for both affected and unaffected leg during walking with and without AFO at baseline assessment of case study 2. | 229 |
| Table 6.11: Modified Rivermead Mobility Index (mRMI) and the Functional Ambulatory Category (FAC) for patient 3 at baseline and outcomes assessments. | 231 |
| Table 6.12: Comparison of temporal parameters assessed with and without AFO for affected and unaffected leg during baseline and outcome assessments for case study 3. | 232 |
| Table 6.13: Comparison of spatial parameters assessed with and without AFO for affected and unaffected leg during baseline and outcome assessment of case study 3. | 235 |
| Table 6.14: Mean (°) and absolute mean (% of range of motion) of standard deviation values for each joint angle for both affected and unaffected leg during walking with and without AFO at baseline assessment of case study 3. | 2341 |
| Table 6.15: Mean (°) and absolute mean (% of range of motion) of standard deviation values for each joint angle for both affected and unaffected leg during walking with and without AFO at outcome assessment of case study 3. | 244A |

List of Abbreviations

| | |
|------|---|
| AFO | Ankle Foot Orthosis |
| AF | Anatomical Frame |
| AJC | Ankle Joint Centre |
| AL | Anatomical Landmark |
| AVPS | Augmented Video-based Portable System |
| CAST | Calibrated Anatomical System Technique |
| CNS | Central Nervous System |
| CM | Centre of Mass |
| CTF | Cluster Technical Frame |
| CVD | Cerebrovascular Disease |
| DOF | Degree Of Freedom |
| FEA | Finite Element Analysis |
| FF | Foot Flat |
| GRF | Ground Reaction Force |
| HJC | Hip Joint Centre |
| IC | Initial Contact |
| ISB | International Society of Biomechanics |
| ISPO | International Society for Prosthetics and Orthotics |
| JCS | Joint Coordinate System |
| KJC | Knee Joint Centre |
| MS | Mid Stance |
| NHS | National Health Service |
| PP | Polypropylene |
| PiG | Plug in Gait |
| PLS | Posterior Leaf Spring |
| RCT | Randomised Controlled Trial |
| ROM | Range Of Motion |
| SD | Standard Deviation |
| SG | Strain Gauge |
| STA | Soft Tissue Artefact |
| SVA | Shank to Vertical Angle |

TC Terminal Contact
TO Toe Off
UCM Uncontrolled Manifold

List of Publications

Journal Articles:

Papi E, Ugbolue UC, Solomonidis SE, Rowe PJ, Quantitative comparison of Plug-In-Gait protocol and a new anatomically based protocol in gait analysis outcomes. (In preparation).

Papi E, Ugbolue UC, Solomonidis SE, Rowe PJ, Comparison of two 3-D motion capture systems. (In preparation).

Ugbolue UC, Papi E, Kaliarntas KT, Kerr A, Earl L, Pomeroy VM, Rowe, PJ, The evaluation of an inexpensive, 2D, video based gait assessment system for clinical use. *Gait & Posture* (Submitted).

Ugbolue UC, Papi E, Kerr A, Earl L, Pomeroy VM, Rowe PJ (2011), Intra and Inter-Rater Reliability Measurements of Kinematic and Temporo-Spatial Parameters of Gait Using a Simple Video Technique. *J Bioengineer & Biomedical Sci*, S1:003.

Conference Proceedings:

Papi E, Ugbolue UC, Solomonidis SE, Rowe PJ (2011), Development of a gait analysis protocol for the evaluation of stroke patients. *23rd International Society of Biomechanics Congress, Brussels (Belgium)*.

Papi E, Rowe PJ, Bowers RJ, Solomonidis SE (2011) Rehabilitation of early stroke patients using custom made solid ankle-foot orthoses: preliminary results of a randomised controlled trial. *1st Conference on Scientific Testing of Orthotic Devices, March, Aix Les Bains (France)*.

INTRODUCTION AND OUTLINE OF THE THESIS

Stroke is a major public health problem causing death and disability worldwide. It is estimated that, just in Scotland, there will be approximately 15,000 new diagnoses each year (SIGN Guideline 64, 2005). The after effects, for those who survive the brain injury, can be widespread and long lasting, requiring clinical care and rehabilitation. One of the most common consequences following the stroke onset is hemiplegia which, at lower limb level, leads to an altered, slow speed and asymmetric gait pattern reducing the patient's independence in daily life. Regaining walking ability is, thus, one of the main goals in stroke rehabilitation. In clinical practice, therapy of these mobility deficits is currently mainly attempted through physiotherapy.

However, the prescription of ankle foot-orthoses (AFOs) as an adjunct to physical therapy is increasing, especially among the chronic stroke population. An AFO is a device which encompasses the ankle joint extending to a point below the knee. Ankle-foot orthoses enhance patients' ambulation by supporting and controlling movements of the patient's lower limb segment. Although nowadays their provision is becoming a more common practice (Best Practice Statement, 2009), questions are still to be addressed to improve appropriate utilisation of AFOs.

A thorough literature review on post stroke rehabilitation and AFO's effects shows a lack of evidence-based research, especially early after stroke. Most researchers have investigated the effect of AFO in chronic stroke patients with evidence of improvements in ambulation (Franceschini et al., 2003; Dieli et al., 1997). The fact that success has been achieved using AFOs in late intervention, together with the promising results from very early mobilisation trials using only physiotherapy (Bernhardt et al., 2004, 2008), raises the question of whether a patient would not have had a better functional recovery if treated at an early stage with an appropriate AFO. The long term effect of wearing an orthosis is not well documented as the majority of studies compared the immediate effects of an AFO against no AFO condition (Tyson and Rogerson, 2009). In addition, regarding the long term use of an ankle-foot orthosis, there is an open debate on the possibility of an AFO to lead to dependency and thus inhibiting recovery. This claim is mainly a concern of

physiotherapists but there is very limited scientific evidence that ankle-foot orthoses may affect negatively calf muscle activity (Hesse et al., 1999). On the contrary, according to an international consensus conference of the International Society of Prosthetics and Orthotics (Condie et al., 2004) the use of an ankle-foot orthosis at an early stage after the stroke should not be discouraged. The use of an AFO as a provisional device during rehabilitation has been suggested with the hope to reduce to a minimum the possibility of producing long term dependency while allowing the patient to mobilise early after stroke.

Only few biomechanical studies (Mc Hugh, 1999; Chu et al., 1995a,b; Yamamoto et al., 1993a;1993b; Bregman et al., 2010) reported on the mechanical properties of the AFO and contribution of the orthosis to the ankle moment. The results from these studies, however, are not applied in clinical practice and the prescription and design of AFOs therefore remain based on empirical techniques.

This study aims to investigate the effects on gait biomechanics of a solid AFO on early stroke patients with usual rehabilitation practice as the control condition, to evaluate the profile of recovery of walking kinematics over a period of 24 weeks and, finally, to measure the loads developed by the AFOs during walking. Participants are randomised into two groups; subjects allocated in the experimental group receive a solid polypropylene AFO with carbon fibre reinforcement, subjects allocated in the control group may receive an AFO if it is deemed appropriate by the Hospital orthotist.

Moreover, to be able to quantify the best rehabilitation practice for stroke patients, valid methods of analysis should be employed in order to obtain relevant information that could be used to refine AFO intervention in clinical practice. A useful tool for the evaluation of stroke gait pattern with and without AFO, for treatment planning and monitoring could be achieved using human movement analysis.

The project thus also aims to explore methodologies and practical issues related to the assessment of stroke patients in a research and clinical environment.

The objective is to introduce a set of methods through which different aspects of the gait can be evaluated from kinematics to motor control, from spatiotemporal

parameters to orthotic loads. The viability of these methods in evaluating the efficacy of AFOs in stroke gait will be investigated through a feasibility study.

This should form a base for future randomised controlled trial planning in order to collect data to establish an appropriate AFO intervention that could be applied in the routine rehabilitation of stroke patients at an acute stage.

The work conducted to pursue the study aims is outlined in this thesis which is articulated as follows:

Chapter 1 presents an overview of stroke and its consequences with particular focus on the management of residual disabilities. The effects of AFOs on gait and mechanical properties of such orthoses are documented based on a survey of the literature. This Chapter concludes with a description of the aspects involved in human motion analysis and with a review of gait analysis protocols that have been introduced to date.

Chapter 2 outlines the steps undertaken to finalize a 3-D gait analysis protocol that could be used for the assessment of early stroke patients. Validations conducted to verify the reliability of the protocol are also described.

Chapter 3 describes the design of a simplified gait analysis protocol that can find readily applicability in a clinical environment. Studies carried out to assess such method are presented.

Chapter 4 focuses on the introduction of a method to calculate AFO contribution to the ankle moment by strain gauging a polypropylene AFO. Tensile tests conducted to characterise the material and verify that strain gauges applied to the AFO record acceptable results are also presented.

Chapter 5 details the design and experimental procedures of a feasibility study involving stroke patients to investigate the effects on gait of AFO during an early rehabilitation phase. In addition, the theory of the uncontrolled manifold approach, for a motor control analysis, is given and what its application involves is described.

Chapter 6 presents the experimental results obtained by the methods outlined in Chapter 5.

Chapter 7 critically discusses the findings reported in Chapter 6 and makes considerations on the methods introduced and utilised. Clinical implications are also discussed.

Chapter 8 concludes the thesis with overall comments on the results and methods and, makes recommendations for further studies.

CHAPTER 1 – LITERATURE REVIEW

1.1 Introduction

In the current chapter, the background of the study and the relevant literature establishing the study rationale are reported.

The first section describes the aetiology and classification of stroke, followed by an overview of stroke incidence and its consequences on the population. Of particular interest to the study is the effect of stroke on gait ability. In this regard, gait abnormalities following the brain incident are described and the current management of those disabilities investigated.

The role of an ankle-foot orthosis (AFO) in stroke rehabilitation is highlighted and studies conducted in this field will be reviewed.

The last section treats human motion analysis as a method of gait assessment. Basic principles are described and consideration is given to the errors associated with this procedure. A survey of gait analysis protocols developed to date is reported.

To conclude, considerations on the literature reviewed are made and the aims of the thesis are outlined.

1.2 Stroke and blood supply to the brain

A stroke is clinically defined as an acute neurologic dysfunction of vascular origin with sudden (within seconds) or at least rapid (within hours) occurrence of symptoms and sign corresponding to the involvement of focal areas in the brain (World Health Organisation, 1989).

The brain, with its billions of neurons, is an active organ which depends upon its blood flow for both oxygen and nutrient supply to function properly. Blood reaches the brain through two main arterial systems: carotid arteries and vertebral arteries (Figure 1.1). The latter fuse to form the basilar artery within the cranium. Carotid arteries (external and internal) and the basilar artery are connected in a ring shaped arterial network at the base of the brain, known as Circle of Willis or arterial circle. Arteries branching from the Circle of Willis are responsible for blood distribution to various area of the brain. The arrangement of arteries into a circle allows for a constant cerebral perfusion even if one of the supplying arteries is occluded or

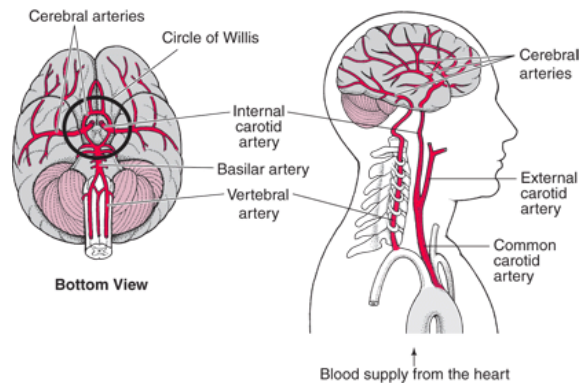


Figure 1.1: Blood supply to the brain. Major arteries and circle of Willis are shown (Figure adapted from: <http://brainmind.net/BrainLecture12.html>).

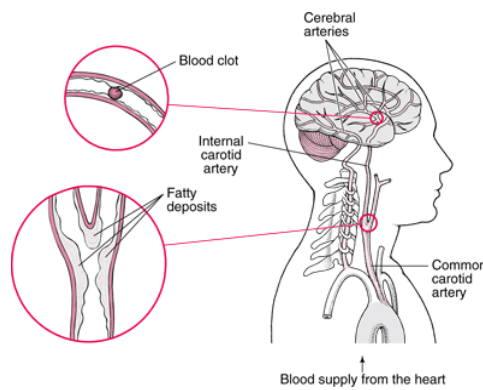


Figure 1.2: Ischaemic stroke causes (Figure adapted from: <http://brainmind.net/BrainLecture12.html>).

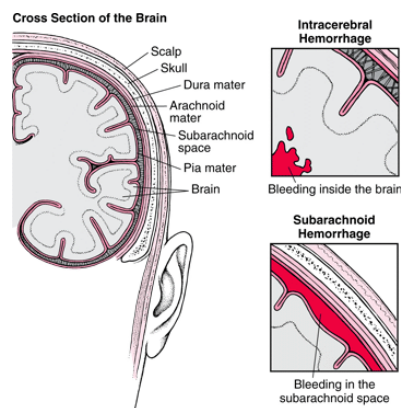


Figure 1.3: Haemorrhagic stroke causes (Figure adapted from: <http://brainmind.net/BrainLecture12.html>).

narrowed. However, interruption of a vessel past the circle can result in serious damage. A reduction or disruption of cerebral blood circulation, if prolonged, can cause brain tissue damage or even death. The severity and clinical features of stroke are determined by the site affected within the brain and by the degree of oxygen starvation.

Stroke can be divided into two broad categories according to the nature of the cerebral lesion: infarcts (ischaemic stroke) and haemorrhages (haemorrhagic stroke) (World Health Organisation, 1989). Ischaemic strokes (Figure 1.2) are the result of the interruption of blood supply to the brain due to a blockage of an artery.

Blockages are blood clots (thrombi) or fatty globules (atheromas) that could develop in the main artery of the brain or in blood vessels in the body and be carried along with the blood stream to the brain (embolus). When the blockage occurs in one of the small penetrating arteries that supply deep area of the brain, stroke is referred as lacunar stroke, 'small, deep infarct'. This sub-category of ischaemic strokes is more likely to be caused by local *in situ* small vessel disease rather than embolism (Warlow et al., 2001). The majority of strokes have been reported to be of the ischaemic type.

Haemorrhagic strokes (Figure 1.3) occur when a blood vessel bursts within the brain (intracerebral haemorrhage) or in the area between the brain and the skull, subarachnoid space (subarachnoid haemorrhage). The expanding blood leakage causes cerebral tissue injuries near the site of the bleeding. Haemorrhagic stroke accounts for nearly 20% of all cases of stroke but are more often fatal compared to ischemic strokes due to the extensive areas of the brain affected.

Blockage of the brain blood supply can also be temporary and lasts for a very brief time, usually 1-2 hours. In this case it is referred to transient ischemic attack (TIA) or mini stroke. Symptoms of TIA are similar to those of an ischemic stroke but the damage is usually small.

The most common symptoms of stroke and temporary ischemic attack are: sudden weakness or numbness of the face, arm or leg, especially on one side of the body, loss of walking function, difficulty in speaking and understanding, loss of vision, poor balance and coordination. The more typical symptoms of haemorrhagic strokes are sudden headache, loss of consciousness, and high blood pressure. However, each

| Medical conditions which favour stroke risk | |
|---|---|
| <p><u>Diabetes Mellitus</u></p> <p>Hyperglycemia can increase the risk of ischaemic stroke especially in large blood vessels.</p> | <p><u>Heart Disease</u></p> <p>Heart diseases have a consistent relationship with risk of stroke.</p> |
| <p><u>High Blood pressure (HBP)</u></p> <p>Hypertension is a major risk factor (70% of all strokes due to HBP).</p> | <p><u>Previous stroke or Transient Ischaemic Attack (TIA)</u></p> <p>A history of prior stroke or TIA increases the probability of subsequent stroke.</p> |
| <p><u>Unhealthy Cholesterol level</u></p> <p>Cholesterol level increases the risk of developing atherosclerosis.</p> | <p><u>Atrial Fibrillation</u></p> <p>Increasing risk for formation of blood clots.</p> |
| Lifestyle choices factors | |
| <p><u>Tobacco use</u></p> <p>Major controllable risk factor.</p> | <p><u>Physical inactivity</u></p> <p>Lack of exercise increases risk of obesity, HBP, and diabetes thus likely stroke occurrence.</p> |
| <p><u>Unhealthy diet/Obesity</u></p> <p>High intake of saturated fat increases blood lipids level and risk of thrombosis.</p> | <p><u>Excessive alcohol intake</u></p> <p>Heavy drinking increases blood pressure, weight and level of triglycerides in the blood.</p> |
| <p><u>Drug use</u></p> <p>Cocaine and amphetamines, in particular, increase risk of stroke.</p> | |
| Uncontrollable risk factors | |
| <p><u>Increasing age</u></p> <p>Stroke is more common in people over 60s.</p> | <p><u>Gender</u></p> <p>Men are more commonly affected by stroke than women.</p> |
| <p><u>Genetic or familial factors</u></p> <p>Stroke more common in people whose relatives have suffered from stroke.</p> | <p><u>Ethnicity</u></p> <p>Blacks, Hispanic Americans, Chinese and Japanese population are at high risk of stroke.</p> |

Table 1.1: Stroke risk factors.

person experiences particular symptoms depending on the area in the brain involved by blockage or bleeding (World Health Organisation, 1989).

Major risk factors that favour stroke occurrence have been summarised in Table 1.1). Although conducting a healthy life style reduces the risk of having stroke there are some risk factors that cannot be altered such as age, genes, gender and ethnic background (www.stroke.org.uk/information/stroke_prevention/index.html, <http://www.isdscotland.org/isd/5783.html>; Mackay and Mensah, 2004).

1.3 Human burden of stroke and its consequences

Stroke is the third most frequent cause of death and the most common cause of major adult disabilities. Stroke is responsible for an estimated 5.7 million deaths worldwide (Strong et al., 2007). About 16 million people have a first-ever stroke every year and more than 30 million are living as stroke survivors (Strong et al., 2007). Although the incidence of stroke is declining in high-income countries, stroke remains a leading health problem in low and middle-income countries, where the incidence of stroke has more than doubled over the past 40 years (The Lancet Neurology, 2011). The number of people living with stroke and its consequences, however, is expected to grow due to population ageing, improvement of services and demographic transition (Mackay and Mensah, 2004; Strong et al., 2007).

Those figures reflect also the prevalence of stroke in Scotland, one of the countries with the highest rates of stroke in the world (Chest, Heart & Stroke Scotland, 2002). This justifies the increasing interest of NHS Quality Improvement Scotland and government on developing evidence-based guidelines and improving specialised stroke units for high quality care across Scotland. It is estimated that seventy thousand Scots are living with stroke and its effects and, each year there will be approximately 12,500 new stroke events (Scottish Intercollegiate Guidelines Network, SIGN 118, 2010). From the latest publication of statistical information from Information Services Division (ISD)'s Heart Disease & Stroke Programme the following key points relating to stroke are highlighted. The last update was on February 2011 (www.isdscotland.org/isd/5782.html):

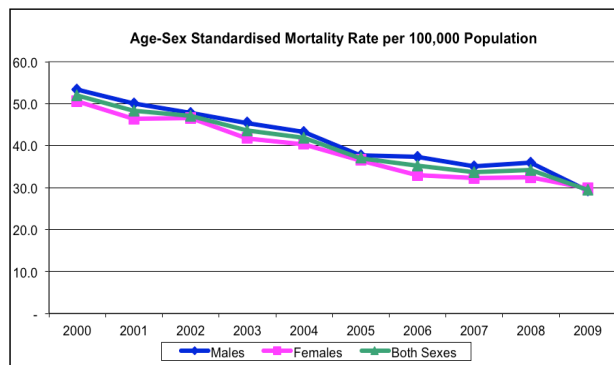


Figure 1.4: Mortality rate for Scottish population between 2000 and 2009 standardised by age and gender (Table MS2 from www.isdscotland.org/isd/5782.html).

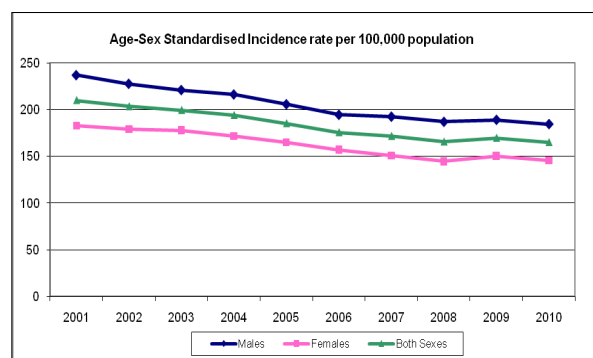


Figure 1.5: CVD rate for Scottish population between 2000 and 2010 standardised by age and gender (Table IS1 from www.isdscotland.org/isd/5782.html).

- The prevalence of stroke was 8.7% in men and 7.5% in women and increased with age, to 35.9% in men and 26.7% in women aged 75 and over (year 2008).
- Mortality following stroke events has decreased; data reported suggest a reduction of 34.6% between 2000 (4,176) and 2009 (2,732) (Figure 1.4).
- Incidence rate for cerebrovascular disease (CVD) diminished by 21.3% between 2000 and 2010 (Figure 1.5);
- Incidence was found to be related to age (Figure 1.6), the rate for under 75s in 2009/10 was 101.1 per 100,000 population and for over 75s for the same period was 1701.1 per 100,000 population and, higher for men than women;

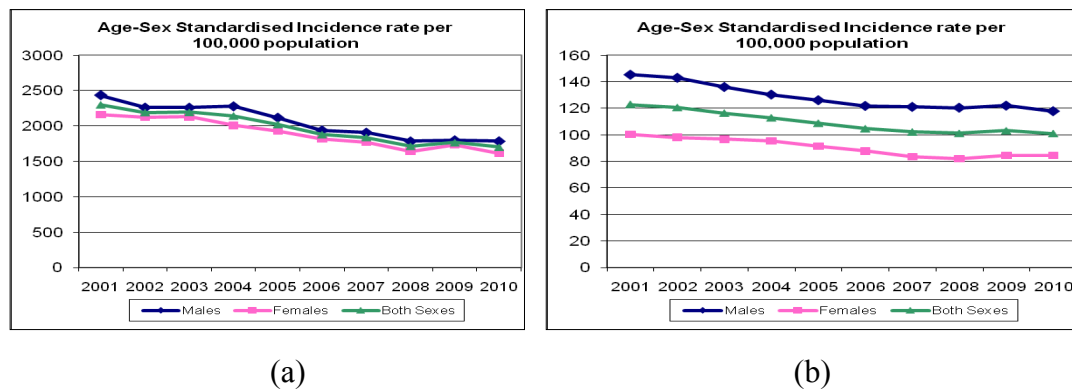


Figure 1.6: CVD incidence for Scottish population over 75 years old (a), and under 75 years old (b) (Table IS1 from www.isdscotland.org/isd/5782.html).

- CVD incidence is also related to the gender of the person, it is higher for men than women (Figure 1.5, 1.6);

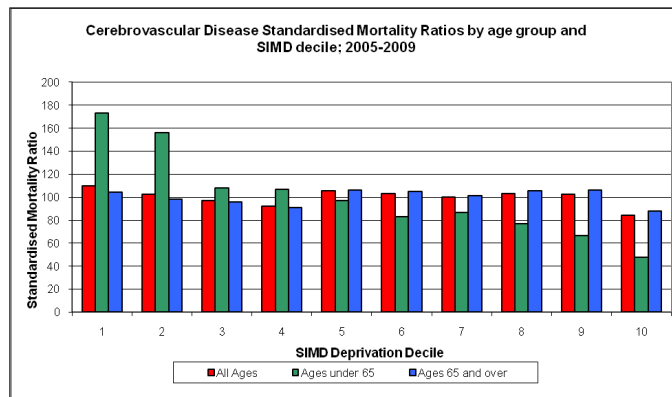


Figure 1.7: Mortality ratio standardised by age and The Scottish Index of Multiple Deprivation (SIMD). SIMD Decile: 1 most deprived to 10 least deprived area (Table DS1 from www.isdscotland.org/isd/5782.html).

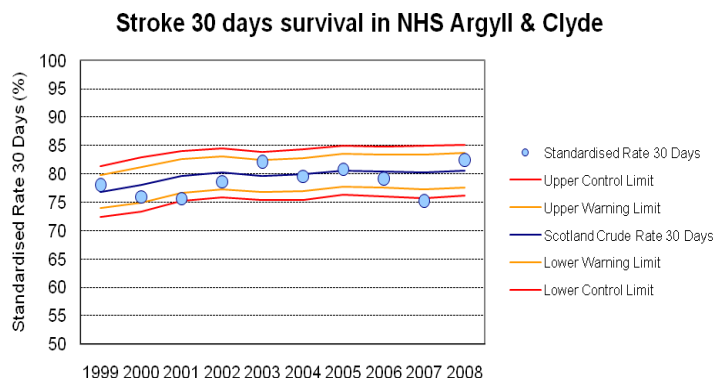


Figure 1.8: Percentage of patients surviving for 30 days after emergency admission due to stroke. Figures are standardised by gender, age and deprivation. (<http://www.indicators.scot.nhs.uk/TrendsJuly09/Stroke.html>).

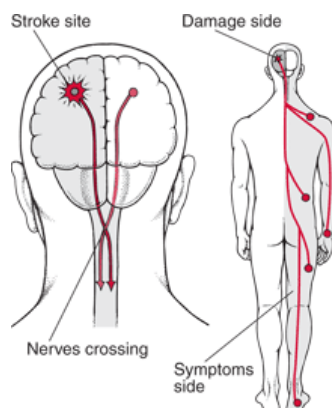


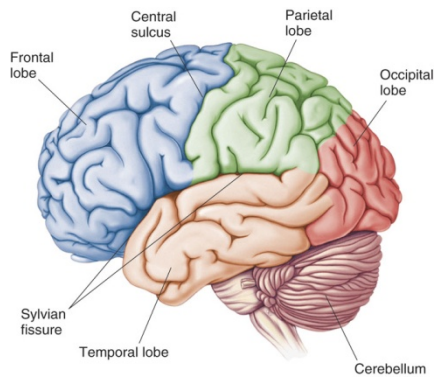
Figure 1.9: Why stroke affect only one side of the body: nerves cross over. (Figure adapted from: www.merckmanuals.com)

- People from deprived areas suffer more from stroke than people from less deprived region (Figure 1.7); the positive relation between mortality and deprivation is particularly noticeable in people under 65 years old;
- Immediate mortality is high and approximately 20% of stroke patients die within 30 days (Figure 1.8);

For those patients who survive the stroke onset, it is estimated that about 40% remains dependent upon other people for their daily activities (Young and Foster, 2007). The recovery time will vary among subjects with only 45 to 60% of survivors being independent a year post stroke (R11 Stroke statistics Resource sheet, 2006). The main burden of stroke is thus the number of survivors left with some degree of functional impairment. Broadly speaking the after effects of the brain injury are:

- Language disorders (aphasia and dysarthria);
- Problem with balance and coordination (ataxia);
- Cognitive problems (loss of memory, poor concentration);
- Problem with swallowing (dysphagia);
- Emotional disturbance/Depression;
- Disturbed vision;
- Continence problems (poor bowel and bladder control);
- Ignoring one side of the body;
- Sensory disturbance (altered ability to feel touch, pain, and temperature);
- Mobility problems due to weakness (hemiparesis) or paralysis (hemiplegia) of one side of the body. Hemiparesis and hemiplegia tends to occur on the side of the body which is opposite from the side of the brain damage (Figure 1.9). This occurs because neurons transporting information from the brain cross over to the other side of the body. As a result, the left side of the body receives information from the right brain hemisphere, and vice versa.

However, the clinical presentation following the stroke onset varies from person to person depending on the site and extent of the brain injury. The brain is composed of different areas, each one associated with a specific function. The largest region of the brain is the cerebrum, divided itself in frontal, parietal, occipital, and temporal lobe, which is involved in the processing of somatic sensory and motor information

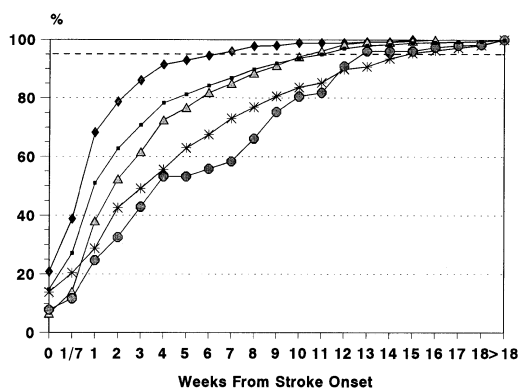


(a)

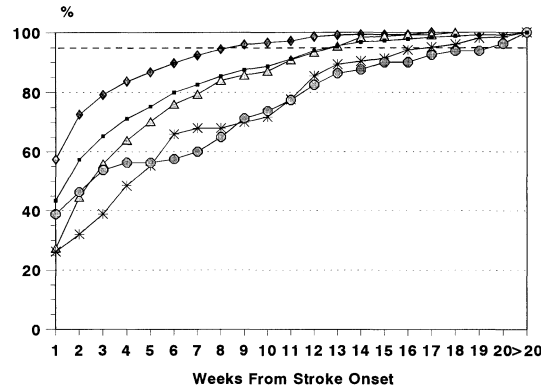
| Lobe | Function |
|--|--|
| FRONTAL LOBE Primary motor Cortex | Voluntary control of skeletal muscles, speech |
| PARIETAL LOBE Primary sensory Cortex | Conscious perception of touch pressure, pain, vibration, taste and temperature |
| OCCIPITAL LOBE Visual Cortex | Conscious perception of visual stimuli |
| TEMPORAL LOBE Auditory cortex and olfactory cortex | Conscious perception of auditory and olfactory stimuli |

(b)

Figure 1.10: Cerebrum lobes subdivision (a) and associated functions description (b) (Martini, 2006).



(a)



(b)

Figure 1.11: Time course recovery of neurological (a) and functional (b) function in subjects with different severity of stroke: ■ all patients, ◆ mild stroke severity, Δ moderate stroke severity, x severe stroke severity, ● very severe stroke severity (Jorgensen et al., 1995b).

(Martini, 2006). The different area of the human cerebrum and the corresponding function are shown in Figure 1.10.

Also the time of recovery is dependent on the extent of the brain damage and, people who survive, recover to a greater or lesser extent also in according to patient's age and general health (Chest, Heart & Stroke Scotland, 2002). Generally, most recovery of neurological, functional/motor functions occurs within 3 months from stroke onset (Jorgensen et al., 1995a). A rapid recovery is seen in 3 month post-stroke, followed by slower and smaller improvements over the subsequent 3 months (Figure 1.11) (Jorgensen et al., 1995a; Verheyden et al., 2008). Further improvement after 6 months can be expected but is mostly limited (Skilbeck et al., 1983; Verheyden et al., 2008). Neurological recovery (Figure 1.11a) is usually faster than functional recovery (Figure 1.11b) (Jorgensen et al., 1995a, 1995b; Newman, 1972). For the best chance of recovery it is now generally accepted that rehabilitation should start as soon as possible as recommended by National guidelines (Scottish Intercollegiate Guidelines Network, SIGN 118, 2010; National Stroke Foundation, 2010; National Stroke Strategy, 2007). However, contradictory results among previously conducted studies have been found in relation to this. Although, the feasibility of this practice has been reported (Bernhardt et al., 2008; Langhorne et al., 2009), what is still uncertain is the contribution made by early rehabilitation to better outcomes in stroke patients. Few studies have reported on the benefit of early rehabilitation in comparison to a delayed intervention (Feys et al., 2004; Indredavik et al., 1999; Ronning and Guldvog, 1998). Due to clinical ethical issues, we remain unable to justify the need for an early rehabilitation practice based on the current available literature (Bernhardt et al., 2009; Bernhardt et al., 2008; Di Lauro et al., 2003). A currently ongoing international trial, named A Very Early Rehabilitation Trial (AVERT) (Figure 1.12), investigates the effect of early rehabilitation versus standard intervention. Phase I (Bernhardt et al., 2004) and Phase II (Bernhardt et al., 2008) provided baseline data on current stroke patients' activity in Melbourne stroke units and results on the feasibility and safety of early rehabilitation. Phase III is now underway aiming to recruit 2,104 stroke patients across Australia, Canada, England, Malaysia, New Zealand, Northern Ireland, Scotland, Singapore, and Wales stroke units. Results are expected by the end of 2011 with the aim to contribute to the

understanding of the efficacy and effectiveness of early rehabilitation to accelerate recovery in stroke patients.

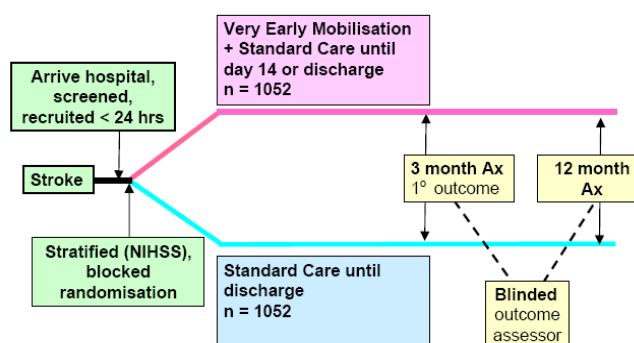


Figure 1.12: AVERT protocol. Patients' assessment is conducted at arrival at hospital and after 3 and 12 months post stroke (AVERT Protocol Summary Version 1.0 - 4 April 2006).

A clear consensus exists on the need for stroke patients to be hospitalized in dedicated stroke units for improved care and better outcomes following the brain injury (Scottish National Report, 2010; Young and Foster, 2007; National Stroke Strategy, 2007, Indredavik et al., 1999). A recent Cochrane review (Stroke Unit Trialists' Collaboration, 2007) screened 31 trials (6,936 patients) comparing stroke unit care with alternative services in providing better recovery following a stroke. It was concluded that stroke patients who receive organised inpatient care in a stroke unit are more likely to be alive, independent, and living at home one year after the stroke. Efforts have been made to improve services across Scotland to save lives and reduce disability and to follow the recent recommendations developed by the Scottish Intercollegiate Guidelines Network (SIGN) and NHS Quality Improvement Scotland (NHS QIS) (SIGN 118, 2010; Better heart disease and stroke care action plan, 2009; Clinical Standards for Stroke Services, 2009; SIGN 64, 2005). The Scottish Stroke Care Audit, which monitors the quality of services provided by NHS hospitals, reported in its last report (Scottish Stroke Care Audit Report, 2010) an increase number of admission in stroke unit between 2005 and 2009 in most of the Scottish hospitals (Figure 1.13) as a reflection of improvement of stroke care.

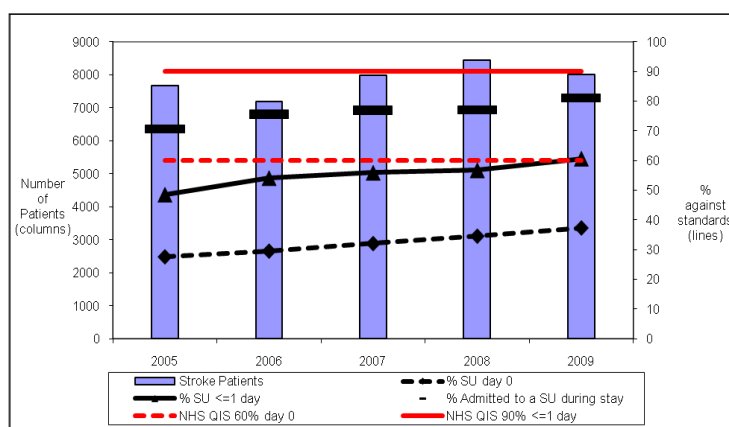


Figure 1.13: Trend in Stroke Unit admission between 2005 and 2009. Horizontal red lines (solid and hashed) reflect NHS QIS standards (2009) to admit 60% of stroke patients on day of admission and 90% within 1 day of admission. (Scottish Stroke Care Audit Report, 2010)

It is also expected that increasing the management of stroke patients in specialised stroke units, the cost of health services will be reduced (National Audit Office Report, Department of Health, 2005). Stroke care costs the NHS approximately £4 billion a year representing the 5.5% of the total UK expenditure on health care (Saka et al., 2009). The expense goes up to £9 billion if cost of informal care and lost of productivity are added (Saka et al., 2009). Encouragement toward more efficient practices will result to potential savings for the NHS as the length of stay in hospital is reduced, in addition to an improved recovery process (National Stroke Strategy, Department of Health, 2007; Scottish Intercollegiate Guidelines Network 118, 2010; Scottish Stroke Care Audit Report, 2010). The increase in number of stroke units is estimated, in fact, to have saved the NHS over £82 million (National Audit Office Report, Department of Health, 2005). Adherence to guidelines is thus crucial for reducing stroke costs. A better understanding of the rehabilitation provided in term of efficacy and cost-effectiveness can further reduce the economic and human burden of stroke if it is clear where to change intervention. To this regard researchers should investigate rehabilitative methods. From a survey of the literature, it is unclear which rehabilitative approach is more effective than another (Pollock et al., 2007; Young and Foster, 2007).

1.4 Stroke and gait abnormalities

The reader is referred to books analysing human locomotion for a thorough description of normal gait (Perry, 1992; Whittle, 2006).

People affected by a stroke, which damages the motor cortex, are characterised by a loss of motor control resulting in the classic hemiplegic presentation of stroke survivors. As already mentioned, the side of the body affected is contralateral to the brain hemisphere damaged. Previously conducted studies involving stroke patients have shown altered kinematic and kinetic gait profiles in both magnitude (range and peak values) and pattern (shape and direction of curves) (Kim and Eng, 2004; De Quervain et al., 1996; Olney and Richards, 1996). Typically the lower limb of hemiplegic patients shows plantarflexion and inversion at the ankle and subtalar joint, extension of the knee and, internal rotation, flexion and adduction at the hip joint (Spence, 1982, Kaplan et al., 2003; Best Practice Statement, 2009). Hemiplegic gait is defined as slow and stiff with poorly coordinated movements of the affected side (Lehmann et al., 1987). It is also typified as an asymmetric gait pattern both in time and space (Saunders et al., 1953; Kaplan et al., 2003; Gard and Fatone, 2004; Esenquazi, 2008). The unaffected limb swings faster minimizing the duration of stance phase of the hemiplegic leg, thus implying also a reduction in the step length of the normal limb (Gard and Fatone, 2004; Esenquazi, 2008). The resultant asymmetries during a gait cycle may be explained by the instability of the affected limb which prompts the patient to shift the weight as early as possible to the sound limb (Lehmann et al., 1987) and by the presence of an extended knee at the hemiplegic side which cause a longer swing phase (Gard and Fatone, 2004). Hemiplegic patients as result, display a very different gait pattern from normal subjects. Moreover, variation in walking patterns has also been noted among stroke patients and related to the degree of recovery (De Quervain et al., 1996; Roth et al., 1997).

Coordination of movements and the ability to move individual joint on the affected side is usually lost (Olney and Richards, 1996; Becher, 2004). Movement of the hemiplegic side is controlled by bulk muscle movement patterns (synergies) leading to impaired gait cycles and requiring compensation (Spence, 1982; Kaplan et al., 2003). Compensation of resulting walking disabilities occurs by the action of the

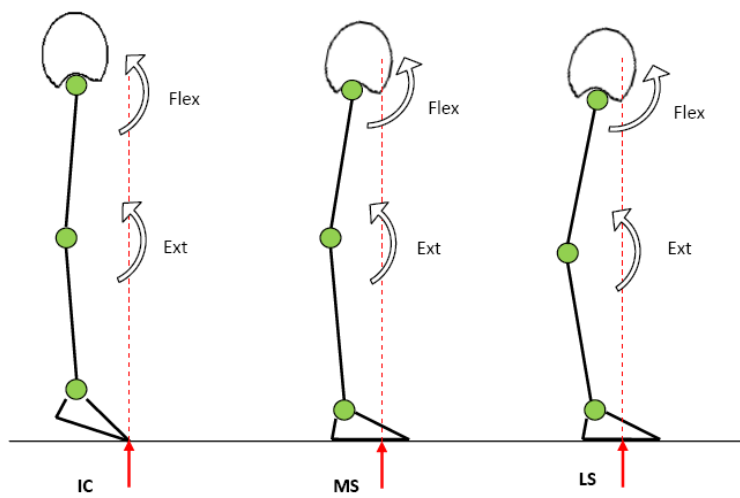


Figure 1.14: Example of a typical stance phase of stroke patients' hemiplegic leg. Wrong position of the GRF creates excessive knee extension and hip flexion at initial contact (IC) and knee extension and hip flexion at mid stance (MS) and late stance (LS) where opposite movement would be expected.

sound limb or by compensatory gait deviations, which increase the energy cost of walking (Olney and Richards, 1996; Gard and Fatone, 2004). Hence, persons with stroke use different strategies to achieve the goal of walking (Kim and Eng, 2004). The prevalence of flexor and extensor synergies usually characterise the hemiplegic gait (Spence, 1982; Yavuzer, 2007). Those synergies result from the collective contractions and relaxation of extensor and flexor muscles. The extensor pattern leads to the simultaneous extension of the hip and knee and plantarflexion of the ankle, whereas the flexor synergy produces flexion of the hip and knee and contractions of the ankle dorsiflexors (Spence, 1982, Kaplan et al., 2003). The flexion synergy is commonly incomplete or totally lost after stroke onset (Spence, 1982; Kaplan et al., 2003; Esenquazi, 2008). The dominance of the extensor pattern usually deprives hemiplegic patients of heel strike (Spence, 1982). Initial contact with the ground occurs with either foot flat or forefoot preventing weight bearing through the heel (Figure 1.14) (Esenquazi, 2008). The foot maintains a plantarflexed position throughout stance and swing phase of the gait with consequences also at the knee and hip joint (Gard and Fatone, 2004; Meadows et al., 2008). During stance phase excessive plantarflexion leads to an abnormal weight bearing through the front part of the foot rather than smoothly allowing the passage of body weight from the heel to over the foot (Meadows et al., 2008; Esenquazi, 2008). In biomechanics terms, this means a deviant alignment of the ground reaction force (GRF) with respect to the lower limb joints and thus erroneous moments and movements (Figure 1.14) (Gard and Fatone, 2004; Meadows et al., 2008). In addition persistent plantarflexion in stance phase resists forward progression of the tibia and consequently the knee is more posteriorly placed (hyperextended) than normal (Best Practice Statement, 2009). The GRF passes in front of the knee causing its extension which, is also enhanced, by the posterior placement of the knee (Best Practice Statement, 2009). A hyperextended knee is maintained also in late stance (Olney and Richards, 1996; Kaplan et al., 2003; Meadows et al., 2008). The orientation of the GRF and the excessive knee extension render hip extension difficult due to the presence of a hip flexion moment (Figure 1.14). The hip is then retracted and flexed during mid to late stance where hip extension would normally be expected (Meadows et al., 2008).

A lack of knee flexion at terminal stance phase accompanied with excessive ankle plantarflexion prevents the leg from being shortened and leads to drop foot (Spence, 1982; Kaplan et al., 2003; Esenquazi, 2008). Toe off and thus floor clearance is impaired. If the patient does not compensate for these abnormalities “toe drag” will occur (Spence, 1982). Compensatory actions for the inability to flex the knee and dorsiflex the ankle on the hemiplegic side are “hip hiking” which results in a flexed hip in terminal stance, “vaulting and circumduction” of the leg or “lean of the trunk” laterally (Spence, 1982; Gard and Fatone, 2004). These mechanisms allow the leg to be swung forward and to clear the ground but increase energy demand (Esenquazi, 2008). Pathologic moments at the knee and ankle lead to the beginning of the stance phase of the sound limb earlier than normal leading to a shorter step length (Gard and Fatone, 2004; Condie and Bowers, 2008), as anticipated earlier.

In addition to a plantarflexed ankle, stroke patients may present a supinated foot throughout the gait cycle (Spence, 1982; Condie and Bowers, 2008). The resultant equinovarus deformity (Figure 1.15) is the most common abnormality seen in stroke patients which creates an unstable configuration of the ankle (Spence, 1982; Esenquazi, 2008). The stance phase, when supination is also present, occurs on the lateral border of the foot. An equinovarus position during swing phase compromises heel ground contact and subsequent weight bearing (Spence, 1982; Esenquazi, 2008).

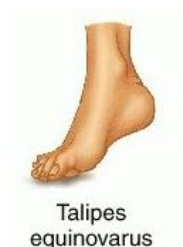


Figure 1.15: Equinovarus position of the foot: Foot inverted, adducted and plantarflexed.

Additional complications in motor function may arise due to the presence of spasticity (Spence, 1982; Kaplan et al., 2003). Spasticity is defined as an uncontrollable, velocity-dependent, increased resistance to passive stretch (Becher, 2008). It manifests as muscle tightness in the affected leg (Becher, 2004). Initially,

the limb will present with a state of flaccidity which is followed by increasing spasticity (Spence, 1982; Kaplan et al., 2003). This abnormal muscle tone may cause pain and may further complicate the timing of flexion and extension during a walking cycle interfering with ambulation (Becher, 2004; Esquenazi, 2008). Finally subjects who have sustained a stroke can also have difficulty during ambulation because of neglect, a reduced vision field, cognitive problems and disturbed balance.

It follows that regaining walking ability is one of the main objectives in stroke patients' rehabilitation in order to produce a more independent life. Rehabilitation for motor disturbances should allow a patient to improve motor control, restore range of movements at joints, and regain muscle power (World Health Organisation, 1989).

1.5 Orthotic management of stroke patients

The management of stroke has been recognised as a clinical improvement priority by NHS Quality Improvement Scotland (NHS QIS) and Allied Health Professionals (AHPs) across Scotland. In particular, the need was highlighted for more consistent advice and guidance on the use of ankle-foot orthoses (AFOs) in the rehabilitation of adults following stroke. A best practice statement (Best Practice Statement, 2009) was then published in August 2009 with the aim of improving practice related to AFOs application following brain injury and to provide guidelines among the variety of current rehabilitation programmes. In the next paragraph a brief introduction to ankle-foot orthoses is followed by a description of the biomechanical principles behind the use of such orthoses. Particularly, the description focuses on how functional problems, which occur after the onset of stroke, can be influenced by AFOs use, followed by a review of studies conducted on the effect of AFOs on walking ability post-stroke and their mechanical properties.

1.5.1 *Introduction and Biomechanical principles of Ankle-foot orthoses*

An orthosis, as defined by the International Standard Organization, is an externally applied device used to modify the structural and functional characteristics of the neuromuscular and skeletal system (ISO 8549-1, 1989). An ankle-foot orthosis, also referred to with the acronym AFO, is an orthosis which encompasses the ankle joint,

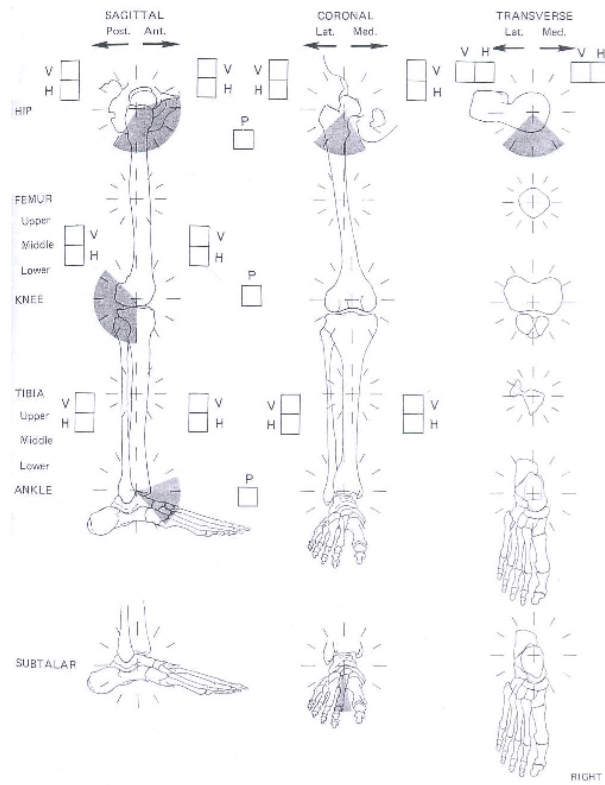


Figure 1.16: Subject's assessment form to record range of motion and muscles power as introduced by the American Academy of Orthopaedic Surgeon.



Figure 1.17: Conventional double upright metal and leather AFO.

the foot in whole or in part and extends up to the shank to a point below the knee (ISO 8549-1, 1989). The use of orthoses was recommended in the management of patients with stroke by a consensus conference of the International Society of Prosthetics and Orthotics (ISPO) (Condie et al., 2004). Ankle foot orthoses are generally prescribed to maintain ankle joint stability in the anterior-posterior and medio-lateral directions during stance phase, to facilitate ground clearance in swing phase, to promote heel strike, to compensate for absent forces due to weakened or absent muscles power and thus restore more normal functions at lower limb level and to support anatomical structure from weight bearing (Lehmann, 1979; Condie and Meadows, 1993; Leung and Moseley, 2003). The effectiveness of an AFO is related to the accuracy with which the functional deficits of the patient have been assessed and by the ability of the device to fulfil these requirements (Condie and Meadows, 1977). Patient assessment should be conducted accurately and include a detailed description of gait deviations with reference to the joint and body segment affected, plane of movements, timing of the occurrence of the deviation during the gait cycle and musculoskeletal impairments, in order to clarify clinical objectives and outcomes desired by the utilisation of an AFO (Condie et al., 2004). The use of standardised screening tool and orthotic referral form is recommended at the stage of AFO prescription (Best Practice Statement, 2009). Charts to record patients' examination have been introduced in the past by the American Academy of Orthopaedic Surgeon (AAOS) (Figure 1.16) or similarly nationally agreed standardised screening and orthotic referral form can be found from the NHS website (www.nhshealthquality.org). Once the objectives of the treatment have been defined, the orthotic prescription can be planned.

Nowadays a large variety of AFOs are available giving the orthotists a wide spectrum from which to choose the correct orthosis treatment. From the early metal and leather AFOs (Figure 1.17), significant changes in materials have led to the development of newly designed orthoses.

The biggest movement in the orthotic technology occurred in the late 70s when thermoplastic materials were adopted in the rehabilitation field (Chu, 2001). Since then, plastic and in particular polypropylene, became one of the mostly used materials in the fabrication of AFOs (Showers et al., 1985; Lin, 2000; Chu, 2001).



Figure 1.18: Example of plastic prefabricated AFOs (www.orthomerica.com; www.optecusa.com).

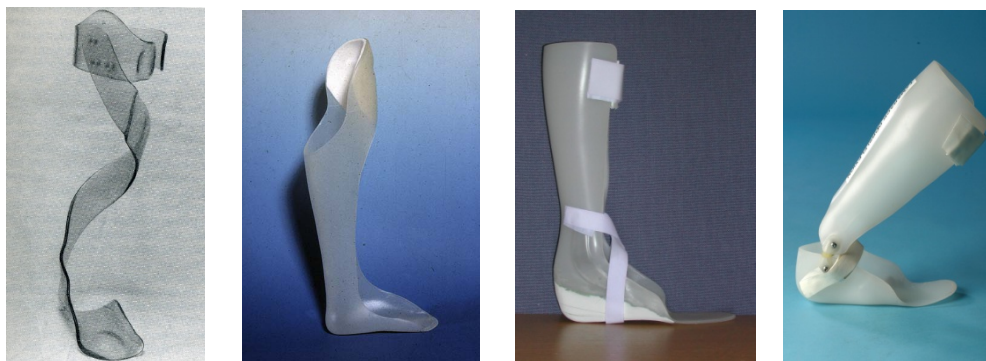


Figure 1.19: Example of custom-made plastic AFOs: Spiral AFO (Condie and Meadows, 1993), Ground reaction orthosis (GRAFO) and Solid AFO (Best Practice Statement, 2009) and articulated AFO (Best Practice Statement, 2009).

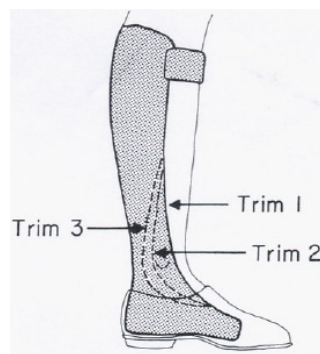


Figure 1.20: Example of three trimlines on a solid plastic AFO (Lehmann et al., 1983).

The use of thermoplastics allows for the manufacture of lighter and more cosmetic devices than metal and leather did in conventional orthoses. Regardless of the type of the orthosis, each AFO is designed to restore functions normally controlled by either passive tissues (ligaments, joint capsules) or active tissues (muscles) and acts through a balanced three or four-force system applied to the patients lower leg (Condie and Meadows, 1993; Lin, 2000). The intimate fit between a plastic orthosis and the patient's leg allows for an even distribution of these forces over a broad area of the lower limb reducing the risk of high pressure and skin damage (Bowker et al., 1993; Lin, 2000; Esenquazi, 2008). Conventional AFOs, on the other hand, have the advantage of durability and adjustability (Esenquazi, 2008). Nevertheless their use has been superseded by more modern plastic devices that obtained higher acceptance by AFO candidates breaking stereotypes set by society (Shamp, 1983) and better match patients' needs. For all the reasons discussed, metal and leather AFO "should be consigned to history" (Condie and Bowers, 2008). The effectiveness of plastic AFOs is strictly related to the correctness of both construction and fit (Condie and Meadows, 1993). Prefabricated ankle-foot orthoses (Figure 1.18) provide less intimate fit when compared to custom-moulded orthosis and thus may result in devices with a limited value in stroke rehabilitation (Best Practice Statement, 2009). Their prescription should be temporary while waiting for a custom-made AFO to be manufactured (Condie et al., 2004).

Various designs of plastic AFOs have been made available and are customarily fitted to the patient's leg (Figure 1.19). They may be characterised by one piece of plastic, a non-articulated AFO, or by two pieces of plastic joined together by mechanical hinges that can be set to allow or prevent movement at the ankle in specific direction, an articulated AFO (Hoy and Reinthal, 2004; Condie and Bowers, 2008; Best Practice Statement, 2009). Control of the ankle joint in a non-articulated AFO is achieved by virtue of the stiffness of the orthosis, which is regulated by the trim line (Figure 1.20) used in its design and by the material used (Lehmann et al., 1983). An articulated AFO, when compared to the non-articulated type may result in a bulky device with a reduced intimacy of fit (Condie and Bowers, 2008) and poor cosmesis. Recommendations on when to prescribe an articulated or non-articulated AFO for stroke patients have been developed during a consensus conference of the

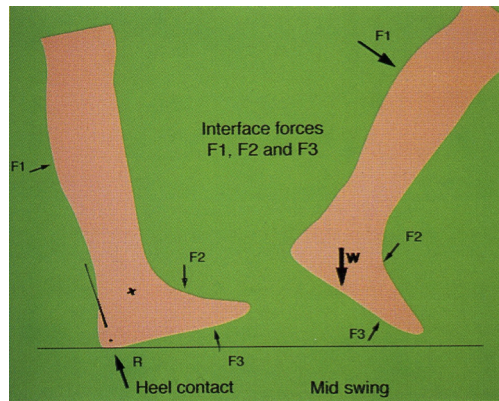


Figure 1.21: Three-force system (F_1 - F_2 - F_3) required to control plantarflexion at initial contact and mid swing. R represents the GRF (Condie and Turner, 1997).



Figure 1.22: Plastic ankle-foot orthosis with a single ankle strap (left) and 'figure-8' crossover strap (right) (Best Practice Statement, 2009).

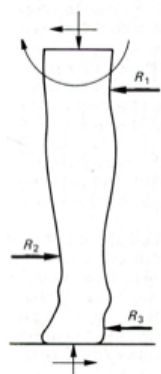


Figure 1.23: Three-force system (R_1 - R_2 - R_3) to prevent supination of the foot (Condie and Meadows, 1993).

International Society of Prosthetics and Orthotics (ISPO) but the final decision is that of the orthotist in charge (Condie et al., 2004).

An ankle-foot orthosis when prescribed to address impairments following stroke should compensate for excessive plantarflexion of the ankle and foot in stance (foot slap) and swing phase (drop foot), correct for foot abnormality (usually equinovarus deformity), improve ground clearance, reduce knee extension and promote hip extension during stance (Condie and Meadows, 1993, Condie et al., 2004, Condie and Bowers, 2008, Best Practice Statement, 2009). This is obtained by virtue of a force systems applied by the AFO to the patient's leg to directly control movements at the foot and ankle and by the indirect action the AFO exerts on the alignment of the ground reaction force with respect to the proximal lower limb joints (Bowker et al., 1993; Condie and Meadows, 1993; Condie and Turner, 1997; McHugh, 1999; Best Practice Statement, 2009).

Excessive plantarflexion during stance and swing phase is controlled by a three-force system as illustrated in Figure 1.21. This system of three forces controls excessive plantarflexion preventing foot slap at the beginning of stance phase and supporting the foot of the swinging leg enabling ground clearance (Condie and Meadows, 1993). This force system is achieved in plastic AFOs through the contact of the posterior calf section (F_1) and the foot piece of the orthosis (F_3) acting in concert with the shoe upper (F_2) (Condie and Meadows, 1993; Meadows et al., 2008). If a subject presents with increased tone, the force F_2 (Figure 1.21), normally provided by the upper of the footwear should be enhanced by the use of an ankle strap (Figure 1.22) (Best Practice Statement, 2009).

The intimate fit provided by plastic AFOs allows also for the application of corrective forces to compensate for the supinated position of the foot. The force system applied to achieve this is shown in Figure 1.23.

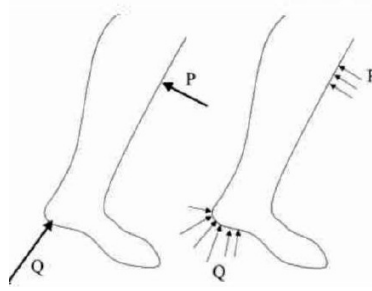


Figure 1.24: Force representations: vector acting in one point (left), distribution of multiple vectors over a broad area (right) (McHugh, 1999).

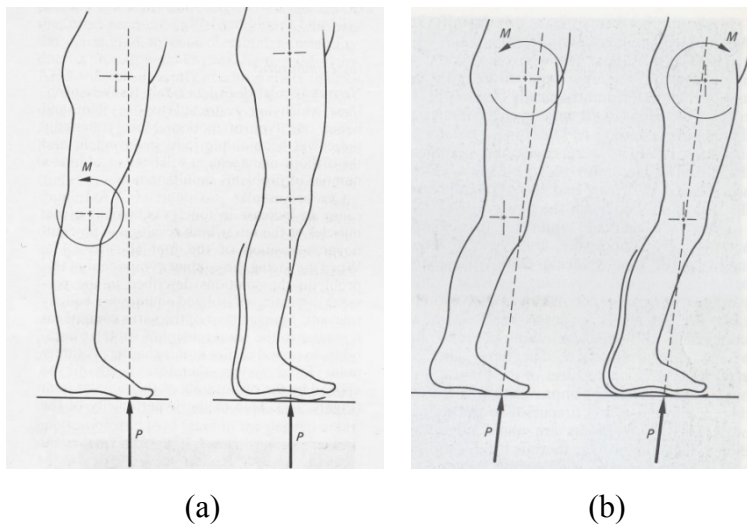


Figure 1.25: (a) Correction of knee hyperextension moment by realignment of GRF through knee joint centre; (b) AFO influence on hip moment: extension is created by the GRF (P) passing behind the hip (Condie and Meadows, 1993).

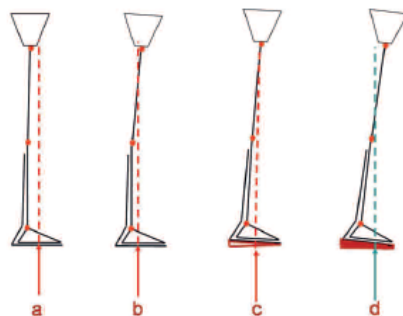


Figure 1.26: Adjustment of the GRF by tuning the AFO (Best Practice Statement, 2009).

Although forces are represented as vectors acting about a single point, it should be noticed that those forces, in reality, are spread over an area of the patients' leg (Figure 1.24) to reduce high pressure and thus patients' discomfort and skin damage (McHugh, 1999).

As anticipated above, an AFO can control movements at the knee and hip by modifying the point of application and the line of action of the ground reaction force (GRF) (Bowker et al., 1993). The AFO reduces knee hyperextension moment during stance phase by moving the GRF backward toward the knee joint centre (Figure 1.25 a). Similarly, the undesirable hip flexion moment during stance is adjusted by aligning the GRF behind the hip joint centre (Figure 1.25 b).

Shank and thigh kinematics (segments inclined or reclined) together with the point of application of the GRF are crucial for obtaining the maximal effects from use of an AFO on the joints not directly encompassed by the orthosis (Meadows et al., 2008). AFOs are used in conjunction with footwear which plays a crucial role on the effectiveness of the AFO itself (Condie and Meadows, 1993; Meadows et al., 2008; Best Practice Statement, 2009). Firstly, the shoe applies forces on the dorsum of the foot which is a component of the three-force system (Figure 1.21). Secondly it regulates GRF alignment with respect of the knee and hip joints. In particular, heel height and sole profile influence GRF point of application and orientation, and lower limb segment kinematics. Footwear should be regarded as an integral part of orthotic fitting (Condie and Meadows, 1993) and when necessary be prescribed by the orthotist (Best Practice Statement, 2009).

When a solid AFO is prescribed, tuning is often performed to optimize the GRF alignment at the knee and hip (Figure 1.26) (Meadows et al., 2008; Best Practice Statement, 2009). The process of tuning involves adding or removing heel wedges to modify the angle of inclination of the AFO and thus the shank to vertical angle (SVA). The latter dictates the position of the GRF with respect to the knee and hip (Figure 1.26). By adding wedges, as shown in the Figure 1.26 the desired alignment, with the GRF passing slightly in front or through the knee and behind the hip (position c and d), can be obtained in contrast to the two previous configurations (position a and b). The importance of correct alignment of the orthosis during late stance and pre swing in producing a more normal step length, gait symmetry, speed

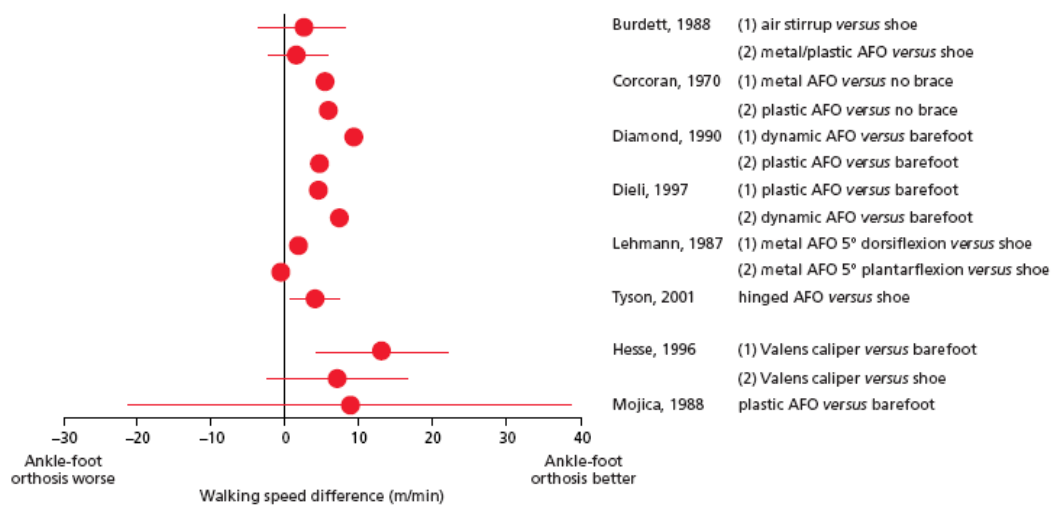


Figure 1.27: Mean difference in walking speed during gait with AFO against barefoot walking or wearing shoes (Leung and Moseley, 2003).

and energy consumption has been highlighted during a consensus conference of the International Society of Prosthetics and Orthotics (ISPO) (Condie et al., 2004). Tuning should be considered at the time of fitting to optimise the stroke patients' gait pattern (Best Practice Statement, 2009).

1.5.2 Research evidence on the use of AFO following stroke

Several studies have been conducted to investigate the effects AFOs have on the walking function of stroke subjects. Aspects generally analysed include: spatial and temporal parameters of gait, lower limb joint kinematics and kinetics, energy expenditure during gait, and subjects' experience. Various designs of ankle-foot orthoses, from conventional metal and leather AFOs to different types of plastic orthoses articulated or not, were used in the studies reviewed. Also research methodologies varied among studies although the majority adopted a cross-over design and thus focusing on the immediate effect of AFO against no AFO condition. Both studies involving acute and chronic stroke patients were found. Research outcomes on the use of AFO following stroke are here reported. To allow a more systematic and organised description of the findings, they will be reported accordingly to the outcome measures.

One of the parameters most commonly reported is walking speed. Research evidence showed that the use of AFOs improved walking speed in stroke survivors. Leung and Moseley (2003), in their systematic review on the impact of AFO on hemiplegic gait, showed that improvement in speed was found in seven out of nine studies which reported this value (Figure 1.27). In these studies different type of AFOs were used: plastic solid AFO (Burdett et al, 1988; Mojica et al., 1988; Diamond and Ottenbacher, 1990; Dieli et al., 1997), articulated AFO (Tyson and Thornton, 2001), metal AFO (Lehman et al., 1987; Hesse et al., 1996) and Air-Stirrup[®] (Burdett et al, 1988).

Similarly to the studies reviewed by Leung and Moseley (2003), other authors suggested improvement in walking speed while wearing an AFO. De Wit et al. (2004), in a randomised cross-over study reported a significant increase in speed with a mean difference in favour of the AFO of 4.8 cm/s versus shoes walking. Overall 20 chronic stroke patients who already wore a plastic non-articulated AFO took part in

the study. Walking speed improved in 12 hemiplegic patients fitted with a custom-made plastic AFO from 19.79 m/min to 26.79 m/min (Franceschini et al., 2001). Subjects were trained for 1-3 weeks after orthosis fitting to optimise AFO effects on daily life activities. The same authors in a subsequent study (Franceschini et al., 2003) reported an increased speed when 9 chronic hemiplegic subjects walked continuously for 6 m wearing an AFO compared with shoes only condition (21.39 m/min; 15.47 m/min respectively). Specifications on the type of the orthosis provided are lacking other than the AFO is adjusted to patients' kinesiological disorder.

Sheffler et al. (2006) evaluated 14 chronic stroke patients, fitted with an AFO prior study commencement, using the modified Emory Functional Ambulation Profile (mEFAP) under 3 test conditions. Firstly they performed the required tasks with shoes only (no device) and then in a randomised sequence with their AFO and with Odstock Dropped Foot Simulator (ODFS). The AFOs previously prescribed to the participants were solid plastic AFOs for 8 of them, 4 received hinged plastic AFOs and the remained 2 a prefabricated AFO. The time to perform each mobility task, was recorded and compared among conditions (Figure 1.28). These values can be considered as an indirect measure of walking speed. The results showed improvements when walking with AFO or ODFS in comparison to no device. Moreover, the time to perform tasks was more reduced with the AFO than with the nerve stimulator, although the differences were not statistically significant.

| Trial | Floor | Carpet | Up and Go | Obstacles | Stairs |
|-----------|------------|------------|------------|------------|------------|
| No device | 15.1 ± 1.9 | 14.2 ± 1.8 | 31.3 ± 4.2 | 44.4 ± 5.9 | 24.0 ± 3.3 |
| AFO | 12.2 ± 1.4 | 11.6 ± 1.2 | 28.3 ± 4.2 | 38.7 ± 4.7 | 21.6 ± 2.7 |
| ODFS | 13.9 ± 1.9 | 12.0 ± 1.3 | 30.6 ± 4.5 | 40.4 ± 4.9 | 22.6 ± 3.1 |

AFO = ankle foot orthosis; ODFS = Odstock Dropped-Foot Stimulator.

Figure 1.28: Mean ambulation time for each task included in the mEFAP. Data for 3 conditions (No device, AFO, ODFS) are shown in seconds ± standard deviation (Sheffler et al., 2006).

In a randomised comparison between metal and Seattle-type polypropylene AFOs, Gok et al. (2003) reported that both types of orthoses increased the walking speed of 12 stroke hemiparetic patients. However, the metallic ankle-foot orthosis, due to its

stiffness, was better at increasing speed than the plastic one. The study population was characterised by a large range of time (30-270 days) since occurrence of the stroke and thus likely to confound results between chronic and acute stroke subjects. In a randomised cross-over study, Wang et al. (2005) investigated the effect of “standard off-the shelf plastic AFOs” on balance and gait of acute (42 subjects) and chronic stroke patients (61 subjects). The results revealed that although the AFO increased walking speed in acute stroke the same effect was not seen in later stage chronic stroke subjects. Controversially, more recently Wening et al. (2009) reported improvement in walking speed with AFO use in both acute (from 35.6 to 44.5 cm/s) and chronic (54.2 to 61.3 cm/s) patients groups. All chronic subjects and 50% of the acute patients were already AFO users but specifications on the orthoses are not provided in the paper. The contrasting results between Wang et al. (2005) and Wening et al. (2009)’s studies can be explained by the different types of AFOs employed and by the fact, that patients in the latter study were, for the majority, accustomed to the use of AFO. In agreement with Wening et al. (2009) are the results obtained by Rao et al. (2008). In this study a significant increase in walking speed was recorded in both acute (13 subjects) and chronic (27 subjects) stroke patients (Figure 1.29) while walking with a custom-moulded polypropylene AFO. The difference in gait velocity before and after AFO was greater in acute stroke patients, 9.86 cm/s against 6.72 cm/s in chronic stroke survivors.

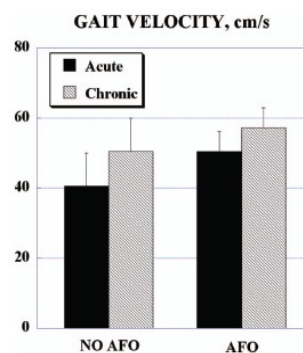


Figure 1.29: Variation in gait velocity with provision of a polypropylene AFO (Rao et al., 2008).

The correctness of AFO prescription as already highlighted in the previous paragraph is fundamental for obtaining positive effects. Another recent study (Tyson and

Rogerson, 2009) found no improvement on gait speed when the participants walked with a posterior leaf spring (PLS) orthosis. The 20 participants involved in the study were chronic stroke patients described as “severely impaired” with a mean Motricity Index of 48/100. The use of such device on these subjects is questionable and could explain this finding even if the authors justified it due to lack of familiarization period of the patients with PLS AFO before testing. Instead, Abe et al. (2009), in their investigation prescribed three different types of AFOs to 16 stroke participants accordingly to their presentation. The AFOs used were Shoe-horn plastic AFO (8 subjects), Gillette double-flexure joint AFO (6 subjects) and Tamarack flexure joint AFO (1 subject). Regardless of the type of orthosis worn, each participant increased walking speed by 126.5 % on average compared to the no AFO condition. Again the subjects involved in the study were a mixture of chronic and acute stroke patients. Similarly, four different types of AFOs, two flexible and two rigid, were used in the study authored by Simons et al. (2009). Twenty chronic stroke patients, fitted with the AFO that matched their impairments, showed a mean walking speed improvement of 0.12 m/s when they walked with the orthosis. Esenquazi et al. (2009) investigated the effect of AFOs in walking parameters of 42 stroke patients but the time elapsed between stroke onset and the test is not reported. Walking speed significantly increased when comparing barefoot walking to using an AFO, a mean velocity of 0.31 m/s against 0.41 m/s respectively was found. However, as the selected participants were already AFO users, a variety of AFO designs were used and details to this regard were not included in the study description.

A variety of other studies reported an increased speed while walking with AFO such as Iwata et al. (2003) who used a PLS orthosis with inhibitor bars attached to the plastic sole, Wang et al. (2007) with plastic AFO, as well as Bregman et al. (2010) who reported on average 0.10 m/s increase in walking speed although 3 (non benefit group) out of the 7 participants (stroke and multiple sclerosis patients) showed a really small change in speed (0.01-0.07 m/s), other studies include Pavlik (2008) with both solid and articulated plastic AFOs, Lewallen et al. (2010) with articulated and PLS AFOs but not with solid plastic AFOs with a trimline anterior to the malleoli, Weiss et al. (2002) who showed improvement in gait speed with two plastic articulated AFOs, one allowing 10° of plantar flexion to 10° of dorsiflexion, and one

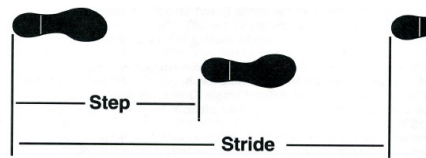


Figure 1.30: Step and Stride length (Perry, 1992).

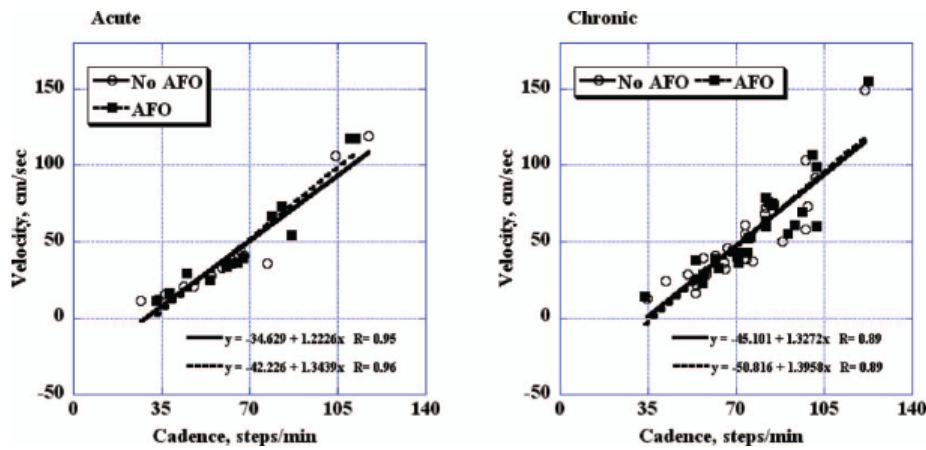


Figure 1.31: Linear regression of gait velocity versus cadence in acute and chronic group patients (Rao et al., 2008).

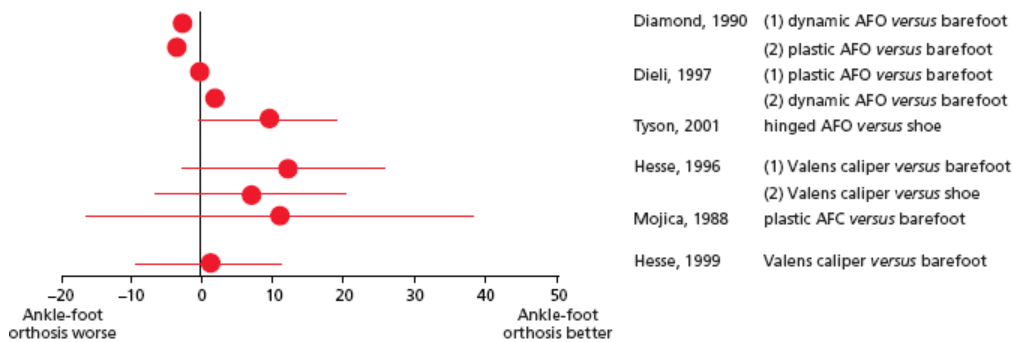


Figure 1.32: Mean difference in cadence during gait with AFO against barefoot walking or wearing shoes (Leung and Moseley, 2003).

restricting plantar flexion at neutral, with unrestricted motion into dorsiflexion but not with rigid AFO at 5° dorsiflexion. Lehmann et al. (1987), used a conventional AFO fixed in 5° dorsiflexion and showed a significant improvement in walking ability in 7 hemiplegic subjects but not if the AFO was set in 5° plantarflexion. Again a plastic AFO in 5° dorsiflexion led to an increase speed in a randomised control trial involving 40 post stroke patients (Beckerman et al., 1996). However, the differences, found between walking speeds with AFO and no device, were not statistically or clinically significant. Similarly, Fatone et al. (2009) reported no significant difference in walking speed neither with a vertically inclined articulated plastic AFO, or one which was anteriorly inclined by 5° to 7°. The poor results of these latter studies may be related to the small tibia inclination obtained. It has been suggested that increased walking speed is related to an angle greater than 5° in dorsiflexion (Bowers et al., 2004; Owen, 2010). In addition, the AFOs prescribed, were not necessarily the most appropriate for the treatment of these participants but, rather, chosen *a priori* for the investigations themselves.

Alongside the calculation of walking speed most of the studies already mentioned, also measured cadence, number of steps per minute, and step/stride length (Figure 1.30).

Improvement in cadence was reported by Iwata et al. (2003) for patients who presented with tonic toe flexion reflex (6.1% increase), Wang et al. (2005) for acute stroke patients only, Rao et al. (2008) who also found a linear relationship (Figure 1.31) between cadence and gait velocity ($R > 0.95$ and $R > 0.89$ for acute and chronic patients with AFO), Esenquazi et al. (2009) for whom analysis also revealed a positive correlation between velocity and cadence, Wening et al. (2009), and Abe et al. (2009). On the other hand, Gok et al. (2003) reported no significant difference in cadence when walking with either a plastic or metal AFO.

The effect of AFO on walking cadence was reviewed by Leung and Moseley (2003) (Figure 1.32). Three (Mojica et al., 1988; Hesse et al., 1996; Tyson and Thornton, 2001) out of the six studies showed a significant improvement of cadence with AFO use, two reported no significant difference (Dieli et al., 1997; Hesse et al., 1999) and one a decrease in cadence (Diamond and Ottenbacher, 1990).

The same authors (Leung and Moseley, 2003) reported also on the influence AFOs have on stride length as found in the papers reviewed by them (Figure 1.33). AFO use was seen to improve both cadence and stride length in the majority of studies.

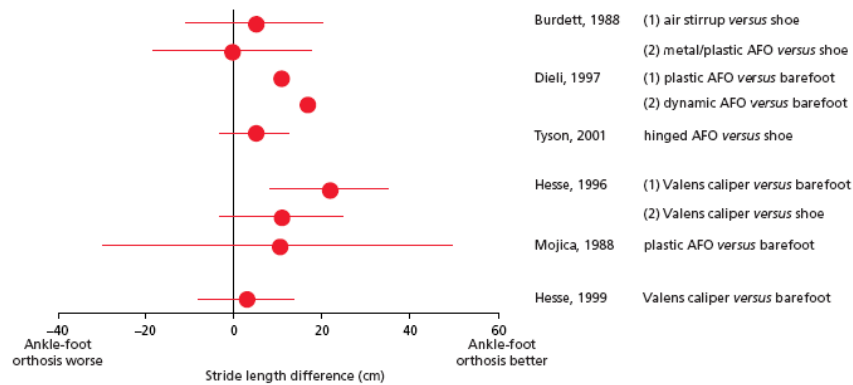


Figure 1.33: Mean difference in stride length during gait with AFO against barefoot walking or wearing shoes (Leung and Moseley, 2003).

Similarly Gok et al. (2003) found a significant difference in step length when chronic stroke patients walked with either plastic or metal AFOs, but no benefits of one type of orthosis over the other were shown. Abe et al. (2009) reported an increased step length in both the affected (119.8 %) and unaffected side (111.8 %) when stroke patients walked with their prescribed AFOs, as also documented by Wening et al. (2009), Rao et al. (2008) and Lewallen et al. (2010) a part from when stroke patients walked with a plastic solid AFO. Esenquazi et al. (2009) measured the percentage step length, defined as step length divided by standing leg length, and reported an increase in that value with the use of an AFO in both the affected and unaffected leg. A mean difference for step and stride length in favor of the AFO was found to be 3.63 and 5.93 cm respectively by Pavlik (2008), with plastic solid and hinged AFOs worn for at least 6 months. Improvements in step length were not found by Tyson et al. (2009) with PLS AFOs used by severely affected stroke patients but, as already discussed earlier, the poor appropriateness of the orthosis for the selected participants might be the explanation for this finding. Iwata et al. (2003) calculated stride length showing a significant improvement (8%) for stroke subjects with tonic toe flexion reflex when fitted with a modified PLS AFO. Increased stride length by the use of

AFOs during walking was also reported by Pavlik (2008), Abe et al. (2009), Wening et al. (2009) and Tyson and Thornton (2001) with an articulated AFO.

The effect an AFO has on lower limb joint kinematics and kinetics was also assessed in a few of the studies reviewed. Fatone et al. (2009) reported improvement in ankle kinematics with the use of articulated AFOs. Excessive plantarflexion at initial contact and mid swing was reduced and dorsiflexion increased during late stance. In the same study it was also reported that, although not statistically significant, knee hyperextension during stance is reduced by the AFOs. Likewise, Bregman et al. (2010) reported that ankle kinematics is positively altered by AFO usage (Figure 1.34) in the AFO benefit group but no effects were recorded on the hip and knee kinematics (Figure 1.34) and ankle sagittal moments for both AFO benefit and non benefit group.

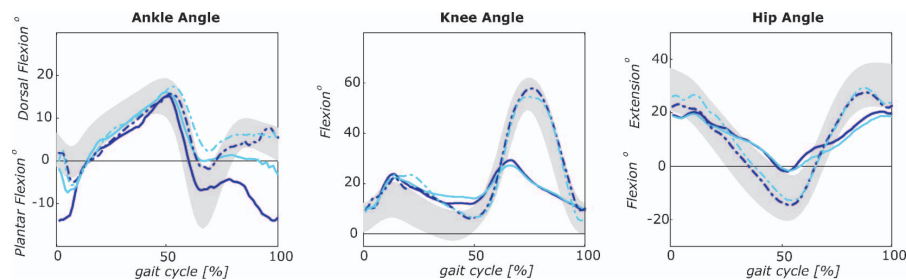


Figure 1.34: Ankle, knee and hip sagittal plane angles for AFO benefit group walking with (light solid line) and without AFO (dark solid line) and AFO non-benefit group walking with (light dashed line) and without AFO (dark dashed line) (Bregman et al., 2010).

Gok et al. (2003) also found an increased ankle dorsiflexion at heel strike and mid swing allowing for a safe toe clearance. Metallic AFO provided greater dorsiflexion (-0.37 degrees) compared to plastic AFO (-6.48 degrees) and this was most likely due to the increased stiffness of the conventional AFO. Knee flexion moments significantly decreased with the metal orthosis only; besides hip, knee, and ankle sagittal moment showed no significant differences when the subjects walked with either of the two types of orthosis.

Hesse et al. (1996) showed that by using a Valens calliper AFO with 19 stroke survivors, all of whom suffered from marked plantar flexor spasticity,

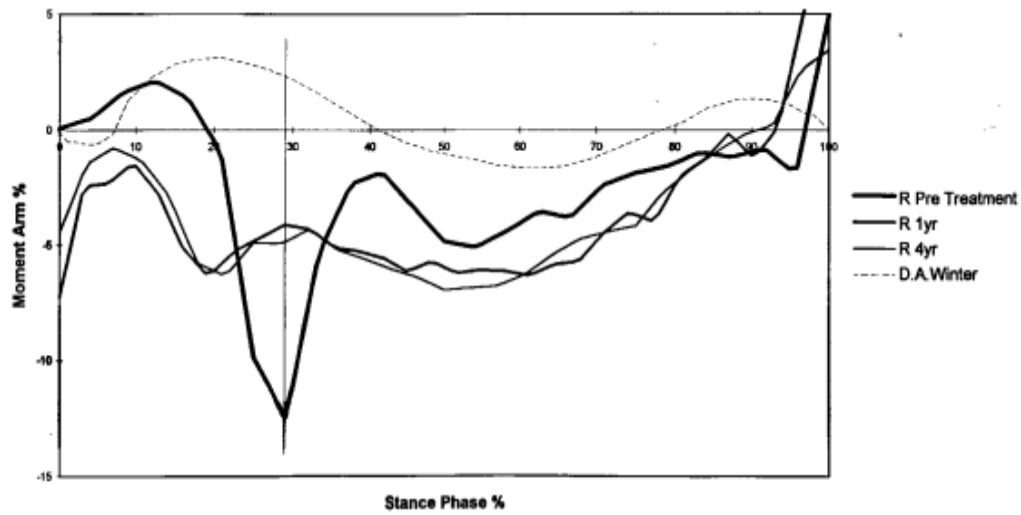


Figure 1.35: Comparison of normalised knee moment arm for the hemiplegic leg.

Data are shown before treatment at 1 year and 4 years and for normal subject as reference. An extending moment arm is represented as a negative value (Butler et al., 1997).

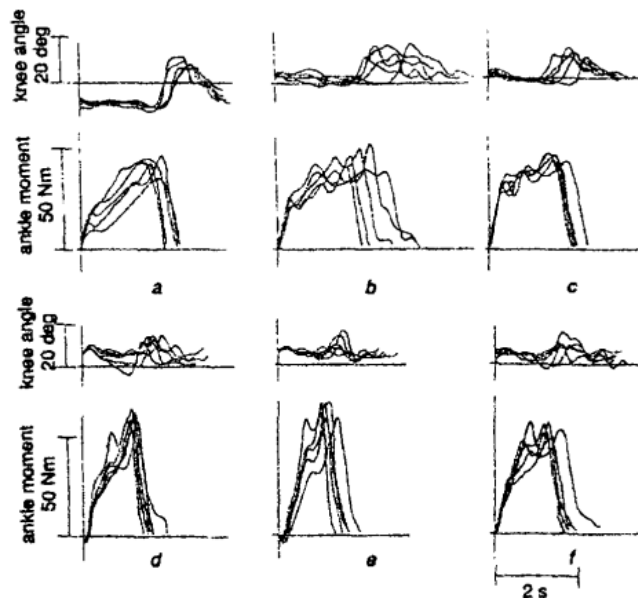


Figure 1.36: Ankle moment and knee angles (positive values correspond to flexion) without AFO (a), AFO without springs (b), AFO with neutral plantar stopper (c),

AFO with moderate stiffness at neutral initial angle (d), AFO with moderate stiffness at 7° dorsiflexed initial angle (e), AFO with slight stiffness at 7° dorsiflexed initial angle (f) (Miyazaki et al., 1997).

equinovarus deformity at the foot can be controlled. The majority of the study participants from being forefoot strikers began to hit the ground with the rear part of the foot while wearing the AFO, primarily by means of reduced plantarflexion during initial contact. In a similar study, a few years later, the same author (Hesse et al., 1999) reported an increase in ankle dorsiflexion during stance (+201.2%) and a decrease in plantarflexion during swing (- 71.2%) when stroke survivors walked with a Valens calliper AFO. The authors also hypothesised that the AFO could have provided a larger flexion at the knee and hip, although this was not measured, to facilitate toe clearance as demonstrated by Lehmann et al. (1987). Their study in fact highlighted the importance of positioning the AFO in dorsiflexion or plantarflexion to obtain a suitable knee flexion moment in stance phase. A 5° dorsiflexed conventional AFO produced a greater flexion moment (11.7 N*m) at the knee than walking without such a device (5.3 N*m) or with the AFO in plantarflexion (7.2 N*m) and thus facilitating the affected leg to swing through.

In a single case study, Butler et al. (1997) demonstrated that the use of a customised thermoplastic AFO with optimally adjusted footwear could correct for excessive knee hyperextension during stance phase of the gait. Knee extending moment arm (Figure 1.35) was reduced when comparing baseline assessment to 1 year and 4 years subsequently examinations after the subject started wearing the orthosis regularly for a year and occasionally for the 3 years to follow. The study however is limited to the results obtained by a single participant, in addition during the test the subject walked barefoot.

Miyazaki et al. (1997) investigated the effect of an experimental articulated AFO with two springs to control dorsiflexion and plantarflexion in 20 hemiparetic subjects. The results from the first 9 subjects tested showed that the AFO assisted dorsiflexion after heel strike but it did not alter plantarflexion activity during stance. The dorsiflexion resisting spring was thus removed for the remained 11 patients' tests. Conducted trials showed that when the subjects walked with a moderately stiff AFO set at neutral angle, ground contact occurred with the heel as shown by the negative values in the ankle moment graph (Figure 1.36 d), moreover with the AFO set at 7° of dorsiflexion the negative moment duration was prolonged and the knee hyperextension corrected (Figure 1.36 e).

Having identified the principles for the construction of an AFO for hemiplegic patients (Yamamoto et al., 1997), a new design of articulated AFO, which incorporate an ankle joint with a hydraulic oil damper, was developed and its efficacy on joint kinematics and kinetics assessed (Yamamoto et al., 2005). The effects of this new AFO, named the ‘Gait Solution’ Orthosis (Figure 1.37) by the authors, were investigated on the gait of three hemiplegic patients (8-18 weeks post stroke). When the subjects walked with the ‘Gait Solution’ Orthosis a reduced ankle plantarflexion during swing and knee extension during stance were noted. In addition changes at the hip moment were observed, with a greater flexion occurring during mid to late stance. An interesting finding, in agreement with a previous study (Yamamoto et al., 1993a), was the relation between AFO flexibility, ankle plantarflexion and knee extension during stance, the greater the movement in the plantarflexion direction, permitted by a more flexible AFO, the greater the extension at the knee. However, when excessive resistance to plantarflexion is applied to the ankle joint, instability of the knee occurs. It is thus important, when trying to address gait impairments following stroke, to control rapid plantarflexion at initial contact but allowing gradual plantarflexion during stance, as the authors concluded. That was possible by the use of the ‘Gait Solution’ Orthosis. The latter is nowadays one of the most used orthoses in Japan for the treatment of hemiplegic patients and it is supplied partially ready for use by Kawamura-Gishi Co. Ltd (Japan).



Figure 1.37: Three different designs of the ‘Gait Solution’ Orthosis as produced by Kawamura-Gishi Co. Ltd, Japan (<http://www.kawamura-gishi.com/product/index.html>)

The same AFO with oil damper (Figure 1.37) was shown to provide sufficient plantarflexion of the ankle and flexion of the knee at initial contact and during late

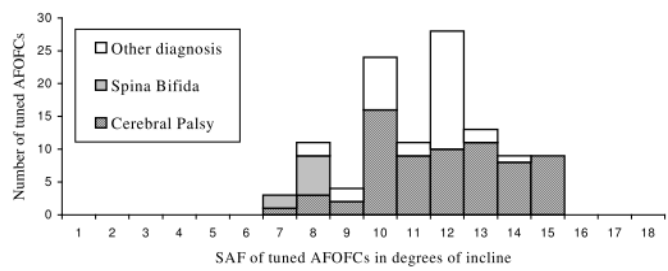


Figure 1.38: Frequency distribution of Shank to Vertical Angle here referred as Shank to Floor angle (SAF), of tuned Ankle-Foot Orthosis Footwear Combinations by diagnosis (Owen, 2004).

stance in two chronic hemiplegic subjects as assessed by Yokoyama et al. (2005). Hyperextension of the knee during mid stance and plantarflexion of the ankle during swing phase were abolished, whereas contrasting results were obtained in the two subjects with regard to the hip flexion angle. Results of these studies on the 'Gait Solution' Orthosis are, however, limited by the small number of patients involved. There is emerging evidence that properly tuned AFO-footwear combinations can improve shank and thigh kinematics and thus the biomechanical alignment of the GRF at the hip and knee and ultimately enhance gait (Bowers and Ross, 2009). However, existing evidence is mostly related to the treatment of cerebral palsy children (Bowers and Ross, 2008) but, eventually, these findings could be extracted and apply to stroke to improve orthotic management in the rehabilitation of adult hemiplegia.

During the International Society for Prosthetic and Orthotics (ISPO) World Congress held in Honk Kong in 2004, Owen et al. (2004) detailed the principles of tuning and highlighted the importance of this process in patients with neurological disorders to avoid missed opportunities in regaining walking ability. A recent paper (Owen, 2010) stressed the importance of obtaining correct shank and thigh kinematics by tuning the AFO and footwear combination to allow a stable stance phase to occur and optimal swing phase initiation. A shank to vertical angle (SVA) of 10-12° incline is the optimum position of the shank during mid stance to provide stability over the stance leg, to allow the thigh to become inclined and to obtain appropriate GRF alignment with respect to the knee and hip (Owen, 2004; Owen et al., 2010). A SVA of 10-12° should be the starting point when tuning AFO and shoes together and, it may be increased or decreased if that value does not represent the optimal position for the particular patients being assessed. In a study (Owen, 2004) involving 74 children affected by cerebral palsy, spina bifida and other conditions for a total of 112 AFOs fitted and tuned, it has been shown that a shank to vertical angle inclined of 10-12° was appropriate for many but not all children (Figure 1.38). SVAs ranged between 7° to 15° inclined with a mean of 11.36° (Owen, 2004).

To obtain the best intervention from tuning, the AFO fitted to the patients should present with appropriate mechanical properties and correct angle at the ankle of the AFO (Owen, 2004; Bowers and Ross, 2008). This means, that even if it is common

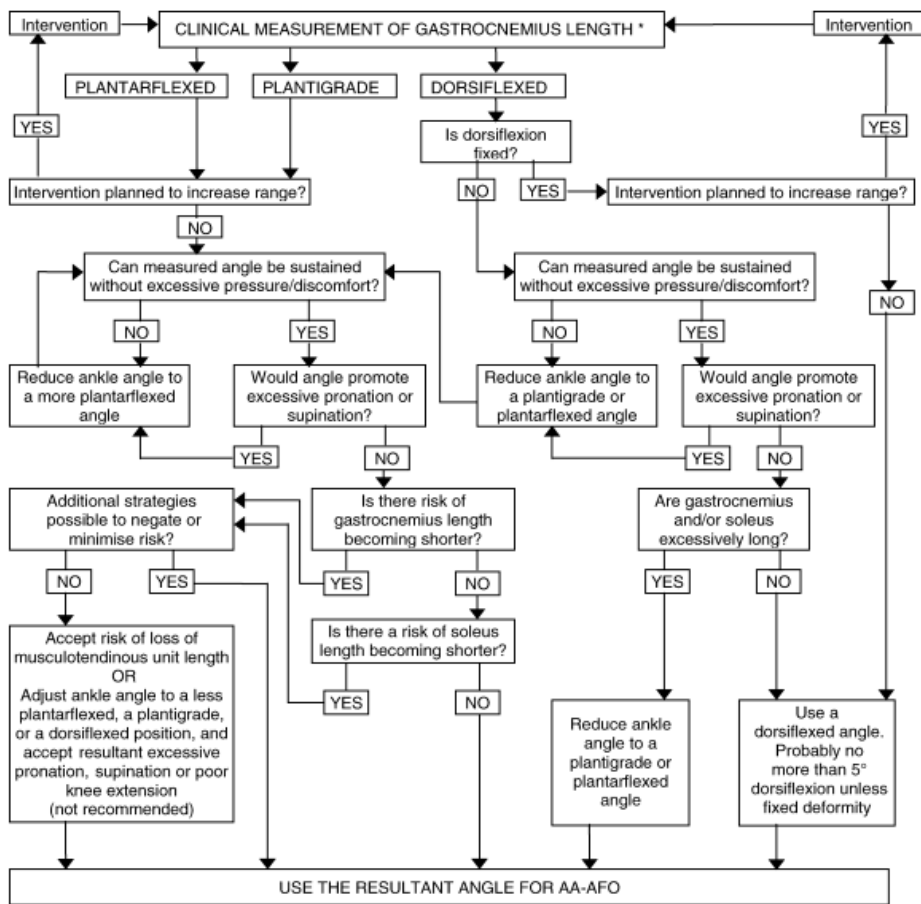


Figure 1.39: Proposed algorithm for deciding AFO casting sagittal angle (Owen, 2005).

| | Without orthosis | | With orthosis | | p-value |
|--|------------------|-------|---------------|-------|---------|
| | Average | SD | Average | SD | |
| Energy cost (ml O ₂ /kg/m) | 0.76 | 0.41 | 0.49 | 0.20 | <0.01 |
| Energy consumption (ml O ₂ /kg/min) | 9.87 | 1.92 | 9.42 | 1.62 | NS |
| Speed (m/min) | 15.47 | 6.95 | 21.39 | 7.30 | <0.001 |
| HR (beats/min) | 89.14 | 13.36 | 87.88 | 13.43 | NS |
| RR (breaths/min) | 22.25 | 3.27 | 23.31 | 4.25 | NS |

Figure 1.40: Effects of AFOs on energy cost and cardiorespiratory parameters (Franceschini et al., 2003).

practice to prescribe AFO casted with the ankle at 90° , AFOs should accommodate for gastrocnemius shortening. They must also be adequately stiff (Owen, 2004; Bowers and Ross, 2008; Best Practice Statement, 2009; Owen, 2010). Casting at 90° in the presence of a gastrocnemius contracture will limit knee extension during stance and will have a detrimental effect on hip and knee kinetics (Owen, 2005; Meadows et al., 2008; Best Practice Statement, 2009). An algorithm (Figure 1.39) to identify the optimal casting angle has been proposed (Owen, 2005), however scientific evidence is still lacking as to the consequences of casting AFO at 90° rather than at gastrocnemius length.

As anticipated earlier, a poor literature has been found to address the effect of tuning AFOs in stroke patients gait pattern. Butler et al. (1997) reported reduced pain at the knee and improvements of the knee extension moment arm (Figure 1.35) when a late hemiplegic patient walked with an optimally adjusted AFO and footwear combination at 1 and 4 year after fitting. However, no information is given on the kinematics and kinetics of the knee. A recent single case study (Jagadamma et al., 2010) with a chronic stroke patient reported, similarly to Butler et al. (1997), alleviation of the pain suffered by the patient at the knee when she wore a tuned AFO and footwear combination (AFOFC). In addition knee kinematics and kinetics benefited from the tuning process as result of a reduction in knee hyperextension during stance. The tuning process was conducted in 4 different steps until the optimum GRF alignment and knee kinematics/kinetics were achieved. The best prescription of the AFOFC for the assessed patients was a plastic AFO tuned at a 14° inclined shank to vertical angle with an added stiff rocker sole. Although this is a promising result and recommendations were made for the routine tuning of AFO in clinical practice in Scotland (Best Practice Statement, 2009), the effect of AFO tuning in stroke still needs to be addressed and thoroughly understood.

Improvement in walking abilities resulting from the use of AFOs have also been reported to lessen the energy expenditure of gait as the challenges the patients need to go through while walking are reduced. Franceschini et al. (2003) to this regard reported improved energy efficiency (Figure 1.40) when subjects wore their AFOs. The AFOs reduced significantly the energy cost of gait without affecting energy consumption or cardiorespiratory response (Figure 1.40) despite an increased in

walking speed. In other words, the body's workload is not affected by higher speed and this can be justified by the facilitating effect the AFOs have on walking.

Similarly, in a previous study, the same authors (Franceschini et al., 2001) reported a decreased energy cost of walking, 0.69 versus 0.46 ml O₂/kg per m, for the same energetic expenditure, 6.07 versus 5.87 ml O₂/kg per min, when 12 hemiplegic patients walked with an AFO. Similar findings concerning the energy cost of walking with AFO in stroke patients have been published in another study (Danielsson et al., 2004) although the AFO was of the carbon composite design. Energy cost significantly decreased by 12% when chronic stroke patients walked with the AFO but oxygen consumption remained almost constant even though walking speed was 20% higher than without the AFO.

More recently, Bregman et al. (2010) reported a reduced energy cost of walking (12.1%) when patients walked with their prescribed AFOs. If one analyses the results more carefully among the 6 subjects that completed the test, it could be noticed that the reduction in energy cost occurred effectively in only 3 out of the overall 6 patients. The controversy in these findings could be explained with the poor appropriateness of orthotic prescription prior to entering the study and thus once again it stresses the lack of clarity in the current clinical practice in prescribing suitable AFOs.

No less important than improvements in gait parameters, are the perceptions AFO users have about their splint. Although a subjective parameter and somewhat related to the ability of the prescribed AFO to match patients' expectation, some studies revealed that AFO wearers were generally happy with the benefits gained by orthotic intervention (Hesse et al., 1996; Tyson and Thornton 2001; De Wit et al., 2004, Pavlik, 2008, Tyson and Rogerson, 2009; Jagadamma et al., 2010). Patients commented on an increased confidence (De Wit et al., 2004; Tyson et al., 2009), increased safety and less difficulties while performing activity that required ambulation (De Wit et al., 2004; Pavlik, 2008; Tyson and Rogerson, 2009). Walking was perceived as near to normal (Hesse et al., 1996; Tyson and Thornton, 2001; Tyson and Rogerson, 2009; Jagadamma et al., 2010) and tiredness was reduced (Pavlik, 2008). Subjects, involved in three of the studies that reported patients' views of AFOs' utilisation were concerned about the cosmetic appearance or weight of the

device provided (Hesse et al., 1996; Tyson et al., 2001; 2009). However, the orthoses used in these three studies were metal and leather AFOs (Hesse et al., 1996) and articulated AFOs (Tyson et al., 2001; 2009) that could easily result in heavier and bulkier orthosis when compared to non articulated plastic AFOs.

Although, beneficial effects on gait ability of people affected by stroke have been demonstrated, some physiotherapists still have reservations on the use of AFOs. They claim that an orthosis is likely to lead to dependency and thus inhibits muscle power recovery. These beliefs however are not scientifically supported by research evidence and should not discourage the use of orthoses early after stroke according to an international conference of ISPO (Condie et al., 2004). Only a few studies have investigated the muscle activity during the use of AFOs and reported inconsistent results (Leung and Moseley, 2003). Controversially a study (Robinson et al., 2008) reported the beneficial effect AFOs had on preventing plantarflexion contracture that could be a rather common problem among stroke survivors (Vattanaslip et al., 2000).

1.5.3 *Mechanical properties of AFOs: a survey of the literature*

Evaluation of the efficacy of AFOs is a two fold process, which requires both assessment of walking ability in terms of improved activity level and re-established kinematics and kinetics at joints, and evaluation of the mechanical characteristics of the specific intervention prescribed. Evaluation and characterisation of the AFO itself will include research questions such as:

- What is the stiffness of the AFO?
- What is the cast angle and the angle of the AFO and footwear combination to the ground?
- What are the loads carried through the AFO?

A search of the literature revealed that few studies were able to answer these research questions even with limitations and, among the clinical evaluations conducted and described above, very few reported the specific details of the AFOs employed.

In relation to these research questions, Yamamoto et al. (1993b) conducted a study to compare the stiffness, in dorsi/plantarflexion and inversion/eversion, of 11 types of plastic AFOs using a muscle training machine. The effective resisting movement of

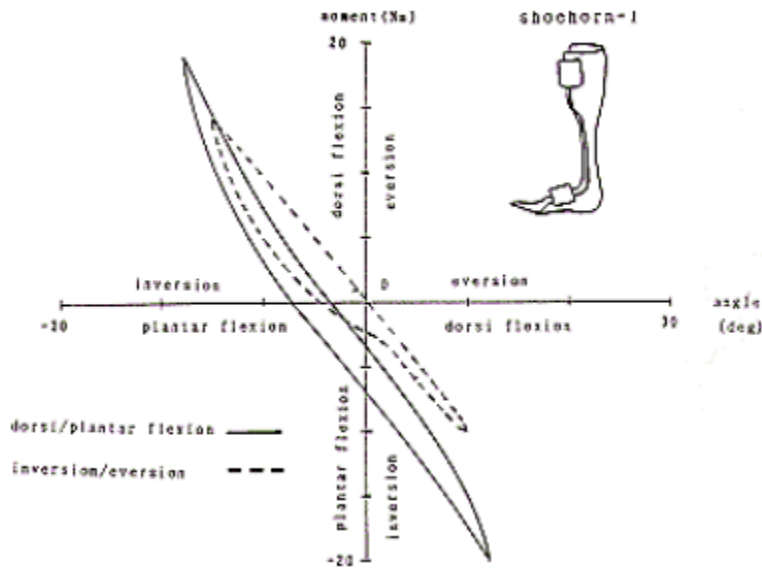


Figure 1.41: Stiffness graph of a shoehorn type AFO. In the abscissa ankle joint angle is represented while the ordinate represents the AFO resistive movement (Yamamoto et al., 1993b).

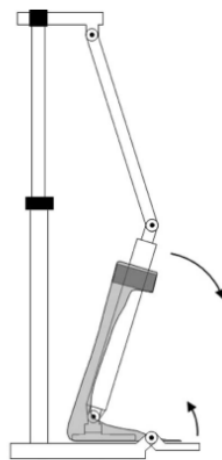


Figure 1.42: Schematic overview of BRUCE. Plantar/dorsiflexion motion at the ankle and flexion/extension at metatarsal-phalangeal (MTP) joint are shown by the 2 arrows (Bregman et al., 2009).

the AFO in these direction was obtained free of muscle and passive tissues resistance. A typical graph obtained is shown in Figure 1.41 for one of the shoehorn types of AFOs tested. A prospect of the flexibility of different AFOs is thus given and one could ideally use the data to choose the correct orthosis to match the degree of paralysis of the patient. However, this is not currently taken into account in clinical practice.

Several other ways have been used in the recent past to assess the stiffness of different AFO designs. These include a simple device which consisted of two metal bars, foot/leg/AFO model and a tensiometer (Sumiya et al., 1996), a test apparatus developed to detect AFO flexibility in 5 degrees of freedom in order to quantify cross-coupled deformation under certain load (Klasson et al., 1998), a mechanical system through which sliding loads deflect the AFO and dummy leg positioned to reflect different phases of the gait cycle (Polliack et al., 2001), a material testing machine (Major et al., 2004) and more complex and reliable developed devices (Cappa et al., 2003; 2005; Bregman et al., 2009). Cappa et al. (2003) developed an AFO testing machine to be operated manually to allow stiffness measurement in 2-Dimension (2D) in a quasi-static manner, and then upgraded the device to allow fully automatic AFOs testing in 3-Dimensions (3D) and dynamically (Cappa et al., 2005). When the two test machines were assessed, results from both showed good reliability with errors in stiffness values less than 4% and approximately 1% for the static and cycling test devices respectively. Reservations to the use of such devices are their applicability in a clinical setting and the definition/convention of ankle angles adopted.

For these systems, the main limitations were the feasibility and accuracy of the measurements and the fact that the movement/force applied to the experimental AFO may not mimic the loading during gait. As an example, during the test conducted by Major et al. (2004), the AFO buckled because they did not use any internal support to represent a patient's leg, this could have altered the results obtained.

An interesting device was proposed by Bregman et al. (2009) called BRUCE, which stands for Bi-articular Reciprocating Universal Com-pliance Estimator (Figure 1.42). A dummy leg and foot are placed inside the AFO to be tested although no contact occurs between the orthosis and the device. This may represent a limitation when

trying to mimic a real situation as for an AFO wearer. BRUCE, however, was shown to reliably measure the stiffness of an AFO at the ankle; moreover, thanks to a movable forefoot plate (Figure 1.42), which can be lifted around the metatarsal-phalangeal (MTP) joint, the stiffness of the sole/forefoot of the AFO or AFO and footwear combination can also be estimated in a reliable manner. Measurements of the neutral angle of the AFO can also be obtained through BRUCE although reliability was found to be dependent on the user. Among the methods proposed to quantify the mechanical characteristics of an AFO, this represents a good compromise that could be incorporated in clinical practice due to the ease of its use and thus provide useful information to improve AFO prescription.

With regard to orthotic load measurement, an analytical analysis was conducted by McHugh (1999) to estimate interface forces in the sagittal plane in the absence of plantarflexion or dorsiflexion muscle power. It was concluded that forces required in late stance when there was a lack of plantarflexors power were greater than forces required for dorsiflexors insufficiency in early stance and swing phase. It followed that in the first situation a more rigid AFO is advisable.

In the late 1960, the strains produced and loads applied to a conventional metal and leather AFO were obtained experimentally by Magora et al. (1968). By attaching 4 strain gauges to each bar of the AFO beneath the ankle joint, strains were measured while three healthy subjects walked with different gait patterns and speeds.

Variations in strains were reported with varying types of gait, foot positions and between the medial and lateral uprights, with the highest loads recorded in the lateral upright. During swing phase no strains were observed. The same method was applied to investigate the stresses generated on conventional AFO by four subjects affected by dorsiflexor paralysis leading to drop foot (Robin and Magora, 1969). It was found that loads applied in a lateral direction by these participants were twice as high as the loads applied by able-bodied subjects measured in the aforementioned study (Magora et al., 1968) and, so were the stresses measured. The reason for this is related to the lateral instability of the foot in presence of calf muscle paralysis. The main aim of these studies was to conduct a mechanical analysis of AFOs under walking conditions in an attempt to improve new AFOs designs and prevent their failure due to the effect of metal fatigue and the high stresses applied to their components. It was

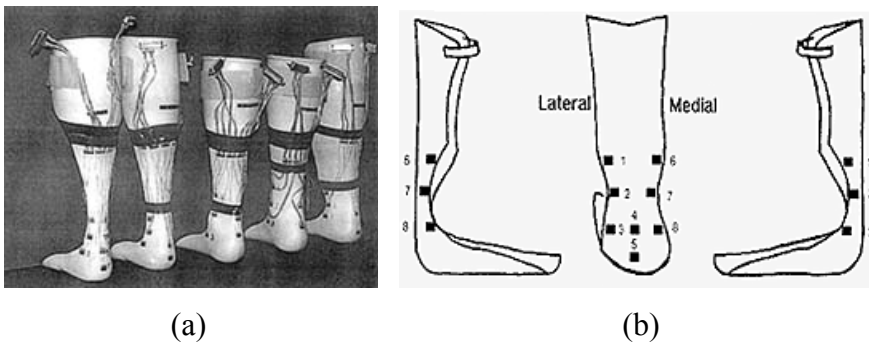


Figure 1.43: (a) AFO types tested with strain gauges attached. The 5 AFOs are (from left) Flex, Standard, Moderate, Solid and Varus AFOs. A schematic view (b) of strain gauges positioning is shown in (from left) medial, posterior and lateral view (Chu and Feng, 1998).

concluded that an AFO with a mechanism to prevent drop foot, operating in swing phase only, would reduce stress development and thus the likely occurrence of a breakage.

A more comprehensive stress analysis of plastic AFOs, has been conducted by a research group at the New Jersey Institute of Technology (Chu et al., 1995a; 1995b; Chu and Feng, 1998; Chu, 2000). Finite element analysis (FEA) was employed to simulate and analyse stress distribution in the plastic AFOs (Chu et al., 1995a; 1995b), and subsequently these results have been validated by experimental investigations (Chu and Feng, 1998; Chu, 2000). A 3D model was developed to represent a polypropylene AFO, and the anatomy of the lower leg (bones and soft tissues) (Chu et al., 1995a; 1995b). Assumptions made considered that the system (AFO and leg) was linear, perfectly elastic and isotropic. Results from a static (Chu et al., 1995a) and quasi-static (Chu et al., 1995b) analysis of normal and pathological (drop foot considered) instants of gait revealed that stress concentration mainly occurred in the heel (compression) and neck region (tension) of the AFO during heel strike and toe off respectively. Stress distribution was shown to be dependent on the point of heel contact, to be asymmetric between lateral and medial side, as found in a conventional AFO along the two side bars (Magora et al., 1968; Robin and Magora, 1969) and, with an inverse relationship to the stiffness of the AFO. Peak tensile stresses were higher when simulating a drop foot. From a separate material simulation test it was found that polypropylene properties are time-dependant and deteriorate with increasing number of test cycles. The analyses conducted provide a picture of stress distribution but are dependent on the major assumptions made which simplify the properties of the material. Moreover dynamic results are not included in these stress analyses a part from stresses developed during the simulation of slow walking. Results from these finite element studies were confirmed through experimental investigations (Chu and Feng, 1998; Chu, 2000). Five types of plastic AFOs characterised by different trimlines (Figure 1.43a) were instrumented with eight strain gauges each (Figure 1.43b) to allow dynamic stress measurements under ten typical motions of stance and swing phase (Chu and Feng, 1998) and while three subjects of various builds donned with the AFOs performed slow walking and a sit to stand movement (Chu, 2000). The procedure used to attach strain gauges on to

polypropylene (Chu et al., 1996) was based on the treatment with UV light at the point on the surface where the gauges are to be positioned. However, neither results on the reliability and feasibility of this technique nor comparisons with other similar procedures were reported. Stress profiles, as calculated through collected strain values, were obtained for each of the five orthosis. Measured stresses varied with AFOs geometry, activities and participants' body weight, although for the latter, changes can not be easily anticipated. In all cases, as predicted by FEA, higher peak stresses occurred in the neighbourhood of the neck region of AFOs and stress distribution was asymmetric. These findings, as suggested by the authors, should serve to predict the fatigue life of the device employed and thus to avoid failure. Results however are affected by various limitations the first of which is the reliability of the strain gauge measurement, and additionally the small number of tests conducted and the not exact fitting of the orthosis as the same devices were given to each subject regardless the shape of their lower limb.

A 3D finite element model of the leg and AFO has been developed more recently by Uning et al. (2008). Differently from Chu et al.'s FE model (Chu et al., 1995a; 1995b), Uning et al.'s model is obtained by 3D reconstruction of CT scan data and thus represents the actual anatomy of the foot and AFO. Friction between the orthosis and soft tissue is also taken into account. Through a dynamic analysis that mimics human gait, stress distribution in the AFO could be obtained. Although more advanced than previous models, the AFO and leg system was still considered linear, uniform, elastic and isotropic. Disappointingly, results from this more promising model were not reported. Material non-linearity was considered in the 3D finite element model developed by Syngellakis et al. (2000). An analysis of AFO behaviour under a static loading condition and with different trimlines was presented. The accuracy of orthosis/tissue interface may be questionable and the reproducibility of a real loading condition was also limited. As pointed out by the authors, the lack of accuracy of the geometry and accurate representation of applied loads could compromise the effectiveness of the procedure when intended to be used as an assessment and design tool prior to AFO prescription and fabrication.

An attempt to measure AFO's corrective moment during gait was pursued by Japanese researchers (Yamamoto et al., 1993a; 1993c; Miyazaki et al., 1993; 1997).

An experimental AFO (Figure 1.44), based on the conventional AFO design with double aluminium uprights, was designed to continuously measure moments generated by the AFO by virtue of two springs which control plantar and dorsiflexion movements. A potentiometer was attached laterally to the mechanical ankle joint of the two aluminium bars to measure the ankle sagittal angle from which AFO's moments were retrieved. A capacitive force transducer attached to the sole of the footwear served to measure the total ankle joint moment as caused by the ground reaction force. The difference between GRF induced moment and AFO moment represent the moment due to muscles and passive tissues around the ankle (Miyazaki et al., 1993).

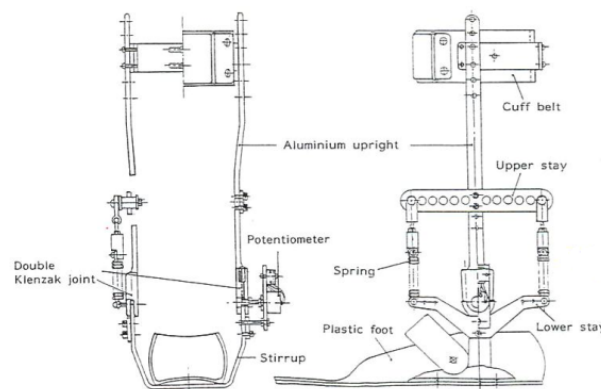


Figure 1.44: Experimental AFO schematic view (Yamamoto et al., 1993b).

From the investigations conducted it was shown that dorsiflexion corrective moment at heel strike was the highest contribution given by the AFO during gait. In comparison plantarflexion corrective moments were really small. These studies pointed out that an increase in walking speed should not be the only parameter to guide the choice of an AFO over another. The effect at initial contact and the improvement in knee joint angle should be valued the most. Although the methodology introduced was shown to be feasible, the AFO used did not represent the plastic AFO most often prescribed in practice and thus results are related to the particular experimental orthosis employed. Even if the instrumented AFO is adjustable, by means that different springs combination can be utilised and set to allow the desire movement in particular directions until the aimed gait pattern is achieved, changing its flexibility resulted in a fairly time consuming procedure that

cannot be used at the time of prescribing an AFO. The authors addressed this issue by adding the springs, previously housed in the joints, to the outside of the AFO. This allowed for easier changes to be made to the stiffness. However, the main problem still remained how to transfer the information gained through the analysis to the fabrication of a plastic AFO commonly provided.

Another study (Johnson et al., 2004) involved four laboratories around Europe and a total of 110 participants. The study tried to measure the loading pattern of a variety of lower limb orthoses including AFOs, knee-ankle-foot orthoses (KAFOs), knee orthoses (KOs) and hip-knee-ankle-foot orthoses (HKAFOs). Their main point was to show that orthotic loads could be determined by using gait analysis techniques. However, this method assumed that all the moments at the lower limb joints were taken by the orthosis that encompassed them. This is not the case in reality where, external forces and moments could still be partially resisted by body tissues either actively or passively. Hence, it is more likely that external loads are opposed by the action of the orthosis and body structures, as indicated in the mathematical model proposed by Miyazaki et al. (1993). Another assumption was to consider the orthosis and the leg as a single rigid body, as it is commonly undertaken to the lower limb segments during motion analysis. In addition, being a multi-centre trial, data from the four laboratories were shared and compared ignoring the errors that could be introduced by undergoing procedures in a slightly different way among different sites. Moreover, the variability of orthoses designs is not taken into account in the evaluation of the estimated orthotic loads. Conclusions from this study should be treated carefully due to the assumptions involved in the methods.

AFO's contribution during gait was quantified by Bregman et al. (2010). Using the previously developed BRUCE device (Bregman et al., 2009), mechanical properties of the AFOs used by the subjects (Multiple sclerosis and stroke) involved in the study were measured. From these values, stiffness and neutral angle of the AFO around the ankle joint, moments and powers provided by the AFOs throughout the gait cycle were derived. Two types of AFOs were used by the 7 participants involved, posterior lead spring (PLS) AFO and an AFO trimmed posterior to the malleoli with dorsal notches for flexibility. It was found that the AFO contribution was small compared to the one provided by the subjects, accounting for only 13.7%

and 7.2% of the total ankle moment in AFO benefit and non-benefit group. Also AFO power contribution to the total power at the ankle was small in both groups. The small AFO moments and powers found in this study should be related to the type of orthoses employed that were of the flexible type with mean measured stiffness of 0.19 N*m/deg. This also explains the non significant difference between AFO and non AFO walking net moments and power and it questions the appropriateness of AFOs prescription. The advantage of this method for quantifying AFO moments and power is that the AFO remains unaltered and assessment is thus performed on the AFO actually worn by a patient. On the other hand, it could be argued that a direct measurement, by means of using an instrumented AFO, would more truly measure the orthotic loads condition than this indirect measurement method requiring stiffness values.

1.6 Human locomotion and its analysis

Locomotion is the act of moving from one location to another. This is achieved by coordinated movements of the lower body segments regulated by the neuromuscular system. Alterations of muscle effectiveness and central nervous system activity thus result in an abnormal ambulation. Assessment on how a diagnosed disorder affects the walking pattern is provided by gait analysis. Gait analysis is defined as the set of methods and techniques aimed at quantitative analysis of human motion (Rose and Gamble, 2005). From this analysis, kinematic and kinetic aspects of the gait can be acquired and used as a clinical tool to quantify a pathological gait pattern. Data gained through motion analysis, provides clinicians and biomechanists with a powerful set of information aimed to assess the locomotor system functions through which prescription of treatments or evaluation (impairment or improvement) of a prescribed treatment can be obtained. The accuracy of such data is of fundamental importance in order to use the obtained results in clinical decision making.

Gait analysis data are obtained both through direct and indirect measurements from a subject. Direct measurement refers to all those quantitative information that can be measured directly using appropriate instrumentations from the subject. Indirect measurements, on the other hand, refer to those quantities obtained by mathematical modelling of the musculoskeletal system and are an estimate. The accuracy of the

results is thus related to instrument errors and the suitability of the biomechanical model employed.

The study of human locomotion can be traced back to the Renaissance with Giovanni Alfonso Borelli (1608-1679), considered the founder of Biomechanics. He first suggested how to measure loads acting on the human body and the determination of the body centre of mass. A first important contribution to the development of kinematics was given by Leonard Euler (1707-1783) who introduced differential equations to describe body movements. Edward Muybridge (1830-1904) and Étienne-Jules Marey (1830-1904) were the first to use photography to quantitatively analyse human locomotion (Figure 1.45).

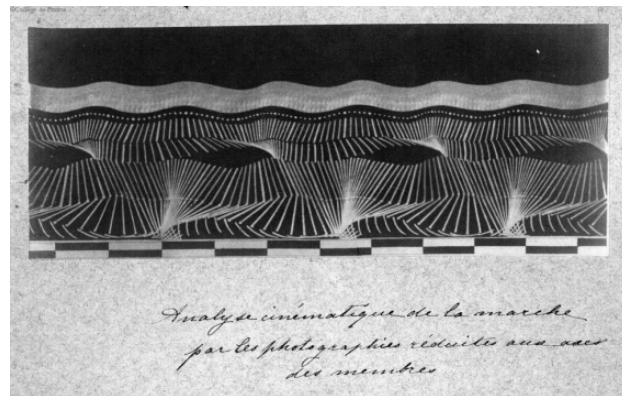


Figure 1.45: Étienne-Jules Marey's photochrononography (Figure adapted from <http://comm02.wordpress.com/2011/02/08/etienne-jules-marey/>).

In his words “Film photochrononography contains the solution of all problems of physiology, physics or of mechanics in which the position of bodies in different points of space and at equal intervals of time must be determined”, Marey described the basic principle of past, present and future Biomechanics. Another assumption, still valid in present biomechanics model, is to consider the human body as composed by rigid segment linked together as recognized by Wilhelm Braune (1830-1892) and Otto Fischer (1861-1917) in the late 1800s. They also contributed to the introduction of photography in 3D space which is the base of stereophotogrammetry used nowadays for body motion capture.

Parallel to the development of body position reconstruction, the precursors of modern force platforms (Marey and Elftman) can be traced back to this time.

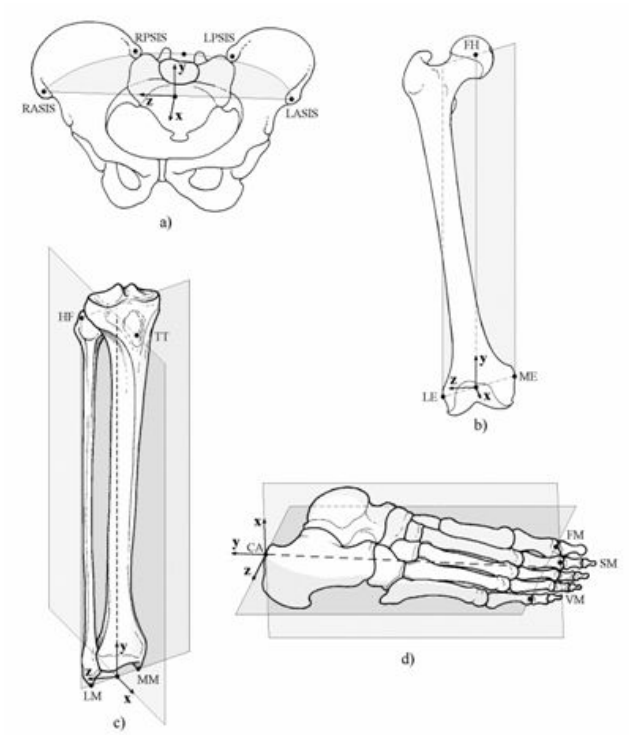


Figure 1.46: Anatomical frames as defined by Cappozzo et al. (1995).

Throughout the years with the aid of more modern technologies, different systems and biomechanical models have been developed with an enhance predictability and accuracy to facilitate the study of human motion and consequently improve the evaluation and treatment of impaired motor activity. However, debates are still ongoing among the biomechanics community to the regard of gait analysis protocols and biomechanical models to be used to pursue significant results. Differences between protocols consist on how a segment is defined anatomically, marker sets used to define bones segment, joint kinematics conventions, joint centre calculation to which rotations are referred, how kinetics are calculated, collection and processing procedures. An overview of the state of the art of human movement analysis relevant to the aim of develop a new protocol in according to the requirements of the current project is presented in the following.

1.6.1 Basic Principles of human motion analysis

A basic objective in movement analysis is the reconstruction of the bone motion in the laboratory reference system (Cappello et al., 1997). This in turn is based on the assumption that the human body can be represented by a series of rigid segments interconnected to each other by joints. Quantities normally extracted through motion analysis and used in research and clinical contexts, such as joint kinematics, required for their determination, the instantaneous position and orientation (pose) of the bone segments involved. Nowadays stereophotogrammetry, a method of motion capture, is used to track the three-dimensional (3D) position of retro-reflective or light-emitting markers assumed to be located in a constant relationship with the underlying bones. Through those markers, reference frames (local frames) are defined to describe the position in time and in space of the body segment they are associated to. Local reference frames can be defined arbitrarily, from markers which have an arbitrary position with respect to the bone (technical frames), or relative to the body morphology. In this latter case, anatomical landmarks are used to identify the so called anatomical frame (Figure 1.46) describing a system of axes which is repeatable among subjects. If anatomical landmarks are defined in a technical frame, instead of positioning a marker directly on them, their trajectories in the laboratory frame can be reconstructed through vector transformations.

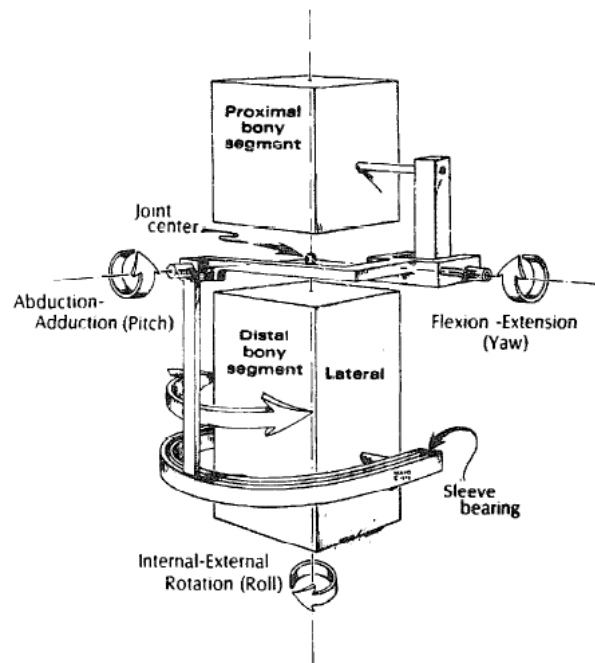


Figure 1.47: Schematization of the mechanism used by the triaxial goniometer which is identical to the Grood and Suntay's convention. (Chao, 1980).

1.6.2 *Joint Kinematics*

Joint kinematics is the description of the relative movement between two adjacent bones in three-dimensional space. Joint motions are thus described by six degrees of freedom, three being translational and three rotational. However, attention has been paid mostly to the relative rotations between two segments and so will be the following analysis. Joint angles/rotations are widely used for clinical decision-making and treatment planning. Their definition should be therefore consistent with the language in use in clinical practice and repeatable to allow intra and inter-subjects comparisons to be performed. A clinical description of joint attitude consists of three components, one in each of the sagittal, coronal, and transverse anatomical planes of the body (Cole et al., 1993). To date various methods have been developed and introduced to measure such joint components. Generally, the movement of the distal segment relative to the proximal segment is described. Among the methods introduced, Cardan/Euler angles are often used for the description of joint kinematics (Tupling and Pierrynowski et al., 1987; Kadaba et al., 1990; Davis et al., 1991). These angles are obtained through three sequential rotations assumed to occur about three distinct axes. If all three axes are different (e.g.:x,y,z), the angles are referred as Cardan angles, otherwise referred as Euler angles (e.g.:x,y,x'). The main limitation of Cardan/Euler angles is related to the sequence dependence of their definition. Twelve different sequences can be applied but the most common used is flexion/extension, ab/adduction, internal/external rotation. The sequence dependence is superseded with the use of the joint coordinate system (JCS) to measure joint angles, proposed by Grood and Suntay (1983). This method through the utilization of a particularly defined coordinate system allows the description of joint rotations which agree with their common anatomical meaning while being sequentially independent. The rotation axes which comprise the JCS are, two fixed in the proximal and distal segments respectively and a third one, 'floating axis', not fixed, perpendicular to the other two. The same concept was applied by Chao (1980) in the design of a triaxial goniometer to measure knee angles (Figure 1.47).

The non orthogonal system, so defined, was first proposed as an application for the evaluation of knee kinematics, but sequentially applied to the other lower limb joints (Siegler et al., 1988; Cole et al, 1993; Stagni et al., 2000; Leardini et al., 2007). In particular, Cole et al. (1993), based on the principles of the joint coordinate system, introduced a standardization proposal for the determination of joint attitudes. The proposal modifies the original angle definitions to make them applicable to all lower leg joints through a selected identification of the body fixed axes. In addition the new formulations prevent the occurrence of the gimbal-lock. This latter singularity condition, a drawback of Euler/Cardan angles as well, presents when the two body embedded axes are parallel or in other words when the ab/adduction angles are 90° . Moreover, the angle equations proposed by Cole et al. (1993) are defined in such a way that they are easily implemented in any software used for gait analysis. Another method introduced to measure joint angles, but which found poor applicability, is the use of a finite helical axis or attitude vector for this purpose (Woltring, 1991; Woltring, 1994). Although this method is not affected by any mathematical singularity, such as gimbal-lock, the significance of the angles so obtained is not well recognized in anatomical language.

It should be noticed that gimbal-lock is mainly a problem which affects upper limb joints, and in particular the shoulder (Chao, 1980). This explains the popularity of Euler/Cardan angles and JCS for the calculation of lower limb joint angles. The accuracy with which those values are obtained is strictly related to the definition of the bone segments coordinate systems, which in turn derive from acquired human motion data.

1.6.3 Associated errors to human movement analysis: measurement and compensation

Marker trajectories reconstruction is often affected by errors that can compromise the estimation of joint kinematics and kinetics. Those errors can be attributed to the instrumentation used, soft tissues artefacts (STA) and to anatomical landmarks misallocation. The first class of errors mentioned, can be compensated through an optimal calibration of the system, ensuring that each marker is seen by at least two cameras and using appropriate filtering and smoothing techniques of the data

acquired. One of the most popular filters used among biomechanists is the generalized cross-validation with splines (GCVSPL) proposed by Woltring (Chiari et al, 2005). For the second class of errors, which is both related to passive and active tissues interposition between the marker and the underlying bone, an accurate, practical and proofed compensation method is yet to be introduced. Filters cannot be used with the intent of minimising this error because STA has a frequency similar to actual bone movements rendering difficult the distinction between the two signals. Skin movements artefacts, thus remain the main source of inaccuracies in motion analysis which have been shown to introduce errors at least an order of magnitude larger than stereophotogrammetric errors (Cappozzo et al, 1996, Reinschmidt et al., 1997). Cappozzo et al. (1996) investigated the magnitude and the pattern of skin movements' artefacts while a subject performed different tasks. The gold standard for this investigation was represented by an external fixator attached directly either to the femur or the tibia of the subject tested. Markers were placed both over anatomical landmarks such as greater trochanter (GT), lateral femoral epicondyle (LE), head of the fibula (HF) and lateral malleolus (LM), and on other locations on the lateral aspect of the shank and thigh. Displacements between skin markers and underlying bone were reported to be in the range between 10-30 mm during walking, with GT and LE markers showing the largest deviations (Figure 1.48).

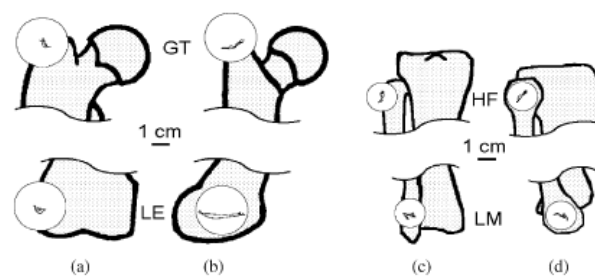


Figure 1.48: Position artefacts trajectories of great trochanter (GT), lateral epicondyle (LE), head of the fibula (HF) and lateral malleolus (LM) skin markers during a walking cycle at natural cadence. (a) and (c) frontal plane, (b) and (d) sagittal plane (Cappozzo et al. 1996).

Smaller artefacts were exhibited by the additional lateral skin markers especially if located on the distal part of the segment. To the regard of STA effects on knee

kinematics it was concluded, after evaluating the effects of different markers cluster combination on bone orientation, that estimation of knee angles may be affected by inaccuracies which could be as big as 10, 50 and 100% of the expected knee rotation range respectively for flexion/extension, adduction/abduction, internal/external rotation.

Similar findings have been reported by Reinschmidt et al. (1997). The aim of this study was to evaluate errors that occur at knee and ankle joint angle when external skin markers are attached over the thigh, shank and shoes of a subject. Six skin markers were located in each segment at standardised distance from anatomical landmarks. The accuracy of joint kinematics obtained by the mentioned markers was evaluated through comparison with joint kinematics derived by “bone markers”. The latter were intra-cortical Hofmann pins with triads of reflective markers inserted into the lateral femoral epicondyle, the lateral tibial epicondyle and the postero-lateral aspect of the calcaneus. With regard to knee rotations, poor agreement was found in the frontal (max difference up to 6°) and transverse plane rotations (max difference up to 10.1°) leading to the conclusion that reliable results at the tibiofemoral joint can only be determined for flexion/extension as errors induced through STA may exceed the actual motion occurring at the knee. The cause of discrepancies between skin and skeletal marker based rotation at the knee was found to be mainly related to skin movement artefacts at the thigh. For ankle joint rotation a better agreement was found between the two measures, although rotations are usually overestimated by the skin markers. Ankle rotation errors were mainly due to shoe markers movements (7° against shank marker movement $2-3^\circ$). It was however concluded that shoe markers can be used to reflect ankle joint motion although the interpretations should be made carefully.

Errors induced by skin mounted markers on shank kinematics and knee kinetics were quantified by Holden et al. (1997). A percutaneous skeletal tracker (PST) specifically designed for this purpose was attached to the distal shank by pins inserted in the periosteum in three subjects. Additionally a surface-mounted target was used to track shank motion. The latter consisted of markers on rigid plates positioned both on the mid shank and on the dorsum of the foot. Kinematic and kinetic data were expressed relative to an anatomically-based segment coordinate system determined from each

target set. Comparisons between set of values from the two anatomical frames were carried out and considered as a measure of STA. Rotations along the medio-lateral (X) and antero-posterior (Y) axes showed an error less than 3° . On the other hand, internal/external rotations errors were more remarkable reaching a magnitude of 8° during terminal stance and most of the swing phase (Figure 1.49). This value represents a considerable percentage of true knee internal/external rotation.

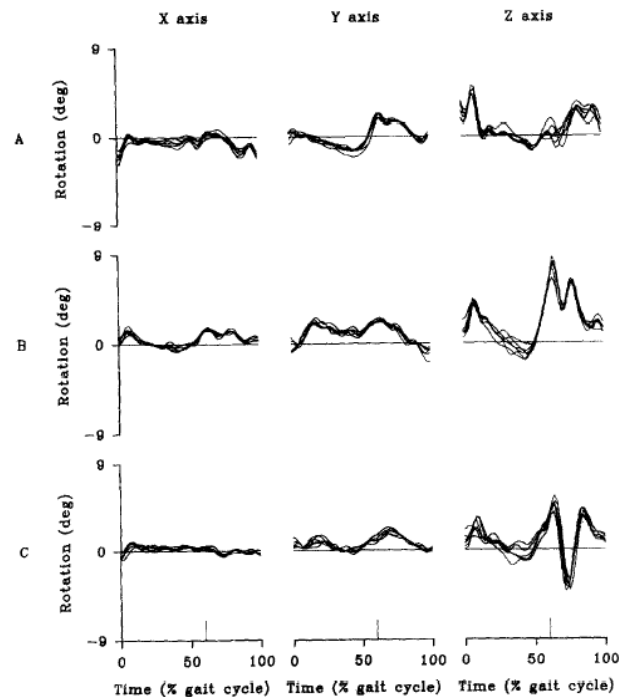


Figure 1.49: Rotational displacements of the surface marker based segment coordinate system with respect to the PST based segment coordinate system of 6 walking trials for three subjects (A, B, C) (Holden et al., 1997).

Displacement of skin based segment anatomical frame origin was higher in the longitudinal direction (10.5mm) than in the transverse and frontal direction ($< 6\text{mm}$). Joint forces and moments estimates derived from surface and bone mounted targets during gait differed mainly during stance phase. Maximum mean differences for any subjects were 39, 16, 9 N for the X, Y, Z force components, whereas the errors transmitted by STA to moments calculation were fairly small: 9, 9, 2 $\text{N}\cdot\text{m}$ for X, Y, Z components respectively.

| Article | Subjects | Motion Analysis | Gold Standard | Motor Task | Result/Conclusion | Limitations |
|------------------------|----------|--|-------------------------------|-------------------------------------|---|---|
| Fuller et al. (1997) | 1 | 3D Arrays of skin markers over thigh and shank | Intra-cortical pins | Walking, swing of each joint | Soft tissue movement is task dependant; Movement up to 20mm; Differences in angular displacement | Invasive and small sample |
| Manal et al. (2000) | 7 | 3D Surface marker arrays over the shank | Percutaneous skeletal tracker | Walking | Max rotational deviation along longitudinal axis during first and last third of stance phase (range 4-7°); Smaller errors in distal constrained markers | Only shank marker error evaluated; Small sample |
| Yack et al. (2000) | 2 | 3D Femoral tracking device (FTD) | Intra-cortical pins | Walking, running, Unloaded pendulum | FTD gave reasonably valid results; 20% error in amplitude in knee kinematics | 85% of stance analysed; Small sample |
| Westblad et al. (2002) | 1 | 3D Marker on the lower leg and heel | Intra-cortical pins | Walking | Tibiocalcaneal rotation RMS differences were 2.5°, 1.7° Dorsi/Plantar, 2.8°Ab/Add; Talocalcaneal RMS difference in Inv/Ever was 2.1° | Only stance phase analysed; Small sample |
| Manal et al. (2003) | 7 | 3D Surface marker arrays | Percutaneous skeletal tracker | Walking | Average peak differences along X, Y, Z were 7.4, 3.7, 2.1 mm respectively; No regular of soft tissue error among subjects; Estimates of tibial translation with a measurement resolution >3 mm are unlikely | Ideal measurement condition examined (slim healthy participants); Small sample |
| Houck et al. (2004) | 2 and 13 | 3D Helen Hayes set and FTD | Intra-cortical pins | Walking | Tibiofemoral joint displacement errors up to 10 mm RMS; Orientation error maximum in frontal plane 1.5° RMS; FTD more accurate than surface marker | 85% of stance phase examined; Small sample; FTD not accurate for swing phase kinematics |
| Benoit et al. (2006) | 8 | 3D Markers array over the thigh and shank | Intra-cortical pins | Walking; lateral cutting manoeuvres | Average rotational error range 2.4-4.4°; 3.3-13.1° and translational 3.3-13mm, 5.6-16.1mm for walking and cutting respectively; Skin marker present limitation in predicting knee kinematics | Small sample; Bone pins failed in rigidity |

Table 1.2: Summary table of studies reporting STA assessment.

Similar findings to the ones just described were reported in several other studies found in the literature (Table 1.2). In these papers STA errors due to skin markers were compared to intra-cortical pins, external fixators, and percutaneous based trackers. Although those methods provide an excellent description of actual bone movements their invasiveness greatly limits their applicability in daily use. In addition, it is likely that patients, who wear those bulky devices, have a non-physiological pattern of locomotion (Leardini et al., 2005). Another drawback of these procedures is the skin motion restriction, caused by the pins, which could limit the realistic quantification of STA during daily life activities (Stagni et al., 2005). An alternative way to investigate the relative movement of the skin to the respect of the underlying bone is to use methods exploiting Roentgen photogrammetry, such as X-ray radiography, fluoroscopy and MRI, as a gold standard to assess STA. Those methods overcome the limitation related to the use of invasive techniques. Recently more studies have been published using radiological techniques than invasive pins (Peters et al., 2010a) for skin movement investigation.

Skin mounted markers used to measure motion at the foot were described by Tranberg and Karlsson (1998) using 2D roentgen photogrammetry (X-ray). Spherical lead markers were attached over the medial malleolus, the navicular, the medial calcaneus, the base and the head of the first metatarsal bone and fifth metatarsal head. X-ray pictures of the medial aspect of the foot were taken in neutral position, 20° of ankle dorsiflexion and 30° of plantarflexion. Proximal markers, the ones close to the medial malleolus, the calcaneus and the navicular bone, deviated from the underlying bone by up to 4.3 mm. Markers placed distally showed a maximal deviation of 1.8 mm. These results can be used to suggest a marker set up at the foot level.

The authors, in addition, found a 2.3° angular error between the line connecting skeletal structures recorded with X-ray and the one identified by marker positioning and motion analysis (Figure 1.50). Angular error should be carefully evaluated as it could increase when the distance between the markers decreases.

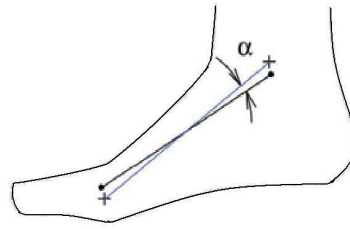


Figure 1.50: Angular deviation (α) between the real line and the one derived by two skin mounted markers (Tranberg and Karlsson 1998).

More recently low dose X-ray radiography was used to compare the displacements of three different markers attachment systems (A, B, C) (Figure 1.51) at different knee flexion angles (Südhoff et al., 2007). Those angles were roughly 0° , 20° , 40° and 70° for each of the 18 subjects tested.

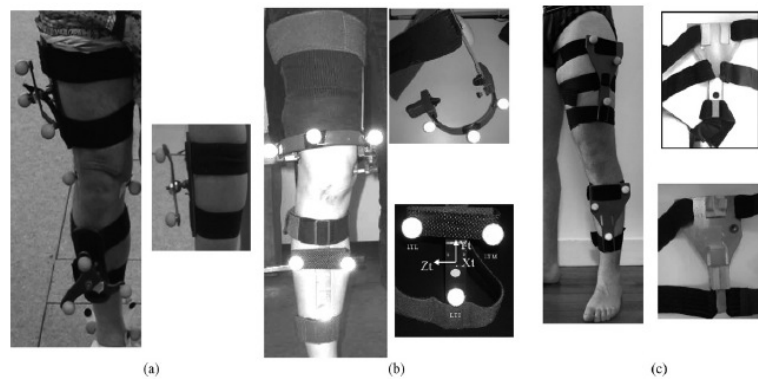


Figure 1.51: Attachment systems used: System A (a), B (b), C (c) (Südhoff et al., 2007).

Tibial and femoral displacements for the three systems between two consecutive positions and overall displacements between 0° to 70° knee flexion were evaluated. Comparisons between systems showed that system B is the most stable, which is also the most invasive. However, each system both in the femur and in the tibia mostly produced relative motion in the transverse plane (mean 6.4° and 6.1° respectively). Motion measurements in the frontal and sagittal plane were precise. The maximum mean displacement in these planes was 1.4° . Elastic strap fixations, thus, limit error in the sagittal and frontal but not in the transverse planes. For this reasons axial

rotation should be evaluated with caution when calculated from stereophotogrammetry system while using elastic bands for fixation.

Fluoroscopy was first used by Sati et al. (1996) to quantify skin movements at the knee. Similarly to the study run by Tranberg and Karlsson for the foot, results from this study could provide guidance in the choice of skin marker positioning for a more accurate knee movement analysis. Radio-opaque markers were individually taped over lateral and medial epicondyles and on lateral aspect of the thigh. The projections of their movement compared to those of the underlying bone were used as a quantification of skin-bone displacement over a knee flexion range of approximately 65°. Lateral marker movements varied from 2.5 mm root mean square (RMS) error to 17 mm RMS, whereas medial marker movements range between 2 to 17 mm RMS. Peak values exceeded 40 mm in the antero-posterior direction. The largest marker movements occurred when markers were placed on the joint line. Marker placement, it was concluded, is a compromise between distance from the region of interest and skin movement error as one approaches this region. This will serve as useful information to keep in mind when using markers to track knee motion.

X-ray can only provide description of STA in 2D and an evaluation limited to static conditions. A combination of stereophotogrammetry with 3D – kinematics reconstruction from fluoroscopic images was used by Stagni et al. (2005). This technique provides skin motion evaluation in unconstrained conditions and during the execution of various motor tasks, and it also overcomes the limit of a restricted fluoroscopic field of view as occurred in the study by Sati et al. (1996). In order to evaluate skin movements at the thigh and shank, markers were spread all over the lateral surface of the subjects' segments. Different technical frames based on possible combination of the markers attached on the thigh and shank were used to define anatomical coordinate systems and then calculate knee kinematics. The standard deviation of the position of each marker in the relevant anatomical frame was calculated for each motor task as a measure of STA errors. Thigh markers clearly moved more considerably than shank ones and their displacements were shown to be task-specific. Choice of different technical frames for the reconstruction of joint kinematics affect knee rotation angles (Figure 1.52).

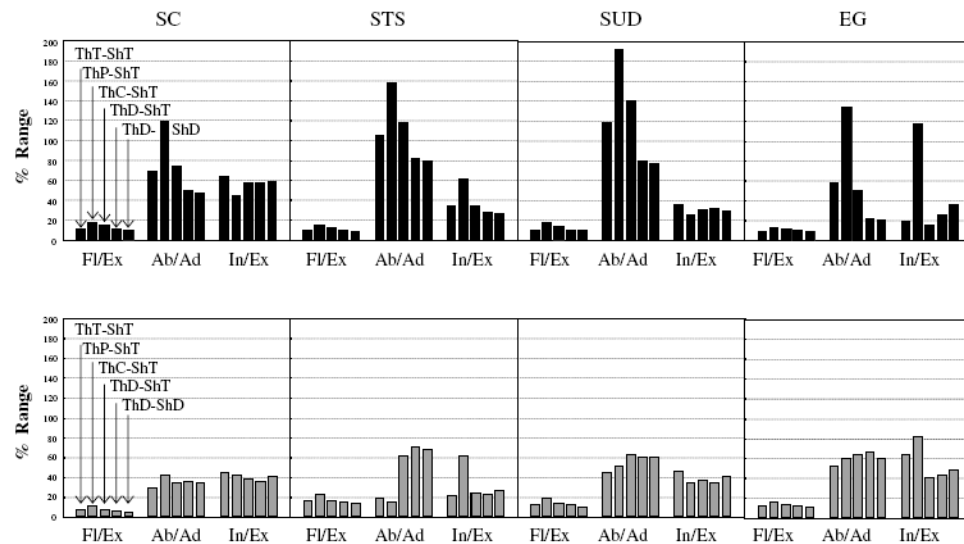


Figure 1.52: RMS difference of knee rotations between 3D fluoroscopy and those evaluated with each cluster combination (ThT–ShT, ThP–ShT, ThC–ShT, ThD–ShT and ThD–ShD) expressed in percentage of the corresponding range. Black and grey bars referred to the two subjects analysed (Stagni et al. 2005).

STA propagation to the flexion/extension angle is limited, whereas the measure of internal/external rotation and adduction/abduction can be invalidated by root mean square errors up to 117% and 192% of the corresponding range, respectively (Figure 1.52). Those more remarkable differences in rotation angles compared to previous studies described, were justified by the authors by the limitation that pins or external fixators may imposed to skin movements. The need of compensation method for skin induced errors is emphasized.

Drawback of fluoroscopy and X-ray is the exposure of the subject to ionising radiation, the use of MRI as a gold standard, however, can avoid this implication. A step back from the measurements of unconstrained tasks as in Stagni et al. (2005) is obligatory when using MRI as the space available is confined. Sangeux et al. (2006) developed a method which uses MRI based bone coordinate systems as a reference to compute the 3D relative movement between bone and external markers. External fixtures with markers attached on them were placed on the subjects' thigh and shank with elastic bands. Participants were asked to perform a knee extension with three pauses before reaching full extension starting from a flexed knee position of approximately 90°. Errors on markers based coordinate systems were expressed as a

translation of the origin and rotation around the 3 principle axes of the reference system. The thigh marker displacements tend to increase with knee flexion angle within a range of 2-22 mm, whereas shank markers were more stable at around 4.5 mm. Relative movement rotation parameters for the thigh were reported to be between 0 to 11°, and for shank markers 0 to 15°. These results are consistent with those of other studies, previously described, and confirm that the relative movement between the bone and the markers represents a major source of error which can highly compromise joint kinematics. Soft tissue displacements should be minimised to mimic the real skeletal movements as accurately as possible.

Analytical methods have been proposed to reduce the propagation of errors due to skin movements to joint kinetics and kinematics. An enhancement of the Calibrated Anatomical System Technique (CAST) (Cappozzo et al., 1995) was introduced by Cappello et al. in 1997 and then improved by the same authors in a later study (2005). This technique recommends a double calibration of anatomical landmarks (ALs), usually identified to describe joint kinematics and kinetics, at the two extremes in the range of the specific task under analysis (Cappello et al., 1997; 2005). The position of the ALs between the two configurations is estimated with Single Value Decomposition (SVD) algorithm (Figure 1.53). Interpolation in the first method (Figure 1.53a) was on a time base, whereas the more recent method (Figure 1.53b) has a flexion/extension angle interpolation.

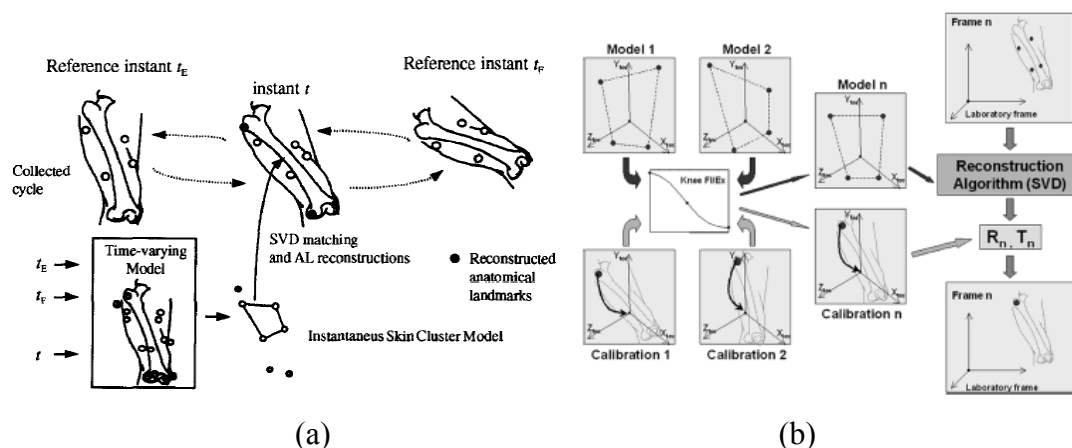


Figure 1.53: Bone pose estimation steps using Double Calibration Technique: first (a) and new (b) methods. t_E and t_F refer to the instants of extension and flexion (Cappello et al., 1997;2005).

Double Calibration was shown to improve the estimates of bone position although it requires additional time for the protocol to be completed.

Similarly, Alexander and Andriacchi (2001) introduced a method based on a point cluster technique (PCT) accounting also for the deformation of the segment as improvement from the original PCT (Andriacchi et al., 1998) to reduce errors due to skin movement artefacts. This technique was shown to improve the prediction of skeletal motion from skin-based markers system but several limitations to this study need to be acknowledged. The overabundance of markers on each segment could lead to difficulties in tracking the markers and requires a time-consuming and careful marker placement. Markers, in fact, should be positioned in a way to prevent cluster of markers having axes of principal symmetry. In addition, the method was tested using simulation trials in which the generated deformation was of the same functional form as the model used for its compensation and validated in an *in-vivo* test on a subject wearing an Ilizarov device which restricts skin motion. Further evaluation of the point cluster technique was performed by Stagni et al. (2003). In their work, Stagni et al. assessed the latter method in real condition highlighting that Alexander and Andriacchi's compensation method is dependant on the modelling form adopted for the Trajectories of the Markers in the Bone Embedded Frame (TMBF). It was then concluded that the correction given through the PCT method does not introduce a significant improvement in bone pose estimation, unless TMBF are accurately known, but this is unlikely in routine human motion analysis.

The compensation methods described so far treat the body segments separately without imposing joint constraints. A different approach, the global optimisation method, was based on the determination of the optimal spatial pose of the multi-link model for each data frame such that the overall differences between the measured and model-determined marker coordinates are minimised in a least square sense, throughout all body segments (Lu and O'Connor, 1999). The latter minimisation technique, imposing joint constraints, removed the possibility of joint dislocation and reduced errors in joint angles of ab/adduction and axial rotation. Global optimisation is at the basis of several compensation methods such as the optimised lower limb gait analysis (OLGA) technique (Charlton et al., 2004). This optimisation method was compared to the Vicon clinical manager (VCM) model, an implementation of the

Newington–Helen Hayes gait model, on roughly 100 gait cycles of a healthy volunteer. Model geometry was better reproduced by OLGA than VCM, knee and ankle cross-talk was eliminated as well as asymmetric hip and ankle internal/external rotation patterns. It has, then, been shown that improvement to gait analysis data can be obtained by applying the OLGA technique.

A similar approach was also suggested recently by Reinbolt et al. (2005). A two-level optimization method was presented to simultaneously optimize joint parameters and motion for multi-joint kinematic models. From test on a single subject the method revealed to be able to reduce root mean square marker distance errors by approximately a factor of two compared to anatomical landmarks method. Although these studies suggested the use of global optimisation methods to reduce STA, their reliability was only obtained through tests with a single normal subject or by simulated data. The application of these methods, therefore, should be carefully evaluated also taking into account the assumptions at the basis of the model adopted for the compensation. In the studies, here described, lower limb joints were all consider as balls and socket joint. This assumption can limit the use of this method when dealing with subject with restricted joint motion or joint deformity. A recent study (Stagni et al., 2009) compared the performance of double calibration technique and global optimisation, highlighting the dependence of the global optimisation to the model exploited for the compensation. Double anatomical calibration results in more reliable compensation techniques than global optimisation, even though it requires additional calibration trials.

Although a STA compensation method is required to quantify accurately joint kinematics, and techniques have been suggested, it is rarely that those methods are applied in current clinical practice. The additional tasks necessary to be performed and the increased amount of time required for data processing may inhibit their introduction in clinical gait analysis. A clinically applicable method to reliably estimate skeletal movement which considers the characteristics of the subject, joint constraints, the motor task under analysis and which is easy to be implemented, is yet to be introduced. However, some strategies can be extracted from the studies in the literature and applied to reduce errors induced by skin movements. The easiest way is to employ a specific marker set which minimizes STA, although there is still a

debate on the best surface-tracking marker set to be used during motion tracking (Manal et al., 2000). The studies, previously presented have gone some way towards enhancing the understanding of which could be the best marker placement area on the subject's lower limb. An immediate suggestion is to consider using the areas least susceptible to tissue movements. Thorough investigations have been conducted analysing the optimal marker set configuration for maximum accuracy. Manal et al. (2000) evaluated 11 different marker sets (Figure 1.54) for tracking motion of the tibia, examining the effect of locations (proximal vs. distal), physical characteristics (constrained vs. unconstrained) and attachment method (underwrap vs. overwrap) to the body segment. As a gold standard to evaluate angular kinematics, a percutaneous skeletal tracker with three tracking markers was attached to the malleoli of 7 subjects. Their results showed smaller deviation when markers were placed distally on the shank, whereas attachment method and physical characteristics didn't show significant effect on rotational estimates. From the evaluation conducted the best marker set was a distal lateral shell underwrapped (DLU). However, even when using this marker array, rotational deviations did occur ($+2^\circ$ about antero/posterior and medio/lateral axes, $\pm 4^\circ$ about longitudinal axes).

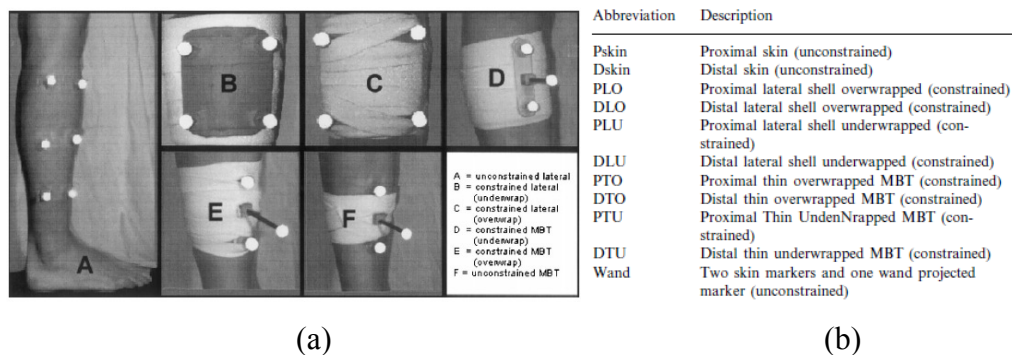


Figure 1.54: (a) Illustration of various marker sets tested. All the 11 sets employed are described on the table (b) (Manal et al., 2000).

Analogous results were found by Holden et al. (1997), who reported smaller errors in identifying the knee joint centre when using neoprene band and rigid cluster of markers rather than using markers directly attached to the lateral aspect of the knee. More recently, a similar study was conducted looking at the estimation of hip axial rotation from 4 different thigh cluster configurations (Schache et al., 2008). Of the

latter, 3 were new designs with specific characteristics (rigid vs. non rigid, thigh wand inclusion vs. exclusion) while one represented the Helen Hayes convention. None of the cluster configurations seemed to represent an optimal solution and clusters were only able to estimate up to 60% of the reference amount of movement. It was however possible to evaluate their performances. The Helen Hayes convention was subjected to the greatest STA, and also if all the other three behaved similarly in reducing the degree of STA, a non-rigid configuration was shown to perform better than a rigid one. Worth notice is that this study lacks a true gold standard measure of hip axial rotations.

Five alternative technical marker sets were evaluated for the motion analysis of the pelvic segment by Fukuchi et al. (2010). Those markers sets differed in markers location at the pelvis (Figure 1.55), hip joint centre estimation (predictive vs. functional method) and markers used to define the thigh technical frame (Helen Hayes vs. rigid cluster as defined by Cappozzo et al. (1995)). Accuracy and precision of these markers sets in evaluating pelvic kinematics was establish through comparisons with the standard pelvic marker set, which involves placing marker on the right and left, anterior and posterior superior iliac spine.

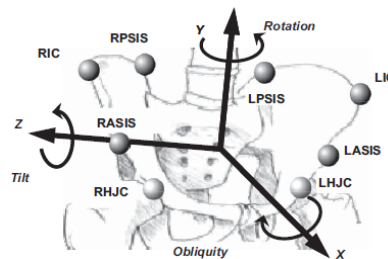


Figure 1.55: Technical points considered to identify pelvic coordinate system. Axes convention is shown (Fukuchi et al.,2010).

All marker sets presented similar precision across trials (about 1°) but different accuracies (ranging from 1° to 3°). As in Schache's study, the Helen Hayes marker set appeared to be the least accurate, in particular for pelvic obliquity and rotation. With regards to the cluster configuration method, Cappozzo et al. (1997) identified design criteria for marker-cluster to be followed to minimize error propagation from marker coordinates to bone-embedded frame position and orientation. A cluster made

up of 4 markers was suggested to be a good solution. The mean radius of the cluster should be greater than ten times the standard deviation of the experimental error and a planar cluster in quasi isotropic position is acceptable. With regards to cluster positioning it was suggested that cluster markers should be attached avoiding areas prone to greatest skin movements such as bony prominences where slipping effects are present. In addition, the longest principal axis should be oriented toward the relevant anatomical landmark.

Despite the suggestions made on optimal marker sets to be used in motion analysis, there are still many uncertainties and discrepancies among currently conducted research which prevent the introduction of a standardised method to be followed to obtain reliable results.

The third class of errors mentioned earlier is the anatomical landmark (AL) misplacement. Error in identifying those key points which, could be either palpable from the body surface or internal, propagates in the definition of anatomical frames and thus to joint kinematics and kinetics. Location of internal anatomical landmarks, mainly joint centres, is pursued through either functional or predictive methods. Restrictions of these methods compromise the accuracy to which joint centres are estimated. Estimation of the hip joint centre was shown to be more critical than the location of knee joint centre, as it affects hip and knee joint kinetics and kinematics quite significantly (Della Croce et al., 2005). A more detailed description on the calculation of joint centres, hip in particular, will be given later on in this chapter. The incorrect location of subcutaneous bony ALs through palpation, on the other hand, can be caused by three main factors (Della Croce et al., 2005):

1. the palpable ALs are not points but surfaces, sometimes large and irregular;
2. a soft tissue layer of variable thickness and composition covers the ALs;
3. the identification of the location of the ALs depends on which palpation procedure is used .

The ability of the assessor to recognise bony landmarks, also plays a role in the precision with which subcutaneous ALs are determined. Few studies focused on the accuracy of the location of those key points, or on the choice of the most suitable AL to reduce error propagation to the anatomical frame definition and joint angles. In their study, Della Croce and colleagues (1999) provided information on the precision

with which the position of lower limb ALs may be determined, intra and inter examiner variability and the effects of errors on bone geometry and joint kinematics. Anatomical landmarks were identified following the CAST method (Cappozzo, 1984) on two subjects with skin marker clusters attached to the pelvis and lower limb segments. The calibration procedure for each anatomical point was performed by six physical therapists with gait laboratory experience. Intra examiner precision was shown to be higher than the inter-examiner precision (range between 6-21mm and 13-25mm respectively). This was explained as being caused by the different examiner interpretations of the instructions given for locating ALs. Pelvic ALs were more dispersed than lower limb ALs, among which the Greater Trochanter was the least precise to be located (root mean square value up to 18 mm). Inaccuracies in identifying ALs lead to errors in the anatomical frame orientation and thus on the definitions of joint angles. Internal and external rotation angles were the most affected, with root mean square (RMS) values comparable to the joint range of motion (Figure 1.56).

| Joint | Intra-examiner | | | Inter-examiner | | |
|-------|----------------|---------|----------|----------------|---------|----------|
| | ab-ad | int-ext | flex-ext | ab-ad | int-ext | flex-ext |
| Hip | 2.5 | 5.3 | 3.9 | 5.2 | 5.6 | 5.0 |
| Knee | 1.7 | 5.8 | 1.0 | 5.2 | 10.4 | 3.7 |
| Ankle | 3.5 | 3.9 | 1.6 | 10.9 | 10.3 | 3.3 |

Figure 1.56: Intra and inter-examiner precision (RMS values) of joint angles during upright posture (Della Croce et al., 1999). Values are in degree.

Results consistent with the latter study were found by Rabuffetti et al. (2002), although their work was related to space applications. Precision of self-marking experimental activity performed by 3 participants on their own body and direct-marking on the same set of anatomical landmarks performed by skilled operators were reported. Self-marking intra-subject precision ranged from 1.8 to 17.5 mm, whereas expert-marking inter-subject precision was between 1.5 and 28.7 mm, similarly to Della Croce et al. results. Lower precision was found in the identification of pelvis and lower limb ALs compared with head and upper body points. The femoral condyles and the greater trochanter appeared to be unfeasible with all precision indices above 10 mm, up to 14.6 and 19.2 mm respectively.

Alternatively to the *in-vivo* pointing technique to identify bony landmarks, medical imaging can be acquired and used for AL locations (Van Sint Jan et al., 2002a, 2003, Taddei et al., 2007). This high resolution calibration procedure is known as virtual palpation. Knowing morphological characteristics of the bone under analysis, through specific software, ALs can be selected at the surface of the model obtained from medical imaging (Figure 1.57).

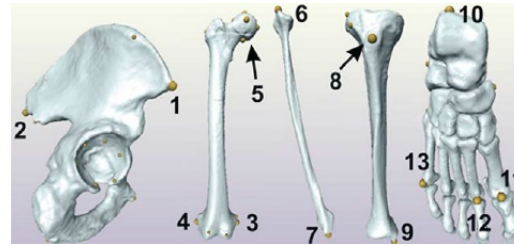


Figure 1.57: The 3D location of the ALs using virtual palpation.

Despite the exact identification of skeletal landmarks obtained through virtual palpation, this method is rarely employed in motion analysis laboratories due to the lack of medical imaging equipment availability and the invasiveness of some of these methods due to their requirement for radiation exposure.

Donati et al. (2007), recently, introduced an alternative anatomical calibration procedure referred to as UP-CAST. This technique is based on the digitization of a bony area over which the position of a large number of unlabelled points (UPs) is acquired. A wand fitted with three markers and a roller sphere tip is used to determine the position vectors of UPs in technical frames defined by cluster of markers attached on the subjects' bony segments. A digital model of a template-bone is selected and ALs identified on it using a virtual palpation technique. The subject specific bone model is obtained through isomorphic deformation and re-orientation of the selected template to optimally match the measured UPs. The location of anatomical landmarks is then made automatically available. The UP-CAST procedure was verified on the femur of two volunteers and on two bare femoral bones. The results obtained showed promising results of the new technique: UP-CAST precision along the anatomical axes (range: subject bones 1.9–7.6 mm, bare bones 0.9-4.6 mm) was higher than that exhibited by the previously described studies. The maximal 3D errors for subjects and bare bones were, respectively, 7.6

and 4.6 mm. In addition, and in contradiction of others studies, differences among examiner were not found and the experience of the examiner was found not to be influential for the precision of the results. Another advantage of this procedure was the short time required to identify ALs compared with conventional anatomical calibration.

The same authors (Donati et al., 2008) also assessed the repeatability of a protocol which applies the new introduced UP-CAST calibration procedure. The investigation was based on five walking trials from each of the five able-bodied subjects who participated to the study. Precision values of UP-CAST in locating ALs were comparable to those found in the previous study with an assessed maximal 3D error of 10.6 mm. Effects of repeated anatomical calibrations on pelvis, hip and knee, posture angles showed a moderate dispersion (less than 3°) for almost all angles except for hip and knee internal–external rotation (6° and 9° , respectively). As shown from the graphs in Figure 1.58 repeatability of joint kinematics was high, with knee ab-adduction and internal–external rotation being the most affected by experimental errors. Inter-operator error and inter-trial error for those two angles ranged between 0.9 and 2.9° , with inter-operator errors which were greater than inter-trials errors.

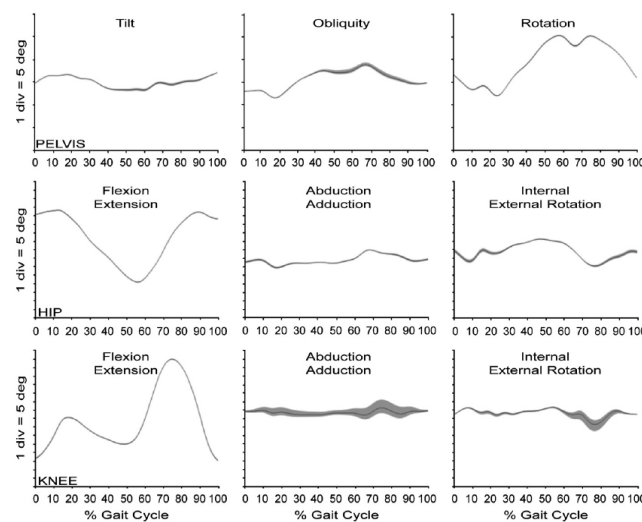


Figure 1.58: Inter-operator variability of the joint kinematics of one subject and one gait cycle (Donati et al., 2008).

For all the other angles inter-operator error and inter-trial error were equal (range 0.1 - 0.9°). Limitations of both the latter studies are mainly related to morphological

differences between the template and the bone of the subjects under analysis and to the requirement that a thin layer of soft tissue cover the area to be digitized, preventing the use of this method with overweight subjects. Although the improvements that could be introduced by the UP-CAST calibration in terms of precision, accuracy and time expenditure, the latter procedure is still far from being introduced in clinical and research practice because of the need of a large database of bone templates and suitable equipments to perform the analysis which are not usually at hand in the majority of movement analysis laboratories and clinical facilities.

Anatomical frame axes are defined from anatomical landmarks. A misallocation of anatomical landmarks, then leads to an erroneous anatomical frame (AF) orientation when related to the relevant bone segment. The error can thus propagate to joint angles calculation giving a misleading joint kinematic evaluation as highlighted in Della Croce and colleagues' study (1999) mentioned earlier. Kinematic data may be affected by errors caused by kinematic crosstalk. Kinematic crosstalk arises when the chosen joint coordinate system is not aligned with the axes about which rotation are assumed to occur. Piazza and Cavanagh (2000) used two-segment mechanical linkages to reproduce knee kinematics. Two devices were used which have 1 and 2 degrees of freedom, respectively, allowing for a controlled range of motion (90° of flexion, 15° rotation). The usual *in-vivo* calibration procedure (CAST) was simulated, by means of identification of anatomical control points (ACPs) in the linkages from which "anatomical axes" of each segment were constructed. Although the ease of locating ACPs joint angles trends deviated from the expected trajectories (crosstalk error). A deviation of 6.4° and 9.7° from the correct axis orientation was found. In addition, a repeated identification of femur epicondyles in a volunteer was performed by 5 observers to quantify the disagreement between knee flexion axis definitions. A mean angle of separation of 7.7° was found. The author warned the readers to have caution about the reliability of small out of plane rotations as they may be the result of cross talk error. This study thus highlights the necessity of accurately defining the rotation axis to avoid crosstalk error but without providing a solution of the problem. The adjustment value to eliminate the crosstalk error was found by performing the correction previously proposed by Woltring (1994). Woltring introduced the concept of the attitude vector (single helical displacement unit) to describe 3D joint angles. In

this study the crosstalk error was tackled from a theoretical and experimental point of view to compare the performance of the orientation vector against the Cardan convention for joint kinematic definition. What the theory predicted was reflected by experimental comparisons of knee angles: crosstalk mostly affected Cardan Convention angles with a deviation increasing as the flexion angle increases. Rotating the embedded coordinate system to zero ab/adduction and zero internal/external rotation while producing maximum flexion, minimized the error but the anatomical meaning of this correction was unclear. The advantages of using the attitude vector over the Cardan convention were presented but this method is still not used because of the difficult physical interpretation of the angles so obtained.

A study was also performed by Kadaba et al. (1990), to investigate the effect of uncertainties in defining anatomical frame on joint kinematics. Although only the results for the knee joint were presented, it is stated that similar results were found at the hip and ankle level for the subject tested. The orientation of the knee flexion axis was varied in a range of $\pm 15^\circ$ at 5° intervals. The results showed significant dispersion in ab/adduction and internal/external rotation angle values from the reference angles. Again a dependency of those minor angles on the flexion angle magnitude was found and the relationship is clearly shown in Figure 1.59. The authors suggested a caution for interpretation of ab/adduction and rotation angles, especially for patients with flexion contractures.

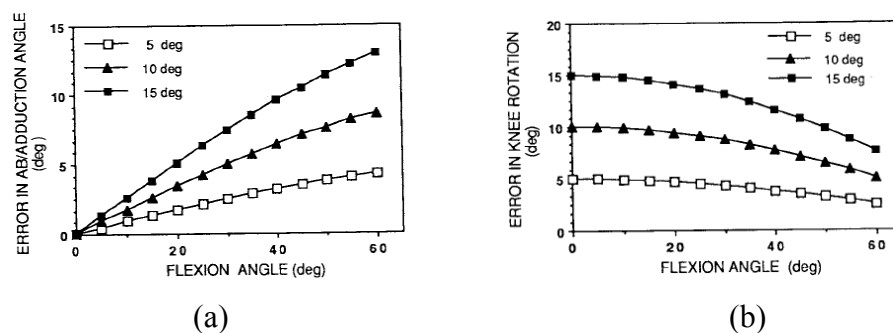


Figure 1.59: Relationship between ab/adduction (a) and internal/external rotation (b) error and knee flexion angles (Kadaba et al., 1990).

A number of different rules for defining the femoral anatomical frame (AF) were assessed by Della Croce et al. (2003) to identify a knee AF which would be the least

sensitive to anatomical landmark location inaccuracies. These authors selected 12 rules which differed in the number of ALs (maximum 8) involved in the construction of the AF, and on the approach, geometric, least squares, singular value decomposition, on which the rules were based. A numerical comparison of the 12 definitions applied to the ALs of a single subject was carried out and conclusions on how to address the effect of AL misallocation were drawn from the results obtained. The authors suggested that in the definition of the knee AF, the longitudinal axes should be taken as the leading axis, and a high number of anatomical landmarks is advisable as redundancy of information reduce error propagation. The rule that showed lowest crosstalk errors used a process to define anatomical frame similar to the one described by Donati et al. (2007), but still its practical application is limited in research environments.

Similarly, Baker et al. (1999) and then Schache et al. (2006) attempted to find a method to reduce crosstalk error introduced by ALs misplacements. In addition, in their publications, attention was also drawn to the effect that a misalignment of the knee flexion axis has on hip axial rotation. Although a number of studies have recently been conducted in this regard, an optimal method of defining the knee axis set is still lacking as pointed out by Schache and colleagues in their brief literature review. The correction method to be applied to a deviated knee flexion axis, as proposed by Baker et al. (1999) was exploited by Schache's team, although with some adjustments, in the attempt to introduce a procedure which would ensure repeatability of hip axial rotation and would minimise crosstalk errors. The optimisation method, through an iterative process, calculates an offset by which the knee flexion axis should be rotated about the longitudinal one to give the minimum variance in knee ab/adduction profile. The adjustments made in respect of the original procedure ensured that only the medio/lateral and antero/posterior axes of the knee anatomical frame were reoriented and not all three axes. Three different methods of defining knee flexion axis were compared: the knee alignment device (KAD) method, a method based on the transepicondylar axis (TEA), and the optimisation method described above. Among the three, the optimisation method was the one with the better repeatability of hip axial rotation and with the lowest crosstalk error. Those results were obtained from a cohort of 20 subjects who were asked to

perform a squat test, non-weight bearing knee flexion, and a walking test. The findings from this study make a noteworthy contribution to the current literature in terms of a solution for orientating the knee joint flexion-extension axis to minimise errors propagation. The optimisation method can be easily implemented through any gait analysis software and adjusted to the needs of the operators to suit their anatomical model if different from the one used by Baker et al.(1999).

The studies reviewed in the last section were related to palpable anatomical landmarks; however, as anticipated earlier, also internal landmarks are required for gait analysis purposes. Among these, the determination of hip joint centre (HJC) is the most debated, as errors in its location influence hip kinematic and kinetic data and also propagate downwards to knee measurements (Stagni et al., 2000). An estimation of 3D HJC location can be accomplished through predictive or functional approaches. In the former, the HJC position is scaled as a function of variables describing the geometry of the pelvis in regression equations. X-rays (Tylkowski et al., 1982), radiographs (Bell et al., 1989, 1990, Davis et al., 1991) and magnetic resonance images (Harrington et al., 2007) of adults and children or measurements taken from cadaver specimens (Seidel et al. 1995) have been used to define regression equation coefficients. The variables mostly used are leg length, pelvic depth, pelvic height, and pelvic width (Figure 1.60) which are correlated differently to the 3D coordinates of the HJC location in the different approaches.

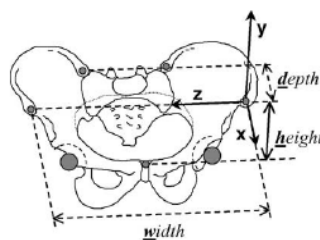


Figure 1.60: Geometrical variables used in predictive methods (Della Croce et al., 2005).

Throughout the predictive methods, Bell et al. (1990) and Davis et al. (1991) are the most widely used but not necessarily the most accurate (Seidel et al., 1995, Harrington et al., 2007, Peters et al., 2010b). Among other observations, Harrington

et al. evaluated those two methods and identified a maximum error of 25 and 31mm respectively when compared with the hip joint centre obtained through MRI scan of healthy adults, children and children with cerebral palsy. Harrington et al.'s method was assessed in a recent study (Peters et al., 2010b). A comparison with 3D freehand ultrasound images of children with gait pathology indicated that Davis et al. equations predicted the HJC location more poorly than Harrington et al.'s method. Mean errors were respectively 22.5 and 14.5 mm. To date it appears that the Harrington et al. method is the most reliable among the predictive ones in estimating hip centre position. Findings of Peters et al. study also shown a better accuracy of the latter method compared to functional approaches. Harrington et al.'s regression equations thus represent an attractive method to calculate the centre of the hip joint. The limitation of predictive approach is the small cohort of subjects from which the regression coefficients have been calculated. This makes the method subject specific for the group analysed and not applicable to all the variety of cases that could be encountered. The use of constants derived from the cohort under analysis in any study would be advisable but not likely to occur as imaging equipments is rarely available. The study with the largest population by Peters et al. has considered 53 subjects and has identified Harrington method as the best choice to determine HJC location. This is also reinforced by the fact that the participants involved suffered from gait abnormalities and thus defining the HJC would be even more critical than for able-bodied subjects. The difficulty in identifying required anatomical landmarks during laboratory sessions is not to be underestimated when those methods are employed. Although the method proposed by Seidel et al. shown better results than Bell et al.'s approach (Seidel et al., 1995; Leardini et al., 1999), this method's use is limited by the necessity of marking the pubic symphysis on the tested subject. Moreover, continuing with the list of limitations, predictive equations do not account for pelvic asymmetry which was found to be on average 12.6 and 6mm (Leardini et al., 1999; Harrington et al., 2007). Not to be forgotten is the erroneous location of markers over the palpable bony landmarks of the pelvis and skin movement artefacts that always represent major issues when aiming for gait analysis valuable data. Despite these drawbacks, predictive equations remain the most common method used

in gait analysis software packages and are the easiest implementation available to estimate HJC location.

An alternative to predictive methods is the functional approach, introduced by Cappozzo et al. (1984) (Della Croce et al., 2005), which can be used to determine the HJC position. The key assumptions of this method are to consider the HJC as a ball-and-socket joint and to consider its centre to be coincident with the pivot point of the movement between the two adjacent segments of pelvis and femur. Several functional methods have been developed which differed mainly on the mathematical algorithm used to locate the pivot point. Those algorithms are given stereophotogrammetric data to calculate the 3D coordinates of the HJC.

Stereophotogrammetric data for this purpose are collected while a subject performs selected movements. The different approaches, that have been developed, can be classified into two main categories, ones which utilise a sphere fitting method (Cappozzo et al., 1984; Leardini et al., 1999; Piazza et al., 2001) and the ones which employ a coordinate transformation method (Piazza et al., 2004; Ehrig et al., 2006). These methods have been evaluated in the attempt to identify the best practice guidelines for the use of the functional approach (Camomilla et al. 2006). Although soft tissue artefacts have not been incorporated into the evaluation, critical aspects (range of motion, marker positioning, algorithms, and number of data points) have been thoroughly examined and an optimized protocol proposed. However, limitations of functional methods still remain partially unresolved. One of the most discussed issues of the aforementioned approaches is how the hip range of motion affects the accuracy with which the HJC is determined. Theoretically reducing the amplitude of the motion at the hip, soft tissue artefact (STA) should also be reduced and so the errors. However, it has been shown that errors in hip joint centre determination increased with a reduction of the range of motion (Piazza et al., 2001; Camomilla et al. 2006, Mac Williams et al., 2008). It should be mentioned that those studies used mechanical analogues of the lower limb. In contrast, a recent *ex-vivo* study (Cereatti et al., 2009), which considered soft tissue artefacts, revealed that hip location errors are not correlated with the movement amplitude when a quartic sphere fit method is used. The latter method was also the one to behave best among the four investigated by Mac Williams et al., (2008). A compromise between range of motion and skin

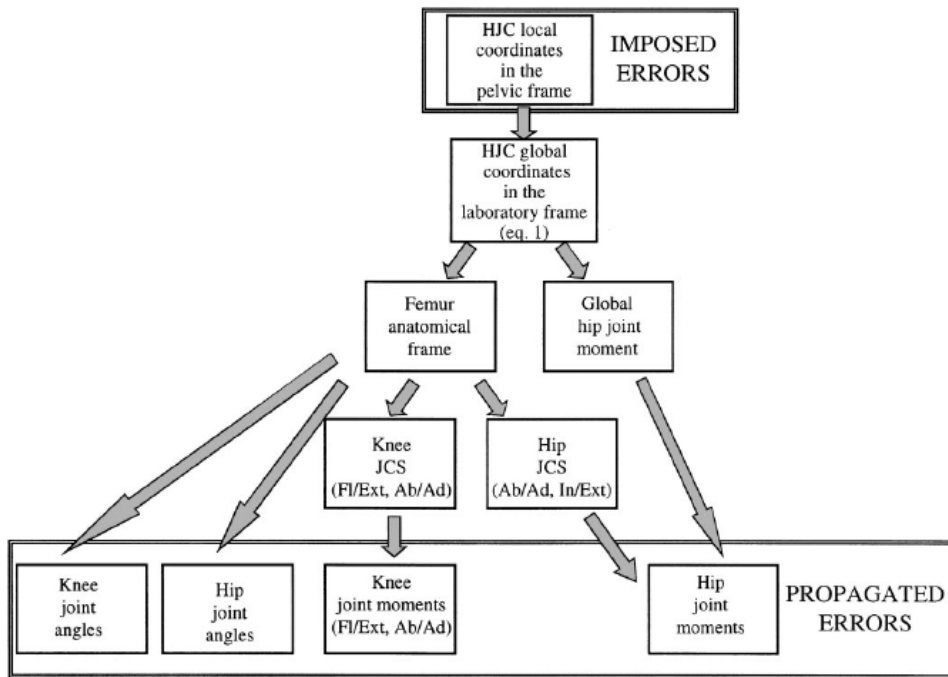


Figure 1.61: Diagram of the propagation of HJC misallocation to hip and knee kinematics and kinetics (Stagni et al., 2000).

tissues artefacts exists and therefore the selection of a certain algorithm over another should be made with caution. However, although a wide range of motion is preferable, HJC can still be estimated using functional methods as acceptable errors have been reported when only a limited movement is achievable (Piazza et al., 2001, 2004; Della Croce et al., 2005), which is the case in patients affected by a reduced mobility at the hip. Another drawback related to the utilization of those methods is the additional task to be performed during test sessions. It has been suggested (Piazza et al., 2004) that usual activities (walking, stairs negotiation) can be used to obviate the need of an extra task to find the hip joint centre. However their data indicated that common activities are not feasible for this purpose. An average error of 70 mm resulted when the HJC was calculated from these trials, thus a special task is required. In contrast to predictive methods, functional methods have the advantage of being subject specific. These methods could be used to gather data on HJC location from different subject populations upon which more specific predictive equations can be built.

Comparative analyses between functional and predictive methods have been conducted. Among those, there are studies (Leardini et al., 1999; Hicks and Richards, 2005) which claimed the supremacy of functional over predictive methods and other studies which supported the opposite (Bell et al., 1990; Peters et al., 2010b).

Different implementations of the functional methods and analyses restricted to healthy subject can explain the discrepancies in the results obtained.

A correct HJC location is crucial in gait analysis as this point is used to define the axes from which the hip and knee kinematics are estimated. Moreover, the HJC is the point from which hip moments are calculated. Therefore, errors in its location can affect hip and knee angles and moments (Figure 1.61).

Holden and Stanhope (2000) investigated the effect of uncertainty in the location of the hip centre on hip moments during walking on 18 subjects at several walking speed. The HJC location was varied plus or minus 20mm in all three directions. Major effects were reported to occur when the HJC was moved in the anterior and posterior direction and when translated medio-laterally at normal walking speed. A/P displacements introduced a change in the peak hip flexor moment of 33% of its value whereas M/L displacements caused a variation of the peak hip abductor moment of

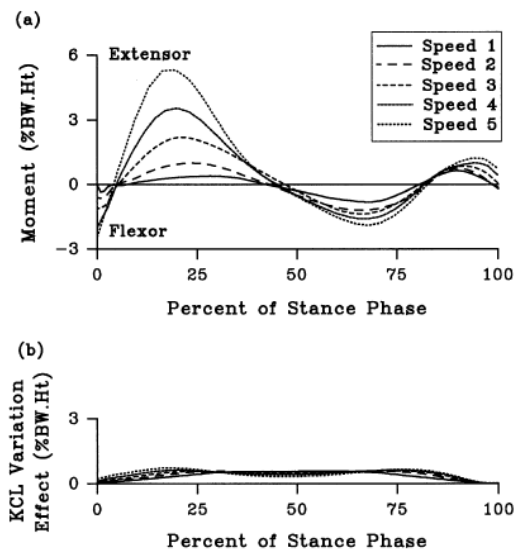


Figure 1.62: (a) Average of net knee moments from 18 subjects at 5 walking speeds (1 the lowest, 5 the fastest); (b) Mean values of KJC variation effect at 5 walking speeds (Holden and Stanhope 1998).

23% of its value. Changes in hip flexor moment increased with a reduction of the walking speed. The authors concluded emphasizing the need of an accurate HJC estimate.

Comparable to these findings were the results reported by Stagni et al. (2000). This study aimed to analyse the effect of HJC misallocation on hip and knee kinematics and kinetics. A superimposed error of ± 30 mm with 6 mm steps was applied to the estimated HJCs of 5 subjects tested. Both, angles and moments, at the hip and knee were affected by an erroneous location of the hip centre, although the effects on angles can be considered negligible. Mostly affected were hip moments. Maximum error occurred at hip flexion/extension moment (22% error) when the maximum displacement was imposed in the antero/posterior direction.

As highlighted from the studies reviewed, the determination of HJC location is important and can alter the outcome measurements, particularly the moments. Results should therefore be considered carefully especially when the method used to determine the hip joint centre introduces error in the antero/posterior direction.

Improvements on the determination of HJC will provide substantial increases in the accuracy of the results; nevertheless if the misallocation error is less than 30 mm, acceptable results can still be obtained on joint kinematics (Stagni et al. 2000).

Less studied in the literature is the definition of knee and ankle joint centres. Those are usually estimated to be the midpoint between the femoral epicondyles and the malleoli respectively. Holden and Stanhope (1998) questioned whether variations in knee joint centre (KJC) location affects knee flexion/extension moments at different walking speeds. KJC translation in the antero-posterior direction of ± 10 mm produced similar effects across subjects (Figure 1.62 b) without affecting the general shape of the moment pattern. However, these effects when expressed as percentage of the net knee moment introduced considerable errors (123% of moment value) especially at lower speed where moment magnitudes are small (Figure 1.62 a). The moments at slow speed cannot then be interpreted with confidence.

Studies on the definition of the ankle joint centre were not found.

1.6.4 *Clinical gait analysis protocols*

A gait analysis protocol, defined upon a particular biomechanical model, is a scheme for data collection, processing and analysis of the results. The uniqueness of each protocol is due to the marker set used to define anatomical segments, how joints kinematics and kinetics are calculated, the estimation of joint centres and degrees of freedom assigned to the joints. Whilst being anatomically accurate and repeatable in the definition of bone segments, a protocol should also allow for an easy and fast marker mounting procedure, a simple analysis and ensure the interpretability of its results. The steps for the design of a gait analysis protocol are summarised in the flow chart in Figure 1.63.

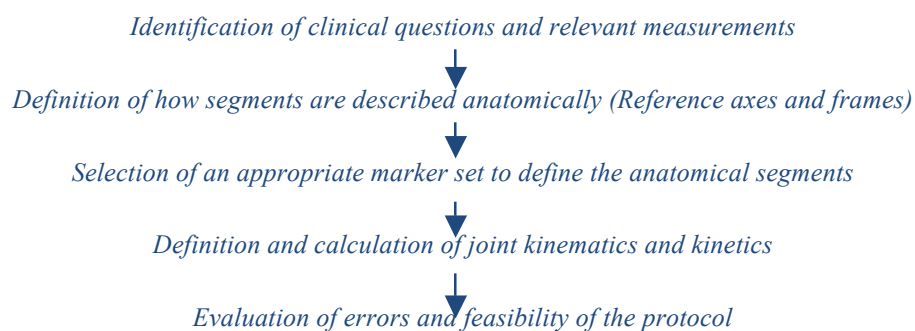


Figure 1.63: Flowchart representing a protocol design process.

Since most of the protocols, so far developed, define anatomical frames based on the reconstruction of the trajectories of retro-reflective markers attached to the human body, attention should be paid to their positioning. In this regard, few requirements which apply to all protocols have been suggested. These are listed as follows (Cappozzo et al., 1995):

- each marker should be within the field of view of at least two cameras at any given time;
- the distance between markers attached to the same segment should be sufficiently large so that error propagation from reconstructed marker coordinates to the bone orientation will be minimal;
- movement between markers and underlying bones should be minimal;

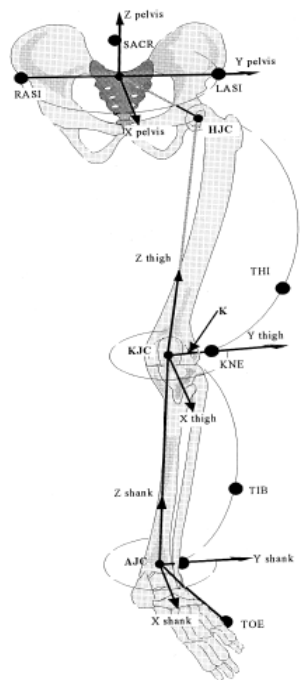


Figure 1.64: Biomechanical model as for the Newington model (Baker et al., 1999).

- it should always be possible to place markers even in the presence of external appliances such as orthoses, prostheses or external fracture fixators;
- mounting the markers on the experimental subject should be a fast and easy operation.

An optimal and standardised protocol for motion analysis is yet to be introduced although numerous procedures, as results of compromises among design criteria, are commonly employed. Currently used gait analysis protocols can be tracked back in time. One of the first proposed protocols is also one of the most commonly used among clinical biomechanics laboratories. This protocol, was originally known as the Newington model, nowadays better known as Plug in Gait (PiG) (Davis et al., 1991). This protocol was first developed by Patrick Shoemaker (1978) at Newington Children's Hospital and then refined by others such as Scott Tashman and Dennis Tyburski (Sutherland, 2002). Later on, Roy Davis added to the original Newington model a subject calibration process based on the use of his newly developed knee alignment device (KAD) to help with the definition of the knee flexion/extension axis. In addition, joint kinetics calculation based on the earlier work of David Winter was incorporated into the Newington model. The Newington model became the basis for commercial software. It was incorporated into Vicon Clinical Manager (VCM) by Oxford Metrics in 1991, and added with the KAD option onto the Workstation platform as Plug in Gait. This protocol is based on a simple marker configuration (Figure 1.64), which however requires high attention with respect to its markers positioning and alignment to obtain accurate bony segments' definition. Limitations of the model reside on the sharing of markers between adjacent segments for their definition, 2D representation of foot and ankle system and a less than fully clear understanding of the biomechanical interpretation of the outputs.

A similar model to the Newington one was developed at Helen Hayes Hospital (Kadaba et al., 1990) and incorporated into clinical software in the late 1980's. The Helen Hayes software was then implemented in 7 different biomechanics laboratories throughout US.

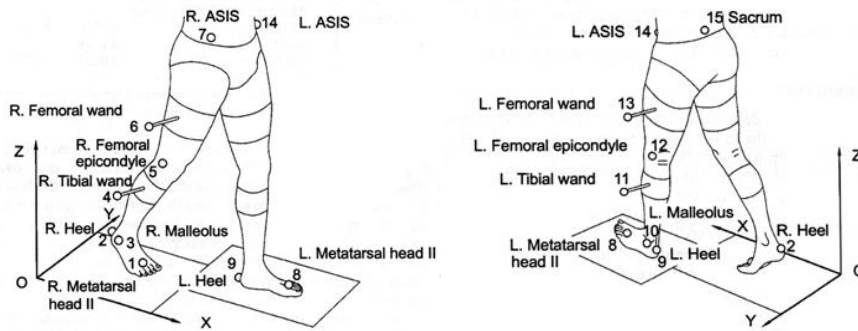


Figure 1.65: Helen Hayes wand based marker set, anterior (left) and posterior (right).

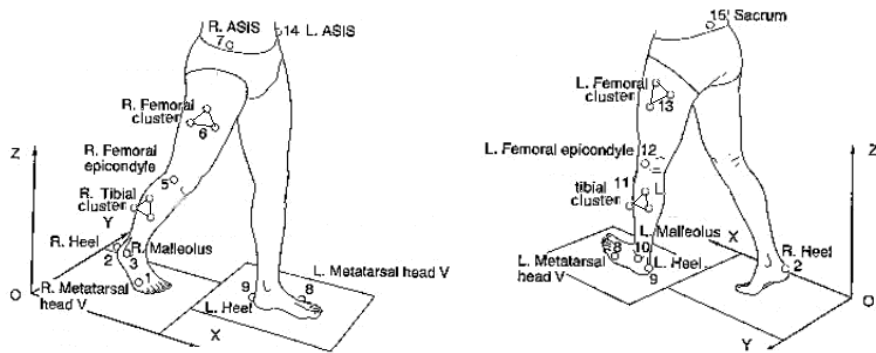


Figure 1.66: Cleveland Clinic Foundation cluster based marker set, anterior (left) and posterior (right).

The main difference between Newington/PiG marker set and Helen Hayes marker set is the use of wand marker in each segment in the latter model (Figure 1.65). This model has been less widely adopted due to concerns regarding the wobble of the wand markers.

Around the same time, in the late 1980's, another model was being developed at the Cleveland Clinic Foundation (Sutherland, 2002) based on the use of cluster of markers as references to identify bone segments (Figure 1.66).

Sutherland (2002) reported higher repeatability in transverse plane kinematics outputs obtained from the Cleveland marker set rather than Helen Hayes set. This was explained with less marker movement achieved by the use of rigid cluster on which markers are fixed.

An improvement to the Newington/PiG model was implemented as a post capture routine in Vicon Clinical Manager. This was achieved by applying to the captured data, an optimisation technique known as Optimised Lower-limb Gait Analysis (OLGA)(Charlton et al., 2004). This procedure, which has been described earlier in this chapter, relies on fitting a lower limb model, with joint constraints, to marker data. The steps of the iterative process which bring about the optimal solution are illustrated in Figure 1.67.

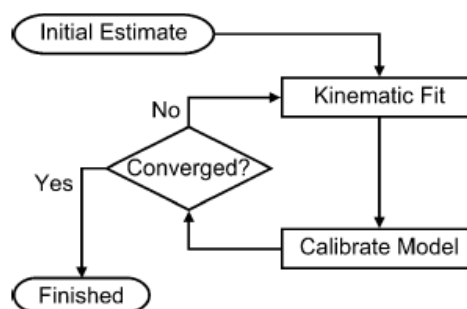


Figure 1.67: Schematic representation of OLGA optimisation procedure (Charlton et al., 2004).

A protocol for gait analysis was also developed at the Bioengineering centre in Milan and thus referred to as Servizio di Analisi della Funzionalità Locomotoria (SAFLO) clinical gait protocol (Frigo et al., 1998). The latter uses a simple marker configuration, as illustrated in Figure 1.68 a, using of fewer bony prominence

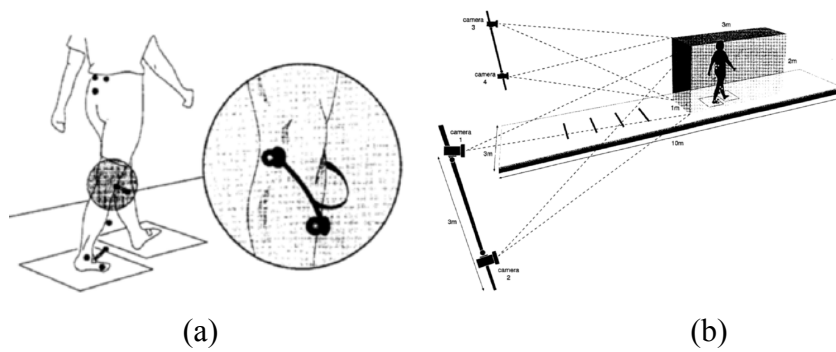


Figure 1.68: (a) Marker set utilises in SAFLO protocol, with the particular of the knee wand shown. (b) Gait laboratory set up (4 cameras) and capture volume (Frigo et al., 1998).

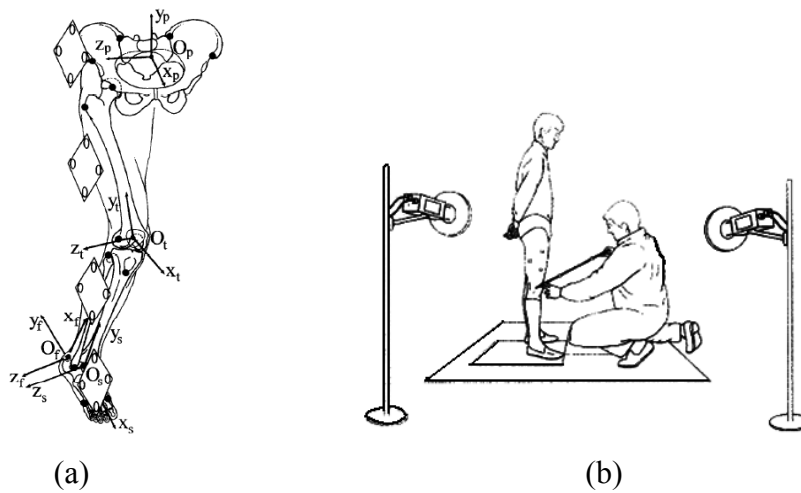


Figure 1.69: (a) Plate-mounted marker configuration and calibrated anatomical landmark (.) (Benedetti et al., 1998); (b) Pointer calibration of the right lateral epicondyle (Cappozzo et al., 1995)

markers and wand markers. The protocol requires a specific capture system arrangement in which four cameras are placed posterolaterally on each side of the subject (Figure 1.68 b). The biomechanical model of SAFLO protocol is based on numerous anthropometric measurements that need to be taken from the test subject, and on functional corrections aimed at improve hip and knee joint centres estimation and knee flexion/extension axis orientation. This protocol was incorporated in into BTS Elite (Italy).

An experimental protocol which is based on a calibration process was proposed by Cappozzo, 1984; 1991) and consequently named CAST (Calibrated Anatomical System Technique) (Cappozzo et al., 1995). The particularity of this approach resides on the utilization of technical markers (plate-mounted markers) and a pointer (Figure 1.69) to identify associated anatomical landmarks on the subject during static calibration trials. Despite the long time required for subject calibration, this technique was shown to be suitable for routine gait tests, although accuracy of knee angles, in the coronal and transverse plane, can be limited (Benedetti et al., 1998). In contrast with PiG technique, the CAST requires less accuracy with respect to marker mounting and alignment by the tester.

The Istituti Ortopedici Rizzoli protocol (IOR Gait) described in Leardini et al. (2007) is an implementation of the CAST procedure with a more efficient marker configuration to shorten the preparation time of the subject (Figure 1.70). This protocol, initially thought to be employed in children, thus represents a good compromise between accuracy and time required for data collection.

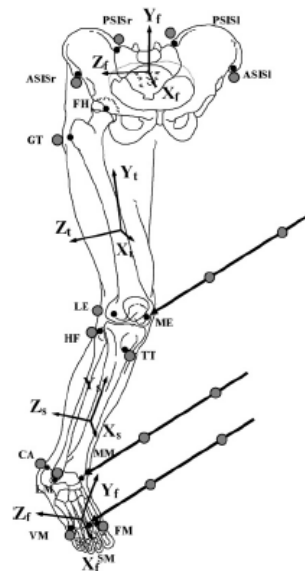


Figure 1.70: IOR Gait marker and calibration set up. Small black circles indicate anatomical landmarks; grey circles represent retro-reflective markers. Three ALs are calibrated in each side by a pointer. Anatomical reference frames for the pelvis, thigh, shank and foot segments are also shown (Leardini et al., 2007).

Similarly Rabuffetti and Crenna (2004) introduced a new protocol for gait analysis in children, referred to as Laboratory for the Analysis of Movement in Children (LAMB) protocol. The modular markers' set up (Figure 1.71), characterizing this protocol, is adaptable to children's body sizes enabling data collection also in small sized subjects. In addition to joint kinematics and kinetics, muscle geometry, centre of mass (COM) kinematics and energetics are estimated.



Figure 1.71: LAMB markers set up: circles indicate anatomical markers, squares technical markers and triangles calibrated anatomical landmarks (Rabuffetti and Crenna, 2004).

The protocol introduced at the Gillette Children's Speciality Healthcare (Schwartz and Rozumalski, 2005) is meant to cope and prevent errors introduced by other protocols which use prediction equations for estimates of hip joint centre (HJC) and anatomical landmark palpation, by using functional range of motion trials to determine specific joint centres and optimal knee flexion/extension axis. The method proposed is also independent from marker placements (Figure 1.72). Although the advantage of being subject specific, the requirement of additional trials can represent a limitation when applying the outlined method in subject with restricted range of motion at selected lower limb joints.

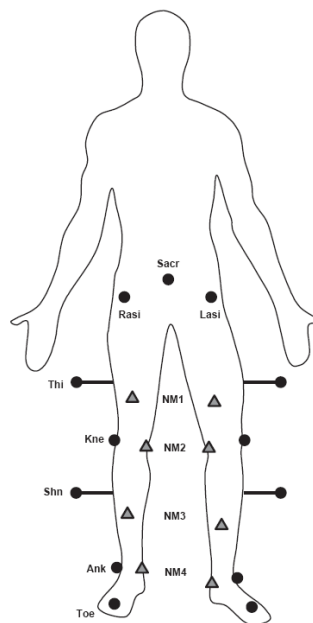


Figure 1.72: Marker set used in Gillette functional model. The set up is the PiG markers (circles) with additional markers (triangles). NM1 and NM3 are arbitrarily placed (Schwartz and Rozumalski, 2005).

1.7 Literature Considerations

Few solid conclusions emerge from the extensive literature review of AFO use in stroke patients' rehabilitation.

Beneficial effects of AFOs have been reported, but research evidence documented in the literature is affected by significant limitations. Most of the studies rely on small patients group, which are often heterogeneous confounding findings between chronic

and acute phase stroke survivors. However, the participants are mainly chronic stroke patients thus, the potentiality of an AFO, as an early rehabilitation aid, is still unknown.

In most studies, pathologies and walking disorders are mixed and analysed together. Moreover, immediate effects of walking with and without AFO are mostly commonly reported whereas, the long-term effects on walking ability remain unresolved.

Randomised controlled trials are lacking with, randomised cross over study being the most common adopted research design.

Description of the AFO utilised is for the majority of studies superficial with lack of prescription details, and in particular with regards to the cast angle, AFO footwear combination, inclination and stiffness. It is advisable to characterise the AFO with as much information as possible if the results obtained are to be use to improve AFO efficacy.

Some papers show strong effects, however, the limited improvements reported in the reviewed papers can indicate these effects are often not achieved probably due to a lack of appropriateness of the AFO prescription and tuning. There is the feeling that some studies were conducted with the aim to assess a certain type of AFO rather than worry about the fact that the supplied orthosis was not the optimal solution for the patient leading to a lack of benefit perceived.

Furthermore to improve orthosis prescription and design and gain a better understanding of the interaction between the orthosis and the lower limb, research should be conducted investigating the AFO's mechanical properties and their biomechanical contribution to the gait cycle as only a few studies have been found attempting to quantify these variables.

In addition to understand which kind of patients may benefit from a particular intervention, study population should be adequately described if the information is to be extracted and applied in clinical practice. It appeared instead, that inclusion and exclusion criteria were not always clearly stated.

The terminology used to describe AFO design and ankle movement should be unambiguously explained to avoid misinterpretation of the results and facilitate data sharing and comparison.

Many of these points were also highlighted during a consensus conference of the International Society of Prosthetics and Orthotics (ISPO) (Condie et al., 2004). To conclude, there are a large variety of walking disabilities experienced by stroke survivors, and numerous possibilities for orthotic intervention. A well designed research study, which describes accurately the study population, and the AFO design used is required to provide knowledge on the efficacy and effectiveness of AFO use and of current AFO practice. Particular stress should be put on the evaluation of the effects an early provision of an AFO has on stroke mobilisation, if, the “window of opportunity” is to be exploited to accelerate recovery. If a rigorously planned research study cannot be achieved the information gained will not strengthen the body of knowledge in the field.

Methods through which valuable information can be extracted are also keys for a successful research. Human gait analysis is one tool that can be used for the assessment of stroke patient. When using gait analysis to tests impaired subjects, compromises have to be taken with the ability of the subjects to stand test sessions while producing reliable results. A review on human motion analysis was conducted with the purpose of screening the methodologies and protocols already developed to verify their applicability with stroke subjects and, the critical aspects involved in the methods themselves (errors, assumptions in biomechanical model, calculations). Moreover, the outputs obtained have to be clinically compliant if they have to be used to improve the clinical practice relatively to the management of stroke gait impairments. This implies definitions of the biomechanical model that beyond allowing mathematical correct descriptions of the movement allows for output to be clinically manageable. Only if clinicians can understand the outcomes provided by the study the gap between research and clinical implications can be reduced, and improvements brought to treatment decisions.

The review presented, thus provided with an insight of the state of art of motion analysis highlighting the more critical aspects involved. This overview should represent the starting point from which emerged problems and limitations should start to be coped to reduce levels of errors in gait analysis data. On the other hand, these studies revision outlines techniques that can be employed and incorporated in further protocol development to remarkably improve data reliability.

All these put the base for the introduction of a new gait analysis protocol with the scope of producing reliable results, being in agreement with the clinical understanding of human gait and overall being applicable to early stroke patients.

1.8 Study Aims

The study aims are two-fold to:

1. Design and run a feasibility study to:
 - Investigate the effects of the early provision of plastic solid AFOs in the gait of acute stroke patients with usual rehabilitation practice as control condition;
 - Evaluate the profile of recovery over a period of 24 weeks;
 - Investigate the orthotic loads during walking using an identical instrumented AFO;
2. Identify optimal methods to address previous objectives and investigate their reliability before being utilised in the feasibility study:
 - Development of a 3-D gait analysis protocol to be used for kinematics and kinetics data collection in the Bioengineering Unit biomechanics laboratory;
 - Development of a simple gait analysis assessment tool to be used in clinical environment;
 - Introduction of a suitable AFO set-up for orthotic loads measurement;
 - Investigation of a technique for motor control analysis.

CHAPTER 2 – DEVELOPMENT AND ASSESSMENT OF A NEW PROTOCOL FOR 3-D GAIT ANALYSIS

2.1 Introduction

The state of art of research on the rehabilitation of the stroke population, the utilisation of ankle-foot orthosis as rehabilitative device and of motion analysis for clinical assessment have been reported in the previous chapter. Key points extracted from the literature review can be listed as follow:

- Regaining walking ability is one of the main aims in post stroke rehabilitation;
- Provision of an ankle-foot orthosis (AFO) to supplement for gait disabilities in stroke affected subjects is now becoming a common clinical practice;
- The utilization of gait analysis as a method to evaluate patients gait abnormalities continue to flourish and its usefulness has been established.

Related to these outlined points, what emerges from the previous chapter is also:

- The limited knowledge available on the optimal rehabilitation programme to be adopted to enhance ambulation for stroke patients;
- Uncertainties on AFO prescription and its biomechanics effects on subject walking pattern early after stroke;
- Lack of evidence on the effects of early AFO intervention on stroke patient gait;
- Necessity of a gait analysis protocol, which is both reliable and repeatable and, easy and fast to be implemented to reduce stroke patients' distress during testing.

All these come together in the aims of the project and thus the first step was to develop a methodology to assess stroke gait with a motion analysis system. Three-dimensional (3-D) gait data set could be then used to evaluate walking recovery of stroke subjects and the effects the use of an AFO can provide.

The sections that follow will take the reader through the process of how the final protocol for 3-D gait analysis was accomplished providing an understanding of the choices made. The first developed method is initially described, followed by an assessment study of its reliability. A comparison between the proposed protocol and the most commonly used protocol in clinical setting, Plug-In-Gait (PiG, Vicon, Oxford Metrics Ltd., UK), is presented. The described study investigates also how two different motion capture systems, an old version and upgraded version of the Vicon systems (Oxford Metrics Ltd., UK), affect gait analysis data. Further features added to the original proposed method are then discussed leading to the final version of the gait protocol which will be employed with each participant during biomechanics test sessions. Finally, results from a preliminary application of the final protocol in able-bodied adult subjects are reported.

2.2 A new protocol and biomechanical model for gait analysis

A new protocol for human motion analysis was designed following the 5 steps identified earlier in this thesis (Chapter 1, Figure 1.63). These steps are here recalled to facilitate the reader in the understanding of this process:

1. Identification of clinical questions and relevant measurements;
2. Definition of how segments are described anatomically (Reference axes and frames);
3. Selection of an appropriate marker set to define the anatomical segments;
4. Definition of joint kinematics;
5. Evaluation of errors and feasibility of the protocol.

1. Identification of clinical questions and relevant measurements

The protocol should allow for the description of lower limb segments during tests of functional evaluation of stroke patients. Assessment of joint kinematics taken at different time during the stroke rehabilitation period provides information on the profile of recovery of walking ability. In addition the biomechanics of gait with and without an AFO can be evaluated.

2. *Definition of how segments are described anatomically (Reference axes and frames).*

Description of joint kinematics requires the reconstruction of bone motion in a three-dimensional space (3-D) and in each sampled instant of time. A global/laboratory reference frame is defined in agreement with ISB recommendations (Wu and Cavanagh, 1995): the x-axis is defined as the direction of progression, y-axis vertical positive upward, and z-axis medio-lateral positive pointing to the right.

Lower limbs are modelled as seven rigid segments, the pelvis, thighs, shanks, and feet, neglecting the deformability of active and passive tissue. For the purpose of bone movement description, anatomical frames of reference are associated to each segment and reconstructed from the known position of anatomical landmarks (ALs). Anatomical frames (AFs) are defined specifically to meet the requirements of intra- and inter-subject repeatability (Cappozzo et al., 2005) and in accordance with the International Society of Biomechanics (ISB) convention of right-handed orthogonal triad (Wu and Cavanagh, 1995). ALs, which are identifiable in a repeatable fashion (Cappozzo et al., 2005), used for the purpose of AFs definition are: anterior iliac spine (ASIS), posterior iliac spine (PSIS), lateral and medial epicondyle (LE, ME), lateral and medial malleolus (LM, MM), calcaneus (CA), first and fifth metatarsal head (FM, VM). These bony points can be identified in both sides of the lower body, left and right, through palpation following the guidelines delivered in the Vakhum EU project (Van Sint Jan, 2002b).

In addition to palpable bony landmarks, location of internal anatomical points, namely hip joint centre (HJC), knee joint centre (KJC), and ankle joint centre (AJC), is necessary to complete the lower limb representation. From the survey conducted on hip joint centre estimation, it was decided to prefer, despite their limitations, the use of one of the predictive models over functional methods. The latter were considered less appropriate in stroke subjects mainly due to the requirement of a sufficient range of motion at the hip that may not be achievable in stroke patients and the requisite of additional tasks to be performed adding burden to these patients. As patients tiredness is one of the main concerns during testing it is advisable to avoid asking for activities other than those absolutely necessary so as to prevent the patient becoming too fatigued to complete the test sessions.

Among the predictive approaches reviewed, it was opted for the recently introduced Harrington et al.'s method (Harrington et al., 2007) to determine the 3-D position of the hip joint centre (HJC). Harrington et al.'s method was shown to perform reliably in comparison to an ultrasound gold standard and was more accurate than most widely used predictive methods, such as those by Bell et al. and Davis et al.'s (Bell et al., 1989; Davis et al., 1991), and other functional methods (Harrington et al., 2007; Peters et al., 2010). In addition, as it is based only on pelvic depth (PD) and width (PW), the identification of posterior and anterior iliac spine on the patient is sufficient to determine these parameters. The practicality of the measurement required for stroke patients, favoured this method over Seidel et al.'s approach (Seidel et al., 1995), which, although accurate, necessitates the identification of an awkward point, the pubic symphysis, on the test subject. The 3-D position of the hip joint centre is estimated with the following equations (in mm) for the right leg:

$$x = -0.24 PD - 9.9$$

$$y = -0.30 PW - 10.9$$

$$z = 0.33 PW + 7.3$$

Equation 2.1

| | |
|--|---|
| | <p>Pelvis</p> <p>Origin: Midpoint between LASIS and RASIS</p> <p>Anterior-posterior (x) axis: Mutual perpendicular to the other two axes</p> <p>Mediolateral (z) axis: In direction from LASIS to RASIS</p> <p>Vertical (y) axis: Perpendicular to the z-axis and the line joining SACR and PELF</p> <p>Virtual points: HJC (left and right) defined as for Harrington's et al (2007) SACR midpoint between PSIS PELF midpoint between ASIS</p> |
| | <p>Femur</p> <p>Origin: KJC (left and right), midpoint between lateral (LEPI) and medial (MEPI) epicondyles</p> <p>Anterior-posterior (x) axis: Perpendicular to y-axis and the line in the right direction joining LEPI and MEPI</p> <p>Mediolateral (z) axis: Mutual perpendicular to the other two axes. Rotated by an angle θ as per Schache et al. (2006)</p> <p>Vertical (y) axis: In direction from KJC to HJC</p> <p>Virtual points: Left and right KJC as defined above</p> |
| | <p>Tibia/Fibula</p> <p>Origin: AJC (left and right), midpoint between lateral (LMAL) and medial (MMAL) malleoli</p> <p>Antero-posterior (x) axis: Perpendicular to y-axis and the line in the right direction joining LMAL and MMAL</p> <p>Mediolateral (z) axis: Mutual perpendicular to the other two axes</p> <p>Vertical (y) axis: In direction from AJC to KJC</p> <p>Virtual points: Left and right AJC as defined above</p> |
| | <p>Foot</p> <p>Origin: Left and right HEEL</p> <p>Antero-posterior (y) axis: In direction from MidFoot to HEEL</p> <p>Mediolateral (z) axis: Mutual perpendicular to the other two axes</p> <p>Vertical (x) axis: Perpendicular to y-axis and the line in the right direction joining MET1 and MET5</p> <p>Virtual points: MidFoot, midpoint between first (MET1) and fifth metatarsal (MET5) markers</p> |

HJC:hip joint centre, KJC:knee joint centre, AJC:ankle joint centre

Table 2.1: Anatomical frames definitions.

x , y , z represent the three coordinates of the right HJC in the pelvis reference frame (Table 2.1). Analogously, the left HJC is determined in the pelvis by negating from Equation 2.1 the z -coordinate (medio-lateral).

Knee joint centre and ankle joint centre are estimated as the mid point between the femoral epicondyles and the malleoli respectively.

Anatomical frames (AFs) as constructed from the specified anatomical landmarks and joint centres are shown for each segment in Table 2.1. AFs were defined in such a way that the y -axis always represents the longitudinal axis of the relative segment. This simplified the computation of joint kinematics into BodyBuilder software (Vicon, Oxford Metrics Ltd., UK) while allowing for a consistent definition with the clinical interpretation of the 3-D rotations at each joint. Pelvic and femoral coordinate systems are defined in accordance with ISB recommendations (Wu et al., 2002). The tibia/fibula and foot coordinate systems, instead, do not follow the definitions proposed by ISB. The reason for this was related to the appropriateness of the bone-embedded axes proposed by ISB in describing knee and ankle rotations in compliance with the clinical terminology (Baker, 2003). The tibia longitudinal axis (y -axis) was therefore defined to pass through the ankle and knee joint centre and not as a line oblique to it; the differences on the foot anatomical frame from ISB convention are to be related to the description of the ankle kinematics and will be explained later in this section.

3. Selection of an appropriate marker set to define the anatomical segment.

A marker set (Figure 2.1) was designed to allow the definition of the described anatomical frame of references.

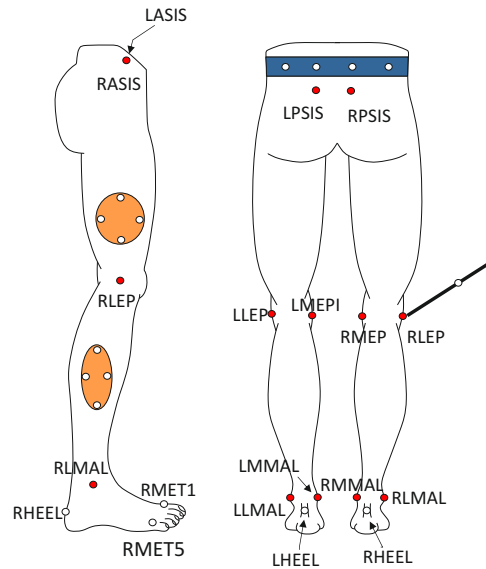


Figure 2.1: Diagram showing the designed marker set. A pointer with two markers used for calibration of anatomical landmarks (red circles) is also shown.

The main source of errors in motion analysis has been identified as skin movement artefacts (Cappozzo et al., 1996). Therefore the chosen position of markers should be made to limit the propagation of errors due to skin movement to the anatomical frames. Studies, presented earlier, which quantified the effect of soft tissue interposition between the marker and the underlying bone reported the greatest movements to be associated with directly attached markers on bony prominences or along the joint line, whereas, the least movement occurred at the distal part of the segments, particularly in the shank. Hence we opted for the use of rigid clusters of markers to identify bone segments, as they were less prone to skin artefacts problems during dynamic trials than single markers on bony points. Four clusters were constructed, following the design criteria identified by Cappozzo et al. (1997), by attaching four 14 mm diameter spherical retro-reflective markers placed onto a rigid curved thermoplastic plate. Clusters were positioned on the distal part of the thigh and shank segments of both legs using a Velcro attachment on elastic bands. Elastic

bands were made from 3mm Neoprene sheets (A. Algeo Ltd., UK) and finished with Velcro strap to allow clusters attachment.

Four markers attached on the back of an elastic band positioned around the subject's waist served as the cluster for the pelvis. Foot segments were identified by placing the markers directly on the foot anatomical landmarks (1st and 5th metatarsal head, calcaneus) where, skin movement is less problematic. Single markers were attached with hypoallergenic double-sided tape.

From the four markers in each cluster, technical reference frames were constructed, and referred to as marker cluster technical frames (CTFs) (Figure 2.2). Markers on the cluster can be tracked during the performance of a dynamic task allowing the construction of CTFs relative to the global/laboratory frame in each instant of the movement captured.

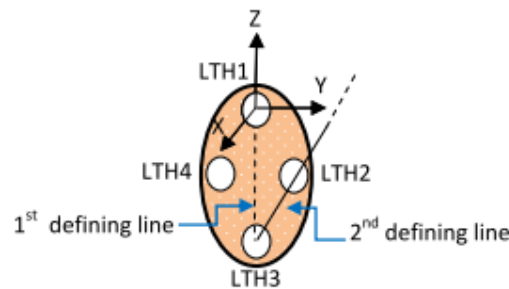


Figure 2.2: Example of how the technical frame was constructed based on the position of the markers in each cluster. Z-axis is coincident with the 1st defining line, x-axis is perpendicular to the z-axis and the 2nd defining line, y-axis is mutual perpendicular to the other two axes.

The position of each of the specified anatomical landmarks, anterior and posterior superior iliac spine, medial and lateral epicondyles, was referenced to the corresponding cluster technical frame during static calibration trials following the Calibrated Anatomical System Technique (CAST) (Cappozzo, 1984; 1991). A calibration pointer fitted with two reflective markers at known distances from the pointer tip was used to point the ALs one after another, while a subject maintained an up-right standing posture. The lateral and medial malleoli positions were calibrated

by locating retro-reflective markers directly on them. These markers were removed prior to capturing dynamic trials.

The purpose of static calibrations was to determine the position and orientation of anatomical landmarks in the relevant cluster technical frame. Specifically: the anterior and posterior superior iliac spine (ASIS, PSIS) coordinates were expressed in the pelvic cluster technical frame, medial and lateral epicondyles in the thigh cluster technical frame and the medial and lateral malleoli in the shank cluster technical frame. From the static pointer calibrations, the position of the selected AL was determined first in the global system (GAL) from the known positions of the markers (p_1, p_2) in the pointer as follows:

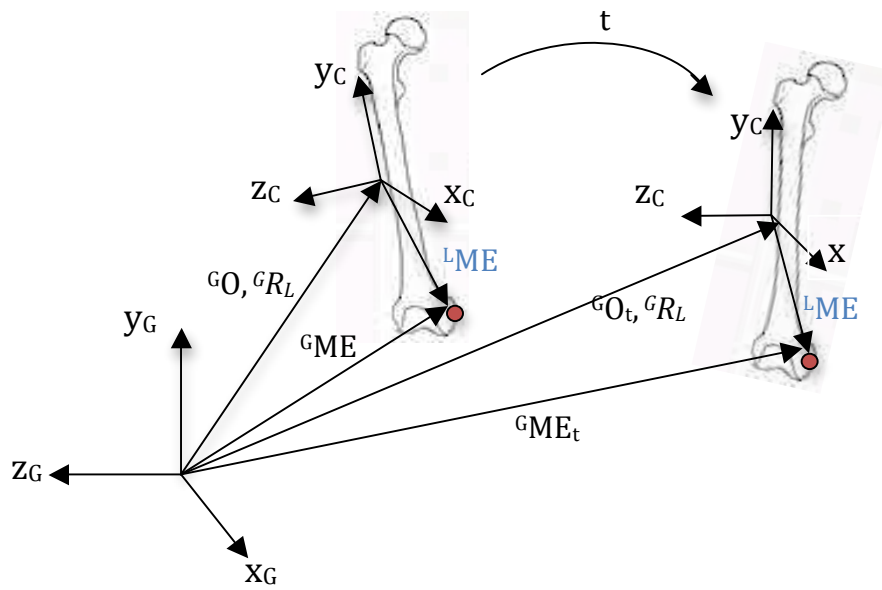


Figure 2.3: Example of AL position reconstruction. Knee Medial Epicondyle (ME) in two different instants of time is shown. The invariant position to the respect of the CTF is in blue font.

$${}^GAL = [(p_1 - p_2)/|p_1 - p_2|] * d + p_1 \quad \text{Equation 2.2}$$

d is the distance between marker p_1 and the pointer tip.

The global coordinates of the AL (GAL) were then transformed into local coordinates of the relative CTF (LAL):

$${}^LAL = {}^LR_G ({}^GAL - {}^G_O) \quad \text{Equation 2.3}$$

Where:

LR_G is the rotation matrix (direction cosine matrix) that transforms the coordinates of any point in the global reference system to the local CTF and, G_O is the position vector which defines the position of the local frame relative to the global (vector between the origins).

The positions and orientations of such ALs to the respect of the corresponding CTFs is invariant assuming a rigid relationship is maintained between ALs and CTFs.

These 3-D coordinates in the CTFs represent the calibration parameters extracted from static trials. Given these calibration parameters (LAL) and knowing the orientation and position of CTFs within the laboratory (${}^GR_L, {}^G_O$) during a dynamic trial, the ALs coordinates in the global/laboratory frame (GAL) can be obtained using coordinate transformation in each instant of time with the following equation (Figure 2.3):

$$({}^GAL = {}^GR_L {}^LAL + {}^G_O)_t \quad \text{Equation 2.4}$$

Where:

GR_L is the rotation matrix (direction cosine matrix), which defines the orientation of the local relative to the global and G_O is the position vector, which defines the position of the local frame relative to the global, t represents the duration of the dynamic trial throughout which the ALs are reconstructed.

Anatomical frames can thus be constructed in each sampled instant of time of the dynamic trials with respect to the laboratory axes and the movement of one bone segment relative to another (joint kinematics) can be determined.

4. Definition and calculation of joint kinematics

For the purpose of defining joint kinematics, the method proposed by Cole et al. (1993) based on the joint coordinate system (JCS) (Grood and Suntay, 1983) was adopted as it represents a mathematically correct and at the same time clinically meaningful representation of what is intended to be measured. As anticipated earlier a clinical description of joint attitude consists of three components, one in each of the sagittal, coronal, and transverse anatomical planes (Figure 2.4) of the body (Cole et al., 1993) and it is fundamental that these components for each joint give results that can be reconciled with conventional clinical terminology (Baker, 2003), if it is intended to use motion analysis as a clinical tool.

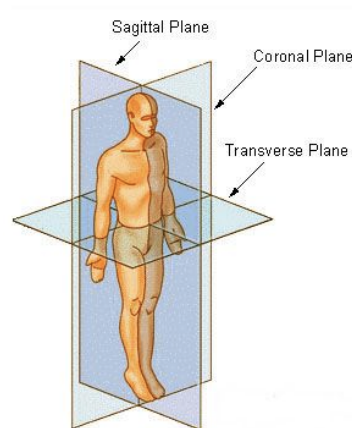


Figure 2.4: Body Planes.

Given two adjacent segments, proximal and distal, the 3-D rotations of the joint interconnecting the two segments are defined as (Baker, 2003):

Flexion/Extension is a rotation in the sagittal plane of the proximal segment,
Ab/Adduction is a rotation out of the sagittal plane of the proximal segment,
Internal/External rotation is the rotation about the longitudinal axis of the distal segment.

In order to quantify joint kinematics as for the JCS approach (Grood and Suntay, 1983), a convenient set of three axes about which the described rotational motions occur has to be defined for each joint articulating two adjacent segments. A joint coordinate system, whose unit base vectors are denoted to as \hat{e}_1 , \hat{e}_2 , \hat{e}_3 , was defined by choosing one axis from each of the AFs characterising the two segments and a

third axis mutually perpendicular to the other two. The two axes embedded in the proximal and distal segment are respectively \hat{e}_1 and \hat{e}_3 (body fixed axes).

\hat{e}_1 was defined as the flexion/extension axis coincident with the medio-lateral axis of the proximal segment; rotations about this axis characterise a rotation within the sagittal plane of the proximal segment and hence the flexion/extension movement of the relative joint.

\hat{e}_3 was defined as the internal/external rotation axis. To comply with the definition of internal/external rotation reported earlier, this axis was chosen as the longitudinal axis oriented lengthwise of the distal segment. Rotations about this axis characterise the internal/external rotator movement of the relative joint.

\hat{e}_2 also referred to as floating axis, is the ab/adduction axis common perpendicular to \hat{e}_1 and \hat{e}_3 . It was defined with the following formula (Cole et al., 1993):

$$\hat{e}_2 = \left(\frac{\hat{e}_3 \times \hat{e}_1}{|\hat{e}_1 \times \hat{e}_3|} \right) * A$$

Equation 2.5

$$A = \begin{cases} -1, & \text{if } ((\hat{e}_3 \times \hat{e}_1) \cdot \hat{t}_j < 0) \text{ and } (((\hat{e}_3 \times \hat{e}_1) \times \hat{e}_3) \cdot \hat{f}_j > 0) \\ 1, & \text{otherwise} \end{cases}$$

Where:

A is a correction factor that allows angle calculations about \hat{e}_2 to be continuous between $-\pi$ and $+\pi$. \hat{t}_j is the “third axis” (Cole et al., 1993) of the distal segment defined as $\hat{t}_j = \hat{l}_j \times \hat{f}_j$, where \hat{l}_j and \hat{f}_j are respectively the longitudinal axis and medio-lateral (flexion) axis of the AF of the distal segment (j).

The floating axis is not fixed in either the proximal or distal segment but it moves along with them while maintaining the condition of orthogonality with respect to \hat{e}_1 and \hat{e}_3 . By saying that, a rotation about \hat{e}_2 occurs in a plane perpendicular to the sagittal plane of the proximal segment since, \hat{e}_1 and \hat{e}_2 are perpendicular by definition. Rotations about \hat{e}_2 describe a rotation out of the sagittal plane of the proximal segment and hence the ab/adductor movement of the joint in agreement with the definition given earlier.

The axes, \hat{e}_1 , \hat{e}_2 , \hat{e}_3 , do not have a common origin and represent a non-orthogonal triad.

Defining joint kinematic as rotation about these axes allowed for the definition of joint angles that are independent from the sequence the rotations were performed and yet clinically relevant. The joint angles of flexion/extension, ab/adduction, and internal/external rotation were derived from a geometrical analysis of the two rotating segments. If a rotation occurred around an axis fixed to the proximal or distal segment (\hat{e}_1 or \hat{e}_3), this segment (proximal or distal) was thought to rotate while the contiguous segment (distal or proximal) remained stationary. To numerically quantify those rotations about the body fixed axes, flexion/extension and internal/external rotations, a ‘reference axis’ in both the proximal and distal segment had to be defined which was taken to be perpendicular to the axis the rotation is about (Grood and Suntay, 1983). In particular, the reference axes (\hat{e}_1^r and \hat{e}_3^r) were defined by the cross product of the longitudinal axis and medio-lateral axis of each segment AFs. The angles between the reference axes in the proximal and distal segments and the floating axis represented flexion/extension and internal/external rotations respectively. The ab/adduction rotation was quantified by the angle between the two body fixed axes, \hat{e}_1 , and \hat{e}_3 .

The formulations, whereby the 3-D angles (α , β , γ) were determined, were extracted from Cole et al. (1993) who extended the method originally proposed for the knee by Grood and Suntay (1983) to be applicable to all joints. In the equations that follow, the reference axes of proximal and distal segment are referred to as \hat{t}_i and \hat{t}_j with i =proximal; j =distal segment and, as anticipated above, they are calculated as $\hat{t}_i = \hat{l}_i \times \hat{f}_i$ and $\hat{t}_j = \hat{l}_j \times \hat{f}_j$. \hat{l} and \hat{f} are the longitudinal and flexion axis of the relative segment.

The rotations angle of flexion/extension (α), ab/adduction (β), and internal/external rotation (γ) are defined as follow (counterclockwise rotations about each axis are considered positive):

α is the angle of flexion/extension, rotation about \hat{e}_1 ,

$$\alpha = \cos^{-1}(\hat{e}_2 \cdot \hat{t}_i) * B$$

Equation 2.6

$$B = \begin{cases} 1, & \text{if } (\hat{e}_2 \cdot \hat{l}_i) > 0 \\ -1, & \text{otherwise} \end{cases}$$

Where:

\hat{t}_i (or \hat{e}_1^i) is the reference axis of the AF of the proximal segment (i) and \hat{l}_i is the longitudinal axis of the AF of the proximal segment; B determines the sign of the angle.

β is the angle of ab/adduction, rotation about \hat{e}_2 ,

$$\beta = \cos^{-1}(\hat{r} \cdot \hat{l}_j) * C, \quad \text{where } \hat{r} = \left(\frac{\hat{f}_i \times \hat{e}_2}{|\hat{f}_i \times \hat{e}_2|} \right)$$

Equation 2.7

$$C = \begin{cases} 1, & \text{if } (\hat{f}_i \cdot \hat{l}_j) > 0 \\ -1, & \text{otherwise} \end{cases}$$

Where:

the vector \hat{r} allows consistency between the sign of the angle and the direction of the rotation around \hat{e}_2 regardless of which axes (x, y, z) are chosen as flexion, \hat{f} , and, longitudinal, \hat{l} , axes in a given anatomical frame (Cole et al., 1993). \hat{l}_j is the longitudinal axis of the AF of the distal segment and \hat{f}_i is the mediolateral axis of the AF of the proximal segment, C determines the sign of the angle.

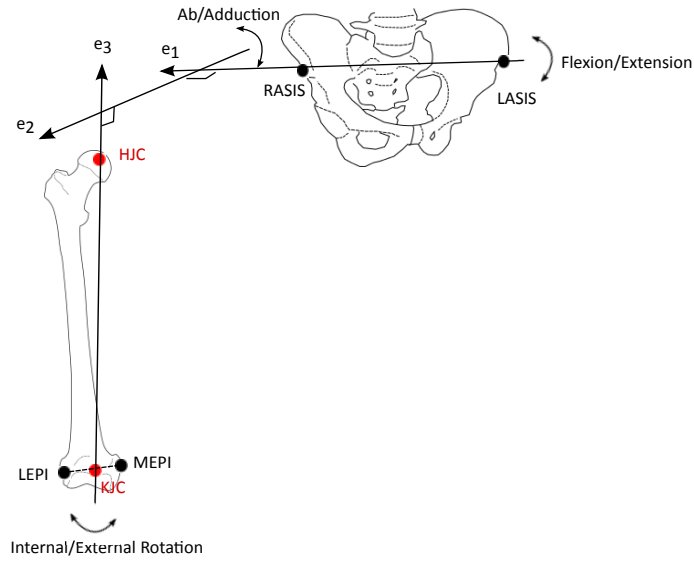


Figure 2.5: Hip joint coordinate system.

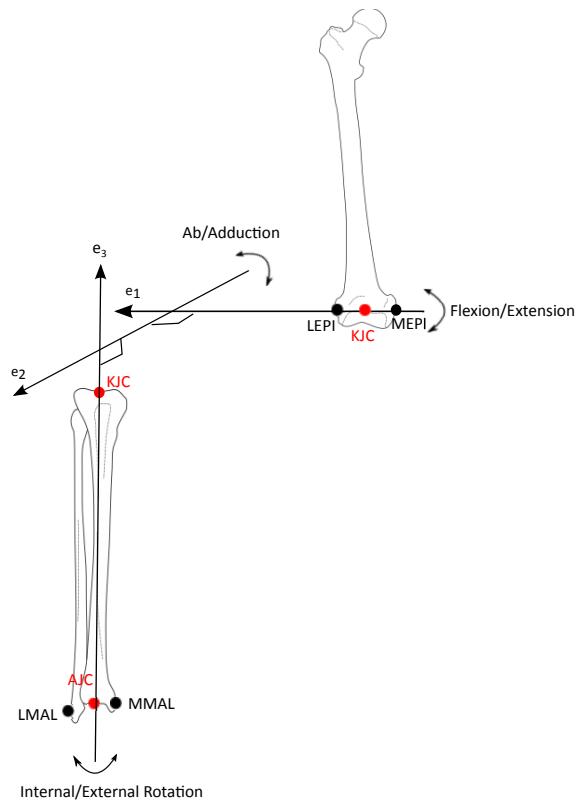


Figure 2.6: Knee joint coordinate system.

γ is the angle of internal/external rotation, rotation about \hat{e}_3 ,

$$\gamma = \cos^{-1}(\hat{e}_2 \cdot \hat{t}_j) * D$$

Equation 2.8

$$D = \begin{cases} 1, & \text{if } (\hat{e}_2 \cdot \hat{f}_j) > 0 \\ -1, & \text{otherwise} \end{cases}$$

Where:

\hat{t}_j (or \hat{e}_3^r) is the reference axis of the AF of the distal segment, \hat{f}_j is the mediolateral axis of the distal segment (j) AF and, D is the sign determinant.

Joint coordinate systems to describe joint movements consistently with the conventional clinical terminology are outlined here after for the hip, knee and ankle joints.

The hip JCS is constituted by the following axes (Figure 2.5):

\hat{e}_1 is the z-axis (medio-lateral) of the pelvis (proximal segment) coordinate system, translated to the hip joint centre as origin. Rotation around \hat{e}_1 describes flexion and extension of the hip joint, rotation in the sagittal plane of the pelvis;

\hat{e}_3 is the y-axis (longitudinal, vertical) of the femur (distal segment) coordinate system. Rotation around \hat{e}_3 describes internal and external rotation of the hip joint; \hat{e}_2 given by Equation 2.5, is the floating axis mutually perpendicular to \hat{e}_1 and \hat{e}_3 . \hat{e}_2 characterises a rotation out of the sagittal plane of the pelvis and thus describes ab/adduction of the hip joint.

The knee JCS is defined by the following axes (Figure 2.6):

\hat{e}_1 is the z-axis (medio-lateral) of the femur (proximal segment) coordinate system. Rotation around \hat{e}_1 describes flexion/extension of the knee joint, rotation within the sagittal plane of the femur;

\hat{e}_3 is the long axis (y-axis) of the tibia coordinate system. Rotation around \hat{e}_3 describes internal/external rotation of the knee joint (tibia rotation relative to the femur);

\hat{e}_2 from Equation 2.5, is the floating axis perpendicular to the plane identified by \hat{e}_1 and \hat{e}_3 . A rotation about \hat{e}_2 represents a rotation out of the sagittal plane of the femur and thus describes ab/adduction of the knee joint.

The ankle joint coordinate system comprises the axes so defined (Figure 2.7):

\hat{e}_1 is the z-axis (medio-lateral) of the tibia (proximal segment) coordinate system.

Rotation about \hat{e}_1 describes a rotation in the sagittal plane of the tibia, dorsiflexion/plantarflexion of the ankle joint.

\hat{e}_3 is the long axis of the foot (distal segment). As previously shown (Table 2.1) it is named y-axis but it is not vertically (proximally) oriented, it lies on the transverse plane of the foot (conventionally speaking x-axis direction, antero-posterior axis).

Rotation around \hat{e}_3 describes internal/external rotation of the ankle joint. These are referred also as inversion and eversion, rotation about the long axis of the calcaneus (Baker, 2003).

\hat{e}_2 given by Equation 2.5, is the floating axis mutually perpendicular to \hat{e}_1 and \hat{e}_3 . A rotation around \hat{e}_2 identifies a rotation out of the sagittal plane of the tibia segment and thus defined ab/adduction of the ankle complex.

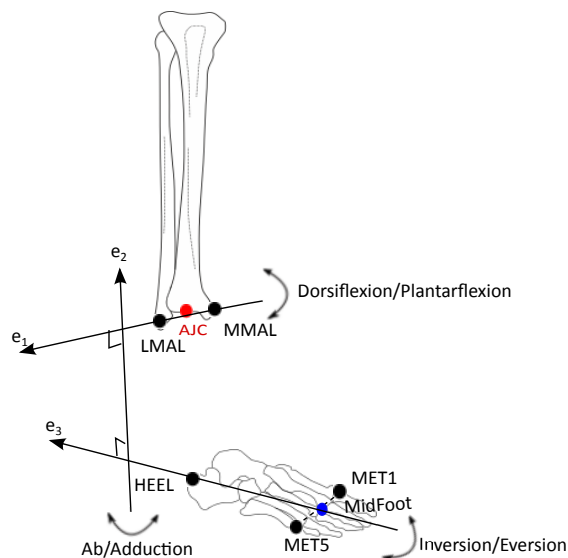


Figure 2.7: Ankle joint coordinate system.

This definition of ankle JCS is different from the one proposed by Wu et al. (2002) as ISB standard recommendation. In their paper, \hat{e}_3 was chosen coincident with the

vertical axis of the foot coordinate system describing internal/external rotation of the ankle. Inversion/eversion was defined as occurring about a floating axis, the common axis perpendicular to \hat{e}_1 and \hat{e}_3 which was not coincident with the long axis of the foot. By definition, internal and external rotation at a joint is stated as the rotation about the longitudinal axis of the distal segment. This rotation for the ankle is inversion/eversion, about the long axis of the foot. The definition given by the ISB convention is thus not in agreement with the conventional understanding of inversion/eversion and does not correlate with the clinical terminology of joint angles (Baker, 2003). The adoption of the ankle JCS as defined by Wu et al. (2002) might lead to misunderstandings with clinicians; the ankle JCS used on the other hand is consistent with clinical terminology and rotation definitions.

The construction of frames of reference and definition of joint angles are obtained by processing reconstructed 3-D marker trajectories with a specifically written BodyBuilder software (Vicon, Oxford Metrics Ltd., UK) code (Electronic Appendix). Implementation of the specified code allows:

1. Definition of lower limb cluster technical frames (CTFs);
2. Calculation of calibration parameters from static trials: invariant positions of anatomical landmarks in the relative CTF;
3. Definition of anatomical frames in the global/laboratory exploiting the information obtained from the calibration procedure and coordinate transformations;
4. Definition of joint coordinate systems (JCSs);
5. Computations of joint kinematics.

Besides, the protocol for data processing includes also the application of an optimisation procedure for orientating the knee joint flexion-extension axis. The method employed is based on the one firstly proposed by Baker et al. (1999) and then slightly modified by Schache et al. (2006) discussed earlier in this thesis. The use of this optimisation technique was aimed to reduce crosstalk errors at knee minor angles, which derived from a misallocation of the knee epicondyles on which the orientation of the knee flexion axis depends on. The knee (femur) medio/lateral axis was rotated in a plane perpendicular to the knee vertical axis by an angle θ .

represents the rotation necessary to minimise knee ab/adduction angle variance (Schache et al., 2006). For more details on this method please refer to Baker et al. (1999) and Schache et al. (2006) papers.

5. Evaluation of errors and feasibility of the protocol

The protocol was assessed through a case study on healthy subjects. How the evaluation was conducted and results obtained is described and discussed in the paragraphs to follow.

2.3 Comparative study of the proposed protocol and Plug-In-Gait protocol and two motion analysis capture systems.

2.3.1 Introduction

The previously described protocol was firstly used with healthy subjects. A study was conducted to assess intra-subject and inter-subject variability of the proposed protocol. In addition, results of this preliminary application were compared to the results obtained by applying the Plug-In-Gait protocol (PiG, Vicon, Oxford Metrics Ltd., UK) to the same gait acquisitions. This allowed for the evaluation of inter-protocol variability. There is a limited knowledge of the effects, different biomechanical model definitions and conventions have on the results produced and their interpretation. Data are shared in biomechanics communities despite differences among protocols.

In addition, the experiment was designed to assess if the use of two different motion capture systems, an old version (Vicon 612, Oxford Metrics Ltd., UK) and upgraded version (Vicon MX Giganet, Oxford Metrics Ltd., UK) of Vicon systems (Oxford Metrics Ltd., UK), affect gait analysis data. The accuracy of these data capture systems mainly depends on the ability of the cameras to calculate the 2-D centroid of markers and the ability of the used software to reconstruct the 3-D marker position from its 2-D centroid. Since bone movement and orientation are derived from the captured position of markers, erroneous estimation of marker 3-D position will affect outcome measurements. The author found no studies in the literature that compared differences between data collected with different systems and thus the current work provides an insight on how upgrading a system can affect data capturing and computations.

3.3.2 Instrumentation and methods

An eight-camera motion capture system (Vicon 612, Oxford Metrics Ltd., UK) and its upgraded version a twelve-camera motion analysis system (Vicon MX Giganet, Oxford Metrics Ltd., UK) were operated in parallel to allow simultaneous marker tracking from both the systems. For the eight cameras system each camera (Vicon V-series, Mcam (50), Oxford Metrics Ltd., UK) had a resolution of 1000x1000 pixels, and they were positioned on adjustable tripods. Camera positions were kept consistent among laboratories sessions creating a capture volume with sides of approximately 4 m in length. The second system (MX Giganet) was connected to six T160 (16 Megapixel) and six T40 (4 Megapixel) cameras (Vicon, Oxford Metrics Ltd., UK) placed in fixed positions on a rail around the laboratory walls. T160 and T40 cameras have a resolution of 4704 x 3456 pixels and 2353 x 1728 pixels respectively. The capture volume had sides of length of 6 m approximately. The laboratory configuration showing cameras placement is illustrated in Figure 2.8. Data sampling was set at 120 Hz and 100 Hz for the old and new motion systems respectively.



Figure 2.8: Laboratory configuration with camera on high tripods (Vicon 612) and camera on the wall trail (Vicon MX Giganet). Not all the cameras connected to the new system are visible.

The two systems were calibrated prior to each test session with calibration tools as suggested by the supplier (Figure 2.9).

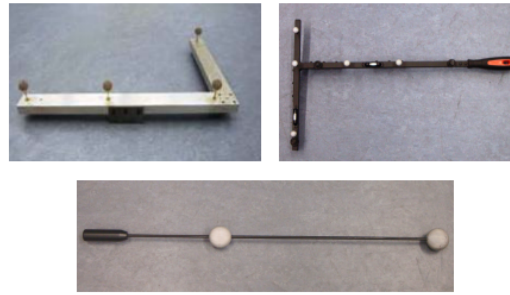


Figure 2.9: Calibration tools: L-Frame (top left corner), 5-marker calibration wand (top right corner), dynamic calibration wand (centre).

Calibration allows each system to define the capture volume and the relative positions and orientations of cameras. A good calibration is crucial for a successful capture. This process requires, in Vicon 612, a static and a dynamic calibration each time. During static calibration, the L-frame (Figure 2.9) is placed on the floor in the centre of the capture volume; the origin of the volume and the orientations of the axes in the 3-D space are thus determined. Dynamic calibration allows the system to calculate the relative positions and orientations of the camera. It is performed by waving the wand in a way that covers the capture volume.

Mx Gigaset system requires only one calibration to set the capture volume and cameras. This involves the movement of a 5-marker calibration wand (Figure 2.9) throughout the capture volume followed by the positioning of the same wand at the origin of the volume.

Reconstruction residuals were used to assess the accuracy of the 3D reconstruction of markers position. The reconstruction residual is defined as the average error distance, calculated by the photogrammetry system, which prevents all camera measurement rays from meeting at an identical point in space (Motion Lab Systems, 2005).

In general, in photogrammetric system, two or more camera rays contribute to the reconstruction of a 3D marker position but they will not necessarily intersect.

Whereas, ideally, if a marker is seen by two or more cameras, it should lie in the intersection of the camera rays. The system should then calculate the locations of the intersection to determine the marker position. The measuring system instead, identifies the best estimate of the marker location, which will be at a certain distance

from the ray (Figure 2.10). The distance from the assumed point location to a given camera ray is reported as a reconstruction residual error.

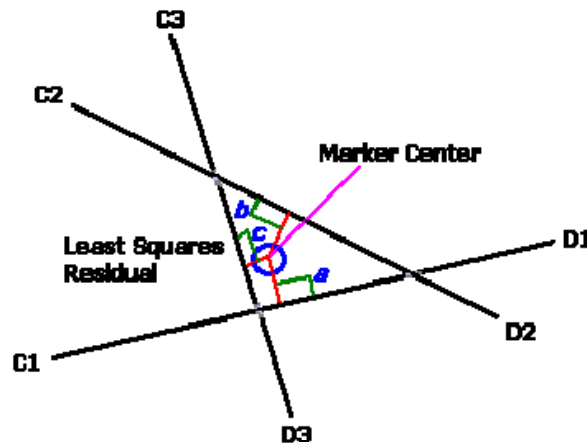


Figure 2.10: Example of marker residual calculation with three camera rays, C1-D1, C2-D2 and C3-D3 (Motion Lab Systems, 2005).

If more than two rays are involved in the reconstruction of a given marker a least-square technique is used by the system to calculate the position of the marker in space and the reconstruction residual.

The smaller the residual is, the more accurate the location of the marker. A residual is measured in millimetres. Residuals of each marker obtained from both motion capture systems were compared for static and dynamic trials. In particular, the averages of the residuals of each marker across all the subjects were kept for the analysis.

A comprehensive marker set was designed by combining markers required by the two protocols, Plug In Gait (PiG-Vicon Motion Systems, Oxford Metrics Ltd., UK) and the cluster method. This included a total of 24 individual retro-reflective markers (14mm diameter) and 4 clusters mounting four, 14 mm diameter markers each. The marker set is detailed in Table 2.2 where individual marker and markers on cluster are reported in reference to the segment they are attached to. With the marker set outlined, both protocols could be implemented simultaneously and recorded with both systems.

| Segment | Marker | Marker Placement |
|----------------------|---------------------|--|
| <i>Pelvis</i> | LASI | Over the left anterior superior iliac spine |
| | RASI | Over the right anterior superior iliac spine |
| | LPSI | Over the left posterior superior iliac spine |
| | RPSI | Over the right posterior superior iliac spine |
| | WAIST 1 | Arbitrarily placed on the back of the waist band on the left side. |
| | WAIST 2 | On the waist band nearly 30 mm apart from WAIST 1 on the right side. |
| | WAIST 3 | On the waist band nearly 30 mm apart from WAIST 2 on the right side |
| | WAIST 4 | On the waist band nearly 30 mm apart from WAIST 3 on the right edge of the band in the back. |
| <i>Thigh</i> | LTHI | Over the lower lateral 1/3 surface of the left thigh |
| | RTHI | Over the lower lateral 1/3 surface of the right thigh (usually higher than LTHI) |
| | LKNE/ RKNE | Over lateral epicondyle of the left and right knee |
| | RTH 1/ LTH 1 | Attached to the thigh cluster, top marker |
| | RTH 2/ LTH 2 | Anti/clockwise marker from R/LTH 1 on the thigh cluster |
| | RTH 3/ LTH 3 | Attached to the thigh cluster, bottom marker |
| | RTH 4/ LTH 4 | Anti/clockwise marker from R/LTH 3 on the thigh cluster |
| <i>Shank</i> | LTIB | Over the lower 1/3 of the left shank |
| | RTIB | Over the lower 1/3 of the right shank (usually higher than RTIB) |
| | RSH 1/ LSH 1 | Attached to the shank cluster, top marker |
| | RSH 2/ LSH 2 | Anti/clockwise marker from R/LSH 1 on the shank cluster |
| | RSH 3/ LSH 3 | Attached to the shank cluster, bottom marker |
| | RSH 4/ LSH 4 | Anti/clockwise marker from R/LSH 3 on the shank cluster |
| <i>Foot</i> | LANK/RANK | Left and right lateral malleolus |
| | LMMAL/RMMAL | Left and right medial malleolus |
| | LHEE/RHEE | On the left and right calcaneus |
| | LMET1/ RMET1 | On the first metatarsal head of the left and right foot |
| | LMET5/ RMET5 | On the fifth metatarsal head of the left foot |

Table 2.2: Marker set used during data collection. The name of each marker and its position is reported relatively to the body segment they are referred to.

Ten able-bodied male subjects with a mean height of 1.77 (± 0.05) m, body mass of 77 (± 9.96) kg and age of 25.1 (± 3.93) years were recruited from the Bioengineering Unit student community. The participants were asked to wear a Lycra suit tight enough to allow markers attachment and visualisation while maintaining their modesty. Markers and rigid clusters were consistently applied to each subject while they kept an up-right natural posture. Individual markers were attached with hypoallergenic double-sided tape whereas clusters were positioned on the distal part of the thigh and shank with Velcro elastic bands. These straps were secured around the subjects' legs to prevent slippage during test sessions.

Anthropometric measurements, required by PiG, were taken from the subject prior data collection. These were knee and ankle width and leg length of both body sides. Right and left anterior superior iliac spine, right and left posterior superior iliac spine, right and left lateral and medial knee epicondyles were located by using a pointer with two markers placed at a known distance from its tip (Figure 2.11) and

recording an identification trial for each anatomical landmark prior to testing. Listed anatomical landmarks were identified by palpation following the methods proposed in the Vakhum Eu project (Van Sint Jan, 2002b).



Figure 2.11: Pointer used for anatomical landmark calibration in static trials.

Two more static trials were performed: one to allow calibration of the malleoli for whom, markers directly attached on them were used rather than the pointer and one for the PiG model as from protocol. These were therefore 10 calibration trials in total. Markers required only for calibration purposes were removed for dynamic data capturing.

Three level walking trials were acquired for each subject simultaneously by both motion analysis systems. Participants walked at their own natural speed wearing their comfortable shoes. Data processing was performed after data collection following procedures characteristic of each protocol using Workstation and BodyBuilder softwares (Vicon, Oxford Metrics Ltd., UK). Marker trajectories were filtered using Woltring's generalized cross-validation with splines (GCVSPL) method with a predicted mean squared error of 15mm (Woltring 1985; 1986). All kinematics outcomes of a gait cycle were time normalised with respect to stride duration time in 101 equal intervals to represent 0% to 100% of a gait cycle using Matlab software (The MathWorks Inc., Massachusetts, US). This allowed averaging across trials and subjects. Left-sided data were chosen for analysis. The same gait cycles were analysed for each protocol and motion capture system, to allow consistency in the comparisons.

Descriptive statistics were applied to the experimental data to assess variability of the measurements. Time series of joint kinematics and extracted discrete parameters at crucial points in the curves were both calculated for analysis. The set of gait parameters used was adapted from the one proposed by Benedetti et al. (1998) and described in Table 2.3. Intra-subject variability was obtained by analysing 3 gait

trials for each subject and, inter-subject variability was assessed by comparison of the averages of the 3 walking trials among the 10 participants. As an indication of variability, standard deviation (SD) and the average of the standard deviation throughout the gait cycle were used. Paired *t*-tests were applied to highlight differences among protocols and systems, hence avoiding the use of ambiguous indices such as intra-class correlation (ICC), coefficient of variance (CV) or coefficient of multiple correlation (CMC). The use of these coefficients has been discouraged lately (Leardini et al., 2007; McGinley et al., 2009) because they result in numbers based on underlying statistical analyses that are often non relevant and, moreover, they are difficult to interpret without any units in relation to the measurement itself.

Paired *t*-tests, at 0.05 level of significance, were performed to determine if significant difference exists between PiG and cluster protocol for kinematic time course. Key kinematic peaks (Table 2.3) were compared. The *t*-test was also applied to data obtained by the two motion capture systems within the same protocol to evaluate the effects cameras accuracy has on outcome measurements.

| Hip angle parameters | | Knee angle parameters | | Ankle angle parameters | |
|----------------------|-----------------------------|-----------------------|-------------------------------|------------------------|---------------------------------|
| H1 | Flexion at heel strike | K1 | Flexion at heel strike | A1 | Flexion at heel strike |
| H2 | Peak stance extension | K2 | Peak flex at loading response | A2 | Max plant.flex loading response |
| H3 | Peak swing flexion | K3 | Peak extension in stance | A3 | Max dorsiflex in stance |
| H4 | Peak stance adduction | K4 | Peak swing flexion | A4 | Peak plant.flex in swing |
| H5 | Peak swing abduction | K5 | Peak stance adduction | A5 | Peak adduction in swing |
| H6 | Peak int rotation in stance | K6 | Peak swing adduction | A6 | Peak stance inversion |
| H7 | Peak ext rotation in swing | K7 | Peak int rotation in stance | A7 | Peak stance eversion |
| | | K8 | Peak ext rotation in swing | | |

Table 2.3: Joint angle parameters. Acronyms and corresponding definitions are reported.

2.3.3 Results

2.3.3.1 Motion Capture systems comparison

In the assessment of the two motion capture systems, from the user experience point of view, Vicon MX Giganet was better at tracking markers during data capturing. When processing the trial data a more careful reconstruction and markers ‘snagging’ procedure was required for data capture with the old Vicon 612 system. This was

needed in order to limit the presence of erratic markers trajectories and avoid gaps in the trajectories due to missed markers.

| | | Residuals from Static trial | | | | | | | | | |
|-----------|--|-----------------------------|------|-------|-------|--------|--------|--------|--------|------|------|
| | | LASI | RASI | LPSI | RPSI | WAIST1 | WAIST2 | WAIST3 | WAIST4 | LTHI | RTHI |
| Vicon 612 | | 1.75 | 1.55 | 1.27 | 2.21 | 2.26 | 1.25 | 1.29 | 2.02 | 1.47 | 1.1 |
| Vicon MX | | 0.59 | 0.55 | 0.4 | 0.36 | 0.5 | 0.6 | 0.4 | 0.52 | 0.59 | 0.48 |
| | | LKNE | RKNE | LTH1 | LTH2 | LTH3 | LTH4 | RTH1 | RTH2 | RTH3 | RTH4 |
| Vicon 612 | | 1.32 | 0.84 | 2.98 | 2.44 | 2.46 | 2.37 | 1.97 | 1.45 | 1.1 | 1.69 |
| Vicon MX | | 0.6 | 0.48 | 0.58 | 0.58 | 0.66 | 0.6 | 0.59 | 0.54 | 0.47 | 0.47 |
| | | LTIB | RTIB | LSH1 | LSH2 | LSH3 | LSH4 | RSH1 | RSH2 | RSH3 | RSH4 |
| Vicon 612 | | 1.45 | 1.46 | 1.43 | 2.14 | 1.9 | 2.44 | 0.98 | 1.34 | 1.76 | 1.09 |
| Vicon MX | | 0.58 | 0.51 | 0.6 | 0.56 | 0.62 | 0.53 | 0.53 | 0.66 | 0.51 | 0.47 |
| | | LHEE | RHEE | LMET1 | RMET1 | LMET5 | RMET5 | LANK | RANK | | |
| Vicon 612 | | 2.55 | 2.45 | 1.78 | 2.45 | 2.06 | 2.7 | 1.87 | 1.66 | | |
| Vicon MX | | 0.59 | 0.63 | 0.7 | 0.7 | 0.59 | 0.56 | 0.64 | 0.61 | | |

Table 2.4: Reconstruction residuals for static trials for all lower limb markers as from Vicon612 cameras and Vicon MX cameras. Values are in mm.

| | | Residuals from Dynamic trial | | | | | | | | | |
|-----------|--|------------------------------|------|-------|-------|--------|--------|--------|--------|------|------|
| | | LASI | RASI | LPSI | RPSI | WAIST1 | WAIST2 | WAIST3 | WAIST4 | LTHI | RTHI |
| Vicon 612 | | 1.8 | 2.21 | 1.92 | 1.86 | 1.37 | 1.5 | 1.7 | 1.59 | 1.65 | 1.69 |
| Vicon MX | | 0.56 | 0.6 | 0.51 | 0.53 | 0.59 | 0.51 | 0.53 | 0.56 | 0.47 | 0.46 |
| | | LKNE | RKNE | LTH1 | LTH2 | LTH3 | LTH4 | RTH1 | RTH2 | RTH3 | RTH4 |
| Vicon 612 | | 1.78 | 1.95 | 2.29 | 1.92 | 1.95 | 2.29 | 2.4 | 2.62 | 2.39 | 2.51 |
| Vicon MX | | 0.52 | 0.52 | 0.57 | 0.58 | 0.56 | 0.55 | 0.59 | 0.57 | 0.53 | 0.55 |
| | | LTIB | RTIB | LSH1 | LSH2 | LSH3 | LSH4 | RSH1 | RSH2 | RSH3 | RSH4 |
| Vicon 612 | | 1.98 | 2 | 2.16 | 2.04 | 2.16 | 2.41 | 2.44 | 2.49 | 2.6 | 2.63 |
| Vicon MX | | 0.53 | 0.53 | 0.57 | 0.6 | 0.59 | 0.61 | 0.53 | 0.67 | 0.57 | 0.54 |
| | | LHEE | RHEE | LMET1 | RMET1 | LMET5 | RMET5 | LANK | RANK | | |
| Vicon 612 | | 2.3 | 2.32 | 2.4 | 2.31 | 2.32 | 2.64 | 1.96 | 2.14 | | |
| Vicon MX | | 0.69 | 0.7 | 0.74 | 0.74 | 0.65 | 0.66 | 0.62 | 0.6 | | |

Table 2.5: Reconstruction residuals for dynamic trials for all lower limb markers as from Vicon 612 cameras and Vicon MX cameras. Values are in mm.

Further the Mx Giganet Vicon system has higher resolution than the Vicon 612. This can be seen in the marker residuals. Table 2.4 shows the residuals calculated by the systems during static trials, when the subjects were standing approximately in the centre of the capture volumes. Table 2.5 reports residual values obtained during dynamic trials, during which the subjects walked across the capture volumes.

Residuals are smaller when using the newer system for both static and dynamic trials (Table 2.4 and 2.5). With the subject standing at the centre of the capture volume, small residuals were obtained; static residuals were generally smaller than dynamic. Only 13 and 12 dynamic marker residuals out of 38 (total number of markers) are greater than correspondent static residuals for Vicon 612 and Vicon MX camera respectively.

In Figure 2.12 joint rotations from PiG processing of data from both systems are illustrated and, in the same way kinematic profiles from the cluster model application are shown in Figure 2.13, allowing comparisons between kinematic time histories, within the same model, derived by the two motion capture systems. Blue solid lines represent kinematics outcomes for the new Vicon MX Giganet system, whereas red dashed lines represent kinematics outcomes for the old Vicon 612 system.

Significant differences between the two motion capture systems, when found from the *t*-test, are shown in the graphs as grey bars through the gait cycle.

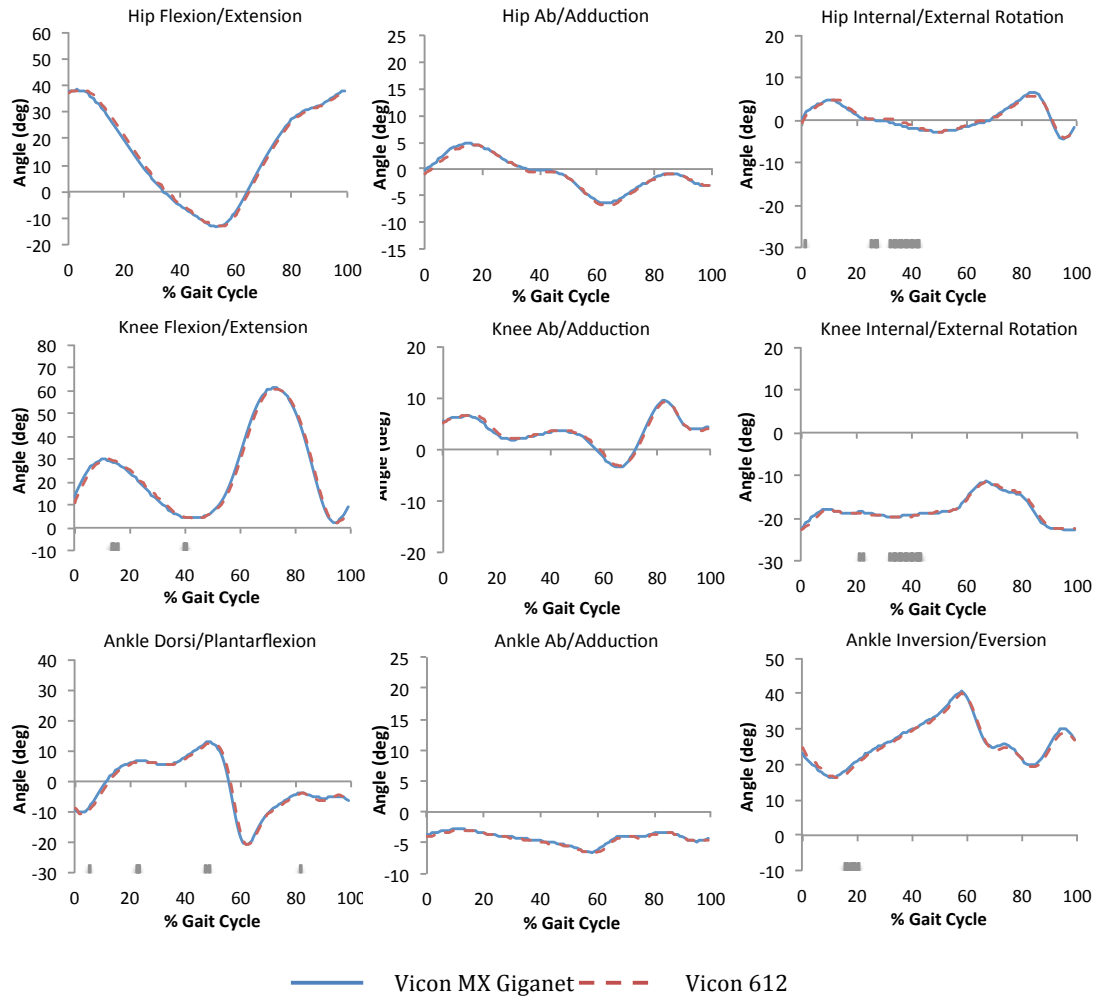


Figure 2.12: Comparison of the two motion capture systems for PiG processed kinematics of a representative subject. *T*-test significant differences throughout the gait cycle are reported at the bottom as grey bars.

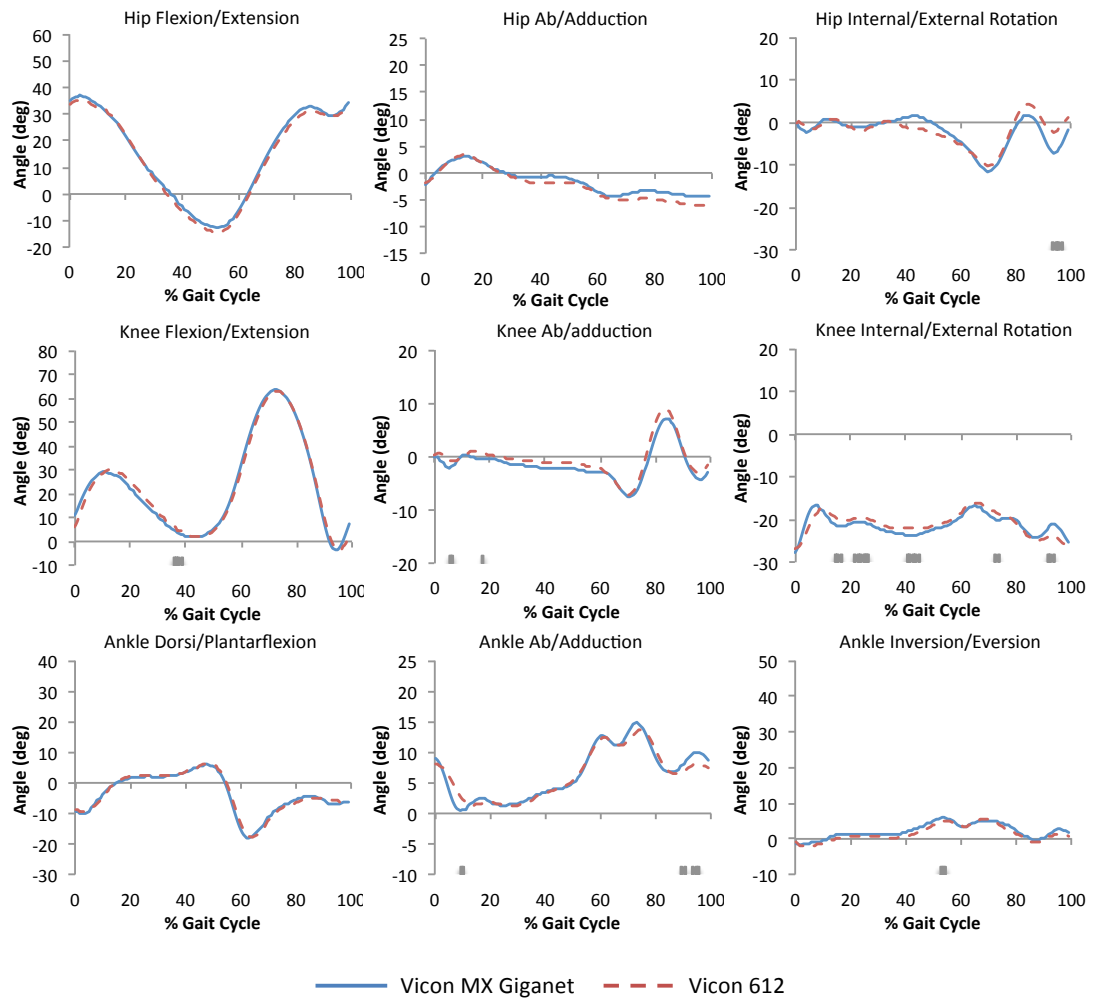


Figure 2.13: Comparison of the two motion capture systems for cluster method processed kinematics of a representative subject. *T*-test significant differences throughout the gait cycle are reported at the bottom as grey bars.

Very good agreement was noticed between motion capture systems (Figure 2.12, 2.13), for both PiG and cluster model processed data. Although generally not significantly, the use of different capture systems seemed to have a slightly more impact on the data processed by the cluster protocol. As for the data of the subject reported here (subject 2), in fact, deviations up to 3° were observed among the other 9 participants in coronal and transverse plane rotations especially.

2.3.3.2 PiG and cluster protocols comparison

Nine kinematics variables were analysed for each subject's left side and comparisons made between protocols. Data obtained from the new Vicon Mx Gigaset system

were used for this analysis. Mean and standard deviation were calculated from three trials.

Joint rotations pattern and range were in good agreement with previously reported kinematic results, displaying typical kinematic patterns in the three, x, y, z directions. Joint angles for hip, knee and ankle in each plane as obtained by PiG and the cluster protocol are shown in Figure 2.14, 2.15 and 2.16 respectively for a typical participant.

Significant differences (p -value < 0.05) between PiG and cluster protocol kinematic variables are highlighted by grey bars in a point by point basis at the bottom of each graph.

Corresponding angle parameters for each joint are reported in the Tables 2.6, 2.7 and 2.8 for the same subject for whom the graphs are given.

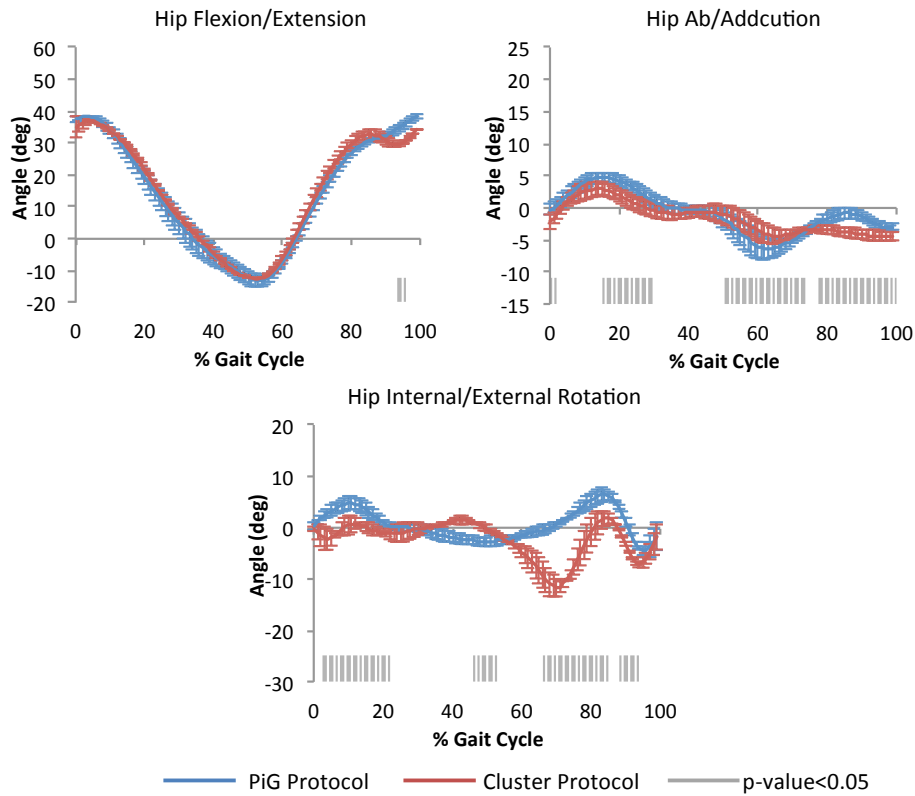


Figure 2.14: Hip joint angles about the three axes (X, Y, Z) as mean (\pm standard deviation bars) over three gait cycles for PiG protocol (blue solid line) and cluster protocol (red solid line) of a representative subject. Statistical significant differences throughout the gait cycle are reported as grey bars.

| Hip angle Parameters (°) | Protocols | | T-Test p-Value |
|--------------------------|--------------------|--------------------|----------------|
| | PiG | Cluster | |
| H1 | 37.5 (\pm 1.0) | 34.9 (\pm 3.2) | 0.16 |
| H2 | -13.2 (\pm 1.9) | -14.0 (\pm 0.0) | 0.68 |
| H3 | 38.2 (\pm 0.7) | 36.1 (\pm 0.1) | 0.07 |
| H4 | 4.7 (\pm 0.8) | 2.9 (1.1) | 0.34 |
| H5 | -6.4 (\pm 1.6) | -4.5 (\pm 0.7) | 0.32 |
| H6 | 4.8 (\pm 1.3) | 1.5 (\pm 0.8) | 0.08 |
| H7 | -4.5 (\pm 0.8) | -11.7 (\pm 1.7) | 0.06 |

*Statistically significant difference

Table 2.6: Hip joint angle parameters of a representative subject as mean (\pm SD) over 3 gait cycles calculated by the PiG and cluster protocol.

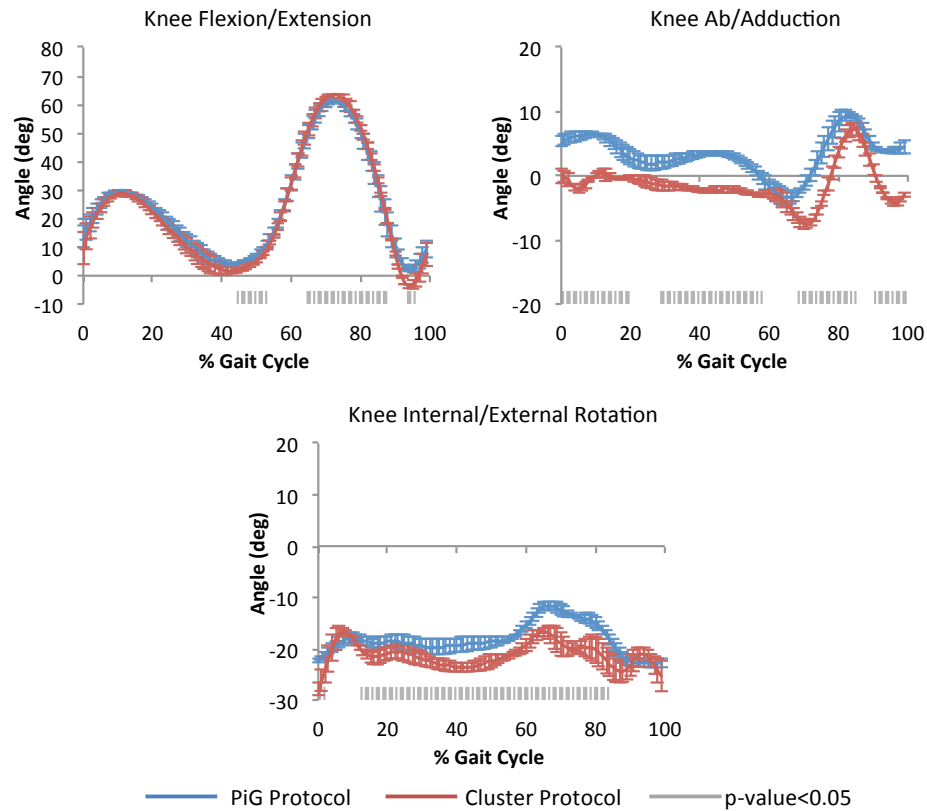


Figure 2.15: Knee joint angles about the three axes (X, Y, Z) as mean (\pm standard deviation bars) over three gait cycles for PiG protocol (blue solid line) and cluster protocol (red solid line) of a representative subject. Statistical significant differences throughout the gait cycle are reported as grey bars.

| Knee angle Parameters (°) | Protocols | | T-Test p-Value |
|---------------------------|--------------------|--------------------|----------------|
| | PiG | Cluster | |
| K1 | 13.6 (\pm 3.9) | 12.1 (\pm 3.1) | 0.66 |
| K2 | 29.8 (\pm 0.6) | 28.9 (\pm 0.9) | 0.26 |
| K3 | 4.1 (\pm 0.8) | 1.7 (\pm 1) | 0.04* |
| K4 | 61.1 (\pm 0.5) | 63.4 (\pm 0.14) | 0.01* |
| K5 | 6.5 (\pm 0.3) | 0.31 (\pm 1.7) | 0.02* |
| K6 | 9.7 (\pm 0.8) | 7.2 (\pm 0.96) | 0.03* |
| K7 | -15.3 (\pm 0.7) | -16.6 (\pm 0.9) | 0.12 |
| K8 | -22.9 (\pm 0.9) | -25.9 (\pm 1.9) | <0.00* |

*Statistically significant difference

Table 2.7: Knee joint angle parameters of a representative subject as mean (\pm SD) over 3 gait cycles calculated by the PiG and cluster protocol.

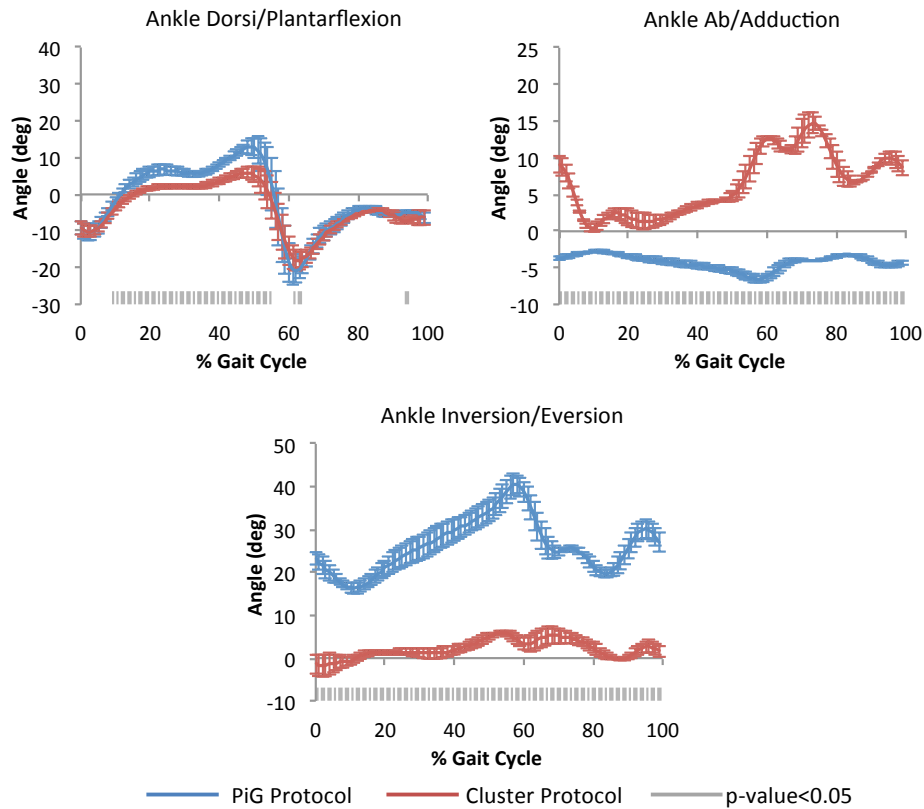


Figure 2.16: Ankle joint angles about the three axes (X, Y, Z) as mean (\pm standard deviation bars) over three gait cycles for PiG protocol (blue solid line) and cluster protocol (red solid line) of a representative subject. Statistical significant differences throughout the gait cycle are reported as grey bars.

| Ankle angle Parameters (°) | Protocols | | T-Test |
|----------------------------|--------------------|--------------------|---------|
| | PiG | Cluster | p-Value |
| A1 | -9.2 (\pm 1.9) | -9.2 (\pm 1.9) | 0.90 |
| A2 | -10.3 (\pm 2.2) | -10.1 (\pm 1.4) | 0.92 |
| A3 | 12.9 (\pm 2.2) | 5.9 (\pm 1.6) | 0.01* |
| A4 | -20.9 (\pm 3.4) | -18.1 (\pm 2.4) | 0.31 |
| A5 | -3.2 (\pm 0.1) | 14.8 (\pm 1.4) | <0.00* |
| A6 | 40.7 (\pm 2.2) | 6.0 (\pm 0.4) | <0.00* |
| A7 | 19.6 (\pm 0.9) | -0.37 (\pm 0.1) | <0.00* |

Table 2.8: Ankle joint angle parameters of a representative subject as mean (\pm SD) over 3 gait cycles calculated by the PiG and cluster protocol.

Although these graphs and tables refer to only one subject they were found to represent well the overall group of subjects and analyses.

The following general findings were found:

1) A change in gait analysis protocol caused different graphs of joint kinematic throughout the gait cycle in all subjects, some of which were statistically significant.

2) Sagittal plane rotations were the least affected by a change in protocol when compared to transverse and coronal plane rotations. The time histories of hip and knee joint angles in the coronal and transverse plane showed the same path throughout the gait cycle but with an offset in all subjects. This could be as low as 5° but up to 20°.

3) Ankle out of sagittal plane rotations (inversion/eversion; ab/adduction) showed the lowest agreement between protocols among the measured kinematic variables, with curves being far apart and with different trends (Figure 2.16). All transverse and coronal plane parameters extracted from the curves, A5, A6, A7 were significantly different between PiG and the cluster method ($p\text{-value} < 0.05$). This was related to the different convention adopted by PiG and the cluster protocol in the evaluation of the foot and ankle complex.

Interestingly, it was found PiG to predict high knee adductions in swing phase (K6) where lower value would be expected and were obtained by the cluster protocol (Table 2.7). Differences in knee swing adductions were significant for 7 out of 10 subjects ($p\text{-value} < 0.05$) (Table 2.7).

| Subjects | Knee adduction peaks (°) | |
|----------|--------------------------|-------------|
| | PiG | Cluster |
| 1 | 24.9 (±1.0) | 6.3 (±0.6) |
| 2 | 9.7 (±0.8) | 7.2 (±0.9) |
| 3 | 14.4 (±0.3) | 9.03 (±1.6) |
| 4 | 1.9 (±0.4) | 7.02 (±1.0) |
| 5 | 10.6 (±1.2) | 6.1 (±0.5) |
| 6 | 6.3 (±0.3) | 6.9 (±1.5) |
| 7 | 19.3 (±0.5) | 7.5 (±1.2) |
| 8 | 8.2 (±1.8) | 4.5 (±0.9) |
| 9 | 9.3 (±8.4) | 5.2 (±1.0) |
| 10 | 24.8 (±0.9) | 6.1 (±2.5) |

Table 2.9: Mean (\pm SD) of knee adduction peak values in swing phase over 3 gait cycles expressed in degrees ($^{\circ}$) calculated with the PiG and cluster protocol for each participant (1 to 10).

The lowest consistency in adduction rotations during swing between the two protocols was obtained in subject 1 (Figure 2.17), 7 and subject 10 with differences in a range of 11 to 19 $^{\circ}$.

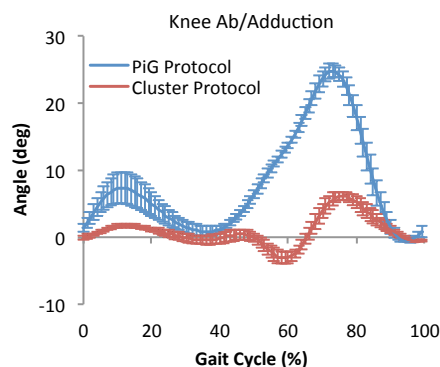


Figure 2.17: Knee Ab/Adduction angles of subject 1 as obtained by PiG (blue solid line) and Cluster protocol (red solid line). SD bars are also illustrated along each corresponding curve.

The comparison between PiG and cluster protocol revealed inter-protocol differences to be more evident than intra-subject (Figure 2.14, 2.15, 2.16) and motion analysis systems discrepancies (Figure 2.12, 2.13). A small intra-subject variability was observed for each kinematics outcome in both protocols over 3 repetitions performed by the same subject. Standard Deviation (SD) bars, in the figures reported above, provide information on the dispersion of the time histories of each measure for one representative subject. Variability of extracted joint angle parameters for the same

subject can be extracted from the standard deviations reported in brackets in the Tables 2.6, 2.7, 2.8. The small standard deviations are indicative of a good repeatability of the protocols outcomes.

To allow an overall analysis of intra-protocol variability, repeatability of joint angles calculation within a protocol for each subject was summarised in the average value of the standard deviation of each joint angle throughout the gait cycle and by the absolute mean standard deviation. Absolute mean standard deviation represents the standard deviation normalised to the range (max-min) of motion of the relative measure and expressed as its percentage. These values are reported in Table 2.10 for hip rotations and in Table 2.11, 2.12 for knee and ankle respectively.

| Subjects | HIP Rotations SD (°,%) | | | | | |
|----------|------------------------|------------|------------------|------------|----------------|-----------|
| | Ab/Adduction | | Int/Ext Rotation | | Flex/Extension | |
| | PiG | Cluster | PiG | Cluster | PiG | Cluster |
| 1 | 0.7(5.6%) | 0.8(6.5%) | 1.1(7.8%) | 0.5(4.2%) | 1.9(4.2%) | 1.6(3.8%) |
| 2 | 0.9(8.4%) | 0.9(13.0%) | 0.9(8.2%) | 1.1(8.9%) | 1.6(3.0%) | 0.7(1.4%) |
| 3 | 1.2(13.9%) | 0.9(13.1%) | 1.0(8.6%) | 1.3(8.2%) | 1.0(2.5%) | 1.1(2.6%) |
| 4 | 0.5(4.8%) | 0.6(8.5%) | 0.5(5.7%) | 0.8(8.3%) | 1.0(2.3%) | 0.9(1.9%) |
| 5 | 1.2(9.6%) | 1.0(15.0%) | 0.7(4.9%) | 0.9(6.7%) | 1.6(3.9%) | 1.0(2.7%) |
| 6 | 1.3(23.1%) | 1.2(13.9%) | 1.5(14.8%) | 1.6(17.6%) | 1.3(2.9%) | 1.9(4.7%) |
| 7 | 0.5(9.9%) | 0.6(8.9%) | 0.6(6.5%) | 0.7(9.0%) | 1.3(2.9%) | 1.3(3.1%) |
| 8 | 0.8(6.9%) | 0.8(7.4%) | 1.5(7.4%) | 1.2(9.3%) | 1.9(4.3%) | 1.3(3.2%) |
| 9 | 1.6(16.9%) | 0.5(7.1%) | 0.8(5.5%) | 1.0(7.1%) | 1.1(2.7%) | 1.1(2.6%) |
| 10 | 1.2(8.3%) | 1.0(6.3%) | 1.3(7.2%) | 1.4(14.8%) | 2.4(5.7%) | 2.9(8.5%) |

Table 2.10: Mean (°) and absolute mean (% of range of motion) of standard deviation values for hip joint angles for all study participants (1-10) for both PiG protocol and cluster protocol.

| Subjects | KNEE Rotations SD (°,%) | | | | | |
|----------|-------------------------|------------|------------------|------------|----------------|-----------|
| | Ab/Adduction | | Int/Ext Rotation | | Flex/Extension | |
| | PiG | Cluster | PiG | Cluster | PiG | Cluster |
| 1 | 1.1(4.4%) | 0.6(6.5%) | 0.7(3.8%) | 0.7(5.9%) | 2.0(3.3%) | 2.0(3.1%) |
| 2 | 0.8(6.2%) | 0.6(4.0%) | 1.0(9.0%) | 1.4(13.0%) | 1.7(2.9%) | 1.5(2.2%) |
| 3 | 0.5(5.0%) | 0.8(4.7%) | 1.2(5.2%) | 1.7(9.2%) | 2.0(3.1%) | 2.3(3.4%) |
| 4 | 0.4(4.0%) | 0.4(3.3%) | 0.9(5.6%) | 1.0(5.8%) | 1.8(3.3%) | 1.8(3.0%) |
| 5 | 0.8(6.3%) | 0.7(7.8%) | 0.6(3.5%) | 1.0(4.0%) | 2.5(4.4%) | 1.7(2.8%) |
| 6 | 0.7(5.0%) | 1.0(12.4%) | 1.4(4.6%) | 1.5(8.5%) | 2.2(3.4%) | 2.1(2.9%) |
| 7 | 0.4(2.6%) | 0.6(6.5%) | 1.0(4.8%) | 1.0(6.9%) | 1.7(2.7%) | 1.7(2.4%) |
| 8 | 1.2(10.3%) | 0.5(9.4%) | 1.6(6.5%) | 1.2(5.3%) | 3.4(6.1%) | 1.5(2.3%) |
| 9 | 3.8(57.7%) | 0.4(10.2%) | 6.5(88.9%) | 1.4(10.4%) | 3.2(6.2%) | 2.5(4.0%) |
| 10 | 1.8(7.1%) | 1.1(10.4%) | 0.9(5.8%) | 1.0(6.8%) | 3.2(5.6%) | 2.6(3.8%) |

Table 2.11: Mean (°) and absolute mean (% of range of motion) of standard deviation values for knee joint angles for all study participants (1-10) for both PiG protocol and cluster protocol.

| Subjects | ANKLE Rotations SD (°) | | | | | |
|----------|------------------------|------------|------------------|------------|----------------|-----------|
| | Ab/Adduction | | Int/Ext Rotation | | Flex/Extension | |
| | PiG | Cluster | PiG | Cluster | PiG | Cluster |
| 1 | 0.5 (13.9%) | 0.8(5.3%) | 2.6(13.9%) | 1.5(13.9%) | 1.0(4.4%) | 1.1(4.1%) |
| 2 | 0.3(8.2%) | 0.7(5.2%) | 2(8.3%) | 1.1(15.1%) | 1.8(5.3%) | 1.3(5.3%) |
| 3 | 0.3(10.9%) | 0.9(6.3%) | 2.3(10.5%) | 1.4(13.7%) | 1.2(4.3%) | 0.9(3.4%) |
| 4 | 0.3(5.8%) | 0.7(9.0%) | 1.9(5.8%) | 1.6(15.4%) | 1.1(3.5%) | 0.9(3.9%) |
| 5 | 0.3(5.9%) | 0.7(4.2%) | 1.6(6.0%) | 1.0(9.1%) | 1.3(3.9%) | 1.3(5.0%) |
| 6 | 0.3(6.0%) | 1.2(13.6%) | 1.8(6.0%) | 1.1(7.7%) | 1.2(5.4%) | 1.6(7.4%) |
| 7 | 0.1(9.2%) | 0.7(4.8%) | 1.6(9.2%) | 1.4(8.3%) | 1.1(4.5%) | 1.2(4.3%) |
| 8 | 0.7(6.4%) | 0.9(8.3%) | 2.4(6.5%) | 0.8(5.8%) | 1.6(6.0%) | 0.9(3.8%) |
| 9 | 1.3(30.7%) | 1.2(8.5%) | 6.6(30.7%) | 1.6(10.9%) | 1.5(5.5%) | 1.6(5.0%) |
| 10 | 0.3(9.3%) | 0.8(8.6%) | 1.7(9.4%) | 1.0(7.9%) | 1.9(7.5%) | 1.9(7.4%) |

Table 2.12: Mean (°) and absolute mean (% of range of motion) of standard deviation values for ankle joint angles for all study participants (1-10) for both PiG protocol and cluster protocol.

Overall a good repeatability was observed among the measured variables for both methods, despite high absolute standard deviation values observed for subject 9 for knee internal/external rotation and ab/adduction. Standard deviation mean value (in degree) was confined to 3° for all rotations among all subjects for the cluster method and to 7° for PiG. The maximum mean SD for the cluster method was of 2.6° for knee flexion/extension, whereas for the PiG method the highest mean standard deviation corresponded to 6.6° found for ankle inversion/eversion measurement. Minimum mean SD was 0.4° for knee ab/adduction of the cluster protocol and 0.1° for ankle ab/adduction of the PiG protocol.

When expressing the average standard deviation values as percentage of the allowed range of motion at each joint and anatomical plane, the highest repeatability (lowest % values) was observed in both protocols for sagittal plane rotations since greater ranges of motion are allowed at the joints in that plane. In particular, lowest absolute SDs were obtained for hip and knee flexion/extension angles; absolute standard deviation values as low as 1.4% and 2.3% for cluster and PiG respectively. Less repeatable were instead coronal and transverse plane rotations with a variability as great as 17.6% for the cluster and as 88.8% for PiG.

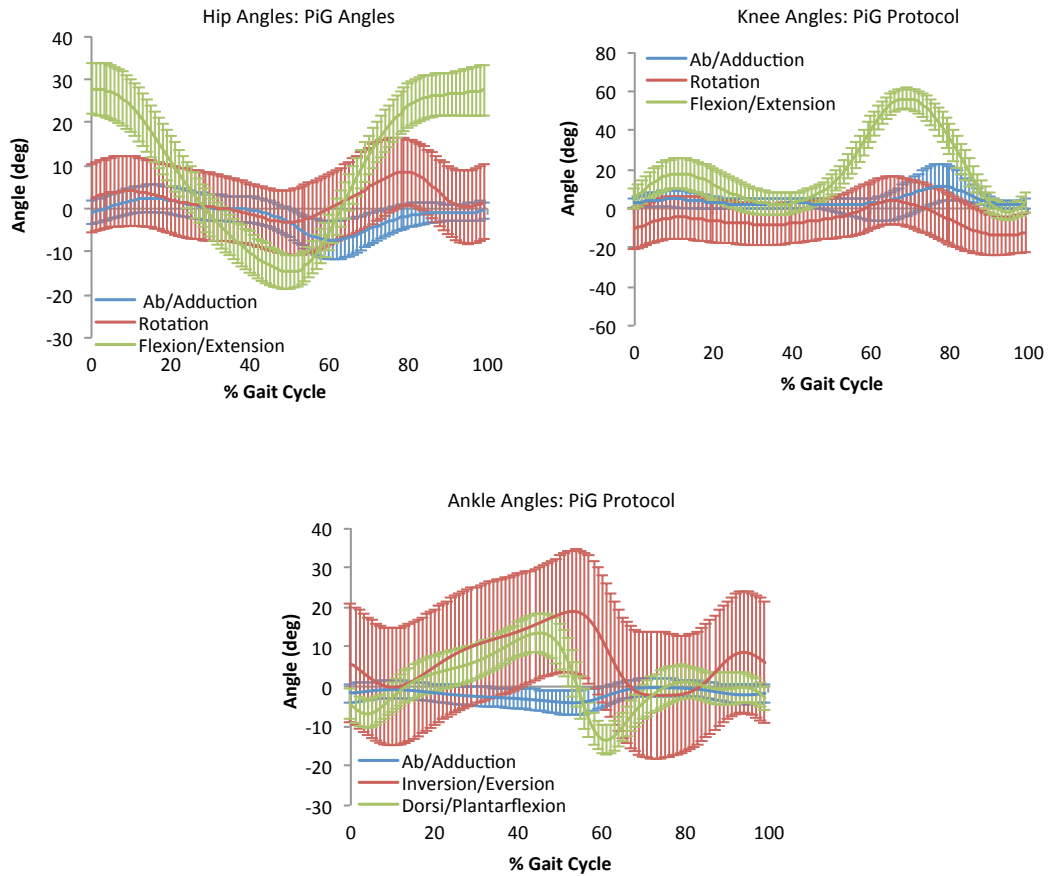


Figure 2.18: Hip, knee and ankle kinematics for PiG protocol as mean over 3 gait cycles for all 10 participants. SD bars are shown along each curve throughout the gait cycle.

Kinematics outcomes were also analysed to assess inter-subject variability. The mean and standard deviation over 3 trials for all ten participants of joint kinematics is shown in Figure 2.18 for the PiG protocol and in Figure 2.19 for the cluster protocol.

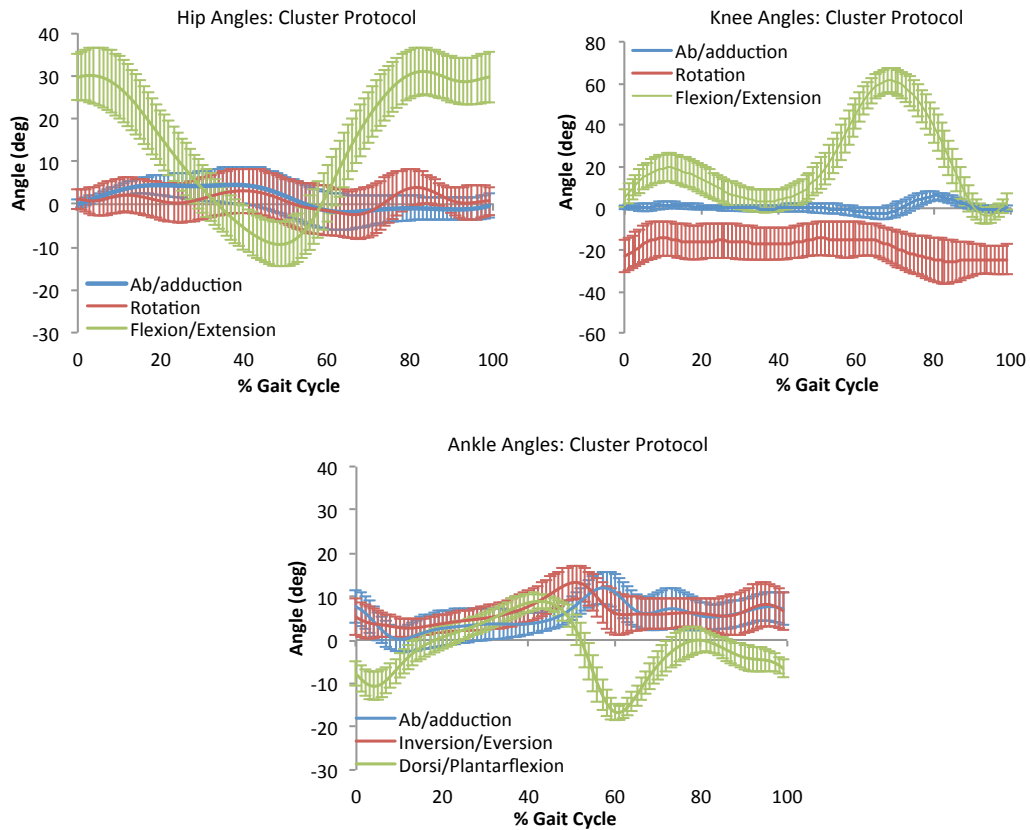


Figure 2.19: Hip, knee and ankle kinematics for cluster protocol as mean over 3 gait cycles for all 10 participants. SD bars are shown along each curve throughout the gait cycle.

Relative joint angle parameters as mean across all subjects are reported in Table 2.13 for the PiG and cluster protocol. Differences in joint parameters with a change in protocol were mostly evident in transverse and coronal plane (p -values <0.05), similarly to what obtained for a single subject comparison. However, ankle parameters in the sagittal plane (A1, A2, A3, A4) were also significantly different between the two protocols.

| Joint Parameters (°) | Protocols | | T-Test |
|----------------------|-------------|-------------|---------|
| | PiG | Cluster | p-Value |
| Hip (°) | | | |
| H1 | 27.7 (5.9) | 29.7 (5.3) | 0.44 |
| H2 | -15.1 (3.6) | -9.9 (5.1) | 0.02* |
| H3 | 28.6 (5.8) | 32.1 (5.5) | 0.19 |
| H4 | 2.6 (3.0) | 5.74 (3.4) | 0.04* |
| H5 | -7.5 (4.5) | -3.2 (3.2) | 0.02* |
| H6 | 4.6 (8.1) | 5.1 (3.6) | 0.84 |
| H7 | -1.8 (7.7) | -4.2 (5.4) | 0.43 |
| Knee (°) | | | |
| K1 | 5.1 (5.6) | 4.9 (4.3) | 0.92 |
| K2 | 18.0 (7.8) | 19.5 (6.7) | 0.66 |
| K3 | 1.8 (5.7) | 2.9 (5.4) | 0.67 |
| K4 | 56.7 (5.4) | 61.7 (5.8) | 0.06 |
| K5 | 6.9 (5.7) | 1.8 (1.7) | 0.02* |
| K6 | 12.5 (8.0) | 6.5 (1.7) | 0.04* |
| K7 | 0.9 (12.8) | -11.5 (8.5) | 0.03* |
| K8 | -18.5 (5.8) | -28.4 (8.9) | 0.02* |
| Ankle (°) | | | |
| A1 | -4.42(3.8) | -7.9 (2.8) | 0.03* |
| A2 | -6.9 (3.6) | -10.8 (3.3) | 0.02* |
| A3 | 13.9 (4.8) | 9.3 (1.6) | 0.01* |
| A4 | -13.7 (3.6) | -16.9 (1.8) | 0.02* |
| A5 | 0.024 (2.1) | 10.8 (3.8) | <0.00* |
| A6 | 19.8 (15.6) | 13.6 (3.8) | 0.25 |
| A7 | 4.1 (14.7) | 3.4(2.9) | 0.14 |

*Significant difference (p -value < 0.05) for PiG against Cluster

Table 2.13: Mean (SD) for joint angle parameters across all subjects for PiG and cluster protocols. T-test results are shown in the last column.

Inter-subject variability (Figure 2.18, 2.19, Table 2.14) as expected was higher than intra-subject variability as it accounts for the intrinsic variation among subjects gait patterns. Mean standard deviation and absolute mean standard deviation values among 10 subjects for joint kinematics of both protocols are reported in Table 2.14. Comparable values of standard deviations between the two protocols were mostly observed (Table 2.14).

| Protocols | HIP Rotations SD (°,%) | | | KNEE Rotations SD (°) | | | ANKLE Rotations SD (°) | | |
|-----------|------------------------|----------------|----------------|-----------------------|-----------------|----------------|------------------------|-----------------|----------------|
| | Ab/Add | Rot | Flex/Ext | Ab/Add | Rot | Flex/Ext | Ab/Add | Rot | Flex/Ext |
| PiG | 3.1 (32.2%) | 8.0 (68.5%) | 5.0 (11.9%) | 4.7 (49.1%) | 11.1 (62.0%) | 6.3 (10.9%) | 2.4 (63.3%) | 14.9 (70.7%) | 4.3 (15.8%) |
| Cluster | 3.1 (49.4%) | 4.6 (72.8%) | 5.9 (14.7%) | 1.9 (23.3%) | 8.3 (74.1%) | 6.5 (9.8%) | 4.1 (29.2%) | 4.4 (33.7%) | 2.7 (10.4%) |

Table 2.14: Mean (°) and absolute mean (%) values of angle standard deviation among the ten participants for both protocols.

For the cluster protocol, mean standard deviation maximum and minimum values were respectively 8.3° (knee int/external rotations) and 1.9° (knee ab/adduction). Maximum and minimum values of mean standard deviation for joint rotations as calculated by PiG protocol for the 10 participants were instead 14.9° for ankle inversion/eversion and 2.4° for ankle ab/adduction respectively. As for the cluster protocol, however, also knee rotation for PiG shown high variability among subjects (11.1°).

To the regards of absolute standard deviation, the lowest repeatability (high %), as also found for within subjects comparisons, was obtained for coronal and transverse plane rotations rather than sagittal plane angles. Values of mean absolute standard deviation for coronal and transverse plane rotations could overcome 70% of the relative range of motion for both PiG and cluster protocols.

Inter-subject variability in angle peaks parameters is shown by the standard deviation in brackets in Table 2.13. Comparable variability can be observed between the two protocols, although for all parameters but H2, H4, K4, K8, A5, standard deviations from PiG protocol were smaller than the one given by cluster protocol. A higher degree of inter-subject variation is apparent for out of the sagittal plane parameters rather than for flexion/extension peaks.

2.3.4 Discussion and Conclusion

Motion capture system comparison revealed that 3-D trajectories from the T160 and T40-based system, as one would expect, were more accurate than the one obtained by MCam-based system. Reconstruction residuals either static or dynamic were always under 1 mm for the T160 cameras, whereas MCam residuals went up to almost 3 mm. This is due to the more performing specifications of the T-series cameras. The higher resolution (more megapixels) and the grayscale marker fitting allow markers to be seen from greater distance and more precisely, reducing also the presence of ghost and merging markers. Moreover the superior number of cameras, 12 T-series against 8 MCam, increased the likelihood of one marker to be seen simultaneously by more than two cameras to contribute to the calculation of the 3-D reconstruction.

The accuracy with which the markers centroids were calculated was also reflected in the kinematic profiles obtained from data collected by both systems and processed with a same protocol. Differences, although for the majority not significant, were observed in the data from the two systems, mostly in planes other than sagittal and for cluster outcomes. Since anatomical frame position and orientation is derived from captured markers in each sampled instant of time, differences in the coordinates of markers detected by the two camera types directly affect kinematic outputs as shown in the study results. More markers are involved in the definition of anatomical frames in the cluster model and thus this may explain why differences were more noticeable for this protocol outputs rather than in PiG outcomes.

Kinematic outputs were system dependent and thus a powerful capture system with cameras positioned to allow marker tracking from more than 2 cameras simultaneously and well calibrated, will benefit to the accuracy of the measurements. If an accurate marker position reconstruction can be obtained, the instrumentation error introduced by the capturing system, will be lessen to a minimum.

One of the main aims in gait analysis is to obtain reliable measurements, which could be safely used for clinical decisions. This should be pursued, in addition to the use of an accurate data collection system, through procedures that, despite the fact of being subject-specific, are repeatable among individuals and easy and rapid to be implemented. Joint angles as obtained by the cluster protocol, for the able-bodied population analysed, were found to be mostly in agreement with previous studies and consistent across subjects. Comparison of the present results for the ankle out of sagittal plane angles, however, is difficult due to the lack of studies that used the same definition for ankle rotation. Only one study (Schache and Baker, 2007) has been found describing ankle kinematic similarly to the cluster model and results provided are comparable to the one obtained in the current study.

Although knee ab/adduction, is generally stated to be affected by errors deriving by knee flexion/extension axis misalignment leading to high peak of adduction in swing phase, this was not observed in knee angles calculated with the cluster model.

Similar knee ab/adduction trends were observed throughout the gait cycle among the 10 participants with an average peak value in swing phase achieved of 7.5° with a variation of 1.7° across the ten subjects.

Similarly to what has been reported in other studies, quite high values were found for knee internal/external rotation. It is difficult to properly describe the real movement allowed at the knee joint in the transverse plane. However, a general trend could be appreciated among subjects in knee transverse rotation pattern. Evaluation of this kinematic parameter remains controversial and attention should be paid when calibrating anatomical landmarks used to define the knee joint coordinate system. Good intra and inter-subject variability was achieved when processing the data with the cluster biomechanical model with mean standard deviation values confined to 3° for all rotations within a subject, and, to 10° across the group. Higher repeatability was observed in sagittal plane kinematics.

A protocol that described in a repeatable manner joint rotations, in adherence with the clinical understandings, has been proposed. The underlying biomechanical model is partially based on anatomical frames defined in standard recommendations to facilitate data sharing and comparison across laboratories. As highlighted elsewhere (Ferrari et al., 2008) in fact, the protocol used can affect measured outcomes and lead to misleading interpretation of the results. This was, once again, confirmed through the conducted comparison of PiG and cluster protocol kinematic outcomes.

Differences in kinematic profiles were found between the two protocols particularly in coronal and transverse planes. This however was expected and the reasons for this finding can be related to the differences in the assumptions of each protocol. To start with, the hip joint centre (HJC) is calculated by different regression equations in the two models. Whereas PiG bases the HJC calculation on Davis et al.'s method (Davis et al., 1991), the cluster protocol exploits the equations introduced by Harrington et al. (2007). Unfortunately, there is not such a conventional and agreed method to calculate hip centre of rotation. However, based on the review conducted, Harrington et al.'s method was found to be the more accurate among predictive and, functional methods as well (Peters et al., 2010). Due to a biomechanics model being a 'downstream' model, errors or differences at proximal segments propagates down to distal segment definitions and computations. Having different HJC coordinates influences, in fact, both hip and knee anatomical frames and thus the relative kinematics. This could be one of the reasons that justify the differences in the kinematic profiles derived by the two protocols. Moreover, discrepancies exist also

on the kinematic convention/definition adopted by the two models for computing joint angles; one method using the joint coordinate system convention, and the other, PiG, Euler angles definition as reported by Kadaba et al. (1990) and Davis et al. (1991).

Different anatomical frames are used to define ankle-foot complex movement explaining the large diversion between ankle transverse and coronal plane rotations. The definition proposed for the foot axes, contrarily to PiG, is based on the anatomy of the segment and it is fully 3-D. The correctness of PiG ankle angles other than dorsiflexion/plantarflexion is questionable.

High peak of knee adduction during swing were observed in the data analysed with PiG but not in the cluster processed data. Adduction values obtained at the knee with the former protocol in swing were as high as 25° but the relative measure with the cluster was smaller. This might be explained with the definition of the knee flexion/extension axis and related cross talk at the joint coronal rotation and, also by erroneous marker positioning.

Although PiG is based on a simple marker set which requires a maximum 16 markers on the lower legs of the test subject, making a fast implementation possible and an advantage of this protocol in routine experiments, the position of these markers is crucial for the correctness of the outcomes. PiG markers are used to both define anatomical landmarks and planes where joint centres lie. In contrast with the cluster method, the PiG model seemed to be greatly affected by a wrong markers alignment either being ALs markers or technical ones. This was verified by a further investigation conducted on the latter method. Varying a single marker in segment definitions and joint centre calculation, differences were observed in joint kinematics trends. Marker clusters position on the other hand, does not represent a limitation for model accuracy and the use of such rigid plates is meant to reduce skin movement artefact mostly associated with single markers attachment in the proximity of joint, as required in the PiG marker set. A proper awareness of how this protocol works, without rushing to markers attachment, is necessary to avoid poor quality data and misleading results. However, incorrect location of anatomical landmarks represents a source of errors in gait analysis independently from the protocol employed and thus attention should be always paid during their identifications.

The advantage of PiG is the fast implementation, as it does not require more than one calibration trial, while 9 were necessary for the cluster method using the calibration pointer. On its side, the latter method, to counter balance that, calculates automatically anthropometric measurement from the known position of calibrated anatomical landmarks. PiG instead requires these values to be taken from the subject and then input before running the model; some time saved is then lost while taking these measurements. However, this process could be not relevant for the patient as they can sit while anthropometric data are measured but of more concern could be standing still while the pointer calibrations are conducted. During a first attempt of collecting data with a stroke patient, the volunteer, in fact, showed tiredness and difficulties in maintaining a standing position while performing static trials. Avoiding a long calibration process is advisable if the protocol is to be applied with stroke survivors and this should be considered in a further development and improvement of the cluster protocol.

Both protocols behaved well in terms of intra-subject and inter-subjects variability, although slightly higher value of standard deviation were observed in PiG protocol. A general acceptable agreement was found across the measured kinematic variables despite the discussed differences between the two protocols. Although the cluster method is characterised by a longer procedure, the time is paid back by an acquired accuracy in the description of joint movement as shown by more realistic measurements of out of sagittal plane rotation when compared with PiG.

If data are to be shared and compared across laboratories importance should be given to a detail definition of the conventions adopted in order to understand and properly interpret the derived outcomes from a gait analysis protocol if the same model cannot be used.

In conclusion, in the study described the effects different capture systems have on produced outcomes were evaluated, a new protocol for gait analysis was presented and its robustness assessed, and finally comparisons of the cluster protocol with a widely used clinical gait analysis protocol, Plug-In-Gait, were discussed. It emerged that reliability of the measurements is based on sound biomechanical assumptions, correct identification of anatomical landmarks and on the capability of the tracking

system. The cluster method shall it be revised on the regards of the calibration trials to accelerate the data collection process.

2.4 Further developments of the cluster protocol

The cluster protocol was slightly modified to better meet the need of an early after stroke population, particularly fast implementation to avoid fatigue. Moreover additional features, such as pelvic angle calculation and kinetic measurements, were added to reinforce the biomechanical evaluation of stroke patient gait. Those characteristics included in the protocol are briefly discussed in the next three sections.

In addition, the previous waist band with four markers attached was substituted by a rigid cluster with four markers on it. This was done to allow a better definition of the pelvis technical frame from the four non collinear markers on the cluster rather than markers placed on the same line as originally done with the previously described and used marker set.

2.4.1 *Anatomical landmark calibration*

The drawback of the original cluster protocol that emerged from the previous study was the long time required for anatomical landmarks calibration. A total of eight static standing trials were required for each subject while the examiner identified anatomical landmark with a pointer. This represents a limitation when using the cluster protocol with stroke survivors who can get tired fairly easily. The use of the pointer for calibration was thus superseded by the use of individual markers (Table 2.15) applied directly on the anatomical landmarks. These static calibration markers were removed during dynamic trials captures. Combining the easy and fast positioning of clusters of markers with directly attached markers for static calibration reduced to a minimum the time required for subject preparation and thus patient discomfort during test sessions. The validity of this procedure, in comparison to the pointer calibrations, was tested in another study, which is presented in the next section (2.5) of this Chapter.

| Marker | Marker Placement |
|-------------|---|
| RASI/LASI | Left/Right anterior superior iliac spine |
| RPSI/LPSI | Left/Right posterior superior iliac spine |
| RLEPI/LLEPI | Left/Right lateral epicondyle |
| RMEPI/LMEPI | Left/Right medial epicondyle |
| RLMAL/LLMAL | Left/Right lateral malleolus |
| RMMAL/LMMAL | Left/Right medial malleolus |

Table 2.15: Anatomical landmarks static calibration markers, name and position are reported.

2.4.2 Pelvic angles

Computation of pelvic rotations with respect to gravity were added to the Body Builder code written for data processing (Electronic Appendix). Such rotations are calculated as the orientation of the pelvis (distal) segment relative to the laboratory frame (proximal segment). Conventionally pelvic angles are described by the Cardan sequence of Tilt, Obliquity, Rotation (TOR) analogue to Flexion/extension, Ab/adduction, Int/External rotation sequence applied for the calculation of the other lower limb joints angles. However, it has been suggested that the use of this sequence for the measurement of pelvic angles lead to results which are not consistent with the clinical understanding of these movements and show low agreement with visual assessments (Baker et al., 2001; Foti et al., 2001; Dickens et al., 2009). The sequence, Rotation, Obliquity, Tilt (ROT) as firstly proposed by Baker et al. (2001), was therefore adopted for the description of pelvic motion as it allows for a more realistic description of pelvic motion. In the convention adopted pelvic rotation are defined as follows (Baker et al., 2001, 2003):

Rotation is the angle of rotation of the pelvis about a vertical axis and which occurs in the horizontal plane by which one point is in front of its mirror image,

Obliquity is the angle of rotation of the medio/lateral axis of the pelvis out of the horizontal plane, by which one point is higher than its mirror image,

Tilt is the angle about the medio/lateral axis of the pelvis.

Accordingly to the ROT sequence and the joint coordinate system convention (Grood and Suntay, 1983), the rotations are described as occurring: the first rotation, around a vertical axis (\hat{e}_1) fixed in the laboratory segment (proximal segment), the third rotation around the medio/lateral axis (\hat{e}_3) of the pelvis (distal segment), and the

second rotation about a floating axis (\hat{e}_2) mutually perpendicular to \hat{e}_1 and \hat{e}_3 . For the definition of pelvic angles, the laboratory frame was defined by considering as the x-axis the actual direction of progression of the subject rather than the global x-axis in absolute terms. The direction of progression was identified as the trajectory of the mid point between the two anterior superior iliac spines, right and left, averaged across seven frames forward and backward to the one being analysed. This allowed to identify the orientation of the progression axis in each sampled instant of time. Rotation, obliquity, tilt angles were computed adapting the formulations extracted from Cole et al. (1993) and previously reported, to the new axes definition.

2.4.3 Joint moments

3-D joint moment estimation was added to the outputs of the code. The inverse dynamics approach (Figure 2.20) was used to calculate the moments at the hip, knee and ankle joints.

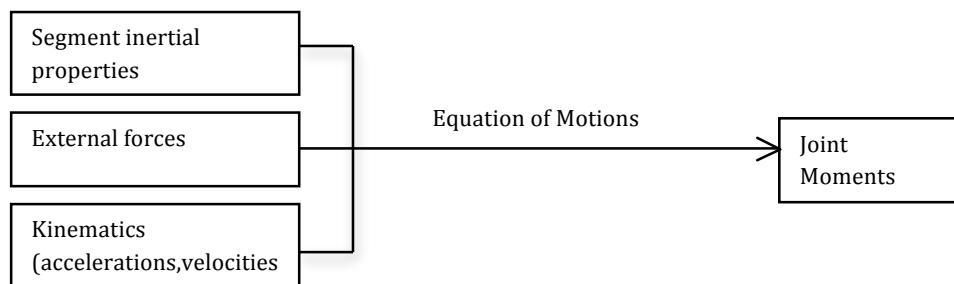


Figure 2.20: Flow chart diagram for the inverse dynamics approach (Hamill and Selbie, 2004).

Inertial and mass properties required for the computation were extracted from Winter (2005). The assumption of rigid body segments was made in the biomechanical model used and thus, all the inertial properties were considered as fixed values. External forces, i.e.: ground reaction forces (GRFs), were measured by force plates. Four force plates (Kistler Instrument AG, Switzerland) were available in the Bioengineering Unit Biomechanics laboratory floor. All four force plates were synchronised with the motion capture system. The last set of data needed for joint moments estimation were kinematic data and in particular segment accelerations. These were calculated by differentiating the

displacement of the segments obtained from the motion capture system. Combining all these data into the equation of motions, internal moments at the lower limb joints can be obtained.

Joint moments as calculated from the written code are expressed in the anatomical frame of the distal segment, of the two segments interconnected by the joint. There is not a universal convention to express joint moment but, to comply with the literature, extension moments are considered as positive as well as abductor and internal rotator moments.

2.5 Validation of the final stroke patient assessment protocol

2.5.1 *Introduction*

A further evaluation of the stroke assessment protocol with the added features discussed previously was undertaken to evaluate the validity of the protocol in estimating pelvis and lower limb joint angles and moments and to determine its ease of use for routine gait analysis of stroke patients.

The protocol was designed to give an accurate and repeatable definition of anatomical segments and a fast and easy implementation. It was designed to reduce subject preparation, which avoids long standing calibration trials, and minimize patients discomfort and tiredness so enhancing their collaboration during test sessions.

The aim of the study was thus to investigate the accuracy and reliability of joint kinematics and kinetics as obtained from the proposed protocol and to evaluate the level of discomfort during the test. With this regard, both pointer calibration trials and anatomical landmark marker calibration trials were performed and the results from both methods compared.

2.5.2 *Methods*

Marker trajectories were captured using a 3-D motion capture system with twelve cameras (Vicon MX Giganet, Oxford Metrics Ltd., UK). Cameras positions were unaltered among test sessions allowing each time a calibrated space of approximately 6 metres in length (Figure 2.21). Ground reaction force data were collected by four

force plates (Kistler Instrumente AG, Switzerland) located in the laboratory floor. Data sampling was set at 100 Hz.

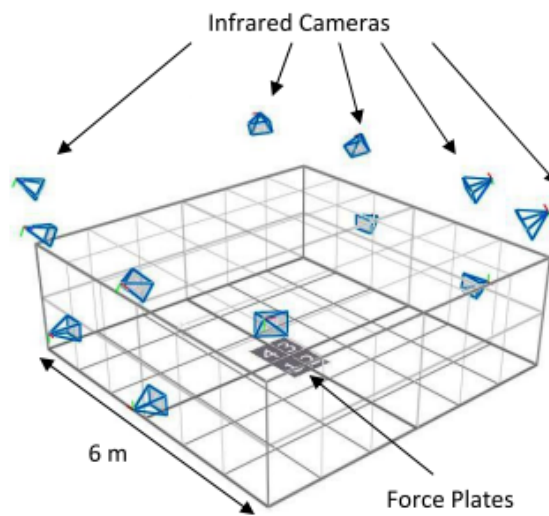


Figure 2.21: Laboratory set up showing the 12 cameras, 4 force plates and the calibrated field of 6 m in length

The marker set (Figure 2.22) previously described was employed for tracking joint movements during barefoot level walking of 6 able-bodied subjects. This consisted of 5 rigid clusters, each comprised of four 14mm diameter markers attached at the distal part of the thigh and shank and on the back of the subject and, three markers on each foot positioned on the first and fifth metatarsal head and on the calcaneus. Twelve skin markers applied on anatomical landmarks (Table 2.15) were used for static calibration purposes and thus removed for dynamic captures. Moreover, a pointer with two markers at a fixed position from its tip, was employed for calibration of the same anatomical landmarks identified by individual skin markers, to allow comparison between the two calibration methods. Clusters and single markers were attached using hypoallergenic double-sided tape and ensuring that a firm positioning was achieved. Neoprene elastic bands were not used to avoid slippages.

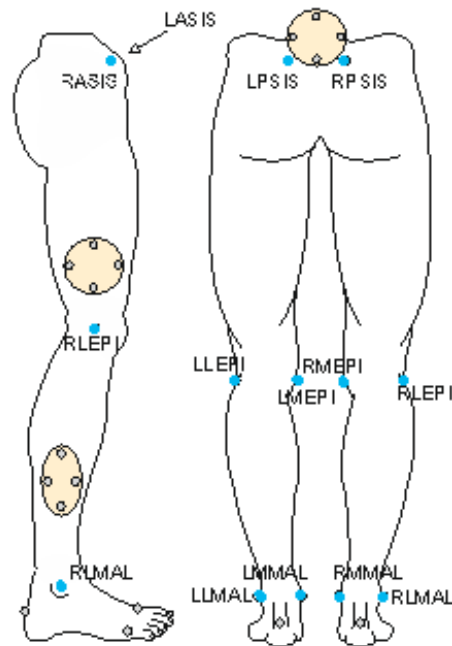


Figure 2.22: Marker set used for data capture. Anatomical landmark markers used for calibration purposes are shown as blue circles.

This marker set allowed the definition of anatomical frames of reference in each sampled instant of time and hence the calculation of joint kinematics and kinetics. The methods and assumptions were as described in the above paragraphs. Six subjects were voluntarily recruited from the Bioengineering Unit community. The participants comprised of three men and three women with a mean height of $168.9 (\pm 10.5)$ cm, body mass of $68.2 (\pm 9.9)$ kg and aged $29.8 (\pm 6.7)$ years. They were asked to wear a tight Lycra suit to facilitate anatomical landmarks identification and clusters and single markers attachments. After completion of subject preparation one static calibration trial was captured according to the final version of the stroke testing protocol and 8 pointer calibration trials were collected as for the original cluster protocol. The subjects stood at the centre of the capture volume for these static trials. Calibration markers were removed prior to acquisition of gait trials. Participants were then asked to walk barefoot at their own normal speed across the capture volume and ten trials for each participant were analysed. Only the trials with a clear heel strike of the left and right foot on one of the four force plates were kept for the analysis. Both right and left gait cycles were evaluated.

Post capture analysis was conducted using Nexus and Bodybuilder softwares (Vicon, Oxford Metrics Ltd., UK). Captured markers coordinates were filtered with Woltring's generalized cross-validation with splines (GCVSPL) method with a predicted mean squared error of 15mm (Woltring 1985; 1986). Kinematic and kinetic data were calculated and time normalised to 101 points. Kinematics outcomes were expressed as a function of 0 to 100 % of the gait cycle and kinetics data as percentage of stance phase.

Time histories of joint angles and moments and related discrete parameters at certain instant of the gait cycle were used for the analysis. The parameters, extracted were those proposed by Benedetti et al. (1998) and used in the previous study (Table 2.3). Kinetics parameters were added and are shown in Table 2.16.

| Hip moment parameters | | Knee moment parameters | | Ankle moment parameters | |
|-----------------------|--------------------------------------|------------------------|--------------------------------------|-------------------------|--------------------------|
| HM1 | Max extensor moment | KM1 | 1 st peak flexor moment | AM1 | Max dorsiflexor moment |
| HM2 | Peak flexor moment | KM2 | 1 st peak extensor moment | AM2 | Max plantarflexor moment |
| HM3 | 1 st peak abductor moment | KM3 | 2 nd peak flexor moment | AM3 | Max adductor moment |
| HM4 | 2 nd peak abductor moment | KM4 | 2 nd peak extensor moment | AM4 | Max abductor moment |
| HM5 | Max int rotator moment | KM5 | Max adductor moment | AM5 | Max invertor moment |
| HM6 | Max extl rotator moment | KM6 | 1 st peak abductor moment | AM6 | Max evertor moment |
| | | KM7 | 2 nd peak abductor moment | | |
| | | KM8 | Max int rotator moment | | |
| | | KM9 | Max extl rotator moment | | |

Table 2.16: Joint moment parameters. Acronyms and corresponding definitions are reported.

Pelvis rotations were also analysed and summary parameters were chosen. They were: maximum rotation in the sagittal plane (P1), maximum and minimum obliquity (P2 and P3) and, finally, P4 minimum rotation in the transverse plane (Benedetti et al., 1998).

Three different types of analysis were performed with the results obtained: 1) intra-subject variability of the stroke testing protocol was assessed by analysing 10 walking trials within the same session of each subject tested; 2) inter-subject variability of the stroke testing protocol was assessed by analysing the average of 10 walking trials across the six subjects; 3) comparison of the joint angles obtained with the two anatomical landmark calibration methods were undertaken. This latter comparison was carried out by analysing 5 walking trials for each methodology

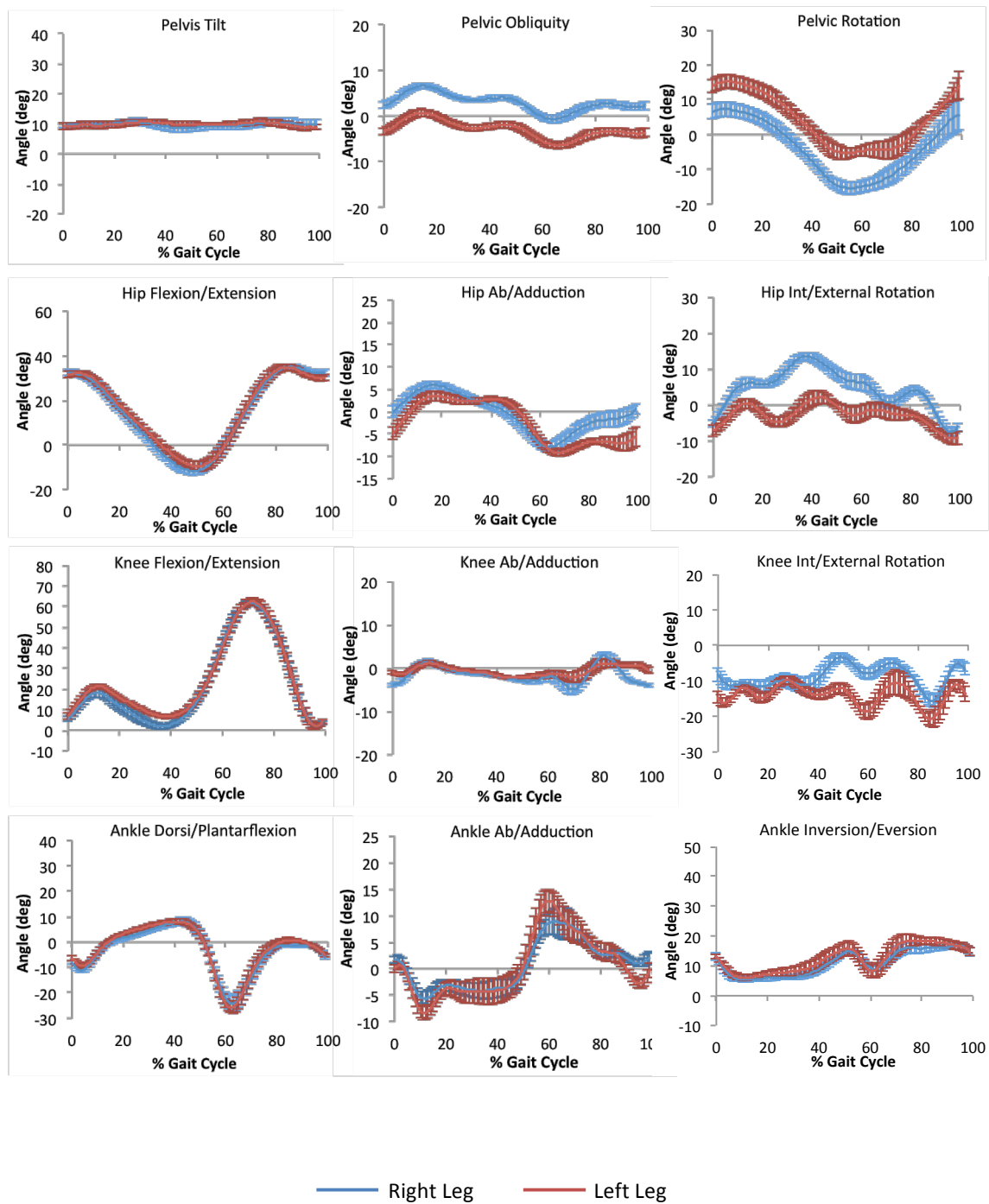


Figure 2.23: Pelvis and lower limb joint angles in each plane as mean plus and minus standard deviation over 10 gait cycles of the left (red solid line) and right (blue solid line) leg of one representative subject.

for each subject. As a measure of variability the standard deviation (SD), average standard deviation and absolute mean standard deviation throughout the gait cycle were used and paired *t*-tests were applied to determine differences between calibration methods. The level of significance was set to 0.05 for all *t*-tests.

2.5.3 Results

Typical kinematic and kinetic patterns in the three planes were observed within subjects and across all participants. In more details:

1) A small intra-subject variability for kinematic and kinetic outcomes was observed for each tested subject over 10 walking trials. This was indicated by the small standard deviation bars observed in every participant for each variable throughout the gait cycle. Figure 2.23 shows the mean and standard deviation of all kinematic variables of a selected subject (subject 5) for right and left leg. They well displayed the typical able-bodied kinematic time histories seen in gait. Few differences could be observed between the two legs and where they existed they were small. Overall a good agreement can be appreciated. Similar results were obtained for the other participants.

Related discrete parameters are reported in Table 2.17 for pelvis, hip, knee and ankle joint angle.

| Pelvis | Angle Parameters (°) | | | | | | | | | | |
|-----------|----------------------|----------------|-----------|---------------|----------------|-----------|----------------|----------------|-----------|----------------|----------------|
| | L | R | Hip | L | R | Knee | L | R | Ankle | L | R |
| P1 | 11.0 (1.0) | 10.7 (0.9) | H1 | 31.5 (1.2) | 32.5 (1.2) | K1 | 6.7 (1.4) | 5.5 (1.2) | A1 | -6.4 (0.9) | -7.9 (0.9) |
| P2 | 0.7 (0.8) | 6.6 (0.5) | H2 | -9.6 (2.1) | -11.7 (1.8) | K2 | 21.4 (1.1) | 18.2 (2.1) | A2 | -9.5 (0.8) | -11.1 (0.9) |
| P3 | -6.5 (0.7) | -0.8 (0.8) | H3 | 34.9 (1.5) | 35.1 (1.1) | K3 | 6.5 (0.9) | 1.7 (1.4) | A3 | 8.1 (1.0) | 8.3 (1.6) |
| P4 | -6.8 (1.9) | -15.3 (1.8) | H4 | 3.5 (1.0) | 5.9 (0.8) | K4 | 62.7 (1.5) | 61.8 (1.2) | A4 | -26.0 (2.4) | -24.2 (3.0) |
| | | | H5 | -9.3 (0.7) | -8.0 (1.2) | K5 | 1.2 (0.5) | 1.4 (0.6) | A5 | 12.9 (2.2) | 9.4 (2.7) |
| | | | H6 | 2.3 (1.9) | 13.7 (1.1) | K6 | 1.6 (0.9) | 2.9 (0.9) | A6 | 16.0 (2.2) | 15.1 (0.7) |
| | | | H7 | -9.6 (1.5) | -7.6 (1.3) | K7 | -9.5 (1.2) | -3.1 (1.4) | A7 | 7.9 (2.5) | 8.9 (0.9) |
| | | | | | | K8 | -21.3 (2.2) | -15.8 (1.8) | | | |

Table 2.17: Mean and standard deviation for the joint angle parameters over 10 repetitions of left (L) and right (R) leg of one subject.

Moreover the repeatability of joint angles calculations for each subject was represented by the average of standard deviation throughout the gait cycle for each outcome variable and absolute mean standard deviation expressed as percentage of each rotation range of motion. These are summarised in Table 2.18, where the averages of all subjects are reported.

| Subj ects | PELVIS Rotations SD (°,%) | | | | | | HIP Rotations SD (°,%) | | | | | |
|--------------|---------------------------|--------------|------------------|--------------|----------------|--------------|--------------------------|--------------|------------------|--------------|----------------|-------------|
| | Obliquity | | Rotattion | | Tilt | | Ab/Add | | Int/Ext Rotation | | Flex/Extension | |
| | L | R | L | R | L | R | L | R | L | R | L | R |
| 1 | 1.3 27.5% | 1.3 30.8% | 2.0 11.9% | 2.4 15.1% | 1.1 47.6% | 1.2 52.7% | 1.7 27.5% | 1.3 9.3% | 1.5 12.8% | 1.6 12.5% | 2.0 4.0% | 1.6 3.1% |
| 2 | 1.2 20.8% | 1.0 19.4% | 2.1 14.7% | 2.1 15.7% | 1.1 52.6% | 1.1 61.1% | 1.5 12.5% | 1.5 14.6% | 1.9 9.7% | 1.6 12.0% | 2.0 3.7% | 2.1 3.9% |
| 3 | 1.0 24.3% | 1.0 24.8% | 1.6 10.2% | 1.7 10.4% | 1.0 54.0% | 0.9 37.9% | 1.0 8.0% | 1.4 11.0% | 1.6 10.1% | 1.9 15.5% | 1.7 3.3% | 1.7 3.3% |
| 4 | 1.0 25.7% | 7.0 21.8% | 1.8 15.0% | 2.0 16.2% | 1.0 87.5% | 0.7 39.6% | 0.9 8.3% | 1.0 10.3% | 1.6 14.8% | 1.4 7.2% | 1.4 3.1% | 1.4 2.9% |
| 5 | 0.8 11.1% | 0.6 9.1% | 1.9 9.5% | 2.1 9.5% | 1.0 52.4% | 1.2 58.3% | 1.0 7.9% | 1.2 8.6% | 1.6 13.5% | 1.4 6.7% | 1.8 4.0% | 1.8 3.8% |
| 6 | 1.0 17.6% | 0.6 10.4% | 1.5 6.2% | 1.5 5.8% | 0.8 10.0% | 0.6 6.6% | 0.9 6.4% | 1.2 7.0% | 0.9 12.3% | 0.8 7.8% | 1.6 2.7% | 1.1 2.8% |
| Subj ects | KNEE Rotations SD (°,%) | | | | | | ANKLE Rotations SD (°,%) | | | | | |
| | Ab/Add | | Int/Ext Rotation | | Flex/Extension | | Ab/Add | | Int/Eversion | | Dorsi/Plantar | |
| | L | R | L | R | L | R | L | R | L | R | L | R |
| 1 | 1.0 18.9% | 0.9 16.4% | 1.6 9.8% | 1.4 10.4% | 2.0 3.1% | 1.9 2.8% | 1.0 6.4% | 1.4 10.0% | 1.5 19.5% | 1.6 10.6% | 1.1 4.3% | 0.9 3.9% |
| 2 | 0.6 9.5% | 0.9 18.0% | 1.6 9.7% | 1.4 8.8% | 2.7 4.8% | 2.4 3.9% | 1.5 8.0% | 1.2 6.1% | 1.5 11.6% | 1.2 14.4% | 2.4 7.3% | 2.4 5.4% |
| 3 | 0.9 15.4% | 1.0 12.5% | 1.9 12.8% | 1.6 16.4% | 2.1 3.7% | 2.0 3.2% | 1.4 10.4% | 1.3 8.9% | 1.7 14.9% | 1.6 13.2% | 1.5 4.0% | 1.6 4.8% |
| 4 | 0.6 8.1% | 0.6 8.8% | 1.0 6.6% | 1.1 8.3% | 1.9 2.9% | 2.0 3.1% | 1.2 13.1% | 0.8 8.2% | 1.3 17.0% | 1.5 19.9% | 1.2 4.7% | 1.2 5.5% |
| 5 | 0.6 19.0% | 0.7 8.8% | 1.7 16.2% | 1.6 12.7% | 1.8 3.0% | 1.9 3.2% | 1.8 8.4% | 1.3 9.1% | 1.8 14.2% | 1.2 10.4% | 1.3 3.7% | 1.4 4.4% |
| 6 | 0.5 5.9% | 0.7 6.1% | 0.9 7.9% | 1.4 10.9% | 1.6 2.4% | 1.4 2.0% | 1.0 8.0% | 0.8 5.0% | 1.3 9.7% | 1.2 10.6% | 0.9 3.2% | 0.8 3.0% |

Table 2.18: Mean values of angle standard deviation (°) and absolute standard deviation (%) throughout the gait cycle for joint angles in each plane for all study subjects. Left (L) and right (R) leg variability are reported.

Overall a low variability over 10 walking cycles was found in each subject (Table 2.18). None of the average standard deviation values exceeded 3°.

The kinematic variable more affected by trial repetitions was for both legs pelvic tilt among all subjects but for subject 6, for whom pelvic obliquity instead was the least repeatable measure. Absolute standard deviations for pelvic tilt were generally higher than 20% of the allowed range of motion to a maximum found in subject 4 of 87% to which corresponded an average SD of only 1°.

Most repeatable outcomes were instead sagittal plane angles that always showed absolute standard deviation values lower than coronal and transverse plane angle SDs of the same joint. Minimum absolute standard deviation value was 2.0% for knee flexion/extension of subject 6.

An analogous analysis to the one presented for kinematics data was conducted for joint moment results. Kinetic profiles as percentage of stance phase duration are shown in Figure 2.24 for one representative subject (subject 5). All values are shown in Nm. In the following graphs, extension (or plantarflexion for the ankle), internal rotation (or inversion for the ankle) and abduction are all positive in the vertical axis.

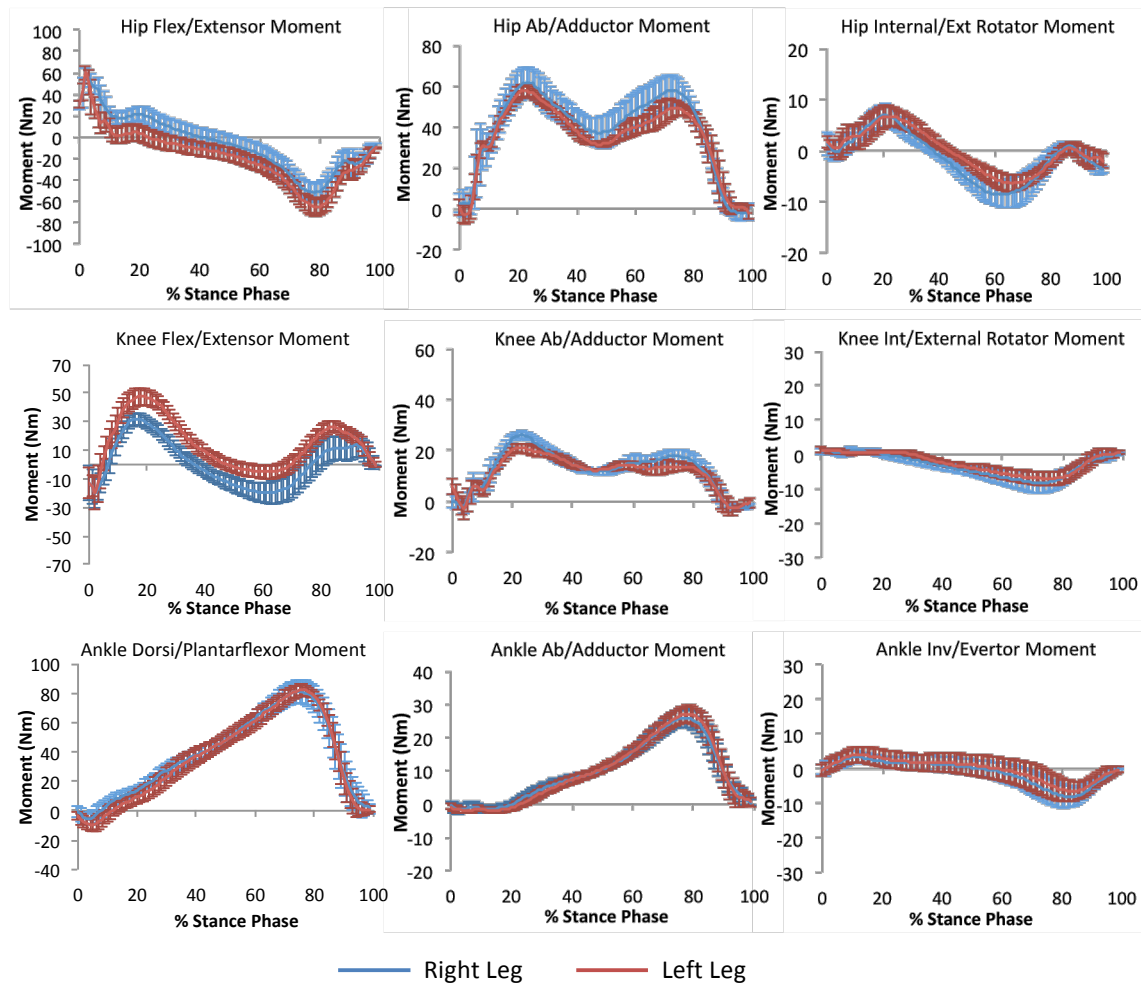


Figure 2.24: Hip, knee and ankle joint moments for left (red solid line) and right (blue solid line) leg of one representative subject. Mean and standard deviation over ten walking cycles.

Joint moment parameters extracted from those curves are detailed in Table 2.19.

| Hip | Joint Moments parameters (Nm) | | | | | | | |
|------------|-------------------------------|----------------|------------|----------------|----------------|------------|----------------|----------------|
| | Knee | | Ankle | | L | | R | |
| | L | R | L | R | L | R | L | R |
| HM1 | 70.2 (11.7) | 68.8 (10.5) | KM1 | -25.3 (8.7) | -25.0 (8.2) | AM1 | -10.9 (4.2) | -6.3 (4.6) |
| HM2 | -66.1 (7.9) | -52.5 () | KM2 | 47.9 (5.7) | 31.9 (4.2) | AM2 | 81.9 (3.9) | 81.3 (10.3) |
| HM3 | 57.9 (2.9) | 62.8 (7.8) | KM3 | -5.5 (4.7) | -20.3 (7.0) | AM3 | -2.4 (0.8) | -2.1 (1.4) |
| HM4 | 50.1 (4.4) | 58.6 (7.2) | KM4 | 27.1 (3.6) | 15.3 (7.9) | AM4 | 27.3 (2.5) | 26.3 (2.6) |
| HM5 | 6.9 (2.0) | 6.9 (2.2) | KM5 | -3.1 (4.2) | -3.2 (4.0) | AM5 | 4.3 (2.4) | 3.4 (1.7) |
| HM6 | -6.4 (1.6) | -8.9 (2.5) | KM6 | 21.2 (1.8) | 26.4 (5.8) | AM6 | -6.9 (2.8) | -8.4 (2.8) |
| | | | KM7 | 15.0 (1.9) | 18.2 (5.8) | | | |
| | | | KM8 | 1.6 (0.6) | 1.5 (0.9) | | | |
| | | | KM9 | -7.2 (2.0) | 8.4 (2.9) | | | |

Table 2.19: Joint moment parameters for the hip, knee and ankle of a representative subject's left (L) and right leg (R). Mean and standard deviation over 10 repetitions in Nm are reported.

Joint moment time histories and parameters reported exhibited a characteristic kinetic pattern comparable to that reported in the literature for able-bodied subjects. This was also found for the other study participants. Good repeatability for kinetic variables was obtained as indicated by low standard deviation values. The average of the standard deviation throughout the stance phase was obtained for each variable and for each subject (Table 2.20). Relatively small values were found for all outcomes. To allow a more comprehensive comparison among these standard deviation values, they were normalised by body mass and thus expressed in Nm/kg. Absolute standard deviation values expressed as percentage of the range of motion normalised by body mass were also calculated and reported in Table 2.20.

| Subjects | HIP Moments SD (Nm/kg, %) | | | | | |
|----------|-----------------------------|-----------------|-----------------|-----------------|-----------------|----------------|
| | Ab/Adductor | | Int/Ext Rotator | | Flexor/Extensor | |
| | L | R | L | R | L | R |
| 1 | 0.05 (3.8%) | 0.04 (2.3%) | 0.03 (9.4%) | 0.03 (6.3%) | 0.07 (3.0%) | 0.07 (3.2%) |
| 2 | 0.15 (12.6%) | 0.16 (15.8%) | 0.04 (10.3%) | 0.04 (11.1%) | 0.14 (6.9%) | 0.17 (7.8%) |
| 3 | 0.09 (8.8%) | 0.07 (5.9%) | 0.03 (9.3%) | 0.03 (10.7%) | 0.13 (5.8%) | 0.13 (5.4%) |
| 4 | 0.05 (4.0%) | 0.09 (7.2%) | 0.02 (8.7%) | 0.02 (8.0%) | 0.09 (3.4%) | 0.10 (4.0%) |
| 5 | 0.05 (5.3%) | 0.05 (4.1%) | 0.02 (10.6%) | 0.01 (4.9%) | 0.10 (4.7%) | 0.09 (5.2%) |
| 6 | 0.05 (4.5%) | 0.04 (4.5%) | 0.02 (8.8%) | 0.01 (6.8%) | 0.09 (4.4%) | 0.09 (4.2%) |
| Subjects | KNEE Moments SD (Nm/kg, %) | | | | | |
| | Ab/Adductor | | Int/Ext Rotator | | Flexor/Extensor | |
| | L | R | L | R | L | R |
| 1 | 0.04 (5.5%) | 0.03 (3.7%) | 0.02 (8.7%) | 0.03 (11.9%) | 0.08 (7.0%) | 0.08 (5.7%) |
| 2 | 0.09 (17.0%) | 0.05 (11.9%) | 0.03 (17.4%) | 0.02 (11.6%) | 0.15 (10.1%) | 0.09 (7.1%) |
| 3 | 0.05 (11.7%) | 0.05 (11.2%) | 0.03 (15.5%) | 0.02 (8.9%) | 0.08 (6.5%) | 0.11 (9.3%) |
| 4 | 0.02 (3.7%) | 0.03 (5.3%) | 0.02 (8.2%) | 0.02 (11.1%) | 0.07 (4.7%) | 0.08 (7.1%) |
| 5 | 0.03 (7.2%) | 0.03 (5.4%) | 0.03 (20.1%) | 0.009 (5.7%) | 0.08 (6.9%) | 0.07 (7.9%) |
| 6 | 0.03 (6.0%) | 0.02 (5.0%) | 0.03 (19.0%) | 0.008 (5.9%) | 0.07 (7.4%) | 0.06 (7.1%) |
| Subjects | ANKLE Moments SD (Nm/kg, %) | | | | | |
| | Ab/Adductor | | Int/Ext Rotator | | Flexor/Extensor | |
| | L | R | L | R | L | R |
| 1 | 0.03 (8.9%) | 0.03 (4.0%) | 0.05 (32.5%) | 0.04 (12.2%) | 0.06 (3.0%) | 0.07 (4.4%) |
| 2 | 0.04 (8.6%) | 0.04 (8.9%) | 0.03 (19.9%) | 0.03 (21.1%) | 0.12 (7.5%) | 0.08 (5.2%) |
| 3 | 0.03 (7.6%) | 0.02 (4.5%) | 0.04 (25.9%) | 0.03 (17.6%) | 0.09 (5.4%) | 0.08 (4.8%) |
| 4 | 0.02 (5.2%) | 0.02 (8.6%) | 0.04 (24.2%) | 0.03 (23.0%) | 0.07 (3.9%) | 0.08 (4.4%) |
| 5 | 0.04 (7.5%) | 0.01 (2.6%) | 0.03 (14.3%) | 0.02 (12.8%) | 0.07 (4.7%) | 0.05 (3.7%) |
| 6 | 0.03 (10.9%) | 0.01 (3.7%) | 0.02 (16.2%) | 0.02 (12.4%) | 0.07 (4.6%) | 0.05 (3.6%) |

Table 2.20: Mean values of joint moments standard deviation throughout stance phase duration for each plane and subjects' left (L) and right (R) leg.

Low intra-subject variability was found for the calculated kinetic variables with peak of variability of maximum 0.15 and 0.17 Nm/kg for left and right leg respectively. In terms of absolute standard deviation the variability was confined to 33% of the relative range of motion with higher values of absolute SDs found in the ankle invertor/evertor moment.

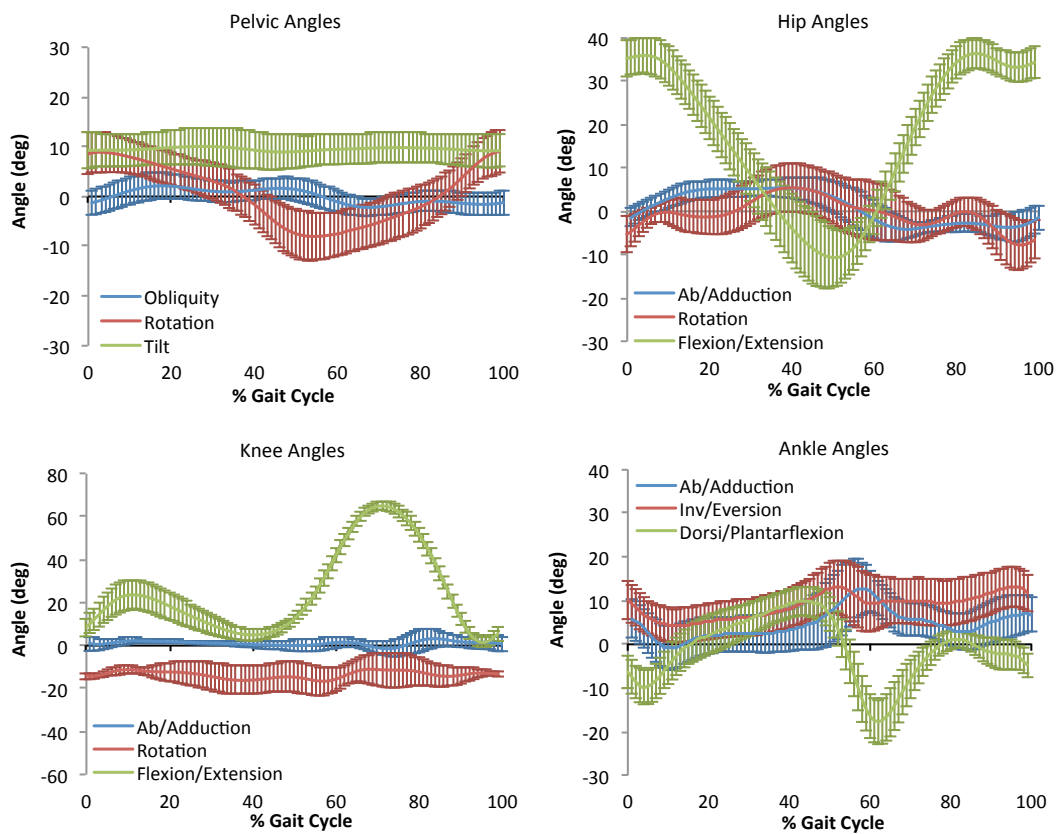


Figure 2.25: Right pelvis, hip, knee and ankle joint rotations in the three planes as mean over 10 repetitions of six subjects. Bars along the lines represent the standard deviation.

2) Inter-subject variability for kinematic and kinetic outcomes was moderate considering that it accounts for the variation of gait pattern from subject to subject. Joint angles and moments as mean plus/minus standard deviation over 10 gait cycles for all six participants' right leg are shown in Figure 2.25 and Figure 2.26, respectively. Similar results were found for the left leg.

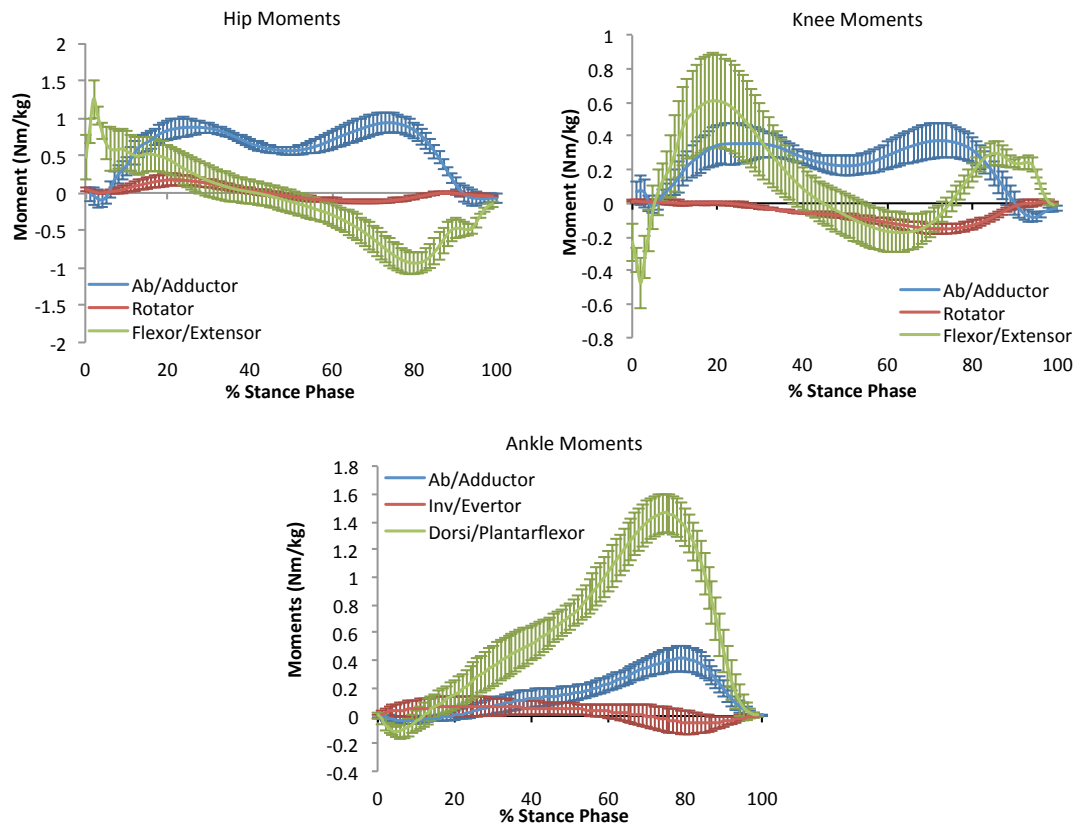


Figure 2.26: Hip, knee and ankle joint moments mean and standard deviation of the right leg of all six subjects.

Corresponding parameters are reported in the Table 2.21 for joint rotations and 2.22 for joint moments.

| Pelvis | Angle Parameters (°) | | | | | | | | | | |
|-----------|----------------------|---------------|-----------|----------------|----------------|----------------|----------------|---------------|-----------|----------------|----------------|
| | Hip | | Knee | | | | Ankle | | | | |
| | L | R | L | R | L | R | L | R | | | |
| P1 | 10.5 (3.4) | 10.5 (3.5) | H1 | 37.2 (6.8) | 35.2 (4.2) | K1 | 9.8 (4.5) | 8.4 (4.1) | A1 | -5.3 (1.5) | -6.2 (3.8) |
| P2 | 2.8 (1.6) | 2.6 (2.6) | H2 | -10.7 (4.7) | -11.2 (6.0) | K2 | 24.6 (5.5) | 23.7 (6.9) | A2 | -9.4 (1.4) | -10.0 (3.8) |
| P3 | -2.5 (2.6) | -2.6 (1.6) | H3 | 39.4 (7.5) | 36.4 (3.5) | K3 | 6.5 (3.5) | 4.6 (2.6) | A3 | 11.3 (2.6) | 10.0 (3.5) |
| P4 | -8.8 (3.9) | -8.3 (4.7) | H4 | 7.1 (4.2) | 6.6 (1.5) | K4 | 65.0 (5.4) | 65.1 (2.0) | A4 | -19.0 (6.9) | -18.1 (5.3) |
| | | | H5 | -4.3 (2.9) | -5.5 (2.1) | K5 | 3.7 (3.1) | 3.7 (3.6) | A5 | 15.2 (4.8) | 13.6 (6.2) |
| | | | H6 | 4.4 (7.3) | 5.9 (5.6) | K6 | 4.0 (3.3) | 4.5 (3.9) | A6 | 13.1 (3.6) | 13.9 (5.9) |
| | | | H7 | -8.3 (6.7) | -8.4 (5.1) | K7 | -9.9 (4.8) | -8.4 (6.5) | A7 | 5.1 (3.1) | 7.6 (4.7) |
| | | | | | K8 | -19.5 (3.3) | -17.0 (7.5) | | | | |

Table 2.21: Joint angle parameters as mean and standard deviation of left (L) and right (R) leg of all subjects.

| Hip | Joint Moments parameters (Nm/kg) | | | | | | | |
|------------|----------------------------------|-----------------|------------|-----------------|-----------------|------------|-----------------|-----------------|
| | Knee | | Ankle | | | | | |
| | L | R | L | R | L | R | | |
| HM1 | 1.26 (0.25) | 1.30 (0.25) | KM1 | -0.49 (0.19) | -0.49 (0.14) | AM1 | -0.16 (0.05) | -0.13 (0.04) |
| HM2 | -1.0 (0.10) | -0.95 (0.14) | KM2 | 0.69 (0.15) | 0.62 (0.27) | AM2 | 1.50 (0.13) | 1.50 (0.15) |
| HM3 | 0.92 (0.15) | 0.90 (0.1) | KM3 | -0.06 (0.1) | -0.18 (0.11) | AM3 | -0.03 (0.01) | -0.04 (0.02) |
| HM4 | 0.85 (0.12) | 0.95 (0.12) | KM4 | 0.40 (0.13) | 0.30 (0.05) | AM4 | 0.40 (0.06) | 0.41 (0.16) |
| HM5 | 0.16 (0.04) | 0.18 (0.08) | KM5 | -0.04 (0.07) | -0.03 (0.03) | AM5 | 0.07 (0.03) | 0.09 (0.05) |
| HM6 | -0.12 (0.04) | -0.12 (0.02) | KM6 | 0.36 (0.06) | 0.38 (0.10) | AM6 | -0.09 (0.03) | -0.07 (0.05) |
| | | | KM7 | 0.37 (0.14) | 0.38 (0.12) | | | |
| | | | KM8 | 0.02 (0.01) | 0.02 (0.01) | | | |
| | | | KM9 | -0.17 (0.05) | -0.15 (0.03) | | | |

Table 2.22: Joint moments parameters as mean and standard deviation, in brackets, of left (L) and right (R) leg of all subjects.

Joint angles and moments profiles and parameters were in agreement and within the range reported in similar conducted studies with able-bodied subjects.

With regard to the measurement repeatability, mean standard deviations values of joint kinematic did not exceed 7° but were no lower than 2° (Table 2.23). In terms of absolute standard deviation, joint angles showed a lower variability in sagittal plane angles of both legs but not for sagittal pelvic movement (pelvic tilt). Due to pelvic

tilt small range of motion, the variability across subjects led to absolute SDs over the 200% of the range (Table 2.23).

Among the kinetic variables (Table 2.24), average standard deviations were within a range of 0.02 and 0.2 Nm/kg.

The least repeatable measure was found to be ankle invertor/evertor moment with an absolute SD value to a maximum of 44.6% of the range. Controversially the most repeatable kinetic outcome across subjects was ankle dorsi/plantarflexor moment with an absolute SD of on average 6.5% (± 1.2) between left and right leg (Table 2.24).

| Leg | PELVIS Rotations SD (°,%) | | | HIP Rotations SD (°,%) | | |
|-----|---------------------------|--------------|-------------|--------------------------|-------------|-------------|
| | X | Y | Z | X | Y | Z |
| L | 2.3 (52.8%) | 3.9 (264.2%) | 3.3 (23.0%) | 3.5 (34.2%) | 6.6 (67.5%) | 5.4 (10.8%) |
| R | 2.2 (51.6%) | 3.3 (298.6%) | 4.0 (23.7%) | 2.5 (26.0%) | 4.6 (35.0%) | 4.9 (10.6%) |
| Leg | KNEE Rotations SD (°,%) | | | ANKLE Rotations SD (°,%) | | |
| | X | Y | Z | X | Y | Z |
| L | 3.5 (129.0%) | 5.6 (104.8%) | 5.0 (8.3%) | 6.9 (48.2%) | 3.5 (40.7%) | 2.6 (8.8%) |
| R | 2.4 (51.1%) | 5.0 (90.5%) | 3.8 (6.0%) | 4.8 (35.0%) | 4.8 (53.9%) | 3.8 (13.7%) |

Table 2.23: Mean values of the standard deviation over the gait cycle for left (L) and right (R) leg joint angles across the six participants, each walking 10 times.

| Leg | HIP Moments (Nm/kg,%) | | | KNEE Moments (Nm/kg,%) | | | ANKLE Moments (Nm/kg,%) | | |
|-----|-----------------------|--------------|-------------|------------------------|--------------|--------------|-------------------------|--------------|-------------|
| | X | Y | Z | X | Y | Z | X | Y | Z |
| L | 0.09 (8.7%) | 0.03 (11.0%) | 0.13 (5.7%) | 0.04 (8.2%) | 0.02 (10.2%) | 0.12 (10.4%) | 0.04 (9.8%) | 0.03 (21.2%) | 0.09 (5.7%) |
| R | 0.09 (9.4%) | 0.04 (12.9%) | 0.17 (7.9%) | 0.07 (16.0%) | 0.02 (10.0%) | 0.13 (12.2%) | 0.05 (11.7%) | 0.05 (44.6%) | 0.12 (7.4%) |

Table 2.24: Mean values of the standard deviation over the stance phase for left (L) and right (R) leg joint moments across the six participants, each walking 10 times.

3) The analysis of kinematic outputs obtained by using two different static calibration methods (one employing 8 pointer trials and the other using one set of static markers directly attached over anatomical landmarks) showed that although differences were observed from the curves they were small and not of relevance. *P*-values from the *t*-tests conducted were all above 0.05 through the gait cycle. Pelvis, hip and knee angles as measured on five repetitions over all six subjects for both methods are reported in Figure 2.27 for the right leg. Ankle angles are not compared

as no pointer calibration is involved in the ankle anatomical landmarks calibration and thus ankle kinematic remains unaffected by the calibration method used.

| Joint Parameters (°) | Protocols | | T-Test |
|----------------------|-------------|-------------|-----------------|
| | No pointer | Pointer | <i>p</i> -Value |
| Hip (°) | | | |
| H1 | 35.2 (4.2) | 34.7 (5.4) | 0.877 |
| H2 | -11.2 (6.0) | -11.7 (7.6) | 0.907 |
| H3 | 36.4 (3.5) | 35.8 (4.9) | 0.827 |
| H4 | 6.6 (1.5) | 6.8 (1.3) | 0.808 |
| H5 | -5.5 (2.1) | -5.2 (2.3) | 0.818 |
| H6 | 5.9 (5.6) | 6.5 (5.6) | 0.908 |
| H7 | -8.4 (5.1) | -9.3 (4.9) | 0.785 |
| Knee (°) | | | |
| K1 | 8.4 (4.1) | 7.1 (4.2) | 0.608 |
| K2 | 23.7 (6.9) | 22.5 (6.6) | 0.775 |
| K3 | 4.6 (2.6) | 3.3 (3.1) | 0.446 |
| K4 | 65.1 (2.0) | 64.6 (1.8) | 0.634 |
| K5 | 3.7 (3.6) | 3.6 (3.9) | 0.978 |
| K6 | 4.5 (3.9) | 4.6 (3.9) | 0.966 |
| K7 | -8.4 (6.5) | -8.4 (6.4) | 0.997 |
| K8 | -17.0 (7.5) | -16.1 (7.4) | 0.883 |
| Pelvis (°) | | | |
| P1 | 10.5 (3.5) | 10.7 (3.9) | 0.929 |
| P2 | 2.6 (2.6) | 3.9 (2.4) | 0.388 |
| P3 | -2.6 (1.7) | -2.4 (2.2) | 0.867 |
| P4 | -8.3 (4.7) | -7.9 (4.8) | 0.881 |

Table 2.25: Mean (SD) for joint angle parameters across all subjects as for pointer and no pointer calibration methods. In the last column *p*-values derived from a conducted *t*-test are reported.

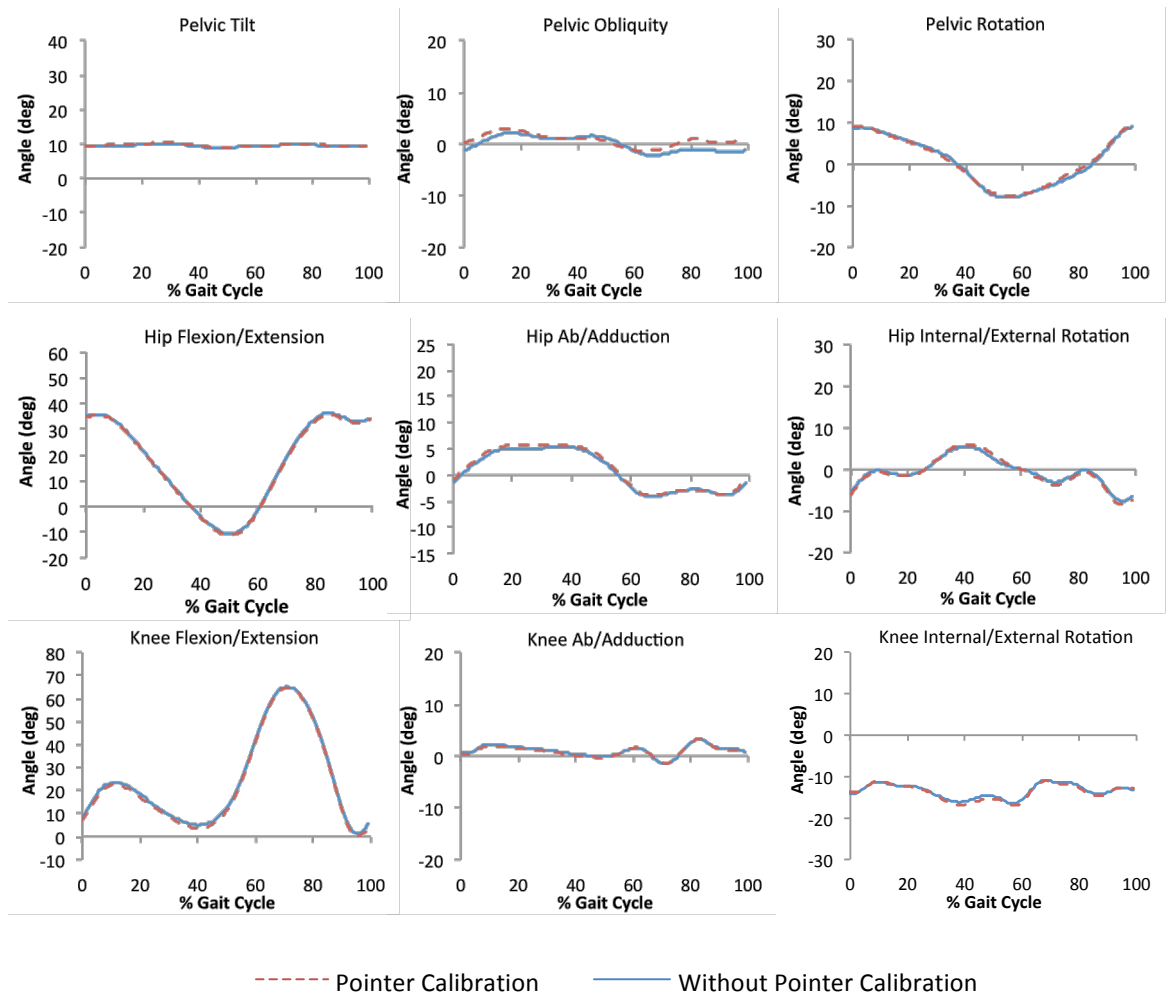


Figure 2.27: Mean pelvic, hip and knee joint angle of the right leg over all subjects for pointer calibration method (red dotted line) and no pointer calibration (blue solid line).

A very good agreement was observed when comparing joint rotations as obtained by the two anatomical landmarks calibration methods. Kinematic curves were superimposed for the majority of the gait cycle duration. Corresponding angle parameters (Table 2.25) were thus really close to each other; p -values for these parameters were all above 0.4 as an indication of a good matching between the two groups (no pointer and pointer calibration).

2.5.4 Discussion and conclusion

The purpose of the study was to introduce a reliable and fast gait analysis protocol that could allow an easy application with disabled subjects. Results gathered showed this aim was achieved. Kinematic and kinetic variables were defined according to sound biomechanical and anatomical principles in order to be described in a way that would be mathematically and clinically correct and to agree with the clinicians understanding of joint rotations and moments. Moreover, anatomical frames were defined according to standard recommendations a part from tibia/fibula and foot coordinate systems, for reasons already explained. This should facilitate data sharing and comparison across laboratories or published reports. The choices made while building up the protocol and the assumptions on which its theory lies on are fully justified by a conducted literature review on motion analysis and fully discussed earlier in this Chapter.

It was thus aimed to propose a method that could satisfy the main study aim and overcome, at least partly, the critical issues, such as reliability, skin movement artefacts, fast implementation, present in human biomechanical models and gait analysis protocols so far introduced.

The variability with which the proposed method calculates kinematic and kinetic variables during walking was used as an indication of the protocol reliability. Joint rotations and moments calculated for the analysed group of six able-bodied subjects were consistent among subjects and in agreement with published gait analysis studies. A good repeatability was showed by the results. Intra-subject variability for joint angles was small and confined to a maximum of 2.7° for all subjects over 10 repetitions for left and right leg. Kinetic variability was generally low (<0.2 Nm/kg) within a subject.

Inter-subject variability was higher than intra-subject variability due to the natural variation in human walking but still moderately small. It was confined to 7° for kinematics and 0.17 Nm/kg for kinetic variables. Overall, variability was found to be lower in sagittal plane kinematics and kinetics when considering the standard deviation expressed as percentage of the relative range of motion. This is also reported in conducted studies. The capability of the protocol in quantifying the gait in a reliable and repeatable manner was thus shown.

The issue of errors derived by skin movement artefact was minimised by the use of rigid clusters firmly attached to the distal part of the segment reducing wobbling occurring in more proximal areas which contain large muscles groups. The use of rigid clusters of markers and attachment at the distal part of the anatomical segment were associated, in fact, with reduced errors due to soft tissues movement in previously conducted studies (Holden et al., 1997; Manal et al., 2000; Leardini et al., 2005).

By eliminating the 8 anatomical landmark pointer static calibration trials, the subject preparation time was reduced making the protocol more bearable for subjects with difficulties in prolonged standing tasks such as stroke patients. All the participants expressed their preference to individual markers attached on anatomical landmarks over the use of the pointer to calibrate those. Results of the comparison of joint rotations between pointer and no pointer calibration methods revealed small or no differences in the outcomes making the new method viable and as precise as the more widely used pointer technique. It should be mentioned, however, that none of the participants was overweight and thus the identification of anatomical landmarks and attachment of the markers was easy. An issue may still remain for people in with big layers of soft tissue covering the underlying bone and for whom the identification of the hidden anatomical landmarks might be more accurate with a pointer. One can always taking into consideration the possibility of using the pointer, when strictly necessary, so as not to compromise the accuracy of the results. For all other occasions using individual markers and thus only one static trial is advisable. In addition, no extra time is required for anthropometric measurements as they are directly calculated from the acquired position of the interested anatomical landmarks. The only compulsory measurement to be taken is body mass.

The driving criteria in the protocol development were accuracy and repeatability of the results, anatomy based definition of bone segments, easy and fast implementation, simple analysis and interpretation of the outcomes. All these criteria were met in the accomplished protocol. The advantages of the gait analysis method introduced can thus be summarised as follows:

- Fast subject preparation;

- Easy marker positioning;
- Soft tissue artefacts minimised;
- Biomechanical model based on easy identifiable anatomical landmarks;
- Segmental and Joint coordinate system consistent with standards (ISB);
- Joint angles which agree with their common anatomical meaning;
- Repeatability;
- Fully 3D, including the foot and ankle;
- Cross talk errors can be minimised at the knee using the optimisation technique by Schache et al., 2006.

On the other hand, the issue of an accurate and certain identification of anatomical landmarks themselves remains unresolved. Practice of the examiner can increase repeatability in this regard. Soft tissue derived errors are minimised but can still partly affect the results. The use of some sort of compensation methods can limit soft tissues artefacts error propagation but, such techniques that could easily be incorporated in the data processing are yet to be introduced.

To conclude, the method described allows for a 3D reconstruction of the pelvis and lower limb segments and a repeatable description of joint motion, both kinematics and kinetics. A reliable method has been developed that is not time-consuming and could be used for the gait analysis of stroke patients as demonstrated by the preliminary application of the protocol in groups of able-bodied subjects.

CHAPTER 3 – DESIGN OF A SIMPLIFIED VIDEO GAIT PROTOCOL FOR KINEMATIC AND TEMPORO-SPATIAL PARAMETERS EVALUATION

3.1 Introduction

In the previous chapter a protocol for 3-D gait analysis has been described. Despite its high potential for assessing a patient, this type of analysis is not easily applicable in a clinical context. Rehabilitation facilities may not have the possibilities to host such laboratories in terms of money and space, and the capability to use the equipment required. This calls for a simple and accessible gait assessment technique that is not costly and could be run by clinicians with no expertise in movement analysis.

In recent years, simpler gait analysis techniques to 3-D human movement analysis have been developed (Hill et al., 1994; Cutlip et al., 2000; Bilney et al., 2003; Menz et al., 2007; Beauchet et al., 2008; Hartmann et al., 2009). Although these methods were able to produce reliable results they still rely on expensive pieces of equipment that require a certain level of technical expertise to operate and interpret the outputs. A system that meets the requirements of accessibility in both cost and operability was developed by Soda et al. (2009). However, this system was only tested with one subject and thus raises concerns about its reliability.

To this end, by exploiting techniques developed by Wall and colleagues (Wall et al., 1997, 2000) a new, simple, low cost, video based portable tool for gait analysis was developed. The method proposed is presented in this Chapter. The reliability of the assembled system in comparison to a 3-D motion analysis system was investigated and its viability within a rehabilitation setting of stroke patients was evaluated. Intra- and inter- rater reliability of the outcome measurements were determined. Two studies were conducted in this regard and are described in the next sections.

3.2 The video gait technique: test apparatus

The equipment necessary for the video gait analysis technique includes a video camera with a tripod, a walkway grid mat, four photoswitches mounted on tripods, a black box with start/stop light bulb indicator, stick-on bull's eye markers and a computer/laptop for subsequent data analysis. This equipment is placed as illustrated in Figure 3.1.

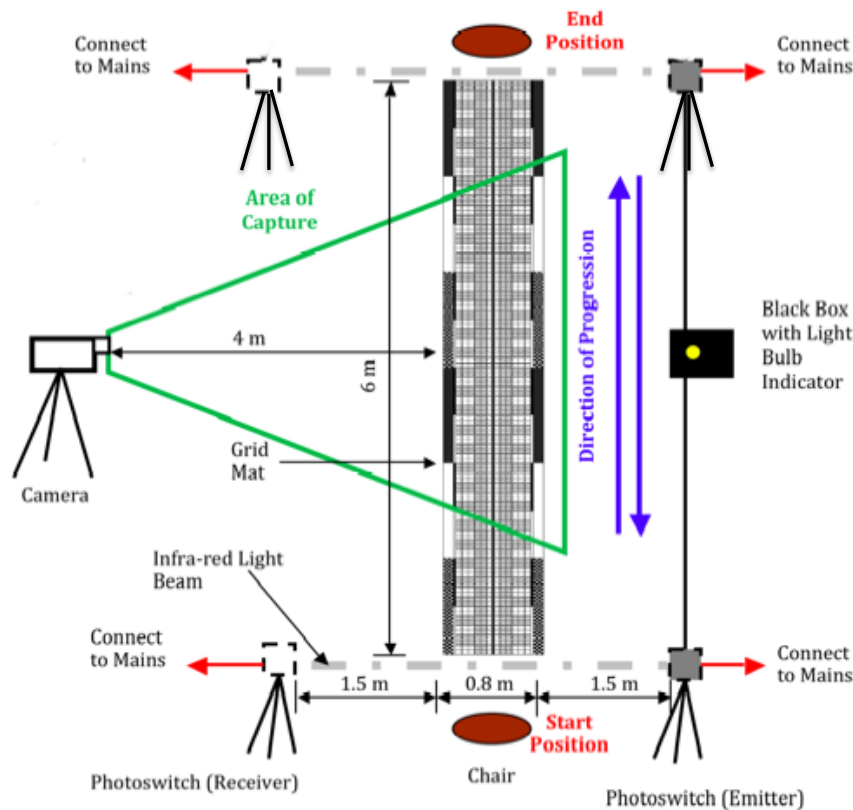


Figure 3.1: Diagrammatic illustration of the test apparatus set up.

Centrally located is the walkway grid mat, a piece of Linoleum of 6 x 0.8 m, designed and manufactured to provide bidirectional measurements to an accuracy of less than 0.01 m. A colour coding grid in black, white and different shades of grey is designed on the surface of the mat to allow estimation of the foot position along its length. The length of the grid mat is divided into six sub-divisions of 1 m set of dimensions. Each 1 m dimension is sub-divided into units of 0.1 m and represented by a lighter shade of grey and white colours. Each 0.1 m dimension is further sub-divided into 0.05 m dimensions and graduated such that measurements to the nearest

centimeter could be obtained. Aligned with the edges of the mat are four E3JM photoswitches (Omron Electronics, IL, USA), two emitters and two receivers placed opposite each other on tripods and connected to a black box light bulb indicator. The latter was wired to function as a flash light triggered by the photoswitches and ultimately as an indicator (start and stop) to estimate the time spent by a subject to walk 6 m. When the emitted infrared right light beam is broken the flash light originates from the black box and it goes off as soon as the infrared light beam is restored. A video camera (EX-FH20 EXILIM, Casio, USA) on a tripod is positioned laterally to the mat to allow recording of the sagittal view of a subject walking. By adjusting the camera zoom, the area of capture can be set. In order to capture 2 to 3 gait cycles one should allow for at least two-thirds of the mat to be within the camera's field of view. Moreover, it should be ensured that the light bulb is clearly visible by the camera to start and stop the time counting.

Bull's eye markers (Figure 3.2) made as sticky labels are used attached to the subject to facilitate the visualisation of lower limb joint centers and feet positions along the mat during post collection analysis.

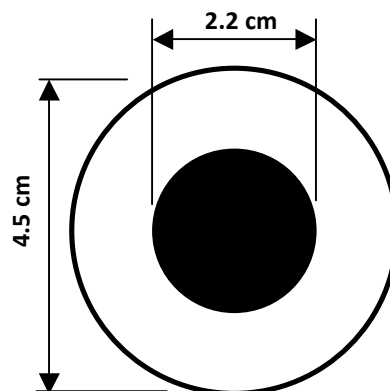


Figure 3.2: Sample of a Bull's eye marker.

A computer which runs Pro Trainer DV motion analysis software (Sport Motion Inc., USA) is used for the video gait data processing. Frames captured are transferred onto the computer and analysed. Using freeze frame and slow motion playback features of the Pro Trainer software the timing of foot falls and their position on the mat can be estimated. Gait events are bookmarked and sagittal joint angles can be quantified using the goniometric tool of the software. Output measurements are copied into a

Microsoft Excel spreadsheet for further calculations and hence the temporal and spatial parameters of gait can be extracted.

3.3 Intra and Inter-Rater reliability measurements of kinematic and temporo-spatial parameters of gait using a simple video gait technique

3.3.1 *Introduction*

Using the equipment described in the previous paragraph (3.2), a simple and cost effective technique to assess gait within rehabilitation clinics and gait laboratories has been developed. The purpose of this study was to evaluate the robustness of such a method in evaluating normal and impaired gait. Intra- and inter- rater reliability of kinematic and temporo-spatial gait parameters obtained by using a walkway grid mat, a video camera and the commercially available Pro Trainer DV motion analysis software (Sport Motion Inc., USA) was therefore determined.

3.3.2 *Methods*

The study was approved by the Bioengineering Unit departmental ethics committee. A total of sixteen subjects were voluntarily recruited. All participants were provided with the study information sheets and completed an informed consent form prior to data collection. The able-bodied group comprised of twelve participants (4 females and 8 males), aged 27.4 ± 3.9 years, height 1.71 ± 0.09 m and body mass 66.75 ± 10.7 kg. The subjects with impaired gait were four patients affected by different levels of stroke severity in a time span of a week from recruitment. These stroke survivors (3 females and 1 male) were aged 55.3 ± 9.5 years, and had a height and body mass of 1.67 ± 0.07 m and 78.67 ± 21.2 kg respectively. They presented with different ability to walk. One of the stroke patients walked with the aid of an assistant, the second patient used a Zimmer Frame, the third stroke patient used a walking stick and the fourth patient walked independently without any aid. Data were acquired using the instrumentations previously described (section 3.2): a walkway grid mat (6 x 0.8 piece of Linoleum), a video camera with high speed

recording mode (EX-FH20 EXILIM, Casio, USA), and four photoswitches (Omron Electronics, IL, USA) on tripods connected to a start/stop light bulb indicator. The equipment was placed in the Bioengineering Unit biomechanics laboratory and in the gym of the clinics, from where patient were recruited, as illustrated in Figure 3.1. Bull's eye marker sticky labels were attached on the subject's lower limb sagittal plane facing the view of the video camera. They were placed on the patient's greater trochanter, lateral epicondyle, lateral malleolus, tip of the shoe on the lateral and medial side and, on the heel (medial and lateral sides) of both left and right legs. Participants were asked to walk back and forth along the mat. A total of six walking trials were captured for each participant, three times with the right leg facing the video camera and three times with the left side facing the video camera. Two chairs were placed at either end of the mat and used for the subject to rest in between trials if necessary. The video data were captured at 210 Hz with a resolution of 480 x 360 pixels.

After data collection, the videos were transferred and played back on a computer with installed Pro Trainer DV motion analysis software (Sport Motion Inc., USA) to be analysed. Temporo-spatial parameters were extracted from the frames captured for each trial and gait events identified. Walking speed was determined by dividing the distance covered by the subjects (6 m) by the duration of the walk, which was identified by the start and stop flashing light (initial and final time). Gait speed symmetry was obtained from the ratio of the walking speeds for the back and forth trials; temporal (step time) and spatial (step length) symmetry measurements were determined by a frame by frame video analysis aimed at identifying the spatial location of the feet with their corresponding temporal parameters. Temporal symmetry was defined as the ratio of step times of the left and right limbs. Spatial symmetry was expressed as a ratio of step lengths of the left and right limbs. Angle of tibia with respect to the vertical at initial contact, foot flat, mid stance and terminal contact of the left and right gait cycle were obtained.

Three different examiners performed the analysis of captured data separately to allow inter-rater reliability to be evaluated. Same gait cycles were kept for post capture processing by each rater. Two of the raters had experience in biomechanical data processing whereas the third one had no experience being a practising clinician.

Since the ultimate goal was to introduce the AVPS (Augmented Video-based Portable System) tool into clinical practice, it was pertinent to test the reliability of measures when used by clinicians. All raters underwent a training session as introduction on how to use Pro Trainer DV motion analysis software prior data analysis.

Descriptive statistics were used to summarise the results. Means and standard deviations for each of the temporo-spatial parameters and kinematic measurements with respect to the trials and between each rater were compared. Mean differences between the three raters were determined and correlations between them were examined. Intraclass correlation coefficients (ICC) for intra-rater reliability were obtained with corresponding 95% confidence intervals. A two way mixed effect model using an absolute agreement definition where rater effects are random and measured effects are fixed was used. SPSS Statistics 19.0 software (IBM, USA) was used to compute the statistical analysis. The reliability of the measurements was interpreted based on the classifications of reliability coefficients developed by Landis and Koch (1977). In accordance with the classification the ICC interpretation scale was represented as follows: poor to fair (below 0.4), moderate (0.41 – 0.60), excellent (0.61 – 0.80), and almost perfect (0.81 – 1.0).

| Measurement Parameters | Healthy Participant Evaluation | | | Stroke Survivor Evaluation | | |
|---|--------------------------------|------------------------|------------------------|----------------------------|------------------------|------------------------|
| | Rater 1 (Mean ± SD) | Rater 2 (Mean ± SD) | Rater 3 (Mean ± SD) | Rater 1 (Mean ± SD) | Rater 2 (Mean ± SD) | Rater 3 (Mean ± SD) |
| Kinematic Parameter | | | | | | |
| Walking Speed (R) (m/s) | 1.38 ± 0.14 | 1.38 ± 0.15 | 1.36 ± 0.14 | 0.24 ± 0.15 | 0.23 ± 0.15 | 0.24 ± 0.15 |
| Walking Speed (L) (m/s) | 1.38 ± 0.14 | 1.37 ± 0.15 | 1.36 ± 0.14 | 0.27 ± 0.20 | 0.26 ± 0.20 | 0.27 ± 0.20 |
| Gait Speed Symmetry | 1.00 ± 0.02 | 1.01 ± 0.02 | 1.00 ± 0.02 | 0.92 ± 0.06 | 0.91 ± 0.07 | 0.96 ± 0.10 |
| Temporo-spatial parameter | | | | | | |
| Left Limb Step Length (m) | 0.76 ± 0.07 | 0.75 ± 0.06 | 0.75 ± 0.07 | 28.64 ± 6.28 | 27.78 ± 6.09 | 28.35 ± 6.22 |
| Left Limb Step Time (s) | 0.53 ± 0.03 | 0.53 ± 0.03 | 0.52 ± 0.03 | 0.92 ± 0.10 | 0.89 ± 0.10 | 0.98 ± 0.50 |
| Right Limb Step Length (m) | 0.77 ± 0.07 | 0.77 ± 0.06 | 0.76 ± 0.07 | 23.15 ± 18.18 | 22.46 ± 17.63 | 22.92 ± 17.99 |
| Right Limb Step Time (s) | 0.53 ± 0.03 | 0.53 ± 0.03 | 0.52 ± 0.03 | 0.92 ± 0.10 | 0.89 ± 0.10 | 0.91 ± 0.10 |
| Temporal Symmetry | 0.99 ± 0.02 | 0.98 ± 0.03 | 0.98 ± 0.02 | 1.45 ± 0.24 | 1.40 ± 0.23 | 1.43 ± 0.23 |
| Spatial Symmetry | 1.01 ± 0.03 | 1.02 ± 0.03 | 1.00 ± 0.03 | 0.64 ± 0.55 | 0.62 ± 0.54 | 0.63 ± 0.55 |
| Tibia Angle of Inclination with respect to Gait Events (°) | | | | | | |
| Tibia inclination angle (at IC) (R) | 22.97 ± 2.31 | 19.94 ± 1.85 | 22.88 ± 2.30 | 13.75 ± 4.72 | 13.86 ± 4.76 | 13.69 ± 4.70 |
| Tibia inclination angle (at FF) (R) | 4.06 ± 2.88 | 2.86 ± 0.54 | 3.94 ± 2.80 | 9.50 ± 4.43 | 9.46 ± 4.41 | 9.23 ± 4.31 |
| Tibia inclination angle (at MS) (R) | 9.64 ± 3.97 | 10.08 ± 3.03 | 9.57 ± 3.94 | 7.50 ± 3.79 | 7.39 ± 3.73 | 7.45 ± 3.76 |
| Tibia inclination angle (at TC) (R) | 54.28 ± 2.61 | 54.22 ± 1.98 | 53.64 ± 2.58 | 38.50 ± 10.38 | 38.43 ± 10.36 | 38.05 ± 10.25 |
| Tibia inclination angle (at IC) (L) | 22.25 ± 1.74 | 19.67 ± 1.85 | 22.16 ± 1.73 | 15.00 ± 8.04 | 15.18 ± 8.14 | 14.94 ± 8.01 |
| Tibia inclination angle (at FF) (L) | 4.31 ± 1.86 | 2.61 ± 0.71 | 4.19 ± 1.80 | 10.50 ± 6.81 | 10.63 ± 6.89 | 10.21 ± 6.62 |
| Tibia inclination angle (at MS) (L) | 10.22 ± 3.52 | 10.56 ± 3.09 | 10.15 ± 3.50 | 8.75 ± 3.20 | 8.73 ± 3.20 | 8.69 ± 3.18 |
| Tibia inclination angle (at TC) (L) | 55.89 ± 2.74 | 55.83 ± 2.15 | 55.23 ± 2.71 | 30.75 ± 11.62 | 30.69 ± 11.59 | 30.39 ± 11.48 |

IC – Initial Contact; FF – Foot Flat; MS – Mid Stance; TC – Terminal Contact; R – Right Leg; L – Left Leg

Table 3.1: Representation of kinematic parameters, temporo-spatial parameters and tibia angle of inclination with respect to gait events showing the mean, and standard deviation for the three raters for the able-bodied and stroke survivors groups.

3.3.3 Results

3.3.3.1 Reliability in healthy participants

With respect to kinematic variables all raters showed similar mean values with low standard deviations (Table 3.1). Mean differences were small and ranged from 0 to 0.02 m/s. For each rater, the temporo-spatial variables with respect to the trials were close as reflected by the size of their standard deviation (Table 3.1). The mean difference for the temporo-spatial variables were also low and ranged from 0.01 m to 0.08 m for the spatial variables and 0.01 s to 0.09 s for the temporal variables. The tibia angle of inclination with respect to the gait events produced small mean differences between raters. Also within the trials for each rater the tibia angle of inclination were similar as indicated by the size of standard deviations (Table 3.1). The results showed high intra- and inter- rater reliability for both the kinematic and temporo-spatial parameters. The ICC value for the intra-rater reliability test was 0.993 for the kinematic variables, and ranged from 0.941 to 0.956 for the temporo-spatial variables and 0.731 to 0.954 for the tibia inclination angle with respect to gait events (Table 3.2). Based on the ICC interpretation scale, the results were classed as either excellent or almost perfect.

Between raters there was a high inter-rater correlation for the kinematic and temporo-spatial variables. Only the tibia inclination angle at initial contact for the left leg and at foot flat for the right leg produced lower correlation values in comparison to the other measurements but still greater than 0.6 for Rater 1 versus Rater 2 and Rater 2 versus Rater 3. Also, it is worth noting that the smallest range of intra-rater correlation values were observed for the tibia inclination angle at initial contact for the left limb. The inter-rater reliability results produced ICC values greater than 0.8 for all the measurement parameters measured (Table 3.3). The smallest inter-rater correlation was found for the angle of tibia to the vertical at foot flat for the right leg with an ICC of 0.822, whereas the highest correlation was for walking speed of the right side trials with an ICC of 0.999.

| Variables | Intra-Rater (ICC Value) | Inter-Rater Correlation | | | 95% Confidence Interval |
|--|----------------------------|------------------------------|------------------------------|------------------------------|----------------------------|
| | | Rater 1 Versus Rater 2 | Rater 2 Versus Rater 3 | Rater 1 Versus Rater 3 | |
| Walking Speed (R) | 0.993 | 0.997 | 0.997 | 0.997 | 0.965 to 0.998 |
| Walking Speed (L) | 0.993 | 0.997 | 0.997 | 0.999 | 0.965 to 0.998 |
| Left Limb Step Time | 0.956 | 0.958 | 0.974 | 0.988 | 0.876 to 0.986 |
| Left Limb Step Length | 0.972 | 0.982 | 0.982 | 0.982 | 0.926 to 0.991 |
| Right Limb Step Time | 0.953 | 0.940 | 0.947 | 0.987 | 0.883 to 0.985 |
| Right Limb Step Length | 0.941 | 0.909 | 0.909 | 1.000 | 0.849 to 0.982 |
| Tibia inclination angle (at IC) (R) | 0.760 | 0.746 | 0.746 | 1.000 | 0.089 to 0.937 |
| Tibia inclination angle (at FF) (R) | 0.805 | 0.614 | 0.614 | 1.000 | 0.504 to 0.938 |
| Tibia inclination angle (at MS) (R) | 0.950 | 0.953 | 0.953 | 1.000 | 0.876 to 0.984 |
| Tibia inclination angle (at TC) (R) | 0.903 | 0.896 | 0.896 | 0.999 | 0.763 to 0.969 |
| Tibia inclination angle (at IC) (L) | 0.731 | 0.693 | 0.694 | 0.999 | 0.071 to 0.926 |
| Tibia inclination angle (at FF) (L) | 0.803 | 0.874 | 0.874 | 1.000 | 0.266 to 0.945 |
| Tibia inclination angle (at MS) (L) | 0.954 | 0.936 | 0.936 | 0.998 | 0.886 to 0.985 |
| Tibia inclination angle (at TC) (L) | 0.938 | 0.951 | 0.951 | 0.999 | 0.824 to 0.981 |

IC – Initial Contact; FF – Foot Flat; MS – Mid Stance; TC – Terminal Contact; R – Right Leg; L – Left Leg

Table 3.2: Intra Rater Reliability (ICC value), Inter Rater Correlation and 95% Confidence Interval for the able bodied group for left and right side measurements.

| Measurement Parameters | Healthy Participant Evaluation (ICC Value) | Stroke Survivor Evaluation (ICC Value) |
|--|--|--|
| Kinematic Parameter | | |
| Walking Speed (R) (m/s) | 0.999 | 1.000 |
| Walking Speed (L) (m/s) | 0.997 | 1.000 |
| Temporo-spatial parameter | | |
| Left Limb Step Time (s) | 0.981 | 0.999 |
| Left Limb Step Length (m) | 0.992 | 1.000 |
| Right Limb Step Time (s) | 0.985 | 0.999 |
| Right Limb Step Length (m) | 0.980 | 1.000 |
| Tibia Inclination Angle with respect to Gait Events (°) | | |
| Tibia inclination angle (at IC) (R) | 0.936 | 0.971 |
| Tibia inclination angle (at FF) (R) | 0.822 | 1.000 |
| Tibia inclination angle (at MS) (R) | 0.983 | 1.000 |
| Tibia inclination angle (at TC) (R) | 0.971 | 0.998 |
| Tibia inclination angle (at IC) (L) | 0.919 | 0.986 |
| Tibia inclination angle (at FF) (L) | 0.914 | 0.999 |
| Tibia inclination angle (at MS) (L) | 0.984 | 0.994 |
| Tibia inclination angle (at TC) (L) | 0.984 | 0.999 |

IC – Initial Contact; FF – Foot Flat; MS – Mid Stance; TC – Terminal Contact; R – Right Leg; L – Left Leg

Table 3.3: Inter-rater reliability for healthy participants and stroke survivors among the three raters.

3.3.3.2 Reliability in stroke survivors

The results for the kinematic variables were very close with the exception of the gait speed symmetry data produced by Rater 3 (Table 3.1). The results showed that Rater 3 produced a mean difference > 0.04 m/s when compared to Rater 1 and Rater 2 for that parameter. There were no statistical differences between Rater 1 and Rater 2 (p -value = 0.147), Rater 2 and Rater 3 (p -value = 0.12) and, Rater 1 and Rater 3 (p -value = 0.224) for the temporo-spatial parameters. All the kinematic and temporo-spatial variables produced very high intra-rater (ICC) values (Table 3.4). Also between raters a strong correlation was observed (Table 3.4). The inter-rater reliability (Table 3.3) analysis for the kinematic, temporo-spatial parameters produced ICC values greater than 0.9. High ICC values were also found at the tibia inclination angle with respect to gait events for both the left (range: 0.986 – 0.999) and right (range: 0.971 – 1.000) leg (Table 3.3).

| Variables | Intra-Rater (ICC Value) | Inter-Rater Correlation | | | 95% Confidence Interval |
|-------------------------------------|-------------------------|-------------------------|------------------------|------------------------|-------------------------|
| | | Rater 1 Versus Rater 2 | Rater 2 Versus Rater 3 | Rater 1 Versus Rater 3 | |
| Walking Speed (R) | 0.999 | 1.000 | 1.000 | 0.999 | 0.986 to 1.000 |
| Walking Speed (L) | 0.993 | 0.999 | 0.997 | 1.000 | 0.995 to 1.000 |
| Left Limb Step Time | 0.999 | 1.000 | 0.999 | 0.999 | 0.979 to 1.000 |
| Left Limb Step Length | 0.997 | 0.996 | 1.000 | 0.999 | 0.928 to 1.000 |
| Right Limb Step Time | 1.000 | 1.000 | 0.999 | 0.999 | 0.999 to 1.000 |
| Right Limb Step Length | 0.999 | 0.999 | 0.999 | 1.000 | 0.994 to 1.000 |
| Tibia inclination angle (at IC) (R) | 1.000 | 0.998 | 0.990 | 1.000 | 0.091 to 1.000 |
| Tibia inclination angle (at FF) (R) | 0.998 | 1.000 | 0.994 | 0.998 | 0.988 to 1.000 |
| Tibia inclination angle (at MS) (R) | 0.997 | 0.993 | 0.997 | 1.000 | 0.984 to 1.000 |
| Tibia inclination angle (at TC) (R) | 0.994 | 0.992 | 0.991 | 1.000 | 0.970 to 1.000 |
| Tibia inclination angle (at IC) (L) | 0.965 | 0.959 | 0.927 | 0.995 | 0.815 to 0.998 |
| Tibia inclination angle (at FF) (L) | 0.990 | 0.996 | 0.996 | 1.000 | 0.901 to 0.999 |
| Tibia inclination angle (at MS) (L) | 0.983 | 0.984 | 0.968 | 0.994 | 0.910 to 0.999 |
| Tibia inclination angle (at TC) (L) | 0.998 | 0.999 | 0.998 | 1.000 | 0.988 to 1.000 |

IC – Initial Contact; FF – Foot Flat; MS – Mid Stance; TC – Terminal Contact; R – Right Leg; L – Left Leg

Table 3.4: Intra Rater Reliability (ICC value), Inter Rater Correlation and 95% Confidence Interval for the stroke survivors group for left and right side measurements.

3.3.4 *Discussion and Conclusion*

Simple gait assessment systems are ideal and preferred within the clinical environment. Although there have been a number of gait analysis systems developed over the years, most of them are impractical and can be considered unsuitable for the fast-paced clinical setting (Mulder et al., 1998; Baker, 2006). The method proposed on the other hand represents a rehabilitation tool that is cost effective and easy to operate both in clinical and research environments to evaluate able-bodied subjects as well as patients with neurological disorders and musculoskeletal deficits with a high level of reliability. This was supported by the results obtained that, revealed a good level of agreement with respect to each trial and between raters for the kinematic, temporo-spatial measurement parameters and tibia to the vertical angles. Good repeatability was shown when comparing the mean differences of the outcome measures and by the small sizes of their standard deviations. ICC intra- and inter-rater reliability was high with all the variables producing ICC higher than 0.73 for both the able-bodied participant and stroke survivor assessments.

The kinematic and temporo-spatial parameter measurements generated from the current study agree well with the results obtained from previously conducted studies (Oberg et al., 1993; Bohannon, 1997; Reid et al., 2005).

While the walkway grid mat and kit is suitable for a simple biomechanical evaluation of gait, the parameters generated from this study have strong clinical implications. Specifically with respect to the derived parameters such as gait speed symmetry, temporal symmetry and spatial symmetry, these values could be used as outcome measures to examine patients with neuromuscular deficits such as stroke patients. Moreover, since both paretic and non-paretic lower limbs can be examined it would be possible to distinguish features from pathological and not pathological joint motions or compensatory actions from that of able-bodied gait. There is a lot of scope for the use of this kit both within and outside the clinical environment. The data acquisition and analysis process was simple to learn by all raters. Pro Trainer DV motion analysis software (Sport Motion Inc., USA) makes the data processing and analysis easy and user friendly although it is manual. This is a drawback of the current system for which post-capturing manipulation of acquired data could be lengthy and repetitive. An automated system would be preferable to a

manual system to reduce data processing duration. A further improvement of the methodology could involve the incorporation of some sort of pattern recognition algorithms into the captured data analysis but without altering the level of complexity in the analysis process. Moreover the system is flexible to allow measurements to be taken by different perspective other than sagittal view. By positioning a video camera in front of the mat or by simply adjusting the camera positioned laterally also step width or ab/adduction angles could be estimated. To conclude, the reliability of a simplified and affordable video technique of gait analysis has been investigated and the capability of the system in producing repeatable and highly reliable data has been proved. The system can thus be used as a simplistic assessment for screening gait as well as targeted rehabilitation in research and clinical settings.

3.4 Evaluation of the concurrent validity of the new video system with the Vicon motion analysis system

3.4.1 *Introduction*

The Augmented Video-based Portable System (AVPS), described previously, which employs a bulls eye ‘paper label’ marker set was used to capture gait data simultaneously to a 3-D Vicon motion analysis system (Vicon, Oxford Metrics Ltd., UK) used with the retro-reflective passive markers set described in Chapter 2. The aim of the study was thus to investigate the reliability of the AVSP in comparison to the Vicon capture system, here considered as a gold standard.

3.4.2 *Methods*

Twelve healthy subjects (6 females and 6 males) from the Bioengineering Unit participated in the study. The subjects were aged 28.6 ± 7 years, with a height 1.71 ± 0.11 m and body mass 68.5 ± 12.1 kg. Approval was obtained from the Bioengineering Unit departmental ethics committee prior commencement and subjects signed a consent form prior to video data collection.

The equipment that constitutes the AVPS is extensively described in paragraph 3.2 and again in 3.3.2. Simultaneously kinematic data and markers trajectories were also acquired with a 12 cameras 3-D motion capture system (Vicon MX Giganet, Oxford

Metrics Ltd., UK). The Vicon cameras located along the perimeter of the laboratory surrounded the AVPS equipment configuration showed in Figure 3.1. These cameras are fastened to suspended steel pipes mounted high around the laboratory walls.

Cameras position was unaltered among test sessions allowing each time a workspace area of approximately 6 meters in length that was calibrated before each test session as from guidelines by the supplier.

Before the main validation on the healthy participants, the AVPS and the 3-D Vicon Motion Analysis System (Vicon, Oxford Metrics Ltd., UK) were concurrently tested, using a two segments rig, designed and developed within the Bioengineering Unit.

The two segments rig secured in a vice, consisted of two 20 cm long segments joined together with an inter-segmental goniometer (Figure 3.3). This hinge joint rig was able to produce accurately measure of angles. Thus, these goniometric angles were used as a reference, to data obtained simultaneously from both the AVPS and the 3D Vicon Motion Analysis System. Bull's eye markers (Figure 3.3) were used for the AVPS while retro-reflective markers were used by the 3-D Vicon Motion Analysis System (Vicon-UK, Minns Business Park, West Way, Oxford, UK). Three bull's eye markers were placed on the rig, one in each segment and a third on the rig joint, imitating the movement of the knee joint. In addition, three retro-reflective markers were mounted on top of the bull's eye markers to allow the simultaneous record of the rig movements from both systems (Figure 3.3). With this set up, angles from both systems were concurrently recorded statically in a range of -90° to $+90^{\circ}$, at 10° increments. For each angle position, three trials of data were captured.

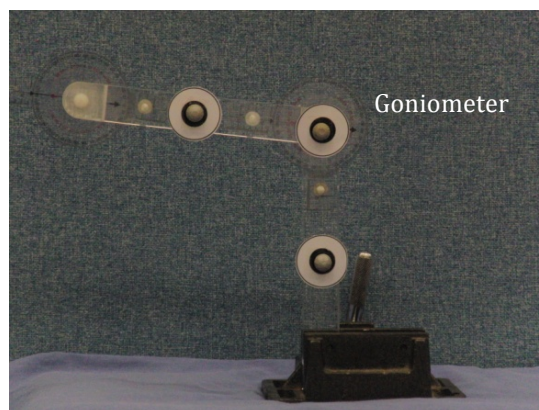


Figure 3.3: Two segments goniometric rig set up with markers attached for data collection.

| Motion and Video Analysis Systems | | | |
|--|---|--|---|
| Augmented Video-based Portable System | | 3D Vicon Motion Analysis System | |
| Sticky bull's eye markers | | Individual retro-reflective markers + clusters of 4 markers each | |
| Marker Name | Location | Name | Location |
| <i>Dynamic trials markers</i> | | <i>Dynamic trials markers</i> | |
| Hip Marker | Great Trochanter | WAIST Cluster | On the back close to the sacrum |
| Knee Marker | Lateral Epicondyle | LTHIGH Cluster (RTHIGH) | Lateral and distal aspect of the left (right) thigh |
| Ankle Marker | Lateral Malleolus | LSHANK Cluster (RSHANK) | Lateral and distal aspect of the left (right) shank |
| Heel Marker | Lateral aspect of the heel | LMET1 (RMET1) | Left (right) 1 st metatarsal head |
| Medial Heel Marker | Medial aspect of the heel | LMET5 (RMET5) | Left (right) 5 th metatarsal head |
| Toe Marker | Lateral side of the 5 th metatarsal head | LHEEL (RHEEL) | Left (right) calcaneus |
| Medial Toe Marker | Medial side of the 1 st metatarsal head | <i>Static anatomical landmark calibration trial markers</i> | |
| All the above are placed on both left and right legs | | LASIS (RASIS) | Left (right) anterior superior iliac spine |
| | | LPSIS (RPSIS) | Left (right) posterior superior iliac spine |
| | | LLEPI (RLEPI) | Left (right) lateral epicondyle |
| | | LMEPI (RMEPI) | Left (right) medial epicondyle |
| | | LLMAL (RLMAL) | Left (right) lateral malleolus |
| | | LMMAL (RMMAL) | Left (right) medial malleolus |

Table 3.5: Marker set used during data collection. Markers are classified in according to the capture system they are used for.

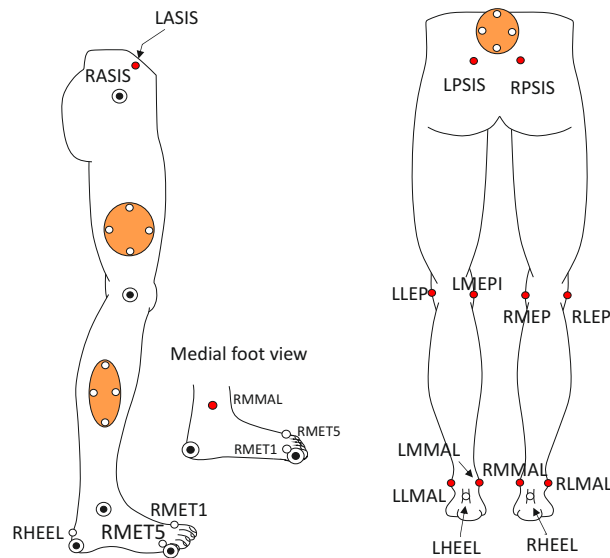


Figure 3.4: Lower limb marker set combining bull's eye markers and 14 mm diameter individual markers and rigid cluster. In red, markers on anatomical landmarks are shown.

A marker set, outlined in Table 3.5, that combined sticky bull's eye paper marker labels and 14 mm diameter retro-reflective markers was used to enable data collection from both systems simultaneously (Figure 3.4). Reflective markers and rigid clusters of four markers each were attached using hypoallergenic double-sided tape.

Each human subject test session commenced with the capture of a static anatomical landmark calibration trial while the subjects maintained an up right position at the centre of the capture volume. Anatomical landmarks markers were removed prior to the dynamic trials. The key anatomical positions with respect to the cluster technical frames, obtained from the static calibration, were used to reconstruct anatomical frames of reference in each sampled instant of time in accordance with standard recommendations (Wu et al., 2002; Baker, 2003) to allow limb joint motion description. A total of six walking trials were recorded by both systems with three times the right leg and then the left leg facing the lateral video camera of the AVPS system. Subjects walked up and down the mat at a self generated speed wearing shoes. Data sampling was set at 100 Hz for the 3-D motion analysis system while video data were recorded at 210 Hz.

3-D markers trajectories were reconstructed after each acquisition and filtered with Woltring's generalized cross-validation with splines (GCVSPL) with a predicted mean squared error of 15mm (Woltring 1985; 1986). Knee joint angles were calculated using the joint coordinate system convention (Grood and Suntay, 1983). Hip centre location was estimated using the methods of Harrington et al. (2007), whereas knee and ankle joint centre were assumed to be the mid point between the two epicondyles and malleoli, respectively. For each trial the temporal events characterising a gait cycle were identified. All computations of data acquired with the 3-D system were performed using Nexus and Bodybuilder softwares (Vicon, Oxford Metrics Ltd., UK). The 3-D coordinates of the lateral epicondyles and lateral malleoli were used to calculate the tibia to vertical angle using simple trigonometry properties, while heel markers coordinates were used to identify the position of the foot on the mat.

Video gait data processing was performed using Pro Trainer DV motion analysis software (Sport Motion Inc., USA). Frames captured were transferred onto a computer and using freeze frames and slow motion playback features of Pro Trainer DV software, gait events and feet position on the mat were determined. Sagittal knee joint angles and tibia to vertical angles were quantified using the software goniometric tool. Measurements extracted from the two systems and kept for statistical analysis were: walking speed, temporal and spatial symmetry of the gait defined respectively as the ratio of step time and step length of the left and right legs, knee sagittal angles at initial and terminal contact and tibia to vertical angle at initial contact, foot flat, mid stance and terminal contact.

All statistical computations were implemented with a commercial statistics software package (SPSS Statistics 17.0, IBM, USA). Descriptive statistics were used to summarise the results. Means and standard deviations for each of the temporo-spatial parameters and kinematic measurements with respect to the trials and between each video/motion system were obtained. Mean differences between both systems were determined and correlations between them were examined.

3.4.3 Results

The AVPS system was validated against a two segments goniometric rig and the 3-D Vicon motion analysis system. The results showed good agreement between both motion analysis systems (Figure 3.5). The AVPS produced a strong correlation with the goniometric rig ($R^2 = 0.999$) and the 3-D Vicon motion analysis system ($R^2 = 0.999$). Based on the two segment goniometric rig range of measure (-90° to $+90^\circ$, at 10° increments), the differences between the measurements from AVPS and the Vicon system were very small and ranged from -0.9 to 0.8° . Differences between angles values obtained from the AVPS and the goniometric rig were also small and ranged from -1.0 to 1.0° . Percentage error between the AVPS and the 3-D Vicon motion analysis systems from 0° to $+90^\circ$ and 0° to -90° were 0.88 and 1.0 respectively. There were no significant differences between the AVPS and the 3-D Vicon motion analysis systems (p -value = 0.206), between the AVPS and the two segment goniometric rig (p -value = 0.578), and 3-D Vicon and two segment goniometric rig (p -value = 0.305).

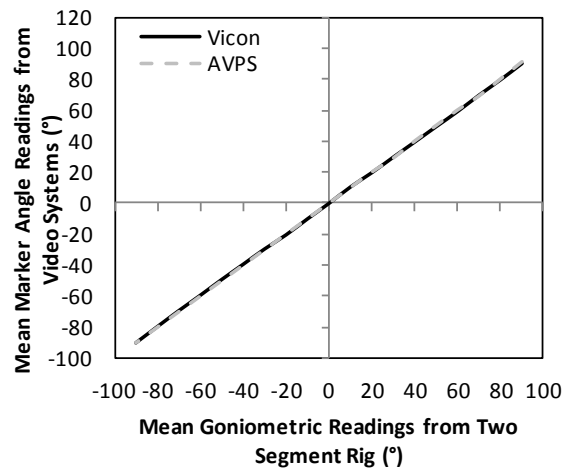


Figure 3.5: Goniometric readings versus angle readings from AVPS (grey dotted line) and Vicon systems (black solid line).

With regards to gait trials, both the AVPS and Vicon system showed a small variability in the outcome measures as indicated by the size of the standard deviations (Table 3.6). There were no significant differences between the AVPS and

the 3-D Vicon motion analysis system with respect to the measured variables (p -values > 0.05) (Table 3.6).

| Variables | Augmented Video-based Portable System (Mean \pm SD) | 3D Vicon Motion Analysis System (Mean \pm SD) | P-Value |
|---|---|---|---------|
| Right Leg Walking Speed (m/s) | 1.2 \pm 0.1 | 1.3 \pm 0.1 | 0.113 |
| Left Leg Walking Speed (m/s) | 1.2 \pm 0.1 | 1.3 \pm 0.1 | 0.122 |
| Right Leg Knee Joint Angle (IC) ($^{\circ}$) | 3.6 \pm 1.8 | 2.4 \pm 1.3 | 0.067 |
| Left Knee Joint Angle (IC) ($^{\circ}$) | 4.1 \pm 2.6 | 2.5 \pm 1.4 | 0.107 |
| Right Leg Knee Joint Angle (TC) ($^{\circ}$) | 48.6 \pm 4.2 | 48.6 \pm 2.3 | 0.986 |
| Left Leg Knee Joint Angle (TC) ($^{\circ}$) | 46.1 \pm 7.0 | 47.7 \pm 2.5 | 0.384 |
| Right Leg Tibia Inclination Angle (IC) ($^{\circ}$) | 23.5 \pm 2.5 | 22.8 \pm 2.2 | 0.053 |
| Left Leg Tibia Inclination Angle (IC) ($^{\circ}$) | 19.9 \pm 2.8 | 20.8 \pm 2.1 | 0.165 |
| Right Leg Tibia Inclination Angle (FF) ($^{\circ}$) | 5.6 \pm 2.2 | 5.1 \pm 1.6 | 0.136 |
| Left Leg Tibia Inclination Angle (FF) ($^{\circ}$) | 3.2 \pm 2.6 | 4.3 \pm 1.5 | 0.079 |
| Right Leg Tibia Inclination Angle (MS) ($^{\circ}$) | 6.1 \pm 1.8 | 6.2 \pm 1.9 | 0.161 |
| Left Leg Tibia Inclination Angle (MS) ($^{\circ}$) | 10.7 \pm 3.0 | 10.3 \pm 2.7 | 0.077 |
| Right Leg Tibia Inclination Angle (TC) ($^{\circ}$) | 51.4 \pm 2.3 | 52.6 \pm 1.7 | 0.110 |
| Left Leg Tibia Inclination Angle (TC) ($^{\circ}$) | 53.8 \pm 2.9 | 53.9 \pm 2.0 | 0.379 |
| Temporal Symmetry | 1.0 \pm 0.1 | 1.0 \pm 0.02 | 0.603 |
| Spatial Symmetry | 1.0 \pm 0.05 | 1.0 \pm 0.02 | 0.920 |

Table 3.6: Outcome parameters from the two systems averaged across the twelve participants. Mean, standard deviation and p -values are reported.

3.4.4 Discussion and conclusion

The analysis conducted showed that the AVPS is capable of generating valid data in a repeatable fashion. Good agreement was shown between the angle values obtained with the AVPS and read from the goniometric rig ($R^2 = 0.999$, Figure 3.5) and, analogously, with the more sophisticated 3-D Vicon system ($R^2 = 0.999$, Figure 3.5, Table 3.6). This gives further strength to the system developed shown already to have good intra- and inter-rater reliability. The drawback of the system still remains the data processing that although simple, for the time being, is still manual.

Customised Microsoft Excel spreadsheets are used to calculate the ultimate outcomes but the values in input are manually identified on the videos through Pro Trainer DV software. To this extent data analysis could be improved to accelerate this process but without adding any difficulties to it.

In conclusion, a gait assessment technique that is simple, portable, cost effective, flexible and yet accurate has been developed. This AVPS is a potential clinical tool kit, which have a simple set up to operate.

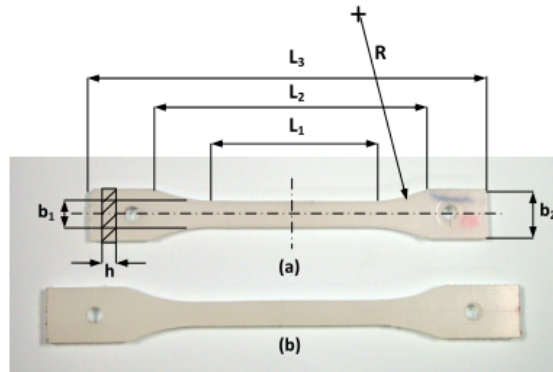
CHAPTER 4 – ORTHOTIC LOAD MEASUREMENT

4.1 Introduction

Few biomechanical studies have attempted the investigation of the loads and stresses acting on an ankle-foot orthoses (AFOs) during gait (paragraph 1.5.3). The limitations characterising these studies leave open for discussion what loads are carried by an AFO and consequently the prescription of the orthosis remain based on empirical techniques. One aim of this project was to investigate a methodology to measure such loads in a reliable manner. Electrical resistance strain gauges attached to the AFO were used for this aim. A similar method was employed by Chu et al. (1996; 1998; 2000). However, in these authors' reports, the accuracy of the methodology was not verified and, moreover, the effect of the UV light treatment required to fix the gauges on to the polypropylene (PP) material was not investigated. UV light exposure to treat the plastic before attaching the strain gauge foil is required to improve the bond between these two elements. Prior to this thesis, in an investigation of the accuracy of strain gauges attached to polypropylene (copolymer), it was found that better accuracy in strain readings was achieved in UV-light pre-treated samples compared to untreated ones (Papi, 2008).

In this chapter, in section 4.2, the tests to establish the tensile properties of the homopolymer polypropylene, from which AFOs are fabricated, are reported. These included tests to determine polypropylene's (PP) viscoelastic nature and Young's modulus, anisotropy and, the effect of UV light irradiation on the material properties. In section 4.3 the assessment of the performance of strain gauges attached to polypropylene is described. This was undertaken with the prospective of using strain gauges to determine orthotic loads generated by the AFO fitted to a subject's leg during normal level walking.

Moreover, test with aluminium samples, both instrumented and not instrumented with strain gauges, were conducted and are discussed in section 4.4. They allowed a verification of the instrumentation used and in particular of the extensometer utilised during the tests of both materials samples.



| <i>Specimen type:</i> | | (a) | (b) |
|-------------------------|---|-----|-----|
| Dimensions in mm | | | |
| L_1 | Length of narrow parallel-sided portion | 60 | 50 |
| L_2 | Distance between broad parallel-sided portions | 108 | 115 |
| L_3 | Overall length | 150 | 165 |
| R | Radius $R = [(L_2 - L_1)^2 + (b_2 - b_1)^2] / 4(b_2 - b_1)^2$ | 60 | 76 |
| b_1 | Width of narrow portion | 10 | 13 |
| b_2 | Width at the ends | 19 | 20 |
| h | thickness | 4.5 | 6 |

Figure 4.1: Test sample dimensions as obtained from the 4.5 mm (a) and 6 mm (b) thick PP sheets.

Moreover, these tests provide an insight into the reliability of strain gauging metals, which is a well-proven technique. They were conducted as a back up alternative to strain gauging an AFO for orthotic load measurement. In case strain gauges fail to measure strain in polypropylene, in fact, the alternative is to attach strain gauges on metal bars and insert them on to the solid AFO.

Finally, in section 4.5, the method for orthotic load measurement consisting of attaching strain gauges into the plastic AFO is described and the results of its preliminary application are reported.

4.2 Material testing

4.2.1 *Materials and Methods*

Tests were conducted on homopolymer polypropylene (PP) specimens under tensile load conditions to investigate material properties, i.e. stress and strain relation, and in addition to determine if sheet orientation affects the PP behaviour and to ensure that UV light treatment does not have a detrimental effect on the material. Two sheets of homopolymer polypropylene supplied by North Sea Plastics Ltd. (Glasgow, UK), with a measured thickness of 4.5 mm and 6 mm were used to obtain the set of samples necessary for the tests. Dumb bell-shaped specimens were cut from polypropylene sheets following the dimensions indicated in the British Standard BS 527-2 (1996) for the 4.5 mm thick sheet and in the American Standard ASTM D638-2008 for the 6 mm sheet (Figure 4.1). This shape was thought to reduce local stress concentration while allowing for an even distribution of stresses in the region where measurement are taken. First, 10 samples were cut from the 4.5 mm sheet, 5 with their main axis parallel to and 5 perpendicular to the main orientation axis of the material piece. This allowed the investigation to determine whether the material is anisotropic or not. Samples cut parallel to the main orientation axis of the PP sheet are referred in the text as standard samples, whereas perpendicular samples are the sample cut perpendicular to the standard ones. Ten more specimens were cut all in the same orientation from the 6 mm thick polypropylene sheet. Five of these were subsequently treated with UV light emitted from a CS410-EC UV curing system (Thorlabs Inc, New Jersey, USA). The samples' surface, where the extensometer

would be attached, was positioned at approximately 25 mm distance from the UV light source for a duration of 30 minutes (Chu et al., 1996).

The PP specimens were tested on an Instron 5800R tensile testing machine (Instron, Norwood, USA) following as far as possible the British Standard BS 527-1 and the American Standard ASTM D638-2008. An extensometer (Instron, Norwood, USA) with a gauge length of 10 mm was used to measure strain during the test. The extensometer was attached on the side of the specimen using rubber O’rings, after the sample had been clamped into the testing machine. Before starting a test the O’rings were checked to ensure they were not loose and the extensometer was firmly attached to the sample so preventing slippages during the data collection. The samples were tested in tension in a stress range between 0 and 2 MPa, which covers the tensile stress likely to be experienced by a plastic AFO in use according to either experimental or finite element analysis studies (Chu et al, 1995, 1998, 2000). A test protocol (Figure 4.2) was created using the software Instron Wavemaker and applied through Instron Waverunner to each sample. The protocol (Figure 4.2) consisted of 200 loading cycles up to 100 N for the 4.5 mm sheet and 120 N for the 6 mm sheet, which correspond to a stress of 2 MPa at the given cross sectional areas of 48.6 mm² (4.5 mm sheet) and 60.22 mm² (6 mm sheet) respectively, followed by a 30 minutes hold step at full load. For each cycle 5 s were allowed for the load to reach the maximum value and 5 s to return to 0 N.

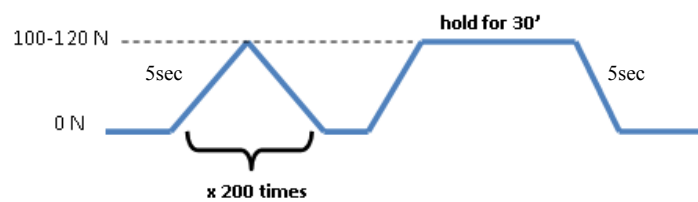


Figure 4.2: Test protocol applied to PP samples with an Instron 5800R tensile testing machine.

Moreover, a continuous tensile load from 0 to 1000 N was applied to one additional specimen with a cross sectional area of 48.6 mm². This maximum load corresponded to a stress of 20 MPa.

Strain data from the extensometer, the corresponding load applied by the testing machine and the crosshead movement were collected at 10 Hz. A statistical analysis was performed using two sample *t*-test at 0.05 level of significance for Young's Modulus of standard PP samples, perpendicular PP samples and UV light treated samples. The Young's Modulus was calculated using the method described in BS 527-1 for computer aided equipment which involved a linear regression procedure applied on the stress-strain curve between two fixed values of strain, 0.0005 and 0.0025. The stress was computed by dividing the loads (N) applied by the initial cross sectional area (mm²) of each sample, whereas strain was calculated by dividing the extensometer readings by its gauge length (10mm).

4.2.2 Results

The experimental findings obtained from tests on the standard, perpendicular and UV treated samples are reported in this section.

Figure 4.3 shows the stress-strain graph of a typical sample for the tensile test. The speed of testing (relative rate of motion of the grips) for the tests conducted was 0.028 (\pm 0.001) mm/min for the 4.5 mm thick standard and perpendicular samples, 0.035 (\pm 0.002) mm/min and 0.08 (\pm 0.001) mm/min for untreated and UV treated 6 mm specimens respectively.

The polypropylene after a preconditioning phase, reached a steady state as the number of cycles increased, with reduced differences among curves.

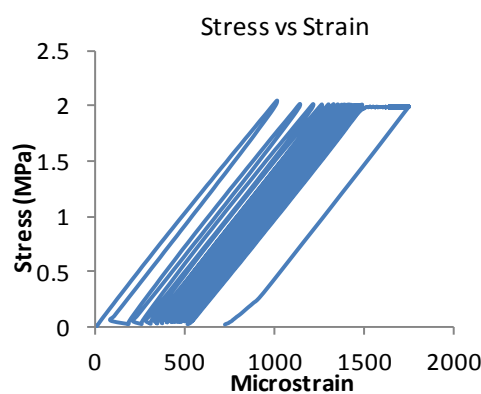


Figure 4.3: Stress-strain graph of a selected polypropylene sample under tensile loads.

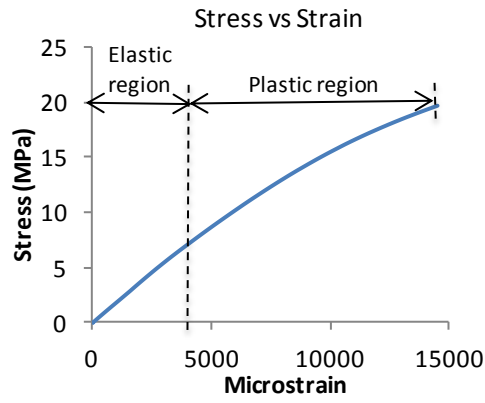


Figure 4.4: Stress-strain graph for the continuous tensile load test up to 1000 N (20 MPa).

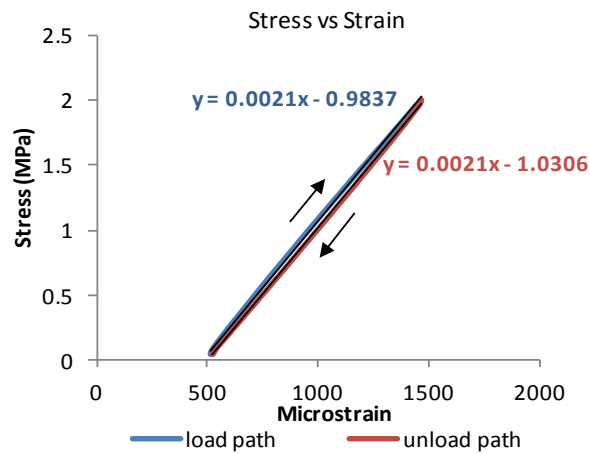


Figure 4.5: Stress-strain graph of the last test protocol cycle of a typical polypropylene sample. Arrows indicate the loading and unloading path. Hysteresis is noticeable.

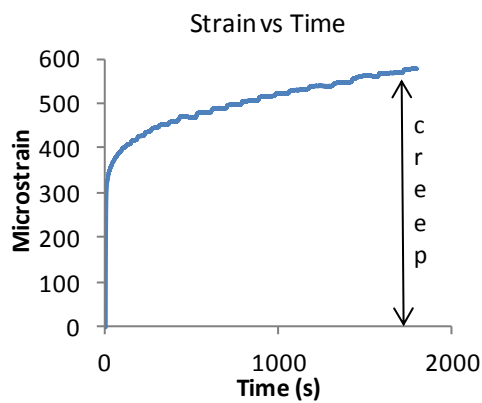


Figure 4.6: Creep during the 30 minutes hold step at 100N for a typical sample.

For the applied test speed between 0 and 2 MPa, the stress-strain relationship for polypropylene is linear and thus Hooke's law applies to determine the Young's Modulus. Under higher loads condition, Figure 4.4, polypropylene showed a non-linear relation between strain and stress beyond a certain limit, indicative of its yield properties. A limit of 7 MPa was identified before the stress-strain curve started to become non linear. A permanent deformation of 1261.9 microstrain (residual strain) was recorded after unloading the sample from a stress of 20 MPa.

Although during the test cycles the sample was stressed within the polypropylene linear region, hysteresis occurred as another manifestation of viscoelasticity. Figure 4.5 presents the stress-strain curve of one cycle of a typical sample highlighting the difference between loading and unloading paths (hysteresis). As can be further noticed from this figure, both parts of the cycle are however near coincident with the relative best trendline by means of a linear stress-strain relation, also confirmed by R^2 values of 0.9995 or higher. The load and unload trendlines are parallel as demonstrated by the same slopes in the equations of the best fitted line, hysteresis is thus low.

When the load was maintained constant during the 30 minutes step hold test, creep was observed (Figure 4.6). An increase in microstrain on average of 504.5 (± 44.3) was recorded across all samples but for UV treated specimens a lower values of 314.4 (± 34.9) was found.

Although these figures refer to a typical sample, stress-strain graphs for the other specimens were similar and comparable to the ones reported.

For each sample, the Young's Modulus was obtained as mean of the moduli of cycles 160, 170, 180, 190 and 200. The higher limit of the strain range between which the Young's Modulus should be calculated, as dictated by BS 527-1, was not achieved with the load applied. It was thus decided to calculate the Elastic Modulus between a strain of 0.0005 and 0.001, instead of 0.0005 and 0.0025. Table 4.1 lists the mean values of Young's Modulus of standard and perpendicular samples obtained from the 4.5 mm thick polypropylene sheet; whereas, in table 4.2 the Young's Modulus of standard and UV treated samples cut from the 6 mm thick polypropylene are reported.

| YOUNG'S MODULUS (MPa) | | | |
|-----------------------|----------------------|----------------|-----------------------|
| Standard: | | Perpendicular: | |
| Sample 1 | 1819.9 (\pm 1.1) | Sample 1 | 1823.9 (\pm 1.8) |
| Sample 2 | N/A* | Sample 2 | 1937.26 (\pm 0.7) |
| Sample 3 | 1810.3 (\pm 1.1) | Sample 3 | N/A* |
| Sample 4 | 1951.5 (\pm 0.4) | Sample 4 | 2029.0 (\pm 1.5) |
| Sample 5 | 1961.8 (\pm 0.6) | Sample 5 | 2085.6 (\pm 0.8) |
| Average | 1885.9 (\pm 81.9) | Average | 1968.9 (\pm 114.4) |

Table 4.1: Mean over 5 cycles of Young's Modulus values found experimentally for standard and perpendicular test samples of 4.5 mm thickness. In brackets the standard deviation is shown.

During the test of two samples (N/A in Table 4.1*) the extensometer came off and thus the values of the Young's Modulus could not be calculated.

| YOUNG'S MODULUS (MPa) | | | |
|-----------------------|----------------------|-------------|-----------------------|
| Standard: | | UV treated: | |
| Sample 1 | 2028.4 (\pm 3.7) | Sample 1 | 1970.7 (\pm 14.3) |
| Sample 2 | 2122.1 (\pm 4.7) | Sample 2 | 2182.1 (\pm 13.9) |
| Sample 3 | 2001.3 (\pm 0.4) | Sample 3 | 2243.6 (\pm 7.2) |
| Sample 4 | 1993.8 (\pm 7.1) | Sample 4 | 2122.9 (\pm 3.9) |
| Sample 5 | 1860.8 (\pm 0.5) | Sample 5 | 2097.16 (\pm 5.7) |
| Average | 2001.3 (\pm 93.7) | Average | 2123.3 (\pm 102.3) |

Table 4.2: Mean over 5 cycles of Young's Modulus values found experimentally for standard and UV treated test samples of 6 mm thickness. In brackets the standard deviation is shown.

Two sample *t*-tests, at 0.05 level of significance on the mean values of Young's Modulus, were conducted between the standard and perpendicular group samples and the standard and UV treated group samples. The *p*-values obtained were respectively 0.28 and 0.09, both greater than the chosen level of significance. The null hypotheses that polypropylene stiffness did not change with sheet orientation or UV light exposure could not be rejected.

4.2.3 Discussion and Conclusion

Polypropylene behaviour under tensile load condition was investigated through the tests conducted. Its viscoelastic nature was revealed showing a linear stress-strain

relation at low stress (0-7 MPa) and an increase of non-linearity as the material was subjected to a higher load condition (Figure 4.4). The onset of a permanent deformation was achieved by moving away from the elastic limit.

Although within the encompassed stress range during the tests, polypropylene was within its linear region, hysteresis was observed and a full recovery of the deformation did not occur when the load was removed. This can be explained by the nature of viscoelastic materials that tend to flow under tensile loads rearranging their polymeric chains. Intermolecular bonds that keep polymers stable in position, break during this process dissipating energy and hence hysteresis. The reestablishment of broken bonds for viscoelastic material is time-demanding and consequentially recovery is slow. To return to its original length each sample would have necessitated a longer time than the one allowed during the performed tests and hence the residual strain observed at zero load condition. As the number of cycles increased, curves in the stress-strain graphs were closer to each other, hysteresis loops overlapped and the residual strain was constant (Figure 4.3). A preconditioned state that corresponds to a certain strain value for a given stress was reached. Preconditioning should be taken into account when testing a polypropylene AFO to avoid misleading results.

Creep, another aspect of viscoelastic material, was observed during hold steps. All samples showed an increase in strain at 2 MPa in the time allowed. UV treated samples showed a smaller strain response at constant load in comparison to untreated samples, 300 microstrain against 500, respectively. A smaller creep is due to a stiffer material. UV treated samples, although not significantly, have higher Young's Moduli in comparison to all other specimens and thus higher resistance to deformations. This can be the explanation for a lower creep in UV treated specimens. The Young's Modulus was calculated experimentally from the stress and strain values obtained from the tests of each sample. The material supplier indicates a Young's Modulus >1300 MPa for homopolymer polypropylene. Low values for polypropylene Young's Modulus are quoted in the literature; however, comparisons with these estimates are difficult due to the numerous variables that can affect it, such as strain rate, temperature, loading history and method of calculation. If a wide range of strain is considered in the determination of the Modulus, it will result in a

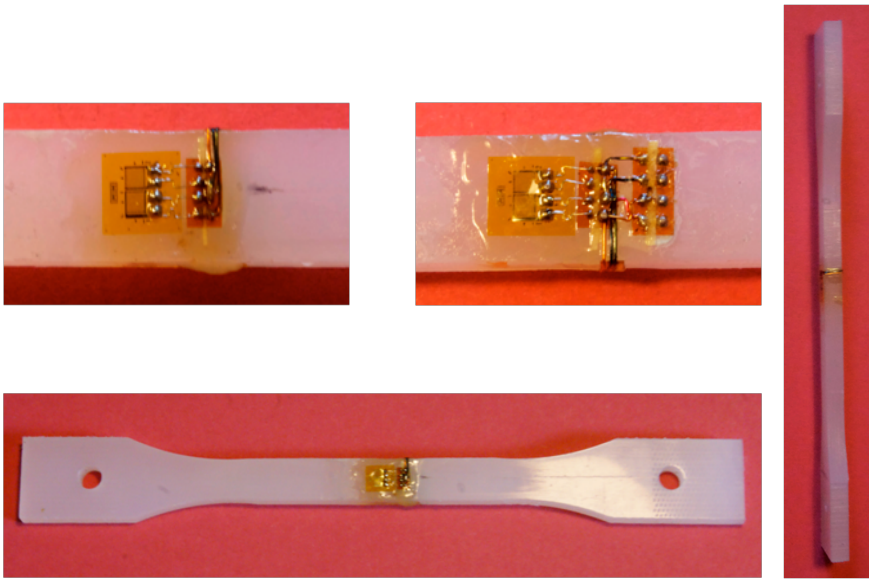


Figure 4.7: A Strain gauged homopolymer polypropylene sample with particulars of strain gauges on the upper and lower surface and side view.

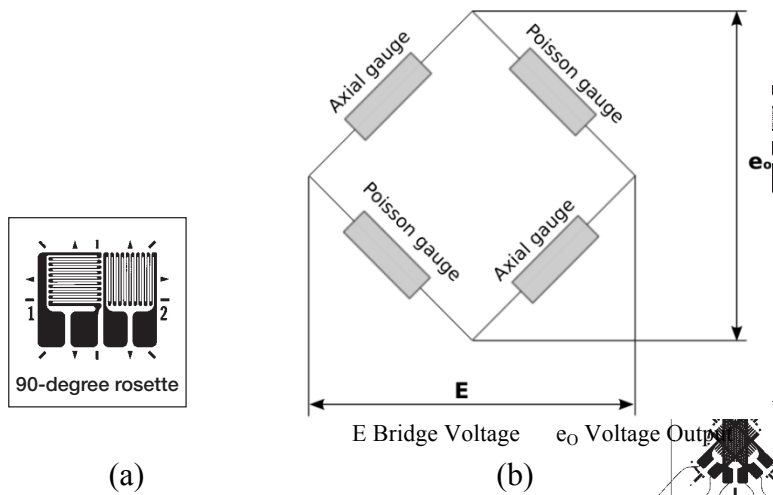


Figure 4.8: (a) Two-element 90° degrees rosette strain gauge used for strain measurement (Vishay Precision Group, Malvern, USA), (b) Wheatstone bridge circuit.

smaller value. Moreover, it is rarely indicated if the reference is to copolymer polypropylene or homopolymer polypropylene. The latter is expected to be stiffer. The values obtained reflect the supplier indication of being overall higher than 1800 MPa. Young's Moduli obtained from the 6mm thick polypropylene sheet were generally greater than the ones obtained from the 4.5 mm polypropylene. This result may be explained with the differences in the speed of testing and thus in strain rate. A viscoelastic material is characterised by a non instantaneous time-dependant response to applied stresses. As a consequence, strains at a given stress differ with changing in strain rate, the higher the rate the smaller the strain, the stiffer the behaviour of the material (Crawford, 1992).

The Elastic Moduli of the perpendicular and UV treated samples were higher than Moduli of standard polypropylene samples; however these differences were not statistically significant (p -values > 0.05). This leads to the conclusion that neither sheet orientation nor UV treatment alter the material behaviour in tension. This allows the utilisation of UV exposure in the preparation of polypropylene surface prior to attachment of strain gauges.

Having highlighted the material properties and the suitability of UV pre-treatment, the next step is to investigate the achievable accuracy of using strain gauging technique on a plastic material before proceeding to the analysis of the loads carried through an AFO.

4.3 Strain gauge testing

4.3.1 *Materials and Methods*

Two strain-gauged samples (Figure 4.7) were tested twice (referred in the text as Test1, Test2) with the test protocol used for the material testing comprising 200 load cycles. Samples were cut to the dimensions indicated in the American Standard ASTM D638-2008 as for the 6 mm thick samples described earlier. The polypropylene was locally treated with UV-light on the part of the surface designated for attachment of the strain gauges. UV light exposure lasted 30 minutes for each of the surfaces (upper and lower) of the samples positioned at 25mm distance from the UV source (Thorlabs Inc, New Jersey, USA) (Chu et al., 1996). Two, two-element 90° degrees rosette strain gauges (Figure 4.8) (Vishay Precision Group, Malvern,

USA) were used and connected so as to create a full Wheatstone bridge circuit. This allowed small changes in electric resistance in the gauge wires to be detected and the strain being determined.

Strain gauges were attached aligned to the principal axes of the sample with cyanoacrylate adhesive on both sides of the sample. Once the adhesive was cured a coating agent was applied over the gauges and lead wires.

The two strain gauged samples so prepared were then clamped into the Instron 5800R tensile testing machine (Instron, Norwood, USA) and the same test protocol outlined earlier was run (Figure 4.2). The extensometer was positioned on the side of the sample allowing a simultaneous measurement of strain along with the strain gauges. The Wheatstone bridge was connected to an amplifier and the outputs, together with extensometer measurements, loads applied and crosshead movement, were transferred into a computer via a data acquisition card (PCI-6040E, National Instruments, Texas, USA). From the computer with a custom-built Labview (Labview software 8.6, National Instruments, Texas, USA) program the four signals were acquired and stored in a Microsoft Excel spread sheet for subsequent data processing. Data sampling was 10 Hz. Data collected were filtered, prior to analysis, to reduce the noise introduced by the recording system used. For this purpose, a custom-made moving average filter implemented via Matlab signal processing software (The MathWorks Inc., Massachusetts, USA), was applied to the data stored. The voltage outputs from the Wheatstone bridge were applied to Equation 4.1 (Papi, 2008), derived from the analysis of the circuit, to calculate strain values:

$$\varepsilon = \frac{2 \cdot e_o}{(1+\nu)E \cdot K_S \cdot G} \quad \text{Equation 4.1}$$

Where: ε = Strain (mm/mm);

e_o = Bridge output (V);

ν = Poisson's Ratio;

E = Bridge voltage (V);

K_S = Gauge Factor;

G = Amplifier Gain.

Amplifier gain (G) and bridge voltage (E) were set at 200 and 3 V respectively. The gauge factor (K_s), provided by the strain gauges supplier, was 2, and a Poisson's Ratio for polypropylene of 0.36 was used (Crawford, 1998).

By dividing the extensometer reading by its gauge length (10 mm), strains from the extensometer were also calculated

The feasibility of the strain measurement obtained through strain gauges attached to polypropylene was assessed by means of a comparison with simultaneously recorded extensometer readings under the given load conditions. The discrepancy between the systems was expressed as percentage difference (Equation 4.2) of the strain range (highest-lowest values) computed with both methods for loading and unloading steps of the test protocol. The percentage was calculated relatively to the strain range obtained by the strain gauges:

$$\% \text{ Difference} = \left(\frac{\text{Strain Gauge Range} - \text{Extensometer Range}}{\text{Strain Gauge Range}} \right) \cdot 100 \quad \text{Equation 4.2}$$

4.3.2 Results

Strains calculated from the Wheatstone bridge output applied to Equation 4.1 were compared to strain values obtained from the extensometer. Although similar trends of strain against time can be generally noticed, with polypropylene reaching a steady state as the number of cycles increase (Figure 4.9 a, b), differences existed in the values of strain measured.

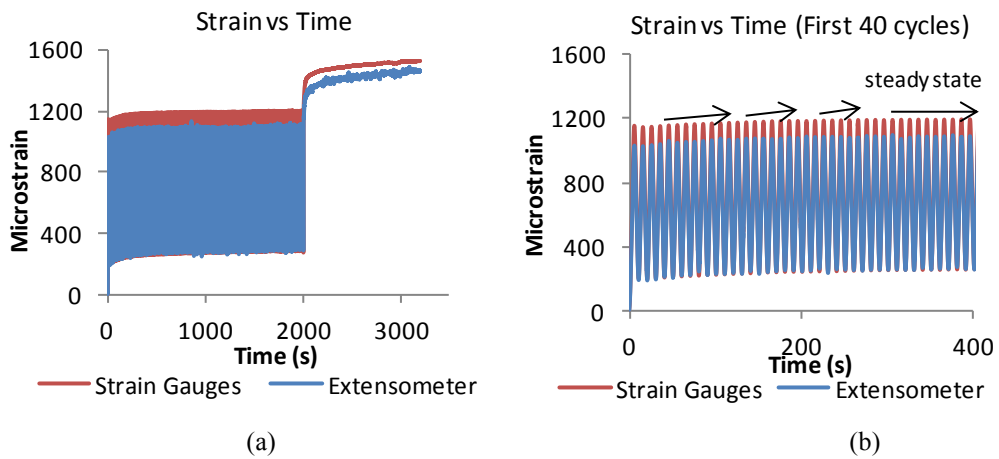


Figure 4.9: (a) Microstrain against time measured by the extensometer (blue curve) and strain gauges (red curve); (b) particular of plot (a) showing the approaching of a steady state. Data are from sample 2 test 1.

The percentage difference in the measurements from the two systems was evaluated separately for loading and unloading path and in the part of the curve where polypropylene was mostly stable. The derived quantities are presented in Table 4.3. These values represent the average percentage differences in the range of measurement (value at 2 MPa – value at 0 MPa) for load and unload for the last 5 cycles as computed from the strain gauges and the extensometer.

| | AVERAGE PERCENTAGE DIFFERENCES (%) | | | |
|------------------|------------------------------------|--------|----------|--------|
| | SAMPLE 1 | | SAMPLE 2 | |
| | Test 1 | Test 2 | Test 1 | Test 2 |
| Loading | 9.2 | 19.6 | 11.6 | 11.6 |
| Unloading | 9.1 | 19.8 | 11.5 | 11.6 |

Table 4.3: Average percentage differences between strain gauges and extensometer values of strain for the last 5 cycles of test in the two samples tested.

On average, a difference of $13.0 (\pm 4.6) \%$ and $13.0 (\pm 4.7) \%$ was obtained between the two measurement systems for loading and unloading paths respectively.

Comparable discrepancies were identified among the tests conducted, although for the second test for sample 1, the divergence was higher. For this mentioned sample (Sample 1, Test 2), the extensometer gave higher values of microstrain in comparison to previous readings, up to nearly 1350 microstrain. At zero load condition, for this sample, values higher than 500 Microstrain were measured throughout the test.

Moreover, it was observed a continuous increasing in strain estimated from the extensometer whereas a more steady state would have been expected and it was instead obtained from the strain gauges. Strain against time for the aforementioned sample and test is shown in Figure 4.10 a. For all the above reasons, for the discrepancies in test 2 of sample 1, the extensometer was thought to give the error due to the odd measurements observed.

Strain gauges readings were found to be higher than extensometer measured values for the first run of the test, whereas for the repeated tests (Test 2) the extensometer gave higher values of strain (Figure 4.10 a). However, for the second test of sample 1 and 2, it was noticed a changing in the path of values measured by the two systems, by mean that first it was the strain gauges to give higher values but as the test proceeded the contrary occurred (Figure 4.10 b). Again the extensometer showed a slight increase in strain rather than an approaching of a constant state although less markedly than test 2 of sample 1 (Figure 4.10 a).

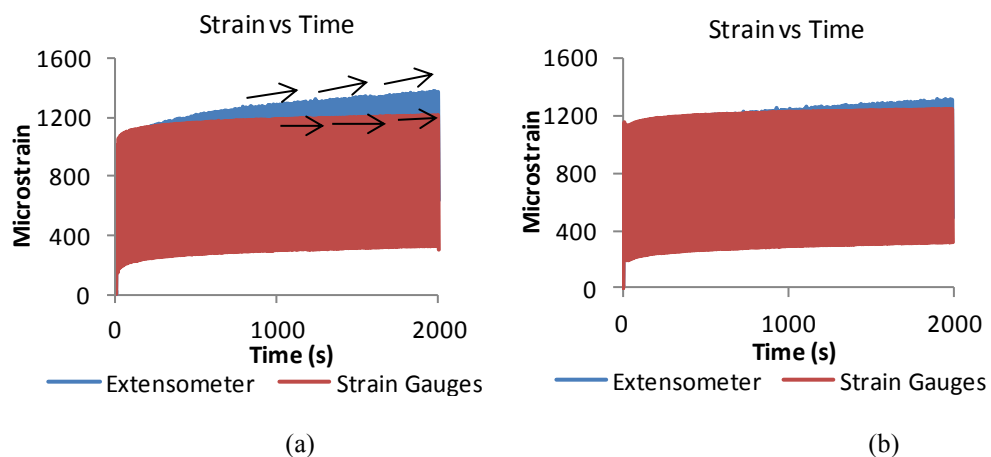


Figure 4.10: Microstrain against time during the 200 load cycles measured by the extensometer (blue curve) and strain gauges (red curve) for sample 1 test 2 (a) and sample 2 test 2 (b).

It was also observed that data measured by strain gauges were more repeatable than values detected by the extensometer and reflected more the results obtained when the sample of the same dimensions were tested without being instrumented. The chart bar in Figure 4.11 allows a comparison of absolute peak strain values as obtained at the end of the 200 cycles for not instrumented and instrumented (strain gauged)

samples. The microstrain obtained as average of microstrains of samples without strain gauges treated and untreated with UV light is assumed to be the reference value (green bars in the chart) to which new measured strains can be compared to. A standard deviation of 37.7 and 137.0 microstrain was found for strain gauges and extensometer measured values respectively. Standard deviation bars are reported in the graph in each mean bar (Figure 4.11).

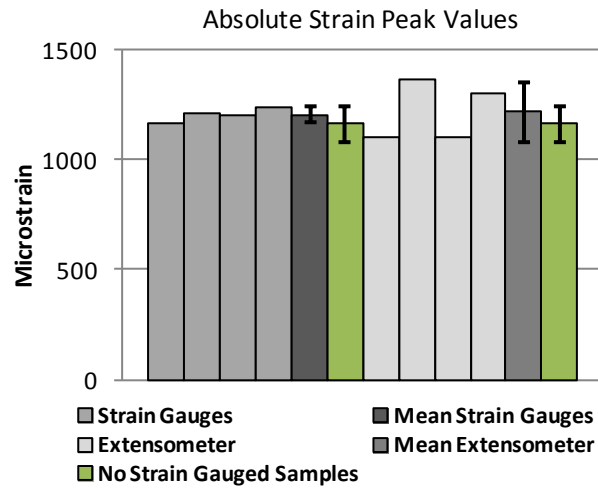


Figure 4.11: Microstrain peak values for the last cycle (200) as measured by strain gauges (grey bars) and extensometer (light grey bars) in the instrumented samples (2 samples, 2 test each). Mean (standard deviation) bars are also shown relatively to the two systems for instrumented samples and for non strain gauged samples (green bar).

The difference between strain gauges and extensometer mean measurements to that of the reference samples (green bar) was quantified as percentage difference. The values obtained are reported in Table 4.4. Negative values indicate a strain measurement from either strain gauges or extensometer higher than the reference strain. The percentage is in terms of the reference strain.

| | PERCENTAGE DIFFERENCES (%) | | | |
|---------------|----------------------------|--------|----------|--------|
| | SAMPLE 1 | | SAMPLE 2 | |
| | Test 1 | Test 2 | Test 1 | Test 2 |
| Strain Gauges | 0.01 | -4.6 | -3.6 | -6.9 |
| Extensometer | 5.2 | -17.5 | 5.1 | -12.3 |

Table 4.4: Percentage differences between strain reference value and strain measured by strain gauges and extensometer for the peak values during cycle 200.

4.3.3 Discussion and Conclusion

Comparison between strains calculated by strain gauges to those measured by the extensometer provided an insight on strain gauges accuracy when attached to a viscoelastic material. The comparison showed that the strain gauges were measuring reasonable results, and the outcomes obtained were comparable with a previous study (Papi, 2008). Good consistency was found among the tests carried out with regards to discrepancy between measures. Results from strain gauges reflected well the outputs from not instrumented samples (Figure 4.11), and more so than the extensometer. The accuracy of the extensometer following the test conducted was questionable. Strain gauges indicated a higher strain than the extensometer at a given stress for two out of four of the tests run. In the other two cases, first it was the strain gauges that measured a higher value but as the number of cycles increased the opposite was observed. This was thought to be an extensometer fault rather than to strain gauges producing wrong strains as the outputs from them showed greater repeatability across tests (Figure 4.11).

The fact that strain gauges gave higher strains than the extensometer was unexpected. Slippages due to poor adhesion between the strain gauges and the sample surface would have caused lower values of strain to be measured by the strain gauges. This would be true also if local or global reinforcement occurred at the surface of the polypropylene (Perry, 1985). The results were a reverse of these expectations and hence it can be concluded that no slippages or reinforcement were observed. At the end of each test the strain gauges were still firmly attached to the specimens. The similar values obtained with those previously conducted tests negate an increase of stiffness.

The extensometer could not be placed directly alongside the strain gauges in the samples and, consequently, the measurements were taken from different positions on the samples, laterally of the specimens by the extensometer and from the anterior and posterior surfaces by strain gauges. The different positioning of the two systems could explain the discrepancy in strain values. Moreover, whereas strain gauges report the average strain over 2mm of length, extensometer readings are representative of an area of 10 mm in length. Given that the material is viscoelastic and thus the strain response is time dependant, averaging the strains over a larger

area (the extensometer) could have resulted in a reduced value of strain in comparison to the value obtained from a more concentrate region (the strain gauge), as this contrarily would have raised the value of strain.

In spite of the discrepancies found, overall the results obtained from the strain gauges were considered acceptable to proceed toward the strain gauging of an AFO.

Test on aluminium samples were however conducted to verify the instrumentation used and particularly the extensometer. These tests are discussed in the paragraph to follow.

4.4 Aluminium tests

4.4.1 *Materials and Methods*

Six aluminium samples without strain gauges were tested on an Instron 5800R tensile testing machine (Instron, Norwood, USA) to characterise the material. The aim of these tests was to identify the linear region of the aluminium to avoid damage to strain gauges once applied on the sample when running a tensile test. The British Standard BS EN 10002-1:2001 was used as a guide in conducting the tests and in the design of test samples. On average the cross sectional area of the dumb bell-shaped specimens was $28.14 (\pm 0.2) \text{ mm}^2$. A test protocol (Figure 4.12) was created with Instron Wavemaker to apply a series of triangular ramps starting from 500 N and increasing the load at every ramp of 500 N in 5 seconds till a maximum of 4500N (160 MPa at the given cross sectional area) and then loading the samples to failure. An extensometer (Instron, Norwood, USA) was mounted laterally to each sample during the tests but removed at the end of the ramp cycles before the sample was loaded till fracture occurred.

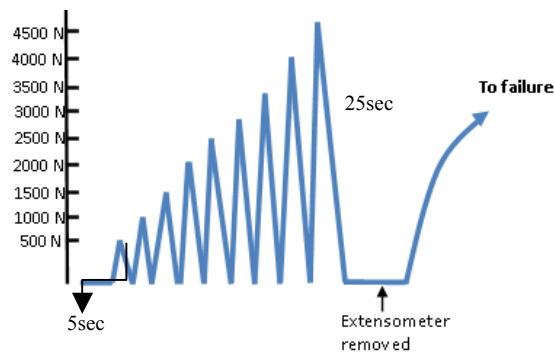


Figure 4.12: Test protocol applied to aluminium samples with the Instron tensile testing machine.

The load at fracture was recorded. The behaviour of the material under tensile load condition was investigated and stress/strain curves derived for each tested sample. Strain from the extensometer, crosshead movement and load applied were recorded at 50 Hz. The Young's Modulus was calculated as the slope of the stress/strain curve of the 2500 N load cycle between 10 and 80 MPa. The lower limit was set in order to avoid errors in the measurement caused by the instrumentation at the beginning of the stress/strain curve while, the upper limit was chosen below the quoted yield stress of the aluminium (Callister, 2000) to ensure a linear relation existed between stress and strain in the part of the curve where the Elastic Modulus was calculated.

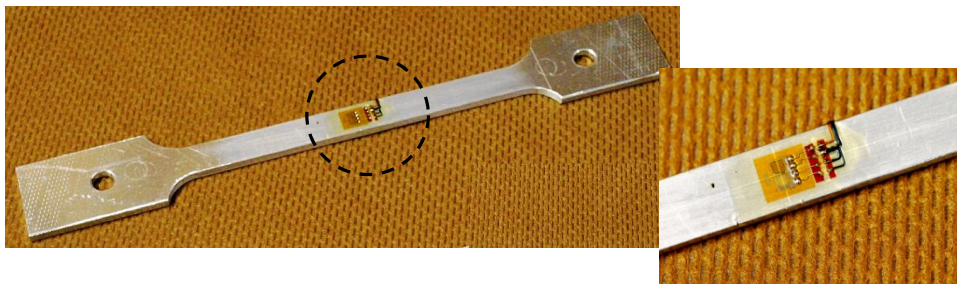


Figure 4.13: An aluminum strain gauged sample. A particular of the attached strain gauges is shown.

Two aluminium samples were strain gauged (Figure 4.13) and a test protocol applied four times in sample 1 and two times in sample 2 to evaluate the differences between calculated strains from strain gauges and extensometer readings. The test protocol designed was a consequence of the results obtained in the previous aluminium tests.

The maximum load applied did not exceed 2500 N for which the aluminium still showed a linear stress/strain relation. The protocol (Figure 4.14) consisted in a series of triangular ramps from 500 N to 2500 N incrementing the load each time of 500 N. Each 500 N was achieved in 5 seconds. The triangular ramp up to 2500 N was repeated for 15 times and then followed by a hold step of the duration of 60 seconds.

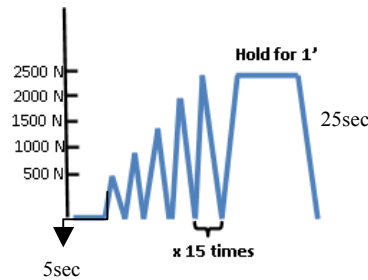


Figure 4.14: Test protocol applied to the strain gauged aluminium samples with the Instron tensile testing machine.

The same type of strain gauges (Figure 4.8) (Vishay Precision Group, Malvern, USA), used for the tests on the polypropylene samples, with a gauge length of 2 mm were attached with cyanoacrylate glue onto the upper and lower surfaces of the aluminium samples and connected to create a full Wheatstone Bridge. The test set up involved the clamping of the specimen into the tensile testing machine, the positioning of the extensometer on the side of the sample with a rubber O'ring and the connection of the strain gauges cable to an amplifier. Bridge voltage was set at 3V and the amplifier gain at 200 for data collection. Data recorded including, extensometer output, strain gauges readings, crosshead movement and, loads from the tensile testing machine, were transferred and stored into a computer with a data acquisition card (PCI-6040E, National Instruments, Texas, USA) and Labview software version 8.6 (National Instruments, Texas, USA) installed on it. The frequency of data sampling was 25Hz. Data were filtered using the same averaging filter used to smooth polypropylene test data. Outputs from the strain gauges were applied to Equation 4.1 to find the resultant strain due to the load applied. A Poisson's ratio of 0.3 was used as quoted in the literature for aluminium (Callister,

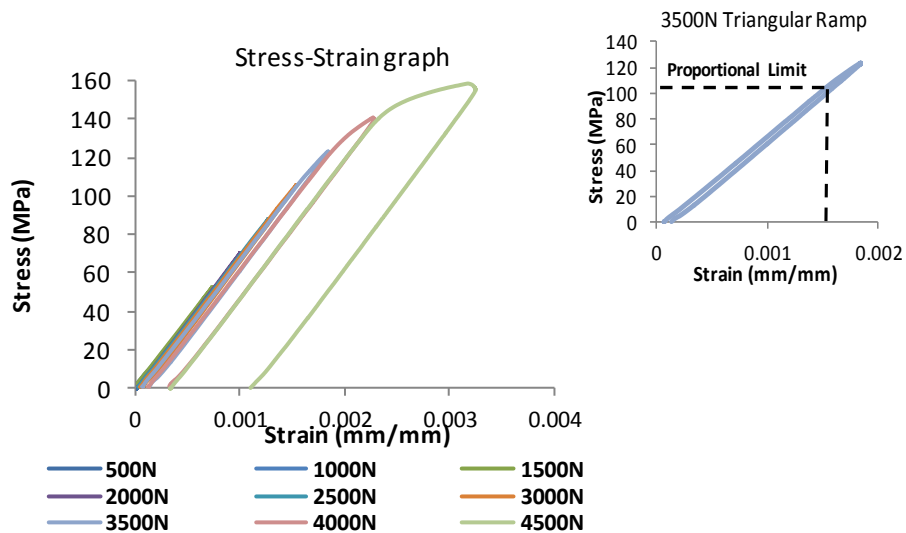


Figure 4.15: Stress/strain graph of a typical sample during the ramp loading steps from 500N to 4500N. On the side (right) the 3500N ramp is shown with the proportional limit being highlighted.

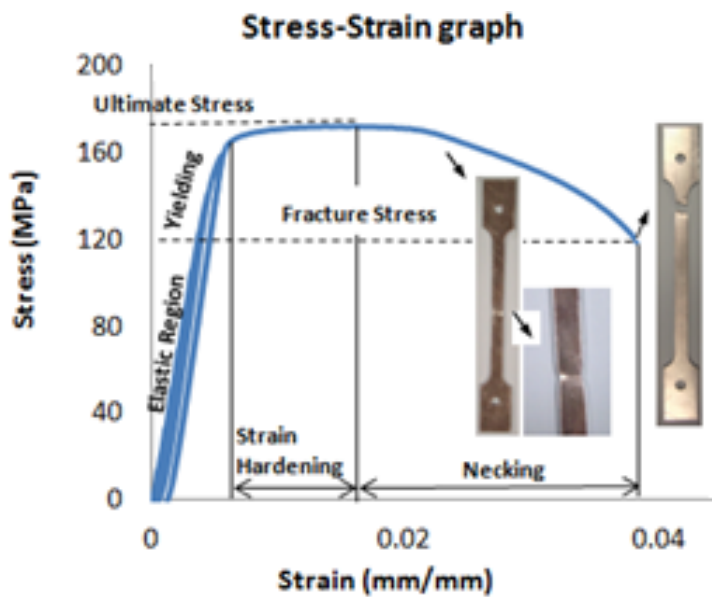


Figure 4.16: Stress/Strain graph of a typical sample during the entire test protocol. The different phases the material went through are highlighted and pictures of the samples shown at key points

2000). Extensometer readings were divided by its gauge length (10 mm) to obtain strain values. The strains so calculated from the two systems were compared.

4.4.2 Results

The first tests conducted on the aluminium samples without strain gauges served to characterise the aluminium alloy from which the samples were made of. A linear relation between stress and strain was observed for applied loads lower to 3000 N. As the load exceeded 3000 N which corresponded approximately to 105 MPa for the given cross sectional area (28.14 mm²), the stress/strain curve started to bend exceeding the proportional limit and permanent deformation occurred (Figure 4.15). In the elastic region of the stress/strain graph the Young's Modulus was computed for each sample and on average it was found to be 73.6 GPa with a standard deviation of 1.88 GPa.

At the end of the ramp cycles, the samples were taken to failure and a typical stress/strain curve for ductile material was observed with the different phases clearly visible in the graphs and in the samples (Figure 4.16). When the elastic and yielding regions were overcome, strain hardening occurred until achieving the maximum load the sample could sustained in tension before necking. A sample with necking is illustrated in Figure 4.16. On average an ultimate stress of 171.8 (± 1.7) MPa was found among tested samples. As the tests continued the samples eventually broke at a fracture stress of 123.3 (± 7.0) MPa. A fractured sample is also shown in Figure 4.16. Having identified the linear region in the stress/strain graph of the aluminium, the test protocol was revised for strain gauged samples to not cause any damages to the strain gauges by applying high loads. It followed that the maximum load applied was 2500 N and instead of breaking the specimens a hold block was added (Figure 4.14). Strain/stress graphs for the tests conducted, for results obtained by both strain gauges and extensometer, showed as expected a linear relation between the two measures (Figure 4.17). Curves for different applied load cycles are overlapping and not distinguishable in the plot (Figure 4.17). It was thus evident that preconditioning did not occur in aluminium samples when loading cycles are repeated. Extensometer and strain gauges curves compared reasonably well, although a difference between the two plots can be appreciated.

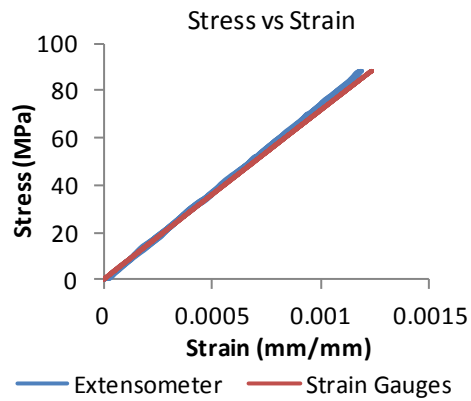


Figure 4.17: Stress/Strain graph for sample 2, test 2 during the ramp cycles for extensometer (blue solid line) and strain gauges (red solid line).

Strain data calculated from strain gauges outputs were then compared to those obtained from the extensometer readings. Figure 4.18 shows microstrain against time of one selected test of the aluminium instrumented sample 2. Results from the other tests conducted were similar to the one reported. Repeatability was observed in microstrain values during the 15 repeated cycles at 2500N for both extensometer and strain gauges. Being in the elastic region for the load range applied, it allowed the samples to recover completely when unloaded; at 0 N, 0 microstrain was recorded as also visible in Figure 4.18 a.

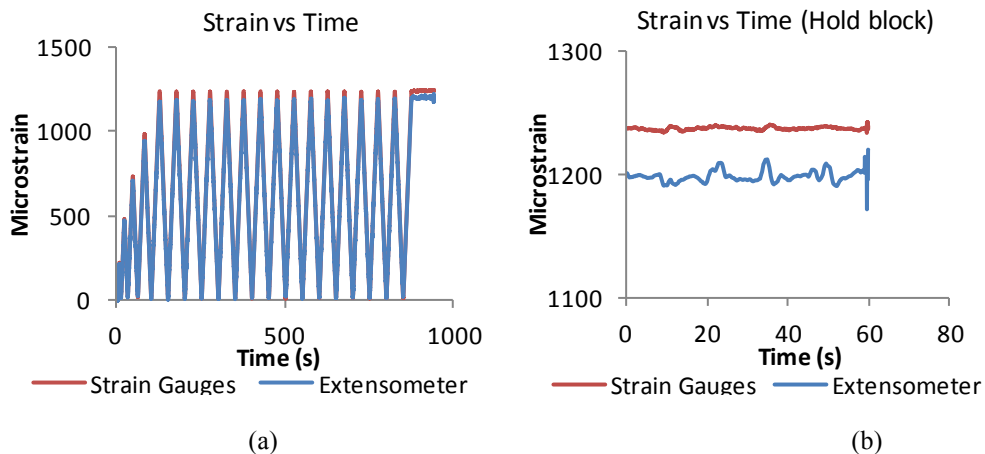


Figure 4.18: (a) Microstrain measured by the extensometer (blue solid line) and strain gauges (red solid line) against time for the aluminium sample 2 test 2. (b) Particular period from graph (a) showing the variation in strain during the 1 minute hold block.

Creep was not present while applying a constant load below the yield point as it is assumed for metallic materials (Figure 4.18 b). Although the two curves, for the extensometer and strain gauges, are not perfectly straight it is noticeable that they float around a constant value of microstrain. These drifts are due to the tensile testing machine attempting to maintain the fixed load (2500 N) to the sample while overshooting it and then tried to home in and hence the spikes.

Microstrain pattern against time for the strain gauges followed the curve of the extensometer. However, the range measured was different between the two systems with strain gauges reading higher values in comparison to the extensometer for both the samples tested in all tests run. Percentage difference of microstrain measured by the extensometer and strain gauges was calculated as for the polypropylene samples (Equation 4.2). The differences found are reported in Table 4.5 for sample 1 and 2 for all the tests run in each specimen.

| | AVERAGE PERCENTAGE DIFFERENCES | | | | | |
|------------------|--------------------------------|---------------|---------------|---------------|---------------|---------------|
| | SAMPLE 1 | | | | SAMPLE 2 | |
| | <i>Test 1</i> | <i>Test 2</i> | <i>Test 3</i> | <i>Test 4</i> | <i>Test 1</i> | <i>Test 2</i> |
| Loading | 8.2 | 7.1 | 13.3 | 7.7 | 5.5 | 4.4 |
| Unloading | 8.7 | 7.3 | 13.6 | 8.1 | 5.4 | 4.4 |

Table 4.5: Average percentage differences between strain gauges and extensometer values of strain for the last 5 cycles of test in the two aluminium samples tested.

For test 3 a high difference ($> 13\%$) was obtained. During this test, the O'ring supporting the extensometer broke and thus a firm attachment of the instrument was not ensured throughout the test. For this reason the results of test 3 were discarded from the final evaluation of the accuracy of the strain gauges. Looking to the other tests conducted, good consistency was observed among the percentage differences calculated. An overall average of 6.6 % and 6.8 % were found for loading and unloading paths respectively for the values listed in Table 4.5.

4.4.3 Discussion and Conclusion

The behaviour of the aluminium samples under tensile load conditions was investigated allowing a characterization of the aluminium alloy the samples were made of. A behaviour, typically observed in metals and in particular ductile

materials, was revealed by the tests conducted (Figure 4.16). When the specimens were loaded to a stress of less than 105 MPa, a linear elastic response was shown in the strain values measured and a total recovery to the samples' original length was obtained. The Young's Modulus computed within the linear region was on average 73 GPa, which reflects the values quoted in the literature (70 GPa) for aluminium (Callister, 2000). As the load applied during the test was increased, the planes characterising the aluminium crystal structure sheared irreversibly leading to a permanent deformation, which manifested more strikingly first as necking and then as fracture if the load exceeded the ultimate stress.

Two strain gauged aluminium samples were tested by applying loads that fell within the elastic region of the aluminium identified in the material tests. An overall 7% difference was achieved between strain gauges and extensometer, making strain gauges accurate enough for strain measurement in aluminium samples. For sample 2 slightly lower discrepancies were found between the two systems than for sample 1. New cyanoacrylate glue, used for strain gauges attachment, was purchased between the tests in the two samples. The use of an old glue for the first specimen could have affected the performance of the strain gauges as the adhesive is recognised as critical for an optimal bonding between the gauges foil and the surface of the sample; therefore the higher differences. Being an actual part of the gauge system the use of an appropriate adhesive is important for the accuracy of strain readings. The persistent difference between the two measurements from strain gauges and extensometer could have also been due to poor gripping of the extensometer in the thin lateral side of the samples.

However, from the tests on the aluminium samples, better accuracy results from the strain gauges and repeatability of the data were obtained than in tests conducted on polypropylene specimens. A linear elastic behaviour thus facilitates strain gauges adhesion and measurement. The ease of instrumenting a metal was confirmed against viscoelastic material in which its time dependent characteristics limit the performance of strain gauges.



Figure 4.19: Medial and posterior view of the strain gauged AFO.

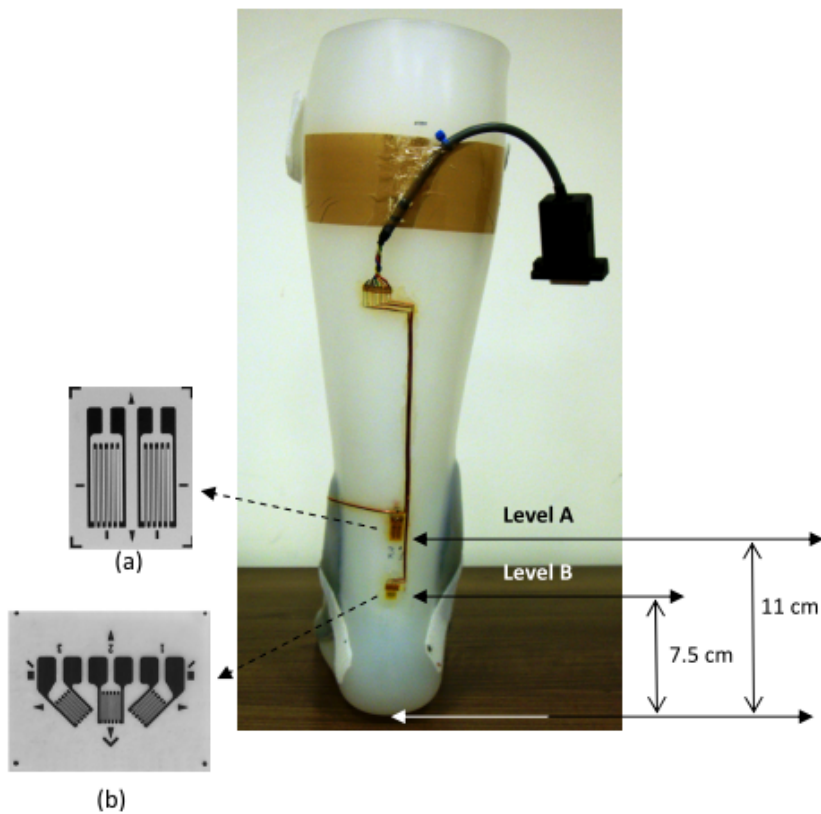


Figure 4.20: 45° three-element rosette (b) and two-element parallel strain gauge (a) used for strain measurements in the AFO (Vishay Precision Group, Malvern, USA).

4.5 Strain gauged AFO

4.5.1 *Materials and Measurement procedures*

An AFO manufactured from a cast of the left leg of an able-bodied subject (Body mass 82 kg) was strain gauged (Figure 4.20) and a preliminary test with the subject walking in the orthosis was conducted.

The AFO was similar to those prescribed to stroke patients, and was made of homopolymer polypropylene (North Sea Plastics Ltd., Glasgow, UK) with carbon fiber reinforcement (PolyCar-C Ankle Inserts, Fillauer Inc., Tennessee, USA) at the malleoli level (Figure 4.19). The strain gauges applied on the calf region of the AFO were a 45° three-element rosette (Figure 4.20 b, Level B) with each element connected to three resistors (bridge complexion resistor, ERA8AEB121P, Panasonic, New Jersey, USA) to complete a full Wheastone bridge circuit to measure axial strains in the y (vertical) direction, in the 45° and -45° to the vertical direction and, two, two-element parallel strain gauges (Figure 4.20 a, Level A) one positioned on the outer and one on the inner surface of the AFO connected together to form a Wheastone bridge circuit for strain measurements due to bending. The surface area of the AFO, where the gauges were to be attached, was exposed to UV-light for approximately 30 minutes. The gauge foils were then attached using cyanoacrylate glue. Strain gauges performance was tested prior to conducting the test with the subject. A calibration (Figure 4.21) was performed by positioning the AFO so as to reproduce dorsiflexion and plantarflexion movement at the ankle and by applying a maximum of 4 kg (39.2 N of force) with an increment of 1 kg every 30 seconds. The weights were added onto a hanger attached to the AFO and then gradually removed. The procedure was repeated two times for each condition. Strain gauges voltage outputs were read through a P3 strain indicator from Vishay Precision Group (Malvern, USA) and the values were stored in a Microsoft Excel worksheet. The outputs from the gauges were plotted against the loads applied to verify if the strain gauges showed a linear behavior.

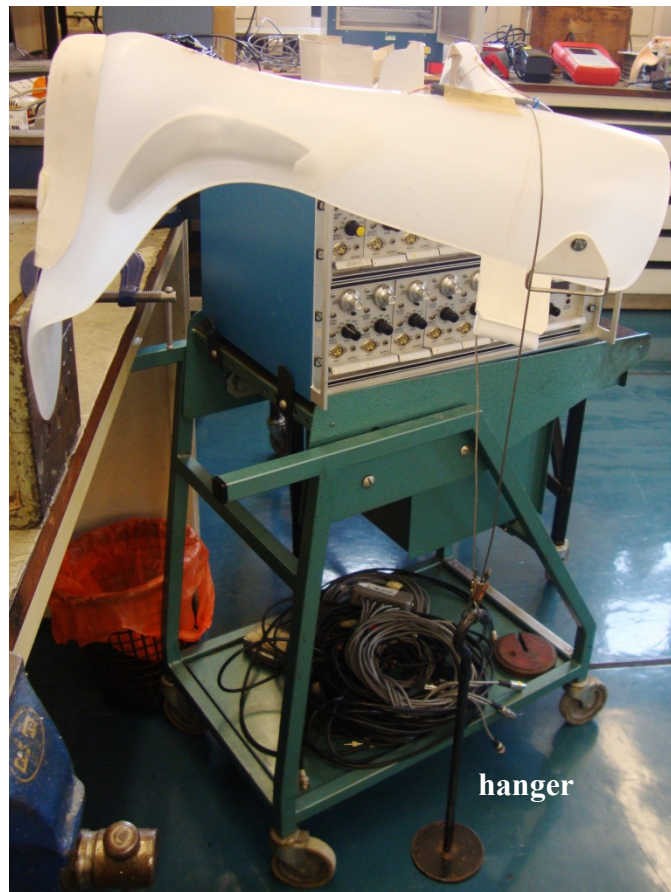


Figure 4.21: AFO plantarflexion calibration set up. 1 kg weights are added on the hanger. For dorsiflexion calibration, the AFO is reversed.

A calibration (Figure 4.21), similar to that conducted to verify the linearity of the gauges, was performed at the end of the subject test to determine the conversion factor that allows the calculation of AFO dorsiflexion and plantarflexion moments from the voltage outputs recorded during walking trials. The strain gauges outputs (Volt), at the known loads applied (1 to 4 kg) during the calibration, were recorded using Nexus software (Oxford Metrics Ltd., UK) installed in the laboratory computer. From these outputs, calibration factors (Nm/V) for dorsiflexion and plantarflexion moment were determined by a linear regression procedure applied to the moment/strain gauges outputs curves. The moment values were obtained by multiplying the loads put onto the hanger by the distance between the strain gauges and the load application point. Calibration factors are used to convert strain gauges output recorded during the subject test into moments quantities (Nm).

A gait analysis test was conducted in the Biomechanics laboratory with the subject fitted with the instrumented orthosis. The AFO was provided with long cables to not restrict subject movements during the test and to prevent additional stress being imposed on the wire connections. Synchronous to the strain gauges outputs, ground reaction forces from four built-in force plates (Kistler Instrumente AG, Switzerland) and 3-D markers trajectories using a 3-D motion analysis system with twelve cameras (Vicon MX Giganet, Oxford Metrics Ltd., UK) were recorded. The cluster marker set and cluster biomechanical model (Chapter 2) were used to obtain the 3-D pose of left and right tibia and feet. With this aim, only two rigid clusters for the distal part of the tibia and individual markers on the feet were used to mark the lower part of the leg of the test subject. Anatomical landmark markers at the knee epicondyles and malleoli were used for static calibration and then removed for dynamic captures. In addition a rigid cluster of four markers was attached on the rear part of the AFO aligned with the three-element rosette. These will be used to construct the strain gauge technical reference frame. The markers and clusters were attached using hypoallergenic double-sided tape.

Before commencing data recording, the subject was given time to get accustomed to the orthosis and to precondition the material. Each strain gauges output, four in total (+45°, 0°, -45° channels from the rosette and 1 from the level A gauges) were connected to an amplifier and then input into the Vicon laboratory computer to allow simultaneous data collection with force plates and 3-D markers trajectories. The bridge voltage and gain settings were set for the four channels at 1 V and 500 respectively. An initial test was conducted to check that these parameters were appropriate. The outputs of each channel were zeroed before starting the test. Data acquisition started with a static anatomical landmark calibration trial and, to follow, dynamic trials were captured. The subject walked at his natural speed across the laboratory with a calibrated field of 6 m in length. Four walking trials with clear heel strikes on separate force plates were used for the analysis. Data from strain gauges, force plates and infrared cameras were sampled at 100 Hz and all acquired using Vicon Nexus software (Oxford Metrics Ltd., UK).

4.5.2 *Data analysis*

Markers trajectories and force plates data were processed using Nexus and Bodybuilder softwares (Oxford Metrics Ltd., UK) with the biomechanical model described in Chapter 2. Woltring's general cross-validatory quintic smoothing spline with a predicted mean-squared error of 15 mm was used to filter coordinate data. The 3-D coordinates of markers in the AFO's cluster and the reconstructed 3-D position of knee and ankle joint centres and lateral and medial malleoli were output for subsequent computations. Internal ankle joint moments calculated by the Bodybuilder model applied to the data were kept for analysis. Moments were expressed in the tibia reference frame.

The analysis of strain gauge outputs was performed with a custom-build Matlab programme (The MathWorks Inc., Massachusetts, US) with the main aim to transform strain gauges output, recorded in the strain gauges reference frame (local technical coordinate system), into the tibia reference frame (local anatomical coordinate system).

The first step of the analysis was to convert the strain gauge output expressed in Volts into moment quantities expressed in Nm by the calibration factors obtained from the calibration of the AFO described earlier.

The Matlab code (Electronic Appendix) receives in input the 3-D coordinates of the four markers in the AFO cluster, left knee and ankle joint centres, left malleoli and moments measured by the strain gauges (SG) in their local frame. The strain gauges reference frame is constructed from the known position of the AFO markers as in Figure 4.22.

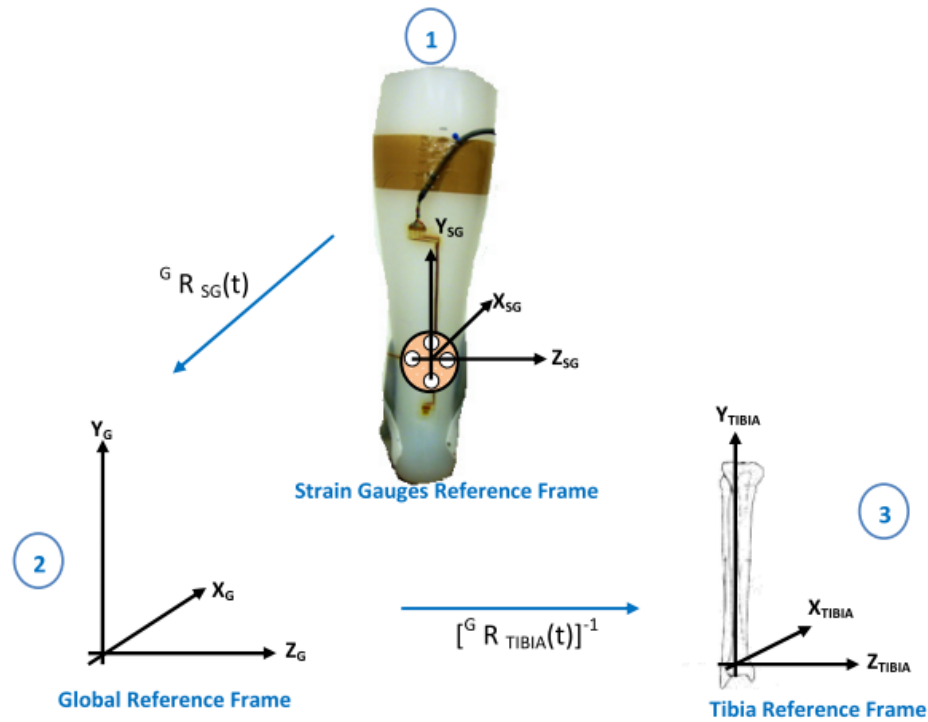


Figure 4.22: Steps followed to transform the strain gauges outputs from the strain gauges reference frame (1) to the tibia reference frame (3). R indicates direction cosine matrix for axes system transformation.

It was assumed, the y-axis of the strain gauges frame coincided with the principal measurement axis of the strain gauges. The cluster in fact was positioned in order to have the two markers that define the y-axis in alignment with the 0° (vertical) strain gauge in the rosette. For this preliminary investigation the outputs from the $+45^\circ$ to the vertical direction and the -45° to the vertical direction strain gauges in the rosette were ignored. Since the strain gauges reference frame was defined by marker positions expressed in the global/laboratory frame, multiplying the measured moments by the y-axis unit vector of the SG frame, results in the transformation of the moments into the global frame (step 2 in Figure 4.22). The final step was to convert these global moments into the tibia axis system. The tibia reference frame was defined as for the biomechanical model adopted (Chapter 2) from the 3-D coordinates of the malleoli, knee and ankle joint centres. A direction cosine matrix was determined to allow the transformation from the global reference frame to that of the tibia (step 3 in Figure 4.22). AFO moments expressed in the tibia reference frame

were finally output from the Matlab programme (The MathWorks Inc., Massachusetts, US).

AFO moments and ankle total moment were time normalised to 100 point so that 100 on the time scale represent 100% of stance phase. The convention used is that of internal moments with plantarflexor moment being represented as positive.

Newton's third law then applies (Equation 4.3) and from the known total ankle moment and AFO moment, the moment due to the anatomy (muscle and passive tissues) can be inferred:

$$M_{TOT} = M_{AFO} + M_{ANATOMY} \quad \text{Equation 4.3}$$

The moment provided by the subject active and passive tissues is referred in this thesis as anatomy moment.

That would be of interest particularly when looking at people with impaired gait for whom muscle power may be lost and the real contribution of the AFO can be better understood.

The stress generated in the AFO at the peak plantarflexor/dorsiflexor moment was calculated from Hooke's law equation (Equation 4.4) assuming that the loads applied on the AFO were within the linear region of polypropylene.

$$\sigma = E\varepsilon \quad \text{Equation 4.4}$$

Where: σ = Stress (MPa);

ε = Strain (mm/mm) measured by the strain gauges;

E = Young's Modulus (MPa) of homopolymer polypropylene obtained from material testing.

The voltage output of the strain gauges was converted into a strain measurement expressed in mm/mm using Equation 4.5 from the quarter bridge definition:

$$\varepsilon_o = \frac{4 e_o}{E K_s G} \quad \text{Equation 4.5}$$

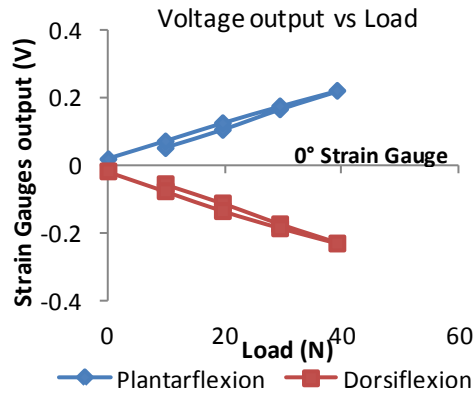


Figure 4.23: Strain gauges outputs of the 0° (vertical) strain gauge of the 45° rosette against load for static AFO calibration in dorsiflexion (blue) and plantarflexion (red).

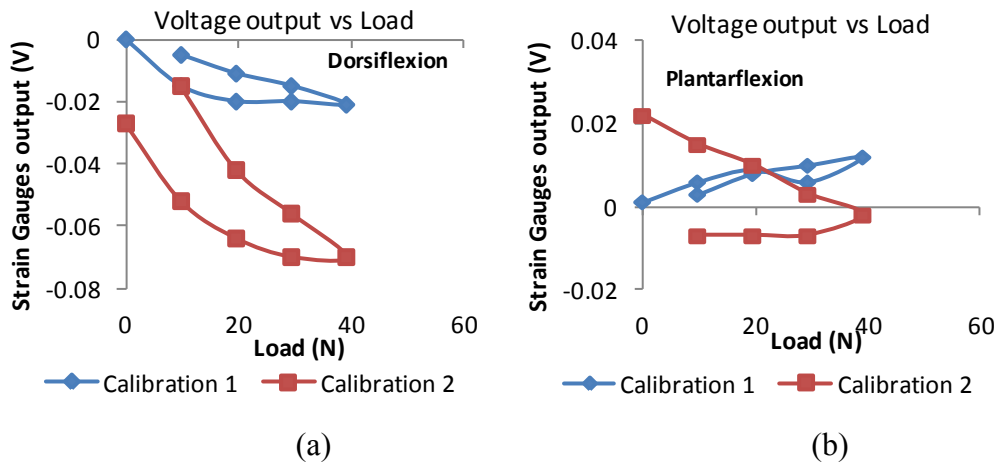


Figure 4.24: Strain gauges outputs of level A strain gauges against load for static AFO calibration in dorsiflexion (a) and plantarflexion (b). Results from the two calibrations conducted are plotted (blue and red curves).

Where: ε_o = Strain (mm/mm);

e_o = Voltage output from the strain gauges (V);

E = Bridge Voltage set at 1 V for the tests;

K_s = Gauge Factor, $1.98 \pm 2.5\%$ as provided by strain gauges supplier;

G = Amplifier Gain set at 500 for the tests.

4.5.3 Results

From the static calibration of the AFO it was revealed that whereas the 45° rosette showed a linear behavior, as shown in Figure 4.23 for the 0° strain gauge on the rosette; odd voltage readings were obtained from the level A strain gauges (Figure 4.24 a,b).

A further test was performed to verify the reason of this behavior. The full Wheastone Bridge was split into four quarter bridges and the output from each recorded in dorsiflexion and plantarflexion loading conditions. The four quarter bridges showed a linear behaviour when separated (Figure 4.25).

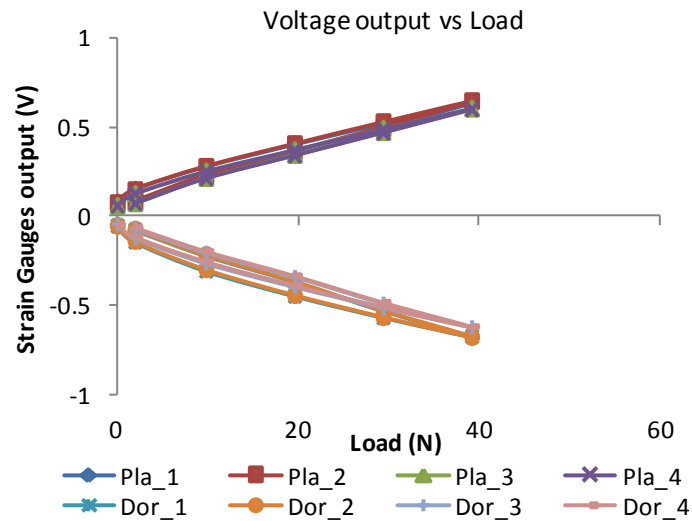


Figure 4.25: Calibration of the four quarter bridges (1 to 4) obtained from the separation of the full Wheastone bridge of the level A strain gauges for plantarflexion (Pla_1:4) and dorsiflexion (Dor_1:4).

The explanation for the erroneous readings during the first tests (Figure 4.24 a,b) was then related to the curvature of the surface where strain gauges were attached

rather than a problem in the attachment of the foils as demonstrated by the latter test (Figure 4.25). The curvature lead to a different variation in the strain gauges resistance of the strain gauges attached to inner and outer surface of the AFO, tending to unbalance the Wheastone bridge and hence the non linearity. Due to these results level A gauges could not be used in the further test with a normal subject. In the processing of gait data, only the output from the vertical gauge in the rosette was considered. A conversion factor in plantarflexion and dorsiflexion of 42.4 Nm/V and 46.6 Nm/V was found from the static AFO calibrations.

Two steps for each of the four recorded walking trial were analysed although, only for one of the two, corresponded force plate data were available. In Figure 4.26, AFO moments in the tibia reference frame throughout the stance phase of the gait are shown for the 8 left steps analysed. Heel strike (HS), foot flat (FF), mid-stance (MS), heel rise (HR) and toe off (TO) events of stance phase are highlighted in the plot.

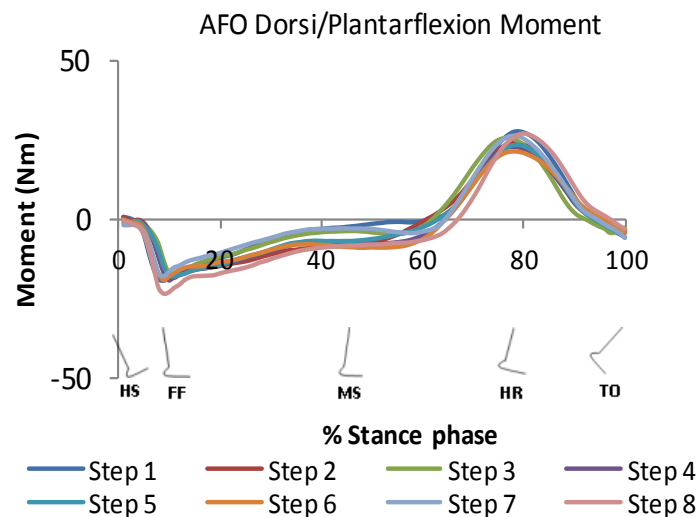


Figure 4.26: Moment measured in the AFO as percentage of stance phase for all the steps recorded (1:8). Two steps for each walking trial were acquired. Positive values represent a plantarflexor moment.

Good consistency was observed among trials with an average standard deviation throughout the stance phase of 2.2 Nm. A peak in the dorsiflexor moment with a mean of $-19.2 (\pm 1.7)$ Nm occurred at foot flat between the 9% and 11% of stance phase of each step. A peak in the plantarflexion direction of on average of $25.0 (\pm$

2.1) Nm was observed at heel rise between 77% and 80% of stance phase of each step. The stress generated in the AFO that corresponded to these two peaks was 3.6 (± 0.3) MPa for dorsiflexion and 5.0 (± 0.4) MPa for plantarflexion.

Mean total moments across four steps for left and right legs are plotted in Figure 4.27. The total ankle moment of the left leg showed a reduced dorsiflexion during early stance phase but higher peaks of plantarflexion in the second half of stance phase when compared to the right ankle moment without orthosis for the four walking trials for whom force plates data were acquired. Moreover a smaller standard deviation (bars in Figure 4.27) was observed for left ankle moment (with AFO) than for the right ankle moment throughout the gait cycle. The average of the standard deviation was 3.5 Nm for the left ankle against 5.3 Nm for the right ankle.

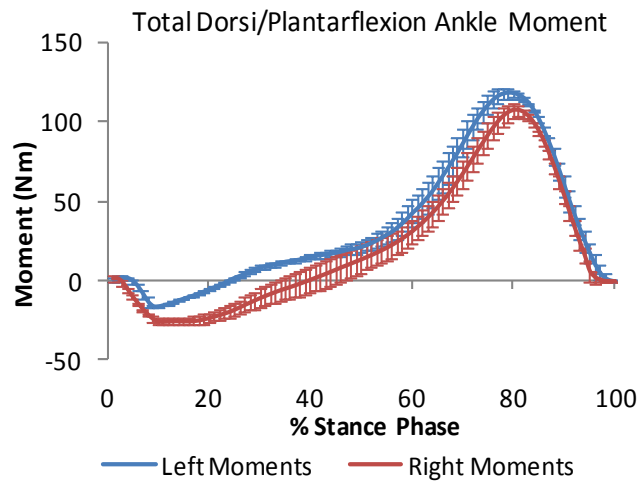


Figure 4.27: Mean (\pm standard deviation) total dorsiflexion/plantarflexion moment at the ankle for left leg with AFO (blue solid line) and right leg with shoe only (red solid line).

The anatomy moment for the left ankle was calculated using Equation 4.3 for four walking trials from the corresponding total ankle and AFO moment. The mean of the anatomy contribution to the net ankle moment throughout stance phase is shown in Figure 4.28. In the same Figure, AFO contribution and left total ankle moments are plotted.

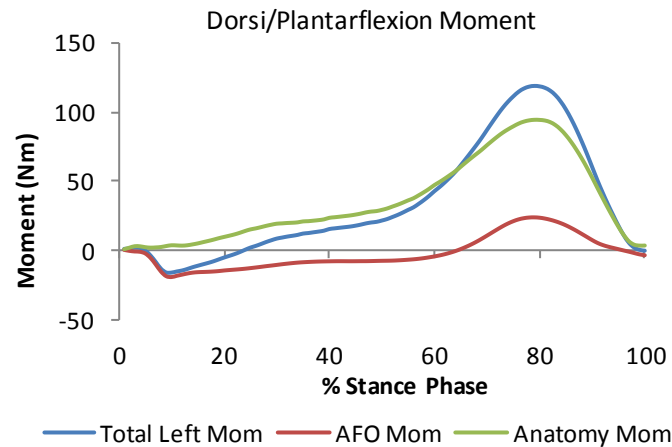


Figure 4.28: Total mean ankle moment of the left leg (blue solid line) and moment contribution of the AFO (red solid line) and anatomy (green solid line).

4.5.4 Discussion and Conclusion

The aim of this investigation was to verify that the method proposed is capable of determining the AFO contribution to the ankle moment during walking. The test conducted revealed that the methodology employed could be used for the estimation of AFO moments. However a problem was encountered with the two-element parallel strain gauges, connected to form a Wheatstone bridge circuit for strain measurements due to bending and, was related to the geometry of the surface where the gauges were applied. The curvature unbalanced the bridge and hence led to the non-linearity of the outputs observed (Figure 4.24). This could be overcome by using a different set up to position the strain gauges on the orthosis where the shape is uniform.

Results obtained from the three element rosette were, instead, encouraging. The method utilized was able to produce repeatable results as shown by the good consistency in the strain gauges measurements across analysed steps (Figure 4.26). The AFO restricted dorsiflexion movements during the stance phase in comparison to the right ankle moment. Constraints in the ankle movements were expected due to the stiffness of the AFO used in this preliminary test. The AFO was of the rigid type with additional reinforcement provided by carbon fiber insertions at the malleoli level. Restriction of the movement at the ankle level is also shown by a reduced standard deviation across repeated gait cycles when compared to the AFO free ankle.

The more reproducible movement at the ankle level is seen as a result of the AFO use.

AFO contribution in this test however could be unrepresentative of the effect AFO has in stroke gait as the subject tested did not present any gait impairments and was capable of full muscles power exertion. However, the results obtained were reasonable and thus the feasibility of the procedure was demonstrated.

To conclude, although strain gauges were attached on polypropylene, a good repeatability in the outcomes measured was obtained verifying the methodology proposed and giving a sensible way to determine AFO contribution to the ankle moment.

This is of particular interest for a better understanding of the AFO interaction with the lower leg with the aim of gathering valuable information to achieve an effective orthosis design.

CHAPTER 5 – RANDOMISED CONTROLLED STUDY METHODOLOGY

5.1 Overview and Study design

Having established suitable outcome measures to explore the efficacy and mechanism of actions of the early use of an AFO in stroke rehabilitation, this study moved on to implement a pilot for an RCT (randomised control trial) of the intervention. It was envisaged that 10 subjects would be recruited within the scope of this feasibility study so testing the feasibility of the RCT design.

If feasibility was established, it was intended to apply for further funding to complete the pilot study and expand it to a full phase II trial of efficacy and mechanism of action under the Medical Research Council (MRC)'s Efficacy and Mechanism Evaluation (EME) scheme as post-doctoral research.

To address research questions (Table 5.1) a single centre randomised control trial design was adopted, in which two different interventions would be compared. A random computerised allocation in block of four was generated to provide bias protection and a randomisation sequence to allocate patients into two equally sized groups, the control and experimental group.

Ethical approval was obtained prior study commencement from the NHS Ethics Committee, West of Scotland REC 3, NHS Research and Development management office and the University of Strathclyde Ethics Committee.

Research Questions:

- What is the effect of early provision of a solid ankle-foot orthosis (AFO) on the walking speed and gait ability (biomechanics) of stroke survivors undergoing early mobilisation?
- Does the early provision of a solid AFO enhance functional recovery compared to the usual clinical rehabilitation practice for stroke survivors?
- How do patients recover over a period of 24 weeks?
- What are the orthotic loads applied by the AFO on the patient's lower leg?

Table 5.1: Research questions.

5.2 Study population

The study population was formed from patients who had sustained a stroke within two months from recruitment. In particular, eligibility to participate to the study was

in accordance to the criteria summarised in Table 5.2. Patients were initially screened from the stroke wards at Stobhill Hospital (Glasgow, UK) and subsequently the enrolment was extended to stroke patients admitted at the Glasgow Royal Infirmary. The recruitment of suitable patients was the responsibility of the research team who personally invited the candidates to take part in the study providing an information sheet and discussing with them what participation would involve. The patients who were interested to be admitted in the study provided signed consent form in order to actively take part to the subsequent trial steps.

| Inclusion Criteria: | Exclusion Criteria: |
|--|--|
| <ul style="list-style-type: none"> • 7 days to 8 weeks after ischemic or haemorrhagic stroke • Medically stable • Aged between 18-90 at the time of stroke onset • Capable of full correction of subtalar joint • No loss of skin integrity over the lower limb • No severe cognitive impairments • Gastrocnemius shortening with plantarflexion contracture (5 degrees of plantarflexion or greater) (criteria removed during recruitment) | <ul style="list-style-type: none"> • Inability to follow simple instructions or to give informed consent • Unstable angina • Cardiac risks • Pain related to walking • Severe spasticity • The need for two assistants while walking • Flexion contracture of hip musculature (greater than 10 degrees hip flexion) • severe proprioceptive sensory impairment |

Table 5.2: Eligibility criteria for subjects' recruitment.

The sample size was decided upon the following formula:

$$n = \frac{7.9 (sd^2)2}{(diff^2)} \quad \text{Equation 5.1}$$

Where *sd* is the standard deviation and *diff* is the difference between two conditions of the main parameter being investigated. Walking speed was considered the key measure for the current trial and the relative *sd* and *diff* values were extracted from conducted studies (Perry et al., 1995; Cooke et al., 2010). Perry et al. (1995) identified that a difference of 0.2 m/s in walking velocity with and without an AFO is clinically relevant. Cooke et al. (2010), in a recent Phase II randomised controlled trial of the efficacy of functional strength training on enhancing lower limb recovery early after stroke, found a within group standard deviation in walking velocity of 0.24 m/s. Considering these values of standard deviation and difference,

and with a power of 80% at 5% significance, the equation 5.1 gave a sample size in each group to be 22. Allowing for drop out, 25 patients should be recruited for each group.

5.3 Experimental procedures and outcome measures

The experimental protocol of the current RCT is summarised in the diagram illustrated in Figure 5.1.

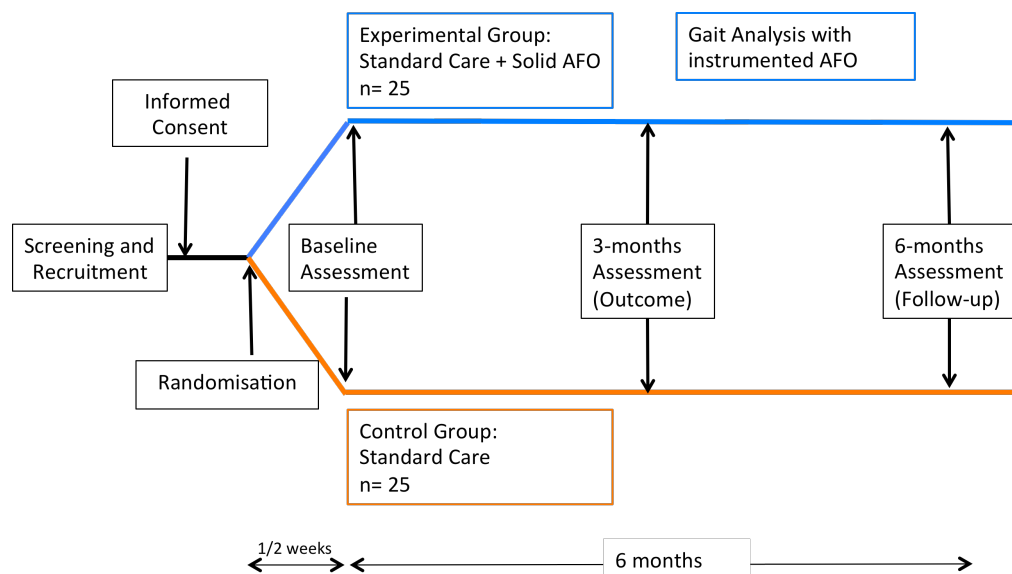


Figure 5.1: Schematic illustration of the study experimental protocol.

After given their agreement to take part in the study patients are randomised into the control or experimental group. The allocation to one group rather than the other discriminates for the post-stroke rehabilitation care provided but not for the assessments that are the same either the group. Participants allocated in the control group receive the usual clinical practice provided by the NHS stroke unit that involves physiotherapy and early mobilisation, as deemed appropriate for each individual impairment. An ankle foot orthosis (AFO) may also be provided when believed appropriate by the NHS orthotist. The experimental intervention, on the other hand, is represented by the provision of a solid AFO as an adjunct to conventional physical therapy. Each participant allocated in the experimental group receives a custom made solid AFOs made from polypropylene (homopolymer) with

carbon fiber reinforcement at the malleoli level (Figure 5.2). The plastic material is provided by North Sea Plastics Ltd. (Glasgow, UK) while the reinforcements from Fillauer Inc. (Tennessee, USA). At the time of fitting, tuning of the AFO with small heel wedges is performed to ensure a right leg alignment/inclination and comfort to the patient during walking. A copy of the prescribed solid AFO will be made and instrumented with strain gauges (Chapter 4) for orthotic load measurement. If a patient regains the ability to walk independently without the AFO aid, its use will be discontinued.



Figure 5.2: Solid ankle foot orthosis provided to the experimental group patients.

The experimental phase of the study for each participant lasts 6 months (24 weeks) with three tests conducted at three months distance from each other, baseline, outcome (3 months) and follow-up (6 months) assessments. These assessments are performed in the biomechanics laboratory of the Bioengineering Department exploiting the 12 cameras Vicon 3-D motion capture system (Vicon, Oxford Metrics Ltd., UK) in conjunction with four built-in force plates (Kistler Instrument AG, Switzerland) and the augmented video-based portable system (AVPS). The marker set comprising 5 rigid clusters and individual anatomical landmarks markers introduced and discussed in Chapter 2 is used for the first mentioned system. For the video gait assessment on the grid mat, the bull's eye paper marker set is employed (Chapter 3). The two systems are run in parallel during test sessions and thus the two marker sets are combined to allow concurrent data collection from both

instrumentations (Table 3.5). Data sampling is set to 100 Hz for the 3-D motion analysis system and force plates and to 210 Hz for the video data recording. Prior to data collection a preparation phase occurs during which time is allocated to allow the patient to get accustomed to the laboratory environment and ask questions; the patient is dressed in shorts or with provided Lycra suits (NIKE, Inc., Oregon, US) to allow marker attachment while maintaining patient modesty; the height and weight of the test subject are taken and the Modified Rivermead Mobility Index (MRMI) and functional ambulation classification (FAC) score are recorded (Appendix 1). Once the markers are positioned over the subject's lower limb, the test protocol follows the procedures described in Chapter 2 and 3 as for each system used. A static calibration trial is first collected followed by dynamic data capturing. Two walking trials are collected while each patient walks at self selected speed with and without an AFO if provided. In addition, for experimental group patients, recordings are made of the subject walking with their strain gauged AFO during the follow-up visit. Data from both the sound and the hemiplegic leg are recorded and kept for post data analysis.

Outcome measures obtained through the 3-D capture system are the kinematics of the lower limb joints and pelvis in the 3 anatomical planes and internal joint moments at the hip, knee and ankle. For the intervention group, the dorsi/plantarflexion moment due to the AFO is also calculated. From the AVPS, temporo-spatial parameters of the gait are measured which include walking speed, temporal and spatial symmetry of the gait, and tibia inclination angle at initial contact, foot flat, mid stance and terminal contact.

5.4 Management of outputs data and statistical analysis

At completion of each test session data are transferred onto a PC with installed Vicon data analysis suite (Vicon, Oxford Metrics Ltd., UK) and Pro Trainer DV software (Sport Motion Inc., US) for data processing. Three gait cycles are extracted from each walking trial performed, for a total of six gait cycles available for statistical analysis for each condition performed: walking with AFO and shoes only.

The raw 3-D motion captured data are first reconstructed and markers labelled using Nexus software (version 1.7) (Vicon, Oxford Metrics Ltd., UK). The Woltring's

generalized cross-validation with splines (GCVSPL) with a predicted mean squared error of 15mm (Woltring 1985; 1986) is used to filter marker trajectories. Heel strikes of each leg are determined, to identify gait cycles, based on force plates data, when possible, and on the minimum acceleration of heel markers. These initial foot contact instances are used to normalise kinematic outputs to 0-100% of the gait cycle duration. Kinetic data are time normalised to 100% of stance phase which is considered the time elapsed between heel strike and toe off. The latter is determined from force plates data and as the instant when front foot markers start to accelerate and move forward. Kinematic and kinetic data are calculated by reconstructing the data and implementing the developed BodyBuilder code (Chapter 2). Data are output in ASCII format and analysed using a custom made application in Matlab (The MathWorks Inc., Massachusetts, US). This normalised the data into either 100% of the gait cycle or stance phase and exports data to customised Microsoft Excel spreadsheets where averages across gait cycles are calculated and graphs of the pelvis, hip, knee and ankle angles and moments are made.

Gait videos from AVPS are played back and analysed using Pro Trainer DV software (Sport Motion Inc., US). Gait events as initial contact, foot flat, mid stance and terminal stance of both legs are identified by visual inspection of the videos. Tibia to the vertical angles, at such instances, are determined with the aid of the goniometric tool of the software which allows the instantaneous calculation of the angle between two drawn lines. Record is kept of the time when the light from the black box first comes on as the initial time to calculate walking speed for each trial. The time when the light comes on for the second time is also recorded as final time. Step length is determined by identifying on the grid of the mat the distance between two consecutive left and right heel strikes. Those values, obtained from the two walking trials recorded, are input into customised Microsoft Excel spreadsheet from where the final outcomes (walking speed, temporal and spatial symmetry, tibia to vertical angles) can be extracted.

Descriptive statistics are used to summarise the results. Mean and standard deviation of every outcome measures are calculated. Outcome parameters during walking with and without AFO are compared. Paired samples *t*-tests at 0.05 level of significance are used for this purpose.

CHAPTER 6 – RESULTS

6.1 Introduction

This Chapter presents the results obtained with the methodology described in the previous section (Chapter 5).

First the progress achieved in the recruitment of suitable participants is discussed.

The section that follows presents the results for three case studies analysed. Within each case study description, first results obtained from the simplified video gait protocol are reported. This included spatio-temporal parameters of the gait and shank to vertical angle during stance phase. Second, pelvis and lower limb joint kinematics from the 3-D gait analysis protocol are shown. For case study one results obtained from a strain gauged AFO are also presented.

In the last section of this Chapter results from the uncontrolled manifold approach are reported. The validation of the geometric model is described and the results of the application of such method to able-bodied subjects and stroke patients are given.

6.2 Study Recruitment

Patients were recruited over a period of time between September 2010 and September 2011.

Although ethical approval was obtained in October 2009, there was a delay until recruitment could actively commence due to service reorganisation and negotiation with the orthotic and physiotherapist stroke service managers of NHS Greater Glasgow & Clyde.

Further, none of the patients screened during the first three months had a gastrocnemius contracture. This was an inclusion criteria for the study and the reason why 0 patients were recruited until December 2010, when this criteria was removed with the approval of the ethics committee. Moreover the NHS stroke service went through a reorganisation process simultaneously to the recruitment for the study. Stroke beds in the stroke rehabilitation ward of Stobhill were reduced. In addition, stroke patients admitted at Stobhill Hospital came from the Royal Infirmary stroke

unit and were sent to Stobhill only if they required prolonged care. This change was brought about by the introduction of Early Supported Discharge.

It followed, that to increase the chance to find suitable participants for the study, amendments were made to the first approved protocol. First of all, the requirement of gastrocnemius contracture was removed from the inclusion criteria and secondly the Royal Infirmary was added as an additional recruitment site. These amendments were approved by NHS Ethics Committee, West of Scotland REC 3, and NHS Research and Development management office in December 2010.

Only three patients were recruited from January 2011 to September 2011, as opposed to the desired 10 patients, and despite 108 stroke patients were admitted at Stobhill Hospital. The reasons for such small recruitment number reside both in the study criteria and in the changes to the NHS stroke service in this period. Patients admitted were too severely affected and hence not able to walk even if with aids or one assistant within two months post stroke. Within this range of time, they presented with insufficient balance and control in standing and this precluded their participation in the study. On the other hand, some of the patients were too good and able to walk freely without the requirement of an AFO. Furthermore, for some patients health complications other than stroke presented in the time they could have been included in the study. Some other patients, although eligible, simply refused to take part in the study or were already enrolled in a different trial and could not participate to the current one. Among the patients admitted in the hospitals, only 19 patients met the criteria but only 3 were included in the study for the reasons just explained.

With the increased awareness of the NHS of the burden of stroke in Scotland improvements were pursued in the emergency care given to stroke sufferers. This could also have diminished the number of patients who require AFO intervention. For all these reasons, in the time available, only three patients were recruited. The reasons for non recruitment will be further expanded in the Discussion Chapter.

6.3 Clinical Case Studies

Results from the three patients recruited are reported separately as single case studies.

In the kinematics graphs, flexion, adduction and internal rotations are shown as positive.

Symmetry ratios for step time and length are calculated as:

$$Ratio = \left(\frac{2 \cdot Affected\ Leg\ Parameter}{Affected + Unaffected\ Parameter} \right) - 1 \quad \text{Equation 6.1}$$

Symmetry is represented by a Ratio equal to zero.

6.3.1 Case Study 1

Case study 1 refers to a 81 years old male of 80 kg body mass and 1.8 m tall affected by stroke on the 21st February 2011. He presented a left side hemiplegia of the upper and lower body. After agreeing to take part in the study, he was randomised into the intervention group. A 5 mm rigid polypropylene AFO with carbon fibre reinforcement and calf and ankle straps was fitted three months post stroke. Heel wedges were provided and the AFO and shoes combination was tuned at 10° of inclination. The patient completed the study. Measurements from baseline (time of fitting of the AFO), outcomes (3 months from baseline), and follow up (six months from baseline) assessments are reported. Baseline assessment occurred 3 months post stroke.

The Modified Rivermead Mobility Index (mRMI) and the Functional Ambulatory Category (FAC) for this subject at the three times points in the study are shown in Table 6.1.

| | Baseline | Outcome | Follow-up |
|-------------|----------|---------|-----------|
| mRMI | 31 | 35 | 38 |
| FAC | 3 | 4 | 4 |

Table 6.1: Modified Rivermead Mobility Index (mRMI) and the Functional Ambulatory Category (FAC) for patient 1.

6.3.1.1 Spatio-temporal parameters and tibia inclination

Two videos of the subject walking back and forth on the grid mat with and without the AFO were recorded in each laboratory session simultaneously to 3-D motion analysis data. From each video, 3 gait cycles of the leg facing the camera were analysed to extrapolate time-distance parameters.

Percentage differences between the two conditions were calculated as follows:

% Difference = $100 * [(\text{mean value with AFO} - \text{mean value without AFO}) / \text{mean value without AFO}]$.

Walking speed profile is shown in Figure 6.1. The speed with AFO increased by 55.6%, 61.8%, and 2.8% at baseline, outcome and follow-up assessments respectively. Although, AFO walking resulted in a faster paced walk, the increases were not significant (Paired T -test: p -value > 0.05).

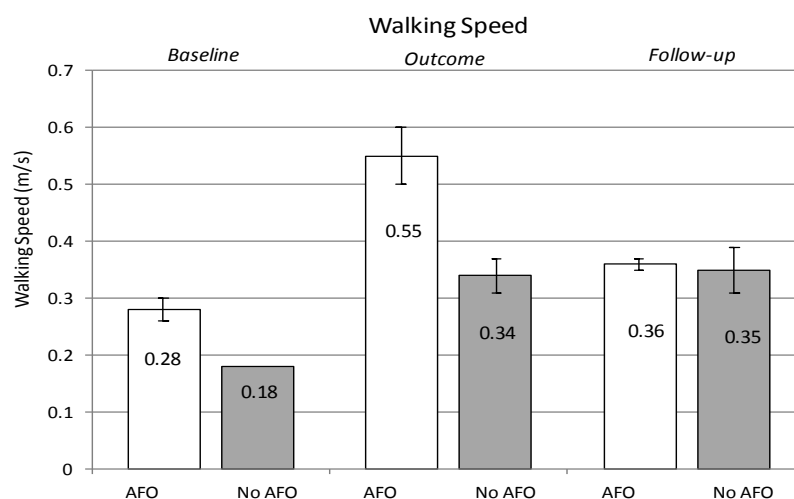


Figure 6.1: Walking speed at baseline, outcome and follow-up assessment for each condition tested. Bars indicate the standard deviation over two trials. For shoes walking at baseline only one trial was performed.

Temporal parameters of the gait cycle are presented in Table 6.2.

A significant reduction in the duration of the gait cycle when walking with AFO, was only found at baseline (-21.4%) when the cycle was measured to the respect of the unaffected leg (Paired T -test: p -value = 0.01). For all other cases, differences in stride duration within each session between AFO and without AFO gait were in the range of 0 to 12.5 % and not significant (Paired T -test: p -value > 0.05). Comparing the

duration of the cycles of the baseline measurement with those of the outcome and follow-up, it can be seen a decrease in stride time for both conditions by 26.7% with AFO and 35.6% without orthosis, on average.

| Temporal Parameters | Baseline Measurement | | Outcome Measurement | | Follow-up Measurement | |
|---|----------------------|-------------|---------------------|-------------|-----------------------|--------------|
| | AFO | SHOES | AFO | SHOES | AFO | SHOES |
| <i>Gait Cycle Duration (s):</i> | | | | | | |
| Affected Leg | 2.1(±0.05) | 2.3(±0.3) | 1.4(±0.07) | 1.6(±0.2) | 1.7(±0.08) | 1.7(±0.09) |
| Unaffected leg | 2.2(±0.09) | 2.8(±0.07) | 1.5(±0.03) | 1.6(±0.04) | 1.7(±0.03) | 1.6(±0.1) |
| <i>Stance Phase (s):</i> | | | | | | |
| Affected Leg | 1.6(±0.09) | 1.7(±0.34) | 0.9(±0.06) | 1.0(±0.12) | 1.1(±0.06) | 0.9(±0.06) |
| Unaffected leg | 1.9(±0.14) | 2.7(±0.11) | 1.1(±0.02) | 1.3(±0.03) | 1.3(±0.01) | 1.3(±0.07) |
| <i>Stance Phase(% of cycle):</i> | | | | | | |
| Affected Leg | 75.1 (±2.7) | 75.8 (±4.4) | 64.3 (±1.3) | 61.0 (±3.8) | 64.7 (±2.6) | 57.9 (±4.5) |
| Unaffected leg | 85.2(±2.8) | 94.0(±1.7) | 76.3(±0.6) | 84.0(±0.3) | 78.9(±1.2) | 83.7(±0.8) |
| <i>Swing Phase (s):</i> | | | | | | |
| Affected Leg | 0.52(±0.05) | 0.55(±0.04) | 0.5(±0.01) | 0.62(±0.1) | 0.6(±0.06) | 0.7(±0.1) |
| Unaffected leg | 0.32(±0.05) | 0.17(±0.04) | 0.36(±0.02) | 0.25(±0.07) | 0.35(±0.03) | 0.26(±0.03) |
| <i>Swing Phase (% of cycle):</i> | | | | | | |
| Affected Leg | 24.9(±2.7) | 24.2(±4.4) | 35.7(±1.3) | 38.9(±3.8) | 35.3(±2.6) | 42.0(±4.5) |
| Unaffected leg | 14.8(±2.8) | 5.9(±1.7) | 23.7(±0.6) | 15.9(±0.3) | 21.0(±1.2) | 16.3(±0.8) |
| <i>Initial Double Support (% of cycle):</i> | | | | | | |
| Affected Leg | 23.9(±1.4) | 21.0(±6.2) | 21.0(±2.8) | 23.0(±4.1) | 25.9(±1.9) | 18.5(±4.2) |
| Unaffected leg | 38.3(±1.6) | 34.4(±12.2) | 18.7(±1.7) | 20.4(±2.6) | 21.0(±2.6) | 22.6(±3.6) |
| <i>Terminal Double Support(% of cycle):</i> | | | | | | |
| Affected Leg | 37.7(±2.9) | 43.5(±11.7) | 20.6(±1.0) | 23.7(±1.4) | 19.6(±2.6) | 21.0(±0.9) |
| Unaffected leg | 22.0(±3.7) | 39.5(±13.7) | 20.8(±1.7) | 21.9(±2.4) | 27.2(±0.8) | 20.0(±2.6) |
| <i>Single Support (% of cycle):</i> | | | | | | |
| Affected Leg | 14.1(±1.9) | 8.6(±3.2) | 23.2(±0.8) | 15.0(±2.2) | 20.0(±1.9) | 17.3(±1.8) |
| Unaffected leg | 24.9(±1.7) | 22.2(±4.5) | 36.2(±2.1) | 40.3(±3.9) | 32.9(±3.2) | 41.6(±4.6) |
| <i>Step Time (s):</i> | | | | | | |
| Affected Leg | 0.80(±0.06) | 1.0(±0.4) | 0.64(±0.05) | 0.59(±0.06) | 0.77(±0.04) | 0.6(±0.04) |
| Unaffected leg | 1.35(±0.06) | 1.6(±0.3) | 0.80(±0.03) | 1.0(±0.08) | 0.88(±0.05) | 1.0(±0.09) |
| <i>Temporal Symmetry:</i> | | | | | | |
| | -0.26(±0.03) | -0.22(±0.2) | 0.12(±0.03) | 0.25(±0.05) | 0.07(±0.04) | -0.27(±0.05) |

Table 6.2: Comparison of temporal parameters assessed with and without AFO for affected and unaffected leg for case study 1.

The patient presented an asymmetric gait in terms of gait cycle phases. The temporal symmetry ratio differed from 0 (symmetry) in each condition at the three time point assessments. The use of the AFO however resulted in an enhanced temporal symmetry throughout the six months of intervention with the smallest ratio (-0.07) obtained at follow up. The differences between AFO and no AFO gait symmetry

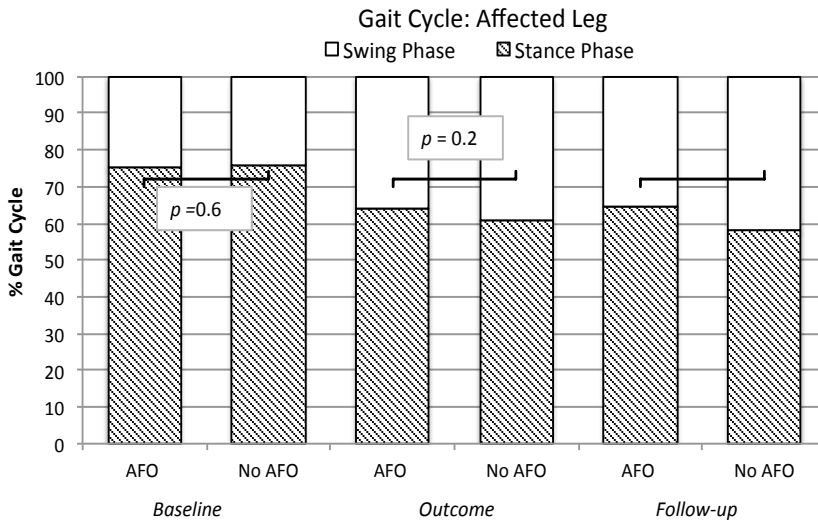


Figure 6.2: Stance (diagonal pattern bars) and swing phase (white bars) duration of the affected leg with and without AFO for the three assessments of case study 1.

Results of the *t*-test are shown for each compared bar.

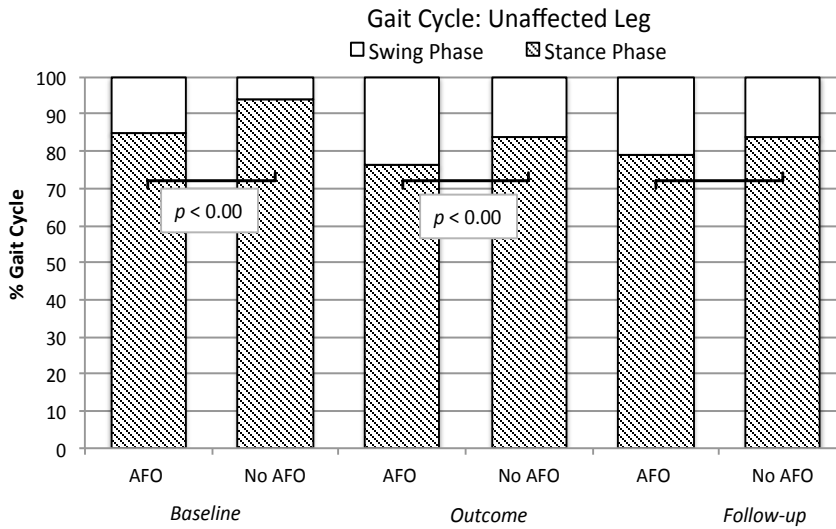


Figure 6.3: Stance (diagonal pattern bars) and swing phase (white bars) duration of the unaffected leg with and without AFO for the three assessments of case study 1.

Results of the *t*-test are shown for each compared bar.

were significant at three (Paired *T*-test: *p*-value=0.04) and six months (Paired *T*-test: *p*-value=0.01) assessments.

The asymmetry of the gait can also be noticed in the altered intervals of the gait cycle from normal level walking. Stance phase duration was generally prolonged when the subject walked with the AFO in comparison to shoes only trials for the affected leg. At baseline, however, only 1% difference was observed, with stance phase being longer with shoes only. The increases for the other two test sessions (11.7% follow-up and 5.4% outcomes) were found to be statistically significant at follow-up (Paired *T*-test: *p*-value=0.04) but not at the outcome assessments (Paired *T*-test: *p*-value=0.2). This is visualised in the Figure 6.2.

Contrarily, the unaffected leg showed a significantly longer (Paired *T*-test: *p*-value<0.05) stance phase when the patient walked without orthosis in each session and the duration of stance phase was prolonged to the respect of affected leg stance for each relative condition (Table 6.2, Figure 6.3).

This, lead also to a short swing phase of the unaffected leg characterising the gait cycle to a minimum of 5.9% of its entire duration at baseline without AFO, to a maximum of 23.7% of the gait cycle with AFO at outcome assessment. A statistical significant difference (Paired *T*-test: *p*-value<0.05) was found in the swing phase of the unaffected leg with and without AFO (Figure 6.3) but the same cannot be stated for the affected leg (Figure 6.2). The sound leg swung faster than the affected leg particularly when the subject walked without AFO. The swing phase was reduced by on average 38.2% ($\pm 4\%$) with AFO in the three sessions and by 65.2% ($\pm 9\%$) with shoes only in comparison to affected leg swing. This, in turn, implied also a short single support phase for the affected leg. On average it represented 19.1% ($\pm 5\%$) of the gait cycle with AFO and 13.6% ($\pm 4.5\%$) of the cycle when the AFO was not worn by the patient. Single support of affected leg was significantly different between the two condition tested in the three sessions (Paired *T*-test: *p*-value<0.05). Single support of the sound leg was always longer than 22% of the gait cycle but limited to the 42% of the cycle. Significant difference between AFO and shoes conditions was found for the sound leg only at follow up (Paired *T*-test: *p*-value=0.03).

A long double support phase, initial and terminal, was observed in both legs for both conditions. It was found to be always greater than 18% of the gait cycle and no significant differences were found between AFO and shoes walking.

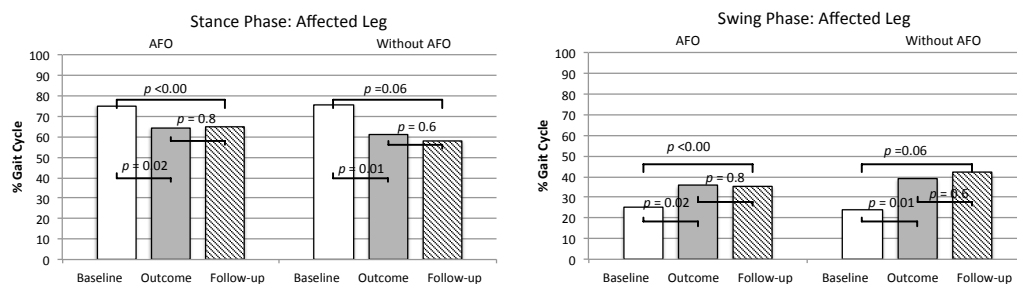


Figure 6.4: Stance phase and swing phase duration of affected leg comparison across baseline (white bars), outcome (grey bars) and follow-up (diagonal pattern bars) assessments with and without AFO of case study 1. Results of the *t*-test are shown.

If the comparisons are made across sessions, stance phase was reduced (Figure 6.4) and swing phase lengthened from baseline measurement to outcome and follow up in both tested conditions for the affected leg (Table 6.2). For AFO walking a reduction of the 15% and 13.7% was achieved for stance phase of the affected leg at outcomes and follow up respectively. For shoes only gait, the stance phase was reduced by 19.5% and 23.6% at the two subsequent measurements from baseline. Stance phase durations of outcome and follow up were significantly different from baseline obtained values for AFO tests (Figure 6.4). The differences in the measurement were smaller if the comparison was done between outcome and follow up measurements (Figure 6.4). Stance phase at follow up was longer by 0.6 % with the AFO, and reduced by 5% with shoes only in comparison to outcomes measurements.

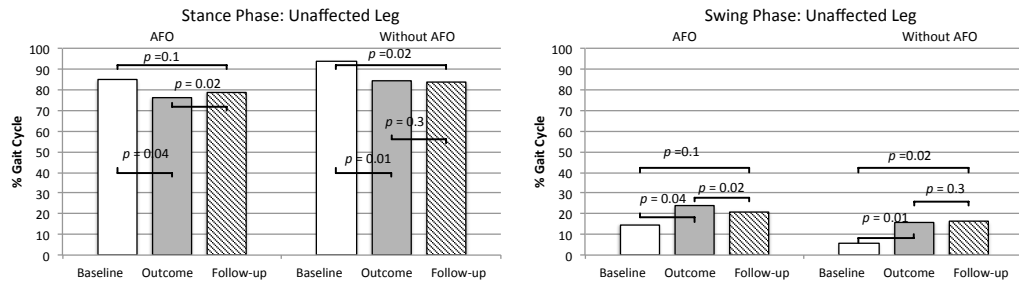


Figure 6.5: Stance phase and swing phase duration of unaffected leg comparison across baseline (white bars), outcome (grey bars) and follow-up (diagonal pattern bars) assessments with and without AFO of case study 1. Results of the t-test are shown.

| Spatial Parameters | Baseline Measurement | | Outcome Measurement | | Follow-up Measurement | |
|--------------------------------------|----------------------|-------------|---------------------|------------|-----------------------|-------------|
| | AFO | SHOES | AFO | SHOES | AFO | SHOES |
| <i>Step Length (m):</i> | | | | | | |
| Affected Leg | 0.24(±0.4) | 0.19(±0.1) | 0.34(±0.4) | 0.10(±0.4) | 0.27(±0.4) | 0.22(±0.5) |
| Unaffected leg | 0.41(±0.5) | 0.27(±0.1) | 0.48(±0.4) | 0.43(±0.3) | 0.38(±0.5) | 0.37(±0.2) |
| <i>Step Length (%Stride length):</i> | | | | | | |
| Affected Leg | 36.6(±1.6) | 40.7(±28.2) | 41.1(±4.2) | 19.8(±5.9) | 41.3(±5.7) | 36.6(±5.1) |
| Unaffected leg | 63.4(±1.6) | 59.3(±28.2) | 58.8(±4.2) | 80.2(±5.9) | 58.7(±5.7) | 63.3(±5.1) |
| <i>Spatial Symmetry:</i> | | | | | | |
| | -0.27(±0.03) | -0.1(±0.5) | 0.18(±0.08) | -0.6(±0.1) | -0.17(±0.1) | -0.27(±0.1) |

Table 6.3: Comparison of spatial parameters assessed with and without AFO for affected and unaffected leg of case study 1.

Similarly a reduction in stance phase duration was observed in the unaffected leg for both conditions. With the AFO, stance phase at outcome and follow up was reduced by 10.5% and 7.4% to the respect of the baseline value; for shoes only the duration was shorten by 10.6% and 10.9% respectively. In the comparison between outcome and follow-up, stance phase increased by 9.7% from outcome to follow-up with AFO but it was reduced by only 0.35% with shoes only. The statistical analysis of these differences is shown in Figure 6.5.

Swing phase was prolonged from baseline duration throughout the six months of intervention in both legs (Figure 6.4, Figure 6.5) with the differences from baseline more noticeable when the subject walked without AFO. At three and six months follow-up, an increase from baseline of on average 42.5 % ($\pm 1.1\%$) and 67.1 % ($\pm 9\%$) was achieved in the affected leg with and without AFO respectively. Similarly, for the unaffected leg, swing phase increased by on average 51% ($\pm 13\%$) and 172% ($\pm 4.8\%$) from baseline when walking with and without AFO respectively. Swing phase was reduced instead with the AFO for both affected (1.1%) and unaffected leg (11.4%) when comparing follow-up measurement to that of the outcome session. This comparison showed also an increase of swing phase at follow up of 7.9% and 2.5% when the subject walked with shoes only for affected and sound leg respectively.

In Table 6.3 spatial parameters of affected and unaffected leg during walking with and without AFO are reported for the three test sessions.

The gait of this patient was characterised also by a spatial asymmetry (symmetry ratio different from 0). A longer step length was observed for the unaffected leg when compared to affected leg (symmetry ratio <0). An improvement in the symmetry ratio was registered at outcome (Paired *T*-test: *p*-value=0.02) and follow-up (Paired *T*-test: *p*-value=0.3) with AFO against no AFO walking. For the affected side, an increase of step length with AFO against no AFO walking was observed at outcome (107.6%) and follow-up (12.8%). The increase was significant at outcome (*p*-value <0.000).

The mean shank to vertical angles (SVA) measured at initial contact (IC), foot flat (FF), mid stance (MS), heel rise (HR) and terminal contact (TC) are represented in

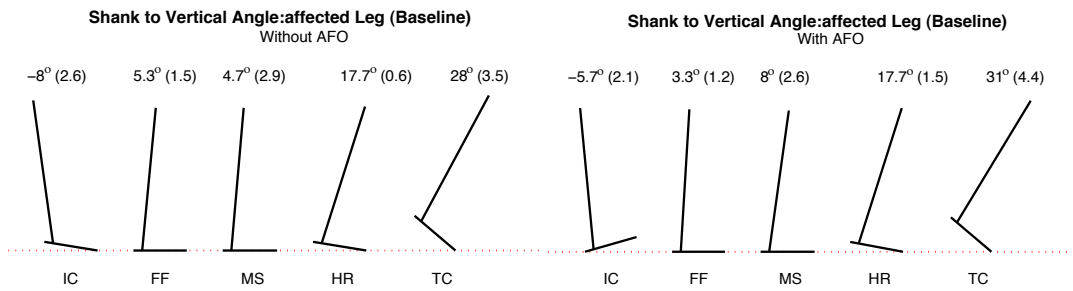


Figure 6.6: Case study 1 baseline shank to vertical angle for affected leg at initial contact (IC), foot flat (FF), mid stance (MS), heel rise (HR) and terminal contact (TC) without (left) and with AFO (right). Angles in degree are reported with values of standard deviation in brackets.

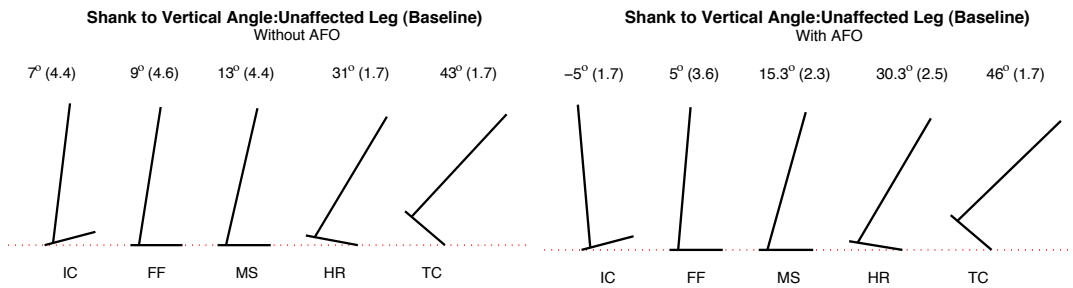


Figure 6.7: Case study 1 baseline shank to vertical angle for unaffected leg at initial contact (IC), foot flat (FF), mid stance (MS), heel rise (HR) and terminal contact (TC) without (left) and with AFO (right). Angles in degree are reported with values of standard deviation in brackets.

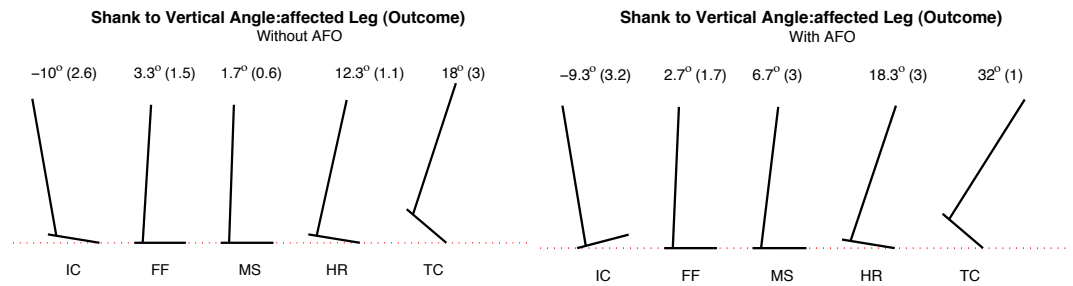


Figure 6.8: Case study 1 outcome shank to vertical angle for affected leg at initial contact (IC), foot flat (FF), mid stance (MS), heel rise (HR) and terminal contact (TC) without (left) and with AFO (right). Angles in degree are reported with values of standard deviation in brackets.

Figure 6.6 for the affected leg at baseline measurement. The figure highlights the movement of the shank showing if it is in a reclined or inclined position.

A reclined position of the tibia was observed at initial contact both with and without AFO. However in the latter case ground contact occurred with the fore part of the foot whereas the AFO allowed for initial contact to occur with the heel and hence a more normal segment kinematics (Figure 6.6) at this point of the gait cycle. A reclined position of the shank could not be achieved at foot flat in either of the two conditions.

Similar tibia kinematics was observed for the sound limb (Figure 6.7). The unaffected leg was able to strike with the heel but when the subject walked without orthosis initial contact occurred with an inclined tibia. This was further evidence of how the affected leg was rushed into stance phase due to the inability of the affected leg to stabilise and support the body weight. With the AFO heel strike could occur with a reclined tibia.

Tibia inclination measurements for outcome assessments are presented in Figure 6.8 for the affected leg. Similar tibia kinematics from baseline was observed. For the AFO condition an enhanced SVA reclined position was observed in comparison to baseline assessments.

Analogously a similar behaviour was observed for the unaffected leg at outcome measurement (Figure 6.9).

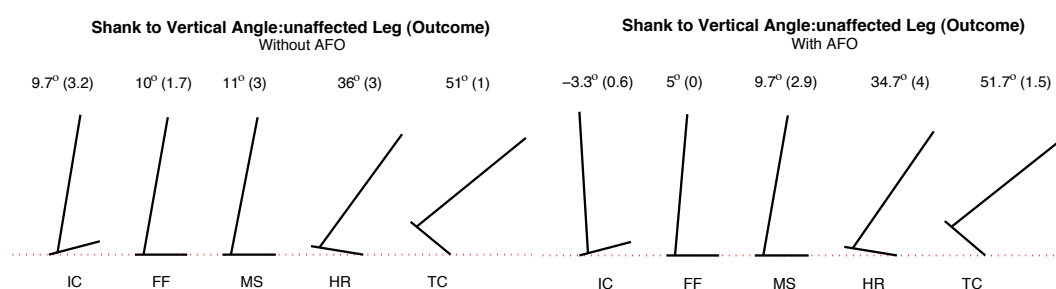


Figure 6.9: Case study 1 outcome shank to vertical angle for unaffected leg at initial contact (IC), foot flat (FF), mid stance (MS), heel rise (HR) and terminal contact (TC) without (left) and with AFO (right). Angles in degree are reported with values of standard deviation in brackets.

The shank to vertical angles for affected and unaffected leg as obtained from the follow-up assessment are shown in Figure 6.10 (a,b). Again the main difference from with and without AFO was at initial contact. The shank was still inclined at foot flat in both conditions for both legs.

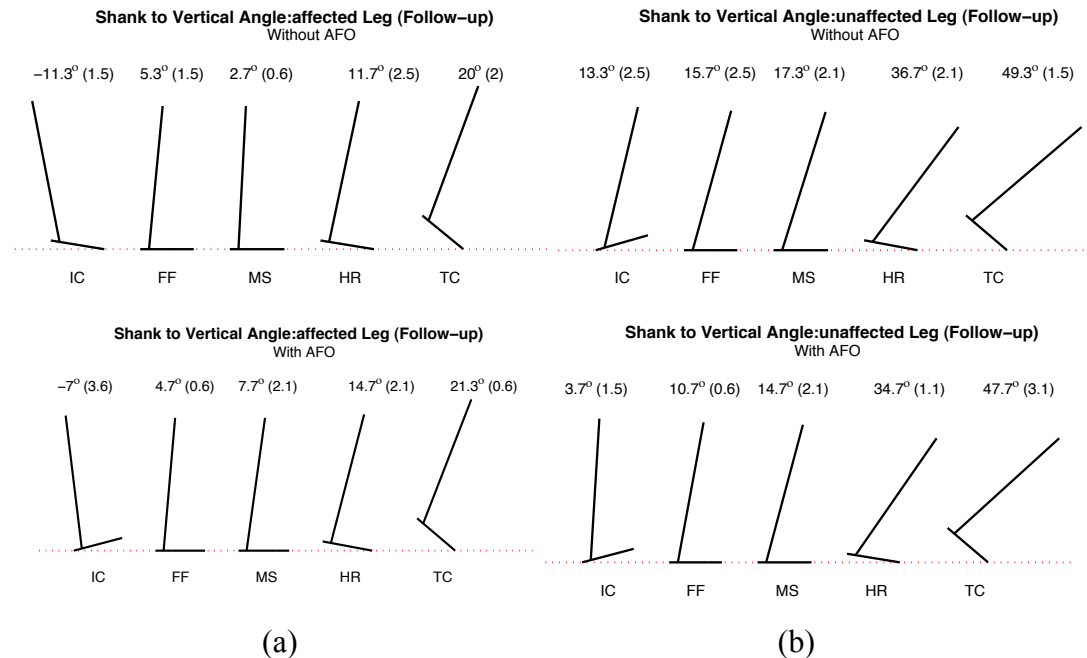


Figure 6.10: Case study 1 follow-up shank to vertical angle for affected (a) and unaffected (b) leg at initial contact (IC), foot flat (FF), mid stance (MS), heel rise (HR) and terminal contact (TC) without (top) and with AFO (bottom). Angles in degree are reported with values of standard deviation in brackets.

6.3.1.2 Kinematic Outcomes

Baseline Assessment:

In the Figures 6.11 to 6.22 kinematic time history of the pelvis and lower limb joints are shown for the baseline assessment. In particular, for each joint rotation, plots are reported which represent the mean and standard deviation when walking with AFO and without AFO for affected and unaffected leg. Comparisons between the two walking conditions for each leg were also plotted. Finally, a summary graph of all joints angle in the three anatomical planes of both legs in both conditions is shown in Figure 6.23.

Pelvic Tilt

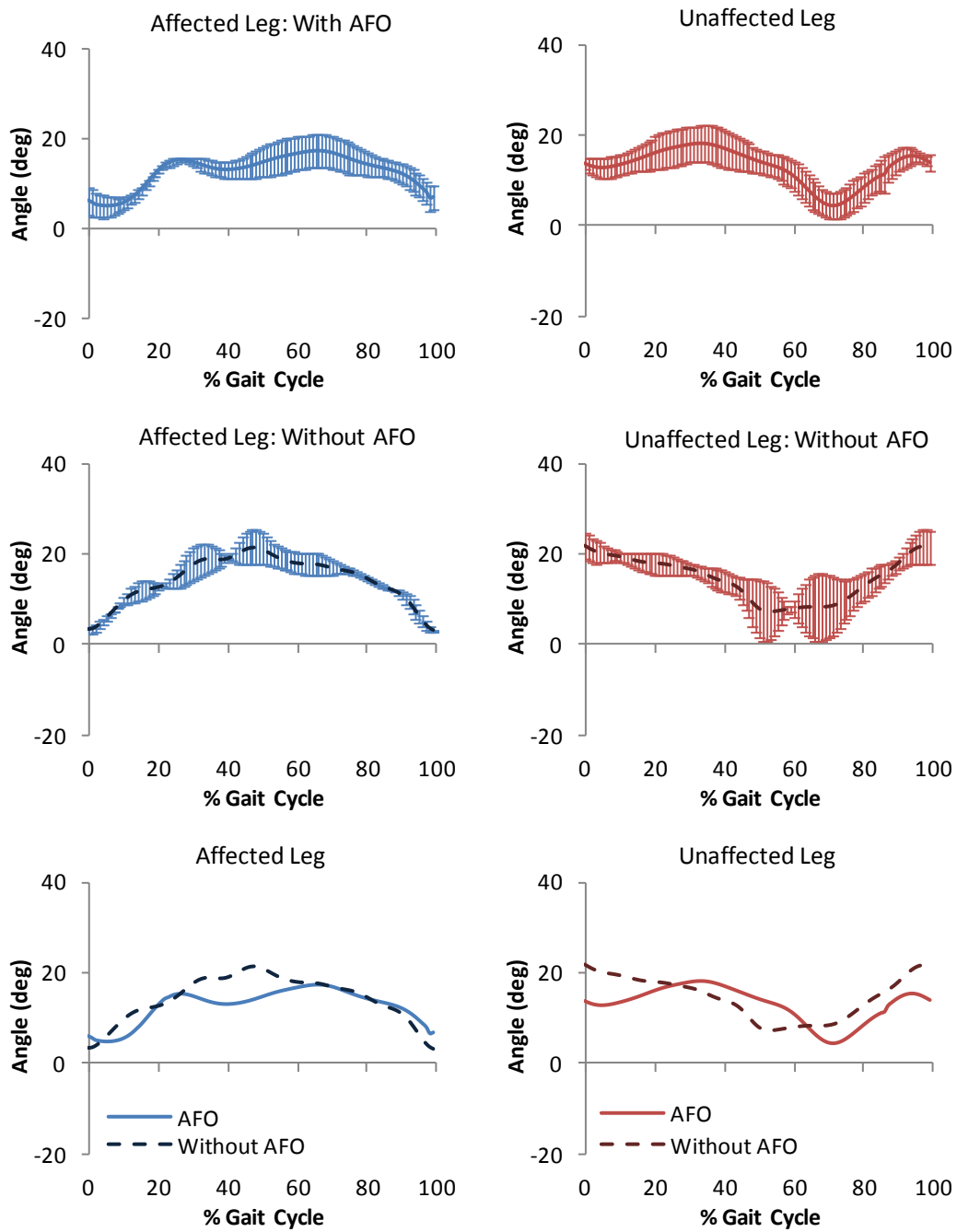


Figure 6.11: Pelvic tilt for baseline assessment of case study 1. Anterior tilt is positive.

Pelvic Obliquity

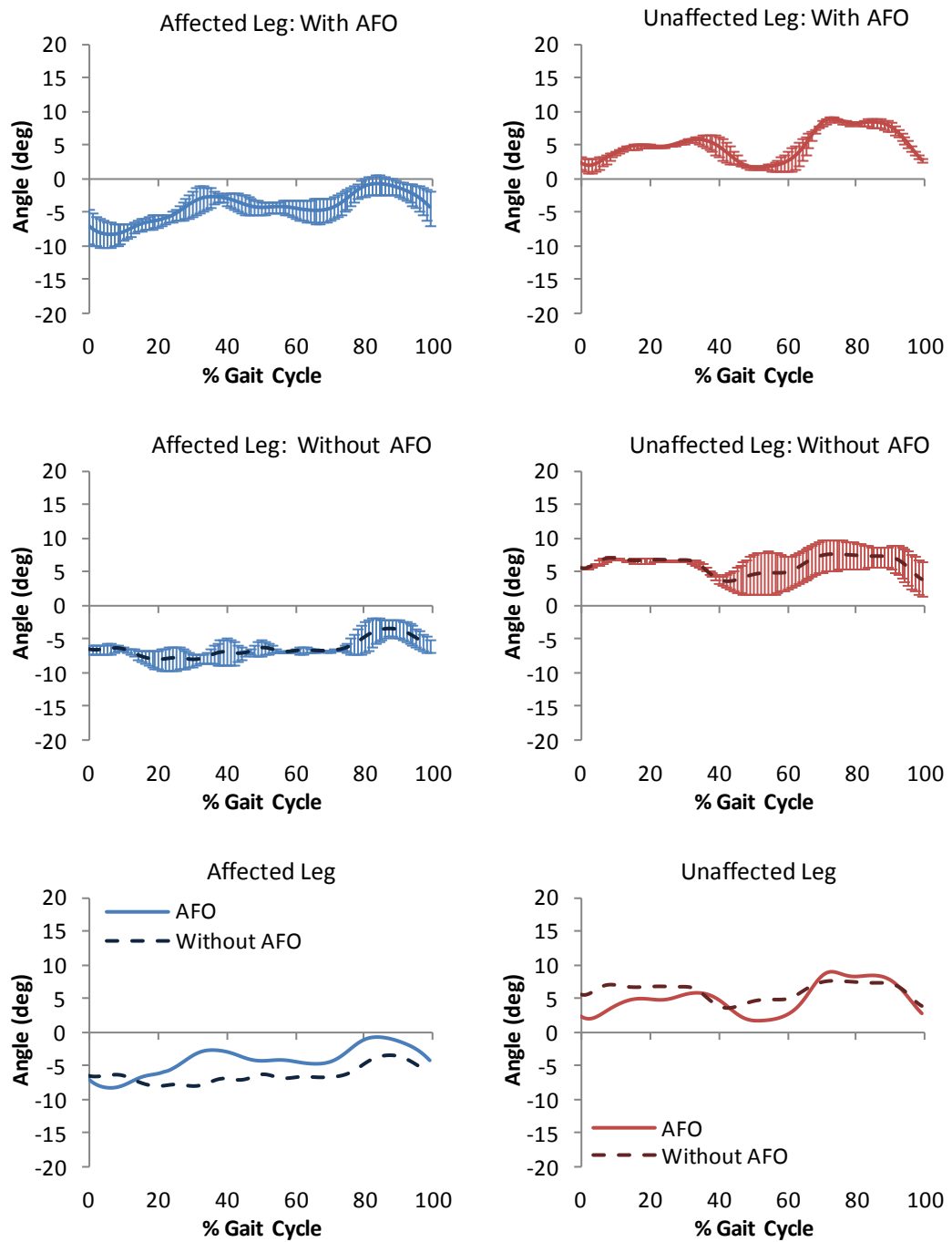


Figure 6.12: Pelvic obliquity for baseline assessment of case study 1. Upward movement is positive in the vertical axis.

Pelvic Rotation

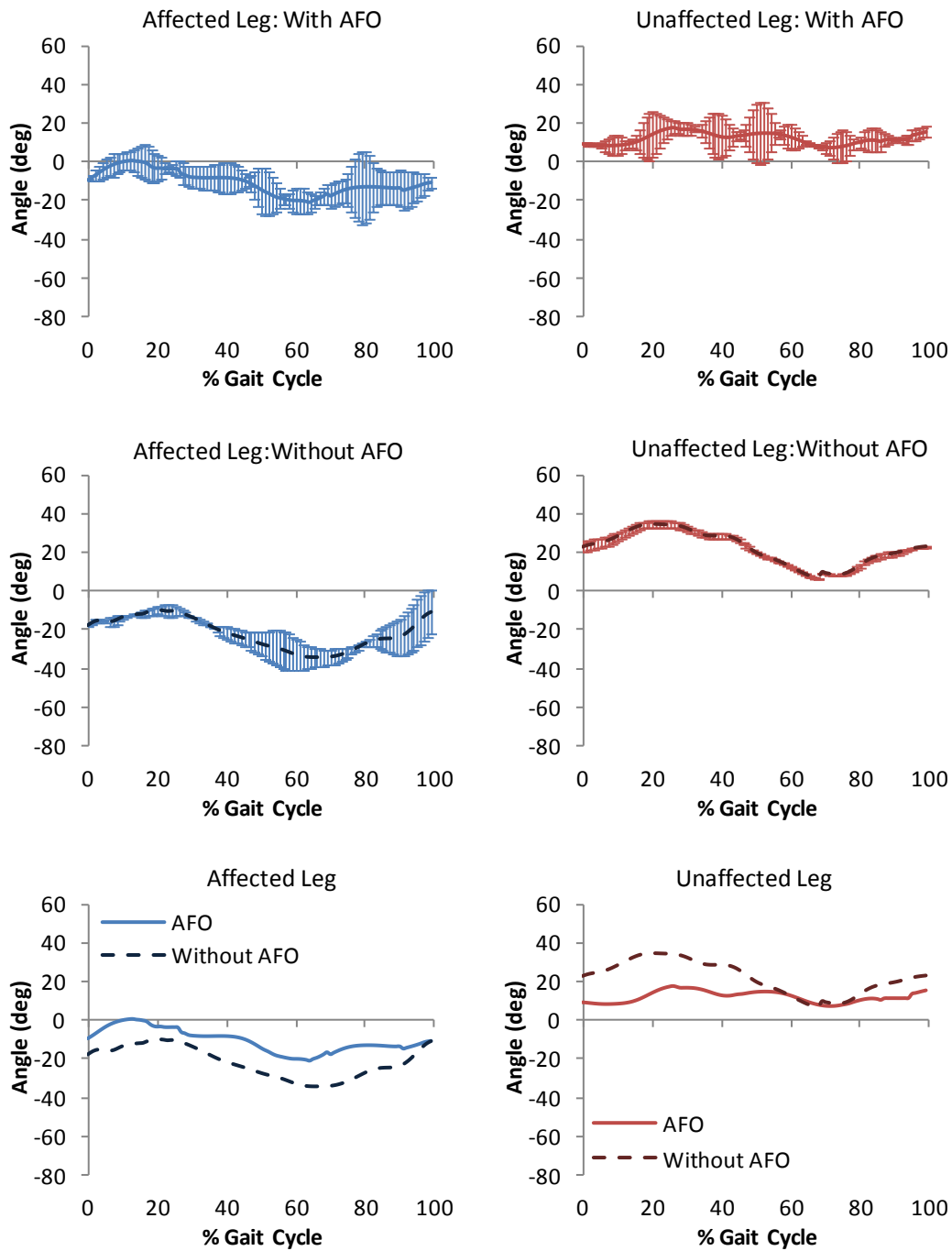


Figure 6.13: Pelvic rotation for baseline assessment of case study 1. Internal rotation is positive in the vertical axis.

Hip Flexion/Extension

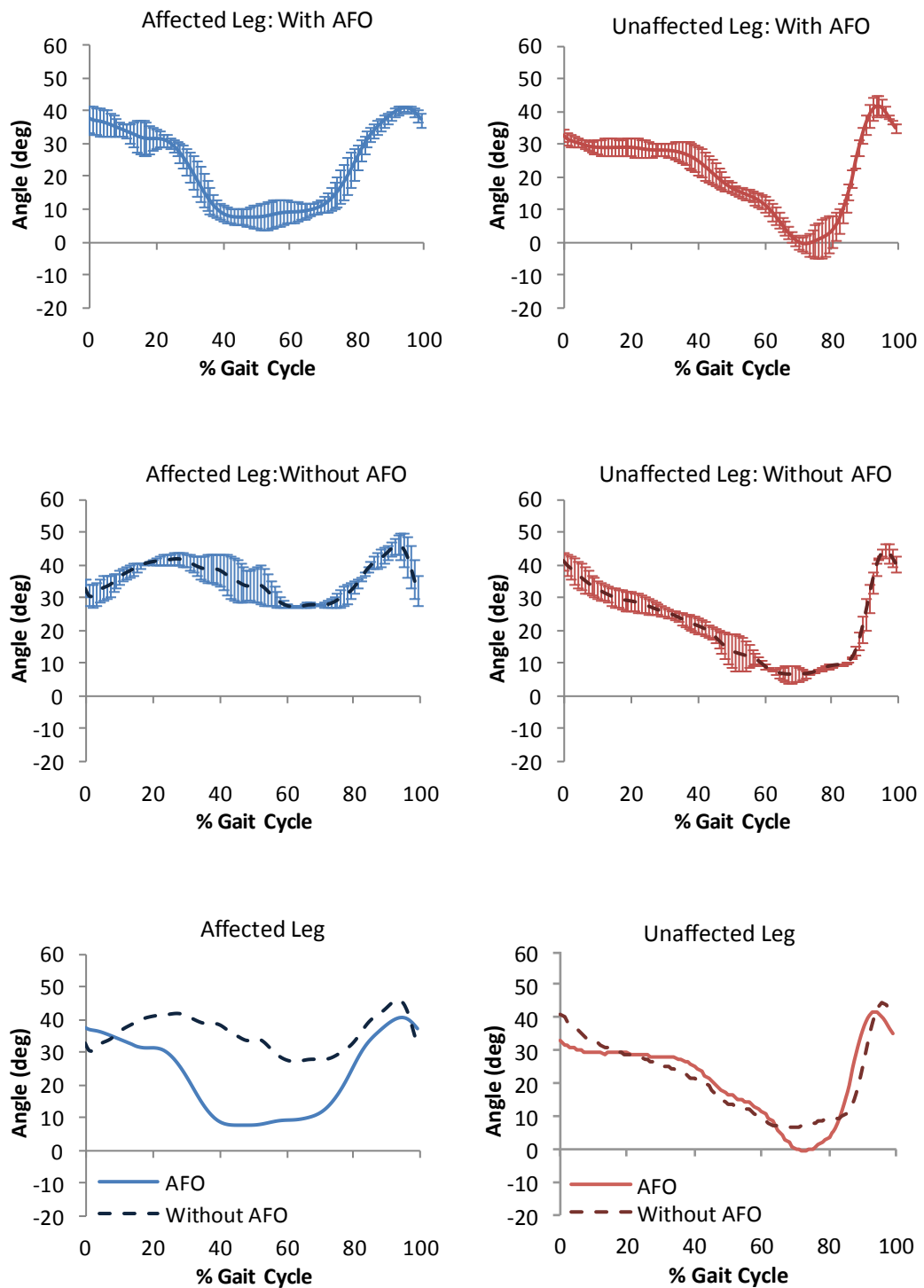


Figure 6.14: Hip flexion/extension angle for baseline assessment of case study 1.

Flexion positive on vertical axis.

Hip Ab/Adduction

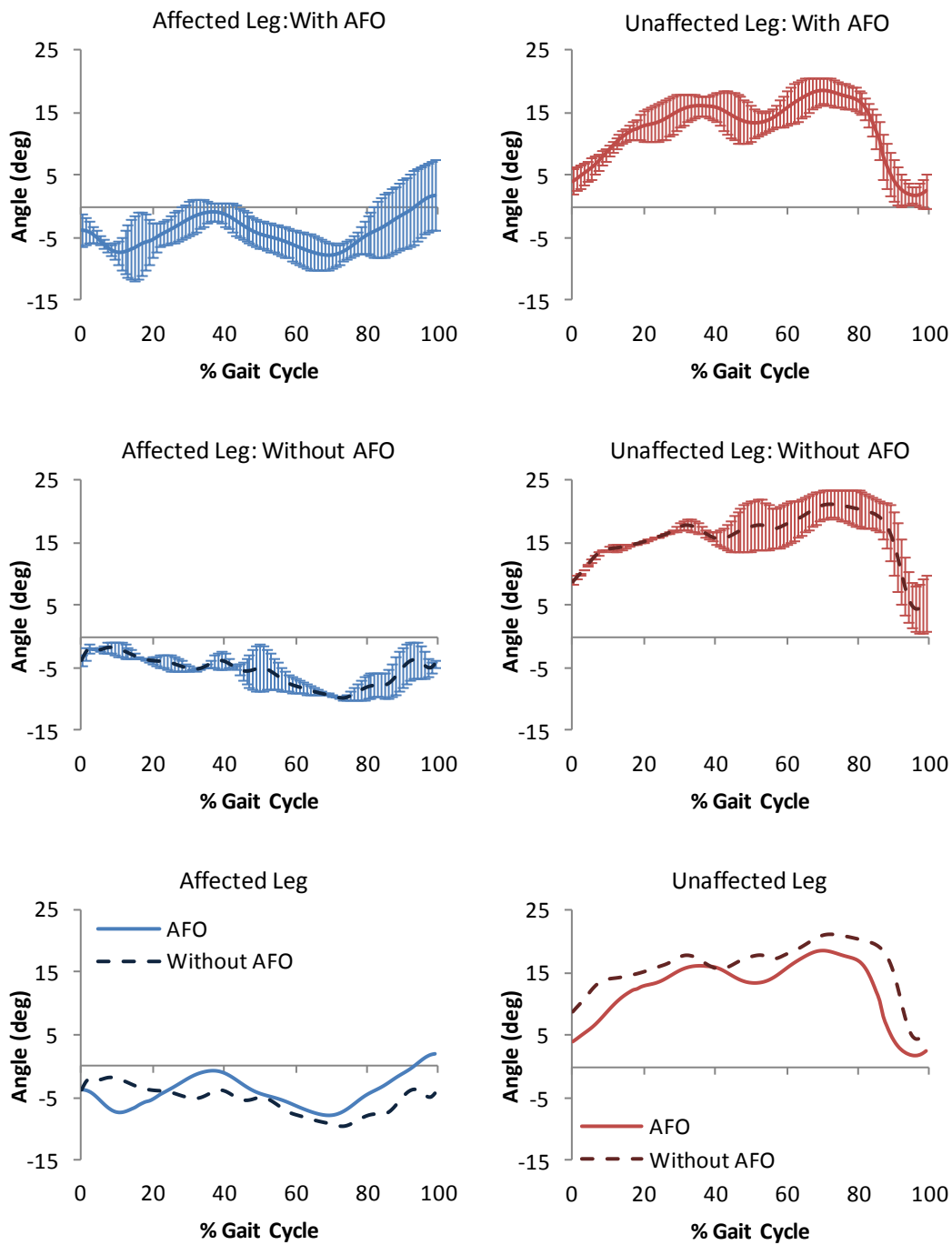


Figure 6.15: Hip ab/adduction angle for baseline assessment of case study 1.

Adduction is represented as positive on the vertical axis.

Hip Internal/External Rotation

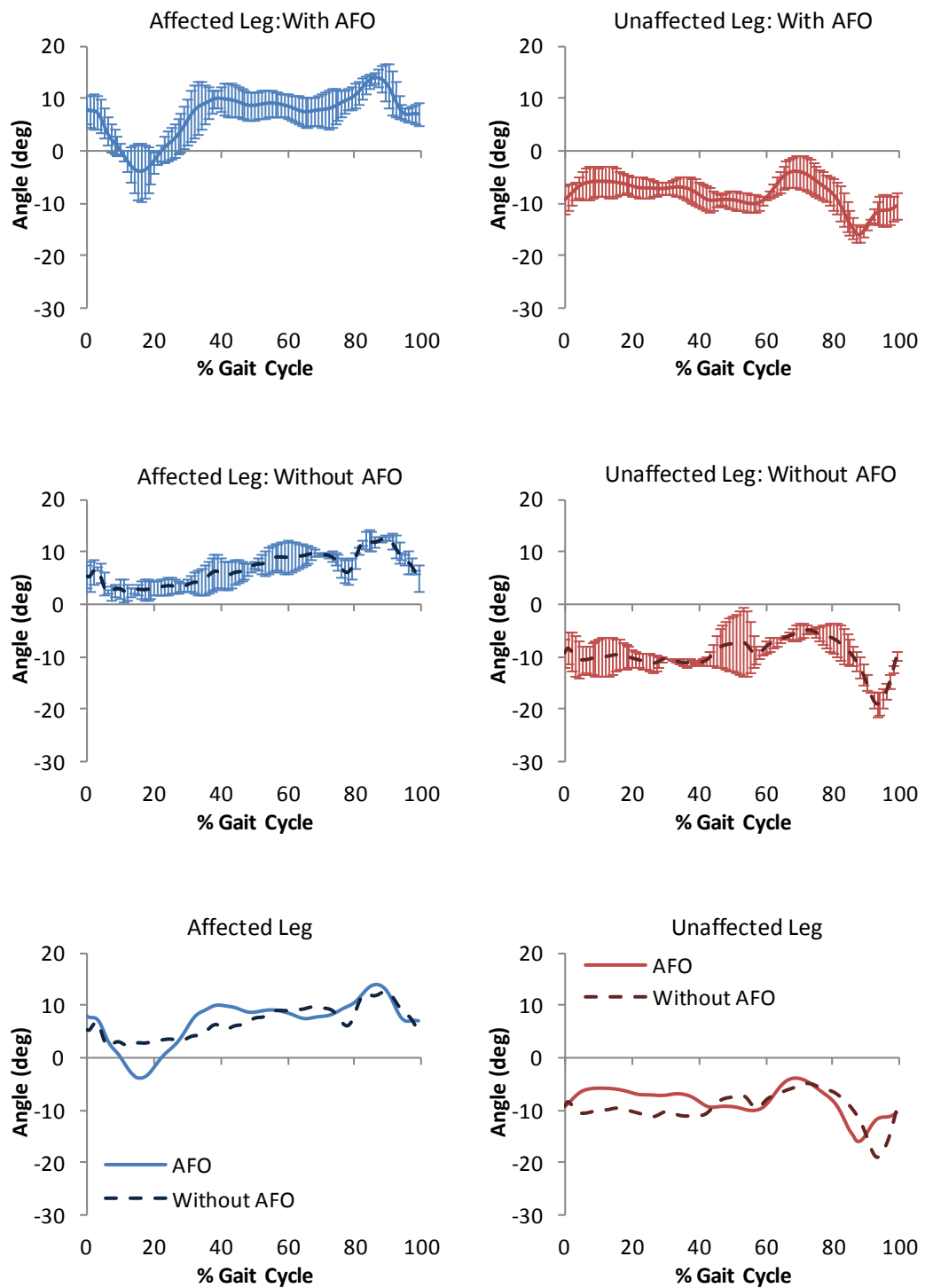


Figure 6.16: Hip internal/external rotation for baseline assessment of case study 1.

Internal rotation is represented as positive on the vertical axis.

Knee Flexion/Extension

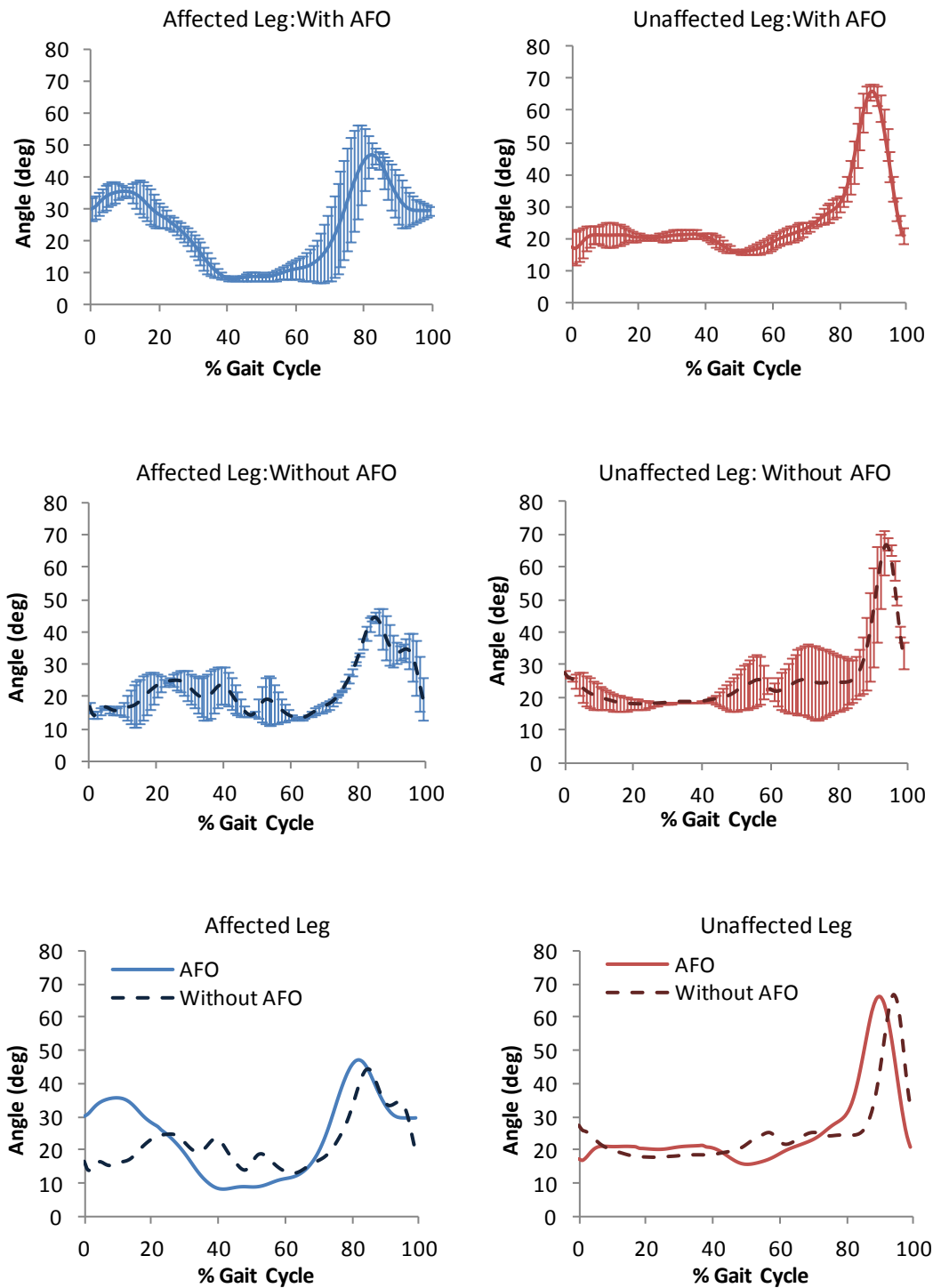


Figure 6.17: Knee flexion/extension angle for baseline assessment of case study 1.

Flexion positive on vertical axis.

Knee Ab/Adduction

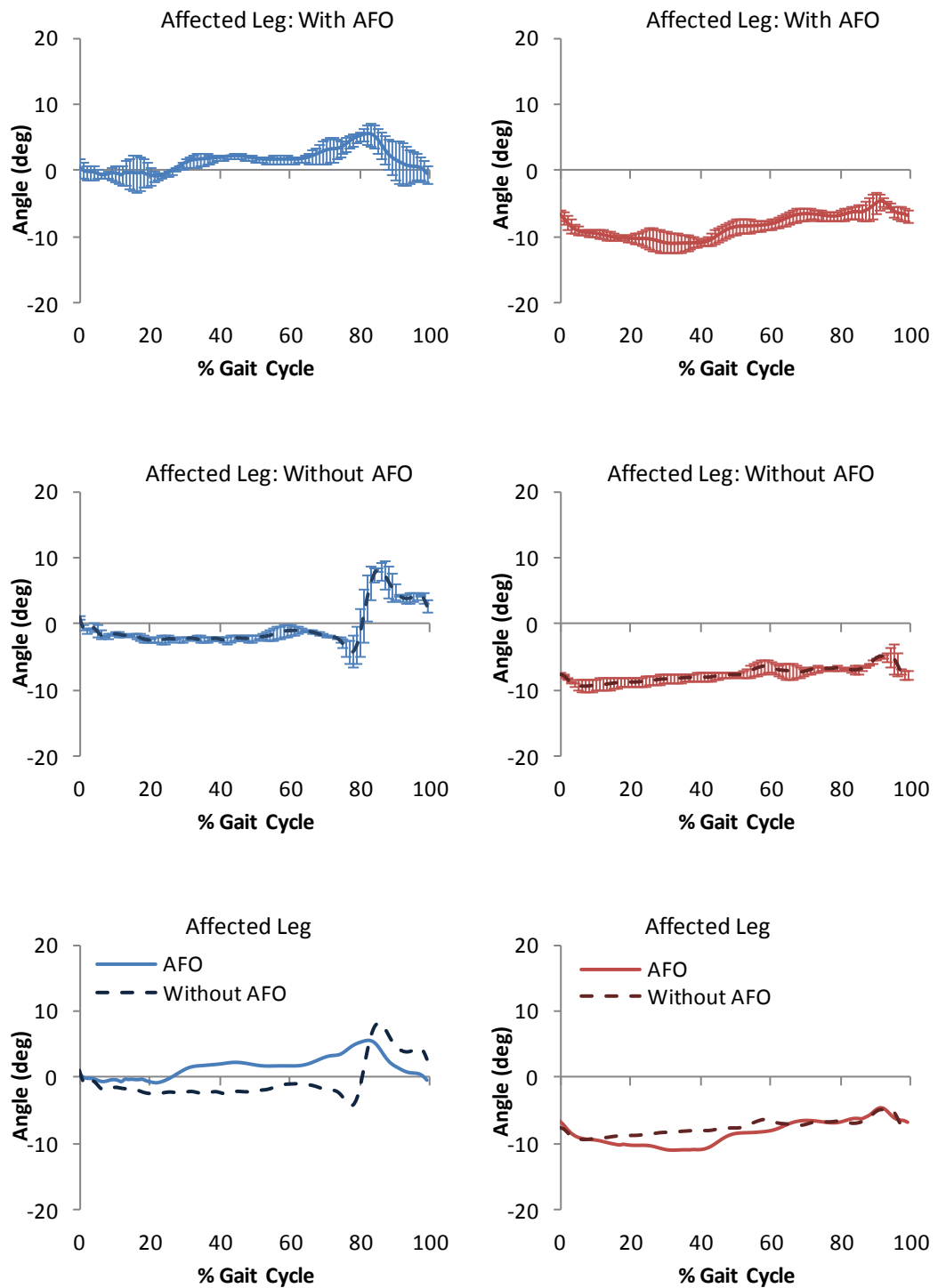


Figure 6.18: Knee ab/adduction angle for baseline assessment of case study 1.

Adduction is represented as positive on the vertical axis.

Knee Internal/External Rotation

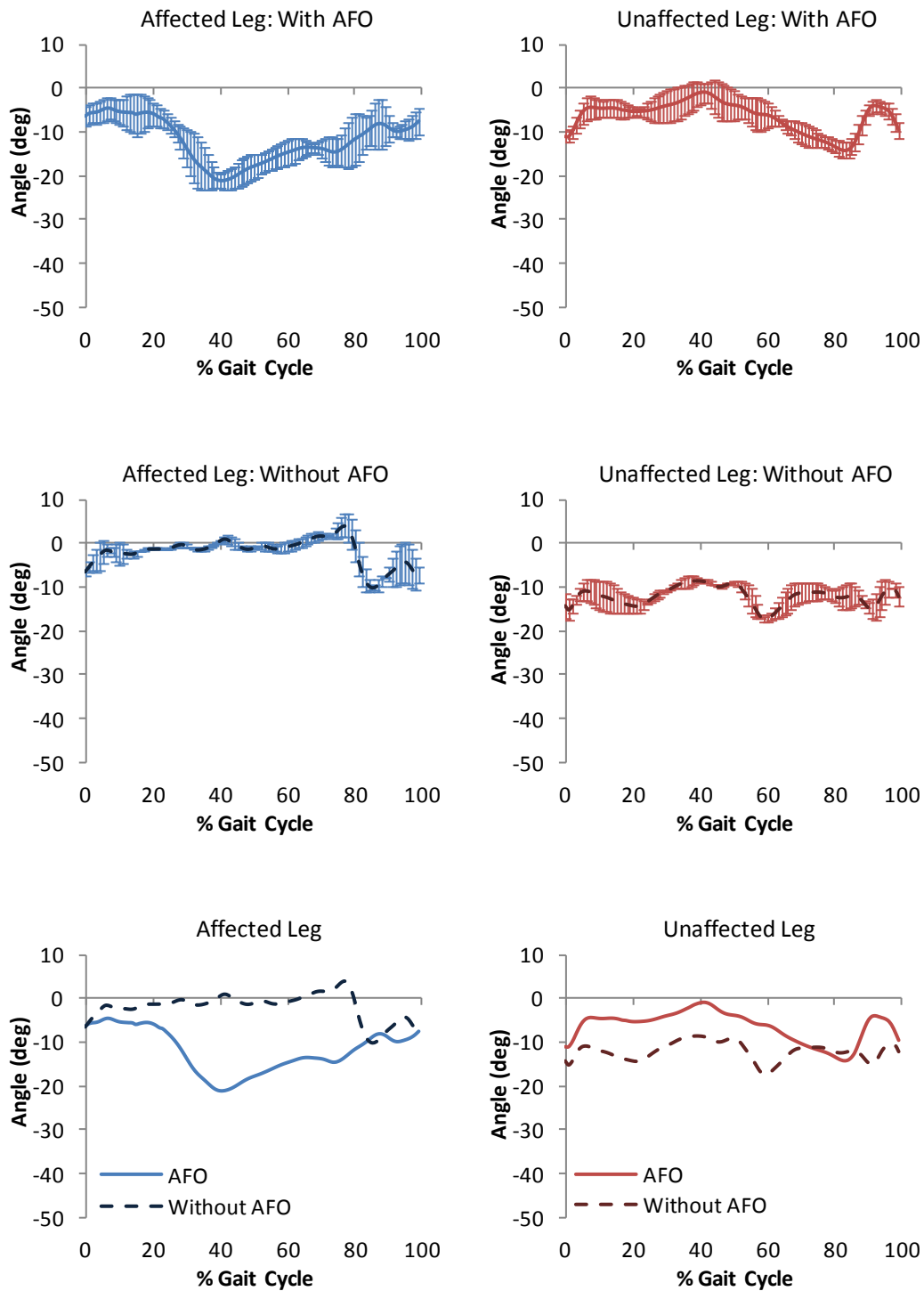


Figure 6.19: Knee internal/external rotation for baseline assessment of case study 1.

Internal rotation is represented as positive on the vertical axis.

Ankle Dorsi/Plantarflexion

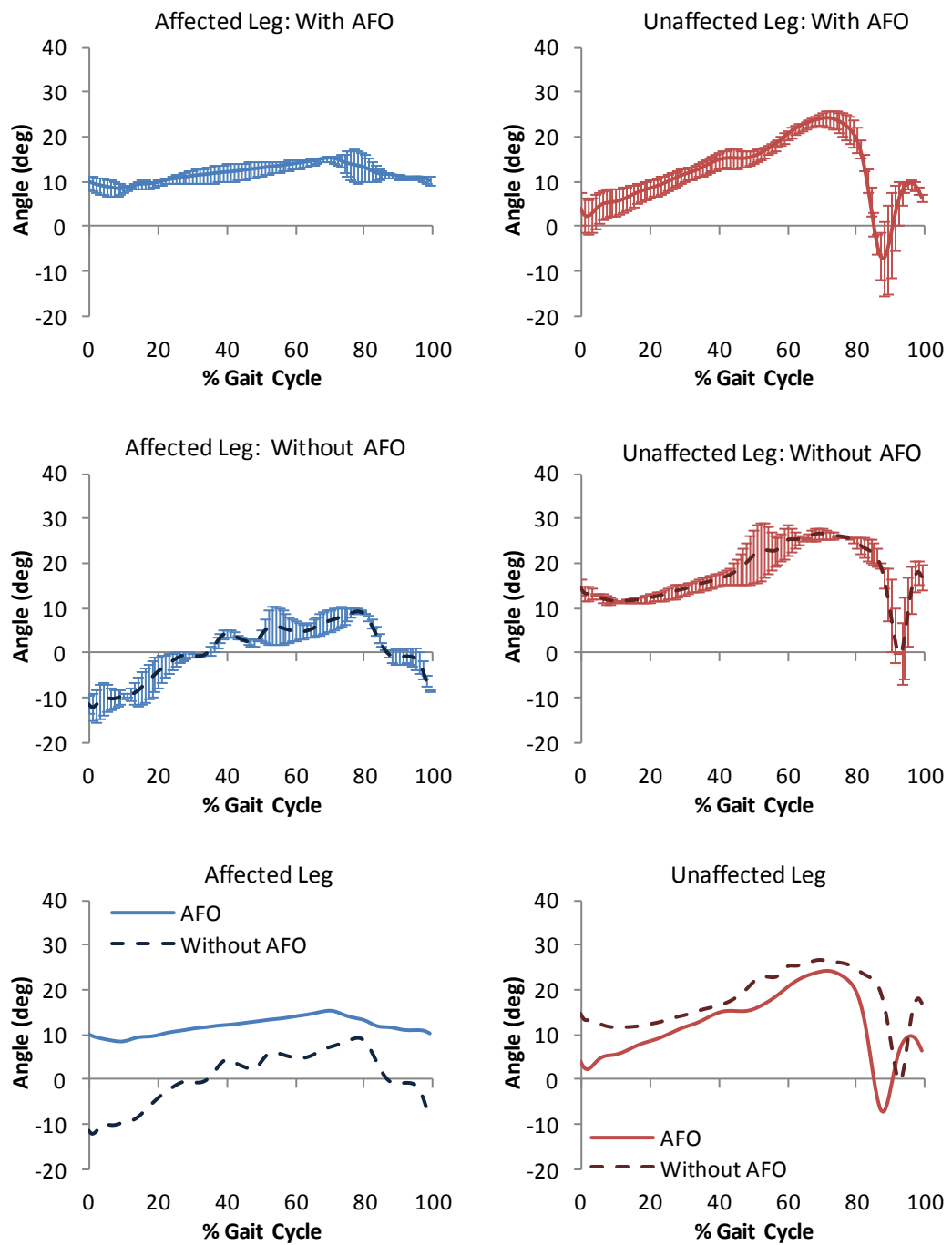


Figure 6.20: Ankle dorsi/plantarflexion for baseline assessment of case study 1. Dorsiflexion is represented as positive on the vertical axis.

Ankle Ab/Adduction

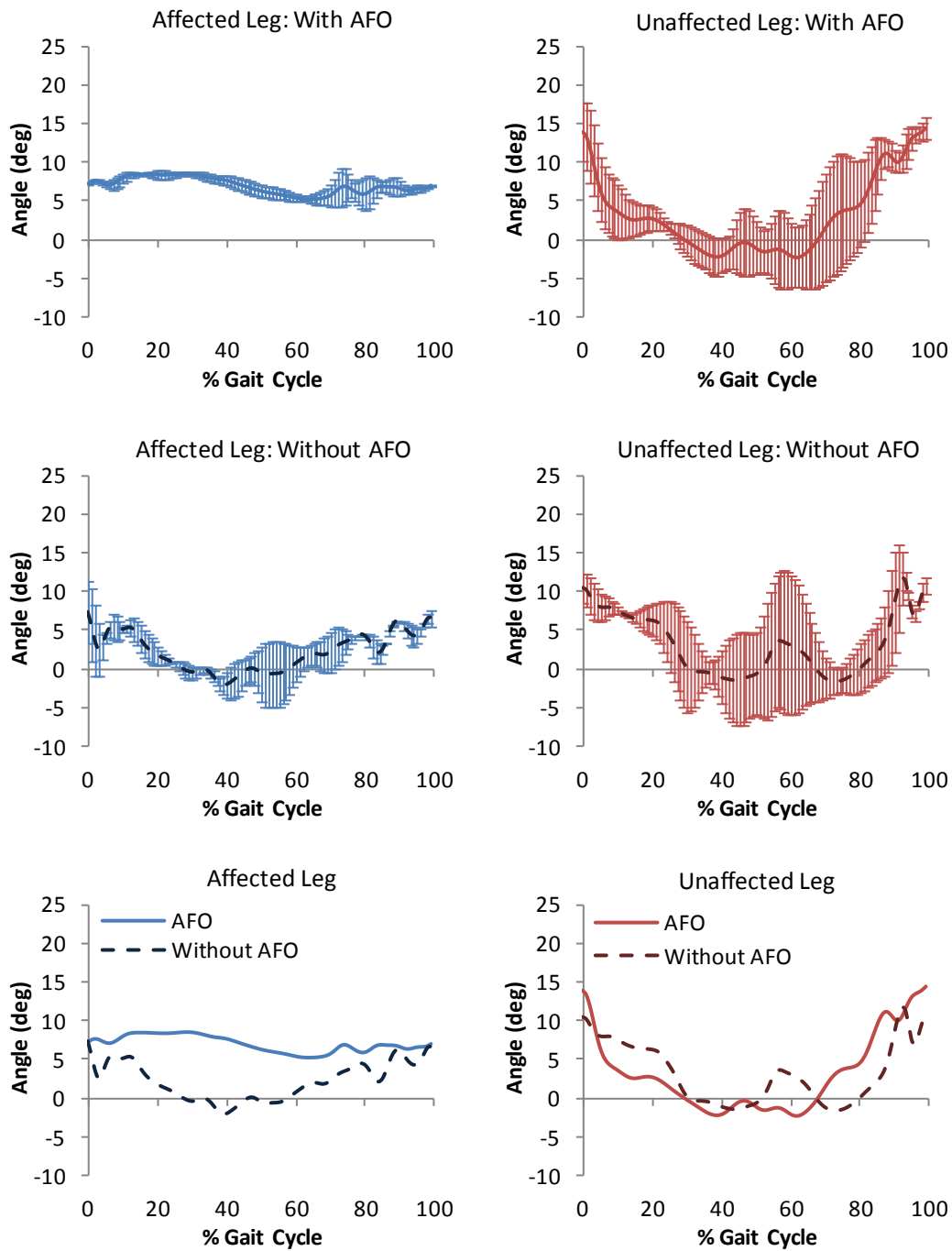


Figure 6.21: Ankle ab/adduction for baseline assessment of case study 1. Adduction is positive on the vertical axis.

Ankle Inversion/Eversion

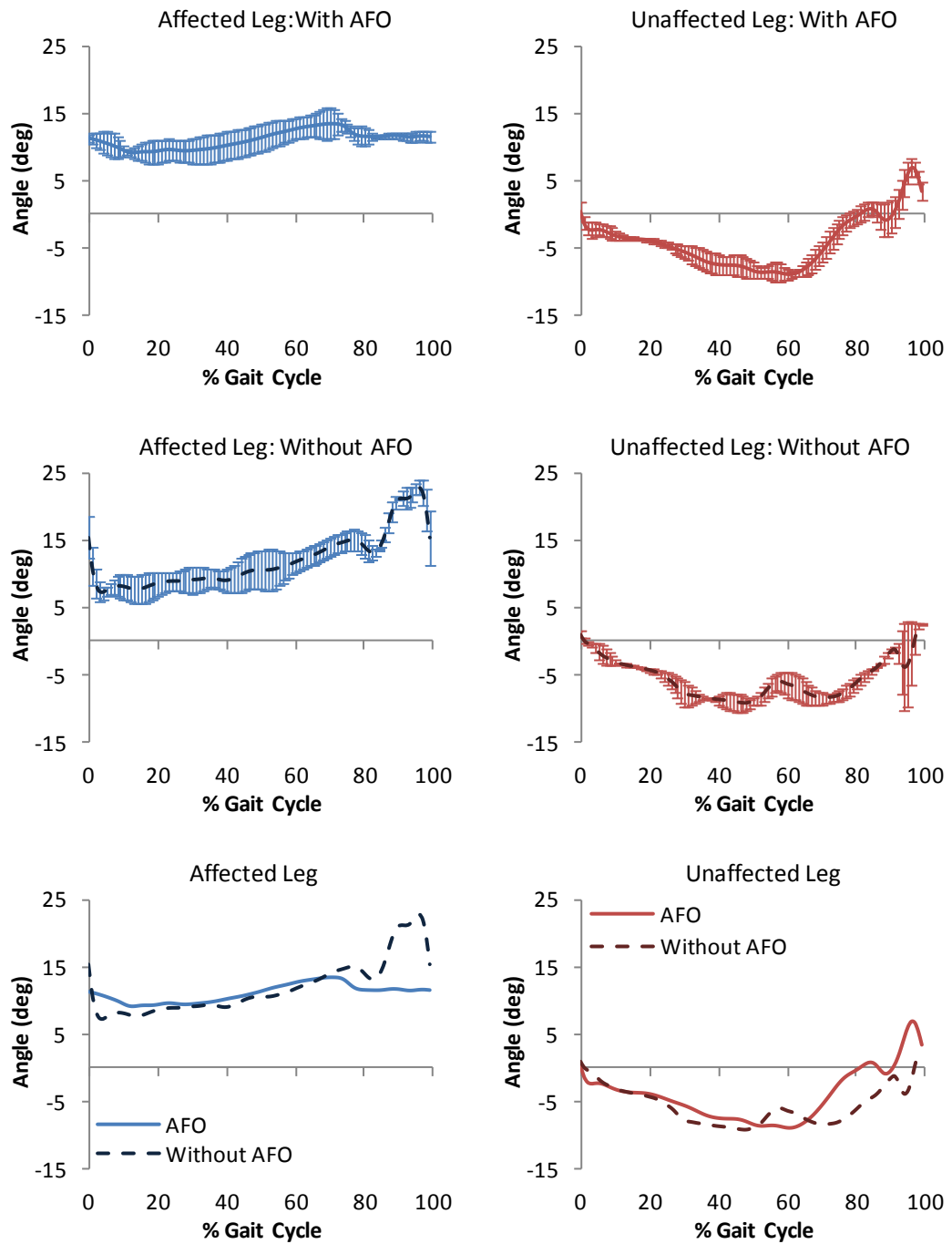


Figure 6.22: Ankle inversion/eversion for baseline assessment of case study 1.

Inversion is positive on the vertical axis.

Baseline Kinematics

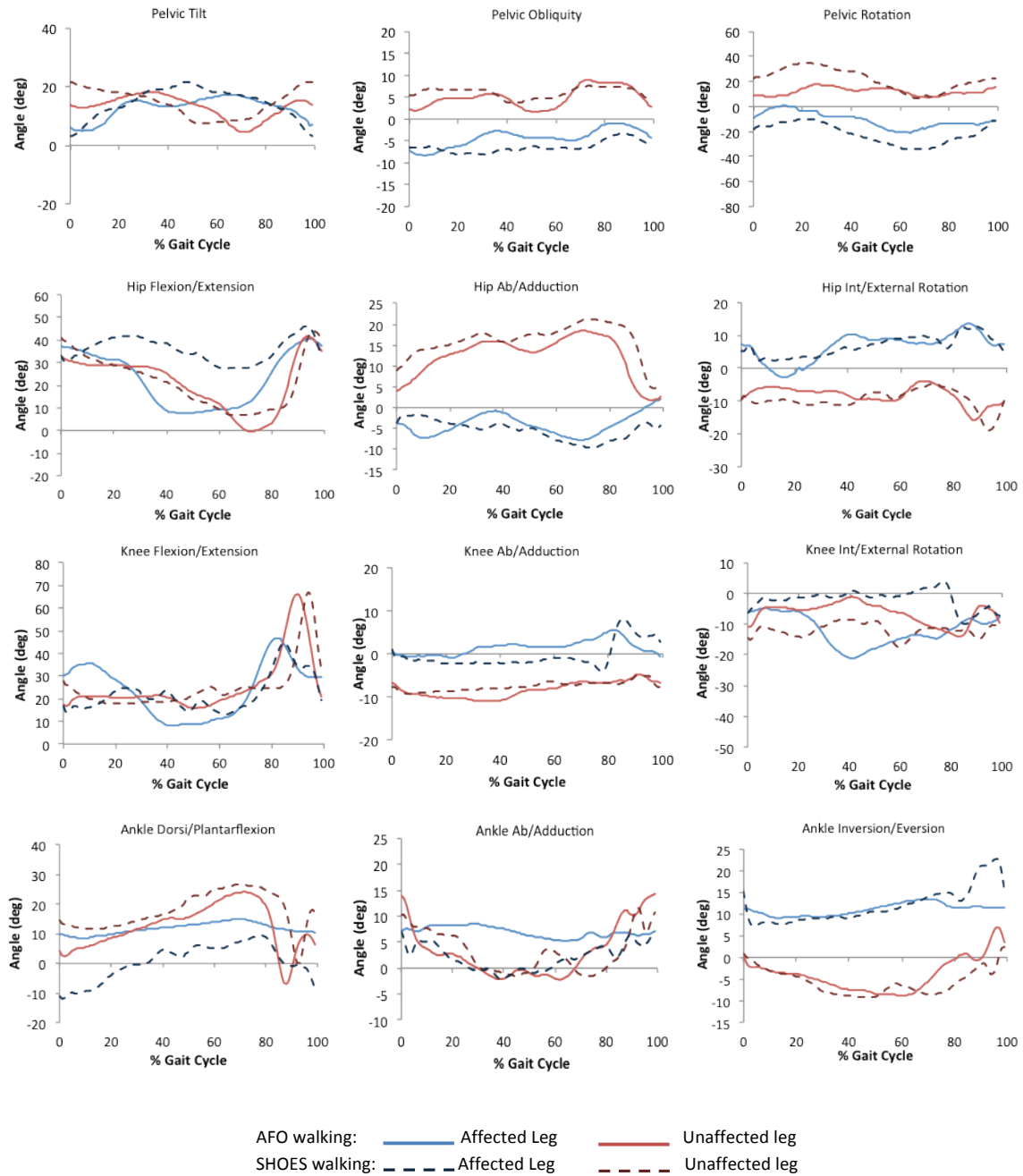


Figure 6.23: Pelvis and lower limb kinematics at baseline assessment for case study 1.

During the baseline test session, the subject was able to perform two walking trials with the AFO and the help of a stick and one walking trial walking with shoes only and the stick. 4 and 2 gait cycles were extracted from the trials with and without the AFO respectively for analysis.

When the subject walked without AFO, initial contact of the hemiplegic leg occurred with the fore and lateral border of the foot with an ankle plantarflexed at $11.3^\circ (\pm 2.1)$ and inverted of $15.3^\circ (\pm 3.0)$ and, the knee unable to extend ($16.7^\circ (\pm 1.8)$ of flexion) (Figure 6.20; 6.22; 6.24 left).

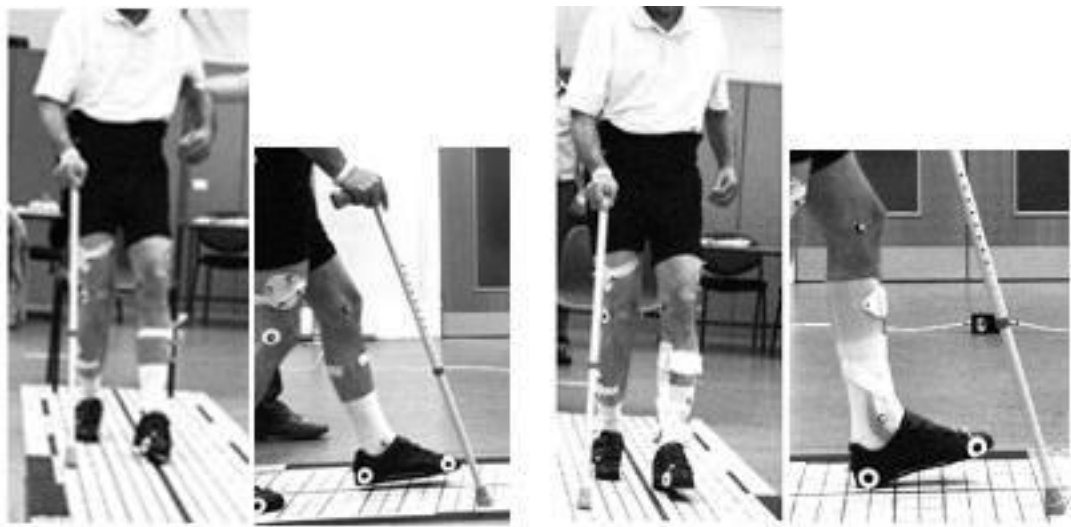


Figure 6.24: Initial Contact: without AFO (left) and with AFO (right) at baseline assessment.

Heel rocker was lost and the acceptance of the weight through the affected leg was slowed down by an inadequate and delayed ankle dorsiflexion. The unaffected leg triggered hip and knee flexion on the hemiplegic side by pushing the body forward (anterior tilt). The ankle passively started to dorsiflex under the action of the hip and knee flexion that inclined the tibia at about the 26% of the gait cycle. At this point of the gait cycle a peak in both hip ($42^\circ \pm 1.9$) and knee ($25^\circ \pm 2.7$) flexion was observed to which corresponded an inversion of the ankle movement from plantarflexion to dorsiflexion. Dorsiflexion peak in terminal stance was small, less

than 10° , at about 75% of the gait cycle. The duration of stance phase for the affected leg was prolonged as already showed in Table 6.2.

The knee remained flexed during stance with a second peak in flexion after toe off of $44.5^\circ (\pm 1.5)$, to which also corresponded a peak in knee adduction of $8.2^\circ (\pm 0.3)$.

The knee was externally rotated during stance starting from $6.4^\circ (\pm 0.9)$ of external rotation at initial contact. The knee was then kept externally rotated to values that did not exceed 2° during the rest of stance and reached a peak of internal rotation ($4.5^\circ \pm 2.7$) followed by a rapid external rotation during swing.

The hip was flexed throughout stance phase (reclined thigh) and not able to extend in mid to late stance while allowing the sound leg to swing forward (Figure 6.14, Figure 6.25a).

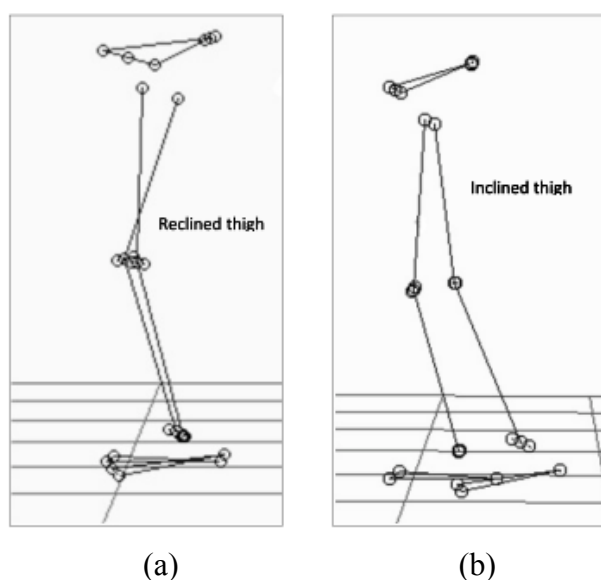


Figure 6.25: Heel Rise: without AFO (a) and with AFO (b) at baseline assessment.

The lack of hip extension disrupted the gait cycle of the unaffected leg which was forced to hit the ground prematurely swinging faster and shortening the step length. The sound leg generally did not advance further than the affected leg (Figure 6.27 left). Initial contact of the unaffected leg occurred with a flexed knee ($27.5^\circ \pm 0.7$) and dorsiflexed ankle ($14.7^\circ \pm 1.8$). The sound leg then rapidly went in to foot flat to release the hemiplegic leg from weight bearing. As can be seen from the Figure 6.17, the knee flexion peak at loading response was missed, an indication of abnormal shock absorption through the sound leg.

This was also accompanied, on the affected side, by a retracted hip. The pelvis was externally rotated in reference to the affected leg and it was anteriorly tilted.

Moreover the hemiplegic hip joint centre was higher than the sound leg hip joint centre (positive pelvic obliquity).

The hemiplegic leg waited for the sound limb to sustain body weight before initiating the swing phase. This explains the long initial double support of the sound leg and terminal double support of the affected limb.

The ankle went into plantarflexion passing through a neutral position in swing phase instead of dorsiflexing in preparation for the subsequent initial contact. In addition, an increase in ankle inversion was clearly observed in swing ($\max 22.8^\circ \pm 1.2$).

This, together with plantarflexion, prevented initial contact through the heel of the foot. The fact that the foot was not dorsiflexed, lead also to an increase in hip flexion to lift the leg up during swing to a maximum of $46.2^\circ \pm 3.0$ at 93 % of the gait cycle to allow ground clearance. Ground clearance was also achieved through hip abduction and pelvic obliquity (hip circumduction). This compensated also for insufficient knee flexion ($\max 44.5^\circ \pm 1.5$) to give a safe ground clearance in swing.

The sound leg had to adjust to the inability of the hemiplegic leg to exert the full range of motion required at each joint for a normal walking pattern. The first consequence, as anticipated above, was an abnormal subdivision of the gait cycle intervals with initial contact that occurred prematurely for a rapid weight bearing. In contrast to the hemiplegic leg, the ankle of the unaffected side could dorsiflex freely to a maximum of $26.6^\circ \pm 1.3$ at 69% of the gait cycle. This allowed for an increased knee flexion that achieved a peak of $67.0^\circ (\pm 1.9)$ in swing and hip ability to extend (reduced flexion visible in the curve in Figure 6.14) during the second half of stance phase. The hip was adducted and always forward with respect to the hemiplegic hip (pelvic rotation positive). It was also noticed that to give stability to the affected leg the subject tended to externally rotate the sound hip and knee; the knee was also abducted.

Swing phase of the unaffected side occurred safely with ankle able to dorsiflex from the plantarflexion position ($0.12^\circ \pm 6.8$) achieved in late stance, and knee able to flex and hip able to extend before going into flexion.

The AFO corrected for excessive ankle plantarflexion at initial contact of the affected leg. Contact occurred through the heel (Figure 6.24 right) when the AFO was worn with an ankle dorsiflexed by $10^{\circ} \pm 1.4$ as compared to the 11.3° of plantarflexion observed at initial contact without the AFO (Paired *T*-test: *p*-value=0.03). Heel rocker was regained although the affected ankle was not able to plantarflex due to the rigid AFO. Only a decrease in dorsiflexion to $8.4^{\circ} (\pm 1.2)$ at 10 % of the gait cycle was observed. Correspondingly at 10 % of the gait cycle, a knee flexion peak was obtained as the load was transferred to the affected leg. The orthosis maintained the foot in dorsiflexion throughout stance phase achieving a maximum of $15.2^{\circ} \pm 0.6$ at 70% of the gait cycle when the ankle dorsiflexion angle is likely to have reached its maximum value. The ankle dorsiflexion allowed the knee to gradually extend to a minimum of flexion of $8.1^{\circ} (\pm 0.7)$ while, also, reducing hip flexion and allowing the hip to go into extension with the AFO reaching a minimum of flexion of $7.7^{\circ} \pm 2.4$. Thigh inclination was achieved unlike in shoes only walking (Figure 6.20b). This gave significant differences between the two conditions (Paired *T*-test: *p*-value <0.05) in mid to late stance in the kinematics curves and facilitated swing phase initiation (Figure 6.26).

The hip was less retracted and thus pelvic rotation was diminished along the entire gait cycle.

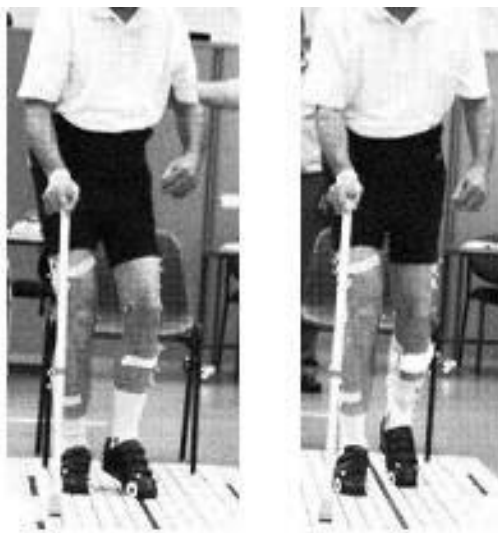


Figure 6.26: Toe Off: without AFO (left) and with AFO (right) at baseline assessment.

During swing phase the ankle was maintained into a dorsiflexed position limiting the toe drag hazard seen without the AFO and allowing for initial contact to occur with the heel. Despite this the knee did not fully extend. $29.5^\circ (\pm 1.4)$ of flexion was noticed at the end of the gait cycle corresponding to the subsequent ground contact of the hemiplegic limb.

Hip abduction persisted as compensation to clear the ground due to an insufficient knee flexion (maximum $46.9^\circ \pm 3.9$), although abduction was reduced with a tendency of going into adduction while approaching the following initial contact.

Pelvic obliquity was also diminished (circumduction of the hip reduced).

The increase of ankle inversion seen without AFO in swing of the affected leg was diminished with the AFO that blocked the ankle in almost steady inverted position. The inversion peak without AFO of 22.8° was brought down to $11.6^\circ (\pm 0.7)$ by the AFO (Paired *T*-test: *p*-value=0.03). Similarly ankle ab/adduction was constrained by the AFO.

The AFO provided stability to the affected leg enhancing also the contralateral leg gait cycle. The sound leg was able to swing freely enhancing step length and eventually overcoming the hemiplegic foot (Figure 6.27) but, still presented with an adducted hip and abducted knee that widened the base of support.



Figure 6.27: Affected leg step length without (left) and with AFO (right).

With regard to variability, for the majority of joint angles similar standard deviation values were obtained without particular differences between walking with and without AFO (Table 6.4). The trend of standard deviation along the gait cycle can be seen in the Figures 6.11 to 6.22. Mean standard deviation and absolute mean standard deviation values throughout the walking cycle are reported in the Table 6.4 for both legs in both conditions tested. Absolute mean standard deviation represents

the standard deviation normalised to the range (max-min) of motion of the relative measure and expressed as its percentage.

| Joint Angles | Affected Leg | | Unaffected Leg | |
|--------------------------------------|--------------|-------------|----------------|-------------|
| | AFO | SHOES | AFO | SHOES |
| <i>Pelvis (°, %range of motion):</i> | | | | |
| Obliquity | 1.4 (18.3%) | 1.0 (20.7%) | 0.6 (8.2%) | 1.4 (35.7%) |
| Rotation | 6.8 (30.8%) | 4.2 (17.3%) | 4.9(46.4%) | 1.1 (3.7%) |
| Tilt | 2.3 (18.2%) | 1.6 (8.8%) | 3.0 (21.8%) | 3.0 (20.8%) |
| <i>Hip (°, %range of motion):</i> | | | | |
| Ab/Adduction | 2.9 (29.5%) | 1.3 (15.9%) | 2.3 (13.6%) | 2.0 (12.1%) |
| Int/External Rotation | 2.8 (15.6%) | 2.1 (17.8%) | 1.7 (15.9%) | 2.1 (14.7%) |
| Flexion/Extension | 3.1 (9.5%) | 2.7 (6.3%) | 2.7 (14.3%) | 2.3 (6.0%) |
| <i>Knee (°, %range of motion):</i> | | | | |
| Ab/Adduction | 1.1 (17.9%) | 0.7 (5.5%) | 0.9 (15.0%) | 0.6 (14.7%) |
| Int/External Rotation | 3.0 (18.6%) | 1.3 (9.0%) | 2.3 (17.6%) | 1.7 (18.6%) |
| Flexion/Extension | 4.6 (11.8%) | 3.3 (10.5%) | 2.5 (4.9%) | 4.7(9.5%) |
| <i>Ankle (°, %range of motion):</i> | | | | |
| Ab/Adduction | 0.7 (21.4%) | 1.5 (16.4%) | 3.4 (20.6%) | 3.7 (28.8%) |
| Inversion/Eversion | 1.4 (31.9%) | 1.7 (11.0%) | 1.1 (7.2%) | 1.0(8.6%) |
| Flexion/Extension | 1.3(19.1%) | 1.8(7.3%) | 2.3(7.3%) | 2.1(7.9%) |

Table 6.4: Mean (°) and absolute mean (% of range of motion) of standard deviation values for each joint angles for both affected and unaffected leg during walking with and without AFO at baseline of case study 1.

As the range of motion varied with and without AFO as can be noticed from the kinematic curves, the proportion of standard deviation in terms of full range of motion was different among conditions and legs although when expressed in degree comparable values were obtained. Careful interpretation of these standard deviation values was required. Higher similarities between AFO and no AFO walking for mean and absolute mean standard deviations were observed for the unaffected leg rather than for the affected leg. Moreover, it was expected that a smaller variability would be observed when the subject walked with the AFO especially at the ankle. This however was not seen when looking at the percentage standard deviation. The AFO restricted the range of motion at the ankle joint and thus the standard deviation resulted in a bigger percentage of the total motion range.

Outcome Kinematics

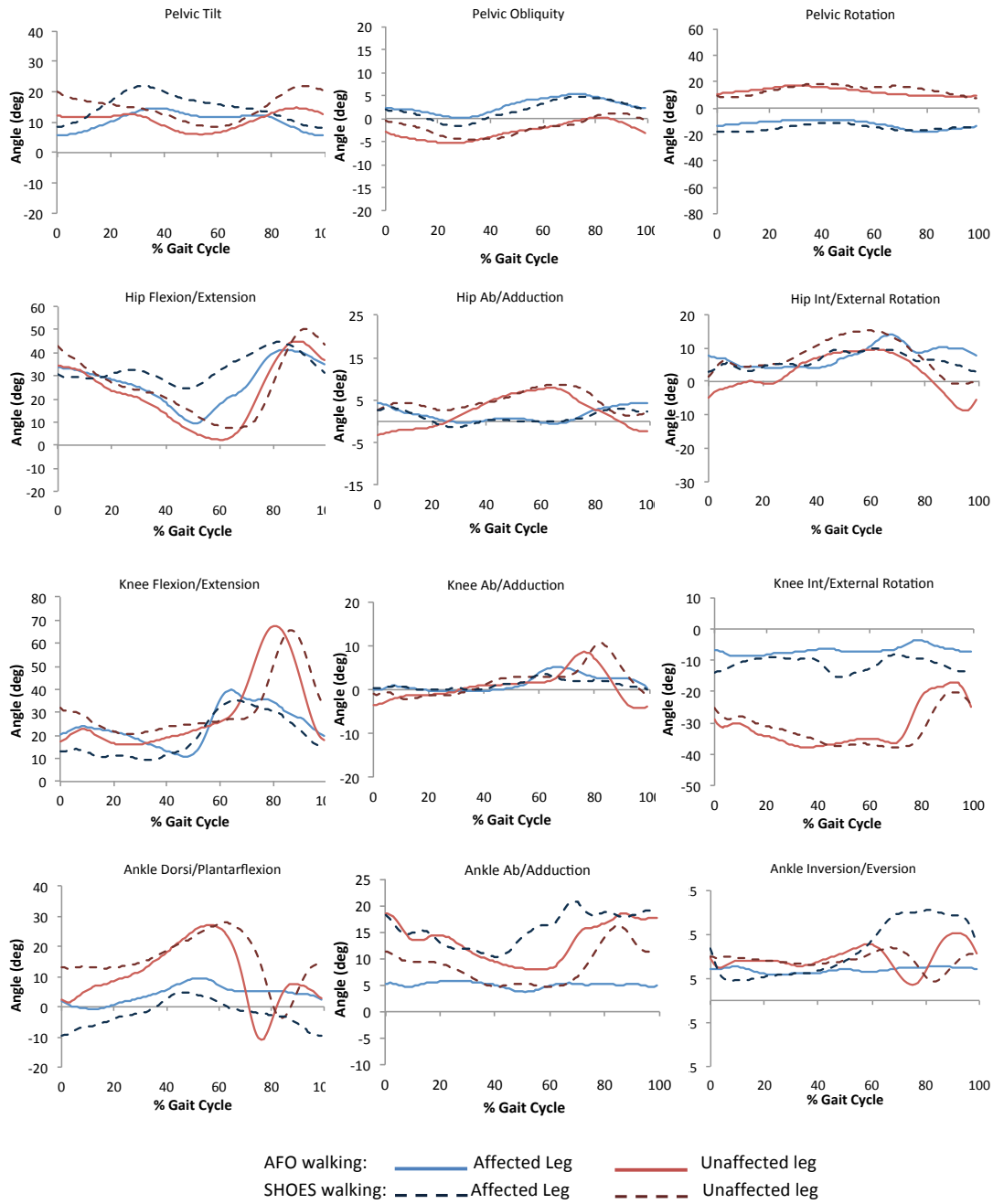


Figure 6.28: Pelvis and lower limb kinematics at outcome assessment for case study 1.

Outcome Assessment:

In Figure 6.28 joint angles in the three anatomical planes for the outcome assessment are shown for both legs for the two walking conditions tested as mean over 5 gait cycles for each condition and leg. The subject walked with the aid of a stick.

The mean trends of affected leg kinematics are represented as blue shade lines whereas unaffected leg kinematics by red shade lines. Solid traces correspond to AFO trials and dotted traces to shoes trials.

Similarities as well as time related changes were noticed between the outcome gait pattern and that the subject had at the time of the baseline assessment. Although common kinematics characteristics were noticed their timing during the gait cycle was different (Figure 6.29) with improved gait timing at this time of the rehabilitation process.

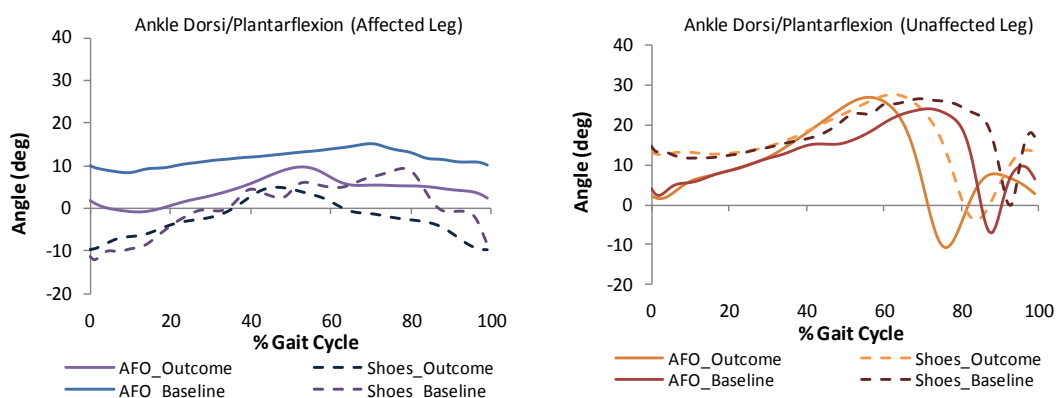


Figure 6.29: Ankle Dorsi/Plantarflexion for baseline and outcome measurements during walking with (solid lines) and without (dotted lines) AFO for affected (left) and unaffected leg (right). Delays among curves can be noticed.

When walking without the AFO at outcome, a lack of ankle dorsiflexion was still observed. Initial contact occurred with fore and lateral border of the foot at 9.5° (± 1.8) of plantarflexion. A peak in dorsiflexion of only 4.8° (± 0.8) was achieved at 47% of the gait cycle after which the ankle went into plantarflexion again. In the coronal and transverse planes, the ankle was adducted and inverted. Inversion rose again during swing to a peak of 20.5° (± 1.9).

Likewise for the knee some similarities with the previous assessment were observed: the knee was flexed above 10° at ground contact, small initial flexion peak of 14.1° (± 2.5) that was just 1° higher than starting knee flexion, inability to extend the knee under 9° of flexion during mid stance and, inadequate knee flexion in swing ($35.4^\circ \pm 5.4$). Moreover, the knee was externally rotated but to a higher extent than at baseline (peak $15.5^\circ \pm 3.1$) and this was clearly noticeable as the foot approached toe off and just after it. The knee was also still adducted throughout the walking cycle although a smaller adduction peak of 3.6° (± 1.3) was achieved.

The hip was flexed at 30.5° (± 2.2) at the start of the gait cycle and was unable to extend below 24.4° (± 4.3) of flexion. Affected limb progression was thus still impaired. The difficulty in initiating the swing phase, as occurred previously, was also presented by a retracted hip; the pelvis was in fact externally rotated. Ground clearance was achieved by virtue of an increased hip flexion (maximum $44.6^\circ \pm 2.3$) that lifted the leg up together with hip hiking (increase in the positive pelvic obliquity) and pelvis anterior tilt. Before preparing to advance forward, the affected leg waited for the contralateral leg to make a full strike on the ground which then implied a shortening of the step length and swing phase of the sound limb. This phase of the gait however was shorter than for baseline walking without AFO (Table 6.2).

Contrarily to what was observed at baseline the hip was not abducted but rather adducted at the beginning of the gait cycle and during swing phase passing through a neutral position during the second half of the stance phase. Internal rotation of the hip was also observed throughout the gait cycle.

The AFO helped the patient in correcting for excessive ankle plantarflexion and lack of dorsiflexion. The gait cycle commenced with the ankle dorsiflexed at 1.9° (± 1.0) to which followed a small plantarflexion movement (peak $0.8^\circ \pm 1.1$) before going into dorsiflexion again. A peak of dorsiflexion of 9.6° (± 0.5) was achieved at 53% of the gait cycle. The ankle then dropped into averagely 5° of dorsiflexion for the duration of the swing phase and ended the gait cycle with 2.4° (± 0.7) of dorsiflexion. Again plantarflexion in swing was prevented by the AFO while allowing for a dorsiflexed foot and hence heel strike rather than abnormal initial contact. Adduction and inversion of the foot were also restricted by the AFO as can be noticed by the flat

curves in Figure 6.28 in ankle ab/adduction and inversion/eversion graphs. Ankle kinematics in sagittal and coronal planes with and without AFO were significantly different for the entire gait cycle (Paired *T*-test: *p*-value<0.00). Significant differences (Paired *T*-test: *p*-value<0.00) in the ankle transverse plane rotations were instead found in swing phase and in the 5 to 20% interval of the gait cycle, only. The enhancements at the ankle level were reflected also in the knee kinematics. A peak of flexion at loading response (8%) could be achieved with the AFO ($23.8^{\circ} \pm 0.7$) contrarily to shoes only walking (Paired *T*-test: *p*-value=0.00). From this flexed position the knee was able to go into extension to a minimum of flexion of 10.8° (± 1.6) to which also corresponded extension of the hip down to 9.4° (± 1.6) allowing for a smoother progression (ankle rocker) of the affected limb. These represented significant improvements compared to without AFO walking trials. Moreover this allowed the sound limb to advance in its swing phase and preparing gradually for the next initial contact without abruptly breaking off into stance as occurred without AFO.

A proper peak of knee flexion in swing could not be achieved with a maximum reachable value of only 39.7° (± 1.3) at 64% of the gait cycle. At this stage of the gait cycle, the hip started to flex to allow for ground clearance with a peak in flexion of 41.1° (± 2.7). Differently from the shoes only condition, although the knee was not fully flexed a safe swing occurred and the ankle dorsiflexed preventing for foot drag. The pelvis remained externally rotated and hip hiking still occurred, as help for advancing the leg toward the subsequent heel strike due to lack of knee flexion. Anterior tilt was diminished throughout the gait cycle as well as knee external rotation of the hemiplegic leg.

As a consequence of the enhanced gait pattern of the affected leg, the sound leg showed improvements, which were mostly time related. The sound limb could divide the different phases of the gait more normally as can be seen from the kinematics curves with AFO compared to those trials without AFO (Figure 6.29).

Moreover, the subject was able to obtain an enhanced up-right posture while walking with the AFO as demonstrated by reduced pelvic tilt for both affected and unaffected legs.

Small variability in joint kinematics was generally found (Table 6.5). Mean average standard deviation did not exceed 4° and 36% when expressed in terms of range of motion.

| Joint Angles | Affected Leg | | Unaffected Leg | |
|---------------------------------------|--------------|-------------|----------------|------------|
| | AFO | SHOES | AFO | SHOES |
| <i>Pelvis (°, % range of motion):</i> | | | | |
| Obliquity | 1.3 (25.9%) | 1.4(22.0%) | 1.3(22.8%) | 1.5(25.4%) |
| Rotation | 1.1(11.6%) | 0.9(13.1%) | 1.4(16.7%) | 2.7(24.5%) |
| Tilt | 1.2(13.0%) | 1.6(11.7%) | 1.2(14.1%) | 1.5(11.0%) |
| <i>Hip (°, %range of motion):</i> | | | | |
| Ab/Adduction | 1.4(28.7%) | 1.6(35.7%) | 1.6(14.1%) | 1.6(22.3%) |
| Int/External Rotation | 1.5(15.6%) | 1.6(22.6%) | 2.3(12.6%) | 2.6(16.8%) |
| Flexion/Extension | 2.3(7.2%) | 2.9(14.2%) | 1.5(3.4%) | 2.3(5.5%) |
| <i>Knee (°, %range of motion):</i> | | | | |
| Ab/Adduction | 0.7(12.9%) | 0.8(21.3%) | 1.0(7.7%) | 1.3(10.0%) |
| Int/External Rotation | 1.8(35.4%) | 2.2(30.0%) | 2.2(10.8%) | 2.5(14.1%) |
| Flexion/Extension | 2.5(8.6%) | 3.5 (13.4%) | 2.2 (4.3%) | 3.1(6.9%) |
| <i>Ankle (°, %range of motion):</i> | | | | |
| Ab/Adduction | 0.7(31.2%) | 2.8(26.6%) | 1.7(16.0%) | 2.4(20.6%) |
| Inversion/Eversion | 0.6(33.2%) | 1.9(20.5%) | 1.0(9.0%) | 1.1(13.8%) |
| Flexion/Extension | 0.9(8.8%) | 1.2(3.1%) | 1.7(11.7%) | 2.8(27.8%) |

Table 6.5: Mean (°) and absolute mean (% of range of motion) of standard deviation values for each joint angle for both affected and unaffected leg during walking with and without AFO at outcome assessment of case study 1.

It appeared that the AFO did not particularly reduced the variability in joint angles, although a reduction in mean standard deviation was observed at the ankle level mostly for ankle ab/adduction of the affected leg.

Follow-up Assessment:

Figure 6.30 shows the pelvis and lower limb kinematic at follow-up assessment. 5 gait cycles were used for the analysis for both legs while the subject walked with and without AFO. A stick was used during the walking task performances. Pelvis and lower limb joint kinematics observed at follow-up assessment showed analogies with the previous two test results and in particular with the outcome measurement.

Follow-up Kinematics

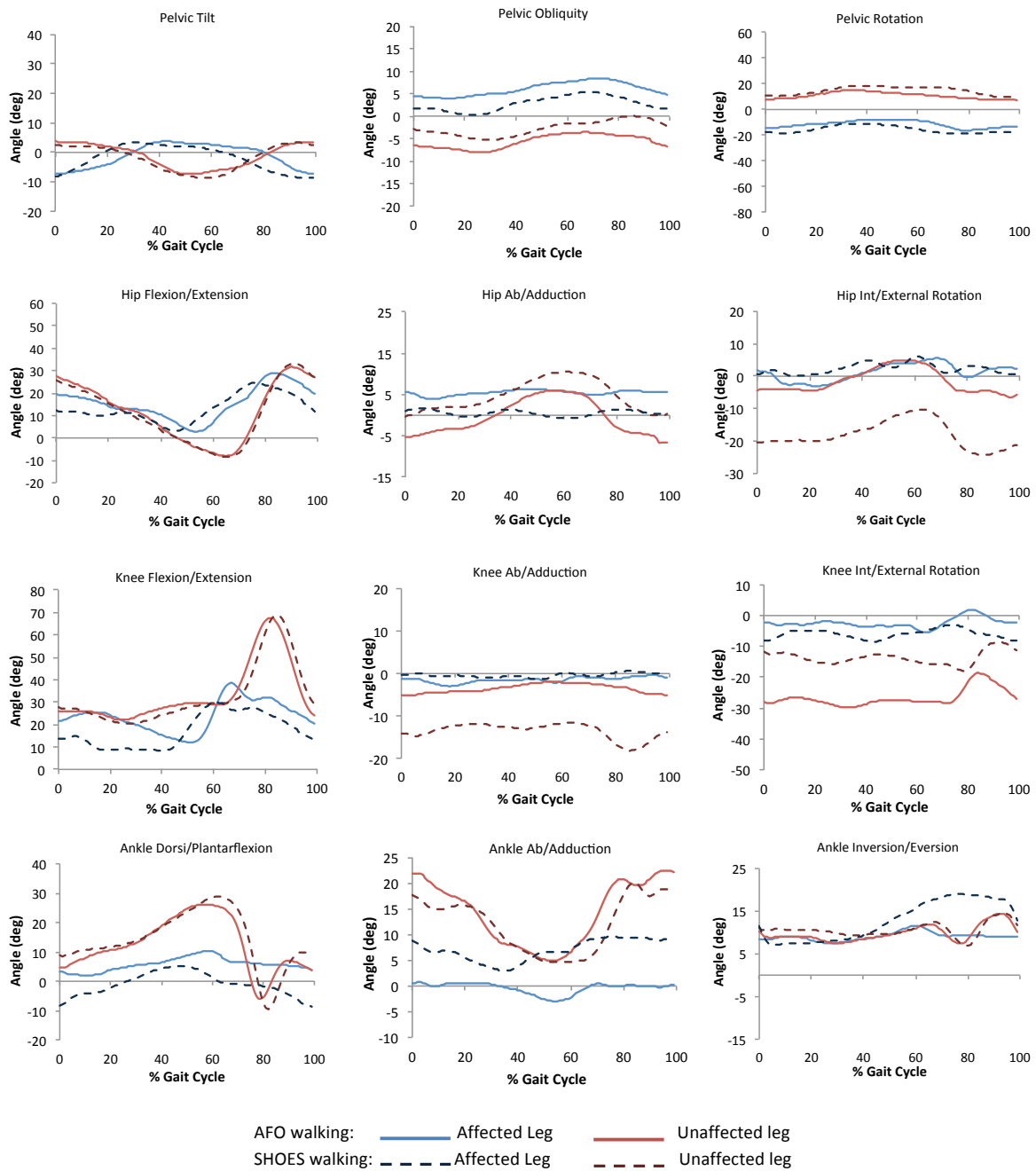


Figure 6.30: Pelvis and lower limb kinematics at follow-up assessment for case study 1.

The improvements observed at outcome from baseline, discussed previously, could be also noticed when comparing baseline and follow-up results.

Good consistency was observed between outcome and follow up kinematics as if a steady state in the rehabilitation process has been reached after the remarkable achievements obtained at 3 months of intervention since baseline assessment. Less noticeable were in fact the changing/improvements between outcome and follow up kinematics. Interestingly what was observed is that the differences in outcome and follow-up when present occurred above the ankle level. Ankle angles either with or without AFO for both legs between the two last assessments showed really close patterns with only a difference in ab/adduction for the affected leg. For the latter, in AFO condition, ankle ab/adduction seemed offset of averagely 5° between the two test sessions. Otherwise, similar ankle angles values were obtained throughout the gait cycle for both legs with and without AFO. In Table 6.6, extracted values from the hemiplegic ankle kinematics are shown to highlight the analogy between outcome and follow up sessions.

| Ankle angle (°): | AFFECTED LEG | | | | UNAFFECTED LEG | | | |
|----------------------------------|--------------|--------|-------------|--------|----------------|--------|-------------|--------|
| | Outcome | | Follow-up | | Outcome | | Follow-up | |
| With AFO | Angle | %Cycle | Angle | %Cycle | Angle | %Cycle | Angle | %Cycle |
| Flexion angle at initial contact | 1.9(±1.0) | 0% | 3.5(±1.6) | 0% | 2.2(±2.7) | 0% | 4.7 (±2.8) | 0% |
| Dorsiflexion peak in stance | 9.6(±0.5) | 53% | 10.3(±0.9) | (58%) | 27.1(±0.7) | (55%) | 26.3(±1.3) | 57% |
| Plantarflexion peak in pre-swing | 5.4(±1.2) | 66% | 6.3(0.9±) | 75% | -10.9 (±2.0) | 76% | -6.2(±2.6) | 79% |
| Rotation at initial contact | 7.2(±0.6) | 0% | 8.2(±0.7) | 0% | 9.5(±2.0) | 0% | 10.4(±1.1) | 0% |
| Peak swing inversion | 7.6(±0.4) | 86% | 9.8 (±1.0) | 67% | 15.2(±1.6) | 92% | 14.4 (±0.6) | 93% |
| Without AFO | | | | | | | | |
| Flexion angle at initial contact | -9.5 (±1.8) | 0% | -8.1 (±0.7) | 0% | 13.2(±3.0) | 0% | 8.8(±2.7) | 0% |
| Dorsiflexion peak in stance | 4.8(±0.8) | 47% | 5.1(±1.5) | 46% | 27.8 (±1.7) | 62% | 28.9(±0.5) | 62% |
| Plantarflexion peak in pre-swing | -0.7(±0.7) | 65% | -0.7(±1.3) | 66% | -3.8(±2.9) | 84% | -9.6(±3.6) | 82% |
| Rotation at initial contact | 11.7(±4.6) | 0% | 11.4(±2.0) | 0% | 10.0(±0.9) | 0% | 11.0(±1.4) | 0% |
| Peak swing inversion | 20.5(±1.9) | 81% | 18.9(±0.9) | 76% | 10.9(±0.4) | 97% | 14.5(±1.2) | 94% |

Table 6.6: Ankle angle in degree and their occurrence as percentage of the gait cycle for outcome and follow up measurements with and without AFO of case study 1.

Worthy of mention it is the ability showed by the subject to extend the hip in mid to late stance differently from outcome evaluation. The unaffected leg went into hip extension down to $8.1^\circ (\pm 2.0)$ and $8.4^\circ (\pm 2.5)$ both at 65% of the gait cycle with AFO and without AFO. Also the affected leg was able to extend in both conditions reaching a minimum of flexion of $2.8^\circ (\pm 2.2)$ at 54% of the gait cycle and $3.2^\circ (\pm 2.4)$ at 46% of the gait cycle respectively with and without orthosis (Figure 6.30). This allowed for a smoother body progression.

Another key factor in walking is knee flexion during swing, this was still inadequate and hence the persistent hip hiking movement to clear the ground and anterior tilting of the pelvis although diminished from previous assessments. The peak knee flexion was of $38.5^\circ (\pm 2.5)$ at 67% of the gait cycle with AFO and $29.9^\circ (\pm 3.0)$ at 61% of the gait cycle without AFO.

Variability of kinematics outcome measurements for follow-up assessment is reported in Table 6.7.

| Joint Angles | Affected Leg | | Unaffected Leg | |
|---|--------------|-------------|----------------|------------|
| | AFO | SHOES | AFO | SHOES |
| <u>Pelvis ($^\circ$, % range of motion):</u> | | | | |
| Obliquity | 0.8(18.7%) | 0.8(15.2%) | 0.9(21.0%) | 0.5(15.2%) |
| Rotation | 2.3(26.0%) | 2.8(34.0%) | 1.3(15.9%) | 3.4(38.9%) |
| Tilt | 1.3(11.9%) | 1.3(10.9%) | 1.1(9.9%) | 1.1(9.6%) |
| <u>Hip ($^\circ$, %range of motion):</u> | | | | |
| Ab/Adduction | 1.1(46.1%) | 1.9(14.7%) | 1.6(65.0%) | 1.8(16.7%) |
| Int/External Rotation | 2.1(24.5%) | 1.6(27.3%) | 2.0(18.1%) | 2.2(15.7%) |
| Flexion/Extension | 2.2(8.3%) | 2.0(9.3%) | 2.5(6.3%) | 2.0(4.8%) |
| <u>Knee ($^\circ$, %range of motion):</u> | | | | |
| Ab/Adduction | 1.0(38.2%) | 0.6(30.8%) | 1.0(30.6%) | 0.9(13.8%) |
| Int/External Rotation | 3.8(50.7%) | 1.9(33.9%) | 2.0(17.7%) | 1.7(18.4%) |
| Flexion/Extension | 2.8(10.5%) | 2.4(6.5%) | 2.9(6.5%) | 2.0(4.2%) |
| <u>Ankle ($^\circ$, %range of motion):</u> | | | | |
| Ab/Adduction | 0.9(25.2%) | 1.4(221.7%) | 3.0(16.8%) | 2.3(14.4%) |
| Inversion/Eversion | 1.1(26.9%) | 1.2(9.9%) | 1.2(17.1%) | 1.0(13.3%) |
| Flexion/Extension | 1.1(13.3%) | 1.3(9.3%) | 2.5(7.7%) | 2.0(5.1%) |

Table 6.7: Mean ($^\circ$) and absolute mean (% of range of motion) of standard deviation values for each joint angle for both affected and unaffected leg during walking with and without AFO at follow-up assessment of case study 1.

Low variability was observed among kinematics variables in both conditions for both legs that did not exceed 4° .

6.3.1.3 AFO and ankle joint moment

Two steps for each of the four walking trials performed by the subject wearing the strain gauged AFO (Figure 6.31) were analysed. Only for one of the two steps force plate data were available. The test was conducted during the follow-up assessment.

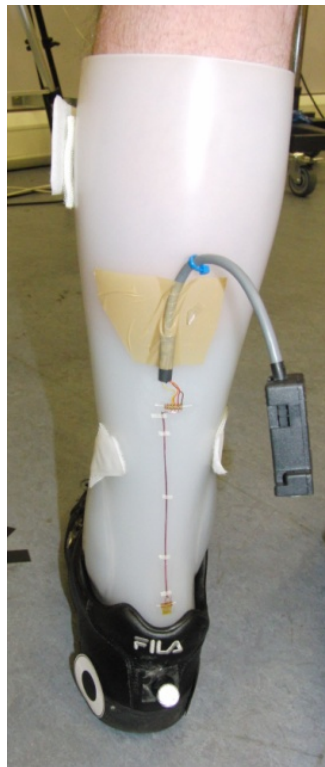


Figure 6.31: Strain gauged AFO fitted on the subject's hemiplegic leg from a posterior view.

A moment conversion factor of 57.8 Nm/V was found for plantarflexion and of 43.5 Nm/V for dorsiflexion from the static AFO calibration.

AFO moments were then calculated using the procedure discussed in Chapter 4 (section 4.5). The resultant AFO moments in the tibia reference frame for the 8 steps analysed are shown in Figure 6.32.

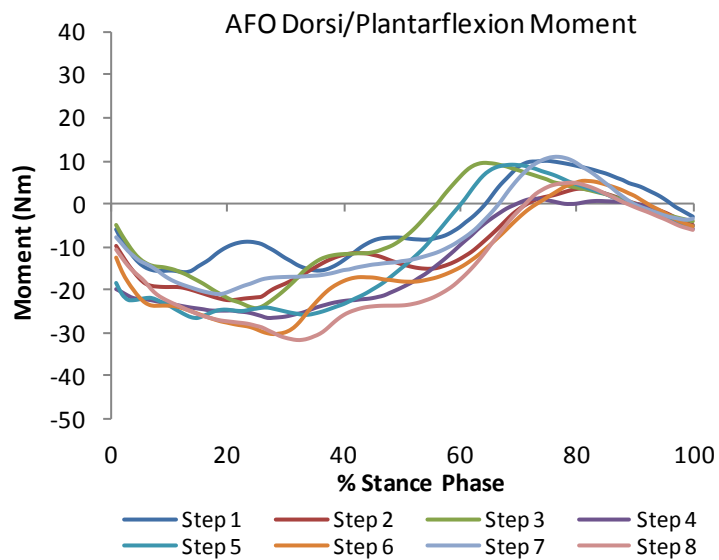


Figure 6.32: Dorsi/plantarflexion moments measured in the AFO as percentage of stance phase for all steps analysed (1 to 8). Plantarflexor moment is positive on the vertical axis.

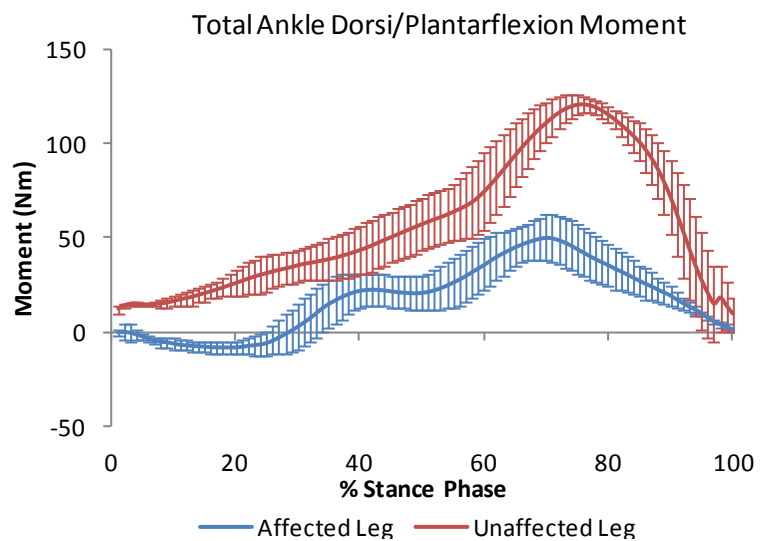


Figure 6.33: Mean (\pm standard deviation) over 4 steps of the total ankle dorsi/plantarflexion moment for affected (blue solid line) and unaffected (red solid line).

AFO contribution was higher in dorsiflexion than in plantarflexion (Figure 6.32). A dorsiflexor peak of on average 24.6 Nm (± 4.9) was recorded in the first half of stance phase. The maximum dorsiflexor moment occurred between the 13 to the 32% of the gait cycle in the 8 steps considered. A peak in plantarflexor moment of 6.6 Nm (± 3.3) was observed in late stance. It occurred after the 64% of stance but before 83% of stance phase.

A stress of 4.7 MPa (± 1.0) and of 1.0 MPa (± 0.5) in the AFO at the level of the gauges corresponded to these two peaks for dorsiflexion and plantarflexion respectively.

The total ankle moments for affected and unaffected leg are compared in Figure 6.33. These data were obtained from the analysis of four steps for each leg for which force platform data were available.

The unaffected leg lacked the dorsiflexor moment at early stance but a high peak in the plantarflexion direction was observed reaching a value of 121.1 Nm (± 4.2). On the other hand the affected leg had a dorsiflexor moment (minimum value 8.2 (± 3.0)) at the beginning of the gait cycle but the peak in plantarflexion did not overcome 50 Nm.

Knowing the total ankle moment of the affected leg and the AFO moment, the contribution from the active and passive tissue of the lower leg to the total moment was calculated using Equation 4.2. This moment is here referred as the anatomy moment. The two components of the net ankle moment, AFO and anatomy are shown in Figure 6.34.

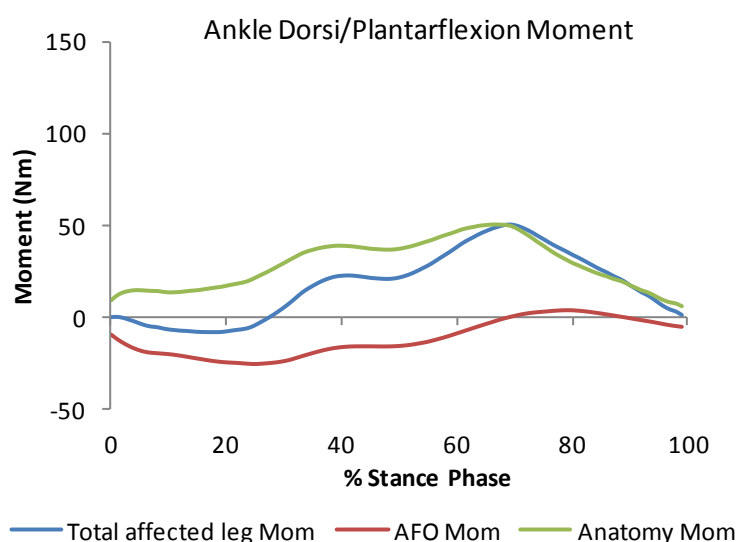


Figure 6.34: Total mean ankle moment of the affected leg (blue solid line) and contributions to the moment by the AFO (red solid line) and anatomy (green solid line).

The affected leg without AFO would have lacked dorsiflexor moment at initial stance as it was derived from the AFO. The major part of the total moment during late stance was instead provided by the subject's muscles and passive tissues (Figure 6.34).

6.3.2 Case Study 2

Case study 2 refers to a 76 years old male (body weight 73kg, height 1.7m) affected by stroke on the 18th of February 2011. The left side of the body was affected by the stroke. The subject, after given consent, was randomised into the intervention group and hence he was provided with a 5mm rigid polypropylene AFO with carbon fibre reinforcement at the ankle level. Calf and ankle strap were attached to the AFO at the time of fitting that occurred three months after stroke onset. AFO and shoes combinations were tuned to 8° of inclination using one heel wedge.

For this participant only baseline data were collected 3 months post stroke. He withdrew from the trial before outcome assessment.

The subject was assigned a Modified Rivermead Mobility Index of 30 and a functional ambulation classification of 3.

Results from the baseline assessment are reported in the following sections. The subject performed the test walking with a zimmer frame.

6.3.2.1 Spatio-temporal parameters and tibia inclination

The subject walked two times back and forth on the grid mat with and without AFO while data were recorded from the sagittal video camera simultaneously with 3-D motion analysis data. Three gait cycles of affected and unaffected leg were analysed for each condition tested and results were extracted from them.

No differences in walking speed were found when the subject walked with and without AFO. An average walking speed of 0.08 m/s (± 0.01) was observed for both conditions.

Temporal parameters extracted from this analysis are presented in Table 6.8.

The gait cycle of the affected leg had a longer duration when the subject walked with AFO (4.2s) rather than without it (3.1s). The difference however was found to be non significant (Paired *T*-test: *p*-value= 0.09). Analogously the step time was longer with the AFO for the affected leg. A 40.2 % difference was found between the two conditions to which corresponded a *p*-value of 0.06 (Paired *T*-test).

The contrary occurred for the unaffected leg, which presented with longer stride and step duration without the AFO. In percentage terms, the difference between the two conditions was of 27.9 and 4.3% respectively for stride and step, both not statistically significant (Paired *T*-test: *p*-value>0.05).

Step time duration was significantly longer (Paired *T*-test: *p*-value<0.05) for the unaffected leg in both conditions in comparison to the affected leg and hence an asymmetric gait pattern (symmetry ratio <0). Gait symmetry improved by the use of the AFO. The AFO reduced the symmetry ratio to -0.3 from -0.5 without the AFO. This was a significant improvement (Paired *T*-test: *p*-value=0.03).

This participant presented an abnormal duration of stance and swing phase for both conditions and both legs. Stance phase was generally prolonged while swing phase shortened. For the affected leg an increase of 6.9% was observed in the duration of stance phase when the subject walked with the AFO and a similar reduction in swing phase was noticed. These differences, however, were not significant (Paired *T*-test: *p*-value=0.1).

| Temporal Parameters | Baseline Measurement | |
|---|----------------------|--------------|
| | AFO | SHOES |
| <i>Gait Cycle Duration (s):</i> | | |
| Affected Leg | 4.2 (±0.6) | 3.1 (±0.1) |
| Unaffected leg | 3.1 (±0.1) | 4.3 (±1.8) |
| <i>Stance Phase (s):</i> | | |
| Affected Leg | 3.6 (±0.7) | 2.5 (±0.05) |
| Unaffected leg | 2.8 (±0.1) | 4.1 (±1.8) |
| <i>Stance Phase(% of cycle):</i> | | |
| Affected Leg | 85.7 (±3.4) | 80.2 (±1.2) |
| Unaffected leg | 90.7 (±2.2) | 94.0 (±1.7) |
| <i>Swing Phase (s):</i> | | |
| Affected Leg | 0.6 (±0.05) | 0.6 (±0.06) |
| Unaffected leg | 0.3 (±0.1) | 0.2 (±0.02) |
| <i>Swing Phase (% of cycle):</i> | | |
| Affected Leg | 14.3 (±3.4) | 19.7 (±1.2) |
| Unaffected leg | 9.3 (±2.2) | 5.9 (±1.7) |
| <i>Initial Double Support (% of cycle):</i> | | |
| Affected Leg | 27.8 (±6.2) | 18.4 (±1.0) |
| Unaffected leg | 51.5 (±0.8) | 62.1 (±15.7) |
| <i>Terminal Double Support(% of cycle):</i> | | |
| Affected Leg | 54.5 (±5.9) | 52.8 (±2.2) |
| Unaffected leg | 21.8 (±1.2) | 15.1 (±6.4) |
| <i>Single Support (% of cycle):</i> | | |
| Affected Leg | 7.3 (±2.9) | 7.5 (±2.0) |
| Unaffected leg | 15.9 (±2.8) | 18.2 (±5.3) |
| <i>Step Time (s):</i> | | |
| Affected Leg | 1.2 (±0.3) | 0.8 (±0.1) |
| Unaffected leg | 2.4 (±0.5) | 2.9 (±1.4) |
| <i>Temporal Symmetry:</i> | -0.3 (±0.1) | -0.5 (±0.1) |

Table 6.8: Comparison of temporal parameters assessed with and without AFO for affected and unaffected leg during baseline assessment for patient 2.

The unaffected leg showed a longer stance phase by 3.5% when the subject walked without AFO and also longer than the affected leg in both conditions. This led to a shortening of sound leg swing phase to 5.9% without AFO and 9.3% of the gait cycle with the AFO. The differences between the two conditions in stance and swing phase duration for the sound leg were statistically significant (Paired T-test: p -value < 0.05). The sound leg, thus, compensated for the inability of the hemiplegic leg to bear weight throughout the gait cycle by reducing the swing time. The impaired weight bearing function of the hemiplegic side can be further noticed from the small single support time of the affected leg that did not overcome 8% of the gait cycle, and by the prolonged double support intervals. This was also reflected on the contralateral side. The AFO did not affect significantly the duration of the single support for the

hemiplegic and sound legs (Paired T -test: p -value >0.05) nor the duration of the double support intervals.

Interestingly it was found that the affected leg always presented a shorter initial double support and a longer terminal double support than the unaffected leg. There was on average a duration difference, in terms of % of the gait cycle, above 30% in both initial and terminal double support between affected and unaffected leg. This could be related to the difficulty of the hemiplegic side in initiating the swing phase and to the fact that the subject pushed first the zimmer frame forward before swinging the affected leg and therefore prolonging this phase of the gait cycle. Spatial parameters of the affected and unaffected leg during walking with and without AFO are presented in Table 6.9.

| Spatial Parameters | Baseline Measurement | |
|--------------------------------------|----------------------|---------------------|
| | AFO | SHOES |
| <i>Step Length (m):</i> | | |
| Affected Leg | 0.10 (± 0.03) | 0.12 (± 0.03) |
| Unaffected leg | 0.12 (± 0.02) | 0.17 (± 0.02) |
| <i>Step Length (%Stride length):</i> | | |
| Affected Leg | 48.7 (± 5.1) | 42.8 (± 8.3) |
| Unaffected leg | 51.3 (± 5.1) | 57.2 (± 8.3) |
| <i>Spatial Symmetry:</i> | -0.03(± 0.1) | -0.1 (± 0.2) |

Table 6.9: Comparison of spatial parameters assessed with and without AFO for affected and unaffected leg during baseline assessment for case study 2.

The subject showed an asymmetric spatial gait with the unaffected leg capable of longer steps (symmetry ratio <0). The AFO improved, although not significantly (Paired T -test: p -value=0.1), the symmetry of the gait reducing the ratio nearly to 0. Step length of the affected side increased with the AFO by a 13.7% of the step length without AFO (Paired T -test: p -value=0.1). Contrarily step length of unaffected leg was reduced (26%) when the subject walked with the AFO (Paired T -test: p -value=0.1).

In general, however the gait of this participant was slow (0.08 m/s) and characterised by short steps, less than 0.2 m in each leg and condition. This could be related to the fact that he walked with the zimmer frame that constrained the forward movement while providing support and, added the task of pushing the frame forward during the gait cycle time.

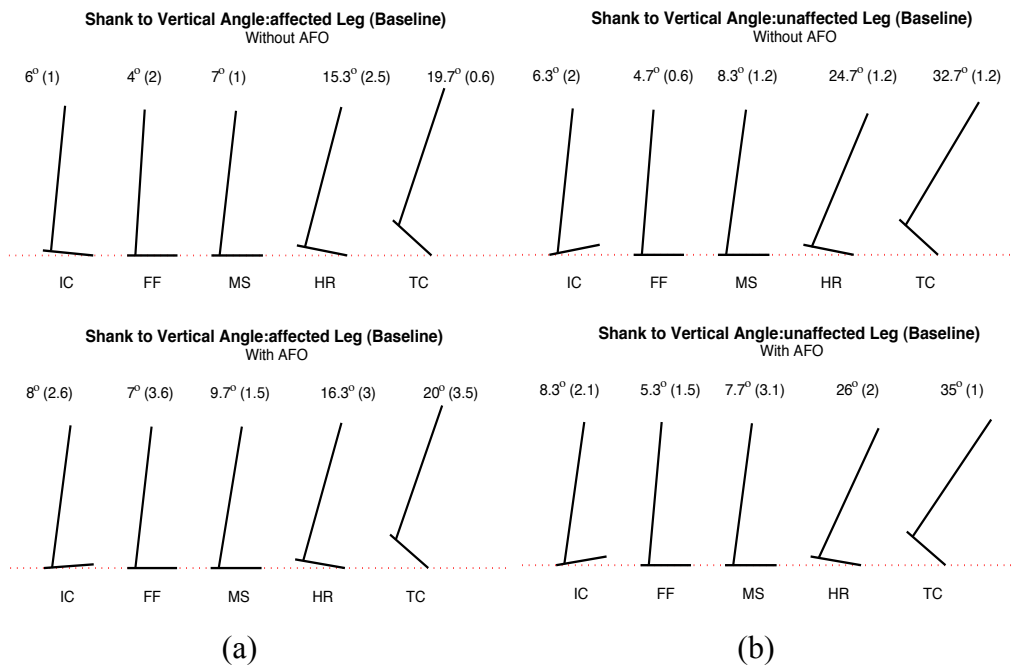


Figure 6.35: Case study 2 baseline shank to vertical angle for affected (a) and unaffected (b) leg at initial contact (IC), foot flat (FF), mid stance (MS), heel rise (HR) and terminal contact (TC) without (top) and with AFO (bottom). Angles in degree are reported with values of standard deviation in brackets.

The shank to vertical angle at initial contact (IC), foot flat (FF), mid stance (MS), heel rise (HR) and terminal contact (TC) was measured for both legs in the two conditions tested. The mean values over three gait cycles are shown in Figure 6.35 (a) for the affected leg and Figure 6.35 (b) for unaffected leg.

The tibia was inclined at initial contact for each condition and leg although initial contact occurred slightly through the heel for the unaffected side and affected side with AFO. The tibia remained inclined for the rest of stance phase. No differences were found between conditions within leg comparisons (Paired T -test: p -value >0.05). Significant differences were instead found when comparing the two legs with and without AFO at heel rise and terminal contact. The p -value was smaller than 0.03 in each comparison (Paired T -test).

6.3.2.2 Kinematic Outcomes

Pelvis and lower limb joint kinematics in the three anatomical planes for this participant are shown in Figure 6.36. The subject walked aided by a zimmer frame. The average over 5 gait cycles for both legs in both conditions tested are plotted against the % of the gait cycle. The mean trends of affected leg kinematics are represented as blue shade lines whereas unaffected leg kinematics by red shade lines. Solid traces correspond to AFO trials and dotted traces to shoes trials. The gait kinematic pattern of this participant was influenced, other than by the stroke, by the use of the zimmer frame that dictated also short steps and time requiring gait cycles.

Baseline Kinematics

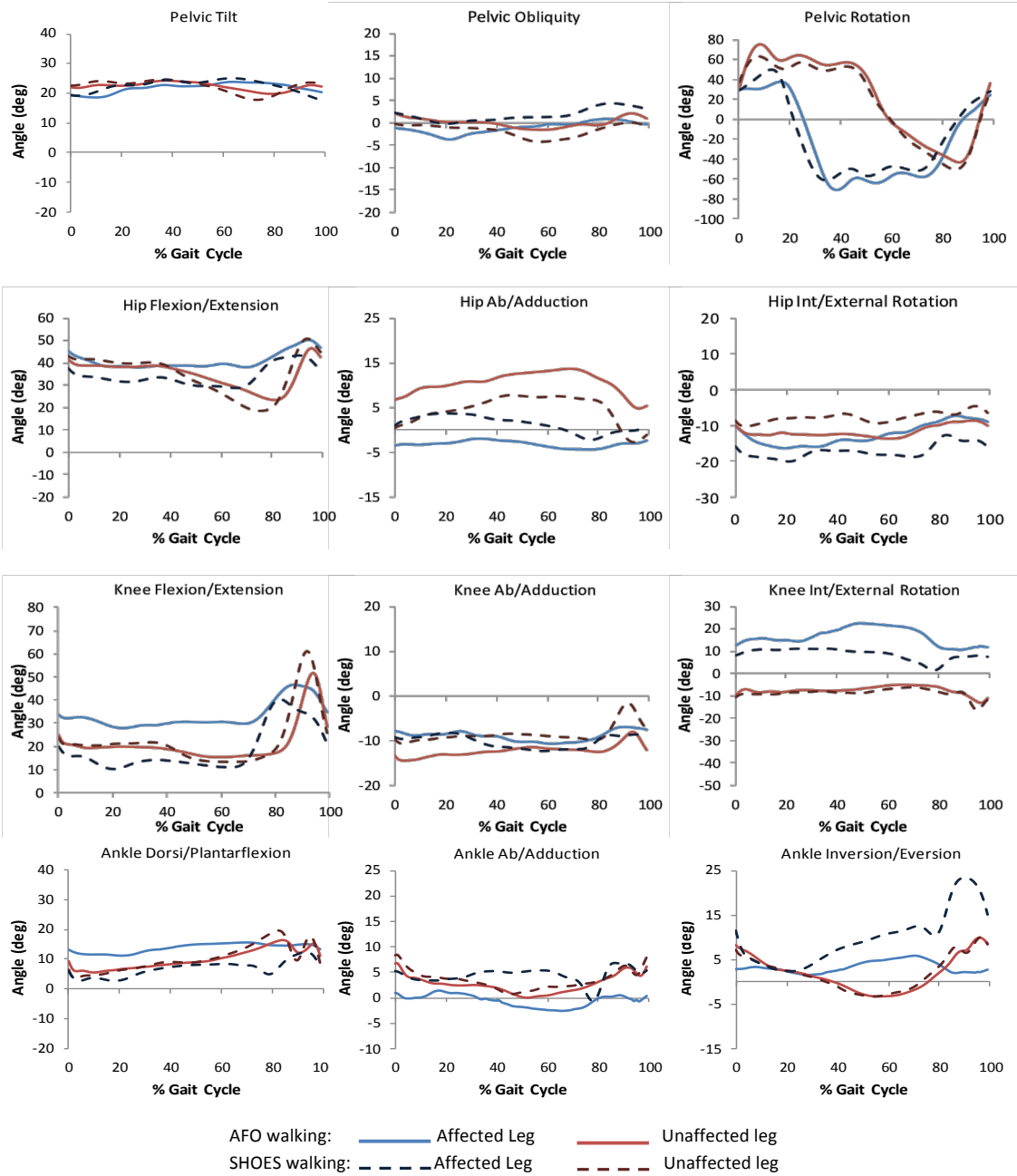


Figure 6.36: Pelvis and lower limb kinematics at baseline assessment for case study 2.

By supporting himself mostly through the zimmer frame the subject tended to lean his body forward instead of acquiring an upright posture. Almost constant values of anterior tilt as indicated by the small range of motion ($ROM < 7^\circ$), were found for each leg and condition. The anterior tilt graph showed curves fluctuating around 20° through the gait cycle.

The gait cycle for the affected leg, without AFO, was initiated by hitting the ground with the lateral border of the foot (Figure 6.37). The ankle was internally rotated to $11.5^\circ (\pm 1.9)$, adducted to $8.3^\circ (\pm 1.0)$ but, dorsiflexed at $6.0^\circ (\pm 1.6)$.



Figure 6.37: Initial Contact through lateral side of the foot without AFO of the affected leg for case study 2. Sagittal and posterior view.

The ankle then went into plantarflexion to a minimum of dorsiflexion of $2.9^\circ (\pm 1.5)$ within the first 20% gait cycle interval. A dorsiflexion position was afterwards observed until reaching a maximum of $8.5^\circ (\pm 0.6)$ at 62% of the gait cycle. The ankle dropped into plantarflexion during late stance before dorsiflexing again in swing phase. The subject was able to lift the foot up to $12.4^\circ (\pm 0.7)$ at 92% of the gait but ground clearance was impaired by the presence of an inverted and adducted foot (max inversion $23.4^\circ (\pm 1.2)$; max adduction $6.8^\circ (\pm 2.9)$).

The affected knee was flexed at initial contact to $20.1^\circ (\pm 2.1)$. As the foot was on the ground, while the ankle was plantarflexing, the knee went into extension down to a minimum flexion of $10.3^\circ (\pm 3.9)$ at 20% of the gait cycle. The knee was then locked

into extension of on average a value of $12.7^\circ (\pm 1.1)$ until the 65% of the gait cycle after which it rapidly started to flex in preparation for swing phase. A $40.5^\circ (\pm 1.4)$ flexion peak was achieved at initial swing (82%). It followed a gradual extension going back to $21.3^\circ (\pm 3.1)$ of flexion for the subsequent initial contact. The extension phase of the knee corresponded with increased knee abduction phase of on average 12° . During swing the knee went into adduction.

Internal rotation of the knee was mostly observed through the gait cycle although a tendency to externally rotate was observed in late stance (60 -80% of gait cycle). The hip commenced the gait cycle at $37.7^\circ (\pm 2.4)$ of flexion. Analogously to the knee and ankle, in the first 20% of the gait cycle, the hip slightly extended. This position was maintained until the hip started to flex again to initiate the swing phase.

A proper hip extension was not achieved in mid to late stance but rather a steady hip position was assumed by the subject. This was due to the locked knee and retracted hip (external rotation of the pelvis) that made thigh inclination difficult and hence gave poor extension. The hip moved into flexion capable of achieving a peak of $49.8^\circ (\pm 1.4)$ in swing.

With regard to the coronal and transverse plane rotations, the hip was adducted and externally rotated during stance but switched into abduction and internal rotation during swing.

For all the joints and in particular for sagittal plane rotations stationary positions were observed (flat curves) due to the affected leg retarding swing phase initiation assuming a fixed position while the contralateral leg completed its swing phase. A double support phase occurred during which the zimmer frame was pushed forward and the hemiplegic leg started to lift the foot from the ground and go into swing.

The unaffected leg had to adjust to the affected leg and hence a short swing phase and to the zimmer frame which limited its movement. This can be seen by a premature stance phase starting with a knee still in flexion ($23.7^\circ \pm 3.2$) from the previous swing. The presence of the zimmer frame did not allow room for the unaffected leg to swing forward. The reduced capability to bear the weight through the hemiplegic leg forced the sound leg to terminate the swing phase early.

A part from prolonged stance phase duration, the unaffected ankle showed similar to normal joint rotations in the three planes. The knee instead, lacked flexion shock

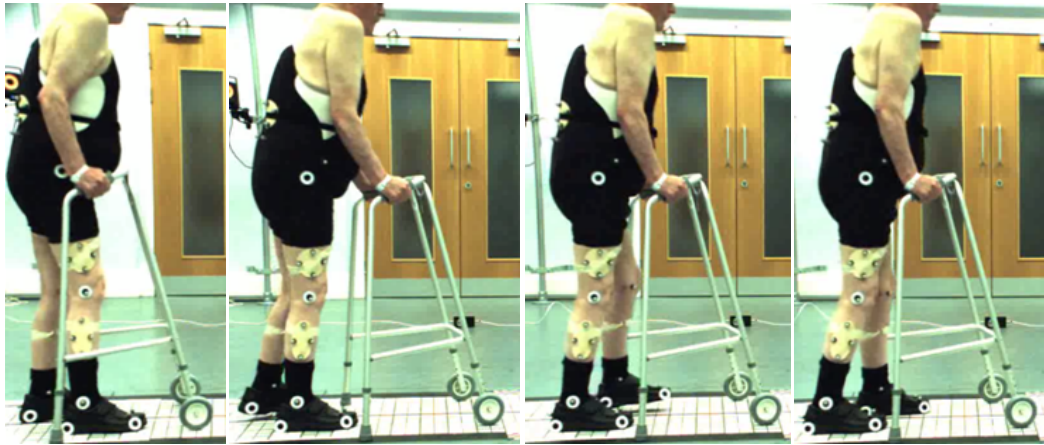


Figure 6.38: Initial to late stance phase of the unaffected leg during walking without AFO.

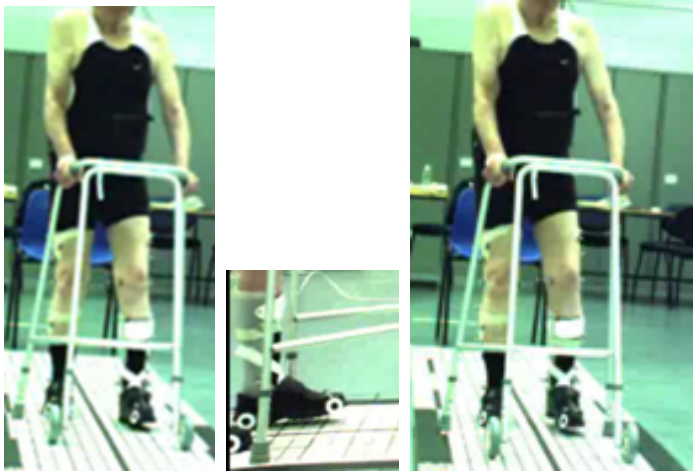


Figure 6.39: Case Study 2 initial contact frontal and lateral view and mid swing frontal view.

absorption peak and was extended until about the 40% of the cycle at on average $21.1^\circ (\pm 0.6)$. A further extension down to a minimum of flexion of $13.4^\circ (\pm 1.3)$ was observed while the hemiplegic leg raised the heel (61% of gait cycle). There followed a gradual flexion between the 67% and 82% of the gait cycle before, rapidly achieving a peak of $60.7^\circ (\pm 2.3)$ (92% of gait cycle) that allowed a safe ground clearance.

Meanwhile, the hip on the sound side kept a steady flexed position for the first 40% gait cycle interval at about $41.2^\circ (\pm 1.0)$, and then starting to extend while the hemiplegic leg swung forward. The hip could only extend to a minimum flexion of $20.6^\circ (\pm 2.2)$ at 78% of gait cycle. The thigh inclined (as the knee extended), although to a small extent, and hence limited extension of the hip. However, the forward movement of the thigh was limited by the hemiplegic leg short step length that, kept the sound leg from using the full hip extension range of motion.

These sequences of events in the hip and knee joints of the unaffected side are illustrated in the Figure 6.38.

The sound hip flexed for a safe ground clearance initiation to a peak of $49.8^\circ (\pm 1.4)$ and then, together with the knee, extend again to be prepared for the following initial contact.

During stance the sound knee was internally rotated with a tendency to externally rotate in late stance (downward peak in the curve) while being constantly abducted (mean $9.2^\circ \pm 0.5$). The sound hip was externally rotated moving toward internal rotation in swing. Adduction of the hip was also observed increasing to a maximum of $7.7^\circ (\pm 2.5)$ before starting to abduct in swing.

When the subject walked with the AFO restriction of the movements at the ankle of the hemiplegic leg was observed whereas no differences could be noticed for the unaffected leg in ankle kinematics. Differences in ankle kinematics for the affected leg between with and without AFO walking were, instead, significant ($p\text{-value} < 0.05$).

In particular the AFO allowed for initial contact to occur through the heel (Figure 6.39) and kept the ankle in a steady dorsiflexed position at on average $13.9^\circ (\pm 1.5)$ of dorsiflexion; range of motion was only of 4.5° . Reduced adduction as well as

inversion was observed. The inverted foot was avoided in swing phase (Figure 6.39right).

Interesting was the increased flexion position of the knee ($33.8^\circ \pm 1.7$) at the starting of the affected leg gait cycle (Paired *T*-test: *p*-value=0.03). The knee showed some extension with a minimum flexion of $27.9^\circ (\pm 4.1)$ at 24% of the gait cycle and then remaining in that position throughout the duration of stance phase. This was explained as an effect of the AFO that pushed the tibia forward in addition to, the long lasting stance phase and, hence, the hemiplegic knee was held into a prolonged flexed position while the contralateral leg terminated the swing phase and started a new gait cycle.

This affected also the hip kinematics that showed a locked flexed position in stance phase until about 74% of the gait cycle and on average $39.1^\circ (\pm 1.5)$. The hip flexion value was higher than that observed without AFO (Paired *T*-test: *p*-value<0.05). The forward position of the knee rendered difficult hip extension as well as thigh inclination. The thigh was more reclined with the AFO than without (Figure 6.40).

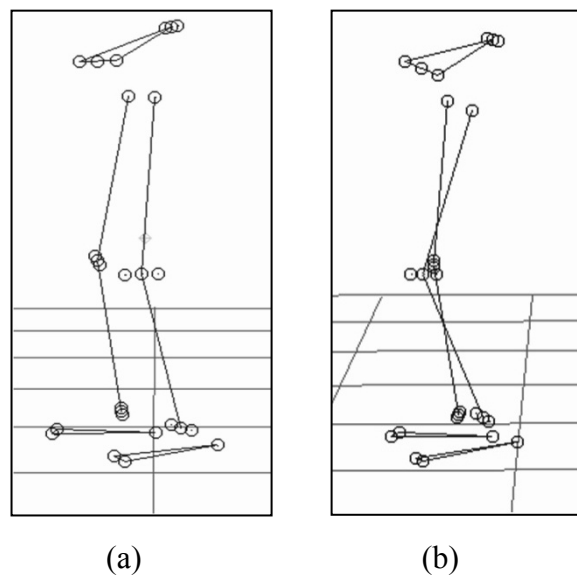


Figure 6.40: Caste study 2 heel rise: without AFO (a) and with AFO (b) at baseline assessment. Thighs are reclined.

No major effects were noticed in the sagittal angles of hip and knee of the unaffected leg with the AFO.

With regards to the coronal plane rotation of the affected leg, the AFO put the knee and the hip into abduction. Internal rotation of the knee increased in stance while the hip was more externally rotated.

For the unaffected leg, in the coronal plane knee adduction and hip abduction increased by 5°; the relative curves with and without AFO were offset from each other.

Pelvic tilt and rotation for both legs were generally unaffected by the orthosis, while the tendency to raise the affected hip was reduced as seen without the AFO.

The zimmer frame provided the patient with the same posture in the gait cycles. Moreover, the zimmer frame regulated the forward progression of the subject and hence the similarities (pattern of the curves) in the kinematics of both conditions within legs and the repeatability of the results. Indications of the repeatability of joint kinematics are shown through the Table 6.10 where mean (°) and absolute mean (% of range of motion) standard deviation values are reported for each leg and condition.

| Joint Angles | Affected Leg | | Unaffected Leg | |
|--------------------------------------|--------------|-------------|----------------|-------------|
| | AFO | SHOES | AFO | SHOES |
| <u>Pelvis (°, %range of motion):</u> | | | | |
| Obliquity | 1.6 (33.5%) | 0.9 (21.2%) | 0.8 (21.6%) | 1.0 (25.5%) |
| Rotation | 12.5 (11.4%) | 10.2 (9.4%) | 8.4 (7.0%) | 10.1 (8.9%) |
| Tilt | 1.4 (25.4%) | 1.9 (25.8%) | 1.3 (29.3%) | 2.2 (30.7%) |
| <u>Hip (°, %range of motion):</u> | | | | |
| Ab/Adduction | 0.7 (27.7%) | 1.6 (27.3%) | 3.8 (%) | 1.8 (17.1%) |
| Int/External Rotation | 1.8 (20.5%) | 1.9 (25.6%) | 1.5 (30.4%) | 2.2 (37.4%) |
| Flexion/Extension | 2.5 (20.0%) | 3.0 (20.9%) | 3.8 (16.8%) | 2.1 (7.3%) |
| <u>Knee (°, %range of motion):</u> | | | | |
| Ab/Adduction | 1.4 (38.9%) | 0.8 (19.8%) | 0.9 (15.1%) | 1.0 (11.4%) |
| Int/External Rotation | 3.0 (26.8%) | 1.9 (19.7%) | 1.6 (20.0%) | 1.0 (10.2%) |
| Flexion/Extension | 2.5 (13.3%) | 3.2 (10.5%) | 2.7 (7.4%) | 1.9 (4.1%) |
| <u>Ankle (°, %range of motion):</u> | | | | |
| Ab/Adduction | 0.8 (20.0%) | 1.3 (17.9%) | 1.4 (20.0%) | 1.0 (13.5%) |
| Inversion/Eversion | 0.7 (17.7%) | 1.0 (5.0%) | 1.1 (8.5%) | 0.9 (6.6%) |
| Flexion/Extension | 0.7 (15.4%) | 1.3 (13.8%) | 1.7 (16.0%) | 0.9 (5.6%) |

Table 6.10: Mean (°) and absolute mean (% of range of motion) of standard deviation values for each joint angle for both affected and unaffected leg during walking with and without AFO at baseline assessment of case study 2.

Good variability was observed across the 5 gait cycles analysed for affected and unaffected leg with and without the AFO. A maximum absolute mean standard deviation value of 37.4% was found in hip internal/external rotation of the unaffected leg while the subject walked without the AFO; for all other cases absolute standard deviation was below that value but higher than 4% of the relative range of motion. Maximum mean standard deviation when expressed in degrees was as high as 12.5°. This value was observed in pelvis rotation of the affected leg with the AFO but, similar high values, above 8°, were found for the other cases analysed. However, they do not represent more than 12% of the pelvis rotation range of motion observed for this subject. The high values of such rotations derived from the definition of the joint coordinate system used for the pelvis angles calculation and in particular from the direction of progression axis.

The latter was defined as the average direction of the mid point between the two anterior iliac spines. Different numbers of frames were used to determine the orientation of the axis from 7 to a maximum of 200 frames. In spite of this, when visualising the progression axis it could be noticed that its direction varied often and abruptly as the subject walked no matter how many frames were considered. It was thus decided to use 150 frames as for the other subjects tested.

If the pelvis rotations are left out, the mean standard deviation in degree was confined to 4°.

6.3.3 Case Study 3

Case study 3 refers to a 51 years old female with a 78 kg body mass and 1.6 m tall. She was affected by stroke on the 21st February 2011 and she was left with right hemiplegia of the upper and lower body. After giving consent, she was allocated into the control group. However, she received a rigid 4mm polypropylene AFO from the NHS without reinforcements at the ankle level. The trim line of the AFO however did cover partially the malleoli. The patient attended the biomechanics laboratory two times for her baseline and outcome assessment. She was then excluded from the study before the follow-up appointment due to a hip replacement surgery which she had a week before the follow-up test was scheduled. Baseline occurred 3 months from stroke onset.

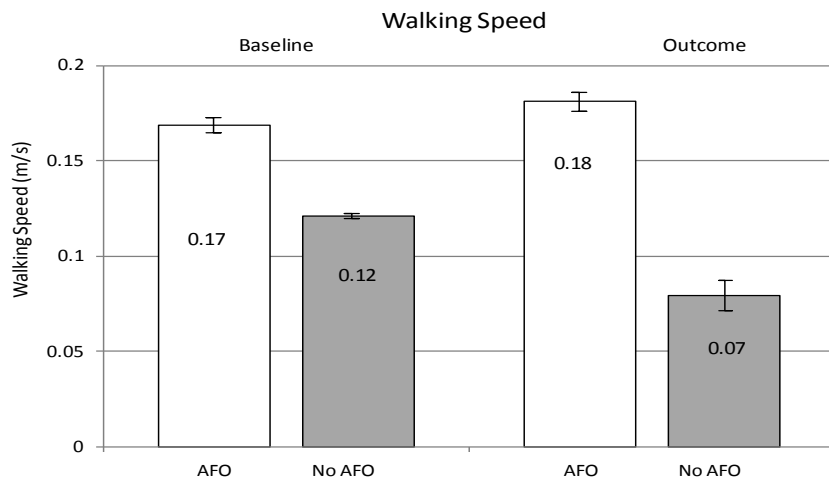


Figure 6.41: Walking speed at baseline and outcome assessment for each condition tested. Bars indicate the standard deviation over two trials.

The Modified Rivermead Mobility Index (mRMI) and the Functional Ambulatory Category (FAC) for this subject at the two assessments three months apart from each other are shown in Table 6.11.

| | Baseline | Outcome |
|-------------|----------|---------|
| mRMI | 35 | 34 |
| FAC | 4 | 4 |

Table 6.11: Modified Rivermead Mobility Index (mRMI) and the Functional Ambulatory Category (FAC) for patient 3 at baseline and outcomes assessments.

6.3.3.1 Spatio-temporal parameters and tibia inclination

Two walking trials back and forth on the grid mat were performed by the subject with and without AFO while data were recorded from the sagittal video camera simultaneously with the 3-D motion analysis data. Three gait cycles of the affected and unaffected leg were analysed for each condition tested. The subject walked with the aid of a stick during both assessments.

The patient showed a slow-paced walk with a velocity no higher than 0.2 m/s. Walking speed profile is shown in Figure 6.41. A significant increase in walking velocity (Paired T -test: p -value<0.05) was found when the subject walked with the AFO. At baseline an increase of 40.2% of the speed without AFO was obtained and as much as 127.7% increase at outcome. With time within conditions the speed did not increase. Similar values were obtained at baseline and outcome assessments (Paired T -test: p -value>0.05) in both conditions.

Temporal parameters extracted from the gait cycles analysed are presented in Table 6.12

The duration of the gait cycle was longer for each leg when the subject walked without the AFO. A reduction of the 21.8% was achieved with the AFO for the affected leg at baseline (Paired T -test: p -value=0.02) but for the unaffected leg the duration was diminished only by the 3.8% (Paired T -test: p -value=0.07). At outcome, a mean significant (Paired T -test: p -value<0.00) reduction of 40.3% (\pm 0.4) between the two conditions for both sides was found.

| Temporal Parameters | Baseline Measurement | | Outcome Measurement | |
|---|----------------------|--------------------|---------------------|--------------------|
| | AFO | SHOES | AFO | SHOES |
| <i>Gait Cycle Duration (s):</i> | | | | |
| Affected Leg | 2.5 (± 0.5) | 3.2 (± 0.1) | 1.9 (± 0.1) | 3.2 (± 0.2) |
| Unaffected leg | 2.5 (± 0.0) | 2.6 (± 0.2) | 2.1 (± 0.1) | 3.5 (± 0.1) |
| <i>Stance Phase (s):</i> | | | | |
| Affected Leg | 1.8 (± 0.4) | 2.6 (± 0.1) | 1.6 (± 0.1) | 2.9 (± 0.2) |
| Unaffected leg | 2.2 (± 0.1) | 2.4 (± 0.2) | 1.9 (± 0.1) | 3.4 (± 0.1) |
| <i>Stance Phase(% of cycle):</i> | | | | |
| Affected Leg | 71.6 (± 5.0) | 81.1 (± 0.4) | 80.2 (± 1.1) | 90.0 (± 1.4) |
| Unaffected leg | 88.4 (± 0.9) | 93.7 (± 0.9) | 88.1 (± 0.8) | 95.5 (± 0.7) |
| <i>Swing Phase (s):</i> | | | | |
| Affected Leg | 0.7 (± 0.1) | 0.6 (± 0.0) | 0.4 (± 0.0) | 0.3 (± 0.0) |
| Unaffected leg | 0.3 (± 0.0) | 0.2 (± 0.1) | 0.3 (± 0.0) | 0.2 (± 0.0) |
| <i>Swing Phase (% of cycle):</i> | | | | |
| Affected Leg | 28.4 (± 5.0) | 18.9 (± 0.4) | 19.8 (± 1.1) | 10.0 (± 1.4) |
| Unaffected leg | 11.6 (± 0.9) | 6.3 (± 0.9) | 11.9 (± 0.8) | 4.5 (± 0.7) |
| <i>Initial Double Support (% of cycle):</i> | | | | |
| Affected Leg | 20.2 (± 4.3) | 20.8 (± 1.0) | 30.8 (± 1.3) | 42.2 (± 3.8) |
| Unaffected leg | 42.5 (± 1.5) | 50.6 (± 2.0) | 35.8 (± 1.9) | 35.4 (± 3.6) |
| <i>Terminal Double Support(% of cycle):</i> | | | | |
| Affected Leg | 41.2 (± 3.6) | 54.5 (± 0.6) | 37.0 (± 2.0) | 42.7 (± 4.5) |
| Unaffected leg | 25.0 (± 0.7) | 22.0 (± 1.9) | 33.9 (± 1.0) | 48.9 (± 2.8) |
| <i>Single Support (% of cycle):</i> | | | | |
| Affected Leg | 10.9 (± 1.2) | 6.0 (± 0.7) | 12.1 (± 0.6) | 4.8 (± 0.6) |
| Unaffected leg | 24.7 (± 5.2) | 20.0 (± 1.5) | 19.0 (± 1.6) | 10.6 (± 1.2) |
| <i>Step Time (s):</i> | | | | |
| Affected Leg | 0.8 (± 0.2) | 0.8 (± 0.1) | 0.9 (± 0.1) | 1.7 (± 0.2) |
| Unaffected leg | 1.6 (± 0.1) | 2.1 (± 0.3) | 1.1 (± 0.0) | 1.7 (± 0.2) |
| <i>Temporal Symmetry:</i> | | | | |
| | -0.3 (± 0.1) | -0.5 (± 0.0) | -0.1 (± 0.0) | 0.0 (± 0.1) |

Table 6.12: Comparison of temporal parameters assessed with and without AFO for affected and unaffected leg during baseline and outcome assessments for case study 3.

While the same time was required by the subject to complete the affected leg gait cycle without the AFO at baseline and outcome, the patient reduced by 24% the duration of the cycle when walking with the AFO between the two assessments. In respect of the cycle timing, the gait cycles of the patient were characterised by long stance phases and short swing phases for both legs. Even longer stance and shorter swing were observed when the subject walked with shoes only. The patient showed a more continuous gait with the AFO as a consequence of a better stability and visibly enhanced weight bearing through the affected leg instead of seeking all

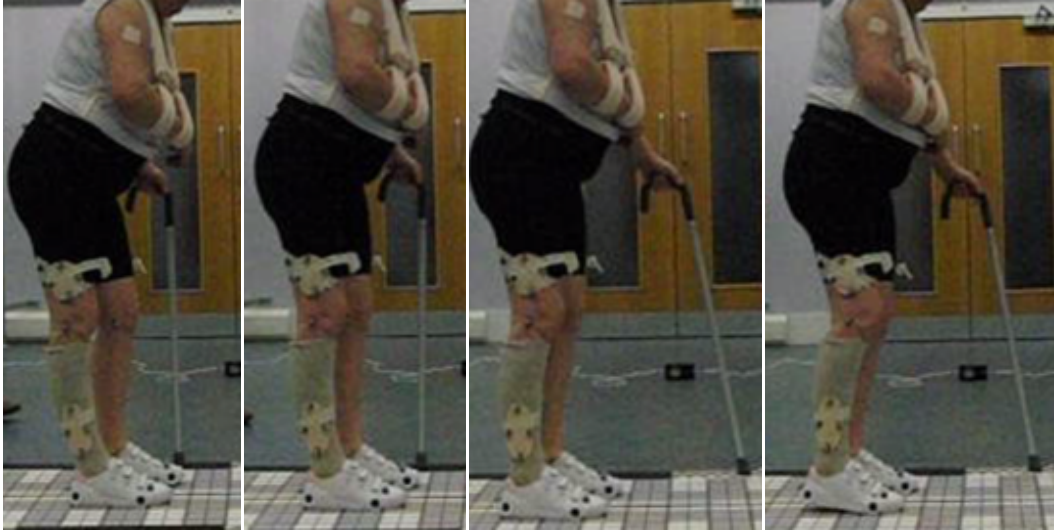


Figure 6.42: Sequence of instants of the unaffected leg without AFO preparing for swing phase initiation. Contralateral leg initial contact, the patient then raised a bit her body, moved the stick forward and finally raised the heel from the ground.



Figure 6.43: Sequence of instants of the unaffected leg with AFO preparing for swing phase initiation. Contralateral leg initial contact and heel rise simultaneous to the stick forward movement.

the support through the stick while the sound leg swung forward. This was particularly noticeable when the unaffected leg contacted the ground, at this stage the hemiplegic leg was still on the floor waiting to swing forward. When with shoes only (Figure 6.42), the subject had to redistribute the weight from the stick to the unaffected leg in search of a new balanced position; after which she could move the stick forward and start the heel rise toward swing phase.

With the AFO (Figure 6.43) all these times were reduced and the subject could start to raise the heel simultaneously to the movement of the stick, hence reducing the stance phase. This was observed in both the assessments although the pictures (6.42, 6.43) refer to the baseline data acquisition.

At baseline, for the affected leg (Figure 6.44a), the differences in stance and swing duration between with AFO and without AFO walking were not significant (Paired T -test: p -value=0.09) but a significant difference was found for the sound leg (Paired T -test: p -value<0.00) (Figure 6.44b). The latter had a stance phase longer than the affected leg in both conditions tested (Paired T -test: p -value<0.00).

At outcome, differences in stance and swing duration between with AFO and without AFO walking were significant (Paired T -test: p -value<0.01) for both legs (Figure 6.44).

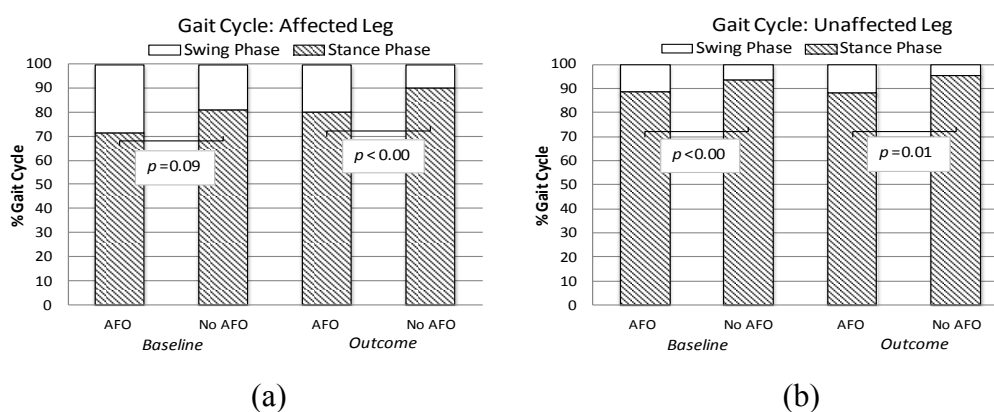


Figure 6.44: Stance (diagonal pattern bars) and swing phase (white bars) duration of the affected leg(a) and unaffected (b) with and without AFO for the two assessments of case study 3. Results of the t-test are shown for each compared bar.

This way of walking with the affected leg waiting for the contralateral leg before initiating swing phase also implied long terminal double support time of the affected

leg above 30% of the gait cycle and long initial double support phase for the unaffected leg also above 30%. The affected leg showed a terminal double support longer than initial double support whereas the contrary was observed for the unaffected leg.

At baseline the AFO lead to a significant reduction of terminal and initial double support for affected and unaffected leg respectively (Paired T -test: p -value=0.02). At outcome, for the affected leg the initial double support phase was reduced significantly (Paired T -test: p -value=0.02) and for the unaffected leg the terminal double support phase was also reduced significantly (Paired T -test: p -value=0.01). Single support was enhanced significantly for both legs at the two assessments when the subject walked with the AFO. The duration of such intervals however did not account for more than 13% of the gait cycle for the affected leg and 25% for the unaffected leg.

It followed also that the unaffected leg presented with a step time longer than the affected leg, particularly at baseline, and hence an asymmetric gait pattern with symmetry ratio below 0 was present. Gait symmetry was improved by the AFO (Paired T -test: p -value=0.01) during baseline but at outcome, the subject walked more symmetrically without the AFO (Paired T -test: p -value=0.01) showing a symmetric gait as the ratio approached 0.

Gait symmetry improved from baseline to outcome measurements significantly for each condition (Paired T -test: p -value<0.00).

Consistent improvements were not observed in the gait cycle intervals duration between the two assessments. Comparable values in fact were found.

In Table 6.13 spatial parameters for the affected and unaffected leg for the two conditions tested are reported for baseline and outcome assessment.

Short steps characterised the gait pattern of this participant. She could not pass the affected foot when the unaffected leg swung forward either if she walked with or without AFO at baseline and at outcome assessment.

With the affected leg, she performed steps of maximum 0.1 m in length when walking with AFO. For the unaffected leg a step of 0.3 m was achieved in both conditions.

| Spatial Parameters | Baseline Measurement | | Outcome Measurement | |
|--------------------------------------|----------------------|---------------------|---------------------|---------------------|
| | AFO | SHOES | AFO | SHOES |
| <i>Step Length (m):</i> | | | | |
| Affected Leg | 0.07 (± 0.02) | 0.04 (± 0.01) | 0.1 (± 0.02) | 0.05 (± 0.02) |
| Unaffected leg | 0.3 (± 0.05) | 0.3 (± 0.01) | 0.3 (± 0.02) | 0.2 (± 0.03) |
| <i>Step Length (%Stride length):</i> | | | | |
| Affected Leg | 18.3 (± 5.8) | 10.4 (± 3.3) | 31.5 (± 4.0) | 21.9 (± 10.4) |
| Unaffected leg | 81.7 (± 5.8) | 89.5 (± 3.3) | 68.5 (± 4.0) | 78.1 (± 10.4) |
| <i>Spatial Symmetry:</i> | -0.6 (± 0.1) | -0.8 (± 0.1) | -0.4 (± 0.1) | -0.6 (± 0.2) |

Table 6.13: Comparison of spatial parameters assessed with and without AFO for affected and unaffected leg during baseline and outcome assessment of case study 3.

The AFO significantly increased step length for the affected leg in the two assessments (Paired T -test: p -value <0.01) but only at outcome for the unaffected leg (Paired T -test: p -value=0.01).

Unaffected step length was greater than affected step length and therefore an asymmetric gait in terms of spatial parameters. The AFO enhanced the symmetry of walking significantly compared to the without AFO condition during baseline and outcome measurement (Paired T -test: p -value=0.04).

Moreover, a significant difference was found when comparing the symmetry with AFO and without AFO respectively, between baseline and outcome assessments (Paired T -test: p -value <0.04).

Across sessions a significant difference was found for affected leg step length when the patient walked with AFO (Paired T -test: p -value <0.00) but not when with shoes only (Paired T -test: p -value=0.1). The unaffected leg was found to improve significantly only when the subject walked without the AFO (Paired T -test: p -value <0.00).

The mean shank to vertical angles measured at initial contact (IC), foot flat (FF), mid stance (MS), heel rise (HR) and terminal contact (TC) are represented in Figure 6.45 for the affected leg (a) and unaffected leg (b) at baseline measurement.

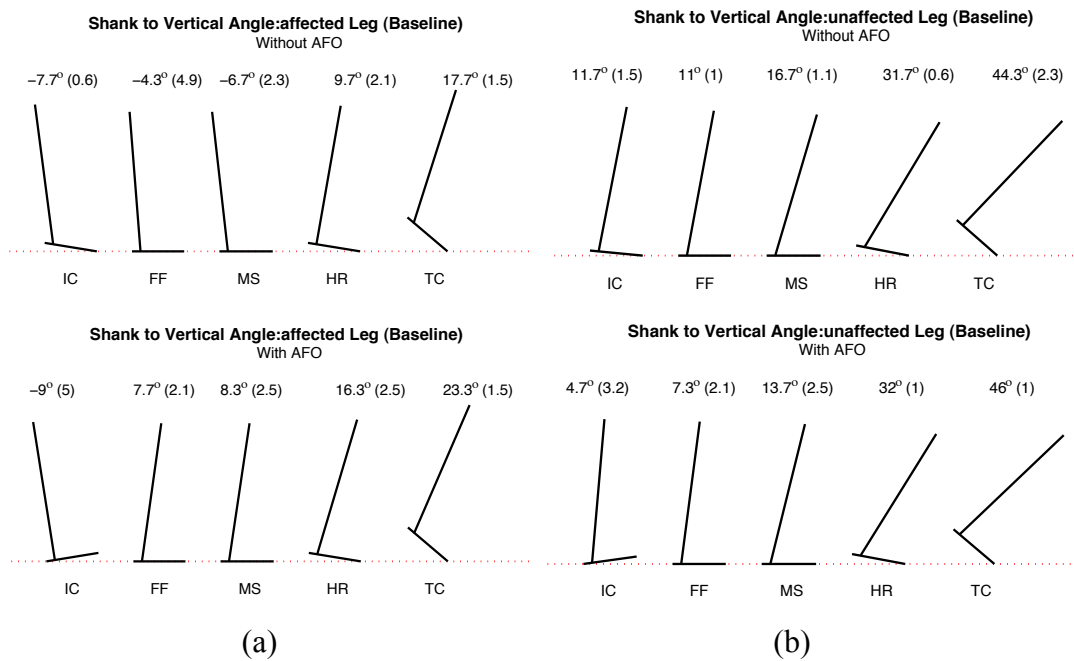


Figure 6.45: Case study 3 baseline SVA for affected (a) and unaffected (b) leg at initial contact (IC), foot flat (FF), mid stance (MS), heel rise (HR) and terminal contact (TC) without (top) and with AFO (bottom). Angles in degree are reported with values of standard deviation in brackets.

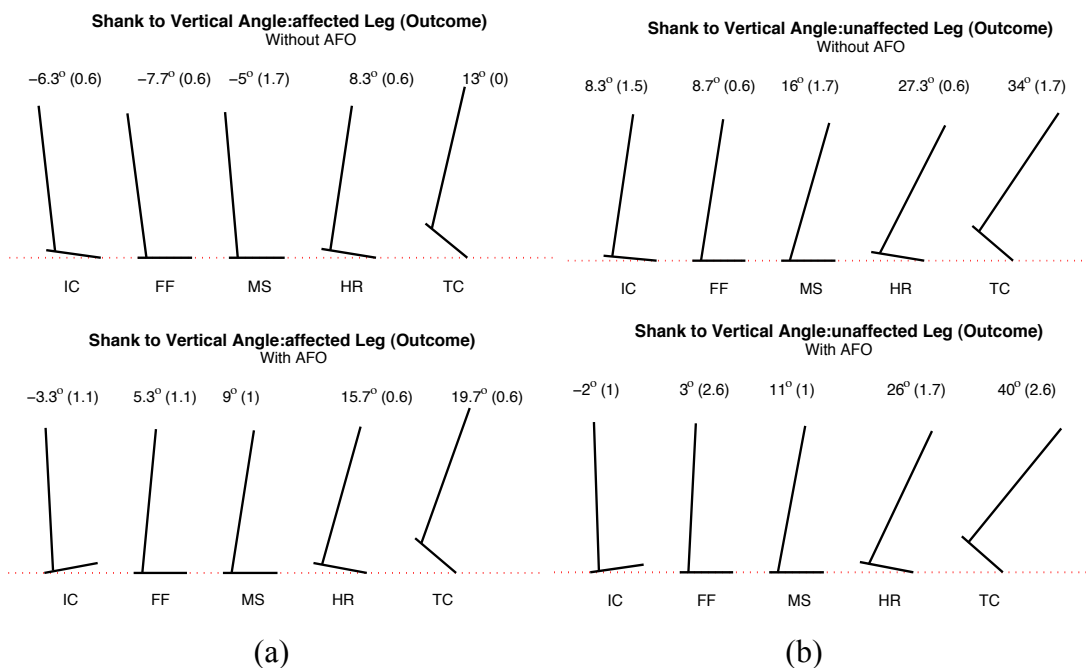


Figure 6.46: Case study 3 outcome SVA for affected (a) and unaffected (b) leg at IC, FF, MS, HR and TC without (top) and with AFO (bottom). Angles in degree are reported with values of standard deviation in brackets.

Without the AFO, the affected leg, showed a reclined tibia for most of the stance phase. Initial contact occurred through the forefoot but the AFO allowed a proper heel strike (Figure 6.45a).

Tibial kinematics of the unaffected leg were also altered because the leg had to adjust itself to the inability of the affected limb to sustain long single support interval and hence initial contact with an inclined tibia (Figure 6.45b).

Similar behaviour of tibia kinematics was observed at outcome assessment (Figure 6.46). At outcome, although to a small extent, the tibia was reclined with the AFO at initial contact in both legs. Reclined tibia could not be achieved at foot flat.

6.3.3.2 Kinematic Outcomes

Baseline Assessment:

Pelvis and lower limb kinematics at baseline assessment are presented in Figure 6.47. Mean over 5 gait cycles for each leg during walking with and without AFO are plotted. The subject used a stick during the test.

The gait cycle of the affected leg, when walking without the AFO, started with forefoot (Figure 6.48) contact with the ankle plantarflexed at 3.4° (± 2.0) and hip and knee flexed respectively at 55.2° (± 2.1) and 27.6° (± 4.7). This was followed by a rapid foot drop that brought the ankle into a neutral position.



Figure 6.48: Initial contact for case study 3 without AFO (left) and with AFO (right) during baseline assessment.

Baseline Kinematics

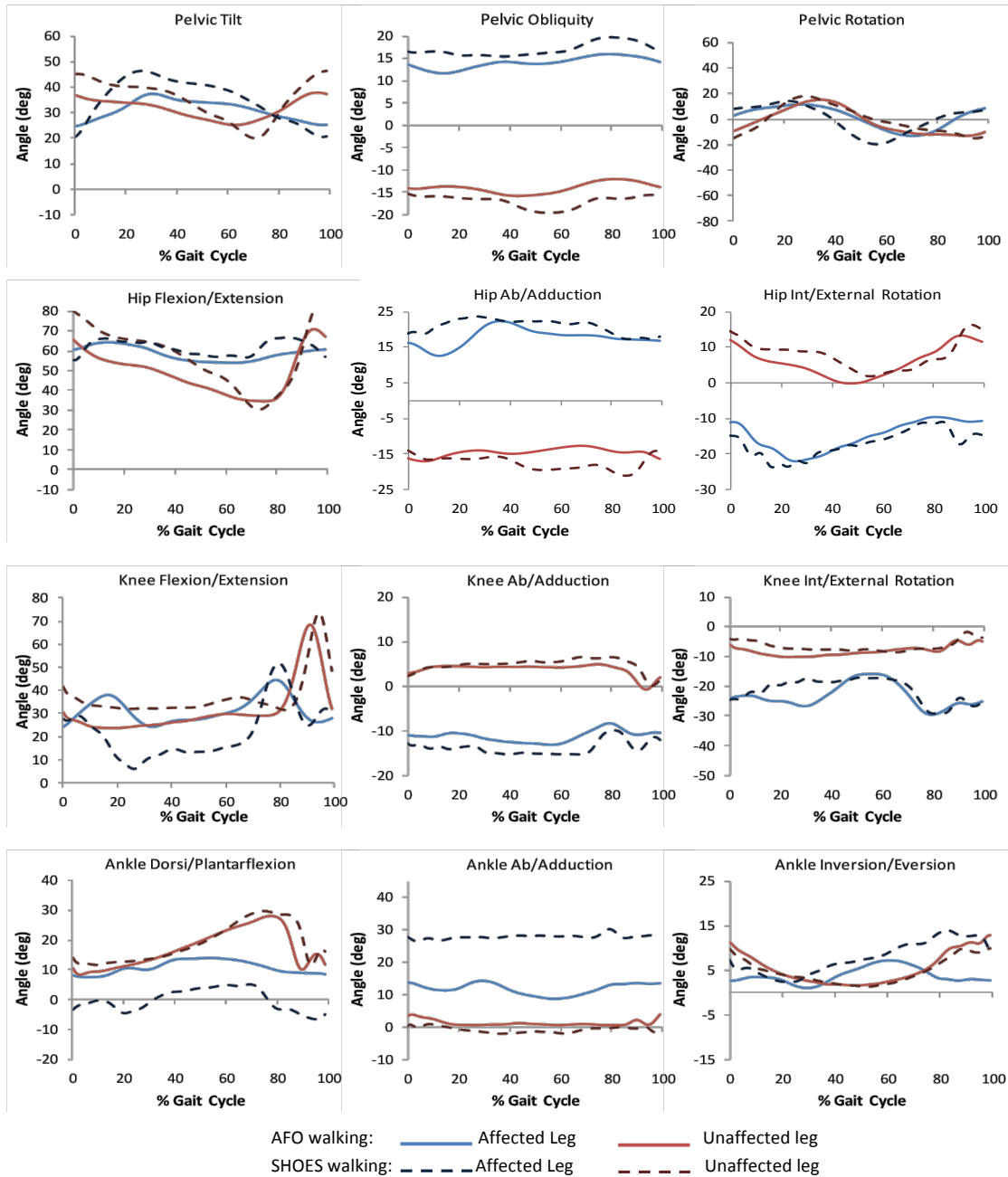


Figure 6.47: pelvis and lower limb kinematics at baseline assessment for case study

3.

The presence of a plantarflexed ankle between the 10 to the 30% of the gait cycle inhibited tibia progression. Ankle rocker was absent. The patient instead hyperextended the knee with a visible reduction in flexion to $5.94^\circ (\pm 1.8)$ at 26% of the gait cycle and leaned the trunk forward with anterior tilt of the pelvis (Figure 6.49). A peak in anterior tilt of $46.2^\circ (\pm 1.1)$ was achieved at 26% of the gait cycle. Locking the knee into extension and forward lean of the trunk helped the patient to maintain balance while the contralateral leg swung forward. The swing phase of the unaffected leg was shortened as the step length. The leg was forced into stance to assist the hemiplegic leg, which was unable to extend the hip in terminal stance and hence advance the body.

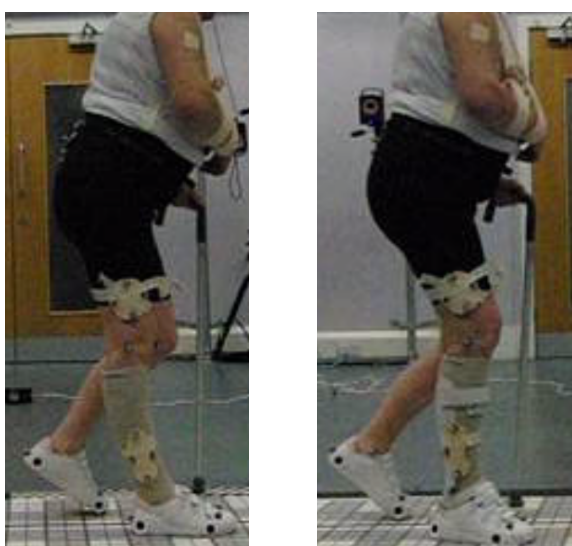


Figure 6.49: Knee hyperextended and anterior tilt in stance phase without AFO (left) and relative instant with AFO (right) at baseline.

When both leg were on the ground the patient was able to assume a more upright posture (reducing of anterior tilt), the hip was maintained in a flexed position of on average $58.3^\circ (\pm 1.6)$, the knee was kept in extension at a flexed position of $14.6^\circ (\pm 1.9)$ and the ankle passively dorsiflexed (peak $5.2^\circ \pm 6.8$) under the effect of the fairly noticeable knee flexion increase that inclined the tibia. During this phase of the gait the stick was brought forward; the knee and the hip could begin to flex (69 % of the gait cycle) A late heel rise of the affected leg occurred. The knee achieved

rapidly a peak of flexion of 51.5° (± 2.1) and, simultaneously (80% of the gait cycle) the hip reached 66.7° (± 2.7).

As the foot was lifted from the ground it dropped into plantarflexion with a peak of 6.6° (± 1.6) and remained plantarflexed through swing phase (Figure 6.50). At the same time inversion of the ankle increased to a peak of 13.9° (± 1.4).

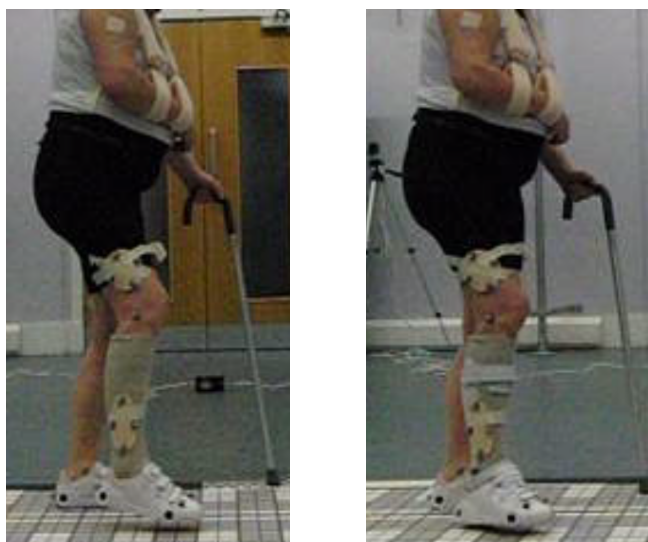


Figure 6.50: Mid Swing without AFO (left) and with AFO (right) at baseline test of patient 3.

A flexed hip was used to clear the ground as well as hip hiking (hip obliquity positive). The knee progressed into extension but started to flex again as the forefoot approached initial contact (jump in the knee/flexion extension curve in Figure 6.47). In the coronal plane the hip was kept in an adducted position in stance and abduction to of a minimum of 17.3° (± 1.7) of adduction in swing facilitating ground clearance. External rotation of the hip was observed during the gait cycle.

The knee was abducted and externally rotated in stance. These movements were enhanced for a safer swing.

The ankle was constantly adducted during the gait cycle with a peak at the end of stance (79%) of 30.2° (± 1.7). The patient had also an inverted foot.

The pelvis went from being internally rotated to external rotation to attain an internal rotation position again by the end of the cycle.

The unaffected leg had to compensate for the impaired leg. As a consequence the unaffected leg gait cycle was characterised by a premature initial contact that occurred with the hip at a high flexion position ($80.3^\circ \pm 3.4$) as well as the knee ($41.4^\circ \pm 3.5$) and the ankle dorsiflexed at $14.1^\circ (\pm 2.9)$. This implied a swing phase reduced to a minimum. The knee flexion peak was missed at loading response as shock absorption occurred through the stick and only after the weight was transferred to the sound leg to allow the movement of the stick. The second peak of knee flexion was as high as $73.4^\circ (\pm 1.2)$, thanks to the ability of the ankle to dorsiflex freely to a maximum of $29.7^\circ (\pm 0.7)$ at 75% of the gait cycle. This allowed a gradual advancement of the tibia and the possibility to extend the hip but only to a minimum of flexion of $30.4^\circ (\pm 1.6)$. To initiate swing phase a rapid hip flexion to lift the leg from the ground was required. Maintaining the leg at high values of flexion at the hip and at the knee lowered the hip joint centre and hence gave negative pelvic obliquity. In terms of coronal and transverse plane rotations of the lower limb joints, for the unaffected leg, stationary positions were kept through the gait cycle (noticeable as flat curves in the relative graphs of Figure 6.47). Movement was only observed for hip rotation during the gait cycle.

The effect of the AFO on the affected leg at the ankle level was noticeable at initial contact. Initial contact occurred through the heel (Figure 6.48) with a dorsiflexed ankle of $8.3^\circ (\pm 0.5)$. Dorsiflexion was maintained throughout the gait cycle preventing plantarflexion.

Adduction of the ankle was reduced by $15.8^\circ (\pm 1.9)$ and the inverted position of the foot was corrected. Significant differences were found for the ankle kinematics during the gait cycle (Paired *T*-test: *p*-value < 0.05). Heel rocker was attained during initial stance and the knee was able to flex for shock absorption. The first knee flexion peak was of $38.1^\circ (\pm 0.7)$ at 17% of the gait cycle. Extension of the knee followed to a minimum of flexion of $24.3^\circ (\pm 3.5)$ (33% gait cycle). The second peak of flexion of the affected knee was of only $44.6^\circ (\pm 3.2)$ at initial swing (78%). However the presence of a dorsiflexed ankle prevented toe drag and swing could occur safely. Knee abduction was reduced significantly whereas external rotation increased during the first half of stance phase after which a similar pattern as seen without the AFO was obtained.

The hip presented in high flexion at the start of the gait cycle with this increasing it to a maximum of 64.5° (± 0.6) in correspondence with the knee first flexion peak.

The hip remained flexed for the rest of the gait cycle reaching a minimum value of 53.7° (± 0.7) in late stance (63% of the gait cycle). The patient was unable to extend the hip as the thigh remained reclined.

The AFO did not particularly affect hip kinematics in the transverse and coronal plane.

The pelvis was still anteriorly tilted, obliquity was reduced as well as hip retraction (pelvic rotation).

Terminal stance was still compromised by the inability to advance the body forward while the contralateral leg swung. A late heel rise still occurred although was anticipated in comparison to walking without the AFO. Hence producing a reduced stance phase duration and a less disrupted swing phase for the unaffected leg. The AFO showed positive effect in early stance but late stance was still abnormal with an impeded progression.

The unaffected leg showed similar kinematics pattern to those seen without the AFO with the persistent necessity to cope with the hemiplegic leg.

The variability of the kinematics measurements of pelvis and lower limb joints is shown by mean standard deviation and mean absolute standard deviation values reported in the Table 6.14.

The subject was generally able of a consistent gait pattern among cycles and within each condition and leg. Standard deviations values did not exceed 5.5° , maximum value of variability found in pelvic rotation which corresponded to 16.6% of the entire range of sound leg when walking with shoes. On the other hand, a value in degrees as small as 1.3° represented the 42.3% of sound leg ankle ab/adduction range. For the majority of kinematics outputs values of absolute standard deviation less than 20% of the relative range were found.

| Joint Angles | Affected Leg | | Unaffected Leg | |
|---------------------------------------|--------------|-------------|----------------|-------------|
| | AFO | SHOES | AFO | SHOES |
| <i>Pelvis (°, % range of motion):</i> | | | | |
| Obliquity | 0.6 (14.3%) | 1.2 (27.6%) | 0.6 (15.3%) | 1.1 (27.3%) |
| Rotation | 2.8 (11.6%) | 4.7 (13.7%) | 4.0 (14.3%) | 5.5 (16.6%) |
| Tilt | 1.6 (12.6 %) | 2.6 (10.2%) | 1.3 (10.0%) | 2.6 (9.8%) |
| <i>Hip (°, %range of motion):</i> | | | | |
| Ab/Adduction | 1.2 (12.7%) | 1.5 (24.0%) | 1.0 (24.4%) | 1.4 (19.4%) |
| Int/External Rotation | 1.5 (12.2%) | 1.8 (14.0%) | 1.1 (8.5%) | 1.6 (10.7%) |
| Flexion/Extension | 1.2 (11.3%) | 4.0 (34.9%) | 2.3 (6.3%) | 4.1 (7.8%) |
| <i>Knee (°, %range of motion):</i> | | | | |
| Ab/Adduction | 0.9 (19.0%) | 0.8 (15.3%) | 0.7 (12.3%) | 0.7 (10.7%) |
| Int/External Rotation | 3.5 (25.4%) | 1.5 (12.6%) | 1.1 (20.5%) | 1.0 (16.0%) |
| Flexion/Extension | 3.8 (18.9%) | 3.6 (7.9%) | 2.5 (5.6%) | 2.3 (5.4%) |
| <i>Ankle (°, %range of motion):</i> | | | | |
| Ab/Adduction | 0.8 (14.7%) | 1.3 (35.0%) | 1.2 (36.8%) | 1.3 (42.3%) |
| Inversion/Eversion | 1.0 (17.5%) | 1.7 (14.6%) | 1.1 (10.2%) | 0.9 (10.5%) |
| Flexion/Extension | 1.5 (24.3%) | 3.4 (28.7%) | 1.3 (6.5%) | 2.0 (29.7%) |

Table 6.14: Mean (°) and absolute mean (% of range of motion) of standard deviation values for each joint angle for both affected and unaffected leg during walking with and without AFO at baseline assessment of case study 3.

Outcome Assessment:

Figure 6.51 shows the pelvis and lower limb joint kinematics of affected and unaffected leg during walking with and without the AFO for the outcome assessment. The patient at this time still walked with a stick. Five gait cycles for each condition and leg were analysed and mean values obtained from them are plotted in Figure 6.51.

From the previous assessment, the patient did not show improvements in the way she used to walk either with or without AFO.

Outcome Kinematics

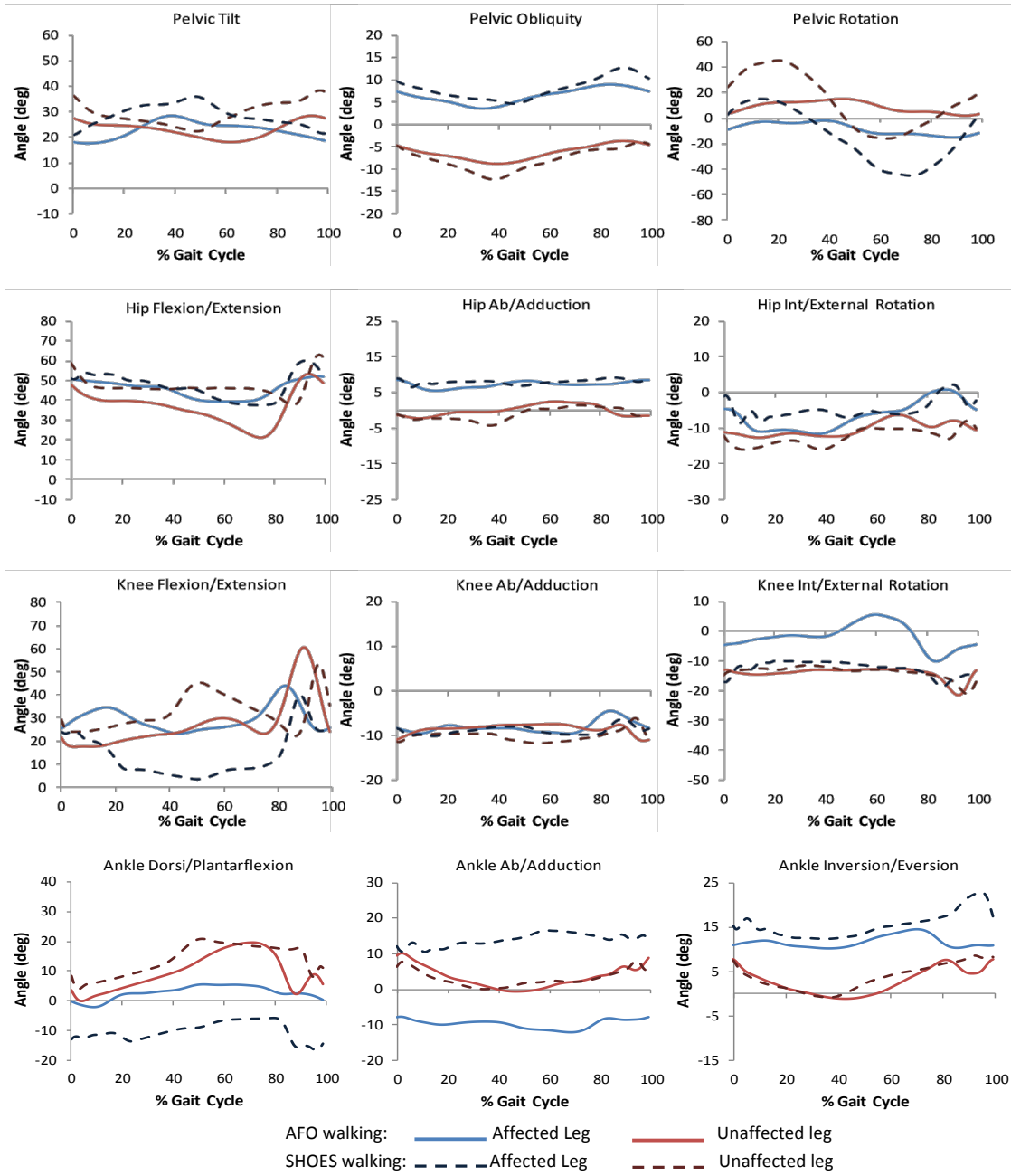


Figure 6.51: pelvis and lower limb kinematics at outcome assessment for case study

3.

During shoes only walking, the ankle of the affected leg was permanently plantarflexed during the gait cycle preventing initial contact from occurring through the heel. The tibia was reclined and, was only able to incline and go passively into dorsiflexion, due to the knee being pushed forward with respect of the ankle joint centre in late stance while the foot was still on the ground and started to raise the heel. At 80% of the gait cycle a peak in plantarflexion (dorsiflexion direction) of 5.7° (± 2.0) was achieved; that corresponded also to the instant from which the knee started to rapidly flex ($12.9^\circ \pm 2.8$) to initiate swing phase. As the rear part of the foot was lifted from the ground due to increased knee flexion, the ankle dropped into plantarflexion again and remained plantarflexed in swing phase.

The foot still presented with an inverted position which increased in swing and an adducted position that was kept throughout the gait cycle.

Similarly to the baseline assessment, the knee was abducted, externally rotated and could not be prevented from going into hyperextension during stance. A value of extension to a minimum peak of flexion of 3.5° (± 0.7) was reached at the 50% of the gait cycle. This extended position of the knee together with anterior tilt represented the mechanism by which the patient stabilised herself while the contralateral leg swung forward and she sought support through the stick. Anterior tilt peak was obtained at 48% of the gait cycle for a value of 36.2° (± 1.7).

Pelvic obliquity was still observed with a tendency to increase toward swing phase as hip hiking helped the patient to go through swing more safely. A peak of 12.7° (± 1.6) at the moment of toe off (89% of the gait cycle) was achieved.

As the hemiplegic foot was on the ground, hip retraction was also observed. High values of external pelvic rotations were measured. These high values could be influenced by the way joint coordinate system for the pelvis was defined as also noticed for case study 2.

The hip at the start of the gait cycle was flexed at a value of 51.2° (± 0.7). The high hip flexion allowed the leg to be pushed further forward. During stance hip extension was limited and a minimum value of 37.7° (± 3.6) of flexion could be achieved in late stance (74% of cycle) before the hip started to flex again to initiate swing phase. The increased flexion of the hip compensated for the inadequate knee flexion and a peak

of hip flexion of 62.9° (± 2.9) was achieved in swing that allowed the leg to clear the ground reducing stumbling hazard.

The hip was adducted and externally rotated although to a lesser extent than at baseline.

The unaffected leg gait cycle was controlled by the inability of the patient to support the weight through the hemiplegic leg and hence the short swing phase of the sound leg and the late heel rise of the affected leg.

A new flexion peak was observed in the unaffected leg in correspondence to affected leg initial contact (Figure 6.52). The flexion of the sound knee helped the patient to advance her body further for the subsequent affected leg ground contact.

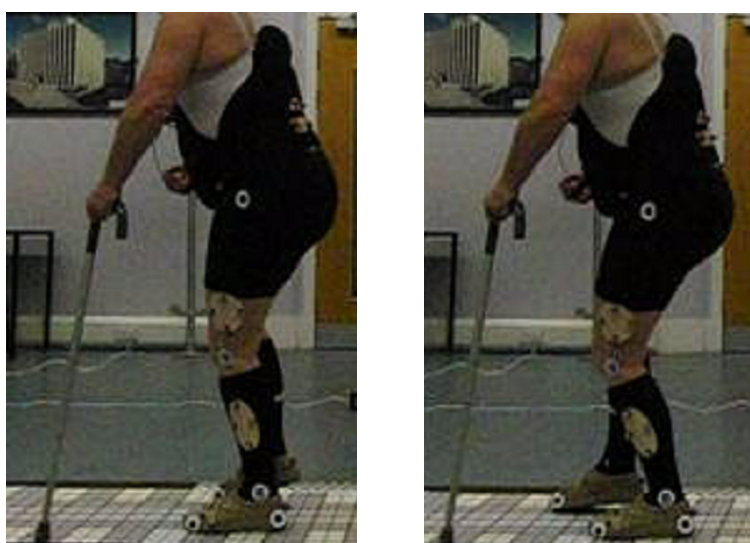


Figure 6.52: Sound leg mid stance just prior affected leg initial contact and increase unaffected knee flexion.

When wearing the AFO the patient was able to dorsiflex her ankle starting the gait cycle with the ankle at almost a neutral position of 0.22° (± 0.7) and with initial contact through the heel. There followed a gradual plantarflexion to a minimum of 2.2° (± 0.2). Heel rocker was possible and a knee flexion peak at loading response was observed ($34.4^{\circ} \pm 0.5$ at 17% of the gait cycle). The ankle then went into dorsiflexion, maintaining a dorsiflexed position through the rest of the gait cycle. Knee extension in stance was reduced and the second peak of flexion enhanced. The maximum extension of the knee achieved was of 22.9° (± 1.4) of flexion at 43% of

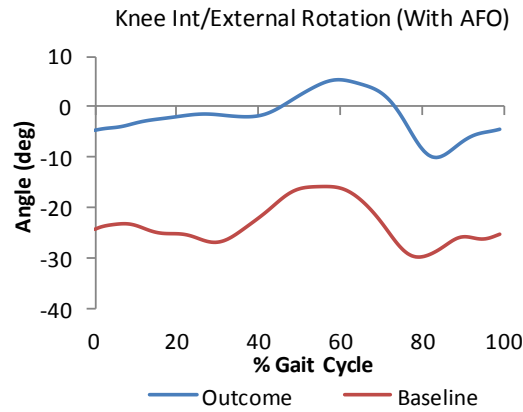


Figure 6.53: Knee internal/external rotation for outcome (blue solid line) and baseline (red solid line) AFO walking.

| Joint Angles | Affected Leg | | Unaffected Leg | |
|---------------------------------------|--------------|-------------|----------------|-------------|
| | AFO | SHOES | AFO | SHOES |
| <i>Pelvis (°, % range of motion):</i> | | | | |
| Obliquity | 0.5 (9.9%) | 1.4 (16.9%) | 0.6 (12.2%) | 1.3 (15.3%) |
| Rotation | 1.7 (12.5%) | 4.4 (7.4%) | 2.0 (15.4%) | 5.4 (8.8%) |
| Tilt | 0.9 (7.8%) | 1.7 (11.0%) | 0.8 (8.0%) | 2.0 (12.9%) |
| <i>Hip (°, %range of motion):</i> | | | | |
| Ab/Adduction | 0.7 (23.1%) | 2.0 (71.8%) | 0.9 (18.4%) | 1.9 (33.8%) |
| Int/External Rotation | 1.5 (11.9%) | 1.4 (13.2%) | 1.2 (17.7%) | 1.2 (14.5%) |
| Flexion/Extension | 1.3 (10.4%) | 1.2 (3.6%) | 2.5 (11.3%) | 2.9 (11.5%) |
| <i>Knee (°, %range of motion):</i> | | | | |
| Ab/Adduction | 0.5 (10.4%) | 0.8 (19.7%) | 0.5 (12.5%) | 0.7 (12.3%) |
| Int/External Rotation | 2.0 (12.8%) | 1.0 (11.6%) | 0.9 (10.2%) | 0.9 (9.1%) |
| Flexion/Extension | 1.8 (8.7%) | 2.8 (7.7%) | 1.5 (3.4%) | 1.7 (5.4%) |
| <i>Ankle (°, %range of motion):</i> | | | | |
| Ab/Adduction | 0.5 (12.4%) | 1.9 (31.8%) | 1.0 (9.0%) | 0.8 (9.6%) |
| Inversion/Eversion | 0.4 (10.0%) | 0.9 (8.4%) | 0.8 (9.0%) | 0.6 (6.6%) |
| Flexion/Extension | 0.8 (10.6%) | 1.8 (16.5%) | 1.1 (5.6%) | 1.3 (7.7%) |

Table 6.15: Mean (°) and absolute mean (% of range of motion) of standard deviation values for each joint angle for both affected and unaffected leg during walking with and without AFO at outcome assessment of case study 3.

the gait cycle and the maximum value of flexion was of $43.9^\circ (\pm 0.8)$ at 83% of the cycle.

This resulted also in a reduced hip flexion during initial stance. The ability to extend the hip was compromised even with the AFO as thigh inclination could not be achieved. The hemiplegic leg in fact still waited for the unaffected leg to reach the ground before swinging forward (late heel rise). Hip flexion in swing was also reduced but it was still as high as $51.8^\circ (\pm 0.7)$ to ensure a safe ground clearance. Leaning of the trunk forward was diminished but still noticeable.

The differences described between with AFO and without AFO condition in the sagittal plane were statistically significant (Paired *T*-test: *p*-value < 0.05).

In the coronal plane the main effect of the AFO was to bring the ankle from an adducted position to an abducted position. This represented a difference also from baseline AFO walking.

In the transverse plane, main changes were reduction of ankle inversion and external rotation of the knee, increasing of hip external rotation during the first half of stance phase and reduction of hip retraction (pelvic rotation).

Interestingly, a similar trajectory shape was observed between baseline and outcome measurement for the knee internal/external rotation for AFO walking with the exception that the outcome curve was shifted upward by on average $21.6^\circ (\pm 2.4)$ (Figure 6.53).

The affected leg improved pelvis, hip, knee and ankle kinematics in the sagittal plane; whereas no major effects were found in the other two planes, coronal and transverse, a part for pelvic rotation that was reduced.

Good repeatability in pelvis and joint kinematics at outcome assessment was found. Values of mean standard deviation and absolute standard deviation are shown in Table 6.15. A 71.8% of variation was found for hip/adduction of affected leg when walking without AFO. A small range of motion (2.8°) was found for this angle and hence the high percentage. In terms of degrees the maximum value of mean standard deviation found was of 5.4° for pelvic rotation of the unaffected leg without the AFO.

6.4 Summary

Each of the three subjects who participated in the study was able to successfully complete a test session and allow data collection.

Results from the tests conducted with each patient were reported. The gait of the subjects was characterised with and without AFO analysing spatiotemporal parameters, shank to vertical angles and lower limb and pelvis kinematics.

The effects an AFO had on patient gait were identified and mostly observed in the sagittal plane kinematics. Direct effects of the AFO at the ankle level were noticed by a reduced plantarflexion and inverted position of the foot. Indirect effects at the affected pelvis, hip and knee were also identified. The subjects walked maintaining an improved upright posture hence diminishing the trunk forward leaning (pelvic anterior tilt). Hip extension was promoted and retraction reduced (pelvic rotation). At the knee, the first flexion peak was achieved, hyperextension was reduced and the second flexion peak increased. Besides, the kinematics gait pattern of the unaffected leg benefitted from the effects AFO had on the hemiplegic side.

Shank kinematics was also improved with the AFO, although a reclined position at foot flat was not achievable.

Temporal subdivisions of the gait cycle were refined towards a more symmetric gait. Walking speed, despite being still low in comparison to able-bodied subjects velocity, increased but not for case study 2. Step length was increased, although short steps tended to characterise those patients gait.

For subject 1 the contribution of the AFO to the ankle moment was measured. The AFO provided the patient with a corrective dorsiflexion moment for about the first 60% of stance phase.

CHAPTER 7 – ANALYSIS OF GAIT DATA IN MANIFOLD SPACE

7.1 Introduction

Motor control is a primary issue for people who have suffered from stroke. Knowledge on what the central nervous system (CNS) tries to control during post-stroke walking is important for a better understanding of which rehabilitation practice is beneficial for which patients.

The theory of the uncontrolled manifold (UCM) has been recently introduced (Scholz and Schoner, 1999; Latash et al., 2007) to investigate how the CNS acts in respect of selected motor tasks by choosing combinations of different musculoskeletal elements that may be involved in that performance. One combination rather than another may lead to a different or the same end solution. Exploiting this approach it is possible to hypothesise which motor variable the CNS controls and what are the elements/degree of freedoms (DOFs), the central nervous system has to organise for that particular output. This theory can thus be seen as an analysis of the variability of a particular functional task in a multi-degree of freedom system. The variability can either be good, if the ultimate task remains unaltered, or bad, if deviations from it occur. The UCM itself is a subspace of all possible combinations of motor elements (elemental variables) that lead to a consistent value of a performance variable (task variable) (Figure 7.1).

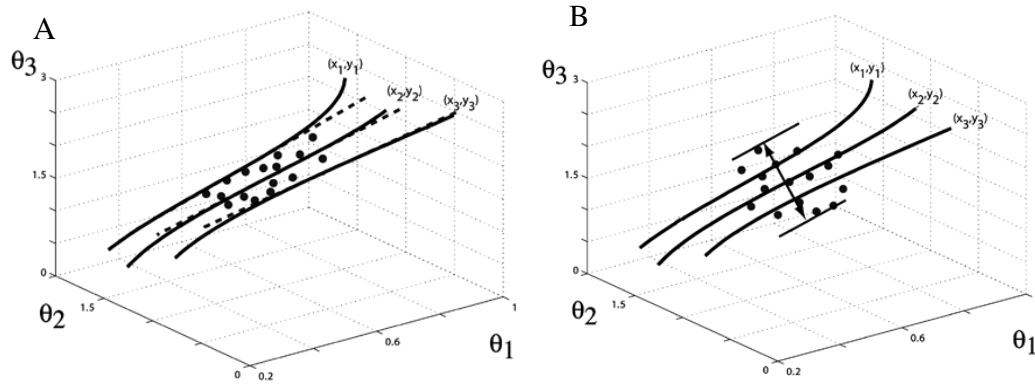


Figure 7.1: Uncontrolled manifolds corresponding to three position (task variable) (x_1, y_1) , (x_2, y_2) , and (x_3, y_3) are shown as solid lines. The positions are functions of three angles Θ_1 , Θ_2 , Θ_3 (radians) representing the elemental variables. Dashed lines, in A, represent a linearization of each UCM. In A, the points in the graph are distributed along the UCM of position (x_2, y_2) ; the end-effector position remains constant. In B, the points are more widespread perpendicularly to the UCM of (x_2, y_2) leading to a change of the end-effector position (Schoner and Scholz, 2007).

It is defined uncontrolled because the control of the variability within it is unnecessary as all the combinations picked within that subspace preserve the task variable value. Saying that, the UCM approach can also be seen as a method to quantify synergies. In this context a synergy refers to an organization of elemental variables that stabilises an important performance variable (Latash and Anson, 2006). The variability of the performance variable is partitioned, with the UCM theory, into two components that lies within or perpendicular to the UCM. These two variabilities expressed as indices of variances across repetitions of the same task are used to verify the hypothesis about what functional task is mostly controlled by the CNS. If the variance within the UCM is bigger than the one perpendicular to it, the hypothesis about the control of the selected motor task is accepted. The purpose of having different synergies (i.e.: Different combinations of angles to achieve that posture) is thus to make as much of the variability a “good” variability as possible; in other words to move along the manifold rather than at right angle to it. The UCM method of analysis has recently been used to verify the control of various motor tasks mostly related to upper extremity and sit-to-stand performances of able-

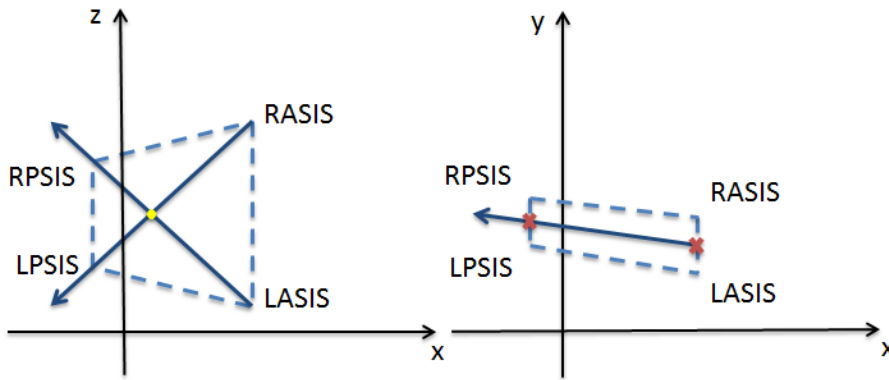


Figure 7.2: Representation of the approximation of the centre of mass definition (yellow dot) and projection line connecting the mid points (red crosses) between anterior and posterior iliac spine.

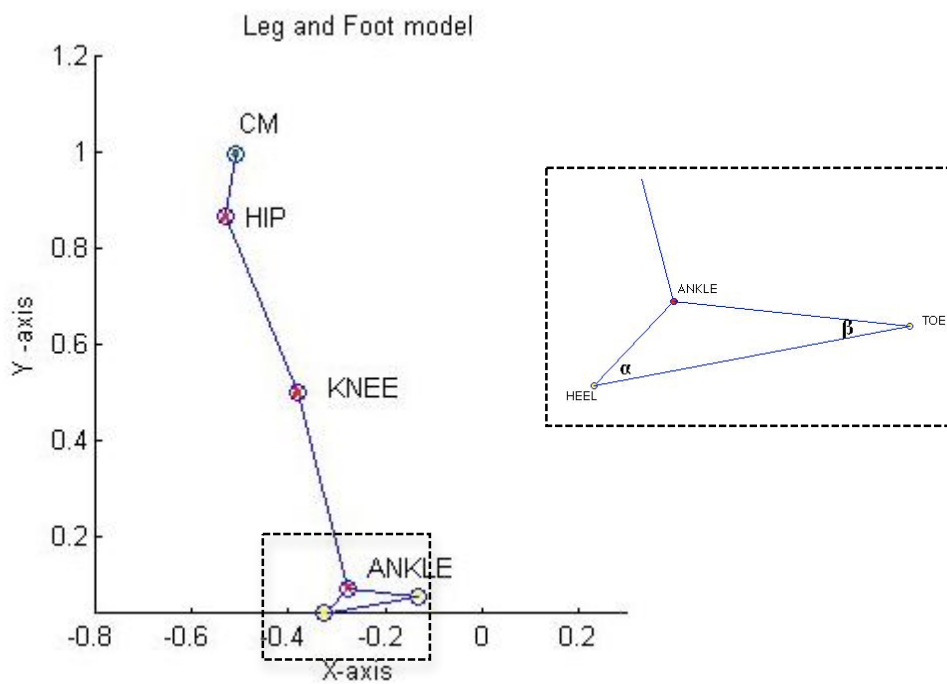


Figure 7.3: Leg and foot stick model.

bodied and impaired subjects (Scholz and Schoner, 1999; Domkin et al., 2002; Reisman and Scholz, 2003; Scholz et al., 2003; Yang et al., 2007; Hsu et al., 2007). Only one study was found to apply the UCM approach to gait (Black et al., 2007). However, the analysis was concentrated at one instant of the gait cycle, heel strike, rather than the entire time history of the walking cycle.

In the paragraph that follows the mathematical formulations on which this approach is based and the steps required for its application are discussed relatively to the application of the method to analyse gait data. The last paragraph describes how the developed method was applied to healthy and stroke subjects.

7.2 Uncontrolled Manifold approach formulation

The first step was to define the hypothesis about the controlled variable. It was hypothesised that the CNS during walking acts to stabilise the centre of mass (CM) trajectory. Hence, the task variable was the CM movement and the elemental variables were all the lower limb joint rotations that could affect this position. As a preliminary development of the UCM method for gait, it was decided to solve the problem in 2 dimensions considering only sagittal plane movements and to approximate the CM as a fixed point in the pelvis (Figure 7.2). This point was defined by the intersection between the two lines identified by the right anterior superior iliac spine (RASIS) and left posterior iliac spine (LPSIS) and the left anterior superior iliac spine (LASIS) and right posterior iliac spine (RPSIS) respectively. The y-coordinate of the CM approximation was obtained by projecting the point of intersection of these lines in the transverse plane onto the line connecting the midpoints between anterior and posterior iliac spine (Figure 7.2 right).

To estimate how the variability of joint angles influences the position of the CM, a geometric model that links hip, knee and ankle rotations to the CM position throughout the gait cycle was defined (Figure 7.3).

A model was created starting from the position of the foot and then scaling up joint by joint to define the CM coordinates in x and y directions. The second step was thus to express the x- and y-coordinates of CM in terms of the corresponding joint angles:

$$(x_{CM}, y_{CM}) = f(\theta_G, \theta_A, \theta_K, \theta_H) \quad \text{Equation 7.1}$$

Where:

θ_G is the angle between the sole of the foot and the ground, θ_A is the ankle dorsi/plantarflexion angle, θ_K is the knee flexion/extension angle and θ_H is the hip flexion/extension angle. Since the position of the CM depends also on the position of the foot on the ground and in particular on the angle between the sole of the foot and the ground, θ_G was considered an elemental variable. θ_G was defined as the angle between the vectors \vec{a} , characterising the sole of the foot, and \vec{b} representing the ground (Figure 5.6):

$$\theta_G = \arcsin(\vec{a} \times \vec{b}) \quad \text{Equation 7.2}$$

The first consideration in the formulation of the model equations was to consider the position of the foot on the ground during walking, from which the position of the ankle joint centre is defined. Three main cases were identified (Figure 7.4):

- 1- the heel is in contact with the ground: $\theta_G > 0$,
- 2- the foot is entirely on the floor: $\theta_G = 0$,
- 3- the fore part of the foot is on the ground $\theta_G < 0$.

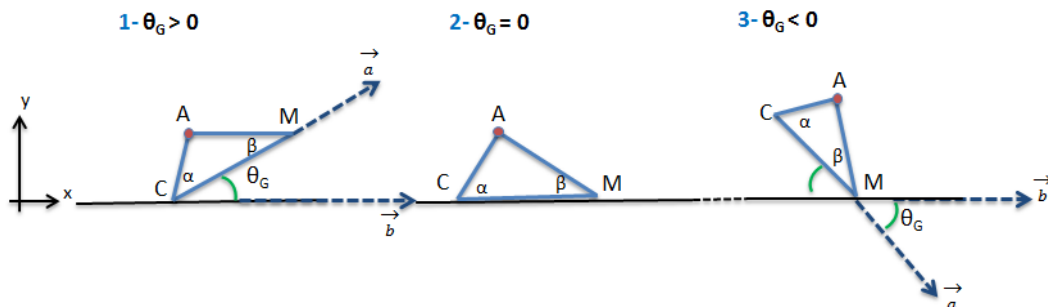


Figure 7.4: Positions of the foot on the ground at the identified 3 key points depending on θ_G value.

If $\theta_G \geq 0$ the x- and y-coordinates of the ankle joint centre are defined as follow:

$$x_A = x_c + CA \cos(\alpha + \theta_G) \quad \text{Equation 7.3}$$

$$y_A = y_c + CA \sin(\alpha + \theta_G) \quad \text{Equation 7.4}$$

Where:

α is the angle at the rear of the foot (Figure 7.4) and the points A and C are the ankle and the calcaneus respectively.

If $\theta_G < 0$ the following equations are used:

$$x_A = x_M - MA \cos(\theta_G - \beta) \quad \text{Equation 7.5}$$

$$y_A = y_M - MA \sin(\theta_G - \beta) \quad \text{Equation 7.6}$$

Where:

β is the angle in the fore part of the foot (Figure 7.4) and the point M is the mid point between the 1st and 5th metatarsal head.

Similarly, through a trigonometric analysis by knowing the sagittal angles of the joints also the 2-D coordinates of the knee and hip centres were determined to finally express the CM position in the sagittal plane as:

$$\begin{aligned} x_{CM} = & \\ & x_A + AK \cos(\theta_G + \theta_A + \pi/2) + KH \cos(\theta_G + \theta_A + \theta_K + \pi/2) + \\ & HCM \cos(\theta_G + \theta_A + \theta_K - \theta_H + \pi/2) \end{aligned} \quad \text{Equation 7.7}$$

$$\begin{aligned} y_{CM} = & \\ & y_A + AK \sin(\theta_G + \theta_A + \pi/2) + KH \sin(\theta_G + \theta_A + \theta_K + \pi/2) + \\ & HCM \sin(\theta_G + \theta_A + \theta_K - \theta_H + \pi/2) \end{aligned} \quad \text{Equation 7.8}$$

Where:

θ_G is the foot/ground angle, θ_A is the ankle dorsi/plantarflexion angle, θ_K is the knee flexion/extension angle, θ_H is the hip flexion/extension angle, AK is the shank segment length, KH is the thigh segment length, HCM is the hip centre to CM segment length. The geometric model was validated by comparing the hip, knee and ankle joint centres defined geometrically to the ones calculated by the Cluster model (Chapter 2) applied to the same normal subjects' walking.

The third step required for this approach was the linearization of the UCM (Latash et al., 2007). This was necessary because the concept of variance is a linear concept while, the UCM, and in particular the geometric model defined, is not linear. The

linearization implies the definition of the Jacobian matrix, $J(\theta)$, and the computation of its null space, $N(J)$. The UCM is linearly approximated by this latter subspace. The Jacobian matrix (Equation 7.9) is a matrix of all first-order partial derivatives of the CM coordinates with respect to the elemental variables. Changes in joint angles and changes of the CM trajectory are linked through the Jacobian matrix.

$$J(\theta) = \begin{bmatrix} \frac{\partial x_{CM}}{\partial \theta_G} & \frac{\partial x_{CM}}{\partial \theta_A} & \frac{\partial x_{CM}}{\partial \theta_K} & \frac{\partial x_{CM}}{\partial \theta_H} \\ \frac{\partial y_{CM}}{\partial \theta_G} & \frac{\partial y_{CM}}{\partial \theta_A} & \frac{\partial y_{CM}}{\partial \theta_K} & \frac{\partial y_{CM}}{\partial \theta_H} \end{bmatrix} \quad \text{Equation 7.9}$$

The null space (Equation 7.10) of the Jacobian matrix, spanned by the basis vectors ε_{n-d} , is the linear subspace of all joint angles combinations that leave the CM coordinates unaffected. The dimensions of this subspace are $(n - d)$ where n is the number of elemental variable (DOFs) and d is the number of dimensions of the task variable. The null space in the current case has the dimensionality of 2 ($4 - 2$).

$$0 = J(\theta) \cdot \varepsilon_{n-d} \rightarrow N(J) = \begin{bmatrix} \varepsilon_{11} & \varepsilon_{12} \\ \varepsilon_{21} & \varepsilon_{22} \\ \varepsilon_{31} & \varepsilon_{32} \\ \varepsilon_{41} & \varepsilon_{42} \end{bmatrix} \quad \text{Equation 7.10}$$

The linearization is performed around a reference configuration. The reference configuration was defined as the mean joint configuration across trials. This is assumed to represent the set of angles that lead to the CM position it should be aimed for. The Jacobian matrix, $J(\bar{\theta})$, was calculated to the respect of this point. The computation of the Jacobian matrix and then of its null space is performed for each time point throughout the stance phase of each trial analysed and hence they continuously vary.

The fourth step was to calculate the deviation (Equation 7.11) of the joint configuration at each sampled instant of time of the stance phase of each trial $(\theta_G, \theta_A, \theta_K, \theta_H)$, from the corresponding mean joint configuration $(\bar{\theta}_G, \bar{\theta}_A, \bar{\theta}_K, \bar{\theta}_H)$.

$$DV = \begin{bmatrix} \theta_G - \bar{\theta}_G \\ \theta_A - \bar{\theta}_A \\ \theta_K - \bar{\theta}_K \\ \theta_H - \bar{\theta}_H \end{bmatrix} \quad \text{Equation 7.11}$$

The obtained deviation vector is then decomposed into a component that is within the null space:

$$\theta_{\parallel} = \sum_{i=1}^{n-d} (N(J)_i^T \cdot DV) N(J)_i \quad \text{Equation 7.12}$$

and perpendicular to it:

$$\theta_{\perp} = DV - \theta_{\parallel} \quad \text{Equation 7.13}$$

Scalar values are obtained from these projections that represent to what extent the trial joint configuration is consistent or not with the relative reference configuration.

The variances (Equation 7.14 and 7.15) of the vector projections, θ_{\parallel} and θ_{\perp} , are finally calculated. Since the null space (linearized UCM) and its complement have different dimensions, the variances were normalised per degree of freedom of each subspace. The variance across trials within the linearized UCM, σ_{\parallel}^2 , is estimated as:

$$\sigma_{\parallel}^2 = \frac{\sum_{i=1}^N \theta_{\parallel N}^2}{(n-d)N} \quad \text{Equation 7.14}$$

Where:

θ_{\parallel}^2 is the squared length of the projection vector lying within the UCM, N is the number of trials kept for the analysis, n is the total number of elemental variables ($n = 4$) and d is the dimensionality of the task variable ($d = 2$).

Analogously, the variance across trial per degree of freedom orthogonal to the UCM, σ_{\perp}^2 , is:

$$\sigma_{\perp}^2 = \frac{\sum_{i=1}^N \theta_{\perp N}^2}{dN} \quad \text{Equation 7.15}$$

The variances within the UCM and its complement are compared to draw the conclusion on the initial hypothesis about the control of the CM trajectory.

A balanced ratio defined as in Equation 7.16 was also introduced to describe and summarise the results obtained from the application of the described method.

$$Ratio = \left(\frac{2\sigma_{\parallel}^2}{\sigma_{\parallel}^2 + \sigma_{\perp}^2} \right) - 1 \quad \text{Equation 7.16}$$

In particular, if more than one hypothesis is tested, the balanced ratio allows the comparison among the results of each control hypothesis, although this is beyond the aim of this thesis.

Matlab (The MathWorks Inc., Massachusetts, US) was used for the computations of the variances. A code (Electronic Appendix) was written that allows the calculation of the good (parallel) and bad (orthogonal) variability at each time point of the stance phase data (lower limb joint angles and markers trajectories) normalised to 100 points. The application of the UCM approach is not confined to a single instant of the gait cycle but to the entire duration of the stance phase, from initial contact until ground clearance.

7.3 Verification of the Uncontrolled Manifold approach

The introduced approach was applied to the data collected with the 3-D motion analysis system (Vicon, Oxford Metrics Ltd., UK) for the study described in section 2.5 which involved six able-bodied subjects, 3 females and 3 males (height 168.9 (\pm 10.5) cm, 68.2 (\pm 9.9) kg, 29.8 (\pm 6.7) years). From the static trial of each participant the 3-D coordinates of the following anatomical landmarks and virtual points were output: right and left anterior superior iliac spine (RASIS, LASIS), right and left posterior iliac spine (RPSIS, LPSIS), hip, knee and ankle joint centres (HJC, KJC, AJC), left and right heel (LHEEL, RHEEL) and left and right foot midpoint (LMidFoot, RMidFoot). The positions of these points were used to calculate invariant values such as, α and β angle of the foot and the length of body segments (shank, thigh, hip to CM, foot and shoes segments, Equation 5.4 ÷ 5.9) that are required for the application of the UCM approach dynamically. These parameters together with normalised sagittal hip, knee, and ankle angles were input in the

Matlab code for the numerical computations of the variance per degree of freedom within and orthogonal to the UCM. Ten walking trials for each subject were analysed and left leg data were used for the application of the UCM method. σ_{\parallel}^2 and σ_{\perp}^2 were compared throughout the stance phase of each participant and the balanced ratio compared among subjects. Mean and standard deviation of joint angles and CM trajectories as calculated from the geometric model, were also used for data analysis. Data analysis was conducted by first looking at the variability of joint angles and CM trajectories and then by looking at the UCM analysis, σ_{\parallel}^2 and σ_{\perp}^2 , to verify if the variability in the CM position was of the good or bad type. If $\sigma_{\parallel}^2 > \sigma_{\perp}^2$, the hypothesis about the control of the CM movement during gait was accepted. The same method and type of analysis was applied to the stroke patients who entered the RCT study (paragraph 5.3). Two conditions were analysed: walking with and without AFO. For both conditions six gait cycles were extracted at each test session and data kept for the analysis. The results from the two conditions were compared against each other.

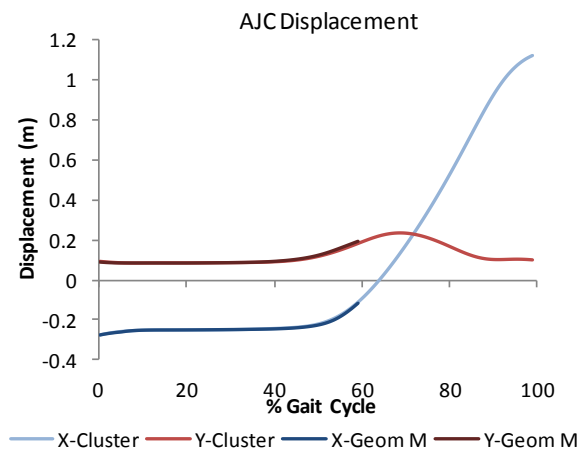
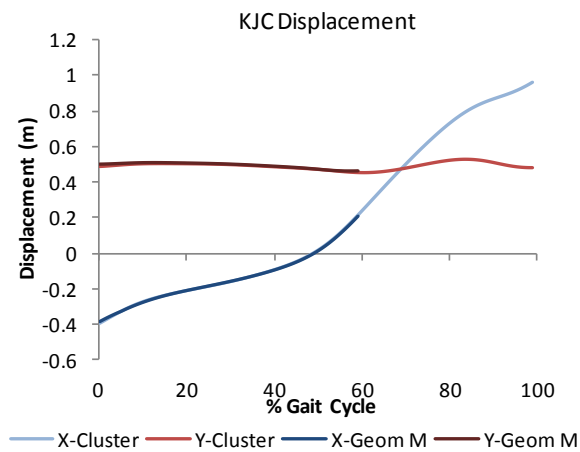
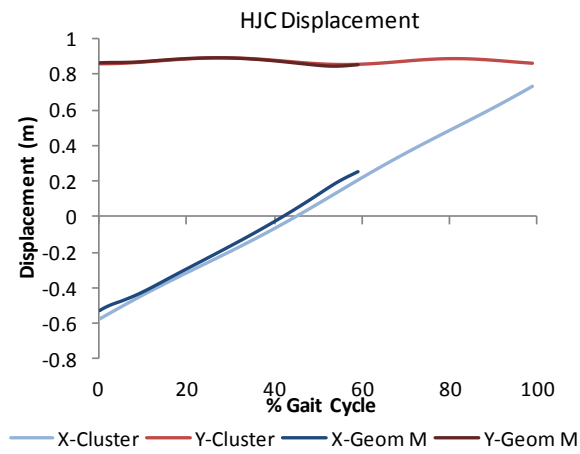


Figure 7.5: Hip, knee and ankle displacement in the x and y direction for one representative subject as obtained from the Cluster protocol and the geometric model.

7.4 Results

7.4.1 *Validation of the geometrical model*

To verify the geometrical model, the x and y coordinates of the hip, knee and ankle joint centres calculated using Equation 7.5 to Equation 7.8 were compared to the coordinates of the joint centres calculated by the Cluster protocol (Chapter 2) in the normal subjects during gait.

In Figure 7.5 hip, knee and ankle joint centres x and y trajectories of one selected subject are shown. From the geometric calculation joint centre displacements are calculated for stance phase only.

Very good agreement was obtained from the two methods of calculation as observed by the curves that are superimposed through stance phase.

7.4.2 *UCM analysis for able-bodied subjects*

Results of the application of the manifold approach are reported in this section for 6 able-bodied subjects. This data analysis is conducted by looking first at the variability of the joint kinematics in the sagittal plane and centre of mass displacement in x and y directions and secondly to the structure of variance within and perpendicular to the manifold. These data are thus reported sequentially.

7.4.2.1 *Joint Kinematics and centre of mass displacement variability*

Figure 7.6 shows hip, knee and ankle sagittal angles normalised to the duration of stance phase to 101 points as mean over 10 walking trials for the left leg for the six subjects tested. Variability of these outcomes is represented through the standard deviation bars in each plot.

Similarly the centre of mass displacements in the x (forward) and y (vertical) direction are illustrated in Figure 7.7. Mean and standard deviation bars from 10 walking trials are shown for each subject.

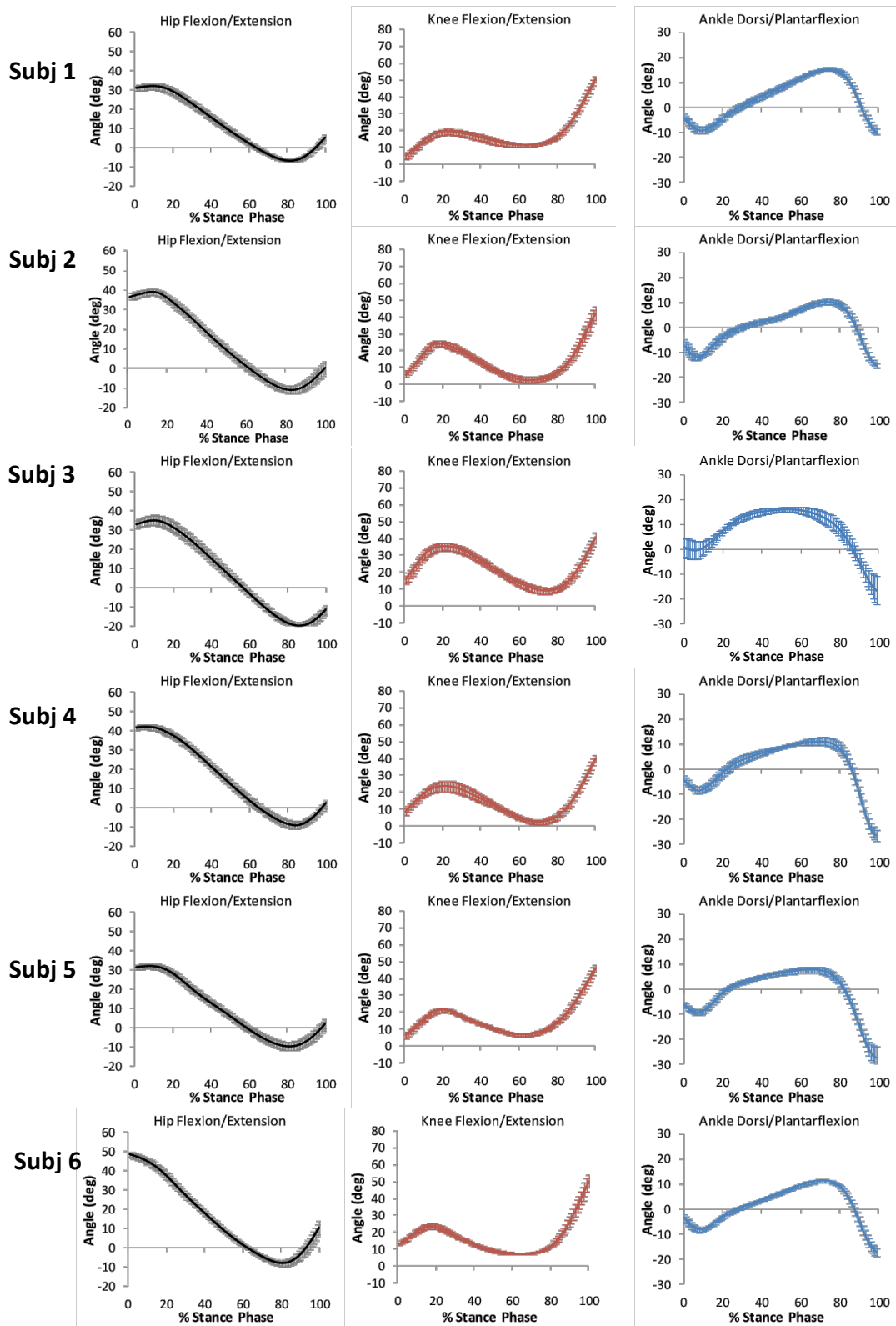


Figure 7.6: Mean and standard deviations bars of sagittal hip, knee and ankle joint kinematics of six normal subjects during stance phase.

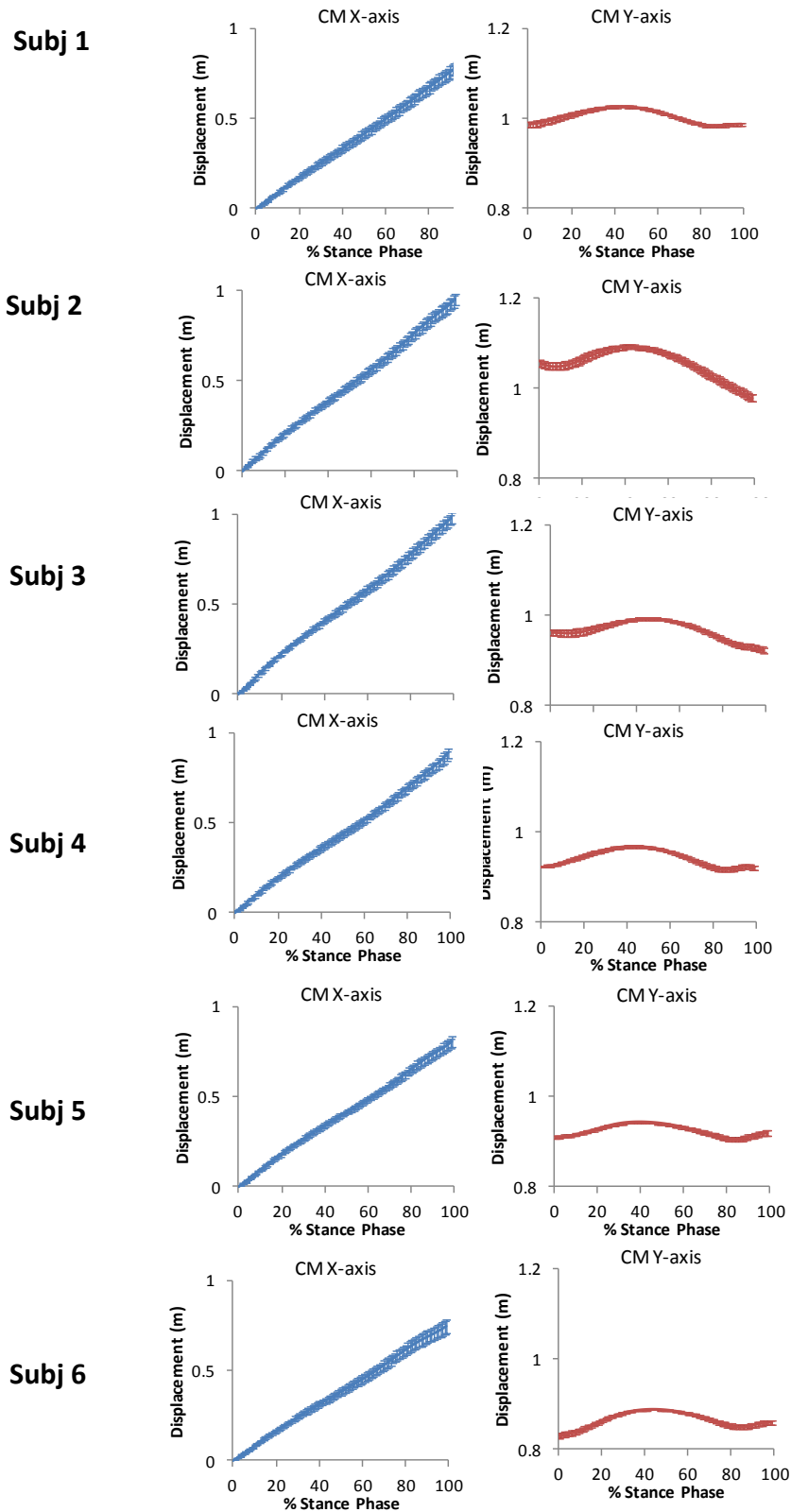


Figure 7.7: Mean centre of mass displacement during stance in the x and y directions for the six normal subjects. Standard deviation bars are shown.

7.4.2.2 Structure of joint configuration variance

With the UCM analysis, variability in joint kinematics is related to the variability of the CM position. The variance partitions per degree of freedom within (σ_{\parallel}^2) and perpendicular (σ_{\perp}^2) to the linearized manifold for the hypothesis about the control of the CM are shown in Figure 7.8. For each subject σ_{\parallel}^2 and σ_{\perp}^2 time series (% stance phase) are plotted. In the graphs, σ_{\parallel}^2 is indicated as Vucm whereas σ_{\perp}^2 as Vort.

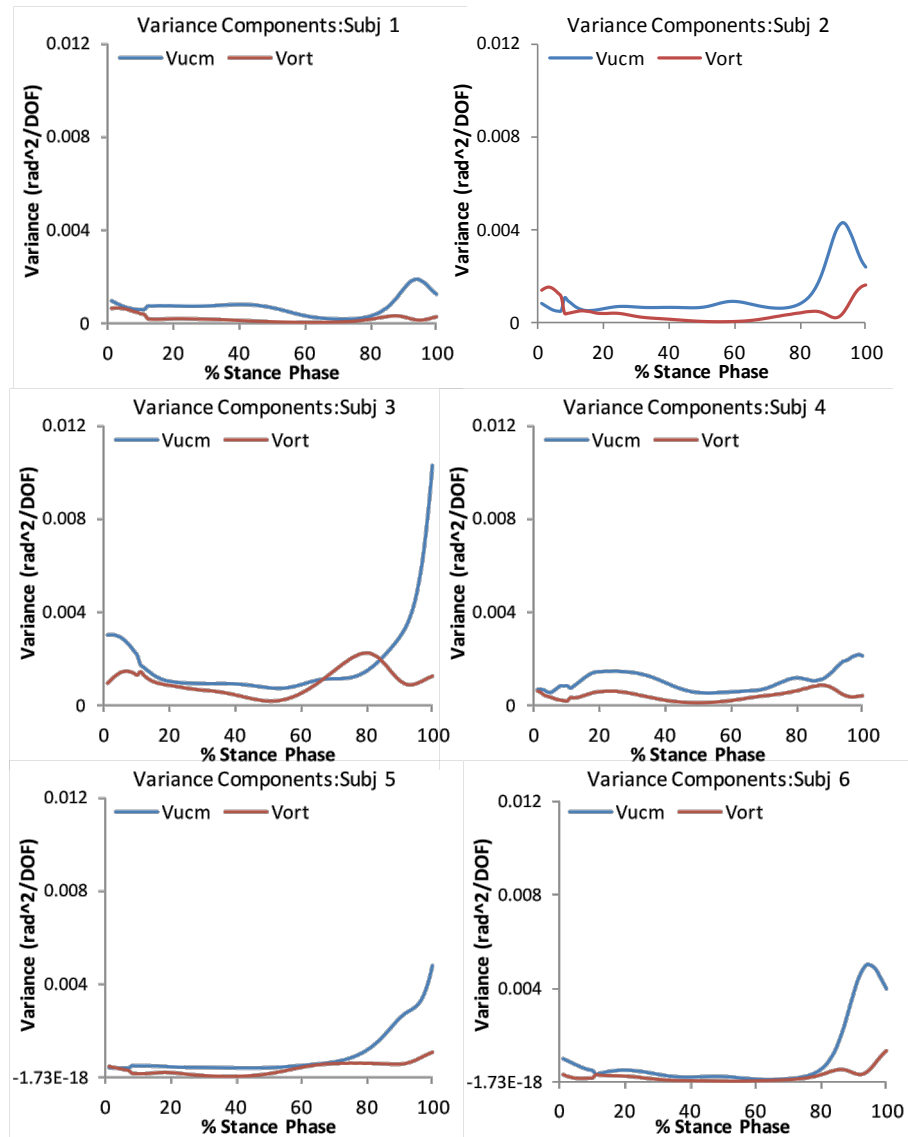


Figure 7.8: Variance components within (Vucm, blue solid line) and perpendicular (Vort, red solid line) to the linearized UCM.

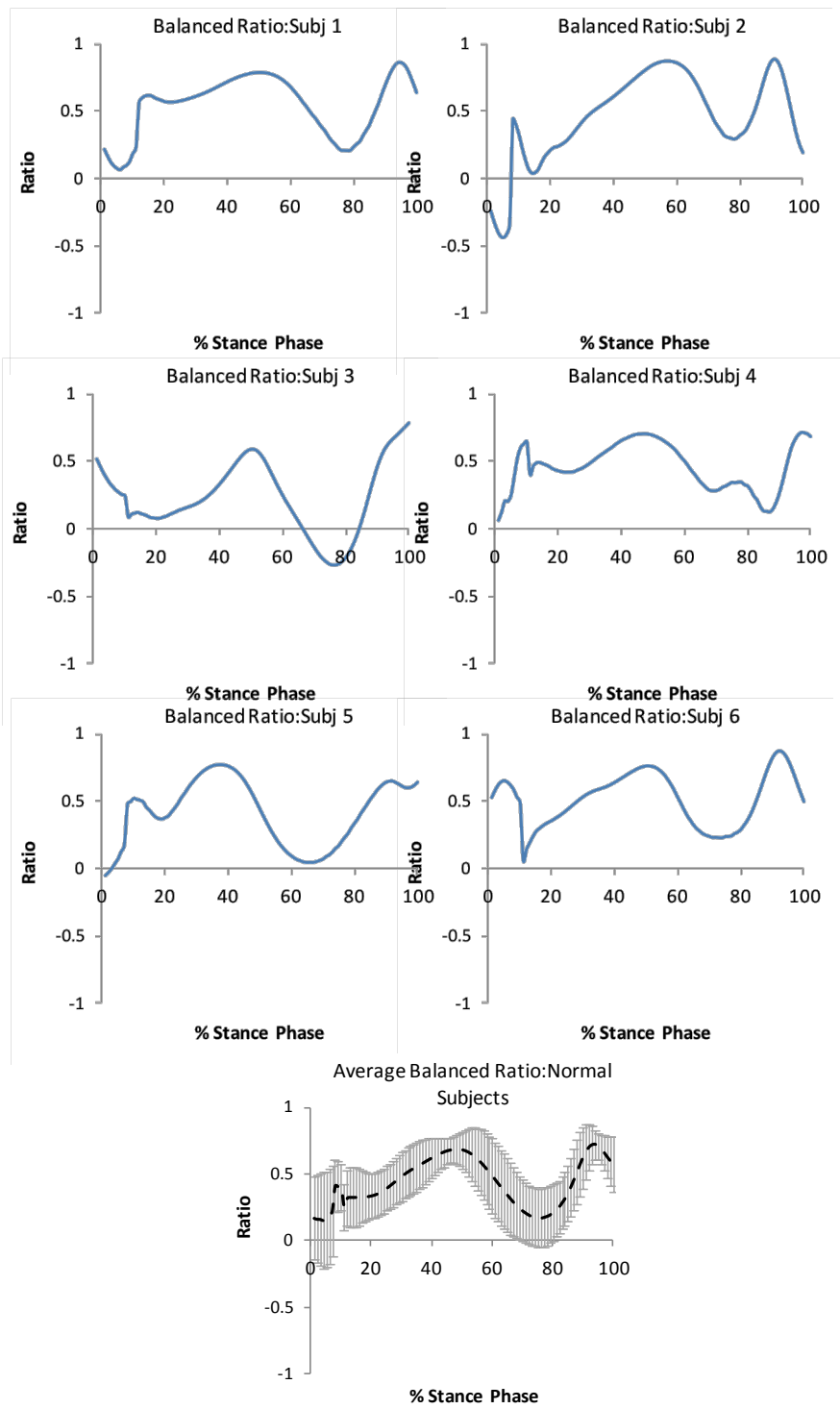


Figure 7.9: Balanced ratio for the six normal subjects.

The balanced ratios calculated from Equation 7.16 are plotted in Figure 7.9 for each participant. Values above or equal to 0 indicate that the hypothesis about the control of the CM can be accepted.

7.4.3 UCM analysis for stroke subjects

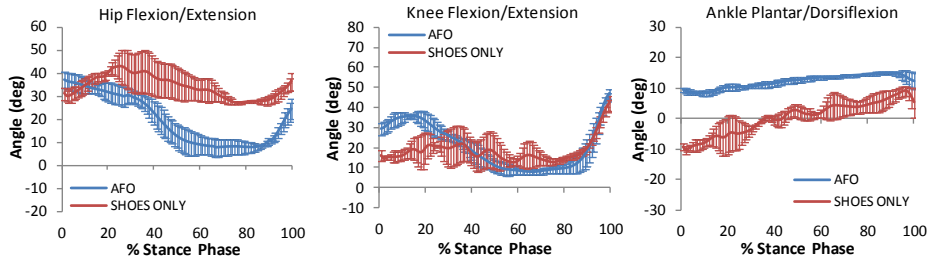
Results of the application of the manifold approach are reported in this section for the three stroke patients recruited for every assessment conducted. Variability of the joint kinematics in the sagittal plane and centre of mass position in x and y directions are firstly reported. Secondly the structure of variance within and perpendicular to the manifold are shown.

7.4.3.1 Joint Kinematics and centre of mass displacement variability

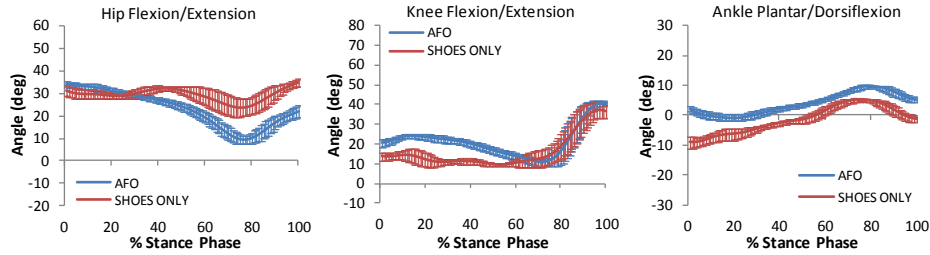
Figure 7.10 shows hip, knee and ankle sagittal angles normalised to the duration of stance phase to 101 points as mean over 6 gait cycles for the affected leg of the three stroke participants. Two conditions were analysed: walking with AFO and without AFO. Variability of the kinematic variables is represented through the standard deviation bars in each plot.

The centre of mass displacements in the x (forward) and y (vertical) direction are illustrated in Figure 7.11. Mean and standard deviation bars from 6 gait cycles with and without AFO, are shown for each subject and test session.

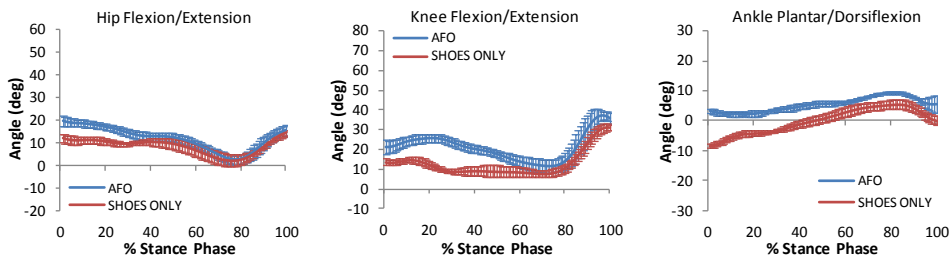
Case Study 1: Baseline



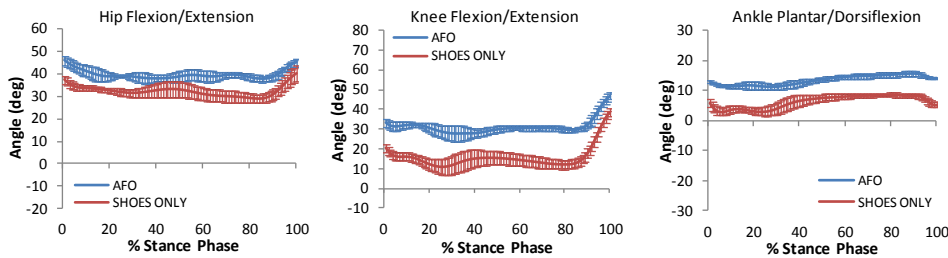
Case Study 1: Outcome



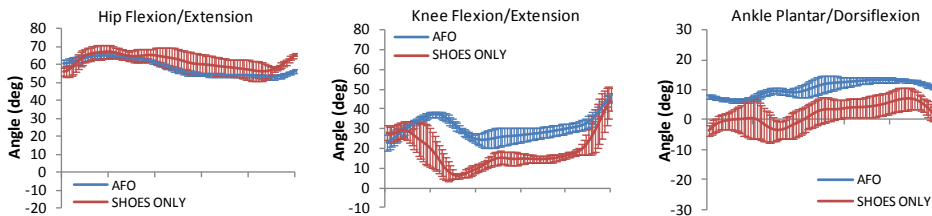
Case Study 1: Follow-up



Case Study 2: Baseline



Case Study 3: Baseline



Case Study 3: Outcome

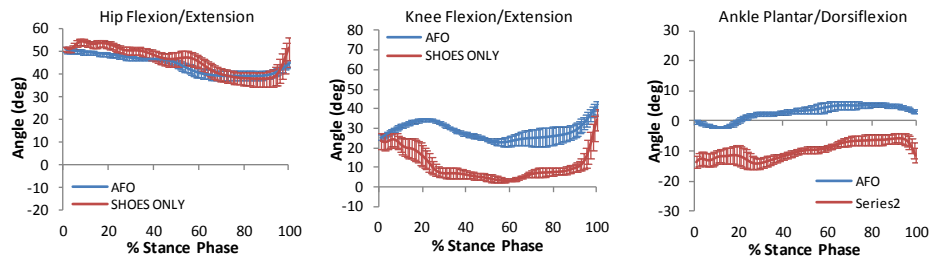


Figure 7.10: Mean and standard deviations bars of sagittal hip, knee and ankle joint kinematics with (blue solid line) and without AFO (red solid line) for 3 stroke patients during their assessment.

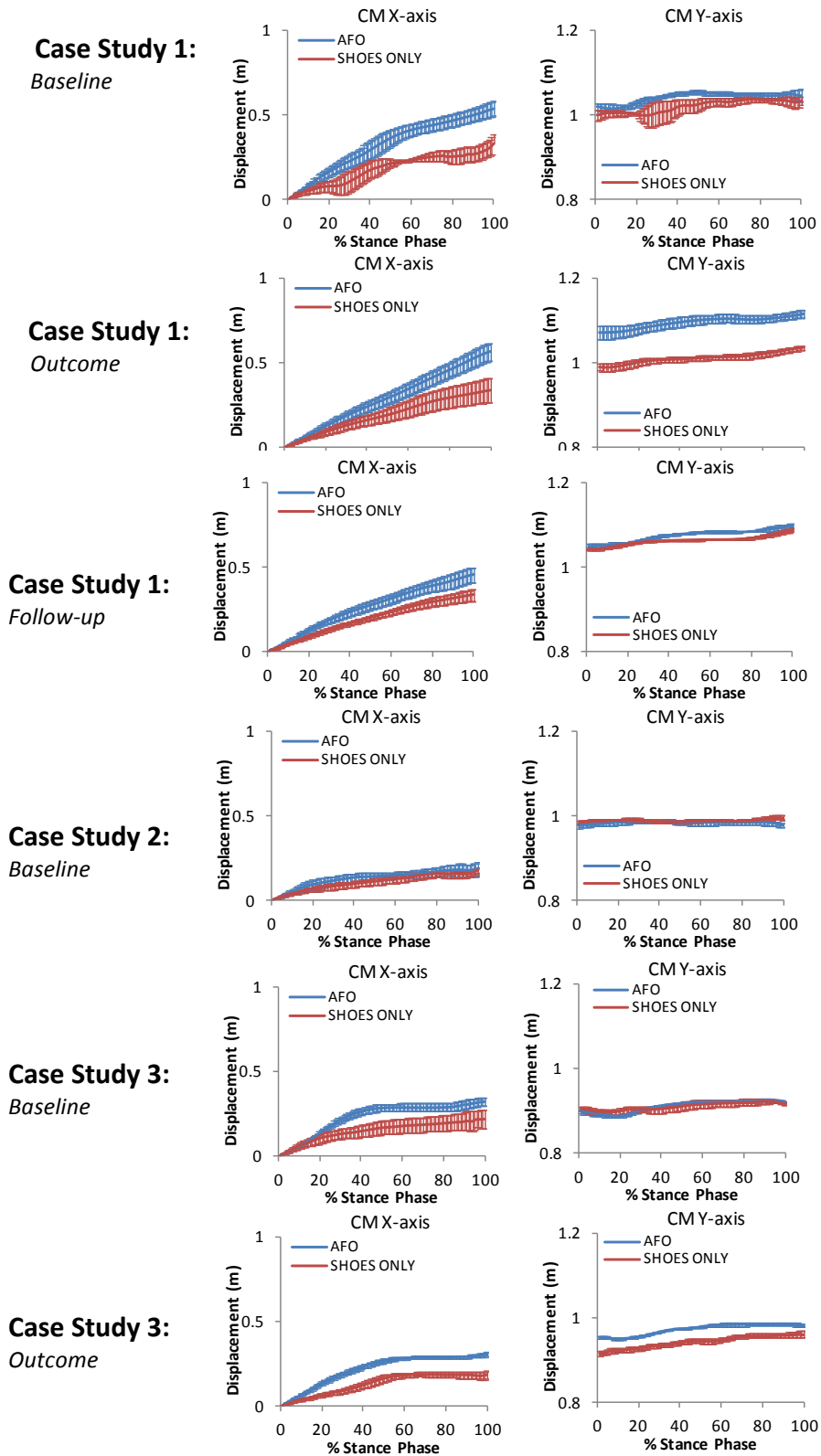


Figure 7.11: Mean centre of mass displacement during stance in the x and y directions for the three stroke subjects. Standard deviation bars are shown.

7.4.3.2 Structure of joint configuration variance

The variances per degree of freedom within (σ_{\parallel}^2) and perpendicular (σ_{\perp}^2) to the linearized manifold for the hypothesis about the control of the CM were calculated in each instant of time for gait cycle conducted with and without AFO. The time series (% stance phase) of the variances (σ_{\parallel}^2 , σ_{\perp}^2) for each stroke patient are presented in the graphs in Figure 7.12.

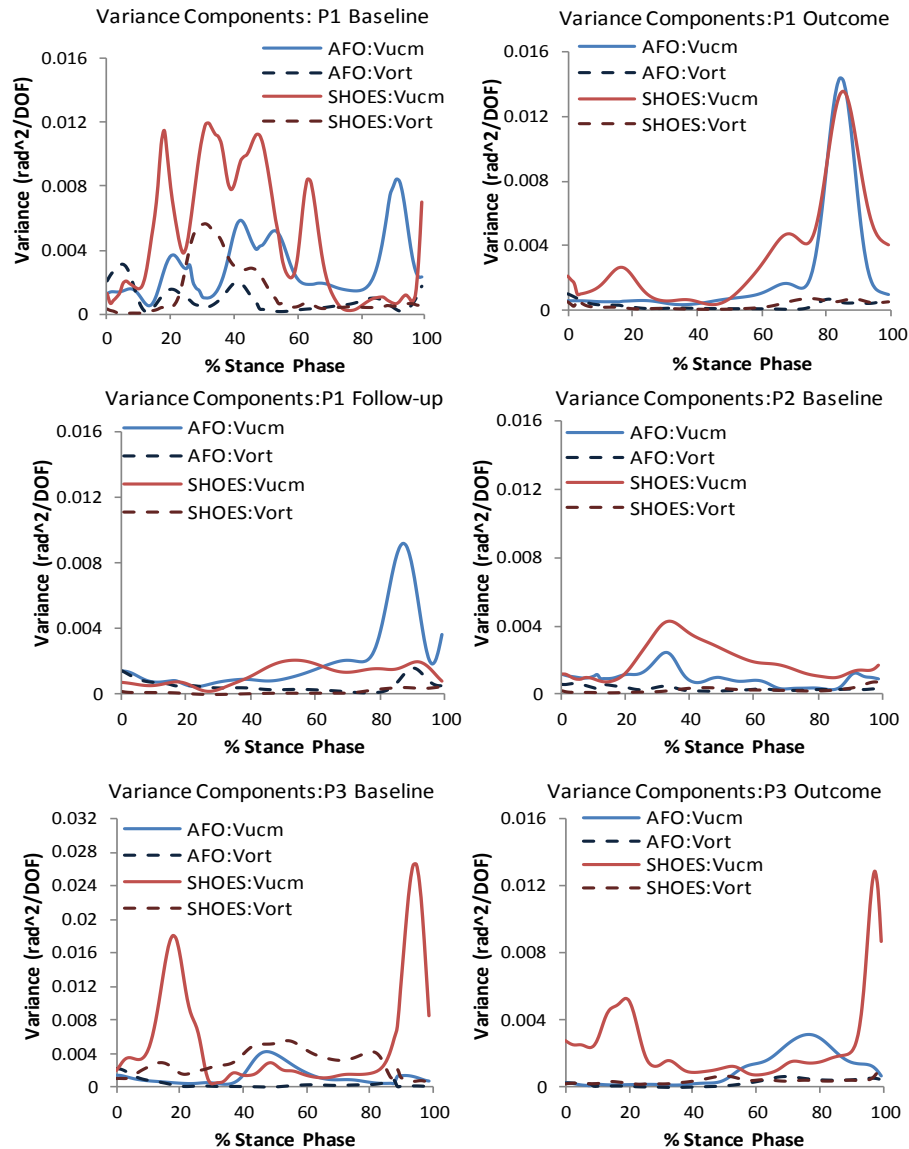


Figure 7.12: Variance components within (Vu cm, blue solid line) and perpendicular (Vort, red solid line) to the linearized UCM for the three stroke patients (P1,P2,P3).

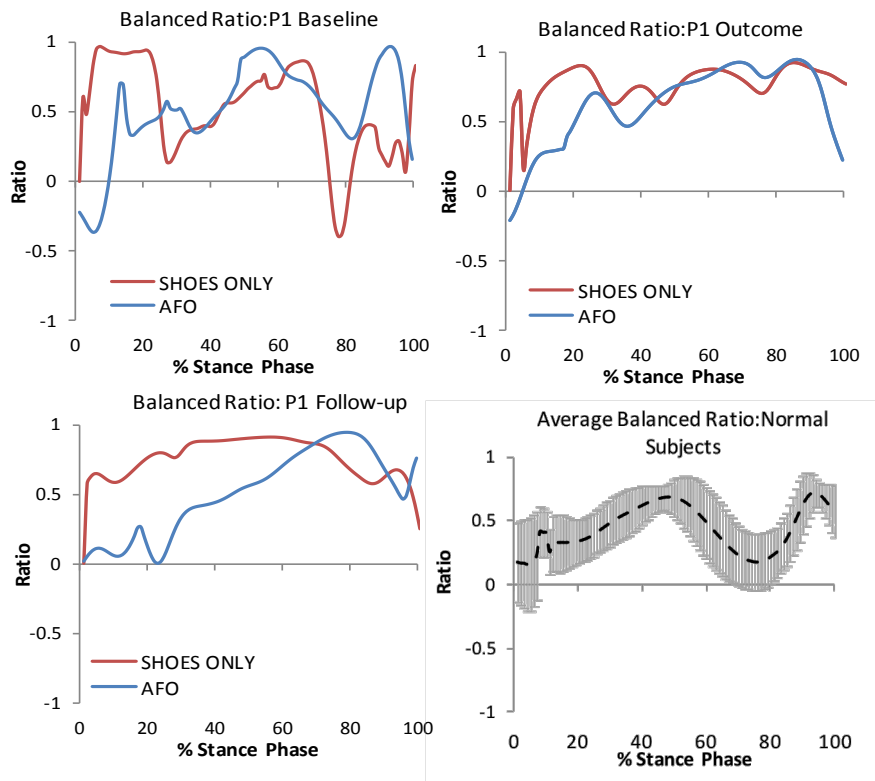


Figure 7.13: Balanced ratio for case study 1. Mean balanced ratio of normal subjects is shown as reference.

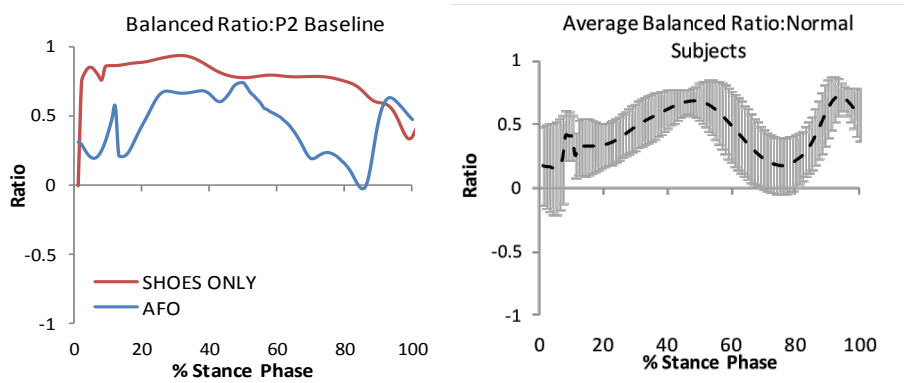


Figure 7.14: Balanced ratio for case study 2. Mean balanced ratio of normal subjects is shown as reference.

Figures 7.12, 7.14, 7.15 show the balanced ratios calculated from Equation 7.16 for the first (P1), the second (P2) and the third (P3) participant respectively, during the assessments they attended. Values above or equal to 0 indicate that the hypothesis, about the control of the CM, can be accepted.

The first patient walked in a controlled fashion to the respect of the CM position during gait with and without AFO as identified by balanced ratio above 0 (Figure 7.13) in all three assessments. The variability in joint angles, generally higher without AFO (Figure 7.10), was used by the participant to attain a stable position of the CM. The control of CM when the patient worn the AFO was reduced through the time (from baseline to follow-up); on the contrary, the control imposed without the AFO was always high. Confidence and stability acquired when walking with the AFO allowed the patient to be less vigilant with regards to the CM displacement. A similar trend to the normal subjects mean ratio can be appreciated particularly at follow-up, although time differences were present.

Similarly, subject 2 (Figure 7.14) controlled the CM position while walking in both test conditions. Without AFO, a great attempt was used by the participant in maintaining a firm CM position. Ratio values were well above 0. With the AFO, a close to normal subjects mean ratio was obtained for this subject.

Case study 3 showed some difficulties in controlling the CM position in mid to late stance without AFO (Figure 7.15). The balanced ratio was below 0 in the interval between 30 to 85% of stance phase at baseline assessment. Variations in the joint sagittal angles (Figure 7.10), for that interval, affected the CM position compromising patient balanced postures during stance phase. The poor balance, showed by subject 3, improved with the AFO. Despite the orthosis, bad control was observed at initial stance but overall the CM position was more controlled and, ratio values above 0 were observed. At outcome assessment further improvements were seen with the patient capable to attain a stable CM position through most of the stance phase. Poor control at initial stance with the AFO was still present.

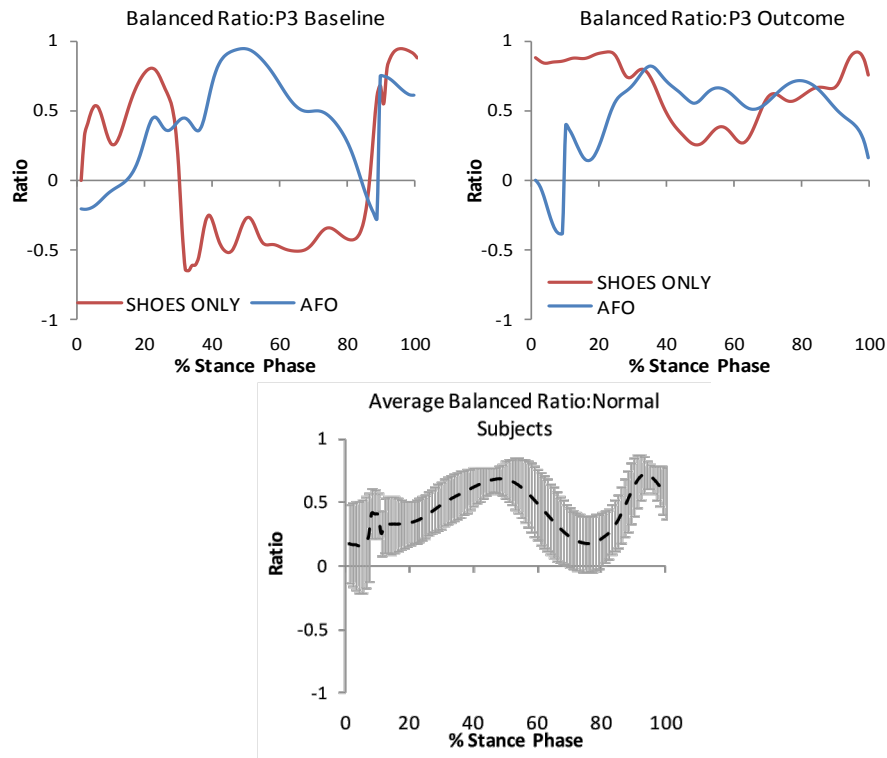


Figure 7.15: Balanced ratio for case study 3. Mean balanced ratio of normal subjects is shown as reference.

The control of the CM was among stroke subjects and normal subjects progressively increased until mid stance when single support of the analysed leg occurred. Control of CM increased again towards toe off when the leg was preparing to initiate swing phase and the weight was transferred to the contralateral leg.

It is worth to point out when analysing UCM approach results, that a more controlled variable (here CM), does not necessarily mean a good biomechanical walking pattern. The analysis provided explanation to the variability of the outputs of the biomechanical analysis and an understanding of the stroke subjects' strategy of walking.

7.5 Discussion

Through the uncontrolled manifold approach the variability obtained in the centre of mass displacements in x and y direction during stance phase while the stroke patients walked with and without AFO was classified accordingly to the subject ability to

maintain a stable or deviant centre of mass (CM) position from the reference configuration.

Hip, knee, ankle sagittal kinematics showed variability through stance phase in each stroke patient and particularly when the patients walked without the AFO. The different combinations of joint angle derived from this variability however were used by the subjects to maintain a stable centre of mass position across gait cycles. In UCM terms this is seen by higher values of the variance within the linearized UCM in comparison to the variance perpendicular to it or by a balanced ratio above 0. The findings confirmed the hypothesis about the control of the centre of mass and hence the variability observed was classified as a good variability. Only subject 3, at baseline when walking without AFO, presented with a variance perpendicular to the UCM greater than the parallel one and thus a CM position that deviated from the reference configuration.

Both able-bodied subjects and stroke patients have, overall, a variance within the UCM greater than its complement and hence stable CM position despite stroke patients presented with a higher variability of joint kinematics. This indicated that the stroke subjects adopted a way of walking which utilised more joint configurations without altering the final outcome, CM position.

Not a strikingly consistency was found when comparing the variances of the two conditions among subjects. Although a tendency of increasing the variance within the linearized UCM (or increasing the balanced ratio) when the subjects walked without AFO was observed. Without AFO, therefore, a major effort was put in the control of the CM position than when walking with an AFO. The AFO seemed to give the patients confidence such that they were willing to lower the control imposed on the CM position (i.e.: lower the balanced ratio) and walk in a more relaxed fashion.

The analysis of variance however is here limited to only 5 gait cycles. The subjects in fact had a limited autonomy before becoming too tired during the performance of the tests.

The aim of applying this approach was also to introduce a method, applied already to more stationary tasks, to gait in order to have a better insight on how this patient control selected performance variables and provide explanation to the variability at

the level of the elemental variables. The UCM analysis thus can provide information on if the variability of elemental variables is functionally employed with the purpose of achieving a successful task performance. To the regard of the rehabilitation practice it can be employed to verify if, for example, AFO intervention hinder or improve the achievement of a certain performance variable or more variables if more than one hypotheses are tested. It can be verified how a successful task performance is achieved by restricting the variance perpendicular to the linearized manifold or increasing the variance within it.

CHAPTER 8 – DISCUSSION

8.1 Introduction

The aim of this thesis was to explore methods with which gain an insight into how plastic AFOs, provided as rehabilitation aids, affect the walking ability of patients who had recently sustained a stroke and hence improve post stroke rehabilitation practice.

Consideration was given to the methodologies, and in particular movement analysis, that should be implemented in order to obtain valuable, meaningful and reliable results for this aim to be pursued.

A discussion of the findings from the three stroke patients recruited for whom the methods described were utilised is presented.

Moreover, in this Discussion, general comments on the methods proposed, gait analysis protocols, orthotic load measurements and uncontrolled manifold approach, are discussed to appraise the usefulness of such methods in evaluating stroke patients walking performances and AFO effects.

8.2 Case studies

Outcomes evaluation of the trial is limited to the three subjects recruited of whom only one completed the six months follow up.

8.2.1 *Gait analysis protocols outcomes discussion*

Hemiplegia following stroke impairs the walking ability of affected subjects with a first consequence of a decreased walking speed and reduced step lengths.

Moreover gait symmetry is compromised both in temporal and spatial terms due to the inability of the hemiplegic leg to cope with forward body progression. All three patients tested, and at the different time points, showed these characteristics in their gait. Without an AFO their walk was characterised by an asymmetric slow-paced sequence of gait cycles with restricted length.

Stance phase was prolonged and swing phase shortened on the affected side. This alteration was even more noticeable in the unaffected leg for which swing intervals

of 5% of the gait cycle were found. The long stance phases were due to the inability, on the affected side, of a smooth leg progression and efficient body weight transfer. The subjects tended to wait for the contralateral leg to fully strike on the ground before initiating swing phase preparation. Late stance and pre-swing of the affected leg occurred with the sound leg already on the floor. Only when both legs were on the ground did the patients start to raise their heel, hence long stance phases characterised by prolonged double support phases. For the affected leg, the terminal double support was of longer duration, whereas, for the sound side it was the initial double support that was the longest of the two. Consequently, the single support phases of the legs were reduced and particularly on the affected side.

Step length was also compromised by the instability and reduced mobility of the affected side. Lack of stability led the unaffected leg to accelerate its swing phase toward an anticipated heel strike to relieve the affected leg from weight bearing and therefore a short step length of the unaffected side. Reduced mobility, by means of a decreased leg lengthening prior to heel strike of the affected side, led to a reduced step length of that leg (hemiplegic). Moreover, for the second case study described, the fact that the patient had his gait regulated by a zimmer frame reduced the step length of the unaffected side due to restricted room for that leg to swing forward. These time and space characteristics of the gait derived from an altered lower limb kinematics of primarily the affected side but also of the unaffected side as this leg had to adjust to the impairments due to hemiplegia. Mainly kinematic deviations occurred in the sagittal plane of the joints although variations from normal kinematics were also seen in coronal and transverse plane of rotations for each participant. For these rotations however less consistency was found across subjects in comparison to sagittal plane movement.

The subjects showed an excessive ankle plantarflexion that led to initial contact occurring with the fore part of the foot or lateral border of the foot when the ankle was also inverted. This compromised heel rocker and shock absorption. Evidence of this was the lack of the first knee flexion peak in early stance in the three patients' knee sagittal kinematics and the failure to keep the tibia reclined until foot flat. The advancement of the affected leg was compromised by the inability to dorsiflex the ankle and bring the tibia into a proper anteriorly inclined position in mid stance.

The hip was flexed and retracted during stance and therefore also the advancement of the thigh was hindered. This slowed all the stance phase instants. Moreover, to gain stability while the contralateral leg swung forward the patients tended to lock their legs into a stationary position with the knee extended to different extent in the three patients. For the third patients described in Chapter 6, knee hyperextension was clearly visible.

Having the hemiplegic leg locked in stance phase constrained hip extension and therefore reduced the possibility of the unaffected side advancing further, under the pushing effect of the affected leg lengthening while maintaining contact with the ground. The unaffected leg was forced to terminate swing phase and shorten the step length while the contralateral leg waited with the entire foot on the ground.

An inadequate second knee flexion peak and a plantarflexed ankle compromised swing phase and put the leg on to toe drag hazard. The patients tried to compensate for these by increasing hip flexion that lifted the leg up and by more energy requiring actions such as hip hiking and hip circumduction for a safer ground clearance.

The subsequent initial contact was shortened by an incomplete knee extension in late swing; the knee was always flexed at initial contact.

Moreover, the subjects showed the inability to walk while maintaining an upright posture but rather they leaned the trunk forward. Anterior tilt accompanied with positive obliquity and negative rotation characterised the movement of the affected pelvis.

Positive effects on lower limb joint kinematics were observed when the subjects walked with the AFO.

First of all plantarflexion at the ankle was controlled allowing initial contact to occur through the heel rather than the fore part and lateral border of the foot. Heel rocker was regained and tibia progression enhanced although a reclined position at foot flat could not be achieved. This is to be related to the neutral angle of the tibia given by the AFO and footwear combination and tuning effect when performed. The AFO thus provide an inclined position of the tibia to start with.

Weight acceptance through the affected leg was refined with a knee flexion peak achievable in early stance although simultaneous plantarflexion at the ankle was limited by the AFO. It was observed that for the patients who were randomised into

the intervention group and received a rigid AFO with carbon fibre reinforcement (case study 1 and 2), plantarflexion of the ankle could not be achieved, as the AFO maintained the joint in a dorsiflexed position. For the third participant, at outcome assessment, plantarflexion at loading response was observed but not in late stance. This is explained by the different stiffness of the orthosis provided to this subject. The rigid AFO related to the intervention group is characterised by an increased stiffness which held the ankle into a firm position through the gait cycle as also noticed for ab/adduction and inversion/eversion plots of the ankle in which almost flat curves were obtained.

Dorsiflexion of the ankle was achieved through stance phase increasing the peak at terminal stance obtained without AFO and tibia inclination in mid to late stance. At the ankle level the AFO also corrected in each patient the inverted position of the foot preventing the peak usually observed in swing phase which imperilled ground clearance.

Knee hyperextension was controlled and knee flexion enhanced in late stance; although in comparison to able-bodied subjects knee flexion was still inadequate but sufficient for a safe swing phase initiation.

Hip flexion was reduced at initial contact as was extension achieved in mid to late stance, although this was different among the three subjects. The better outcome in terms of hip extension was achieved by the patient of case study 1. The thigh was able to move from a posteriorly inclined position to an anteriorly inclined position with the AFO encouraging extension and facilitating limb advancement. For this subject a progressive improvement was observed from baseline to follow up assessment in the hip's capability to extend.

In case study 2, controversially hip extension did not improve with the AFO but the hip remained locked into a flexed position. Thigh inclination could not be achieved in subject 2 for who the thigh resulted even more reclined than without AFO.

This demonstrated that the AFO can have effects at the hip but, for these effects to be of benefit to the patients, a correct tuning is fundamental. For patient 2 in fact the forward inclination of the tibia resulting from enhanced dorsiflexion and the increased knee flexion position, transferred the knee joint centre further hindering hip extension and thigh inclination in late stance.

This should explain the undesired effect of the AFO for subject 2 who may have benefitted for a smaller neutral inclination of the tibia given by the tuning process. For subject 3, hip extension was improved when the patient walked with the AFO, although to a lesser extent than for subject 1. The knee was held into a sustained flexed position in mid to late stance making it more difficult for hip extension to occur. As for subject 1 the effect of the AFO at the hip was maximised at outcome assessment. For all subjects however, the reduced ability to extend the hip was also due to an affected retracted hip, even if hip retraction was diminished when the subjects walked with their AFO.

Swing phase occurred safely although hip hiking was still observed and the knee could not extend completely for the subsequent heel strike.

During the gait cycle forward lean of the trunk was lessened as a consequence of an acquired stability during stance of the affected leg in supporting the body weight without compromising the patient balance. Subject 2 did not show any improvements in anterior tilt with the AFO as his posture derived mainly by the use of the zimmer frame and hence remained constant among walking trials.

Minor influences of the AFO in ab/adduction and internal/external rotations were observed for pelvis, hip and knee. However, at the foot significant variations were observed in these two planes, as already mentioned.

The sound leg kinematics deviated from normal subjects' joint motion in an attempt to compensate for the affected leg in both tested conditions, with and without the AFO. Kinematics curves closer to a normal lower limb kinematics pattern were observed in the sagittal plane in comparison to the affected leg although shock absorption was often altered, the presence of a flexed knee was observed during stance and, hip extension was reduced. Only for subject 3 at the follow up assessment, knee flexion peak at loading response and hip extension in terminal stance were observed for the unaffected leg when walking with an AFO. The unaffected leg's coronal and transverse plane rotation patterns showed adjustments for the affected leg seeking for stability by widening the base of support using hip or knee abduction and by externally rotating the knee.

The improvements in lower limb kinematics achieved with the AFO were reflected also in the spatio-temporal parameters of the gait. Walking speed was increased in

two out of three patients tested but the velocity achievable was still low in comparison to able-bodied subjects. The subject for whom no increase in velocity was found walked with the zimmer frame that seemed to regulate the timing of his gait cycle.

Stance phase duration was decreased for both legs and swing phase consequently prolonged although the differences between the two tested conditions were not always statistically significant. Single support phase of the affected leg was increased significantly with AFO for subject 1 and 3 whereas, comparable results were found between the two conditions for subject 2.

In spite of the improvements achieved with the AFO in the gait cycle intervals, these subdivisions were still different from normal able-bodied phases and only for subject 3 at follow up could close to normal stance and swing phase durations be obtained with and without the orthosis.

Gait symmetry was also enhanced significantly by the AFO in all three subjects although for subject 3, at outcome assessment, a more symmetric gait was achieved without AFO.

The AFO also increased the step length of the affected side as a result of increase stability of the leg but step length of the unaffected side was not always longer with the AFO due to the persistent inability of the unaffected swinging leg to extend the knee allowing a more advanced initial contact. Step length of the sound leg was however greater than for the hemiplegic leg resulting in a spatial asymmetry of the gait even if enhanced in comparison to shoes only walking.

Worthy of mention is the effect the AFO had over time in the two participants who were possible to assess at different time points during their rehabilitation process. Improvements were observed from baseline and outcome in both subject 1 and subject 3. Moreover, subject 1 was able to further improve at follow up from outcome test session although the progress was reduced in comparison to what was achieved at outcome from baseline. Also when walking without an AFO, the patient could do it better at follow up than at baseline and outcome assessment.

Although only three subjects were analysed in this study and hence conclusion cannot be drawn on the actual effect of the AFO on stroke gait, a few points emerged that relate to data gathered from the literature.

Through this study it was seen that the AFO influenced the way a subject walked at the ankle level but also at the knee, hip and pelvis.

Direct effects of the AFO were confirmed as the ability of an acquired dorsiflexion position of the ankle in stance encouraging heel contact as start for a new gait cycle and decrease of plantarflexion in swing for a safe ground clearance. This agreed with reported literature (Lehmann et al., 1987; Hesse et al., 1996, 1999; Gok et al., 2003; Fatone et al., 2009; Bregman et al., 2010). In addition correction of foot inversion particularly in swing could be observed from the results obtained although conducted studies are limited to the description of sagittal ankle kinematics. Only one report mentioned a reduction in inversion of the foot when subjects walked with Air-Stirrup[®] (Burdett et al., 1988).

Indirect effects of the AFO were also noticed in the sagittal plane kinematics of the hip and knee and less for the other two planes of rotations. To this regards, only a few studies were found to report on sagittal knee and hip kinematics and none on coronal and transverse plane rotations.

The effect achievable at the knee was to decrease knee hyperextension as also commented in previous studies conducted by Lehmann et al. back in the 80s and more recently by Butler et al. (1997), Miyazaki et al. (1997), Yamamoto et al., 2005, Yokoyama et al. (2005), Fatone et al. (2009), but also to re-establish shock absorption through the first knee flexion peak. On this, only one group of researchers (Yamamoto et al., 2009) gave account, showing improvements in knee flexion at loading response. The second knee flexion peak in late stance was also enhanced by the AFO in the current study but no reference on this was found.

At the hip level, less consistency was found in the outcomes attainable through the use of an AFO in this study but what is interesting and emerged from the results is that the AFO can influence also hip kinematics as potentially believed from evidences in cerebral palsy children (Bowers & Ross, 2009) and as highlighted as an issue to be addressed during a consensus conference of the International Society of Prosthetics and Orthotics (ISPO) (Condie et al., 2004).

Among the studies who reported the effect on the hip, one (Bregman et al., 2010) did not find any influence in hip flexion/extension when the test subjects walked with the AFO and another one (Yokoyama et al., 2005) reported two contrasting

achievements in the two subjects tested, an increase and a decrease in hip flexion in swing. In the current study the main influence the AFO had on hip kinematics was to modify extension in mid to late stance and reduce flexion during swing as a consequence of a decreased demand for lifting the leg up through greater flexion at the hip to clear the ground.

The capability of the orthosis in affecting hip sagittal angles was found to be dependent on the appropriateness of the AFO prescribed and its inclination following the tuning process. For subject 2, an undesirable hip flexion was achieved in stance preventing extension to occur. Although increased dorsiflexion at the ankle level was observed the position acquired may have been too much for the patient leading to an increased forward movement of the knee and backward position of the hip inhibiting extension from occurring.

Careful attention should be paid at the time of fitting to obtain a maximal beneficial effect from an AFO without focusing only on the most obvious corrections achievable at the ankle level as this can affect other joint kinematics. A tailored AFO to each subject's impairment should not compromise leg advancement as partially found in subject 2. If the AFO is able to positively change hip sagittal angles, leg advancement results enhanced with a positive effect on all body progression processes, smoother and less tiring gait for the patient and the possibility that compensating actions may not be required anymore.

Improvements in patient posture during walking as observed for the participants of the trial were only reported by Yamamoto et al., (2009).

Moreover, the studies previously conducted do not take into account the unaffected leg for which results are discarded from the analysis while it is believed that also the unaffected leg has an important role in the overall improvement of stroke patient gait although it reflects the achievements gained in the hemiplegic leg.

The slow pace and short step length and asymmetric gait both in time and space that characterised stroke patients way of walking was turned into a more symmetric and faster sequence of longer steps by the AFO. However, the differences in spatiotemporal parameters between AFO and shoes only walking were not consistently significant across subjects and sessions. These discordances were found also in the literature where only some studies showed significant improvements

accomplished by the use of the AFO (Leung and Moseley, 2003; Gok et al., 2003; Franceschini et al., 2001, 2009; De Wit et al., 2004; Wang et al., 2005; Fatone et al., 2009; Abe et al., 2009; Bregman et al., 2010). Again the correctness of the AFO to cope with subjects' deficits played an important role in the outcomes obtained in the current study and in the reports of the literature.

Limitations of this study and other studies in the literature (Chapter 1) are the relatively small number of patients recruited. Further investigations are required to clarify the benefits achievable from the AFO in order to maximise stroke patients' recovery in terms of gait ability. The methods developed in this thesis are capable of clarifying these benefits.

It should also be considered that the aim of AFO intervention is to obtain the best outcomes for each patient to gain stability and a safe and efficient leg advancement rather than aiming a priori to a normal gait pattern that will be difficult to restore.

7.2.1.1 AFO dorsiflexion/plantarflexion moments

For the first case study presented, the subject also completed the kinetic protocol with a strain gauged AFO. Hence plantarflexion/dorsiflexion moments exerted by the AFO were measured.

The main contribution of the AFO was to provide a dorsiflexion corrective moment at initial stance. The contribution in late stance was in a plantarflexion direction and was minimal. This correlated well with the findings reported in the literature by a research group of the Tokyo University (Miyazaki et al., 1993; 1997; Yamamoto et al., 1993) for which a higher dorsiflexion contribution in early stance was found in comparison to plantarflexion in late stance; however they used an experimental AFO design that approximated the rigidity of a plastic AFO through the use of springs.

The plantarflexion peak in the affected ankle total moment was achieved by virtue of the patient's muscle power and passive tissue resistance since no contribution was provided by the AFO. The peak achieved however did not exceed a mean of 50 Nm. This was explained as a diminished proportion of body weight supported through the affected leg. The body weight was also being sustained through the stick.

A higher peak in plantarflexion was instead achieved in the unaffected leg although it lacked of initial dorsiflexion moment. The initial contact of the unaffected leg,

although it occurred through the heel was followed by a rapid foot flat that kept the ground reaction force forward with respect to the ankle joint together with the presence of the stick on the same force platform.

The stress registered in the AFO in correspondence of the dorsiflexion peak was found to be higher ($> 4\text{MPa}$) in comparison to the values experimentally found in the literature for which values of maximum 2MPa were reported (Chu et al., 1998; 2000). However this could be related to the different geometry of the AFO tested and condition of the tests and most probably from the calculations performed. In the current study, the fact that the stress was calculated using an experimental Young's Modulus may have biased the results. The Young's modulus used was as high as 2062.3MPa . This value multiplied by the strain could have produced a higher stress value than if a smaller Young's Modulus would have been used. No details of the calculations are given in the published reports.

The use of this method to estimate orthotic loads was found to produce reasonable results with a good level of repeatability given the material properties and the impaired gait of the participant tested. Valuable information can be extracted and the contribution of this type of AFO at early stance was highlighted providing the patient with improved ankle kinetics in addition to ankle kinematics as already discussed.

8.3 Methodological considerations

8.3.1 *Gait analysis protocol*

Two protocols for gait analysis were proposed in this thesis. Firstly the cluster method which relies on sophisticated technology providing a 3-D description of the pelvis and lower limb kinematics and kinetics and, second an Augmented Video-based Portable System (AVPS) simpler requiring only a video camera and a grid mat for the evaluation of spatiotemporal parameters and shank to vertical angles. Both protocols were shown to produce reliable results in a repeatable manner (Chapter 2, Chapter 3) and, therefore, the decision to use such protocols to investigate stroke patients' gait. Standard deviation in joint kinematics for the first protocol was confined to 3° and also small sizes of standard deviations were found for the parameter evaluated with the AVPS that were well below 1cm for length values, and around 0.1 s for temporal parameters.

Whereas the 3-D gait analysis protocol, cluster method, provides an objective description of the human movements and helped in the explanation of the reasons why certain impairments could be seen, the AVPS technique provides more immediate patients screening that helped in the quantification of when certain events occurred in the gait cycle. Although the outputs of each protocol could stand on their own, they are correlated and information when analysed together provide a more comprehensive understanding of the way stroke patients walked.

From a more practical point of view the AVPS, being a simpler method, allows for a faster implementation than the cluster protocol reducing to a minimum patients' effort during a test session. In return, the cluster method, although requiring additional time for patient preparation, provides outcomes that are keys for the understanding of stroke gait biomechanics. Quantification of pelvis and lower limb kinematics of stroke patient when walking with and without AFO allows the identification of the differences, if there are any, between the two conditions tested and thus the benefit an AFO may provide can be inferred. These results can be more explanatory of the actual effects of the orthosis on gait rather than only simple spatiotemporal parameters. One can walk with longer steps and faster but it could be the way the subject walked which is of primarily value rather than only the step length and the velocity. This could be important in stroke patients as they have to start to relearn how to walk and the improvements achievable can be maximise if correct biomechanical principles can be applied along with the rehabilitation practice. 3-D gait analysis provides evidence for this and guide patient, therapist and orthotist as to what is wrong and what must be practiced to put it right.

Ideally it should be possible to use both the methodologies to gain a wider perspective on the walking ability of the test subject. Studies on stroke patients are often limited to reports of walking velocity and spatial parameters of gait. The few reports of the kinematics of gait in stroke lay particular emphasis on sagittal plane kinematics. The advantage of using the cluster method is to provide a full 3-D description of joint kinematics and kinetics, provided the patient is capable of a single strike on a force plate. To these, spatiotemporal parameters and shank to vertical angles can be added by using for example the AVPS method. Shank to vertical angle (SVA) also represents an interesting parameter for stroke patients as

SVAs reflect the ability of the subject to progress the tibia during stance and evidence of heel and ankle rocker capability.

Some limitations also characterised the methods adopted.

The cluster method is prone to error as consequence of misplacements of anatomical landmarks from which the rotation axis of the joint are defined. Careful identification of bony prominences should be performed but, their location is not always easily identifiable, especially in overweight subjects. However, the cluster method allows the flexibility of using a pointer to identify anatomical landmarks if strictly necessary. That presents as a good compromise to maintain the reliability of the results in spite of the additional time required for subject calibration.

Skin movement artefacts, also if minimised by the use of rigid cluster positioned on the distal part of the body segments, can still be present and introduce errors.

Finally, the identification of the hip joint centre is not subject specific since the use of a predictive method was chosen over functional methods. This represents however a common practice among motion analysis protocols to avoid additional tasks to be performed and to avoid the limitations that could derive from patients with a restricted range of motion at the hip and the difficulties of some patients to support themselves on a single leg.

Regarding the AVPS method, apart from the already commented long post-collection data analysis (Chapter 3), limitations rely on the subjectivity that could affect the identification of gait cycle instants. This however was found to be marginal as a small inter-rater variability was obtained in the preliminary study conducted. To further avoid errors one should clearly clarify what is intended to be identified in the gait cycle and allow consistency in the measurements. This can be addressed by a descriptive protocol in which definitions are given for the instances of the gait cycle to be marked in the trial.

Overall, two gait analysis methods were introduced capable of detecting impairments characterising stroke gait either with or without AFO. Moreover, the protocols were suitable for the assessment of early stroke patients, who were able to complete the test session to which they took part.

8.3.2 *Orthotic load measurement*

A methodology that can be used to estimate the fraction of the ankle joint moment attributable to the AFO was introduced in Chapter 4. The method was applied to a normal subject and a stroke subject and while preliminary, the findings suggested that the method is feasible for the determination of plantarflexion/dorsiflexion moment contribution of the AFO.

Repeatable results were found in the outcomes from strain gauges attached on polypropylene despite its viscoelastic nature. This enabled an unmodified AFO to be used without the need to insert metal bars on which strain gauges reliability is widely recognised. The fact that alterations of the AFO were not necessary allows for the test to be conducted on the actual AFO provided to the patients and thus more realistic estimations of the AFO moments can be obtained. The AFO maintains its properties and the loads applied to it are under real walking condition and, the moments are obtained directly from strain gauges measurement.

Previous conducted studies that attempted the determination of AFO moments and stress developed in the orthosis were limited by the use of modified/experimental orthosis (Yamamoto et al., 1993a; 1993b; Miyazaki et al., 1993; 1997) or conventional metal and leather AFO (Magora et al., 1968; Robin and Magora, 1969), nowadays superseded by plastic AFOs; simulation of loads applied in finite element analysis studies based on restrictive assumptions (Chu et al., 1995a; 1995b; Syngellakis et al., 1998; Uning et al., 2008) or through muscle-training machine (Chu and Feng, 1998) to mimic gait movements; or by the use of indirect method exploiting ankle joint angle and AFO stiffness, not always easy to quantify, for the calculation of AFO moment (Bregman et al., 2010).

The method proposed seemed to fit well in the limitations found among published studies and the potential of the method in quantifying AFO moment was revealed. Knowledge of the AFO contribution to the ankle moment represents an important parameter for the understanding of the effect an AFO has on the gait of stroke patients. Being able to quantify such a variable will be of value to refine AFO prescription to better match the patient need with the AFO mechanical properties. Ideal it would have been if also the stiffness of the orthosis was available. AFO with different stiffness contribute differently to the ankle moment and at various instants

of the gait cycle (Yamamoto et al., 1993; Sumiya et al., 1996); knowing also this measure will allow for an even more conscious AFO prescription decision.

8.3.3 *Uncontrolled Manifold analysis*

The uncontrolled manifold (UCM) approach was formulated to be applied on gait analysis data to test the hypothesis about the control of the centre of mass (CM) position (Chapter 7). This was done with the perspective of establish if the CM movement is of concern in stroke patient gait by characterising the nature of the variability of its position.

The geometric model, used to link variations in joint angles to that of the CM position in the current analysis, was shown to be a realistic representation of a subject lower limb body as demonstrated by the comparison of joint centre locations obtained geometrically and through the cluster method.

The model, however, was based on the assumption that the CM is at a fixed point in the pelvis. This choice was made to simplify the formulations of the UCM approach in a first instance. Calculation of the CM as a sum of each body segment centre of mass weighted with respect to segments' mass could be included as further development of this approach.

Another limitation of the method was to confine the analysis only to the xy plane (sagittal) and to the duration of stance phase.

The method introduced, although simplistic, showed reasonable results. Consistency was found in the variance outcomes obtained from the UCM analysis of normal and stroke subjects' gait. Generally, results confirmed the CM position being a controlled variable as the variance within the linearized UCM was greater than the variance perpendicular to it.

The advantage of the method proposed over studies already conducted is the ability to perform the analysis through a period of time rather than be concentrated to only instances of the motor task performed and its applicability to gait where most of the studies concentrated on upper body tasks and sit to stand performances (Scholz and Schoner, 1999; Domkin et al., 2002; Reisman and Scholz, 2003; Scholz et al., 2003; Yang et al., 2007; Hsu et al., 2007).

The UCM analysis allows a classification of the variability of a selected control variable with respect to the elemental variables and it can be seen as a tool to appraise the effect of rehabilitation over time or in different conditions (as for the current study) such as walking with and without an AFO. Its utility is to provide explanation on how the central nervous system act to cope with the different degree of freedom available for the walking task and how it compensates if impairments at the elemental variable level are present. It is another form of analysis to be added to the results of 3-D gait analysis in the process of evaluating stroke gait kinematics for which a retrospective analysis is conducted through the UCM.

In summary, all the methods discussed, gait analysis protocols, instrumented AFO test, UCM approach, even if they looked at different aspects of the gait, were able to provide reliable and valuable outcomes for the scope of characterising stroke patients walking performances.

The question now lies on if all these data are necessary for the evaluation of stroke gait. For the purpose of rehabilitation and motor relearning, therapist and orthotist should focus on a sound biomechanical gait that allows these patients to cope safely with daily life activities. In order to verify the biomechanics of gait and how this can be influenced through intervention such as the provision of an AFO or simply dedicated physiotherapy treatment, or how gait changes over a period of time, 3-D kinematics (and kinetics) data are of most value. They allow a quantification and description of a good or bad gait biomechanics differently from only spatiotemporal parameters. An increase in walking speed, for example, may not necessarily imply an enhanced gait pattern. Systems such as the AVPS can provide a temporary evaluation of the gait when application of 3-D motion analysis protocol is difficult. Moreover they could be used for qualitatively monitor the subject, over time, in between to 3-D analysis sessions as the latter are more time consuming and less likely to be repeated on a regular basis.

UCM approach should be considered in accompanying 3-D kinematics analysis to provide a more thorough evaluation of stroke patient gait. The UCM can be used to explain the mechanisms of movement described by kinematics data. The strategy utilised by stroke patients during walking can be determine with reference to certain

established task variables which performance depend on correlated elemental variables. In the current study, elemental variables were joint angles; an intervention that affects those can compromise the task performance (CM position). Being able to verify this can help in the guidance of a rehabilitation technique to be adopted. In the author's opinion, if a research has to be conducted to have an impact in clinical practice with regards to stroke rehabilitation, 3-D motion analysis should be employed as first choice of analysis method since it provides a detailed description of stroke gait attitude. UCM approach can be applied to the outcomes, so obtained, for an ulterior characterisation of the gait without requiring additional data collection. With one set of data, collected by one 3-D capture system, two types of analysis can be conducted, kinematics (and kinetics) and UCM analysis.

From research outcomes, factors (guidelines), one should look at, can be extracted and used to accelerate patient care and treatment decision making. Then, simpler system than 3-D motion capture, such as AVPS, can be employed to verify the correctness of the treatment provided in clinical environments for routine care and monitor the patient over time. With AVPS and a careful analysis of the video also sagittal angle at the lower limb joints can be estimated providing an approximate evaluation of sagittal limb kinematics to add to spatiotemporal parameters assessment. This represents a compromise when a more accurate assessment through 3-D motion analysis cannot be performed. In this way, the AVPS represents the link between research outcomes and clinical practice, allowing safe implementations of the results obtained through a rigorous research. The latter is fundamental to provide evidences that can be useful and valuable to improve clinical rehabilitation practice of stroke patient.

8.3.4 Recruitment and RCT design

Although stroke represents a health-threatening problem of primarily importance in Scotland and Glasgow, only three patients were found to meet the study criteria. The reason for this was mainly related to the small window of time allowed between stroke onset and study recruitment. Subjects who would have benefit from an AFO, within two months post stroke, were only starting their mobilisation rehabilitation and hence not in the stage to walk as yet. On the other hand, some of those who were

able to walk within two months from onset could do it independently without the need of an AFO that may have restricted their movements.

Other factors, that negatively influenced study recruitment, were related to the NHS reorganisation of stroke units between Stobhill and Royal Infirmary and to medical changes to the care of stroke survivors. These included the introduction of a rapid response team and paramedic team, availability of rapid MRI scanning facilities, administration of thrombolytic therapy for ischemic stroke patients and intensive first 24 hours care. All these contribute to limit residual neurological damages to the patients who survive the stroke onset. The fact that patients were first admitted to the Royal infirmary, when at the beginning recruitment was only based at Stobhill Hospital, together with the introduction of an early discharge policy could brought missed opportunities of recruitment.

Moreover, the current study was a non-funded trial and hence NHS staff was resistant in helping with recruitment since it was seen as an additional unpaid effort and they were not willing of having research staff on a regular basis in the stroke units. The poor collaboration with clinical staff could also justify the small number of patients recruited.

All these aspects should be carefully consider in future arrangements of a research trial for a successful recruitment.

Having undertaken a feasibility study, although limited to a small patient group, with the perspective of conducting a RCT provides us with valuable information for future planning. The study highlighted the importance of conducting research in the field of early rehabilitation in stroke patients but also the difficulties may be encountered during the progress of an RCT study, first of which is recruitment, as anticipated earlier in this section.

With regards to this, the time frame allowed for patients' enrolment should be revised. Mobilisation for stroke survivors occurs at different time from the stroke onset according to its the severity, the more severe the stroke the more prolonged is the time between onset and when patients can start to be mobilised. Early mobilisation is thus subject specific. Expanding the time window for recruitment increases the chance of finding suitable study candidates while still allowing the effect of AFO in early rehabilitation/mobilisation to be explored.

Moreover, one may want to consider the involvement of nurses, physiotherapists or physical therapists based on the Hospital structure where recruitment is addressed to. This in turn may involve the adoption of the study from funding bodies so that to provide an extra payment to these people and make them more willing to collaborate. Having a contact directly in the Hospital should also reduced the possibility of missed recruitment due to early discharge to patient's home or other care facilities. The aim of providing an AFO is to afford the patient with the ability to restart walking in an efficient and safe fashion. The AFO for this scope should be tailored to each patient's impairment for the best outcome achievable. This has to be taken into account when defining the intervention of a RCT. Prescription of more than one type of AFO may confound the results but, if common characteristics can be identified among the gait of groups of participants, at the end of the trial it should be possible to clarify who will benefit for what. A spectrum of possible AFO intervention to address certain impairments can be defined. If that would be possible the outcomes from the research will find an actual application in clinical practice.

Adding the measurement of the orthosis mechanical properties (stiffness, stress, and orthotic load) will supply with additional characteristics to classify the intervention provided and help in future choices.

The methods introduced are applicable for the evaluation of early stroke patients and can thus be safely employed in a RCT.

Although only one patient could complete the study protocol to the follow-up assessment, this should not discourage an RCT which involves a follow-up study as the information obtained are important to establish the long term effect of the AFO and thus start thinking of the orthosis as a provisional device if the patient improves to the stage of walking independently without it.

8.4 Implications for clinical practice

The benefits achievable when stroke patients are prescribed an AFO were shown in the outcomes of the conducted study. Results are however limited to 3 patients and hence findings should be treated carefully and evidences to confirm such results should be sought through further trials.

Nevertheless, if an AFO is proved to help stroke patients to regain walking ability during their acute rehabilitation phase, the prescription of an AFO should be introduced in the treatment of such patients. The provision of the orthosis will be a duty of the orthotic service of the Hospital where patients were admitted in. The orthotic department in NHS facilities is in continuum expansion and especially relatively to the management of stroke patients since the publication of the “Best Practice Statement” (2009). However, although this document encourages the use of AFOs early after stroke, research evidence to support the outlined guidelines needs to be established. A research as the one proposed can address this issue.

If necessary, casting of the AFO should be delivered at patients’ home as portable tools are only required. The fitting of the AFO instead, may require gait analysis tests to be conducted to verify the appropriateness of the orthosis.

If what discussed earlier will be possible (conducting a RCT) and guidelines for AFO provision extracted from a sound conducted research, only a simple gait analysis protocol such as AVPS would be sufficient for the verification of the AFO fitting and tuning processes. The use of such system is applicable in clinical environment and could be adapted to be applied in patients’ homes if room is available to position the mat and the camera. This should be however the last solution as patients are more likely to be still hospitalised at the time fitting or able to be transported from one place to another where AVPS can be used.

Monitor of the patient over time should also be considered in clinical practice if there is the possibility to discharge these patients from the use of the orthosis.

Finally, the AFO capability to accelerate walking recovery will also have the advantage to reduce costs, both in time and money, related to the physical therapy sessions needed for these subjects.

CHAPTER 9 – CONCLUSIONS AND RECOMMENDATIONS

9.1 General Conclusions

One of the aims of the current thesis can be described broadly as the development of methodologies that can be utilised for the assessment of stroke patient during the performance of walking tasks. In Chapter 2 and Chapter 3 this issue has been addressed and two protocols for gait analysis have been introduced and validated. One protocol is a 3-D gait analysis protocol from which kinematics and kinetics data of the lower limb joints and pelvis can be obtained in a reliable and repeatable manner; the other, is a 2-D gait analysis protocol from which spatiotemporal parameters of the gait and shank to vertical angles can be reliably extracted. A combination of the two protocols, producing different outcomes, allows a comprehensive examination of the test subject walking capability providing information of clinical relevance when evaluating rehabilitation interventions and walking improvements of the patients through a period of time.

The other aim of the thesis was, in fact, to evaluate the efficacy of AFO in early stroke patients' gait. Using the two protocols of gait analysis introduced, it was possible to identify differences between walking with and without AFO at different time points within a period of six months of intervention. Moreover, to the evaluation of the effect AFO has on the walking ability of a stroke patient, a method was introduced to estimate the actual contribution of the AFO to the net ankle moment. Although this method was only tested with one normal subject and one stroke patient, the potential it has to determine the orthotic contribution to the ankle dorsi/plantarflexor moment was verified. Also this type of analysis provides valuable information in order to enhance AFO prescription and so obtain an optimal effect from its use by stroke survivors.

Furthermore, with regards to the methods that could be use in the evaluation of the gait of stroke patients during the rehabilitation process, the uncontrolled manifold approach was explored and applied to verify the centre of mass displacement control

by the central nervous system. With the uncontrolled manifold method, explanation on how the patients control their gait can be gathered.

A feasibility study was run that employed these four methods for the outcomes evaluation of early stroke patients walking ability. In particular, the interest was to assess the effect, a rigid plastic AFO with carbon fiber reinforcement, has on walking in contrast to shoes only and usual clinical rehabilitation practice post stroke. Only three patients, however, entered the study. Two of them received the experimental AFO whereas one patient received a solid AFO from the NHS. Due to the restrict number of patients involved in the trial the findings cannot not be generalised. The comparison between groups was abandoned but rather it was focused on the effect rehabilitation and AFO had on each participant.

The amount of outputs obtained with the methods utilised, allowed a comprehensive examination of the walking ability of the participants. Not only the direct effects of the AFO at the ankle were shown but also the indirect effects at the more proximal joints (hip and knee) and pelvis could be observed in a full 3-D perspective.

Common characteristics were found in the way the AFO influenced the walking capability of these subjects otherwise characterised by short steps that follow each other at slow speed due to altered lower limbs joints kinematic postures during the gait cycle.

The AFO generally brought beneficial changes in lower limb joint and pelvis kinematics, with which stroke participants walked, by:

- Enhancing initial contact to occur through the heel;
- Correcting for excessive plantarflexion while allowing for dorsiflexion to occur;
- Reducing ankle inversion particularly in swing;
- Preventing drop foot in swing for a safe ground clearance;
- Improving shank to vertical angles. Tibia could move from a reclined to an inclined position in stance;
- Allowing knee first flexion peak as demonstration of weight acceptance enhancement;

- Reducing knee extension in mid stance and enhancing knee flexion in late stance although the peak achieved was still small in comparison to normal subjects;
- Promoting hip extension in mid to late stance;
- Lessening the trunk forward leaning (pelvic anterior tilt);
- Diminishing hip retraction (pelvic rotation);
- Improving joint kinematics through time as observed when it was possible to run tests with 3 months gap from each other.

These implied also improvements, although not always significant, in the spatiotemporal parameters of the gait. These included:

- An enhanced gait symmetry both in time and space;
- An increased walking velocity even if still small in comparison to able-bodied subjects speed;
- An improved subdivision of gait cycle phases: reduction of stance phase and double support times, increase of swing phase and single support;
- An increased step length.

As consequence of such improvements also the walking pattern of the unaffected leg resulted enhanced.

The AFO contributed positively at the ankle sagittal kinetics by providing a corrective moment in the dorsiflexor direction as verified by the test conducted on one stroke participant with the instrumented AFO.

Stroke patients gained confidence when walking with the AFO reducing the effort paid in maintaining a stable CM position during gait as highlighted through the UCM analysis.

Finally, it was also emphasised by the results that the appropriateness of the AFO is key to maximize the effects achievable through the AFO intervention and thus a research as the one conducted, is valuable for the clinical application of this practice to obtain the best outcomes.

9.2 Recommendations for further study

The methods proposed were found feasible for early stroke patients' assessment and capable of producing reliable results that addressed research aims in investigating the

effect of AFO in stroke population gait. The use of such methods, from gait analysis protocols to strain gauged AFO and uncontrolled manifold approach, could be used in future study to enhance the quality of research and ultimately be able to extend the results found into clinical practice.

The use of the uncontrolled manifold approach could be expanded and applied to verify different hypotheses relevant to the gait and linked to lower limb kinematics or simply modify the one proposed from a 2-D to a 3-D analysis of the CM displacement.

Estimation of AFO contribution to the ankle dorsi/plantarflexor moment may well be accompanied by an evaluation of AFO stiffness to widen the mechanical characterisation of the AFO employed.

Finally, if future studies are to be conducted with early stroke patient one may consider extending the recruitment period to, at least, 3 months post stroke. This will increase the chance to find suitable patients but without losing the “window of opportunity” and gather enough results to be able to generalise the findings and establish the effect AFO has on stroke gait. It is important, however, that the AFO is tailored to the patient need, and also the tuning process is conducted properly. This may require tests to be conducted and data being analysed before the final choice is made for the most appropriate AFO.

REFERENCES

- Abe H, Michimata A, Sugawara K, Sugaya N, Izumi S. 2009, Improving gait stability in stroke hemiplegic patients with a plastic ankle-foot orthosis. *Tohoku J Exp Med* 218(3):193-199.
- Alexander EJ, Andriacchi TP 2001, Correcting for deformation in skin-based marker systems. *J Biomech* 34: 355-361.
- Andriacchi TP, Alexander EJ, Toney MK, Dyrby C, Sum J 1998, A point cluster method for in vivo motion analysis: applied to a study of knee kinematics. *J. Biomech. Eng* 120: 743-749.
- ASTM D638 2008, Standard Test Method for Tensile Properties of Plastics. ASTM International, West Conshohocken, PA 19428-2959.
- AVERT Protocol Summary Version 1.0 - 4 April 2006. Available from url: <http://www.nsri.org.au/pics/clinical-trials/pdf/Protocol2006.pdf>
- Baker R 2001, Pelvic Angles: A mathematically rigorous definition which is consistent with a conventional clinical understanding of the terms. *Gait & Posture* 13: 1-6.
- Baker R 2003, ISB recommendation on definition of joint coordinate systems for the reporting of human joint motion-part I: ankle, hip and spine. *J Biomech* 36: 300-302.
- Baker R 2006, Gait analysis methods in rehabilitation. *J Neuroeng Rehabil* 2:3-4.
- Baker R, Finney L, Orr J 1999, A new approach to determine the hip rotation profile from clinical gait analysis data. *Hum Mov Sci* 18: 655-667.
- Beauchet O, Herrmann FR, Grandjean R, Dubost V, Allali G 2008, Concurrent validity of SMTEC footswitches system for the measurement of temporal gait parameters. *Gait & Posture* 27: 156-159.
- Becher JG 2004, Understanding tone and spasticity. In 'Report of a consensus conference on the orthotic management of stroke patients', ed Condie L, Campbell J, Martina J. International Society of Prosthetic & Orthotics, Copenhagen, ISBN 87-89809-149.

- Beckerman H, Becher J, Lankhorst GJ, Verbeek AL 1996, Walking ability of stroke patients: efficacy of tibial nerve blocking and a polypropylene ankle-foot orthosis. *Arch Phys Med Rehabil* 77:1144-1151.
- Bell AL, Brand RA 1989, Roentgenographic changes in proximal femoral dimensions due to hip rotation. *Clin Orthop Relat Res* 240: 194-199.
- Bell AL, Pedersen DR, Brand RA 1990, A comparison of the accuracy of several hip center location prediction methods. *J Biomech* 23(6): 617-621.
- Benedetti MG, Catani F, Leardini A, Pignotti E, Giannini S 1998, Data management in gait analysis for clinical applications. *Clin Biomech* 133: 204-215.
- Benoit DL, Ramsey DK, Lamontagne M, Xuf L, Wretenberg P, Renströma P 2006, Effect of skin movement artifact on knee kinematics during gait and cutting motions measured in vivo. *Gait & Posture* 242: 152-164.
- Bernhardt J, Dewey HM, Thrift A, Collier J, Donnan G 2008, A Very Early Rehabilitation Trial for Stroke (AVERT): Phase II Safety and Feasibility. *Stroke* 39: 390-396.
- Bernhardt J, Dewey HM, Thrift A, Donnan G 2004, Inactive and alone: Physical activity within the first 14 days of acute stroke unit care. *Stroke* 35: 1005-1009.
- Bernhardt J, Thuy MN, Collier JM, Legg LA 2009, Very early versus delayed mobilisation after stroke. *Cochrane Database Syst Rev* 21(1).
- Best Practice Statement 2009, Ankle Foot Orthoses following stroke. NHS Quality Improvement Scotland. Available from url:
<http://www.stroke.scot.nhs.uk/docs/UseOfAnkle-FootOrthosesFollowingStroke.pdf>
- Better heart disease and stroke care action plan 2009. Available from url:
<http://www.scotland.gov.uk/Resource/Doc/277650/0083350.pdf>
- Bilney B, Morris M, and Webster K 2003, Concurrent related validity of the GAITRite walkway system for quantification of the spatial and temporal parameters of gait. *Gait & Posture* 17: 68-74.
- Black DP, Smith BA, Wu J, Ulrich BD 2007, Uncontrolled manifold analysis of segmental angle variability during walking: preadolescents with and without Down syndrome. *Exp Brain Res* 183(4):511-521.

Bohannon RW 1997, Comfortable and maximum walking speed of adults aged 20-79 years: reference values and determinants. *Age Ageing* 26: 15-19.

Bowers RJ 2004, Non-articulated ankle-foot orthosis. In 'Report of a consensus conference on the orthotic management of stroke patients', ed Condie L, Campbell J, Martina J. International Society of Prosthetic & Orthotics, Copenhagen, ISBN 87-89809-149.

Bowers RJ, Ross K 2009, A review of the effectiveness of lower limb orthoses used in cerebral palsy. In: 'Recent developments in healthcare for cerebral palsy; implications and opportunities for orthotics', ed. Morris C, Condie D, International Society of Prosthetic & Orthotics, Copenhagen. p. 235-297

Bowker P, Condie DN, Brader DL, Pratt DJ 1993, The Biomechanics of Orthoses, Ankle-Foot Orthoses, in 'Biomechanical Basis of Orthotic Management', ed Bowker P, Condie DN, Brader DL, Pratt DJ, Wallace AW, Butterworth-Heinemann, Oxford.

Bregman DJJ, Rozumalski A, Koops D, de Groot V, Schwartz M, Harlaar J 2009, A new method for evaluating Ankle Foot Orthoses characteristics: BRUCE. *Gait & Posture* 30:144-149.

Bregman DJ, De Groot V, Van Diggele P, Meulman H, Houdijk H, Harlaar J 2010, Polypropylene ankle foot orthoses to overcome drop-foot gait in central neurological patients: a mechanical and functional evaluation. *Prosthet Orthot Int.* 34(3):293-304.

BS 527-2 1996, Plastics-Determination of tensile properties-Part 2:Test conditions for moulding and extrusion plastics. British Standard Institution, London.

BS 10002-1 2001, Metallic materials - Tensile testing - Part 1: Method of test at ambient temperature. British Standard Institution, London.

Burdett RG, Borello-France D, Blatchly C, Potter C 1988, Gait comparison of subjects with hemiplegia walking unbraced, with ankle-foot orthosis, and with air-stirrup brace. *Physical Therapy* 68: 1197-1203.

Butler PB, Farmer SE, Major RE 1997, Improvement in gait parameters following late intervention in traumatic brain injury: a long-term follow-up report of a single case. *Clin Rehabil* 11(3):220-226.

Callister WD 2000, Materials science and engineering: An Introduction, 5th edition. John Wiley and Sons, New York.

- Camomilla V, Cereatti A, Vannozzi G, Cappozzo A 2006, An optimized protocol for hip joint centre determination using the functional method. *J Biomech* 39:1096-1106.
- Cappa P, Patanè F, Pierro MM 2003, A novel device to evaluate the stiffness of ankle-foot orthosis devices. *J Biomech Eng* 125(6):913-917.
- Cappa P, Patanè F, Di Rosa G 2005, A continuous loading apparatus for measuring three-dimensional stiffness of ankle-foot orthoses. *J Biomech Eng* 127(6):1025-1029.
- Cappello A, Cappozzo A, La Palombara PF, Lucchetti L, Leardini A 1997, Multiple anatomical landmark calibration for optimal bone pose estimation. *Hum Mov Sci* 16(2-3): 259-274.
- Cappello A, Stagni R, Fantozzi S, Leardini A 2005, Soft tissue artifact compensation in knee kinematics by double anatomical landmark calibration: performance of a novel method. *IEEE Trans Biomed Eng* 52(6):992-998.
- Cappozzo A 1984, Gait analysis methodology. *Hum Mov Sci* 3: 25-54.
- Cappozzo A 1991, Three-dimensional analysis of human walking: Experimental methods and associated artifacts. *Hum Mov Sci* 105: 589-602.
- Cappozzo A, Cappello A, Della Croce U, Pensalfini F 1997, Surface-marker cluster design criteria for 3-D bone movement reconstruction. *IEEE Trans Biomed Eng* 44: 1165-1174.
- Cappozzo A, Catani F, Croce UD, Leardini A 1995, Position and orientation in space of bones during movement: anatomical frame definition and determination, *Clin Biomech (Bristol, Avon)* 10(4): 171-178.
- Cappozzo A, Catani F, Leardini A, Benedetti MG, Croce UD 1996, Position and orientation in space of bones during movement: experimental artefacts. *Clin Biomech (Bristol, Avon)* 11: 90-100.
- Cappozzo A, Della Croce U, Leardini A, Chiari L 2005, Human movement analysis using stereophotogrammetry Part 1: theoretical background. *Gait & Posture* 21:186-196.
- Cereatti A, Donati M, Camomilla V, Margheritini F, Cappozzo A 2009, Hip joint centre location: An ex vivo study, *J Biomech* 427: 818-823.

- Chao EY (1980) Justification of triaxial goniometer for the measurement of joint rotation. *J Biomech* 13(12): 989-1006.
- Charlton IW, Tate P, Smyth P, Roren L 2004, Repeatability of an optimised lower body model. *Gait & Posture* 20: 213-221.
- Chest, Heart and Stroke Scotland 2002, Stroke Strategy for Scotland. Available from url: <http://www.scotland.gov.uk/library5/health/chds.pdf>
- Chiari L, Della Croce U, Leardini A, Cappozzo A 2005, Human movement analysis using stereophotogrammetry Part 2: instrumental errors *Gait Posture* 21: 197-211.
- Chu TM 2000, Determination of peak stress on polypropylene ankle-foot orthoses due to weight change using strain gage technology. *Experimental Techniques* 24(2): 28-30.
- Chu TM 2001, Biomechanics of Ankle-Foot Orthoses: Past, Present, and Future. *Topics in Stroke Rehabilitation* 7(4): 19-28.
- Chu TM, Feng R 1998, Determination of stress distribution in various ankle-foot orthoses: experimental stress analysis. *J Prosthet Orthot* 10:11-16.
- Chu TM, Gent AN, Sukthankar S, Reddy NP 1996, Bonding Methods for Strain Gages on Polypropylene Material. *Experimental Techniques*, 20(5): 29.
- Chu TM, Reddy NP 1995b, Stress distribution in the ankle-foot orthosis used to correct pathological gait. *Rehabil Res Dev*32(4):349-360.
- Chu TM, Reddy NP, Padovan J 1995a, Three-dimensional finite element stress analysis of the polypropylene, ankle-foot orthosis: static analysis. *Med Eng Phys* 17(5):372-379.
- Clinical Standards for Stroke Services: Care of the Patient in the Acute Setting 2009. Available from url: http://www.healthcareimprovementscotland.org/previous_resources/standards/clinical_standards_for_stroke.aspx
- Cole GK, Nigg BM, Ronsky JL, Yeadon MR 1993, Application of the Joint Coordinate System to Three-Dimensional Joint Attitude and Movement Representation: A Standardization Proposal. *J Biomech Eng* 1154A: 344-349

Condie L, Campbell J, Martina J (editors) 2004, Report of a consensus conference on the orthotic management of stroke patients. International Society of Prosthetic & Orthotics, Copenhagen, ISBN 87-89809-149.

Condie ME, Bowers RJ 2008, Lower limb orthoses for persons who have had a stroke. In: 'Atlas of orthoses and assistive devices', ed Hsu J, Michael J, Fisk JR, 4th edition, American Academy of Orthopedic Surgeons, Philadelphia; pp 433-440.

Condie DN, Meadows CB 1977, Some biomechanical considerations in the design of ankle-foot orthoses. *Orthot Prosthet* 31: 45-52

Condie DN, Meadows CB 1993, Ankle-foot orthoses, in 'Biomechanical Basis of Orthotic Management', ed Bowker P, Condie DN, Brader DL, Pratt DJ, Wallace AW, Butterworth-Heinemann, Oxford. pp. 99-123.

Condie DN, Turner 1997, *An Atlas of Lower Limb Orthotic Practice*. Chapman & Hall, London.

Cooke E, Tallis RC, Clark A, Pomeroy VM 2010, Efficacy of functional strength training on enhancing lower limb recovery early after stroke. A Phase II randomised controlled trial. *Neurorehabilitation and Neural Repair* 24(1): 88–96.

Crawford RJ 1998, *Plastics Engineering*, 3rd edition, Butterworth-Heinemann, Oxford.

Cutlip RG, Mancinelli C, Huber F, and DiPasquale J 2000, Evaluation of an instrumented walkway for measurement of the kinematic parameters of gait. *Gait & Posture* 12: 134-138.

Davis RBI, Ounpuu U, Tyburski D, Gage JR 1991, A gait data collection and reduction technique. *Hum Mov Sci* 10: 575-587.

Della Croce U, Camomilla V, Leardini A, Cappozzo A, 2003 Femoral anatomical frame: assessment of various definitions. *Med Eng Phys* 25: 425-431.

Della Croce U, Cappozzo A, Kerrigan DC 1999, Pelvis and lower limb anatomical landmark calibration precision and its propagation to bone geometry and joint angles. *Med Biol Eng Comput* 37: 155-161.

Della Croce U, Leardini A, Chiari L, Cappozzo A 2005, Human movement analysis using stereophotogrammetry Part 4: assessment of anatomical landmark misplacement and its effects on joint kinematics. *Gait & Posture* 21: 226-237.

- De Quervain IA, Simon SR, Leurgans S, Pease WS, McAllister D 1996, Gait pattern in the early recovery period after stroke. *J Bone Joint Surg Am* 78(10): 1506-1514.
- De Wit DCM, Buurke JH, Nijilant JMM, Ijzerman MJ, Hermens HJ 2004, The effect of an ankle-foot orthosis on walking ability in chronic stroke patients: a randomized control trial. *Clin rehabil* 18:550-557
- Diamond MF, Ottenbacher KJ 1990, Effect of a tone-inhibiting dynamic ankle-foot orthosis on stride characteristics of an adult with hemiparesis. *Phys Ther* 70(7): 423-430.
- Dickens W, Pratt E, Davenport C et al. 2009, A comparison of two sequences of pelvic angle calculation in patients with a stiff hip. *Gait & Posture* 30S: S37
- Dieli J, Ayyappa E, Hornbeak S 1997, Effect of Dynamic AFOs on Three Hemiplegic Adults. *Journal of prosthetics & orthotics* 9(2): 82-89.
- Di Lauro A, Pellegrino L, Savastano G, Ferraro C, Fusco M, Balzarano F, et al., 2003, A randomized trial on the efficacy of intensive rehabilitation in the acute phase of ischemic stroke. *J Neurol.* 250(10): 1206-1208.
- Domkin D, Laczko J, Jaric S, Johansson H, Latash ML 2002, Structure of joint variability in bimanual pointing tasks. *Exp Brain Res* 143:11-23.
- Donati M, Camomilla V, Vannozzi G, Cappozzo A 2007, Enhanced anatomical calibration in human movement analysis. *Gait & Posture* 262: 179-185.
- Donati M, Camomilla V, Vannozzi G, Cappozzo A 2008, Anatomical frame identification and reconstruction for repeatable lower limb joint kinematics estimates. *J Biomech* 4110: 2219-2226.
- Ehrig RM, Taylor WR, Duda GN, Heller MO 2006, A survey of formal methods for determining the centre of rotation of ball joints. *J Biomech* 9(15):2798-2809.
- Esenquazi A 2008, Assessment and orthotic management of gait dysfunction in individuals with traumatic brain injury. In: 'Atlas of orthoses and assistive devices', ed Hsu J, Michael J, Fisk JR, 4th edition, American Academy of Orthopedic Surgeons, Philadelphia; pp 433-40.
- Esquenazi A, Ofluoglu D, Hirai B, Kim S 2009, The effect of an ankle-foot orthosis on temporal spatial parameters and asymmetry of gait in hemiparetic patients. *PM R* 1(11):1014-1018.

- Fatone S, Gard SA, Malas BS 2009, Effect of ankle-foot orthosis alignment and foot-plate length on the gait of adults with poststroke hemiplegia. *Arch Phys Med Rehabil* 90(5):810-818.
- Ferrari A, Benedetti MG, Pavan E, Frigo C, et al. 2008, Quantitative comparison of five current protocols in gait analysis. *Gait & Posture* 28(2):207-216.
- Feys H, De Weerdts W, Verbeke G, Steck GC, Capiou C, Kiekens C, et al. 2004, Early and Repetitive Stimulation of the Arm Can Substantially Improve the Long-Term Outcome After Stroke: A 5-Year Follow-up Study of a Randomized Trial. *Stroke* 35: 924-929.
- Foti T, Davis RB, Davids JR, Farrell ME 2001, Assessment of methods to describe the angular position of the pelvis during gait in children with hemiplegic cerebral palsy. *Gait & Posture* 13: 270.
- Franceschini M, Massucci M, Ferrari L, Agosti M, Orsic M, Paroli C 2001, Gait with custom-made orthosis in hemiplegic patients: preliminary data. (abstract) *Gait & Posture* 2001,13(2): 139-140.
- Franceschini M, Massucci M, Ferrari L, Agosti M and Paroli C 2003, Effects of an ankle-foot orthosis on spatiotemporal parameters and energy cost of hemiparetic gait. *Clinical Rehabil* 17:368-372.
- Frigo C, Rabuffetti M, Kerrigan DC, Deming LC, Pedotti A 1998, Functionally oriented and clinically feasible quantitative gait analysis method. *Med Biol Eng Comput* 36: 179-185.
- Fukuchi RS, Arakaki C, Veras Orselli MI, Duarte M 2010, Evaluation of alternative technical markers for the pelvic coordinate system. *J Biomech* 43: 592-594.
- Fuller J, Liu LJ, Murphy MC, Mann RW 1997, A comparison of lower-extremity skeletal kinematics measured using skin- and pin-mounted markers. *Hum Mov Sci* 16: 219-242.
- Gard SA, Fatone S 2004, Biomechanics of lower limb function and gait. In 'Report of a consensus conference on the orthotic management of stroke patients', ed Condie L, Campbell J, Martina J. International Society of Prosthetic & Orthotics, Copenhagen, ISBN 87-89809-149.
- Gok H, Kucukdeveci A, Altinkaynak H, Yavuzer G, Ergin S 2003, Effects of ankle-foot orthoses on hemiparetic gait. *Clinical Rehabil* 17:137-139

Grood ES, Suntay WJ 1983, A joint coordinate system for the clinical description of three-dimensional motions: application to the knee. *J Biomech Eng* 105(2): 136-144.

Hamill J, Selbie WS 2004, Three-dimensional kinetics. In: 'Research methods in biomechanics', ed Robertson DGE, Caldwell GE, Hamill J, Kamen G, Whittlesey SN, Champaign, IL. pp 145–160.

Harrington ME, Zavatsky AB, Lawsonb SEM, Yuanb Z, Theologis TN 2007, Prediction of the hip joint centre in adults, children, and patients with cerebral palsy based on magnetic resonance imaging. *J Biomech* 40:595-602.

Hartmann A, Luzi S, Murer K, de Bie RA, and de Bruin ED 2009, Concurrent validity of a trunk tri-axial accelerometer system for gait analysis in older adults. *Gait & Posture* 29: 444-448.

Hesse S, Luecke D, Jahnke MT, Mauritz KH 1996, Gait function in spastic hemiparetic patients walking barefoot, with firm shoes, and with ankle-foot orthoses. *Int J Rehabil Res.* 19: 133-141.

Hesse S, Werner C, Matthias K, Stephen K, Berteau M 1999, Non- velocity-related effects of a rigid double stopped ankle foot orthosis on gait and lower limb muscle activity of hemiparetic subjects with an equinvarus deformity. *Stroke* 30(9):1855-1861.

Hicks JL, Richards JG 2005, Clinical applicability of using spherical fitting to find hip joint centers. *Gait and Posture* 22: 138-145.

Hill KD, Goldie PA, Baker PA, Greenwood KM 1994, Retest reliability of the temporal and distance characteristics of hemiplegic gait using a footswitch system. *Arch Phys Med Rehabil* 1994: 75: 577-583.

Holden JP, Orsini JA, Siegel KL, Kepple TM, Gerber LH, Stanhope SJ 1997, Surface movement errors in shank kinematics and knee kinetics during gait. *Gait & Posture* 5: 217–227.

Holden JP, Stanhope SJ 1998, The effect of variation in knee center location estimates on net knee joint moments. *Gait & Posture* 7: 1-6

Holden JP, Stanhope SJ 2000, The effect of uncertainty in hip center location estimates on hip joint moments during walking at different speeds. *Gait & Posture* 11, 120-121.

- Houck J, Yack HJ, Cuddeford T 2004, Validity and comparisons of tibiofemoral orientations and displacement using a femoral tracking device during early to mid stance of walking. *Gait & Posture* 191: 76-84.
- Hoy DJ, Reinthal MA 2004, Articulated ankle foot orthoses designs, in 'Report of a Consensus Conference on the Orthotic Management of Stroke Patients', ed Condie E, Campbell J, Martina J, International Society for Prosthetics and Orthotics, Copenhagen. pp 95-111.
- Hsu WL, Scholz JP, Schöner G, Jeka JJ, Kiemel T 2007, Control and estimation of posture during quiet stance depends on multijoint coordination. *J Neurophysiol* 97(4):3024-3035.
- Indredavik B, Bakke RPT, Slørdahl SA, Rokseth, Håheim LL 1999, Treatment in a combined acute and rehabilitation stroke unit: which aspects are most important? *Stroke* 30: 917-923.
- International Organization for Standardization (ISO) 1989, General terms for external limb prostheses and external orthoses. ISO 8549-1:1989. Prosthetics and orthotics - vocabulary.
- Iwata M, Kondo I, Sato Y, Satoh K, Soma M, Tsushima E 2003, An ankle- foot orthosis with inhibitor bar: effect on hemiplegic gait. *Arch Phys Med Rehabil* 84(6):924-927.
- Johnson GR, Ferrarin M, Harrington M, Hermens H, Jonkers I, et al. 2004 Performance specification for lower limb orthotic devices. *Clin Biomech* 19(7):711-718.
- Jørgensen HS, Nakayama H, Raaschou HO, Vive-Larsen J, Støier M, Olsen TS 1995a, Outcome and time course of recovery in stroke. Part I: Outcome. The Copenhagen Stroke Study. *Arch Phys Med Rehabil*, 76(5): 399-405.
- Jørgensen HS, Nakayama H, Raaschou HO, Vive-Larsen J, Støier M, Olsen TS 1995b, Outcome and time course of recovery in stroke. Part II: Time course of recovery. The Copenhagen stroke study. *Arch Phys Med Rehabil*, 76(5):406-412.
- Kadaba MP, Ramakrishnan HK, Wotten ME, Gainey J, Gorton G, Cochran GVB 1990, Measurement of lower extremity kinematics during level walking. *J Orthop Res* 8(3): 383-392.

- Kaplan P, Cailliet R, Kaplan C 2003, Rehabilitation of stroke. Butterworth-Heinemann Ltd, London.
- Klasson B, Convery P, Raschke S 1998, Test apparatus for the measurement of the flexibility of ankle-foot orthoses in planes other than the loaded plane. *Prosthet Orthot Int.* 22(1):45-53.
- Kim CM, Eng JJ 2004, Magnitude and pattern of 3D kinematic and kinetic gait profiles in persons with stroke: relationship to walking speed. *Gait Posture* 20(2): 140-146.
- Jagadamma KC, Owen E, Coutts FJ, Herman J, Yirrell J, et al. 2010, The Effects of Tuning an Ankle-Foot Orthosis Footwear Combination on Kinematics and Kinetics of the Knee Joint of an Adult with Hemiplegia. *Prosthet Orthot Int* 34(3): 270-276.
- Landis JR, Koch GG 1977, The measurement of observer agreement for categorical data. *Biometrics* 33(1): 159-74.
- Langhorne P, Coupar F, Pollock A 2009, Motor recovery after stroke: a systematic review. *Lancet Neurol* 8: 741-754.
- Latash ML, Anson JG 2006, Synergies in health and disease: relations to adaptive changes in motor coordination. *Phys Ther* 86(8):1151-1160.
- Latash ML, Scholz JP, Schönner G 2007, Toward a new theory of motor synergies. *Motor Control* 11(3):276-308.
- Leardini A, Cappozzo A, Catani F, Toksvig-Larsen S et al. 1999, Validation of a functional method for the estimation of hip joint centre location. *J Biomech* 32(1):99-103.
- Leardini A, Chiari L, Della Croce U, Cappozzo A. 2005 Human movement analysis using stereophotogrammetry. Part 3. Soft tissue artifact assessment and compensation. *Gait Posture* 21: 212-225.
- Leardini A, Sawacha Z, Paolini G, Ingrosso S, Nativo R, Benedetti MG 2007, A new anatomically based protocol for gait analysis in children. *Gait & Posture* 26:560-571.
- Lehmann JF 1979, Biomechanics of ankle foot orthoses prescription and design. *Arch Phys Med Rehabil* 60:200-207.

- Lehmann JF, Condon SM, Price R, DeLateur BJ 1987, Gait abnormalities in hemiplegia: their correction by ankle-foot orthoses. *Arch Phys Med Rehabil* 68(11): 763-771.
- Lehmann JF, Esselman PC, Ko MK, Smith JC, DeLateur BJ, Dralle AJ 1983, Plastic ankle-foot orthoses: evaluation of function. *Arch Phys Med Rehabil*, 64(9): 402-407.
- Leung J, Moseley A 2003, Impact of Ankle-foot Orthoses on Gait and Leg Muscle Activity in Adults with Hemiplegia. Systematic literature review. *Physiotherapy* 89(1): 39-55.
- Lewallen J, Miedaner J, Amyx S, Sherman J 2010; Effect of Three Styles of Custom Ankle Foot Orthoses on the Gait of Stroke Patients While Walking on Level and Inclined Surfaces. *J Prosthet Orthot* 22(2): 78-83.
- Lin RS 200, Ankle-foot orthoses, in 'Orthotics and Prosthetics in Rehabilitation' ed Lusardi MM, Nielson CC, Butterworth Heinemann, Boston. pp:159-175.
- Lu TW, J O'Connor JJ 1999, Bone position estimation from skin marker co-ordinates using global optimisation with joint constraints. *J Biomech* 32: 129-134.
- MacWilliams BA 2008, A comparison of four functional methods to determine centers and axes of rotations. *Gait & Posture* 28: 673-679.
- Mackay J and Mensah G 2004, Risk Factors, in 'The atlas of heart disease and stroke', ed World Health Organisation, The Hanway Press, London.
- Magora A, Robin GC, Adler E, Libai A., Eitan A 1968, Dynamic strain analysis of below-knee orthopaedic braces. *Am J Phys Med* 47(1): 31- 40.
- Major RE, Hewart PJ, MacDonald AM 2004, A new structural concept in moulded fixed ankle foot orthoses and comparison of the bending stiffness of four constructions. *Prosthet Orthot Int* 28(1):44-48.
- Manal K, Davis IM, Galinat B, Stanhope S 2003, The accuracy of estimating proximal tibial translation during natural cadence walking: bone vs skin mounted targets. *Clin Biomech* 182:126-131.
- Manal K, McClay I, Stanhope S, Richards J, Galinat B 2000, Comparison of surface mounted markers and attachment methods in estimating tibial rotations during walking: an in vivo study. *Gait & Posture* 11(1): 38-45.

- Martini F 2006, *Fundamentals of Anatomy & Physiology*, 7th edition. Pearson/B. Cummings, San Francisco.
- McGinley JL, Baker R, Wolfe R, Morris ME 2009, The reliability of three-dimensional kinematic gait measurements: a systematic review. *Gait & Posture* 29: 360-369.
- McHugh B 1999, Analysis of body-device interface in the sagittal plane for patients wearing ankle-foot orthoses. *Prosthet Orthot Int*, 23:75-81.
- Meadows B, Bowers RJ, Owen E 2008, Bioemchanics of the hip, knee and ankle. In: 'Atlas of orthoses and assistive devices', ed Hsu J, Michael J, Fisk JR, 4th edition, American Academy of Orthopedic Surgeons, Philadelphia; pp 433-40.
- Menz HB, Latt MD, Tiedemann A, Mun San Kwan M, and Lord SR 2004, Reliability of the GAITRite walkway system for the quantification of temporo-spatial parameters of gait in young and older people. *Gait & Posture* 20: 20-5.
- Miyazaki S, Yamamoto S, Ebina M, Iwasaki M 1993, A system for the continuous measurement of ankle joint moment in hemiplegic patients wearing ankle-foot orthoses. *Front Med Biol Eng* 5(3):215-232.
- Miyazaki S, Yamamoto S, and Kubota T 1997, Effect of ankle-foot orthosis on active ankle moment in patients with hemiparesis. *Med Biol Eng Comput* 35: 381-385
- Mojica JAP, Nakamura R, Kobayashi T, Handa T, Morohashi I, Watanabe S, 1988 Effect of ankle-foot orthoses on body sway and walking capacity of hemiparetic stroke patients. *Tohoku J Exp Med*, 156(4): 395-401.
- Motion Labs System 2008, *The C3D File Format User Guide*. Motion Lab Systems, Inc., Baton Rouge, LA. Available from url: http://www.motion-labs.com/support_docs_manuals.html
- Mulder T, Nienhuis B, and Pauwels J 1998, Clinical gait analysis in a rehabilitation context: some controversial issues. *Clin Rehabil* 12: 99-106.
- National Audit Office Report, Department of Health 2005, *Reducing Brain Damage: Faster access to better stroke care*. Available from url: http://www.nao.org.uk/publications/0506/reducing_brain_damage.aspx.

- National Stroke Foundation 2010, Clinical Guidelines for Stroke Management. Available from url: <http://www.strokefoundation.com.au/>.
- National Stroke Strategy 2007. Available from url: http://www.dh.gov.uk/en/Publicationsandstatistics/Publications/PublicationsPolicyAndGuidance/DH_081062.
- Newman M 1972, The Process of Recovery: After Hemiplegia. *Stroke* 3: 702-710.
- Oberg T, Karsznia A, Oberg K 1993, Basic gait parameters: reference data for normal subjects, 10-79 years of age. *J Rehabil Res Dev* 30: 210-23.
- Olney SJ, Richards C 1996, Hemiparetic gait following stroke. Part I: Characteristics. *Gait & Posture* 4(2):136-148.
- Owen, E 2004, The point of 'point-loading rockers' in ankle-foot orthosis footwear combinations used with children with cerebral palsy, spina bifida and other conditions. *Gait & Posture* 20(S1): s86.
- Owen E 2005, Proposed clinical algorithm for deciding the sagittal angle of the ankle in an ankle-foot orthosis footwear combination. *Gait & Posture* 22S: S38-S39.
- Owen E 2010, The importance of being earnest about shank and thigh kinematics especially when using ankle-foot orthoses. *Prosthet Orthot Int* 34(3):254-69.
- Owen E, Bowers RJ, Meadows B 2004, Tuning of AFO footwear combinations for neurological disorders. In: Conference Proceedings. International Society for Prosthetics and Orthotics (ISPO) 11th World Congress. Hong Kong. pp 278-279.
- Papi E 2008, Investigate the use of strain gauge technology for the determination of the mechanical characteristics of polypropylene ankle foot orthoses. MSc Thesis, University of Strathclyde, Glasgow.
- Pavlik AJ 2008, The effect of long-term ankle-foot orthosis use on gait in the poststroke population. *J Prosthet Orthot* 20(2):49-52.
- Perry CC 1985, Strain-Gage Reinforcement Effects on Low-Modulus materials. *Experimental Techniques* 9(5): 25-27.
- Perry J 1992, *Gait Analysis: Normal and pathological Function*. SLACK Incorporated, Thorofare, New Jersey.

- Perry J, Garret M, Gronley JK, Mulroy SJ 1995, Classification of walking handicap in the stroke population. *Stroke* 26: 982-989.
- Peters A, Baker R, Sangeux M, 2010b, Determining the best hip joint centre location method for patients compared to 3-dus. *JEGM 2010 Conference Proceedings*.
- Peters A, Galna B, Sangeux M, Morris M, Baker RJ 2010a, Quantification of soft tissue artifact in lower limb human motion analysis: A systematic review. *Gait & Posture* 311: 1-8.
- Piazza SJ, Cavanagh PR 2000, Measurement of the screw-home motion of the knee is sensitive to errors in axis alignment. *J Biomech* 33(8): 1029-1034.
- Piazza SJ, Erdemir A, Okita N, Cavanagh PR 2001, Accuracy of the functional method of hip joint center location: effects of limited motion and varied implementation. *J Biomech* 34: 967-973.
- Piazza SJ, Erdemir A, Okita N, Cavanagh PR 2004, Assessment of the functional method of hip joint center location subject to reduced range of hip motion. *J Biomech* 37(3):349-356.
- Polliack AA, Swanson C, Landsberger SE, McNeal DR 2001, Development of a testing apparatus for structural stiffness evaluation of ankle-foot orthoses. *J Prosthet Orthot* 13(3):74-82.
- Pollock A, Baer G, Langhorne P, Pomeroy V 2007, Physiotherapy treatment approaches for the recovery of postural control and lower limb function following stroke: a systematic review. *Clin Rehabil* 21: 395-410.
- R11 Stroke Statistics resource sheet 2006. Available from url: http://www.stroke.org.uk/information/our_publications/factsheets/stroke_statistics.html.
- Rabuffetti M, Baroni G, Ferrarin M, Ferrigno G, Pedotti A 2002, Self-marking of anatomical landmarks for on-orbit experimental motion analysis compared to expert direct-marking. *Hum Mov Sci* 21: 439-455.
- Rabuffetti M, Crenna P 2004, A modular protocol for the analysis of movement in children. *Gait & Posture* 20: S77-S78.

- Rao N, Chaudhuri G, Hasso D, D'Souza K, Wening J, Carlson C, Aruin AS 2008, Gait assessment during the initial fitting of an ankle foot orthosis in individuals with stroke. *Disabil Rehabil Assist Technol* 3(4): 201-207.
- Reid S, Shaw A, and Haugh LD 2005, Validity and reliability of an internet-based temporal gait assessment tool with healthy adults: a pilot study. *Arch Phys Med Rehabil* 86: 1014-1018.
- Reinbolt JA, Schutte JF, Fregly BJ, Koh BI, Haftka RT, et al. 2005, Determination of patient-specific multi-joint kinematic models through two-level optimization. *Jof Biomech* 38: 621-626.
- Reinschmidt C, van Den Bogert AJ, Lundberg A, Nigg BM et al. 1997, Tibiofemoral and tibiocalcaneal motion during walking: external vs skeletal markers *Gait & Posture* 62: 98-109.
- Reisman D, Scholz JP 2003, Aspects of joint coordination are preserved during pointing in persons with post-stroke hemiparesis. *Brain*, 126: 2510-2527.
- Robin GC, Magora A 1969, Dynamic stress analysis of below-knee drop foot braces; studies on patients with paralysis of the lower limb. *Med Biol Eng* 7: 221-226.
- Robinson W, Smith R, Aung O, Ada L 2008, No difference between wearing a night splint and standing on a tilt table in preventing ankle contracture early after stroke: a randomised trial. *Aust J Physiother* 54(1):33-38.
- Rønning OM, Guldvog B 1998, Outcome of Subacute Stroke Rehabilitation : A Randomized Controlled Trial. *Stroke* 29: 779-784.
- Rose J and Gamble JG 2005, *Human Walking*, Williams & Wilkins, Philadelphia.
- Roth EJ, Merbitz C, Mroczek K, Dugan SA, Suh WW 1997, Hemiplegic gait. Relationships between walking speed and other temporal parameters. *Am J Phys Med Rehabil* 76(2):128-133.
- Saka O, McGuire A, Wolfe C 2009, Cost of stroke in the United Kingdom. *Age and Ageing* 38: 27-32.
- Sangeux M, Marin F, Charleux F, Dürselen L, Ho Ba Tho MC 2006, Quantification of the 3D relative movement of external marker sets vs bones based on magnetic resonance imaging. *Clin Biomech* 219: 984-991.
- Sati M, De Guisea JA, Larouchea S, Drouina G 1996, Quantitative assessment of skin-bone movement at the knee. *The Knee* 3(3):121-38.

- Saunders JB, Inman VT, Eberhart HD 1953, The major determinants in normal and pathological gait. *J Bone Joint Surg Am* 35: 543-558.
- Schache AG, Baker R 2007, On the expression of joint moments during gait. *Gait Posture* 25(3):440-452.
- Schache AG, Baker R, Lamoreux LW 2006, Defining the knee joint flexion–extension axis for purposes of quantitative gait analysis: An evaluation of methods. *Gait & Posture* 24:100-109.
- Schache AG, Baker R, Lamoreux LW 2008, Influence of thigh cluster configuration on the estimation of hip axial rotation. *Gait & Posture* 27(1): 60-69.
- Scholz JP, Kang N, Patterson D, Latash ML (2003), Uncontrolled manifold analysis of single trials during multi-finger force production by persons with and without Down syndrome. *Exp Brain Res* 153:45-58.
- Scholz JP, Schoner G 1999, The uncontrolled manifold concept: Identifying control variables for a functional task. *Experimental Brain Research* 126:289-306.
- Schoner G, Scholz JP 2007, Analyzing variance in multi-degree-of-freedom movements: uncovering structure versus extracting correlations. *Motor Control* 11(3):259-75.
- Schwartz MH, Rozumalski A 2005, A new method for estimating joint parameters from motion data. *J Biomech* 38: 107-116.
- Scottish Intercollegiate Guidelines Network (SIGN) 2002, Update 2005, Management of patients with stroke. Rehabilitation, prevention and management of complications, and discharge planning. (SIGN Guideline 64). Available from url: <http://www.sign.ac.uk/pdf/sign64.pdf>.
- Scottish Intercollegiate Guidelines Network (SIGN) 2010, Management of patients with stroke. Rehabilitation, prevention and management of complications, and discharge planning. (SIGN Guideline 118). Available from url: <http://www.sign.ac.uk/pdf/sign118.pdf>.
- Scottish Stroke Care Audit: 2010, National Report Stroke Services in Scottish Hospitals. Data relating to 2005-2009. Available from url: <http://www.strokeaudit.scot.nhs.uk/Downloads/2010%20report/SSCARReport0610.pdf>.

- Seidel GK, Marchinda DM, Dijkers M, Soutas-Littlepi RW 1995, Hip joint center location from palpable bony landmarks--a cadaver study. *J Biomech* 28(8): 995-998.
- Shamp K, Joanne A 1983, Ankle Foot Orthoses: Metal vs Plastic. *Clinical Prosthetics & Orthotics*, 7(1): 349-351.
- Sheffler LR, Hennessey MT, Naples GG, Chae J 2006, Peroneal nerve stimulation versus an ankle foot orthosis for correction of footdrop in stroke: impact on functional ambulation. *Neurorehabil Neural Repair* 20(3):355-60.
- Showers David C, Strunck Martha L 1985, Sheet Plastics and their applications in Orthotics and Prosthetics. *Orthotics and Prosthetics*: 38(4): 41-48.
- Siegler S, Chen J, Schneck CD 1988, The three dimensional kinematics and flexibility characteristics of the human ankle and subtalar joints - Part I: Kinematics *J Biomech Eng* 110(4):364-73.
- Simons CD, van Asseldonk EH, van der Kooij H, Geurts AC, Buurke JH 2009, Ankle-foot orthoses in stroke: effects on functional balance, weight-bearing asymmetry and the contribution of each lower limb to balance control. *Clin Biomech* 24(9):769-775.
- Skilbeck CE, Wade DT, Hewer RL, Wood VA 1983, Recovery after stroke. *J. Neurol. Neurosurg. Psychiatry* 46: 5-8.
- Soda P, Carta A, Formica D, and Guglielmelli E 2009, A low-cost video-based tool for clinical gait analysis. *Conf Proc IEEE Eng Med Biol Soc* 3979-3982.
- Spence WD 1982, Biomechanical assessment of the polypropylene ankle-foot orthosis. MSc Thesis, University of Strathclyde, Glasgow.
- Stagni R, Fantozzi S, Cappello A, Leardini A 2003, Validation of the Interval Deformation Technique for Compensating Soft Tissue Artefact in Human Motion Analysis. *Surgery Simulation and Soft Tissue Modeling* 2673: 293-301.
- Stagni R, Fantozzi S, Cappello A, Leardini A 2005, Quantification of soft tissue artefact in motion analysis by combining 3D fluoroscopy and stereophotogrammetry: a study on two subjects. *Clin Biomech* 20: 320-329.
- Stagni, R, Fantozzi, Cappello A 2009, Double calibration vs global optimisation: Performance and effectiveness for clinical application. *Gait & Posture* 29(1):119-122.

- Stagni R, Leardini A, Cappozzo A, Benedetti MG, Cappello A 2000, Effects of hip joint centre mislocation on gait analysis results. *J Biomech* 33(11): 1479-1487.
- Stroke Unit Trialists' Collaboration 2007, Organised inpatient (stroke unit) care for stroke. *Cochrane Database Syst Rev* 17(4).
- Strong K, Mathers K, Bonita R 2007, Preventing stroke: saving lives around the world. *The Lancet Neurology* 6(2): 182-187.
- Südhoff I, Van Driessche S, Laporte S, de Guise JA, Skalli W 2007, Comparing three attachment systems used to determine knee kinematics during gait. *Gait & Posture* 254: 533-543.
- Sumiya T, Suzuki Y, Kasahara T 1996, Stiffness control in posterior-type plastic ankle-foot orthoses: Effect of ankle trimline. Part 2: Orthosis characteristics and orthosis/patient matching. *Prosthet Orthot Int* 20:132-137.
- Sutherland DH 2002, The evolution of clinical gait analysis Part II Kinematics. *Gait & Posture* 16: 159-179.
- Syngellakis S, Arnold MA, Rassoulian H 2000, Assessment of the non-linear behaviour of plastic ankle foot orthoses by the finite element method. *Proc Inst Mech Eng H* 214(5): 527-39.
- Taddei F, Ansaloni M, Testi D, Viceconti M 2007, Virtual palpation of skeletal landmarks with multimodal display interfaces. *Med Inform Internet Med* 32(3):191-198.
- The Lancet Neurology 2011, Stroke prevention: the need for a global response. *The Lancet Neurology*, 10 (1):1.
- Tranberg R, Karlsson D 1998, The relative skin movement of the foot: a 2-D roentgen photogrammetry. *study Clin Biomech* 131: 71-76.
- Tupling SJ, Pierrynowski MR 1987, Use of cardan angles to locate rigid bodies in three-dimensional space. *Med & Biol Eng & Comput* 25:527-532.
- Tylkowski CM, Simon SR, Mansour JM 1982, Internal rotation gait in spastic cerebral palsy in the hip. *Proceedings of the 10th Open Scientific Meeting of the Hip Society*. pp:89-125.
- Tyson SF, Thornton HA 2001, The effect of a hinged ankle foot orthosis on hemiplegic gait: Objective measures and users' opinions. *Clinical Rehabil* 5:53-58.

- Tyson SF, Rogerson L 2009, Assistive walking devices in nonambulant patients undergoing rehabilitation after stroke: the effects on functional mobility, walking impairments, and patients' opinion. *Arch Phys Med Rehabil* 90(3):475-479.
- Uning R, Abu Osman NA, Abdul Rahim RB 2008, 3D Finite Element Analysis of Ankle-Foot Orthosis on Patients with Unilateral Foot Drop: A Preliminary Study. *IFMBE Proceedings*, 1, Volume 21, 4th Kuala Lumpur International Conference on Biomedical Engineering 2008, Part 3, Part 7: 366-369.
- Van Sint Jan S, Feipel V, Ciaravella C, Martin S 2002b, Lower limb anatomical landmark definition and identification within different experimental contexts; deliverable of the Vakhum project; [http://www.ulb.ac.be/project/vakhum/public_report/public_report.htm]
- Van Sint Jan S, Hilal I, Salvia P et al. 2003, Data representation for joint kinematics simulation of the lower limb within an educational context. *Med Eng Phys* 25(3): 213-220.
- Van Sint Jan S, Salvia P, Hilal I, Sholukha V, Rooze M, Clapworthy G 2002a, Registration of 6-DOFs electrogoniometry and CT medical imaging for 3D joint modeling. *J Biomech* 35(11):1475-1484.
- Vattanasilp W, Ada L, Crosbie J 2000, Contribution of thixotropy, spasticity, and contracture to ankle stiffness after stroke. *J Neurol Neurosurg Psychiatry* 69: 34-39.
- Verheyden G, Nieuwboer A, De Wit L, Thijs V, Dobbelaere J, Devos H et al., 2008, Time Course of Trunk, Arm, Leg, and Functional Recovery After Ischemic Stroke. *Neurorehabil Neural Repair* 22 (2): 173-179.
- Wall JC, Devlin J, Khirchof R, and Lackey B 2000, Measurement of step widths and step lengths: a comparison of measurements made directly from a grid with those made from a video recording. *J Orthop Sports Phys Ther* 30: 410-417.
- Wall JC, Crosbie J 1997, Temporal gait analysis using slow motion video and a personal computer. *Physiotherapy* 83(3):109-115.
- Wang RY, Yen LL, Lee CC, Lin PY, Wang MF, Yang YR 2005, Effects of ankle foot orthosis on balance performance in patients with hemiparesis of different durations. *Clinical Rehabil* 19: 37-44.

- Wang RY, Lin PY, Lee CC, Yang YR 2007, Gait and balance performance improvements attributable to ankle-foot orthosis in subjects with hemiparesis. *Am J Phys Med Rehabil* 86(7):556-562.
- Warlow CP, Dennis MS, van Gijn J, Hankey GJ, Sandercock PAG, Bamford JM, et al. 2001, *Stroke: a practical guide to management*. Blackwell Science, Edinburgh.
- Weiss W, Mulroy J, Gronley JK, Perry J, Boyd L 2002, Rigid AFO impairs walking ability in individuals with hemiparesis from CVA. *Gait and Posture* 16(Suppl 1): p. S2.
- Wening J, Huskey M, Hasso D, Aruin A, Rao N 2009, The Effect of an Ankle-Foot Orthosis on Gait Parameters of Acute and Chronic Hemiplegic Subjects. *The Academy Today* 5(1).
- Westblad P, Hashimoto T, Winson I, Lundberg A, Arndt A 2002, Differences in ankle-joint complex motion during the stance phase of walking as measured by superficial or bone anchored markers. *Foot and Ankle Int* 239: 856-863.
- Whittle MW 2007, *Gait analysis: An Introduction*. 4th edition, Elsevier, Philadelphia.
- Winter DA 2004, *Biomechanics and motor control of human movement*. 3rd Edition. John Wiley & Sons Inc, New Jersey.
- Woltring HJ 1985, On optimal smoothing and derivative estimation from noisy displacement data in biomechanics. *Hum Mov Sci*,4:229–245.
- Woltring HJ 1986, A FORTRAN package for generalized, cross-validatory spline smoothing and differentiation. *Advances in Engineering Software*, 8:104–113.
- Woltring, H J 1991, Representation and calculation of 3-D joint movement *Hum Mov Sci* 10: 603-616
- Woltring HJ 1994, 3-D attitude representation of human joints: a standardization proposal. *J Biomech* 27:1399–414.
- Wu G, Cavanagh PR 1995, ISB recommendations for standardization in the reporting of kinematic data. *J Biomech* 28(10): 1257-1261.

- Wu G et al. 2002, ISB recommendation on definitions of joint coordinate system of various joints for the reporting of human joint motion--part I: ankle, hip, and spine. International Society of Biomechanics. *J Biomech* 35(4): 543-548.
- World Health Organisation 1989, Stroke--1989. Recommendations on stroke prevention, diagnosis, and therapy. Report of the WHO Task Force on Stroke and other Cerebrovascular Disorders. *Stroke* 20:1407-1431.
- Yack HJ, Houck J, Cuddeford T, Pierrynowski M 2000, Measuring 3D knee motion with surface markers, it can be done. *Gait & Posture* 112: 148-149.
- Yamamoto S, Ebina M, Iwasaki M, Kubo S, Kawai H, Hayashi T 1993b, Comparative study of mechanical characteristics of plastic AFOs. *J Prosthet Orthot* 5: 59-64.
- Yamamoto S, Ebina M, Miyazaki S, Kawai H, Kubota T 1997, Development of a new ankle-foot orthosis with dorsiflexion assist. Part 1: Desirable characteristics of ankle-foot orthoses for hemiplegic patients. *J Prosthet Orthot* 9(4): 174-179.
- Yamamoto S, Ebina M, Kubo S, Kawai H et al. 1993c, Quantification of the effect Dorsi-/Plantarflexibility of ankle-foot orthoses on hemiplegic gait: A preliminary study. *J Prosthet Orthot* 5(3):88-94.
- Yamamoto S, Ebina M, Kubo S, Hayashi T, Akita Y, Nayakawa Y 1999, Development of an ankle-foot orthosis with dorsiflexion assist, Part 2: Structure and function. *J Prosthet Orthot* 11(2): 24-28.
- Yamamoto S, Hagiwara A, Mizobe T, Yokoyama O, Yasui T 2005, Development of an ankle-foot orthosis with an oil damper. *Prosthet Orthot Int* 29(3):209–219.
- Yamamoto S, Hagiwara A, Mizobe T, Yokoyama O, Yasui T 2009, Gait improvement of hemiplegic patients using an ankle-foot orthosis with assistance of heel rocker function. *Prosthet Orthot Int* 33(4):307-323.
- Yamamoto S, Miyazaki S, Kubota T 1993a, Quantification of the effect of the mechanical property of ankle-foot orthotics on hemiplegic gait. *Gait & Posture* 1:27-34
- Yang JF, Scholz JP, Latash ML 2007, The role of kinematic redundancy in adaptation of reaching. *Exp Brain Res* 176: 54-69.
- Yavuzer MG 2007, Walking After Stroke. *J PMR Sci* 1:1-8.

Yokoyama O, Sashika H, Hagiwaya A, Yamanato S, Yasui T 2005, Kinematic effects on gait of a newly designed ankle-foot orthosis with oil damper resistance: A case series of 2 patients with hemiplegia. *Arch Phys Med Rehabil* 86:162–166.

Young J, Forster A 2007, Review of stroke rehabilitation. *BMJ* 13: 86-90.

Web Sites:

<http://brainmind.net/BrainLecture12.html>

<http://comm02.wordpress.com/2011/02/08/etienne-jules-marey/>

www.indicators.scot.nhs.uk

www.isdscotland.org

www.merckmanuals.com

www.orthomerica.com;

www.optecusa.com

Appendix 1

Data Collection Sheet

Date: _____

Subject Trial Number: _____

Subject Group: _____

Test Session: _____

| | | | |
|--------------------------|--|---------------------|--|
| Body Weight (Kg): | | Height (cm): | |
| Hemiplegic Leg: | | | |

The Modified Rivermead Mobility Index (MRMI):

Write the number, between 0 and 5 based on the scoring key below, that best describes the performance of the participant.

| | SCORE |
|--|-------|
| 1. TURNING OVER Please turn over from your back to your stronger side | |
| 2. LYING TO SITTING From lying on your stronger side please sit up on the side of the bed | |
| 3. SITTING BALANCE Please sit on the edge of the bed (The assessor times participant for 10 s) | |
| 4. TRANSFERS Please go from the bed to the chair (Chair placed on participant's stronger side) | |
| 5. SITTING TO STANDING Please stand up from the chair (Participant takes less than 15 s) | |
| 6. STANDING Please remain standing (The assessor times participant for 10 s) | |
| 7. WALKING INDOORS Please walk for 10 metres in your usual way | |
| 8. STAIRS Please climb up and down this flight of stairs in your usual way | |
| TOTAL SCORE | |

Scoring :

- 0 = unable to perform
- 1 = assistance of 2 people
- 2 = assistance of 1 person
- 3 = requires supervision or verbal instruction
- 4 = requires an aid or appliance
- 5 = independent

Scoring of Items:

- If the patient turns over in bed by pulling himself/herself over with his/her unaffected arm, this counts as using an aid. The patient should be asked to roll onto his/her unaffected side first. Both sides can be tested if appropriate;

- The patient should be asked to sit up while lying on his/her unaffected side first; Pulling himself/herself up on the edge of the bed with his/her unaffected arm counts as using an aid.
- The use of the hands to hold on constitutes as aid;
- The use of hands to push up into standing constitutes an aid;
- The patient should start the transfer towards the unaffected side;
- Using a railing constitutes using an aid;
- Supervision or verbal instruction excludes any physical contact.

Functional Ambulation Classification (FAC):

Tick the box that best describes the ambulation performance of participant.

| | SCORE | |
|---|----------|--|
| Non-functional ambulatory Participant cannot walk, walks in parallel bars only, or requires physical assistance from more than one person to walk safely outside parallel bars. <i>Participant clearly requires 2 people to walk.</i> | 1 | |
| Ambulator – dependent on physical assistance - Level II Participant is able to walk outside parallel bars for at least 4 steps but requires continuous manual contact to support body weight as well as to maintain balance or to assist co-ordination during walking. <i>Participant would fall without the physical assistance of another person.</i> | 2 | |
| Ambulator – dependent on physical assistance - Level I Participant can ambulate for 5 metres but requires intermittent or continuous light touch to assist balance or coordination. <i>May include another person helping to move affected leg. Light hand support only, chest or trunk should not need supporting.</i> | 3 | |
| Ambulator – dependent on supervision Participant can ambulate on level surface for 5 metres without manual contacts of another person but requires standby guarding of one person either for safety or for verbal cueing. <i>Participant does not require assistance to move affected leg, nor to support body weight, standing by is allowed. Would be unsafe walking alone.</i> | 4 | |
| Ambulator – independent level surface only Participant can ambulate independently on level surface for 5 metres but requires supervision to negotiate non-level surfaces e.g. stairs, inclines. <i>Using a banister/rail counts as assistance.</i> | 5 | |
| Ambulator – independent Participant can walk anywhere independently, including stairs. <i>Without any form of supervision.</i> | 6 | |

Gait analysis test:

| Calibration trial_Vicon Instrumentation | | | |
|--|-------------|----------|-----------------------|
| Static Stand | | | |
| Walking trial (Tick / R or L)_Vicon Instrumentation | | | |
| | Without AFO | With AFO | With Instrumented AFO |
| Gait 1 | | | |
| Gait 2 | | | |
| Gait 3 | | | |
| Walking trial (Tick)_Gait mat | | | |
| | Without AFO | With AFO | |
| Gait 1 | | | |
| Gait 2 | | | |
| Gait 3 | | | |

Comments:

Appendix 2

Index of Electronic Appendix

BBModel_EP5

Body Builder code for processing 3D capture data for the calculation of joint kinematics and kinetics in according to the protocol described in Chapter 2.

BBMarkerfile_EP5

File containing the list of markers comprised in the utilised marker set for marker labelling in Workstation (to be used with BBModel_EP5).

BBParameterfile_EP5

File in which anthropometric data of the subject tested are saved (to be used with BBModel_EP5).

BBKneeOptimisation

Body Builder code for knee flexion axes optimisation based on the method proposed by Baker et al. (1999) and then modified by Schache et al. (2006).

BBAFOMomentModel

Body Builder code for processing 3D capture data to calculate ankle kinetics and extrapolate the trajectories of markers in the AFO cluster and foot (Chapter 4).

Matlab_AFOStrainGaugesDataAnalysis

Matlab code for the analysis of AFO strain gauges output to finally calculate the orthotic moment (Chapter 4).

MatlabUCM_STATIC

Matlab code which calculates static/constant parameters from markers positions of 3D static trial to be used for the UCM formulations.

MatlabUCM_DynamicVisualisation

Matlab code which allows the dynamic visualisation of the subject walking (one leg only) as a stick figure according to the geometric model in Chapter 5.

MatlabUCMVariance

Matlab code which calculates the variance within and perpendicular to, the uncontrolled Manifold following the formulations in Chapter5. This file exploits two created matlab functions described in other two Matlab files:

MatlabProjectionsfunction,MatlabThetaGround.